International Symposium on

PLUTONIUM FUELS TECHNOLOGY

Horton
Macherey
Allio

Nuclear Metallurgy Committee,
Institute of Metals Division,
The Metallurgical Society of AIME

NUCLEAR METALLURGY, VOLUME 13

Nuclear Metallurgy, Volume 13

International Symposium on

PLUTONIUM FUELS TECHNOLOGY

Edited by: K. E. Horton
R. E. Macherey
R. J. Allio

Proceedings of the 1967 Nuclear Metallurgy Symposium held in
Scottsdale, Arizona on October 4 - 6, 1967

Sponsored by
Institute of Metals Division,
The Metallurgical Society,
American Institute of Mining,
Metallurgical and Petroleum Engineers, Inc.

THE METALLURGICAL SOCIETY

J. Harry Jackson, President
Albert E. Lee, Jr., Past President
Michael Tenenbaum, Vice President
Carleton C. Long, Treasurer
Jack V. Richard, Secretary

INSTITUTE OF METALS DIVISION

Morris E. Fine, Chairman
Julius J. Harwood, Past Chairman
Donald J. McPherson, Senior Vice Chairman
John H. Rizley, Vice Chairman

NUCLEAR METALLURGY COMMITTEE

W. F. Sheely, Chairman
J. L. Klein, Past Chairman
J. T. Waber, Vice Chairman
A. N. Holden, Secretary

FORWARD

The Symposium on Plutonium Fuels Technology was presented in five sessions at the Camelback Inn in Scottsdale, Arizona. The Symposium Chairman was R. E. Macherey, Argonne National Laboratory. Other members of the Symposium Committee were R. J. Allio, Westinghouse, Atomic Power Division, and K. E. Horton, U. S. Atomic Energy Commission. The Chairmen of the various sessions were J. M. Simmons, U. S. Atomic Energy Commission, D. E. Erb, U. S. Atomic Energy Commission, E. A. Evans, Battelle-Northwest, J. H. Wright, Westinghouse Atomic Power Division, and M. V. Nevitt, Argonne National Laboratory.

The Symposium was truly international in context and attendance. There were thirty attendees from seven foreign countries and an overall attendance of 128.

TABLE OF CONTENTS

PLUTONIUM -- THEN AND NOW

R. D. Baker

R. D. Baker is the chemistry and metallurgy Division Leader with the Los Alamos Scientific Laboratory, Los Alamos, New Mexico

It is indeed a pleasure to have the opportunity to open the 1967 Symposium on Plutonium Fuels Technology. During the past few years the effort going into the use of plutonium as a reactor fuel has increased manyfold. It would be difficult for me to say anything new as to why plutonium is important as a nuclear fuel--the two main reasons being, I'm sure: (1) the possibility of lower cost electrical power and (2) the possibility of using all the energy available in natural uranium. It would also be difficult to try to summarize the status of plutonium fuels as of today--this symposium will do much of that in a technical manner. To make any predictions as to the most likely plutonium fuel or fuels of the future could disrupt even this opening session--it might be a bit like criticizing a child in front of his parents.

There is one subject concerning plutonium, however, that I have always found interesting, intriguing and even a bit romantic and that is the history of the element plutonium. It could be that many people now working with the element have never given its history a great deal of thought--perhaps I would not if I had not been introduced to the infant in 1943.

Plutonium was discovered in 1941--only 26 years ago. Even the concept of the existence of transuranium elements began with the discovery by E. Fermi and his co-workers in 1934 that the neutron irradiation of uranium produced radioactive substances. This makes the whole field of transuranium elements only 33 years old--younger than many of the people now working on the problems of using plutonium as a reactor fuel. Plutonium is the first synthetic element to be produced in visible amounts and we all know the importance of the nuclear properties of plutonium-239; both in the past and in the future. The metallurgical and chemical properties of plutonium are more interesting, and at times more baffling than any other element.

In February 1941, plutonium was discovered in the cyclotron by Glenn T. Seaborg and associates at the Radiation Laboratory of the University of California. The isotope first discovered was plutonium-238. The search for the isotope, plutonium-239, was successful and the proof that it would undergo fission was accomplished during the spring of 1941. This proved the value of plutonium as a source of nuclear energy.

In December 1941, the decision was made to undertake a major effort to produce kilogram quantities of plutonium-239. In order to accomplish this, two problems had to be solved; the development of a method of producing large quantities of plutonium and, once produced, the development of chemical and metallurgical methods for the separation, purification and preparation of the element. The magnitude of these problems was tremendous since the element had been discovered only a few months before.

The method of producing large quantities of plutonium was achieved on December 2, 1942 when E. Fermi and his co-workers succeeded in achieving the first self-sustaining chain reaction in a graphite and natural uranium lattice. This historic event led to the development of the world's first reactors--the beginning of what we now know as nuclear power.

The first studies of the chemical and metallurgical properties of plutonium are, to me, the most interesting studies recorded in the two fields of science.

Time does not permit a discussion of the early work in detail but it should be pointed out that the chemistry for a large percentage of the types of processing that have since been worked on in great detail was investigated using trace concentrations of cyclotron-produced plutonium-238. These investigations were under the direction of Glenn T. Seaborg. Without the results of these studies the development of methods for the separation and purification of the larger amounts of plutonium to come would have been delayed. I feel that this fact is often not recognized and should be because it truly was a great technical accomplishment.

After chemical separation and purification came another major problem; that of the preparation on the microgram scale of plutonium metal. Micrometallurgy on the microgram scale was unknown and its development at the University of Chicago represents a great technical achievement in the history of plutonium. The first production of plutonium metal was made in November 1943 at the University of Chicago. Thirty-five micrograms of plutonium tetrafluoride were reduced by reaction with barium metal vapor in the ceramic double-crucible system. Several three-microgram plutonium metal globules were formed with a density of about 16 gm/cm^3. As more reductions on the microgram scale were made, it was found that the density of the tiny metal globules varied from 16 to about 20 gm/cm^3. The melting point was reported as being below $800^{\circ}C$. The data provided from the microscale metallurgical research on plutonium were essential to the development of the macroscale technology of plutonium production that followed very soon at Los Alamos.

During 1944, three short years after its discovery, gram quantities of plutonium produced in the Clinton reactor at Oak Ridge were received at Los Alamos. It was in the form of nitrate which required further purification. The amount of plutonium at Los Alamos during 1944 was not great. The plutonium available had to be recycled many times in order to do the development work necessary for the production of large quantities of the pure metal from nitrate solutions. At Los Alamos the scale for the preparation of plutonium compounds and of plutonium metal increased from the microgram scale used at Chicago to the one-gram scale. Uranium was first used as a stand-in for the development of techniques for the preparation of plutonium metal. As word came from Chicago that the melting point might be as low at $800^{\circ}C$, cerium was also used as a stand-in element. The first successful reduction of plutonium tetrafluoride to plutonium metal at Los Alamos was made using lithium as the reductant. The reduction was carried out using a 900 rpm centrifuge to aid in the collection of the metal. The centrifuge method was shortly replaced by the so-called stationary bomb method using plutonium tetrafluoride, calcium metal as the reductant and iodine as a "booster." This method of producing the metal was successfully used on the 0.5, 1, 10, 25, 100, 250 gram scale.

The first plutonium prepared on the one gram scale was of low density and was malleable. As the purity of the metal increased in later reductions, both the density and brittleness increased. It was suspected that the behavior of the metal was complicated by the existence of polymorphic transformations. The first transition point at about $120^{\circ}C$ was found by measuring the volume change

on transformation in an oil-filled volumetric dilatometer. This volume change was greater than that of any known metal except tin. It was soon found that plutonium metal exhibited five modifications between room temperature and the melting point. These findings gave the metallurgists working on the project the most fascinating subject to talk about that, I'm sure, any group had ever enjoyed. The discovery of the modifications opened up a field of fundamental research which, as you know is still being pursued. By the end of 1945 the transformation temperatures for the five phases, the crystal structure of two of the phases, the densities, the expansion coefficients, the electrical resistivities and the temperature coefficients of resistivity had been determined. It is remarkable that these early values are so close to the ones determined later under far less hectic conditions.

I have reviewed what I believe to be the technical highlights in the first five years of plutonium. They are: its discovery, a method for its production, much of its chemistry worked out on the tracer scale, the development of micrometallurgy and then the large scale production, separation, purification and reduction to metal.

Much was accomplished, much has been accomplished since 1945 and much is yet to be accomplished before plutonium reaches its ultimate use to mankind in the production of cheap, dependable nuclear power.

The use of plutonium as a reactor fuel was recognized very early and people were speculating on the types of fuels to use in 1946. The types of alloys being suggested at that time were as follows:

80% U, 10% Pu and 10% of some other element
Al or Be alloys of Pu
Liquid alloys of Pu
Th-Pu alloys

In 1946, very little was known about any of the alloys of plutonium. The potential use of plutonium as a reactor fuel helped to start many of the early alloy programs both in this country and abroad. The rate of growth of effort on plutonium fuels research was slow for two reasons; the scarcity of plutonium for research purposes and the difficulty of handling the material. However, as plutonium became available and more was learned and published concerning the element, the amount of effort increased rather rapidly to what it is today. An interesting observation is that at the First International Conference on Plutonium Metallurgy in 1957, there were eight technical papers concerning plutonium fuels, at the second conference in 1960, there were nine, and at the third conference in 1965, there were twenty-four papers.

Because of the increase in the amount of research and development on plutonium that has and is taking place, I feel that it is very important to maintain technical communication on the subject. This can be accomplished through publication, by visiting each others' laboratories, and by holding meetings such as this Symposium. I have been delighted with the free flow of information concerning plutonium fuels that has and is taking place throughout the world.

This Symposium is on the use of plutonium-239 as a reactor fuel. Some other isotopes of plutonium may also be the subject of future symposiums as the possible uses for them become more developed. Plutonium-238, the first

isotope of plutonium to be identified, is now being used as a heat source in thermoelectric and thermionic conversion devices. These devices are being used as power sources in the space program. Plutonium-238 is being considered for use in the medical field. The possible uses being investigated at this time are the pacemaker device for heart patients and the artificial heart. Both of these applications, if successful, will be another milestone for plutonium in the affairs of man. Another isotope, plutonium-242, has very interesting possibilities for the future. This isotope is a source material for the production of transplutonium elements. Work on the possible uses of these elements has hardly started at this time. Plutonium--be it 239, 238, or 242--will continue to make technical history--remember what has taken place with this element since its discovery in 1941.

In closing, I would like to wish you all success in your research and development on the use of plutonium as a reactor fuel. I am looking forward to hearing and studying your papers on the subject.

Thank you!

PLUTONIUM RECYCLE IN U. S. THERMAL REACTORS

Myron C. Beekman and Harvey A. Wagner

Abstract

It is estimated that 100,000 kilograms of fissile plutonium will have been recovered from the generation of light water reactors by the end of year 1980. The use of this material and the quantities available for research and development programs, as a fuel material for fast breeder reactors and for recycling in thermal reactors, are discussed. The Edison Electric Institute has programs with two reactor manufacturers to evaluate the economics and technical parameters of recycling plutonium in commercial water reactors. An analysis of future plutonium values has been made with respect to the cost of Uranium 235.

Myron C. Beekman is Assistant to the Executive Vice President for Production of The Detroit Edison Company, and Harvey A. Wagner is Executive Vice President for Production of The Detroit Edison Company, Detroit, Michigan.

INTRODUCTION

Plutonium today is a scarce material and what does become available is easily disposed of at a fixed price under the USAEC's plutonium buy-back policy. However, both of these are short-term conditions. The rapid growth of the light water reactor industry will result in very large quantities of plutonium becoming available in a few years. Furthermore, the USAEC guaranteed buy-back price of $10.00 per gram of the contained plutonium isotopes 239 and 241 as nitrate, expires December 31, 1970. Presumably, after that time, plutonium will be a commercial commodity subject to the laws of supply and demand.

How to efficiently and economically utilize plutonium, what are its nuclear characteristics in fast and thermal spectrums, when and to what extent will it be recycled in thermal reactors, what are the fast breeder reactor requirements and when, and what will be its free market price, are some of the presently unresolved questions facing the nuclear industry. Many of these subjects will be discussed in detail during this meeting.

NUCLEAR CAPACITY GROWTH

Since plutonium is a man-made material and can only be produced in quantities by the operation of nuclear power plants, any estimate of plutonium production and recovery is related to the operating nuclear capacity in a given year. Many estimates of nuclear power growth rates have been made, some of which involved detailed analyses of area fuel costs, economy growth, electric power generation and pooling considerations, air pollution conditions, and other factors. Experience has shown that most of such forecasts have in the past underestimated the actual growth. This might well be expected in this new and continually improving nuclear industry.

Two estimated nuclear capacity forecasts for the years 1965 through 1980 are shown on Figure 1. The most recent USAEC (United States Atomic Energy Commission) forecast of installed nuclear capacity in 1980 indicates between 120,000 and 170,000 megawatts, with 150,000 megawatts being the best single estimate. (The authors have assumed the expansion curves corresponding to these capacities.) A more recent review of this subject, and the one used in this paper, was prepared by the EEI Fast Breeder Reactor Study Group. Their preliminary results of this analysis indicate about 200,000 megawatts of installed nuclear capacity in 1980.

There are too many uncertainties to make meaningful long-range predictions other than that, toward the end of the century, the U. S. may have an installed nuclear capacity of greater than one million megawatts. Many are predicting that by year 2000, about one-half of the total electrical energy produced in the U. S. will be from nuclear plants.

RECOVERED PLUTONIUM

Plutonium production is not only a function of the operating power level, but also of the type and design characteristics of the reactor. Generally, high-thermal-efficiency systems have lower plutonium production rates than do low-thermal-efficiency systems. The design characteristics of present-day light water reactors are such that more plutonium is produced per megawatthour in a pressurized than in a boiling reactor concept. In addition, the fissile part of the plutonium produced, at comparable fuel exposures, is larger for the pressurized water reactor.

For purposes of this study, it was assumed that all nuclear capacity installed prior to 1980 consists of equal amounts of boiling water and pressurized water reactors. It was further assumed that fast breeder reactors will become competitive with light water reactors in the early 1980s and will gradually represent more and more of the annual installed nuclear capacity during that decade.

The designs and fuel exposure warranties of today's light water reactors are such that a plant operating at 80 percent capacity factor will have a combined average discharge of about 0.192 kilograms of fissile plutonium per megawatt per year. Design optimizations in time may result in changing this average production rate. However, no significant departure is expected during the next decade.

The annual and cumulative total fissile plutonium recovered from U. S. civilian power reactors between 1970 and 1990 is shown in Figure 2. In computing these quantities, a two-year lag was assumed between initial reactor operation and discharge of spent fuel, and one year after discharge before the plutonium was recovered. The data indicate that about 100,000 kilograms of fissile plutonium will have been recovered by 1980, and 300,000 kilograms by 1985. Quantities of these magnitudes and the dollars they represent pose significant technical and economic issues.

PLUTONIUM DEMANDS

There appears to be three basic uses of recovered plutonium:

1. For Research and Development
2. As a Fuel Material for Fast Breeder Reactors
3. For Recycling in Thermal Reactors

Substantial quantities of plutonium for research and development programs have been used over the past ten years and there is a continuing need for even greater amounts. A paper by Messrs. D. Boyer and E. Goodman, USAEC, presented at the Brussels Symposium on "Use of Plutonium as a Reactor Fuel" in March 1967, indicated an estimate of the civilian utilization demands through fiscal year 1976. They

have estimated that 11,600 kilograms of plutonium will be required through 1971 and 25,000 kilograms through 1976 for research and development programs. It is apparent, when comparing the quantities of recovered plutonium with the demands for research and development, that the demands cannot be met from plutonium recovered from civilian power reactors. The present USAEC policy, as we understand it, is to make maximum use of plutonium received from domestic licensed reactors, from other overseas' sources, and to provide any remaining deficit from the production reactors.

Technical evaluations indicate that plutonium will be most efficiently used, and consequently have its greatest value, in fast breeder reactors. It is probable that two or more 300-500 Mwe fast breeder reactor demonstration plants will be built and operated in the mid-1970s. It is also probable that fast reactors will not be developed sufficiently to be economically competitive with light water reactors until the early 1980s. During the 1980s, fast breeder reactors will be constructed on some expansion sequence commensurate with electric power industry acceptance and manufacturing capabilities. A large demand for plutonium at a premium price is expected to materialize as the fast reactor portion of the total nuclear capacity increases.

PLUTONIUM AVAILABLE FOR RECYCLE USE

The timing and quantities of plutonium available for recycle use are, therefore, functions of the research and development requirement and the timing and installation rate of commercial fast breeder reactors. A review of these conditions and possibilities indicates that most of the plutonium recovered in the early 1970s will be used for research and development programs. Fast breeder reactor demonstration plants to be operating in the mid-1970s will require substantial amounts of plutonium for inventory and initial reload, but there appears to be excess plutonium available for recycle.

Assuming that early commercial fast reactors can pay $3.00 per gram more for plutonium than its value in thermal recycle, holding the recovered plutonium for two years before selling for fast reactor use would appear to be economically justifiable. If the fast reactor requires purchase of plutonium two years in advance of operation, this would result in a four year advance between recovered plutonium and fast reactor operation. If it is further assumed that commercial fast breeder reactors are operating in 1980 and are installed at the rate of four 1,000 Mw units in the first two years, eight in the next two years, sixteen in the next two, and so on, their demands would leave little, if any, for recycle use after the early 1980s.

Based on these assumptions, which are of great importance to the conclusion, it appears that 60 to 80 metric tons of plutonium should be used in thermal reactor recycle during the latter half of the 1970s and the early 1980s.

RECYCLE OF PLUTONIUM IN THERMAL REACTORS

There appears to be no technical feasibility problem in using plutonium as a reactor fuel in light water reactors, as plutonium exists in all operating plants. However, the efficient utilization of plutonium contained in new reactor fuel is another matter. There are many important factors in recycling plutonium in thermal reactors which are not well understood at this time. Some items of particular concern are the low energy resonances of the plutonium isotopes, their effect on power peaking, the speed of response to control action, plutonium segregation, spectral effects, non-isotopic uniformity, and fuel cycle economics.

Many programs related to the technology of plutonium recycle have been pursued over the years by the USAEC, Battelle Northwest, General Electric, Westinghouse, NUMEC (Nuclear Materials and Equipment Corporation), ESADA (Empire State Atomic Development Associates, Inc.), and others. Probably the largest single effort has been the USAEC's Plutonium Recycle Program. More recently, the partial plutonium loadings in the Saxton Experimental Nuclear Reactor and in the EBWR (Experimental Boiling Water Reactor) will contribute appreciably to this area of technology.

EEI PLUTONIUM RECYCLE PROGRAMS

In 1966 the Edison Electric Institute entered into research and development programs with the General Electric Company and with the Westinghouse Electric Corporation to evaluate the economics and technical parameters of utilizing plutonium as a fuel in large boiling water and pressurized water reactors, respectively. Each of the current programs is a part (Phase I) of total programs leading to commercial loadings of plutonium bearing fuels in large water reactors in the early 1970s, and are financed with each manufacturer on a cost-sharing arrangement.

The scopes of work in the Phase I programs consist of an evaluation of (1) the parameters that influence plutonium fuel cycle economics, (2) the methods of improving plutonium utilization, and (3) the potential problem areas. These programs were originally scheduled as a one-year effort with General Electric and an 18-month program with Westinghouse. Phase I of the General Electric program was essentially completed in September 1967 and the corresponding part of the Westinghouse program should be completed by the end of 1967.

Subsequent Phase II programs would be based on the results of the Phase I efforts as well as other pertinent information available at the time. It was initially envisioned that Phase II would include the design and fabrication of plutonium bearing test fuel assemblies for irradiation in large water reactors. Data from these programs would then provide the basis for the design of economic full reactor loadings. A decision as to whether to support additional work in these programs must await completion and evaluation of the results

of the Phase I studies.

It is premature to discuss any conclusions or results obtained from the Phase I studies, but some general comments appear to be in order.

General Electric Program

A reference fuel fabrication technique has been selected, employing pelletized, mixed-oxide fuel with Zircaloy cladding. It is recognized that, in the long term, physical mixtures of uranium-plutonium oxide powders using vibratory compaction may result in lower fabrication costs. However, the need for additional information on the fast transient performance of segregated plutonium fuels, the results obtained to date in pelletizing mixed oxides, and the large industrial acceptance of pelletized fuel, have led to this design selection for additional in-reactor testing at this time.

An in-reactor test is now being performed in the Dresden 1 reactor which contains four recycle plutonium fuel pins, ranging from 1.4 to 1.7 percent plutonium enrichment. This test represents the first time that plutonium contained in the discharged fuel from a power reactor has been recovered commercially, fabricated into new fuel pins, and re-inserted into the reactor which produced it, thus "closing the loop." This test is considered valuable in that, among other things, it will aid in determining necessary requirements for licensing and transporting recovered plutonium, provide additional performance data, provide substantial information to guide any Phase II irradiation test program, and assist in evaluating new fabrication facilities and fabrication technology using full-size rods and commercially recovered plutonium.

A series of design calculations have been completed to evaluate the nuclear and thermal performance of several alternate fuel bundle designs. As is the case for boiling water reactor uranium-enriched fuel designs, several different plutonium enrichments are incorporated in the reference design to compensate for neutron flux peaking caused by the water gaps at the edge of the bundle. Preliminary economic studies on the estimated value of plutonium have resulted in a wide range of values due to the different fuel bundle loading designs. For the most favorable plutonium design, however, it was found that the value of fissile plutonium is not significantly different than the value of the fissile uranium burned in a typical boiling water reactor design, providing fabrication cost increments for plutonium fuel are not larger.

Westinghouse Program

The primary effort during the first part of this study program was devoted to nuclear engineering, mainly in the development of calculational methods and the planning and evaluation of critical experiments. Plutonium cross section data and nuclear design codes have been evaluated by comparison with the results of the plutonium

critical experiments conducted under an agreement with ESADA.

Under the ESADA program, critical experiments were conducted with two weight percent PuO_2-UO_2 fuel containing either eight percent or twenty-four percent plutonium 240. Single and two-region experiments employing four different lattice configurations were made with each isotopic composition. Power distribution and reactivity data from these experiments have provided valuable information for evaluating nuclear data and engineering design methods.

Fuel cycle parameter studies have been performed to provide a basis for more detailed evaluations of the important fuel cycle variables. A series of equilibrium cycle fuel depletion calculations for variations in hydrogen-to-fuel ratio, specific power, burnup, fuel density and plutonium isotopic content, have been completed. Studies are now in progress to evaluate the relative merits of several fuel management schemes during the transition from a uranium-fueled to a plutonium-recycle core configuration.

Plutonium fuel fabrication techniques and relative costs are also receiving considerable attention. Results have indicated the plutonium fabrication costs are extremely sensitive to plant throughputs and that this may have a greater effect on unit fabrication cost than either the type of fuel or the fabrication process. A cost comparison of four material and fabrication process cases did not indicate a strong economic preference.

The effects on fuel cycle cost and plutonium value of the important economic parameters have been analyzed for equilibrium cycles. Results indicate that, for a typical 1000 Mwe reactor, plutonium values in the $7.00 to $9.00 per gram range may be expected. Variables studied include burnup, fabrication cost, uranium ore cost, specific power, and hydrogen-to-fuel ratio.

THE VALUE OF PLUTONIUM

The 1964-1965 Congressional legislation in the United States, ending mandatory government ownership of nuclear fuels, also established guarantees with regard to plutonium. Although at the present time the guaranteed buy-back price is based only on the fissile isotopes, in the future the price may be applied to all isotopes since plutonium 240 and plutonium 242 do have significant fast fission cross sections.

Completion of the EEI Plutonium Recycle and other current programs will provide more substantial evidence regarding the actual value of plutonium when recycled in light water reactors. However, there are some basic principles against which these values must be measured.

The values of uranium and plutonium are always related since either can be used as the fissile material in thermal reactor or fast breeder reactor fuels. Furthermore, because of the chemical separability of plutonium, its value is proportional to the price of fully enriched

uranium, as opposed to the price of slightly enriched uranium. Hence, as changes occur in the costs of uranium ore, conversion of U_3O_8 to UF_6, and in separative work, these will be reflected in the value of plutonium. Therefore, the most important elements in the long term value of plutonium are its nuclear fuel characteristics as compared to other fissile materials, and its supply and demand. In the near future, during the early years of the plutonium recycle program, such things as lack of performance data, minimal sized fabrication facilities, and shipping and reprocessing complications may result in lowering its competitive value.

One of the larger near term factors that may reduce the value of plutonium is the fabrication cost penalty of this radioactive and toxic material. Considerable work has been done in attempting to assess the cost of performing plutonium fuel fabrication operations. Battelle Northwest Laboratory (formerly Hanford), probably having done the most work in this area, concluded that plutonium enrichment, as compared to uranium enrichment, increases the fabrication cost about 25 percent. A major portion of this differential reflects the cost of converting plutonium nitrate to a usable oxide form. This conclusion is generally supported by others. If this cost differential is realistic, then the plutonium fabrication penalty might reduce the value of plutonium $1.00 per gram. Even if this penalty were doubled, and it may well be in the early years of its use, the resulting plutonium price would still be sufficiently high to warrant its use in a recycle program. In the early part of the 1980s, it appears that plutonium throughputs required by fast breeder reactors or a larger recycle program will be sufficiently great to require large scale fabrication plants. This, plus a more knowledgeable application of plutonium in light water reactors, would somewhat, if not completely, offset the earlier cost penalties.

Plutonium has particularly advantageous properties as compared to uranium 235 in a fast spectrum. For example, the neutrons released per fission for plutonium 239 and plutonium 241 are on the order of 25 percent and 40 percent larger, respectively, than for uranium 235. Furthermore, a high gain breeder provides a fuel cycle cost which is largely insensitive to plutonium price as the credit for excess-bred plutonium offsets the carrying charges on the plutonium inventory. In a mixed reactor complex of thermal and fast reactors, with a balanced plutonium economy, it is logical to assume that the price of plutonium will be established so that the cost of generating power will be a minimum. This situation is, however, affected appreciably by the cost of uranium 235, the supply and demand of plutonium, the doubling time of fast breeder reactors compared to that of the growth rate of the electric power industry, design changes in either reactor type, and other factors. Thus, for a low specific inventory--high breeding ratio fast reactor, the value of plutonium may be as much as 50 percent greater than fully enriched uranium. The net effect of a premium price for plutonium is to reduce the overall cost of electric power generation.

Considering the foregoing comments and evaluating the effect each may have on the price of plutonium, it is estimated that price of fissile plutonium will remain close to 85 percent of the value of fully enriched uranium until the mid-1970s. During the latter part of the 1970s and early 1980s, the price ratio may decrease slightly, after which the demand for fast reactor inventories will increase its price ratio to perhaps 1.5 by 1990.

SUMMARY

The technical and economic development and the commercial acceptance of light water reactors as a means of generating electrical energy have resulted in nuclear capacity growths far exceeding earlier predictions. It is now estimated that about 200,000 megawatts of nuclear capacity will be installed by 1980.

The operation of these units will produce large quantities of plutonium. It is estimated that 100,000 kilograms of fissile plutonium will have been recovered by the end of year 1980. This material will be used for research and development programs, fast breeder reactor inventories, and recycled in thermal reactors. Since it does not appear that large fast breeder reactor requirements will materialize before the early 1980s, a substantial plutonium recycle program will be undertaken to efficiently utilize this material in the interim period.

In view of this, the Edison Electric Institute, the U. S. Atomic Energy Commission, and others have undertaken studies to evaluate the economic and technical parameters of using plutonium in large thermal reactors. Specifically, the EEI programs with General Electric and Westinghouse are scheduled so as to have the information necessary for commercial loadings of plutonium-bearing fuels in large water reactors in the early 1970s.

The values of uranium and plutonium are always related since either can be used as the fissile material in reactors. Plutonium will be needed for research and development programs, perhaps until the mid-1970s, after which there will be a substantial plutonium recycle program prior to the demand created by fast breeder reactors. When used in a fast breeder reactor, its value may be increased to as much as 50 percent greater than that of fully enriched uranium.

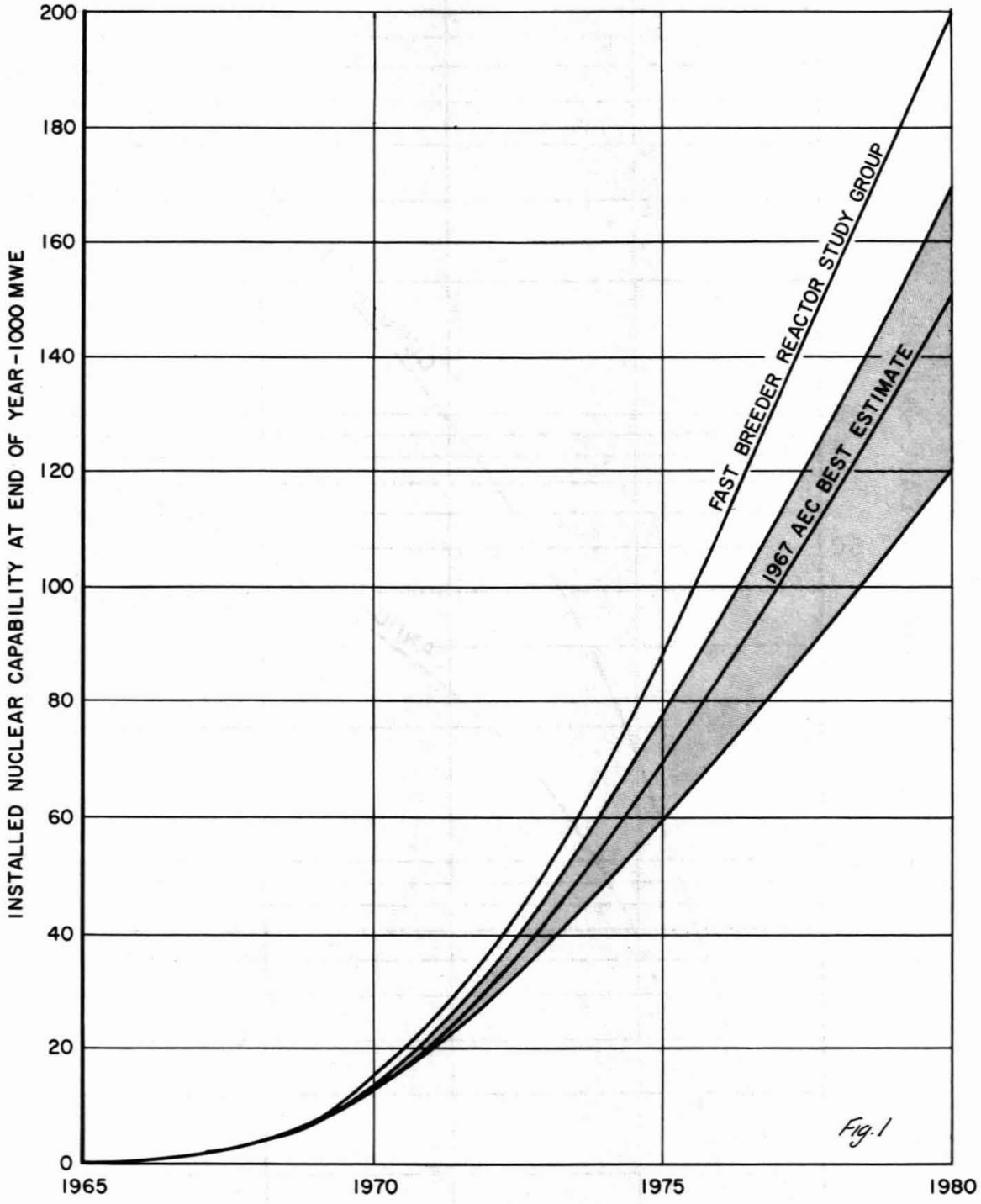
INSTALLED NUCLEAR CAPABILITY AT END OF YEAR-1000 MWE
200
180
160
140
120
100
80
60
40
20
0
1965
1970
1975
1980
FAST BREEDER REACTOR STUDY GROUP
1967 AEC BEST ESTIMATE
Fig. 1

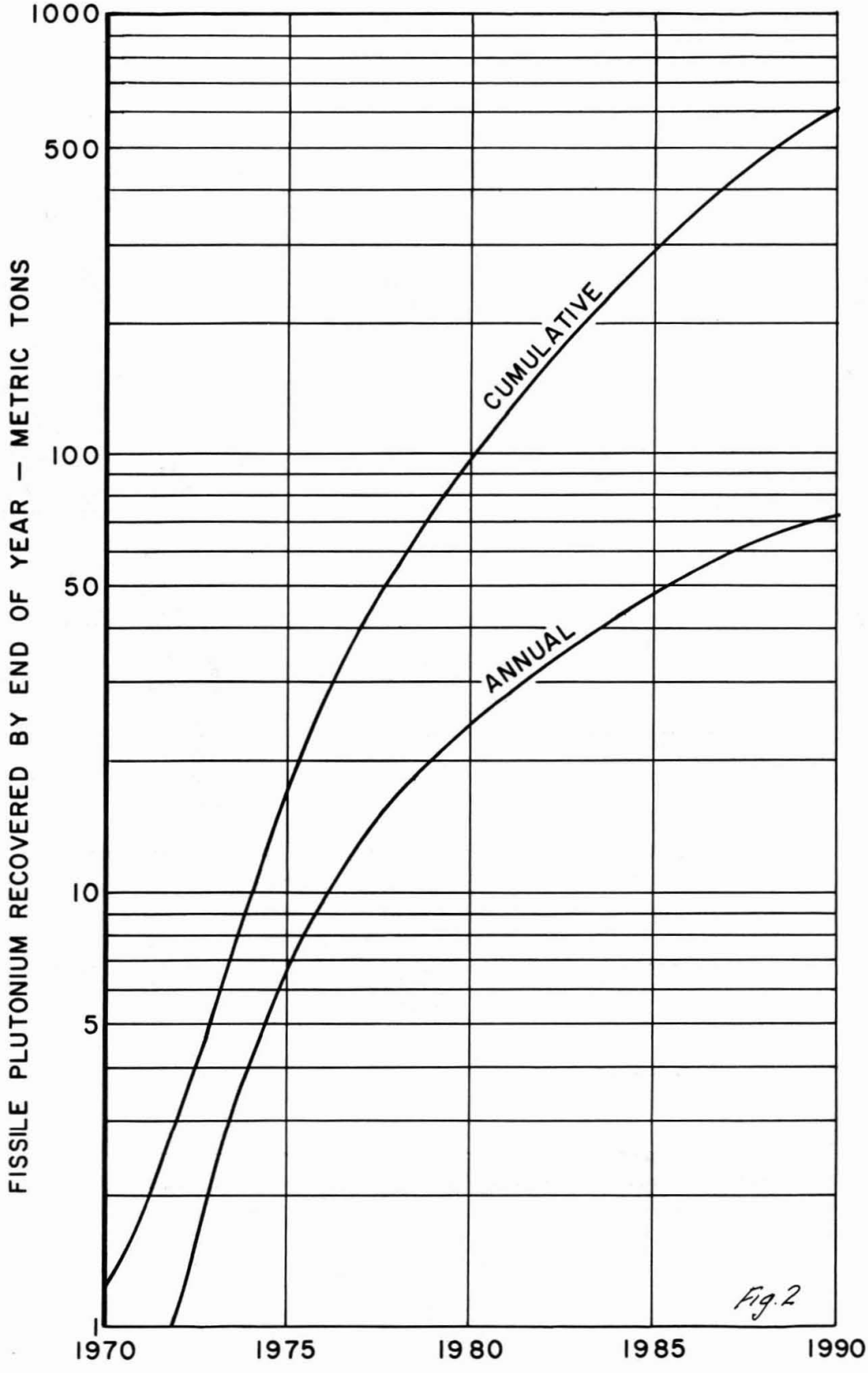
1000
500
100
50
10
5
1
FISSILE PLUTONIUM RECOVERED BY END OF YEAR — METRIC TONS
CUMULATIVE
ANNUAL
1970
1975
1980
1985
1990
Fig. 2

CENTRAL STATION FAST REACTOR FUEL REQUIREMENTS
BELGIAN EXPERIENCE

J. Van Dievoet *
E. Vanden Bemden **

Abstract

The paper gives a description of the fast reactor program for Belgium. This program is subdivided into two parts. The first one is related to a research and development program for the design and the construction of fast reactor prototypes in co-operation with Germany and the Netherlands. The second part is related to the Belgian industrial nuclear power program.

Some considerations about plutonium availabilities and plutonium needs are given on the bases of the above mentioned Belgian program.

The paper shows the incertitudes affecting the establishment of an estimation of future plutonium production and plutonium needs. It concludes upon the necessity to envisage the use of a possible excess of plutonium in thermal reactors and also upon the interest to study an uranium 235 enrichment of the fast reactors in case of a temporary lack of plutonium. Some comments are given about this latter case.

* Directeur at "BelgoNucléaire" S.A. (Société Belge pour l'Industrie Nucléaire), Brussels, Belgium
** Directeur-Adjoint at "BelgoNucléaire"

Research and Development Program

The principal objective of the fast reactor Belgian research and development program is to prepare the Belgian industry to participate in the design and construction of the future commercial fast reactor power station.

The main aspects of this program are briefly described hereunder.

In January 1966, Euratom and the Belgian Government signed an Association contract for the development of fast reactors. It is carried out in co-operation with the Euratom - Germany fast reactor Association. Its first phase amounts to more than 3 million dollars and is supported by Euratom, the Belgian State and the industry. The research and development work has been assigned to BelgoNucléaire and the Centre d'Etude de l'Energie Nucléaire (CEN). One section of that contract is devoted to fast reactor fuel.

Ten years ago, an agreement was signed between Atomic Power Development Associates (APDA) and BelgoNucléaire. The CEN joined this agreement later on. In the scope of this agreement, about ten BelgoNucléaire- and CEN engineers have participated in the design, construction and start up of the Enrico Fermi reactor. They totalize more than 30 years - engineer spent in the United States.

As a continuation of that collaboration, BelgoNucléaire undertook in the framework of the above mentioned Association the study of the plutonium oxide fuel for the second core of the Enrico Fermi reactor. It was considered that the know-how gained in developing the work could be applied afterwards to European programs. A detailed description of the performed work is given in the report entitled "Belgian Experience in Fabrication and Irradiation Performance of Fast Reactor Fuel" prepared for this symposium by J. M. Leblanc, R. Horne and H. Andriessen. This program will be extended during the next Belgian five year plan by a general study of fast reactor fuel elements including plutonium oxides, carbides and a very small effort on nitrides.

BelgoNucléaire is also negotiating, with the full support of the Belgian Authorities, an extended co-operation with the German Consortium Siemens - Interatom and the Dutch Company Neratcom on the design and the construction of a 300 MWe sodium cooled fast reactor prototype to be put in operation at the end of 1973. It will be in the field of the design and construction of the reactor core that the Belgian effort will be mostly concentrated.

Time-scale for the Belgian industrial Fast Reactor Program

As said hereabove, a 300 MWe fast reactor prototype will be built and put in operation at the end of 1973 in the framework of the co-operation between Germany, the Netherlands and Belgium.

As a result of this, a first 1,000 MWe prototype reactor is expected to run in the second half of the next decade.

As far as the later future is concerned, it can be estimated that in somewhat more than 30 years from now on, it is to say at the end of the present century, the power need will request approximately 30,000 installed MWe including probably 20,000 MWe which could be of the nuclear type. In order to reach these requirements, as from 1982 on, 1,000 MWe will have to be installed at the beginning of every two years, afterwards every year and at the end of the century 2,000 MWe will have to be put in operation every year. An important part of these installed capacities after 1982 will probably be covered by fast reactors taking into account the various advantages that one can expect from them, but principally also in respect with plutonium availabilities.

Fuel Requirements for the industrial Fast Reactor Program

In order to start the fast reactors, the plutonium normally requested, will be produced by the existing thermal power stations. The total thermal reactor capacity to be installed in 1980 will amount between 3,500 and 4,000 MWe following approximately the schedule shown in table I. Taking this program as a reference, the quantity of plutonium produced by these thermal reactors and the prototype fast reactors are given in figure 1. An average production of 250 g Pu/MWe installed has been considered. Curve A takes into account an average delay of three years between the production of energy and the availability of plutonium. On the other hand, curve B shows the plutonium availability , taking into account a reduction of that delay to two years. Curve C shows the amount of plutonium needed to fulfil the prototype fast reactor program described above. Curve D shows the same needs , but in the event of a delay of one year in the fast reactor industrial program. On the bases of these curves one can see that up to 1974 there will be probably a lack of plutonium because of the fact that the Research and Development programs will also request plutonium which is not included in the curves.

During a non-defined period after 1974 there will be probably an excess of plutonium. This incertitude is due to the fact that the parameters used for the estimation greatly influence the conclusion and that these parameters are depending on external factors such as :

- general international political situation ,
- possibilities of purchasing plutonium outside of the country,
- speed of development of fast reactors ,
- competition between thermal and fast reactors ,
- evolution of the reprocessing capacity and characteristics,
- etc...

It is quite difficult in these conditions to establish definite conclusions at the present time as far as plutonium availability and plutonium needs are concerned. As a matter of fact we have to consider that following the evolution of the development of the various reactor types and the different factors mentioned hereabove we could have to face in Belgium from time to time a lack of plutonium (this will certainly be already the case during the next six or seven years) or an excess of plutonium (at least during a non-defined period after 1974). Considering these incertitudes and taking into account that Belgium wants to develop largely its nuclear fuel industry, a coordinated program has been decided. As a main objective this program covers the use of plutonium as a fast reactor fuel. But on the other hand it incorporates also a general study of the recycling of plutonium in the thermal reactors and a study on the interest of fuelling fast reactors with uranium 235 instead of plutonium. It has in fact to be considered that the industry must have the necessary knowledge to offer a core for the operating reactors whatever the situation could be as far as plutonium availability is concerned.

The work carried out in Belgium on the recycling of plutonium in thermal reactors has been performed up to now in the framework of contracts concluded with Euratom and the actual conclusions are encouraging. A description of the general program is given in the communication of P. Kruys (Euratom) on the " Euratom Program on Plutonium Recycled Fuels in Thermal Reactors " and in the paper entitled " Irradiation of Plutonium Fuel in the BR - 3 " by H. Bairiot (BelgoNucléaire). Both reports are presented during this symposium.

As said before, in case of a temporary lack of plutonium, a fuelling of fast reactors with uranium 235 could reduce the problem of fuel requirements. Some considerations about this concept are given hereafter.

Interest of fuelling Fast Reactors with Uranium 235

As pointed out above, this solution could be envisaged in case of temporary plutonium shortage. It is for instance supposed that the plutonium produced in a uranium 235 enriched fast reactor is directly recycled in the same one.

A reactor fuelled with uranium 235 is not a true breeder reactor so that during the first cycles an extra amount of plutonium is needed to get the reactor critical, but after a few cycles the quantity of plutonium produced exceeds the requested one. The excess can then be introduced in the core of other reactors.

An analysis of this concept has been made by BelgoNucléaire (1) in the framework of the Euratom - Belgium Association contract taking as a reference the Na l 1, 000 MWe prototype fast reactor studied by the Karlsruhe C enter (GfK - Germany).

One has to consider first that reprocessing of the core and the blankets, either together or not, influences of course the extra quantity of plutonium needed during the first cycles. Three main cases can be envisaged :

case 1 : separate reprocessing of core, axial blanket and radial blanket ,
case 2 : common reprocessing of core and axial blanket, the radial blanket being reprocessed separately ,
case 3 : common reprocessing of core, axial blanket and radial blanket.

Figure 2 shows for the three cases at the upper side of the curves the extra quantity of plutonium needed and at the lower side of the curves the amounts of excess of plutonium produced. It can be seen on the figure that following the reprocessing concept, called case 1, for instance 250 kg of fissile plutonium are needed for the first recycling, somewhat more than 100 kg for the second recycling and approximately none for the third one. At that point the conversion ratio becoming greater than 1, an excess of plutonium is produced.

Table II summarizes for the three reprocessing cases the amounts of plutonium needed and the quantities of that material produced in excess after the first cycles.

Another interesting result is given on figure 3 showing the decrease from cycle to cycle of the U 235 enrichment. Reprocessing the fuel following case 1, a uranium 235 concentration practically equal to the natural value is reached after six recyclings. Following reprocessing case 2 this point is reached after four recyclings and in the latter reprocessing case, the reactor needs only three recyclings to lower the uranium enrichment to the natural value.

As far as economics are concerned, this concept will not alter considerably the cost of the fuel cycle itself. Indeed, it will be applied only in case of plutonium shortage and in such a situation the value of plutonium will be directly determined by that of uranium 235 so that as a principle, in such event the fuel cycle cost of a uranium enriched or a plutonium enriched reactor will be very similar. This of course implies that fast reactors should be close to competition if they are enriched with uranium 235.

Table III gives the average fuel cycle costs (calculated for the various cycles up to the equilibrium).

As a conclusion of the study briefly summarized above, it seems that it is perfectly possible to shift progressively from a uranium enrichment to a plutonium one and this process could be used in temporary cases of plutonium shortage. Nevertheless, we have to consider that :

1) reprocessing the core of the reactor separately allows to use a limited extra quantity of plutonium during the two first recyclings, the residual uranium 235 enrichment reaching the natural value after six recyclings.
This process gives the possibility to recycle all the residual enriched uranium 235 in the reactor. A disadvantage of this comes from the progressive increase of the parasitic isotope uranium 236 with the number of uranium cycles. This phenomenon could force to limit this number and to shift sooner to a full plutonium enrichment.

2) reprocessing the core and the blankets together leads to an increase of the fuel cycle cost due to the reduction of the enrichment of the mixture in uranium 235, but decreases the uranium 236 concentration. This process gives of course a great excess of residual enriched uranium which has to be sold. The extra plutonium quantities needed to operate the reactor during the first recycling is much higher than in the first case mentioned above.

General Conclusion.

A plutonium fuel requirement estimation is difficult to establish far in advance, mainly because of the large incertitudes relative to the development of the different nuclear reactor types (thermal and fast), but also because of external factors which could largely influence the nuclear market. Therefore, we could have to face temporarily either a lack or an excess of plutonium.

Consequenlty, even if we consider that plutonium has to be used in priority in fast reactors, we have to be prepared to absorb a not yet defined plutonium excess in thermal reactors and also to envisage the possibility to fuel fast reactors with uranium 235 in the event of a temporary lack of plutonium.

Both alternatives are technically and seem economically feasible. They will be a complementary insurance against the unforeseeable fluctuation of fissile material availabilities and could therefore decrease the importance of the fuel requirements problem.

REFERENCE

1. Van Dievoet, J. , Eglème, M. , Hermans, L.
Incidence économique du démarrage des réacteurs rapides à l'aide d'uranium 235 sur le cycle du plutonium. Paper presented at the Symposium on the Use of Plutonium as a Reactor Fuel , Brussels, March 13 to 17, 1967 - SM - 88/26

TABLE I

Thermal capacity to be installed in Belgium

Year	MWe	Remarks
1967	145	BR - 3 50 % of the Belgian - French SENA reactor
1972 (	1100 - 1500	Two power stations to be located, one at Tihange and the other at Doel
1973 (		
1976	750	
1979	750	
1980	750	
	3500 - 3900	

TABLE II

Uranium 235 fast reactor enrichment

Number of recyclings	Plutonium needed (kg)		
	case 1	case 2	case 3
1	220	800	1280
2	125	150	75
3	20	-	-
4	-	-	-
	Plutonium in excess		
2	-	-	170
3	60	80	210
4	110	160	225
5	140	190	230
6	170	205	230
7	180	210	230

TABLE III

Uranium 235 fast reactor enrichment - Fuel cycle cost

Actualization yield %	Pu value $/g	Fuel cycle cost (mills/kWh)		
		case 1	case 2	case 3
7	22	0.77	0.72	0.72
11	22	1.12	1.07	1.08

Fig. 1

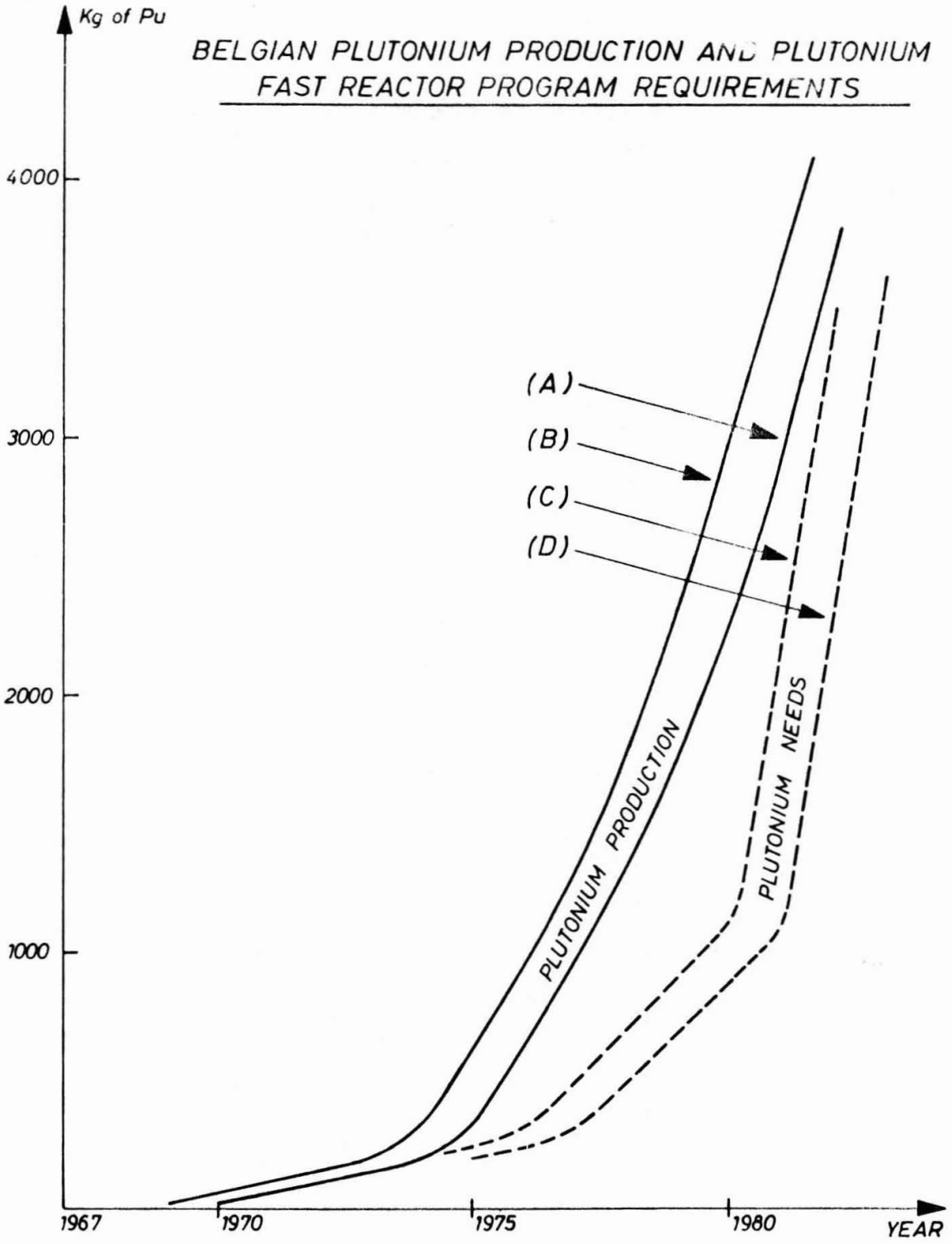
Kg of Pu
BELGIAN PLUTONIUM PRODUCTION AND PLUTONIUM FAST REACTOR PROGRAM REQUIREMENTS
4000
3000
2000
1000
(A)
(B)
(C)
(D)
PLUTONIUM PRODUCTION
PLUTONIUM NEEDS
1967
1970
1975
1980
YEAR

Fig. 2

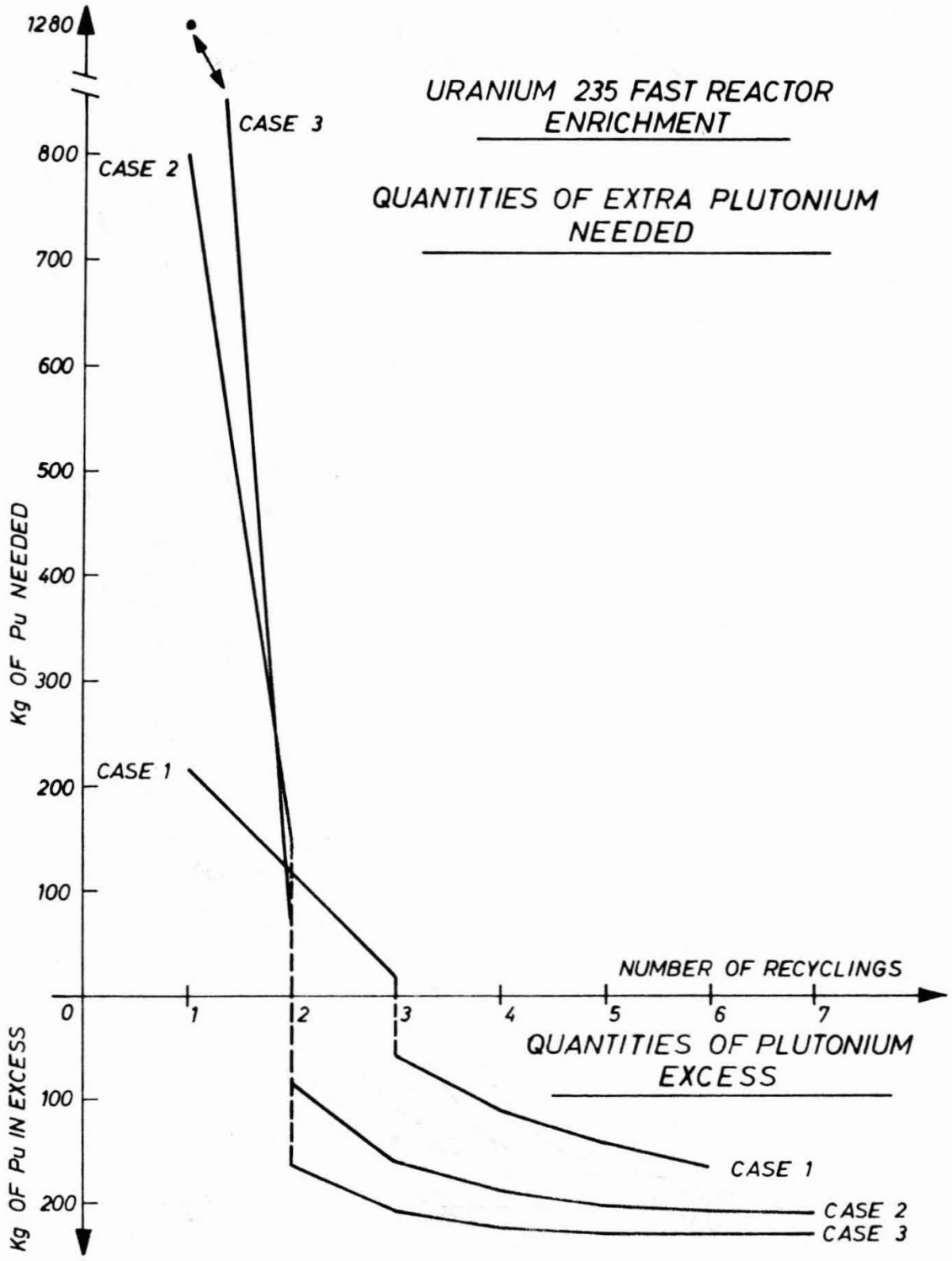
URANIUM 235 FAST REACTOR
ENRICHMENT
QUANTITIES OF EXTRA PLUTONIUM
NEEDED
1280
800
700
600
500
400
300
200
100
CASE 3
CASE 2
CASE 1
Kg OF Pu NEEDED
NUMBER OF RECYCLINGS
0
1
2
3
4
5
6
7
QUANTITIES OF PLUTONIUM
EXCESS
100
200
Kg OF Pu IN EXCESS
CASE 1
CASE 2
CASE 3

Fig. 3

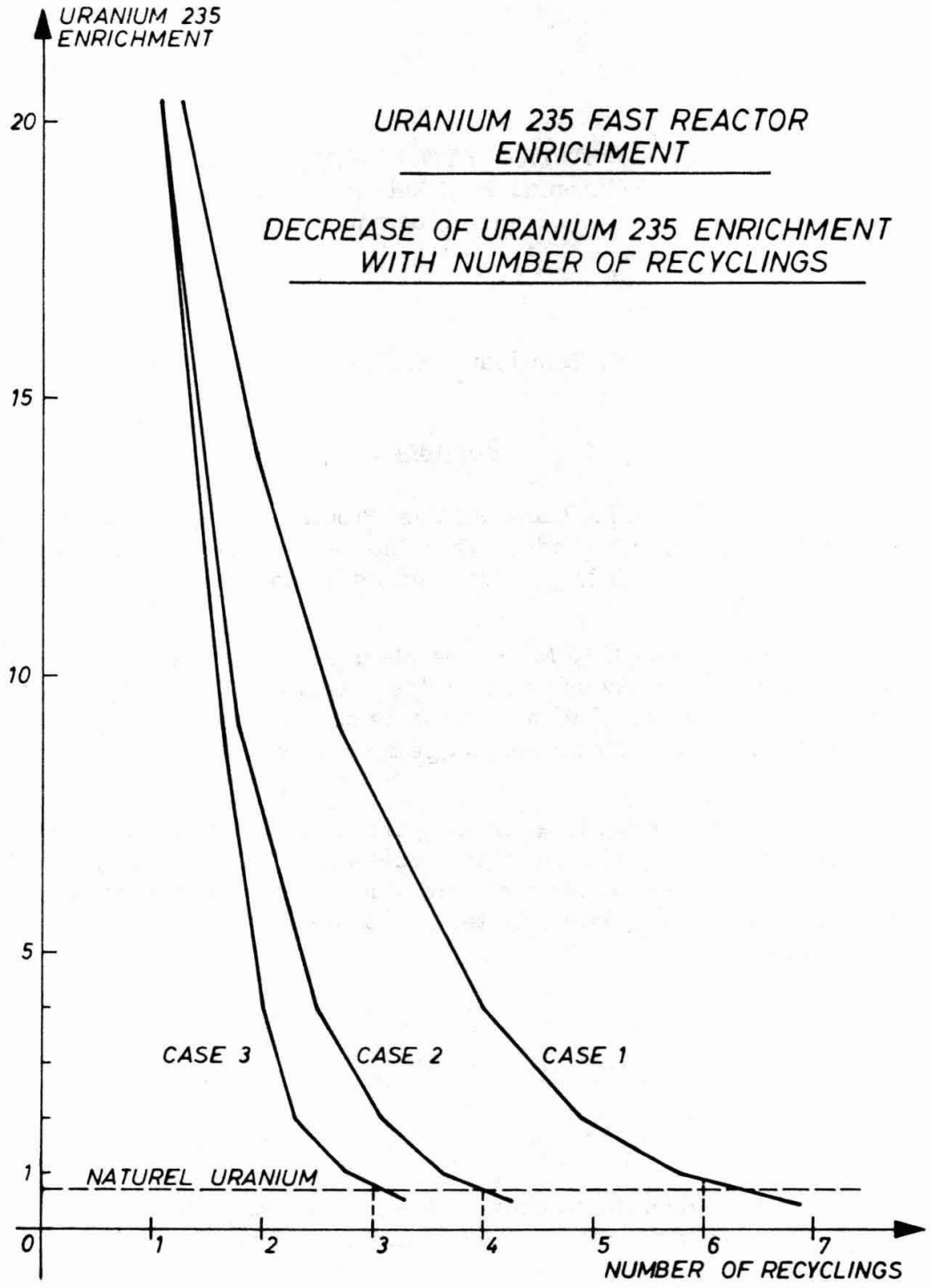
URANIUM 235
ENRICHMENT
URANIUM 235 FAST REACTOR
ENRICHMENT
DECREASE OF URANIUM 235 ENRICHMENT
WITH NUMBER OF RECYCLINGS
20
15
10
5
1
0
CASE 3
CASE 2
CASE 1
NATUREL URANIUM
1
2
3
4
5
6
7
NUMBER OF RECYCLINGS

CENTRAL STATION FAST BREEDER REACTOR
Plutonium Fuel Requirements
French Program

F. Sebilleau - C.P. Zaleski

Abstract

The French Fast Breeder Fuel Program is mainly based on mixed uranium-plutonium oxides. This choice ensures continuity of effort from Rapsodie to the large fast reactors beeing built at the end of the next decade.

For Phenix (250 MWe) the plans are to use pellet type fuel made by a sintering process and stainless steel canning. For economics and fabrication reasons, the main effort is directed towards improvement of industrial stainless steel though noticeable work is performed on nickel based alloys.

On a parallel line, other types of fuels materials : carbides and carbonitrides, other fabrication process like vibrocompaction and other type of fuel like vented fuels are studied. They are considered as solutions which could provide better economics of the fuel cycle for large breeder reactors.

Commissariat à l'Energie Atomique - B.P. n° 6 - 92 Fontenay aux Roses
Association Euratom-CEA - Contrat n° 006/62/1 RAAF

REVIEW OF THE FRENCH PROGRAM FOR FAST REACTOR FUELS.

General trends.

On account of the large amount of effort required for the research and development in the fast reactor field, the French program is mainly concentrated on one reactor type : sodium cooled fast reactors.

As fas as the fuel cycle is concerned, it seems that sodium cooling has greater advantages than vapor or gas cooling, in particular because of the low pressure and small coolant velocity involved. The situation is not the same for other components like heat exchangers for example and more development is needed in this field.

Concentration of efforts requires a continuity in the development which is outlined by the characteristics of the two prototypes preceeding the future large power plants : Rapsodie and Phenix.

Rapsodie is a small experimental reactor, the first of its kind in France. It is expected to provide experience not only on fast core operation but on other components like sodium pumps and heat exchangers. It is also a convenient irradiation facility for testing fuel prototypes for Phenix and future large power reactors.

Phenix will be a demonstration prototype more industrial in character ; it is expected to provide informations on the design and concepts validity of large power stations. Though not economically competitive, it will provide a firm basis for power generation costs evaluations. Because of its industrial character it will probably be less flexible than Rapsodie for irradiation studies but on account of its greater neutron flux it will provide essential informations especially on canning material behaviour.

Fuel types.

In fast reactor fuel development, first priority is given to mixed uranium plutonium oxide fuel with sealed stainless steel cans. Such a design is considered at the moment as sufficiently prooven to constitute a basis for the development of economic fuels for the next future.

On a parallel line a small effort is made on vented fuels. It seems that the main interest of this design lies in the possibility of reducing the fuel length and consequently the core height by suppres-

sion of the gas plenum. That possibility lies in turn on the availability of a reliable venting system other than the diving bell, the development of which requires a great deal of effort. The situation seems to be different for carbide or nitride fuels where the sodium may be allowed to enter in the can thus requiring a simpler venting device.

Fundamental studies of carbides and nitrides are performed on the same level than oxides, but on account of the priority given to oxide the effort on development of carbide fuels is small, as shown in figure 1 which gives the number of irradiated carbide and oxide prototype fuel pins versus time. It is expected that the rate of effort on carbides and nitride will increase in the next few years.

For canning materials, studies are mainly devoted to stainless steels. AISI 316 was choosen for Rapsodie and a similar alloy will be used for Phenix, though the exact grade is not yet determined. Industrial stainless steels exhibit acceptable characteristics for their use as canning material, it seems to us that the first step is to improve these characteristics such as creep strength and irradiation behaviour by alloying additions and modifications of the fabrication process. If the irradiation behaviour of stainless steels cannot be satisfactorily improved, nickel based alloys can be used. Nevertheless these alloys will probably be needed for carbide fuels at high linear power.

An important part of the work on canning materials is concentrated on non destructive testing and fabrication control in order to determine reject criteria compatible with low fabrication costs and reliability.

Fuel fabrication and reprocessing.

The fuel for Rapsodie has been made by sintering, and the same technique will be used for Phenix. The fabrication process is beeing adapted to low density pellets either in the porous or in the annulus form. For Phenix the present plant capacity will be increased by a factor of ten (3 to 30 kg of mixed oxide per day) merely by extrapolation of the actual process.

A discontinuous process rather than a continuous one will be employed, the smaller fissile material concentration allowing increased batch size. This solution has been selected because it is believed that it leads to more reliable and flexible equipment, and in order to take advantage from previous studies for Rapsodie.

A small effort is made on vibration techniques. For mixed

oxide fabrication the question seems to be at present whether this technique provides better fuels from the standpoint of irradiation behaviour rather than economics comparisons between fabrication processes.

Reprocessing of the Rapsodie fuel will be performed in a small pilot plant the capacity of which is 1 kg of mixed oxide per day. For Phenix no decision has been taken up to now, but it is likely that the adopted process will be an aqueous one. Our reprocessing studies include aqueous and dry processes like volatilization of fluorides, the last one needing more development to demonstrate its validity.

EVOLUTION OF FUEL CHARACTERISTICS, EXPECTED OPERATING PARAMETERS FOR LARGE PLANTS.

Burn up.

Economic incentives for high burn up are obvious. Fuel cycle cost evaluations indicate a rapid decrease of costs in the vicinity of 60 000 MWd/t, the curve showing a minimum at about 130 000 MWd/t. Calculations made in France indicate that the fuel cycle cost is 20 % less if the burn up is increased from 70 to 100 000 MWd/t, the gain beeing very low for greater values.

These economic considerations must be faced with technical feasibility. At the moment it seems that 70 000 MWd/t is reasonably attainable with oxide fuel canned in stainless steel, the next step will require more development effort than the first one towards greater burn up in the 90 - 100 000 MWd/t range. The main difficulty lies in improving canning materials properties, especially creep resistance and post irradiation ductility.

In view of these considerations, the design burn up has been chosen as 30 000 MWd/t for Rapsodie, 60 - 70 000 for Phenix and from 70 to 100 000 for the first large power station.

It should be noted that, since increasing the burn up is not the unique way to improve the fuel cycle economy, it may be of greater benefit to act on other reactor characteristics. For example the same 20 % reduction of the fuel cycle cost can be gained by increasing the burn up from 60 to 70 000 MWd/t or by minimising the axial flux distribution factor from 1,3 to 1,17.

Finaly, it seems that burn up values in the range 70 -

80 000 MWd/t must be reached. Higher values are desirable but not necessary since the corresponding loss may be compensated by a better reactor design or a better load factor.

In order to accomodate the swelling some void fraction must be kept in the fuel and two questions arise which had not been given up to now very clear answers : what is the amount of swelling for a given burn up and which is the best void distribution inside the fuel ?

For mixed oxides, at high linear power, it appears from recent experiments that the swelling rate has probably been overestimated and in view of these results one can anticipate a substantial decrease of the void fraction in the fuel from the actual 20 % value. In the case of carbides, more experiments are needed but it already appears that severe temperature limitations will be necessary if reasonable swelling rates are required.

The void fraction may be distributed in the fuel either in the form of a central hole or in the form of uniform porosity. From the heat exchange point of view, these two solutions are very different at the beginning of the irradiation but it is likely that the situation will be approximately the same for both at the end of their life. The choice between the two solutions will therefore be guided by other factors like the stresses induced in the can by fuel swelling and fabrication economics.

Linear power.

With mixed oxide fuels, reasonable linear power can be attained in the 500 W/cm range with fuel diameter 0,5 - 0,6 cm. This leads to 0,7 - 0,8 MW per kg of plutonium. Higher values could be reached provided a certain amount of central melting is not ruled out during the life of the fuel, but more statistical experience is needed in order to determine the exact limits.

As far as thermal bonding is not used, between can and fuel, carbide and nitride performances are not very different from oxide's ones because of severe temperature limitation imposed by swelling. Improvement of linear power for these fuels seems to lie uniquely in increasing fuel density, hence heat conduction, at the maximum value compatible with swelling.

Provided the fuel-canning temperature drop is lowered at a small value, by sodium bonding for example, carbides and nitrides could probably be operated at linear powers in the 1500 - 1800 W/cm range. Difficulties arising from thermal stresses in the can and from

heat extraction in the sub-assembly may well reduce this figure to 1000 W/cm. This high linear power, combined to corresponding larger fuel diameter, is a strong incitation to further studies of these second generation fuels as they have been called by some authors.

Internal breeding gain.

Internal breeding gains not very different from 1 are desirable. This allows to minimise the reactivity loss due to burn up and thus improves the general characteristics of the reactor. One can consider that internal breeding gain values between 0,9 and 1,1 are very suitable ones, 0,8 beeing still acceptable. It seems that one of the better ways to achieve high internal breeding gains is to increase the fuel density and this gives considerable interest to the use of carbides even with medium linear power.

An other way to increase the internal breeding is to increase the fuel proportion in the core at the expense of coolant. The limiting factors in this way are merely of safety concern and it is probable that more reactor operation experience is needed before assigning reasonable limits.

Maximum can temperature.

The maximum can temperature depends upon sodium outlet temperature and hot channel factors. The sodium outlet temperature is determined by the vapor temperature and the trend is obviously to adopt the standard value for conventional turbines which, in France, is 565°C for the 250 and 600 MW power levels.

On the other hand the creep properties of the canning material introduce limitations of the maximum can temperature. For the stainless steels it seems that 700°C is about the upper limit, higher temperatures requiring other material like nickel alloys. The temperature difference 700°C - 565°C = 135°C is sheared in two parts : the temperature drop in the heat exchanger and the hot channel factor.

For the Phenix project, the actual design is :

- sodium outlet temperature : 566°C
- vapor temperature : 512°C
- maximum can temperature : 700°C.

Obviously, except for the maximum can temperature, these temperatures result from optimisation of the heat generation system which

can lead to somewhat different results for larger reactors.

As far as the fuel is concerned, it seems that some improvements could be made in reducing the hot channel factor, especially by a better knowledge of sodium mixing in the sub-assemblies and reduction of other uncertainty parameters. This could lead not only to a higher vapor temperatures but to a lower maximum can temperature ensuring a longer life for the fuel.

Since the incentive for vapor temperatures higher than 565°C is poor, the use of nickel alloy cans would allow some improvements in the can design in account of their better creep properties rather than an increase of the maximum can temperature.

CONCLUSION.

Table I illustrates the evolution of fuel characteristics from Rapsodie to the first large power station in the French program. It is obviously difficult at the present time to know if these evaluations are pessimistic or optimistic, operation of intermediate size plants like Phenix will provide priceless experience in this field. Nevertheless it can be hoped that the main difficulties will be overcome leading to economic power generation by fast reactors in the next future.

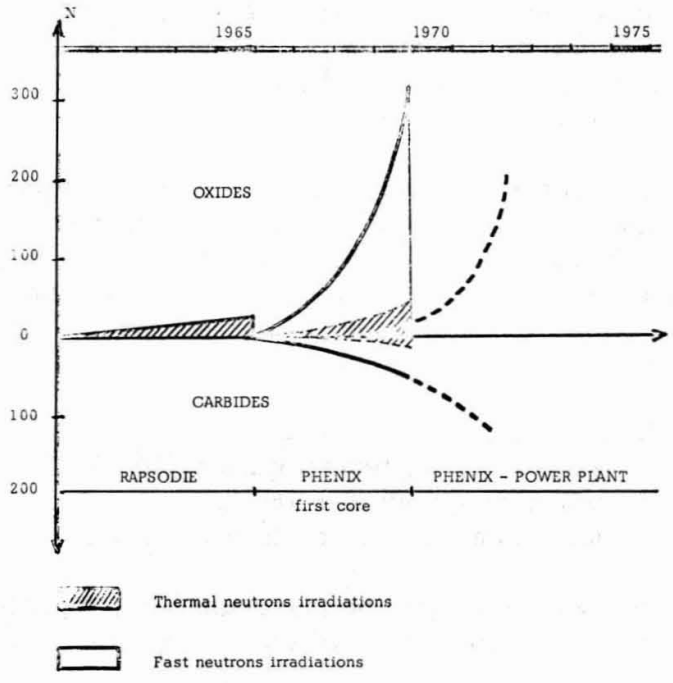

TABLE I - FUEL CHARACTERISTICS

	RAPSODIE		PHENIX		POWER PLANT
	first core	other cores	first core	other cores	
Fuel	UO_2-PuO_2	UO_2-PuO_2 (carbides)	UO_2-PuO_2	UO_2-PuO_2 (carbides)	UO_2-PuO_2 carbides
Canning material	AISI 316	AISI 316 X 18 M (316)	X 18 M (316)	X 18 M (316)	-
Pu/U	1/3	1/3	1/5 - 1/3	1/5 - 1/3	1/3 - 1/5
Maximum can temperature	650°C	700°C	700°C	700°C	700°C
Maximum linear power (W/cm)	340 - 360	400 - 500	430	400 - 600	400 - 600 1000
Burn up MWd/t	30 000	30 - 50 000	60 - 70 000	70 000 - 100 000	70 000 - 100 000
Fuel diameter (mm)	5,7	5,6	5,5	5 - 6	5 - 8
Core height (mm)	340	340 - 600	850	700 - 1000	1000 - 1400
Maximum neutron flux	$2,5 . 10^{15}$		8.10^{15}	8.10^{15}	10^{16}

CENTRAL STATION FAST BREEDER REACTOR PLUTONIUM FUEL REQUIREMENTS *)

K. Kummerer

Abstract

Some basic decisions on fuel and pin type introduce into the field of the principal criteria for the fuel of large fast breeder reactors, which are presently in a conceptional stage. As the German development program pursues in parallel the two lines of a sodium cooled fast breeder and a steam cooled version, the fuel pin requirements are compiled for both cases. The pin layout characteristics translate the requirements to real designs and also to fuel and pin specifications. In conclusion the future development lines concerning fuel types and pin features are shortly mentioned and compared to possible future fuel requirements.

Institut für Angewandte Reaktorphysik
Kernforschungszentrum Karlsruhe
Federal Republic of Germany

*) Work performed within the association in the field of fast reactors between the European Atomic Energy Community and Gesellschaft für Kernforschung m.b.H., Karlsruhe

INTRODUCTION

The fast reactor fuel requirements are evaluated in different stages of development. In the German fast breeder program the first stage was dedicated to some principal selection studies, a procedure, which of course is typical for all large technical development projects. As a first basic decision, oxide type fuel for the fast breeder prototype reactor designs was selected. A metal fuel was considered to be too limitating with respect to the necessary linear power rating at high fuel temperature and to the achievable burnup. On the other hand carbide ceramic is not yet enough experienced, at least not within the available technological know-how for our project. A second approach, however, may be performed with carbide fuel leading to an economically improved fuel cycle.

A further basic decision pertains to the external and internal geometry of the fuel arrangement. Having also studied the feasibility of ball-shaped fuel units, we selected pin type geometry, the latter being more evaluated, both in the inpile cooling behaviour and in the fabrication techniques. The internal geometry is conventional. As we propose a tight free standing strong can, provisions are to be made for the fission gases and vapors and also for the solid fuel swelling in radial and axial direction. Thus the total length of the fuel pin is distributed to the active fuel zone, to lower and upper axial blanket regions and to a fission gas plenum.

The design ideas for fast reactor fuel pins are strongly oriented to our fast reactor design studies for a sodium cooled prototype reactor (1,2,3) and a steam cooled prototype (4). There might be some differences between prototype designs and future central station fast reactors with a capacity of, say, 1000 MWe, mainly concerning the enrichment in fissionable isotopes and the pin length. These differences are considered to be of minor influence to the overall performance of the pin type fuel and hence can be neglected in this state of evaluation. The design principles follow a rather conservative line as far as preparational assumptions for a pin layout are concerned. They are based on some irradiation test pin experience (5), on the single efforts of our fuel development program (6) and also on our irradiation performance considerations and results (7).

The paper here describes at first the basic criteria, which are the starting point for the pin design logic. These lead to the fuel pin requirements for prototype fast reactors. The requirements have to be translated to detailed wording within specifications, some highlights of which we are presenting in the chapter on pin layout characteristics, together with a few typical drawings. In conclusion, there is a discussion on the main limitating factors for a pin layout and on possible future and futuristic development lines.

It should be mentioned, that the requirements concerning the whole subassemblies bring certainly some important enlargement, which refer mainly to the cooling thermodynamics. As the sub-

assembly features are only of minor influence to the pure fuel and fuel pin technique, they are not included here. Above that such subassembly requirements are not yet in a stage of technical evaluation as to be easily expressed in common principles.

BASIC CRITERIA

The basic criteria for the fuel pin design have their sources in the triangle: safety, economy and breeding potential. A forth point of view, which is less scientific - but is of practical importance - is the adjustment to the available development background. The following paragraphs will outline, in more detail, these considerations.

The safety criteria refer to normal reactor operation conditions, if they ask for duly adapted smooth linear power rating distribution. They refer also to possible sudden overpower conditions in the reactor core, when reactivity changes must be outruled by inherent safety features. Their wording might be in short terms:

- The fuel specifications concerning the longitudinal distribution of fissionable material are to be established as to guarantee a smooth heat source distribution over the pin length according to the requirements for the hot channel analysis of the subassembly.
- The reactivity feedback according to an - expectedly - negative temperature coefficient for the Doppler effect in the fuel mixture must become effective within calculated short delay time in a reactor power transient. This asks for specified homogeneity in the plutonium distribution. In this context reference is made to a recent theoretical work (8).
- Another limitation is induced by the socalled "slumping danger". The internal geometry of the fuel pin has to limit axial fuel movement to a specified extent, in order to avoid inherently fuel configurations, which produce an uncontrollable reactivity increase. A general measure in this context is to limit the free volume in the fuel ceramic. This leads to a lower limit for the smeared density of the fuel.

The economic criteria receive their language from different aspects concerning the fuel cycle:

- A plain, but most important truth is, that the fuel pin specifications are to be established as a fit to the whole fuel cycle in an optimized manner.
- There are special limitations due to the fact, that the source material market and prices are not yet developed. Hence the fuel pin requirements get an incentive to proceed in a direction of the "least amount of fuel in the fuel cycle", which may not be the cheapest way.

- Another criterion spells out, that the fuel pin production must be possible at dates according to the time schedule of the prototype planning. Hence the specifications take consideration of the really available techniques and the really foreseeable price situation (9).
- Finally a principle of continuous evolution demands, that the initially established specifications are also applicable to recycle fuel without major economic influence. This means for instance, that a fuel fabrication line, which is adjusted to a set of specifications, can handle also plutonium of equilibrium isotopic composition.

The breeding potential as a target is implicitly involved in the economic criteria. Above the pure economic optimization, however, there is an additional special incentive:

- In order to make comparable the "doubling time" of the future expanding energy demand to the doubling time of an expanding breeder reactor population, a high breeding potential is a separate criterion for the reactor design. Hence the fuel layout via the internal breeding ratio is directly affected. In this context belong also the evaluations - presently underway - for a pure uranium start-up with U 235, in order to soften the conditions of a "dry" plutonium market.

The basic selection criterion with respect to available experimental and technical experience reads e.g. as follows:

- A fuel pin design for a large fast breeder reactor can be based reliably only on a sufficient fabrication experience - at least in pilot plant scale - and on the positive results of irradiation performance tests with a number of pins, which allow at least some statistical judgement.

FUEL PIN REQUIREMENTS FOR PROTOTYPE DESIGNS

The elements of the fuel pin requirements are getting their incentives and limitations by

- reactor physics
- fuel cycle economics
- safety considerations

Taking also into account the basic criteria formulated above, these requirements are outlined and discussed in the following statements.

The enrichment of fissionable material is dictated by the core magnitude and the detailed core design. The content in fissionable Pu is for large fast oxide breeders in the range between 10 and 25 % of total U and Pu contained in the fuel. Normally two radial zones different in the enrichment are provided in order to get a radial power flattening. For a 1000 MWe sodium cooled design e.g. the figures are about 10 % in the central zone

and 14 % in the outer zone, while at typical prototype designs (ca. 300 MWe units) the contents are 15 and 23 %, respectively.

The isotopic composition of the plutonium itself will correspond in the long term range to the related equilibrium conditions of the fuel cycle. At combined core and blanket reprocessing management, there might be a composition of, say, 75 % Pu 239, 22 % Pu 240, 2 % Pu 241 and about 1 % Pu 242. At a separated reprocessing routine the content of higher Pu isotopes in the core cycle will be much higher, of course.

The linear rod power is selected to have values which guarantee no central melting of the fuel. Hence at nominal conditions the maximum figures are in the region of 500 watts/cm. These are the data, which are typical for sodium cooled fast reactors. At the steam cooled version the economically reasonable surface heat transfer makes further limitations to bring the maximum nominal rod power into the range of 350 watts/cm at still reasonable diameters.

The fuel diameter at sodium cooling is determined by the optimized rating value and the selected rod power. At steam cooling the diameter is a compromise between the incentive to a large rating, the feasible steam cooling technique and an economically favoured increased diameter. In both cases the region between 5 and 6 mm in fuel diameter is the result of recent reference design evaluations.

The length distribution of a pin is governed by the request for axial breeder blankets and a fission gas plenum. The volume demand of the latter is in strong relationship to the mechanical pin concept and the internal fuel geometry, see below.

The internal breeding ratio receives its "sources" only from fertile material in the core. Therefore the highest allowable fuel density - each additional density percent is of full benefit to the fertile potential - is aimed for.

The smeared fuel density is a compromise between the necessary porosity in the ceramic body for gaseous and solid fission products - which defines the higher density limit - and breeding loss as well as the slumping danger concerning the lower limit. The most promising density range for oxide type fuel is - according to our knowledge - between 80 and 85 % of theoretical density. For first core equipment of prototypes we propose to use 80 % of theoretical density taking into account a sacrifice in internal breeding. It is hoped that further irradiation performance experience will justify a moderate fuel density increase for later central station fast reactor fuel pins.

The fuel burnup is expected to be in ranges between 50 000 and 100 000 megawatt days per metric ton of heavy elements. A steam cooled reactor might have the schedule at about 60 000 MWd/ton, while a sodium cooled prototype asks for 80 000 to 90 000 MWd/ton, all expressed as maximum burnup values. The requirements for future large central stations may be still somewhat higher.

The level of the cladding temperature distribution is forced to the highest possible data by the required thermal efficiency of the system. The maximum nominal can midwall temperature is

about 600°C for sodium cooling and about 650°C for steam cooling.

The mechanical requirements onto the pins are outlined by the strong can concept. For sodium coolings the necessary mechanical properties are defined by the fission gas pressure buildup during burnup and the thermal stresses in the can wall. The radial solid fission product swelling is considered to be the most dangerous mechanical attack to the cladding wall. The pin lifetime is solely governed by these impacts, if the cladding material layout is to withstand the fission gas and thermal stresses for the expected loadtime at fast neutron environment. Hence the mechanical cladding layout is to be adjusted to the available swelling volume for the solid fission products.

For steam cooling the pressure situation with respect to the cladding is turned around. The high coolant pressure outbalances by far the internal gaseous pressure within the pin. This situation is accompanied by the mechanical creep buckling problem. This instability danger must be handled by additional tubing specifications in high temperature creep strength and in initially limited ovality and also by possible internal support from the ceramic fuel. For steam cooling the "strong can" thinking has lost some of the absoluteness.

The internal geometry of the pin has two main sources of definition. The first one deals with the homogeneity of the fuel mixture. Due to the fact that the inherently acting negative Doppler coefficient shall operate instantaneously, the largest admissible pure PuO_2-particles are in the magnitude of 100 micron. Above that microhomogeneity, there is a request for "macrohomogeneity" in the fuel, which means an overall uniform distribution of the fissionable isotopes in the fertile matrix.
The second source of definition is embedded in the upper and lower density limits, see above. The chosen smeared density can be realized by different fuel densities (for pellet fuel), corresponding to a proper amount of open voids for gap, dishing and central hole. The gap between pellet surface and can, diametrally about 100 to 200 microns, provides for thermal expansion and some fission product swelling. It favours also the pellet fill-in steps at the pin production. According to our knowledge, there is no special incentive for pellet dishing and central hole from the irradiation performance standpoint, if the rod power is high enough to plasticize the central fuel region. The fabrication procedure, however, in some cases may prefer a dished or cored pellet, in order to direct the bulk density of the pellet into higher ranges, where sintering precision is easier to be controlled.

PIN LAYOUT CHARACTERISTICS

In this paragraph it is intended to summarize all actual information concerning the real pin layout. Of course the main examples are taken from the reference design studies (1,2,3,4). Other to some extent very representative examples can be derived

from the layout characteristics for pin irradiation performance tests like the fuel irradiations in the Enrico Fermi Fast Breeder Reactor (EFFBR) (5) and the pin irradiation in a trefoil rig of the Dounreay Fast Reactor in Scotland. All important data are compiled in Tables I and II. There was made a distinction between performance parameters and fabrication parameters. The latter ones constitute the network of pin specifications, while the first ones show the operational conditions in the reactor core or in the irradiation test bed.

The pin data for the Na1 reference design are somewhat futuristic, mainly in the expected maximum burnup compared to the assumed smeared fuel density. The Na2 reference design concentrating now to a prototype reactor of 300 MWe capacity takes more cautious parameters on the basis of very conservative solid fission product radial swelling calculations. The D1 reference design for steam cooling outlines an evaluation comparable to the Na1 stage. The D2 design for the steamcooled prototype, which is presently under evaluation, is not yet included here. There are three examples for irradiation test pins. The two data sets for EFFBR specimens include both a pellet pin version and a pin with vibrocompacted powder fuel. The specimens for the DFR irradiation finally are more developed to a conservative pin layout.

A demonstration of the pin layout in simplified drawings is included in Fig.1 for the reference design pins and for the irradiation test pins. Hence the main geometrical features can be compared.

MAIN LIMITATIONS AND FUTURE DEVELOPMENT

As to the present status of experience we see the main limitations for a high performance oxide fuel pin layout in the radial swelling problem and in the hardly sufficient high temperature creep behaviour of the cladding material. Especially at a steamcooled fast reactor the high external pressure may cause a mechanical instability by creep-buckling.

If a conservative low smeared density for the fuel is taken - in order to provide voidage for the solid fission products - the slumping danger arises. Also the internal conversion ratio is adversely affected. One of the goals of future systematic experimental evaluations is to find the fuel density, just highest possible in view of radial impact on to the cladding. This density figure, of course, will be dependent on a network of parameter constellations like internal fuel geometry, temperature distribution, cladding restraint and burnup level.

The fission gas pressure buildup is partly governing the mechanical analysis of the cladding. But principally in all cases the fission gas plenum can be foreseen large enough, as to shift the critical path for the cladding design to other claims like thermal stresses or radial swelling forces. Therefore the concept of fuel venting get the justification only from space availability arguments, because the pin geometry with fission gas

plenum reduces the axial blanket amount.

The ceramic fuel of the mixed carbide and nitride type is considered to be of remarkable potential for future pin designs. The high heavy metal density is of sensitive benefit to fuel cycle economy, as the breeding ratio is favorable influenced and a higher fuel rating is possible. This trend is fully on the line of future fuel requirements. After the present development efforts, which are mainly directed to specify a uniform production, to investigate the compatibility to cladding and to overcome the large fission product swelling, there may be some switch-over from oxide to these new fuels.

A further field of urgently necessary development is with the tubing material and technology. New alloy types for sodium cooling, as e.g. the vanadium base alloys, are under investigation. But also the class of iron base alloys, the steels, need a "tailormaking" procedure, as the bulk of the now available steels were not developed for reactor design requirements. Especially the fast neutron induced irradiation damages ask for new "streamlined" steel alloys.

REFERENCES

1. D. Smidt and A. Müller, Referenzstudie für den 1000 MWe natriumgekühlten schnellen Brutreaktor (Na1), 1964, KFK-299

2. K. Gast et al., Na2 Design 300 MWe German FCR, ANS Fast Reactors National Topical Meeting, San Francisco, April 10-12, 1967, ANS-101

3. E. Schlechtendahl et al., Safety Features of a 300 MWe Sodium Cooled Fast Breeder Reactor (Na2), Conference on Fast Reactor Safety, Aix-en-Provence, Sept. 19-22, 1967

4. A. Müller et al., Referenzstudie für den 1000 MWe dampfgekühlten schnellen Brutreaktor (D1), 1966, KFK-392

5. G. Karsten and K. Kummerer, Program, Pin Design and Specification for Fuel Irradiation Experiments in the Enrico Fermi Fast Breeder Reactor, 1967, KFK-586

6. K. Kummerer and G. Karsten, Some Results on the Development of a Fast Reactor Fuel Element, BNES Conference on Fast Breeder Reactors, London, May 17-19, 1966, KFK-576

7. D. Geithoff et al., Irradiation Performance of Fast Reactor Fuels, This Symposium, Session E, KFK-662

8. E. Fischer and K. Keller, Einfluß der Entmischung von oxydischem Brennstoff auf den Verlauf von Leistungsexkursionen in schnellen Reaktoren, die durch den Dopplerkoeffizienten abgefangen werden, Nukleonik, 1966, 8, 471

9. K. Kummerer, Production Cost Parameter Analysis for Fast Reactor Fuel Elements, IAEA Symposium on the Use of Plutonium as a Reactor Fuel, Brussels, March 13-17, 1967, KFK-576

Table I PIN LAYOUT FOR REFERENCE DESIGNS

				Na-1 Design (1000 MWe, sodium-cooled)	Na-2 Design (300 MWe, sodium-cooled)	D-1 Design (1000 MWe, steam-cooled)
Operation	Max. Linear Rod Power, nominal		(W/cm)	566	446	326
	Max. Can Midwall Temp., nominal		(°C)	625	627	622
	Max. Can Midwall Temp., hot spot		(°C)	654	696	737
	Max. Internal Gas Pressure		(atm)	70	70	260
	Max. External Pressure		(atm)	4	6	170
	Max. Burnup, axially averaged		(MWd/t_{Metall})	100 000	68 000	55 000
Fabrication Parameter	External Geometry	External Diameter	(mm)	6.7	6.0	7.0
		External Length	(mm)	2672	2475	2155
	Internal Geometry	Wall Thickness	(mm)	0.35	0.38	0.37
		Diametral Gap	(μ)	-	140	180
		Upper Axial Blanket Length	(mm)	400	400	350
		Fuel Length	(mm)	955	950	1510
		Lower Axial Blanket Length	(mm)	400	400	(separate)
		Fission Gas Plenum Position		Bottom	Bottom	Top
		Length	(mm)	800	650	250
	Cladding Material			Incoloy 800	16/13 CrNi	Inconel 625
	UO_2-PuO_2-Fuel	Fuel Shape		Vibro Powder	Pellet	Pellet
		Composition in Zone 1/2	(w/o PuO_2)	16/20	20/30	13/16
		Smeared Density	(% th.d.)	90	80	87
	UO_2-Blanket, Smeared Density		(% th.d.)	90	90	87
	He Filling, initial pressure at room temp.		(atm)	1	1	56

Table II PIN LAYOUT AT PERFORMANCE TESTS

				Test Irradiation in EFFBR		Test Irradiatons in DFR (Trefoil)
				Pellet Fuel	Vibro Fuel	
Operation	Max. Linear Rod Power, nominal		(W/cm)	600	615	500
	Max. Can Midwall Temp., nominal		(°C)	602	602	650
	Max. Can Midwall Temp., hot spot		(°C)			
	Max. Internal Gas Pressure		(atm)	78	78	<100
	Max. External Pressure		(atm)	(low)	(low)	(low)
	Max. Burnup, axially averaged		(MWd/t_{Metall})	50 000	50 000	80 000
Fabrication Parameter	External Geometry	External Diameter	(mm)	6.35	6.35	6.35
		External Length	(mm)	1286	1286	709
	Internal Geometry	Wall Thickness	(mm)	0.40	0.40	0.40
		Diametral Gap	(μ)	150	-	150
		Upper Axial Blanket Length	(mm)	150	150	130
		Fuel Length	(mm)	700	700	360
		Lower Axial Blanket Length	(mm)	-	-	70
		Fission Gas Plenum Position		Top + Bottom	Top + Bottom	Top
		Length	(mm)	188 + 195	188 + 195	130
	Cladding Material			16/13 CrNi	16/13 CrNi	16/13 CrNi
	UO_2-PuO_2-Fuel	Fuel Shape		Pellet	Vibro Powder	Pellet
		Composition	(w/o PuO_2)	15	15	20
		Smeared Density	(% th.d.)	83	85	83
	UO_2-Blanket, Smeared Density		(% th.d.)	83	85	83
	He Filling, initial pressure at room temp.		(atm)	1	1	1

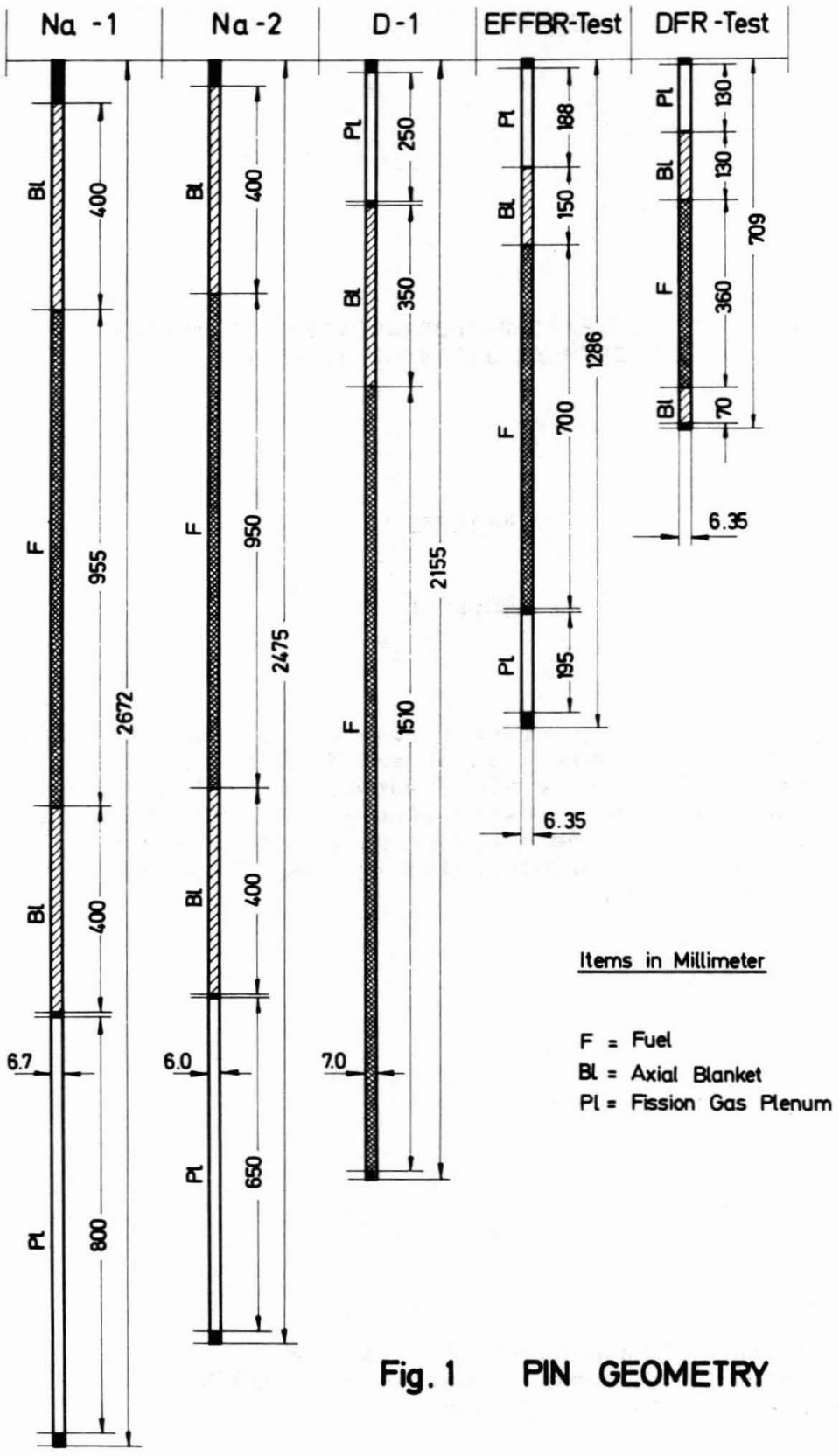

Fig. 1 PIN GEOMETRY

CENTRAL STATION FAST BREEDER-REACTOR PLUTONIUM FUEL REQUIREMENT JAPANESE EXPERIENCE

Y. Nakamura

Abstract

A development program of fast breeder reactors has been initiated by the Power Reactor and Nuclear Fuel Development Corporation with a wider support from JAERI and industries in Japan. Design studies on 1000 MWe breeder are discussed from the stand point of fuel technology. The present status of plutonium fuel development for the JFER are described.

Y. Nakamura is the manager of Plutonium Fuel Development Laboratory, Tokai Works, Power Reactor and Nuclear Fuel Development Corporation, Japan.

1. INTRODUCTION

Japan has to depend upon the nuclear power generation more and more in the future in order to keep its economical growth rate. Light water reactors will be introduced in the near future as the main nuclear power stations. However Japan has very poor uranium resources and no isotope seperation plant, so that the nuclear fuels problems are very serious.

Plutonium should be best used as the fast breeder reactor fuels, and Japan Atomic Energy Commission established a policy to promote fast breeder reactors development in the country. Also JAEC showed another policy to use plutonium as the direct substitute of enriched uranium in order to utilize imported nuclear fuels as effectively as possible in the intermediate future.

The design study of fast breeder has been conducted in the Japan Atomic Energy Research Institute (JAERI). JAERI is now engaging in final conceptional design for the construction of the Japan Fast Experimental Breeder Reactor (JFER). The present plan of the construction;

Completion of Design ----------	Early 1968
Breaking Ground ----------	Early 1969
Fuel Loading ----------	Middle 1972
Dry Critical ----------	Middle 1972
Wet Critical ----------	End 1972
Full Power ----------	End 1973

A prototype breeder reactor will be critical around 1975 under the supervision of a new organization which is established recently to promote the development of FBR and ATR. This new organization,the Power and Nuclear Fuel Development Corporation, PNC is established with an aim that JAEC's policies on these advanced power reactor development are to be realized with a wider supports inside the country including JAERI, AFC, industries and utilities.

1,000 MWe fast breeder design studies have been carried out by JAERI and will be succeeded by P.N.C. No program of fixed central station fast breeder reactor is yet established at the present, but the survey studies by JAERI are very useful. The first conceptual design study on 1,000 MWe fast breeder[1] was completed in April 1966. The second conceptual design study[2] has been finished recently and will be published from JAERI. The results obtained by these design studies are reflected to the detail design of JFER and to the design philosoply of prototype breeder.

As for the plutonium fuel development, main efforts have been paid by the Plutonium Fuel Development Laboratory of the Atomic Fuel Corporation. Three papers were presented by this laboratory to the IAEA Symposium

on the Use of Plutonium as a Fuel, held in Brussels in March 1967. The Corporation is reformed to the above-mentioned new organization. Close co-operation between JAERI and AFC (new organization) are maintained in the field of fuel design and fabrication of these fast breeders.

Plutonium balance between production and requirement in the near future in Japan was reported in Brussels.[3)]

2. JFER AND 1,000 MWe BREEDER DESIGN STUDY, FROM THE STANDPOINT OF FUEL TECHNOLOGY

The purpose of the JFER is to design, construct and operate it at the earliest future in order to use it for fuel testing. Experiences obtained through design and construction are to be used directly for prototype breeder program. The designed thermal out put of JFER is 100 MWt, and future installation of in-core loop is considered. The reactor power was obtained with the bases as follows;

(a) Core height is desired to be 600 mm in order to irradiate fuel elements for prototype breeder in the reactor.
(b) The right cylindrical geometry is desired for the least fissile fuel inventory requirement.
(c) A moderate power density in the core is required in order to irradiate test fuel at shorter period. Thus a moderate linear rod power rating and neutron flux level are obtained.

The design principles of the JFER are in general conservative, as this is the first experience in Japan, and the safety consideration are seriously required against nation's feelings. However we have advantages to use informations and experiences in the advanced countries, and one of the features of the JFER is that the reactor is designed with the most flexibility for fuel testing. As the reactor size is not so large, the peak to average ratio of power rating in the core is inevitably not so small, while it has advantage that the sodium coefficient is enough negative and the reactor is inherently safe. The long burn-up capability of fuel is not necessarily required for the first inventory, and the minimum requirements are to provide stable irradiation behaviours at the designed power level and thus to provide a moderate fast neutron flux for fuel testing.

Specially designed in-core monitoring systems are to be installed, and alpha-gamma monitoring cave capable of some non-destructive testings and necessary mechanical handlings such as the measurement of pressure drop along the fuel element by means of inert gas flowing and minor

repairing, will be constructed adjacent to the reactor. Periodical inspections of fuel assemblies are to be done, and capability for further irradiation is estimated stage by stage. High density pellets might be used for the first loading in order to provide known in-pile properties such as thermal conductivity and thermal expansions and also to provide minimum fuel movement in case of an unexpected reactor abnormal conditions. Lower density pellet is thought to give longer burnup capability, but has many uncertain irradiation behaviours.

Final preference on the pellet density is affected by the availability of data on the irradiation behaviours and by our own irradiation experiences. The final choice is to be done in Mid-1971.

Two kinds of design study on 1,000 MWe breeder reactor have been done by JAERI, based on the sodium cooled, and mixed oxide fuel system. Safety, power generation economy and breeding gain are three components to be considered for such a commerical power breeder plant. The safety aspects of the reactor design give more difficulties as the reactor size becomes large.

The 1st 1,000 MWe breeder design study dealt flat cylindrical (D/H = 2.15) core geometry with an aim that a higher breeding gain could be obtained (1.44). Two-zone enrichment (10.5% and 14.8% PuO_2) was applied to get flat power distribution. Calculated sodium coefficient at the worst case was more than +3$, while it could be less than +1$ in case of loss of sodium in the central 19 channels.

Safety aspects were emphasized in the 2nd design study from the following stand points;

(a) Maximum sodium coefficient was reduced in order to have more nuclear safety margin,
(b) Power density intthe core was reduced in order to have more thermal safety margin,
(c) Clad thickness was increased in order to have more mechanical strength.

A ring core geometry was selected in the 2nd design study.

Main reactor core parameters related to the fuel design and calculated fuel performances in the two design studies are shown in Table 2.

3. FUEL FOR THE JFER

Key parameters of JEFBR design are shown in Table 4.

The enrichment of fuel is 30 ~ 35 a/o fissile as shown in Table 4. The weight percentage of PuO_2 is changed in accordance with the isotopic ratio of plutonium which is used for the reactor. If the plutonium from the Tokai Reactor of Japan Atomic Power Company, a Calder Hall Type

Reactor of 166 MWe, is used for this purpose, the weight percentage of PuO_2 in UO_2-PuO_2 is about 40. The mixed oxide of this range is easy to be reduced during sintering, and the stoichiometry in the pellets becomes less than 2.00. The hypo-stoichiometric UO_2 -40% PuO_2 has two phases at room temperature, while it has single phase at high temperature, as shown in the Vienna Panel of IAEA.[4]

Minor changes were observed by X-ray diffractometry, dilatometry and differential thermal analysis in our laboratory. The differential thermal analysis, and X-ray diffractometry are carried out to study the materials in detail. The thermal cycling effects are being investigated and short period irradiation testings in a thermal material testing reactor are planned.

However if we should avoid the less-known metallographical and thus irradiation behaviours of this composition of the mixed oxide, and this will be more realistic from the standpoint of plutonium availability at the planned construction stage, we must consider the enrichment both by U-235 and Pu-239 enrichment which means less content of U-238, and the Doppler dependency from reactor safety standpoint must be reestimated. Fission paterns in mixed oxide crystals are different in 239-238 system and 235-239-238 system.

As for the designed thermal performances of fuel pins and fuel pins assemblies of JFER, the levels are almost of the same order expected in the prototype or demonstration reactor. So we expect that we could proceed to the prototype reactor fuel development without greater difficulties.

4. PRESENT STATUS OF FAST REACTOR FUEL DEVELOPMENT IN JAPAN

As described in the introduction, detail design of fuel element for JFER, hydraulic studies, and mechanical assessments of fuel assembly are being carried out in JAERI. Fuel material development and studies are mainly done by the Plutonium Fuel Development Laboratory of PNC. Studies on cladding materials and basic studies on mixed carbide and nitride and some of mixed oxide are to be done by the metallurgy group in JAERI. Inspection techniques have been developed and are applied in the Inspection Laboratory of PNC.

An irradiation testing of fuel pins in the Enrico Fermi Reactor is planned by the collaboration of JAERI, PNC and the Japan Central Research Institute of Electric Power Industry (CRIEPI).[5] The fuel test assembly contains 24 fuel pins sub-assembled in 4 thimbles. The combination of sample pins is planned to obtain informations as much as possible from the single test assembly irradiation. As there are the reactivity limits both of upper and lower value for the in-reactor irradiation, and we must consider fissile material availability, two kinds of enrichment were selected, that are 40% PuO_2-UO_2

(20% U-235 enriched) and 20% PuO -UO_2 (90% U-235 enriched). The maximum linear rod powers at the reactor overpower are 320 w/cm and 540 w/cm, and 240 w/cm and 420 w/cm at normal condition, respectively. Seven types of fuel specimens are planned.

Type II ; 40 w/o PuO_2-UO_2 (20% EU)
Vibratory compacted, 80% Smeared density with crush and sintered particles.
Clad O.D. 6.30 ± 0.05 mm
Clad thickness 0.40 ± 0.05 mm

Type III; 40 w/o PuO_2-UO_2 (20% EU)
90% T.D. pellets, 5.5 mm diameter mechanically blendent and sintered.

O/M $2.00 \begin{smallmatrix} + 0.01 \\ - 0.02 \end{smallmatrix}$, AISI 316 clad

Clad O.D. 6.30 ± 0.05 mm
Clad thickness 0.35 ± 0.05 mm

Type IV ; 40 w/o PuO_2-UO_2 (20% EU)
Holed 90% T.D. pellets, 80% Smeared density 5.5 mm
O.D. pellet mechanically blended and sintered.
Same O/M ratio.
Clad thickness 0.40 ± 0.05 mm

Type V ; 40 w/o PuO_2-UO_2 (20% EU)
Vibratory compacted to 80% Smeared density with Sol-Gel UO_2-PuO_2 particles.
Clad O.D. 6.30 ± 0.05 mm
Clad thickness 0.40 ± 0.05 mm

Type VI ; 40 w/o PuO_2-UO_2 (20% EU)
90% T.D. pellet with low O/M (1.93 ~ 1.96)
Clad O.D. 6.30 ± 0.05 mm
Clad thickness 0.40 ± 0.05 mm

Type VII; 20 w/o PuO_2-UO_2 (90% EU)
90% T.D. pellet, O/M $2.00 \begin{smallmatrix} + 0.01 \\ - 0.02 \end{smallmatrix}$
Clad O.D. 6.30 ± 0.05 mm
Clad thickness 0.35 ± 0.05 mm

Type VIII; 20 w/o PuO_2-UO_2 (90% EU)
83% T.D. pellet, O/M $2.00 \begin{smallmatrix} + 0.01 \\ - 0.02 \end{smallmatrix}$
Clad O.D. 6.30 ± 0.05 mm
Clad thickness 0.35 ± 0.05 mm

Test specimens are examined at several burnup levels.

Another series of irradiation testing in the Dounreay Fast Reactor is being planned. The first program is to be done with a main emphasis of the investigation on the cladding material. AISI 316

stainless steel pipes of different grain size, cold drawn and solution treated, will be irradiated at the higher temperature in the reactor. Natural Uranium Dioxide pellets and control orificing of sodium flow are used to keep clad temperature at designed levels. Mixed oxide fuel pins of the design for first loading of JFER are to be irradiated in the second program.

Studies on mixed carbide and nitride are not yet started in the present. However JAERI is modifying research facilities for this purpose. Uranium carbide and nitride have been investigated for these years both by JAERI and private compaines. Interests are being shown to the nitrocarbide.

5. ACKNOWLEDGEMENTS

The auther would like to appreciate advices for the preparation of this article to Dr. Masao Nozawa, JAERI.

REFERENCES

(1) JAERI-MEMO-2244. A 1,000 MWe Fast Breeder Design Study (Japanese)

(2) JAERI-MEMO-2654. The Second 1,000 MWe Fast Breeder Design Study (Japanese)

(3) IAEA Panel on Thermodynamics of Nuclear Materials, with an Emphasis of UO_2-PuO_2 Mixed Oxide. held in Vienna 1966.

(4) "Plutonium Fuel Development in Japan." Y. Imai, Y. Nakamura and R. Ueda, SM88/36, IAEA Symposium on the use of Plutonium as the Reactor Fuel. March 1967.

(5) AFCPU-REPORT-09 "Design and Specifications of Fuel Pins for CRIEPI Irradiation in the EFFBR" Dec., 1966.

Table 2. Main Reactor Core Parameters Related to the Fuel Design

			1st Design		2nd Design
Reactor power MWt			2,500		2,500
Active core height		cm	80		80
Core outher diameter		cm	264.8		324.4
Core inner diameter		cm	-		160
Core volume		ℓ	4,400		5,000
Length of axial blanket		cm	40		40
Thickness of radial blanket		cm	40		40
Core composition Fuel		%	44		41.4
Sodium		%	39		36.2
Structural		%	16		21.6
Fuel material			PuO_2-UO_2		PuO_2-UO_2
Enrichment (Pu fissile %)			I 10.5		13.0
			II 14.8		
Isotopic composition of Pu	239		77.4		77.4
(Initial)	240		17.7		17.7
	241		4.3		4.3
	242		0.5		0.5
(Discharged)	239		75.4	74.7	70.8
	240		19.8	20.2	23.3
	241		4.0	4.4	4.8
	242		0.7	0.7	1.1
Fuel inventory Pu-239, 241, kg			1,930		2,335
Total Pu, kg			2,350		2,858
Breeding ratio			1.44		1.29
internal			0.96		0.81
blanket			0.48		0.48
Power peaking factor			1.6		1.55
Specific power MWt/kg fissile			0.65		0.96
Power density MW/ℓ -core			0.50		0.45
Number of fuel assemblies			337		390
Number of radial blanket assemblies			234		312
Number of pins per fuel assembly			265		265
Pin pitch		mm	7.7		7.7
Fuel assembly pitch		mm	135		135
Fuel pin					
Outer diameter		mm	6.4		6.4
Clad thickness		mm	0.275		0.35
Inner diameter		mm	5.85		5.7
Pellet diameter		mm	5.8		5.6
Active core length		cm	80		80
Axial blanket length		cm	40 x 2		40 x 2
Gas reservoir		cm	60		60
Total length		cm	220		220
Coolant sodium					
Velocity		m/sec	8.0		4.8

Flow rate	t/sec	12.3	9.86
Pressure drop	kg/cm^2	10.0	5.0
Inlet temp.	°C	400	400
Outlet temp.	°C	550	600

Table 3. Designed Fuel Performance

		1st Design	2nd Design
Fuel material		PuO_2-UO_2	PuO_2-UO_2
PuO_2 content	%	I 12.8 II 18.1	15.9
Density	g/cc	10	10
Cladding material		AISI 316	AISI 316
Av. linear rod power	w/cm	312	272
Max. linear rod power	w/cm	500	420
Peak/Average		1.6	1.54
Max. fuel temp.	°C	2,358	2,556
Max. clad temp.	°C	684	723
Max. thermal stress in clad kg/cm^2		795	711
Max. pressure stress in clad kg/cm^2		424 (610 °C)	588
Av. burn up	MWD/T	86,300	83,000
Max. burn up	MWD/T	100,000	100,000

Table 4. Design Parameters of JFER

<u>Plant performance</u>		
Reactor power	MWt	100
Core power	MWt	93
Reactor inlet temp.	°C	350
Reactor outlet temp.	°C	500
Core region coolant velocity	m/sec	5
Primary system allowable pressure drop	kg/cm^2	6
Core pressure drop (grid spacer)	kg/cm^2	3.2
<u>Dimensions</u>		
Core volume (including control rods)	ℓ	200
Pitch of fuel assemblies (triangular)	mm	80
Pitch of fuel pins (triangular)	mm	7.7
Clad outer diameter	mm	6.3
Clad thickness	mm	0.35
Fuel diameter	mm	5.5
Core height	mm	600
Axial blanket height	mm	400 x 2
Radial blanket height	mm	1,400
Gas reservoir height	mm	200
<u>Core Performance</u>		
Core average power density	MW/ℓ	0.45
Core material		PuO_2-UO_2
Enrichment		0.35
Core volume fraction Fuel/Na/SS		38/38/23

Core fuel density	g/cc	10
Number of core fuel assemblies		55
Number of control rod		6
Number of radial blanket assemblies		257
Number of fuel pins per core assembly		88
Max. fuel pin linear power	w/cm	500
Peak to average power ratio in core		1.6
Max. heat flux at pin surface	w/cm^2	250
Max. clad surface temperature	^oC	580
Max. fuel temperature	^oC	2,300
Max. burnup	a/o	5

CENTRAL STATION FAST BREEDER REACTOR PLUTONIUM FUEL REQUIREMENTS - U. S. EXPERIENCE

J. H. Wright

The near term use for plutonium in fast breeder power plants is expected to be quite modest from now until the mid 1980's, two to three tons per year covering the foreseeable situation. Plutonium requirements for the anticipated fast growing breeder capacity in the late 1980's may exceed the supply from all sources on an annual basis but a modest holding time could cover the possible shortage without undue economic penalty.

The amount of plutonium required as initial inventory and produced annually by the fast breeder is a function of the breeder design parameters of which specific power and breeder ratio are most significant. The developing status of breeder technology leaves open at this time the ultimate choice of breeder fuel material, but economic and performance objectives stress the desirability of a high performance ceramic fuel.

J. H. Wright is a senior consultant for the Atomic Power Divisions, Westinghouse Electric Corporation, Pittsburgh, Pennsylvania.

Introduction

The U.S. experience in plutonium requirements for central station breeder reactors has been essentially non-existent. Whereas some fast breeders have been operated, these reactors have either been fueled with U-235 or cannot be characterized as central station power plants. This paper is concerned only with the future requirements of plutonium and the design characteristics of the breeder which will affect these requirements.

Influence of Breeder Design Characteristics

The design characteristics of the breeder determine how much plutonium is required for initial inventory in the core and in the total fuel cycle, and its doubling time determines the rate of new material production.

The net plutonium balance for a large (1000 MWe) breeder reactor is illustrated in Figure 1. In this illustration an in-core specific power of 1 MW thermal per kilogram of fissile plutonium was used and an additional one third of core for out-of-pile inventory was assumed. From this we find that 3.3 tons of plutonium are required as an initial investment. The compound doubling times of 6 to 12 years were used to illustrate the net cumulative plutonium production available from one reactor after reprocessing. As can be readily seen, the actual time required to recover the initial plutonium requirements is from 9 to 18 years. This example shows the importance of understanding the "doubling time" parameter. (The rate of plutonium production from a uranium fueled PWR is shown by dashed line for comparative purposes.)

The compound doubling time assumes that the plutonium dividends are being reinvested in other new breeders having the same rate of return as the present breeder, whereas the simple doubling time does not include interest on the dividends. Doubling times are also quoted with and without out-of-core inventory. Broad definitions covering most of the more commonly used doubling time expressions are summarized in Table I.

Further refinements such as average bred plutonium, time-composition function to reach equilibrium, etc., can be incorporated to improve accuracy but these are more difficult to apply and require much more detailed information on the fuel cycle, thus losing the desirable characteristic of a simple and easily applied criterion for breeder performance evaluation. This author has chosen definition no. 4 as the most meaningful, yet simple, approximate criterion for breeder performance. The out-of-pile inventory is included for obvious reasons, and the compound expression more accurately depicts plutonium gain when the breeder reactors are being built in large numbers. All the fast breeder concepts which have been conceived to-date will

probably have higher capital costs than the present and future water reactors, thus emphasizing the critical importance of the fuel cycle economics.

The breeder doubling time is more than a statement of plutonium gain potential; it is also an index to the economic potential of the fuel cycle. For example the plutonium credit from a breeder can be accurately approximated by the following expression:

$$\text{Net Pu credit, mills/kwhr} = \frac{0.045\ (BR-1)}{\epsilon} \times \text{Pu Value, \$/gm}$$

Furthermore, the inventory cost, expected to be the largest single component in the breeder fuel cycle cost, is an inverse function of specific power making it similar to the doubling time expression:

Unit inventory cost at 80% load factor

a) in-core inventory:

$$I_c = \frac{1}{S} \times \frac{1}{\epsilon} \times (\chi)\ (\gamma)\ \frac{10^3}{7000} \text{ m/kwhr}$$

S = Specific Power MWt/kg Pu fissile
ϵ = thermal efficiency
χ = Pu value, \$/gm fissile
γ = annual charge for non-depreciating assets
10^3 = mills/\$
7000 = hours/yr at 80% factor

b) out of core inventory

$$I_o = I_c \quad \frac{F_T - F_c}{F_c} \quad \text{m/kwhr}$$

F_T = Total fuel in cycle
F_c = In-core fuel

c) inventory on Bred Pu

I_B = function of detailed fuel cycle characteristics influenced by residence time, burnup, breeding ratio, fuel relocation, etc.

$$= \frac{0.12 \times 10^{-3}\ (BR-1)\ (1-a)\ (\chi)\ (PF)}{(1+F)\quad(\epsilon)}$$

d) total inventory costs

$$I = I_C + I_O + I_B \text{ mills/kwhr}$$

Thus, as the core design parameters are altered to improve (reduce) doubling time, the economics of the fuel cycle are advantageously affected. Figures 2, 3 and 4 show graphically these effects. In Figure 2 the inventory costs are related to the plutonium specific power; separately, the plutonium credit is shown also as a function of specific power. In this graph plutonium value is taken at 10$/gm fissile and annual charges at 10%. In Figure 3 the net plutonium costs (inventory cost less credit) are plotted with specific power again using 10% annual charges but showing two values for plutonium. Here, the advantages to fuel cycle cost for high specific power and breeding ratio are clearly indicated.

The ultimate purpose of any new reactor system, including breeder, is purely economic. The breeders developed for utility use should serve three important and related functions:

1. They should be economically attractive compared to all other power sources at the time of installation.
2. They should have fuel cycle characteristics which provide for continuing good economics independent of future uranium or plutonium prices. Failure to achieve this objective removes most of the incentive of any breeder system.
3. The breeder should create a more stable fuel cycle environment for all existing reactors. The breeder can accomplish this if it reduces the future demand for large quantities of uranium and if it provides a truly premium market for plutonium from other reactors. It can eventually supply an adequate but alternate source of fissile material in competition with enriched uranium.

Figure 4 indicates the net plutonium unit cost as a function of plutonium value for some selected values of breeding ratio and specific power. Here we note that a breeder having a specific power of 1.1 and a breeding ratio of 1.4 would have zero plutonium costs independent of the value placed on the plutonium. This corresponds to a high gain breeder having a seven year doubling time according to definition (4). These design parameters would then meet all three of the breeder objectives.

Breeder Design Considerations

From the foregoing discussion the plutonium costs are minimized in designs having high specific power and high breeding gain. To reduce unit fabrication costs and extend operating intervals between refueling, there is considerable economic incentive for high burnup fuel. In the

ideal case the core composition would be limited to uranium and plutonium atoms. Each additional substance added has the effect of reducing spectral hardness and, consequently, breeding ratio. Metal cladding and structural material take their toll in performance downgrading in two ways - softening the neutron spectrum by elastic and inelastic scattering and by absorption of neutrons. Spectral hardness is also affected by the composition of the fuel material. For example, the reduction in heavy metal atom density and increased scattering that occurs when fuel in the form of uranium-plutonium dioxide is used causes a reduction of the ideal or theoretical breeding ratio by as much as 40 - 50%. This dilution of fuel concentration and the resulting reduction in breeding ratio requires a compensating increase in the ratio of plutonium (fissile) to uranium (fertile) material to maintain criticality for the desired fuel lifetime. The use of more dense fuel materials, such as carbides and nitrides, minimizes this effect.

One of the chief detractors from the breeder performance is the effect of the coolant. In this regard helium has the least effect and steam the greatest with sodium somewhere in between. It is conceivable that various breeder reactors will be built in the U.S. using each of these coolants, but further remarks in this paper will be limited to sodium cooled systems for many reasons, principally among which is the fact that the LMFBR program is most likely to achieve early success because of their advanced technical position and the huge domestic and international effort in this area. Similarly, ceramic fuels seem to be the almost unanimous choice as breeder fuel in spite of extensive and somewhat encouraging results obtained with metalic fuels.

Within the framework of sodium cooled ceramic fueled breeders, the plutonium enrichment requirement is one of the most important parameters to the performance of the breeder. When plutonium loading requirements go up beyond the 8 - 10% minimum requirement, two adverse effects are noted on breeder performance:

1. the internal breeding ratio is reduced as noted in Figure 5, adversely affecting not only the breeding gain but causing a reactivity drop with burnup. This latter effect requires additional plutonium loading in order to provide reactivity through the lifetime of the fuel charge. This results in excess reactivity at the beginning of life and gives rise to certain potential accidents which must be considered and provided for in the design.

2. the fissile plutonium specific power rating of a fuel having a defined upper thermal limit is reduced as plutonium is substituted for U-238.

Thus, increasing the plutonium loading adversely affects specific power, breeder ratio, doubling time and economics. Why, then, would

one not use the minimum enrichment of plutonium? The answer, which is transitory in nature, is related to the current understanding of safety characteristics in large breeders. A large breeder core, cooled by sodium, will exhibit a positive sodium temperature and void characteristics if designed for minimum plutonium content, because, in order to use the minimum plutonium content, it is necessary to minimize the neutron leakage; this is done by minimizing the surface to volume ratio. In such a core the internal breeding ratio is high but the sodium provides significant spectral softening during normal operation. On the loss of sodium, the neutron energy spectrum tends to harden, and the reactivity increases. Present technology has not determined exactly how much reactivity increase from this source can be satisfactorily dealt with by other safety mechanisms (Doppler coefficient, thermal expansion, fast acting rods, etc.) nor how much reactivity increase will actually occur. Therefore, it may seem prudent to avoid the problem at this time by designing cores having higher neutron leakage resulting in negative sodium coefficients but requiring higher plutonium loading.

A general picture of the enrichment requirement shown as a function of surface to volume (leakage) ratio is given in Figure 6 where it can be noted that current designs require 15 to 18% plutonium loading. Figure 7 gives a general relationship of breeding ratio versus surface to volume ratio (leakage). Although this figure indicates that the loss of internal breeding ratio may be compensated by additional breeding in the blanket, it is important to note that the blanket must be much larger and more costly and that the increased enrichment required for this abortive design reduces the specific power drastically.

It is both likely and imperative that the necessary answers to the safety questions be soon forthcoming and breeder design development be pushed more toward the optimum. Eventually, the answer must be found in the overall power coefficient rather than in the one term, sodium coefficient.

The specific power design of the breeder is subject to all of the usual materials constraints - fuel center temperature limit, maximum allowable clad temperature, clad thermal stress, fuel swelling and gas release, irradiation embrittlement of clad and structural materials, etc. The design influence of two of these limitations, fuel center temperature and fuel clad temperature, are illustrated in Figures 8 and 9.

Although ceramic fuels have found widespread use in the growing nuclear power systems throughout the world, the performance demanded of these fuels has been modest compared to fast-breeder fuel requirements. Specific power and burn-up requirements for breeder fuels will exceed the performance previously demanded of nuclear fuels by a factor of three or four.

When fission heat is liberated within a ceramic fuel pellet, the temperature of the fuel must rise until all of the heat generated is conducted out of the fuel, through the cladding, and into the coolant. The temperature rise within the fuel is dependent upon the amount of heat being generated, the amount of fuel through which the heat must be conducted (pin diameter), the thermal conductivity of the fuel clad, the gap between the fuel and clad, and the heat transfer coefficient and bulk temperature of the reactor coolant.

With liquid sodium used as reactor coolant, excellent heat transfer from clad to coolant exists, but care must be taken to prevent the sodium temperature from rising to its boiling point. The clad material (usually 316 stainless steel) adds further constraints on the temperature profile by imposing maximum clad temperature limits. This limit for stainless steel is thought to be in the range of 1300-1400 degrees F and is determined, in part, by the temperature-dependent rate of nickel removal by sodium.

With a fixed maximum clad temperature, the reactor sodium temperature must be well below this point. The relationship between average sodium outlet temperature, average sodium temperature rise, deviation of hottest part of core from core average (hot channel factor), and maximum clad temperature is shown in Figure 8. For example, with an average outlet sodium temperature of 1000 degrees F, a sodium temperature rise of 250 degrees F, a hot-channel factor ($F_{\Delta H}$) of 2.0, the maximum sodium temperature is 1250 degrees F for an inlet sodium temperature of 750 degrees F (Fig. 8). With a sodium flow of 3×10^6 pounds/hr-ft^2 and a heat flux of 2×10^6 Btu/hr-ft^2, the maximum clad temperature will be 1310 degrees F (Fig. 8).

To minimize the temperature rise across the clad-to-fuel-pellet gap, this gap is filled with sodium.

The temperature rise from the outside to the center of a cylindrical fuel pellet is given approximately by the formula,

$$\Delta T_{pellet} = \frac{Q}{4k} r^2$$

where ΔT is the temperature difference between the outside and center of the pellet, Q is power density in the fuel (Btu/ft^3-hr), r is the radius of the fuel pellet, and k is the average thermal conductivity of the fuel material.

The thermal conductivity of many ceramic materials, including uranium and plutonium compounds, changes with temperature; therefore, a simpler expression, kilowatts (thermal) per foot of rod length is often used to describe thermal performance capability of fuel rods.

If center fuel melting is to be avoided for all fuel during normal operation, a design basis for steady-state operation must be established that is well below the melting point. One such criterion might

be to allow center fuel melting only at 15 percent over-power. In such a case, the maximum thermal rating per unit length of fuel rod can be established. The specific power of the total fuel then becomes a function of the fuel pin diameter. A plot of this relationship is shown in Fig. 9 for three ceramic fuel materials.

An example will illustrate the application of the specific power-fuel rod diameter curve. For a mixed carbide fuel with a fuel pin diameter of 0.300 inch, the maximum specific power, limited by the center melting criteria previously described, is 0.65 MWt per kilogram of total fuel material (Fig. 9). This maximum specific power, divided by F_Q, the heat generation hot channel factor (Fig. 9), gives an average specific power for the fuel of 0.2 MWt. To get specific power per unit of fissile plutonium, average specific power of the rod is divided by the plutonium content of the fuel (Fig. 9) to get 1.5 MWt per kilogram of plutonium. And finally, this value is corrected for the applicable fuel density (Fig. 9).

At this time all of these relationships are under development and therefore are being continually revised as more is learned in experimental work. For example, hot channel factors are empirical in nature, and vary from one reactor design to another with such factors as total size, core geometry and fuel assembly design. Hence, a full-sized prototype fuel assembly can provide accurate values for a significant part of the overall performance evaluation.

Also, there are many other constraints on fuel pin diameter in addition to center temperature, which may turn out to be the controlling factors; for example, fuel swelling or gas release, because of the extremely high burnups that are being sought, may become limiting factors. However, the relationships illustrated by these curves point out the desirability of high fuel density, high thermal conductivity, low plutonium enrichments, and low hot-channel factor in obtaining larger, more economic fuel pin diameters.

One of the most critical aspects of attaining really high thermal and neutronic performance is in reducing the plutonium loading by more profound safety design criteria.

Future Plutonium Requirements

From the previous sections of this paper the parameters affecting the inventory and production rates of breeder reactors have been discussed. In order to discuss the plutonium requirements for future breeders it is necessary to make some estimates on performance characteristics and rate of breeder installations.

Near Term

For the next 8 to 10 years plutonium requirements for fast breeder

reactors will be quite nominal. Principal users in the near future will be the Fast Flux Test Facility, the Enrico Fermi Fast Breeder Reactor, and a small number of sodium prototype plants and, perhaps, steam and gas cooled breeder experiments. Critical facilities will require a few tons of plutonium and fuel experiments will add only slightly to the total requirement. Rough estimates of these requirements are tabulated in Table II.

The figures in Table II indicate that FBR plants will require approximately 2 to 2.5 tons of plutonium annually in the near future. This estimate is on the high side because it includes rather optimistic assumptions for the experimental breeder projects and optimistic scheduling of LMFBR prototype plants.

The source of plutonium during this period will be the production in water reactors. The composition of the water reactor plutonium, having about 70% fissile atoms, will charge only slightly during its irradiation in the core, but the new blanket plutonium will be much higher, >95%, in fissile content. Depending on the management of the various fuel streams recovered, the composition of the equilibrium breeder core plutonium may be quite similar to that from water reactors. This would be the case if the core and axial blanket are combined and the radial blanket separated for use elsewhere. In this case the fissile plutonium content would still be about 70%, but there would be a shift in isotopic distribution toward Pu-239 at the expense of Pu-241. Generally speaking, plutonium from or recycled in water reactors tends to build up in the heavier isotopes, and that recovered from breeder cores is altered slightly in the same direction, while the new blanket plutonium is predominantly Pu-239. It is, therefore, evident that water reactor plutonium can be most satisfactorily used for starting up breeders and will be the dominant source of plutonium in the United States for a great many years to come.

The growth rate of breeder capacity will occur in three time phases, each phase subject to different constraints as noted in Figure 10.

Phase I Technical Limitations

First, the growth rate is technologically limited at the present time. Although a large breeder could be built with present day knowledge, attaining economic attractiveness from the breeder depends on further technical progress. This paper assumes that prototype breeders will become operational in the mid 1970's and that marginally attractive breeders will become operational in the late 1970's.

Phase II Transition Period

It is reasonable to expect that some transitional period will exist between the start-up of the first marginally economic

units and full scale growth. This period may be from five to eight years duration. During this period additional breeders will be placed into operation, but they will be bucking the more established types and regarded by many as a more risky investment. A few years of successful operation will be required to surmount these financial and psychological limitations. New units are expected to add only 2000 MWe annually during this transitional phase.

Phase III Electrical Growth Rate and/or Plutonium Limitations

By the mid 1980's it is expected that a large flow or orders will begin for breeders causing a strong upward surge in breeder on-line capacity by 1990.

From this point on and assuming a continuation of economic attractiveness and good technical performance, the growth of breeder capacity can be expected to accelerate subject only to the continuing demands for electricity, plutonium availability and the manpower and facilities required to fill the orders.

Barring major catastrophe it is a foregone conclusion that the demand for increased electrical capacity will continue at or near its present pace for many decades. In Figure 11 the total nuclear capacity is shown derived from an estimate that nuclear power will account for approximately 60% of all new generating capacity. The large initial capacity of water reactors dwarfs the breeder capacity for many years to come; the estimate given here is that a 50 - 50 water reactor-breeder mix may occur around the turn of the century.

The future plutonium requirements can now be found by combining the growth rate curves with the breeder design parameters. In Figure 12 the plutonium production and requirements are summarized. These curves are based on available plutonium obtained from a displacement in time of the production curves to allow for core operation, cooling and reprocessing. Plutonium requirements for the breeder are based on a design having a specific power of 1 MWt per kilogram of fissile plutonium and one third of a core out of core inventory coupled with the growth rate predictions in Figure 11. It was assumed that the plutonium would be required one year before plant operation. The curve indicates minimal requirements until the mid 1980's. The acceleration of breeder growth is illustrated by the steepness of the annual requirements from 1985 to 1995. Toward the end of this period, new breeder additions will have reached 45,000 MWe per year, and that rate may be expected to hold with only slight increase for the succeeding 10 or 20 years.

During this period plutonium production comes from two sources, water reactors and breeders. The water reactor production rate, shown

in Figure 1, for a single plant, is based on 85% plant factor. The total annual production curve, Figure 12, is shown to take a dip in 1990, reflecting a slight reduction of load factor for water reactors. The breeder plutonium production is based on a design having a 7 year compound doubling time (example: breeding ratio 1.4, specific power 1.1, one third of core out of reactor). With a longer doubling time the bred plutonium would be reduced.

For this particular set of assumptions it can be noted that the amount of water reactor plutonium is considerably in excess of breeder requirements until the late 1980's, shortly after which there may be a brief period of time when the plutonium requirements exceed the production. Most of the breeder fuel will come from water reactor plutonium throughout this century. Figure 13 illustrates the net difference between total plutonium available and fast breeder requirements. On a year by year basis a deficit could appear in the early 1990's. This curve illustrates that a brief holding period, say 5 or 6 years, would provide plutonium for continued expansion of breeder capacity during these years. The curve also indicates that there will be approximately 300 tons of water reactor plutonium which will be in excess of breeder requirements and, therefore, available for recycle in water reactors. This recycle plutonium will reduce the uranium requirements during that period by as much as 60,000 tons. This curve also shows that plutonium will be in excess again by the late 1990's, thus providing a replacement for 10,000 tons/year of uranium by the turn of the century and going up sharply thereafter.

These indicated requirements are subject to many envolved assumptions. For example, this apparent plutonium shortage would not exist if

1. the water reactors continued through 1995 at 80 - 85% load factor,
2. higher specific power designs are developed for the breeder,
3. the growth of breeder capacity is smaller than projected.

On the other hand the apparent plutonium deficiency could become serious if,

1. breeders having worse performance characteristics are used,
2. water reactor capacity does not grow as anticipated,
3. breeder growth rates are greatly accelerated.

In the case of a sustained plutonium deficiency, breeder reactors could be initially fueled with enriched uranium, but a significant economic penalty would result.

Plutonium fuel fabrication volume is given in Figure 14. The annual volume of plutonium bearing fuel, tons/year, is plotted on the basis that

all breeder fuel contains 15% fissionable plutonium and that water recycle requires 3% fissionable plutonium loading. The water recycle plutonium is included for comparative purposes. The fabrication requirement for breeder fuel is quite nominal until the mid 1980's after which it rises sharply and continuously.

The annual fabrication volume of plutonium recycle in water reactors is expected to reach a peak of more than 1,500 tons by the mid 1980's but may drop sharply thereafter due to the anticipated demand for plutonium in the start-up of new breeder reactors. Some level of plutonium recycle is expected to continue indefinitely. In Figure 14 the volume of re-recycle plutonium fabrication is estimated. It is more likely that new plutonium would be preferable in water reactors to the second and third recycling of water reactor plutonium in order to limit the build-up of heavy isotopes. The curve only serves to identify this plutonium of somewhat different composition as being available with the expectation that the best method of utilizing it will be determined later.

The curves in Figure 15 give estimates of the total fuel fabricated for the nuclear-electric industry through the turn of the century and provide a relative comparison of the water reactor and breeder fuel fabrication requirements. Whereas the total water reactor fuel volume may be expected to reach 15,000 tons/yr, it is important to note that the plutonium recycle fuel for water reactors does not exceed 15% of the total water reactor fuel during any year, and the fast breeder fuel will not reach even the 1975 volume of water reactor fuel during the remainder of this century.

Doubling Time Expression	Approximate Formula	Example*
1. Simple Doubling Time, core inventory only	$SDT^{**}_{core} = \frac{3.2}{S\,(BR-1)}$	8.0
2. Simple Doubling Time, including out-of-core inventory	$SDT_{total} = \frac{3.2}{S\,(BR-1)}\frac{(F_T)}{(F_C)}$	10.7
3. Compound Doubling Time, core inventory only	$CDT_C = \frac{\ln 2}{\ln\left(1+\frac{1}{SDT_C}\right)}$	5.9
4. Compound Doubling Time, including out-of-core inventory	$CDT_T = \frac{\ln 2}{\ln\left(1+\frac{1}{SDT_T}\right)}$	7.8

*The example uses the same reactor design in all four cases:

Specific power 1 MW thermal/kg fissile Pu
Breeding ratio 1.4
Refueling cycle 1/3 of core and blanket annually

Where S = Specific power, MW thermal/kg Fissile Pu in core
BR = Breeding ratio
F_T = Total fuel in cycle
F_C = Fuel in core

**Explicit form is

$$SDT = \frac{2.6}{L.F.\ S\,(BR-1)}\quad\frac{1+F}{1+\alpha}$$

Where F is fast fission effect in U-238
and α is capture to fission ratio in Pu

Assumption in Formula
1. 80% load factor
2. $\frac{1+F}{1+\alpha} \sim 1.0$

TABLE I

	Pu ENRICH.	1971	1972	1973	1974	1975	1976
EFFBR	40%	800	400	150	150	-	-
FFTF	25%		625	625	400	110	110
LMFBR PROT. #1	15%		900	300	-	-	-
LMFBR PROT. #2	15%			900	300	-	-
LMFBR PROT. #3	15%				900	300	-
SCRE	25 - 40%	400	140	140	15	15	15
GCRE	50 - 80%		400	200	150	150	150
LMFBR PDR #1	15%					1800	600
LMFBR PDR #2	15%						1800
NET Pu REQUIREMENTS, TONS/YR		1.2	2.4	2.3	1.9	2.3	2.5

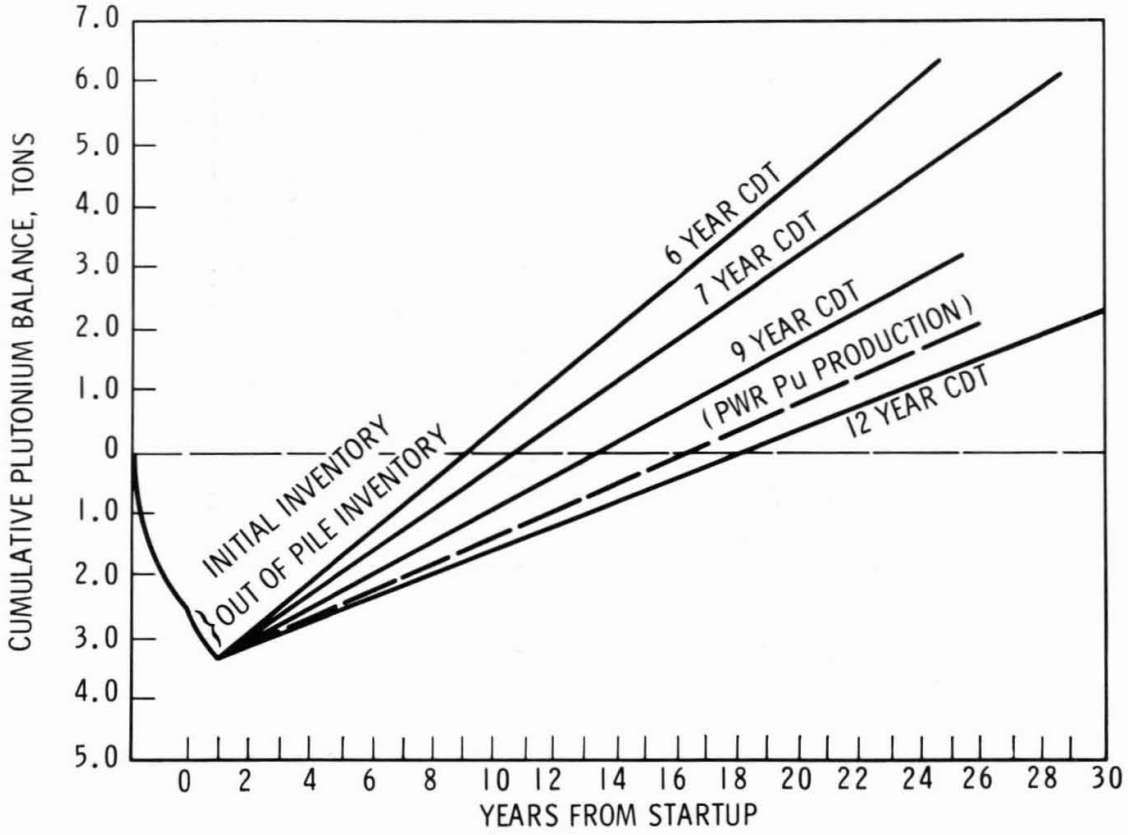

Figure 1. Plutonium Production from Breeder Reactors

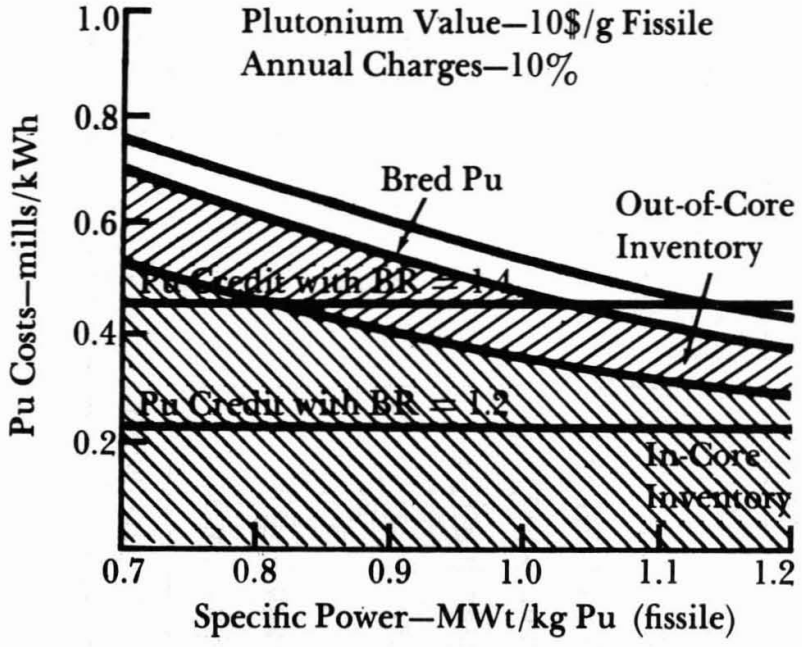

Figure 2 Plutonium Effect in FBR Fuel Cycle

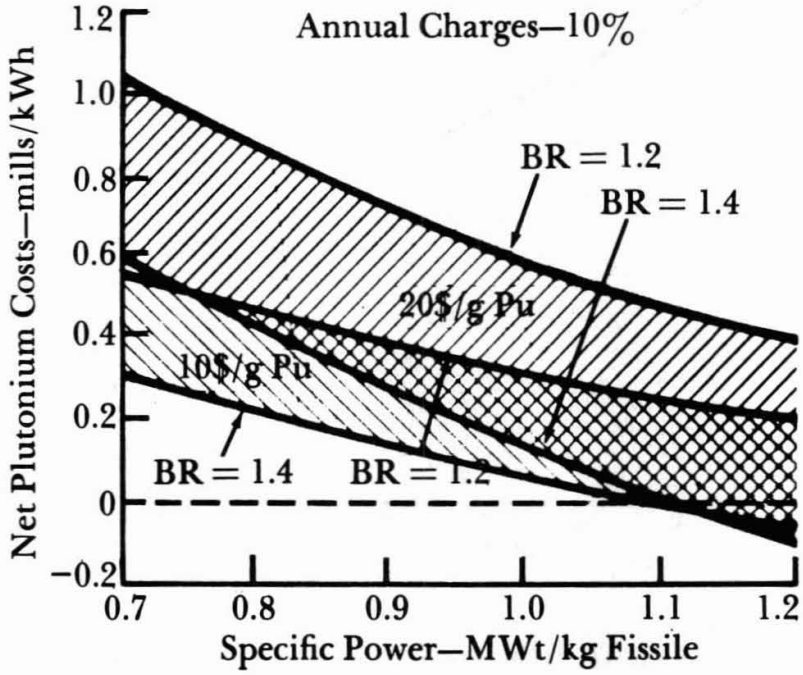

Figure 3 FBR Fuel Cycle Net Plutonium Costs vs. Specific Power

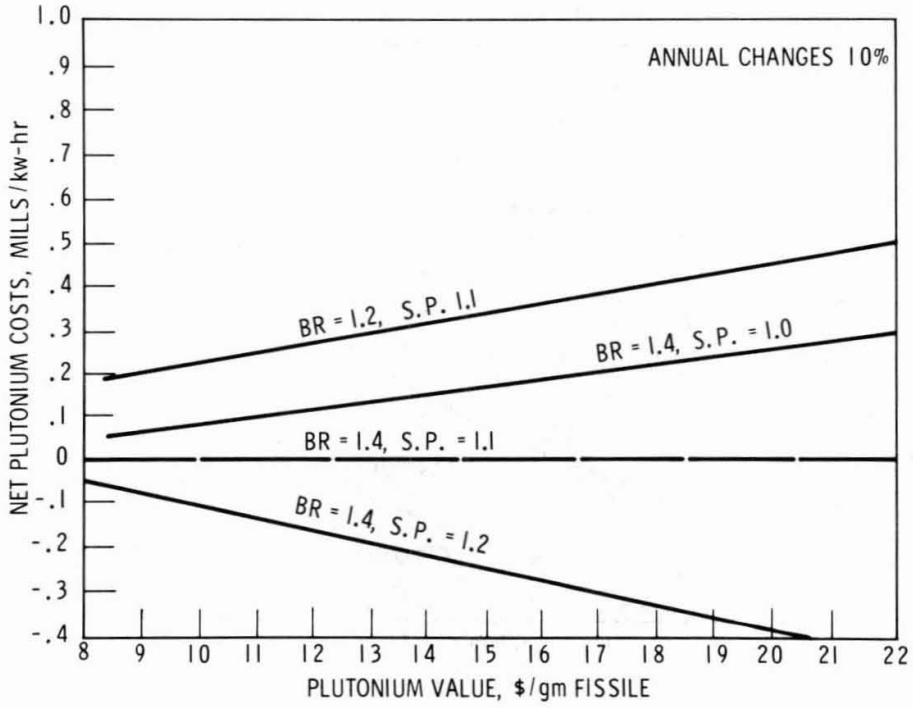

Figure 4. Net Plutonium Cost vs. Plutonium Cost and Specific Power

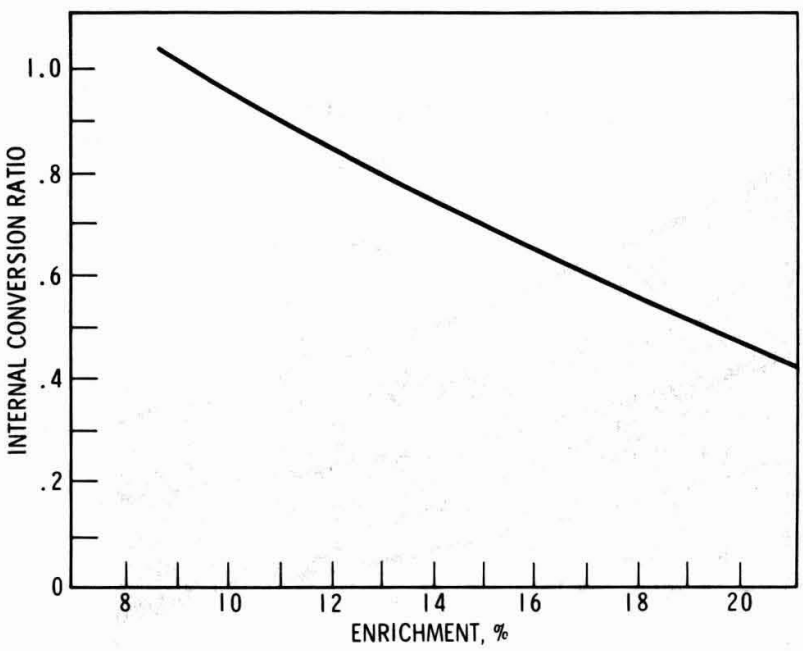

Figure 5. FBR Core Conversion Ratio

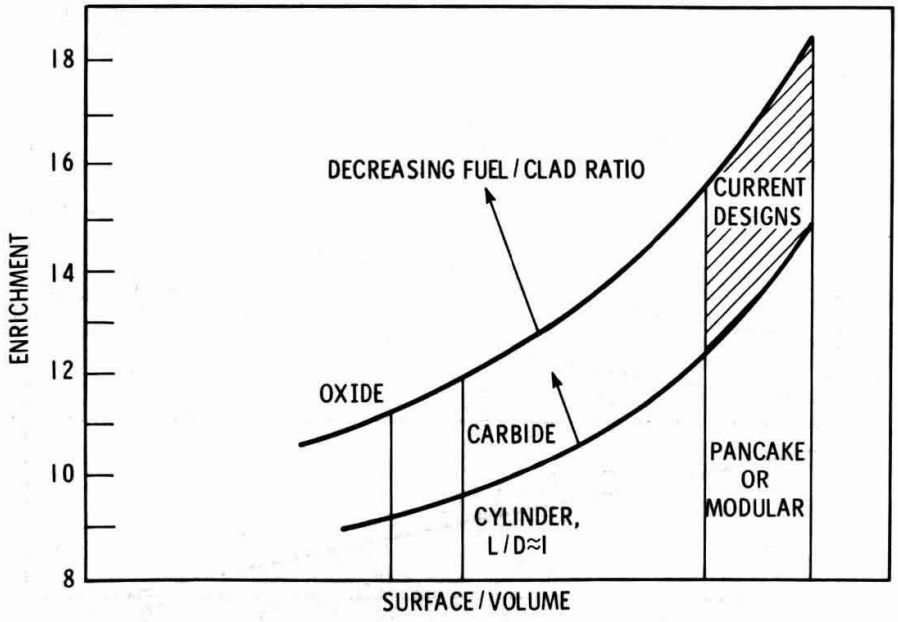

Figure 6. FBR Fissile Enrichment

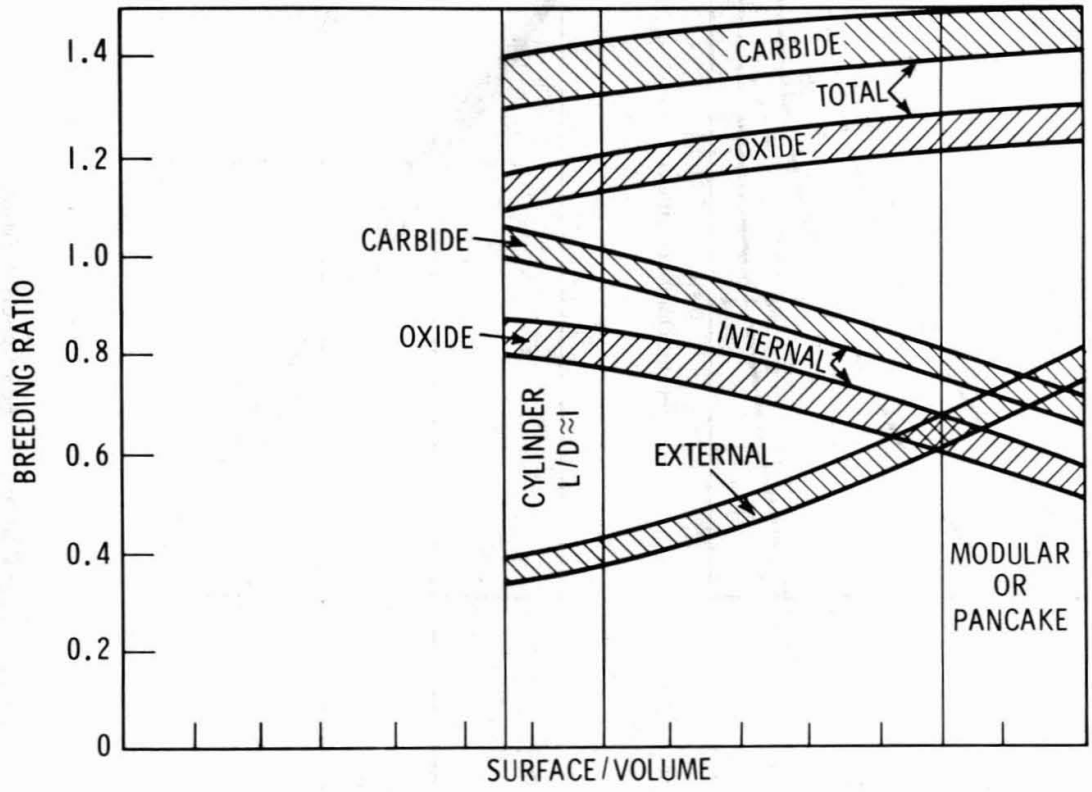

Figure 7. FBR Breeding Ratio

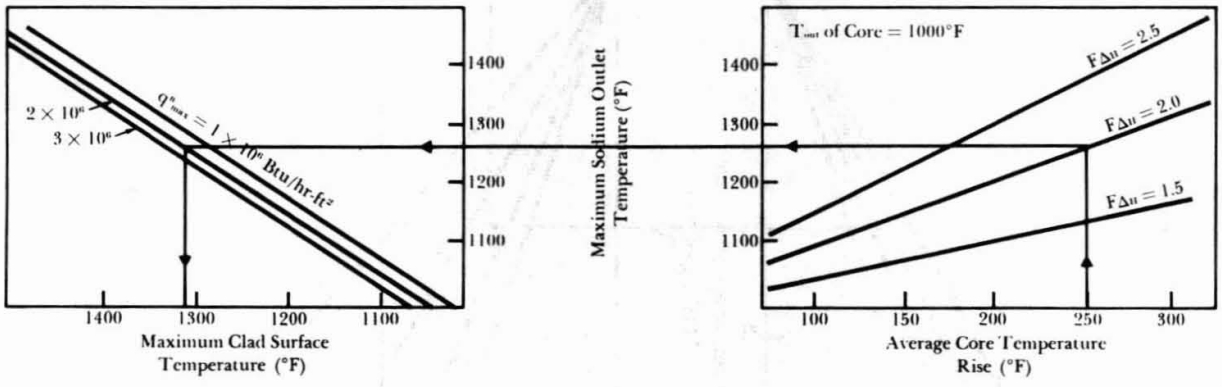

Figure 8 FBR Maximum Sodium and Clad Surface Temperatures

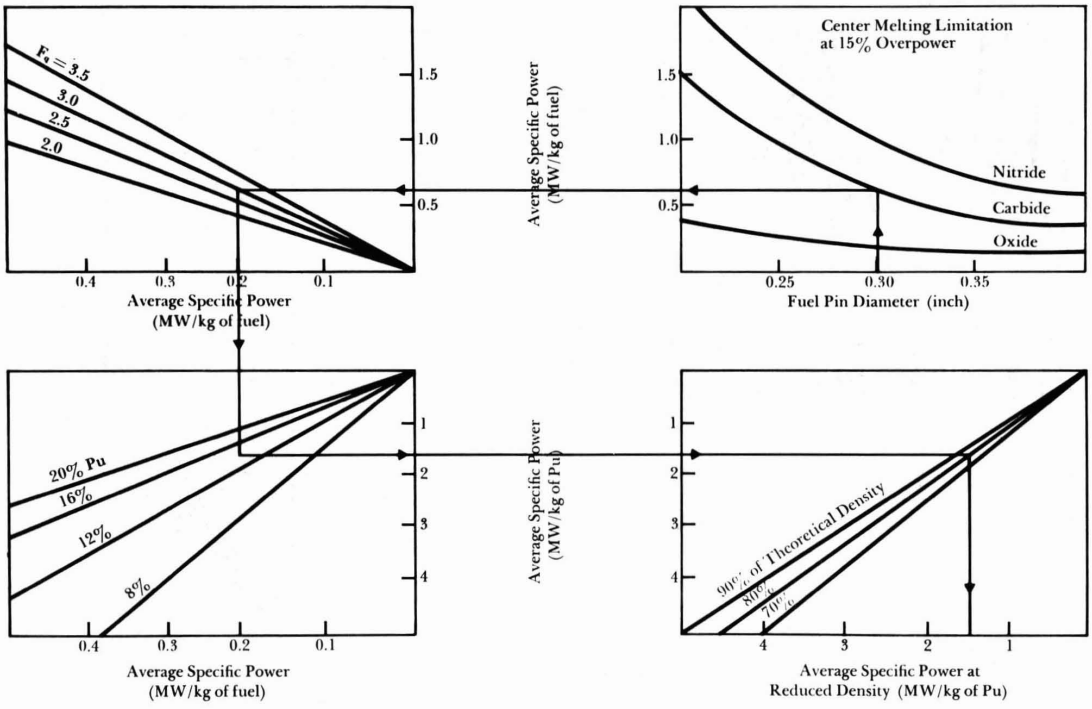

Figure 9 FBR Specific Power

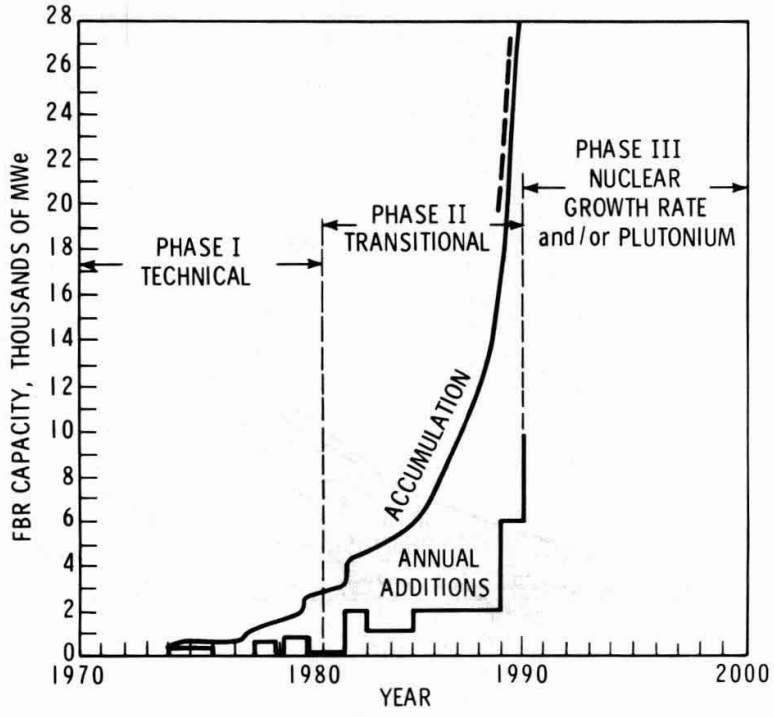

Figure 10. FBR Capacity Next 30 Years

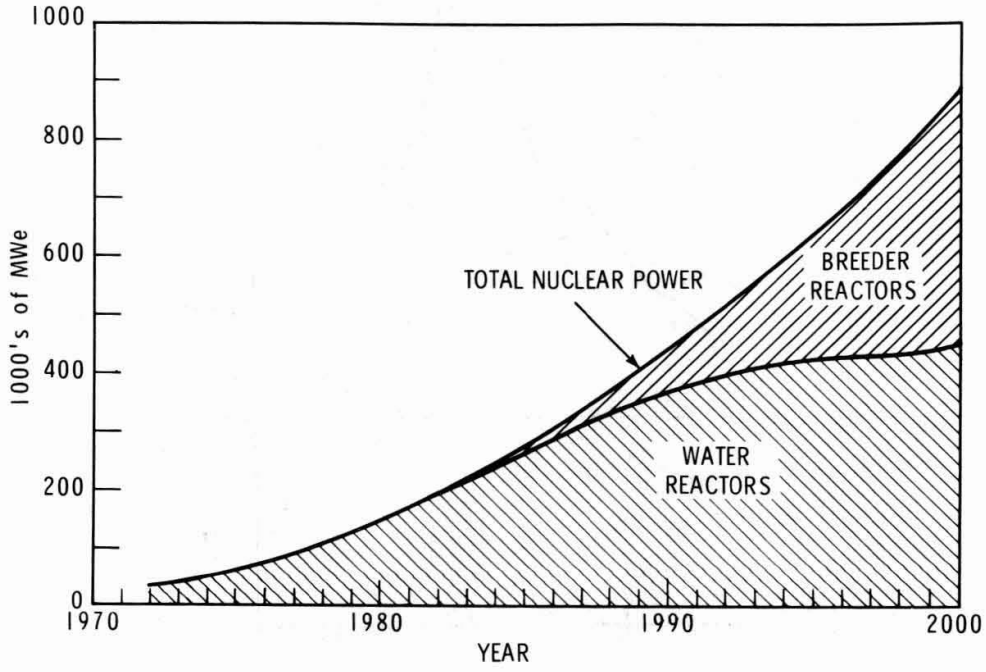

Figure 11. Nuclear Electrical Capacity

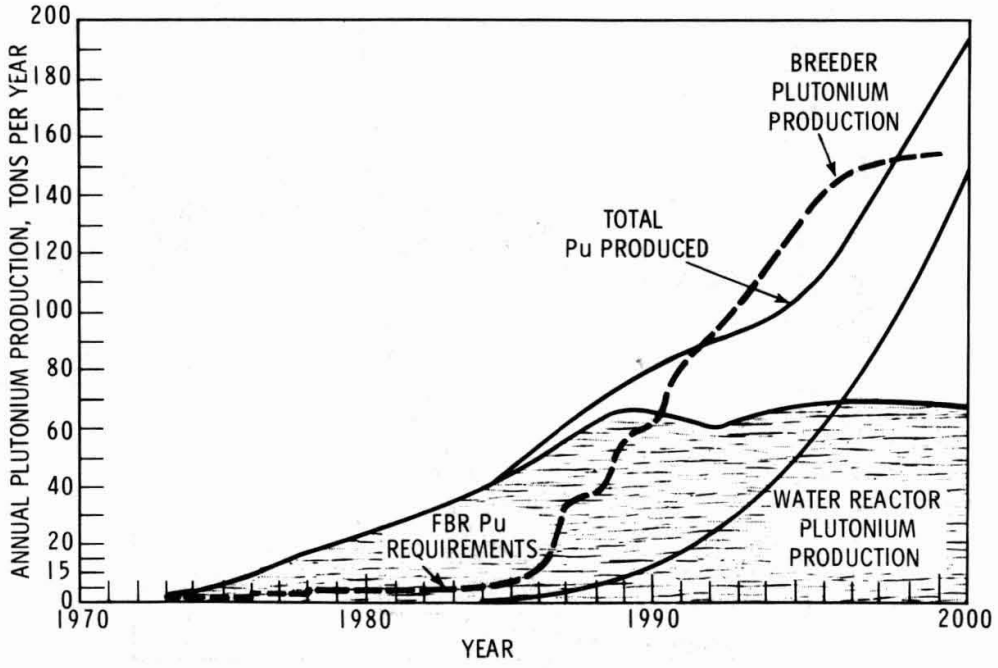

Figure 12. Annual Plutonium Production and Requirements

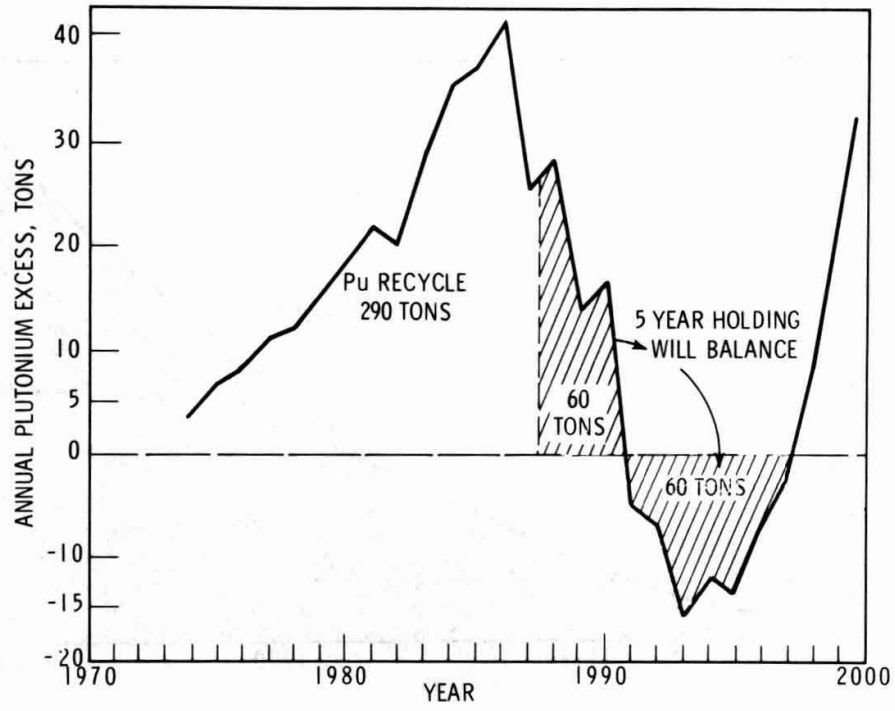

Figure 13. Annual Plutonium Production in Excess of Breeder Requirements

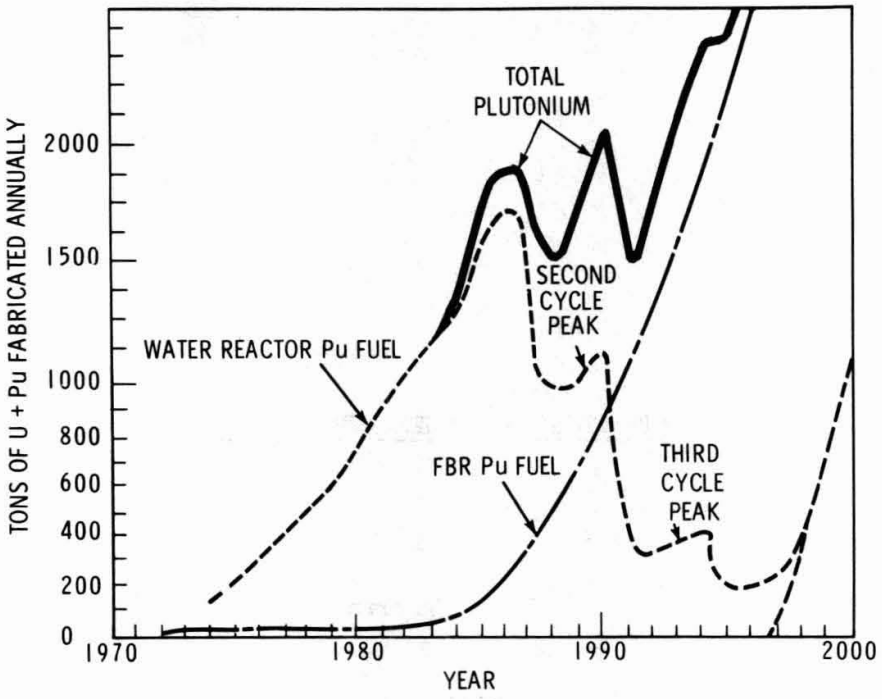

Figure 14. Annual Plutonium Fuel Fabrication Volume

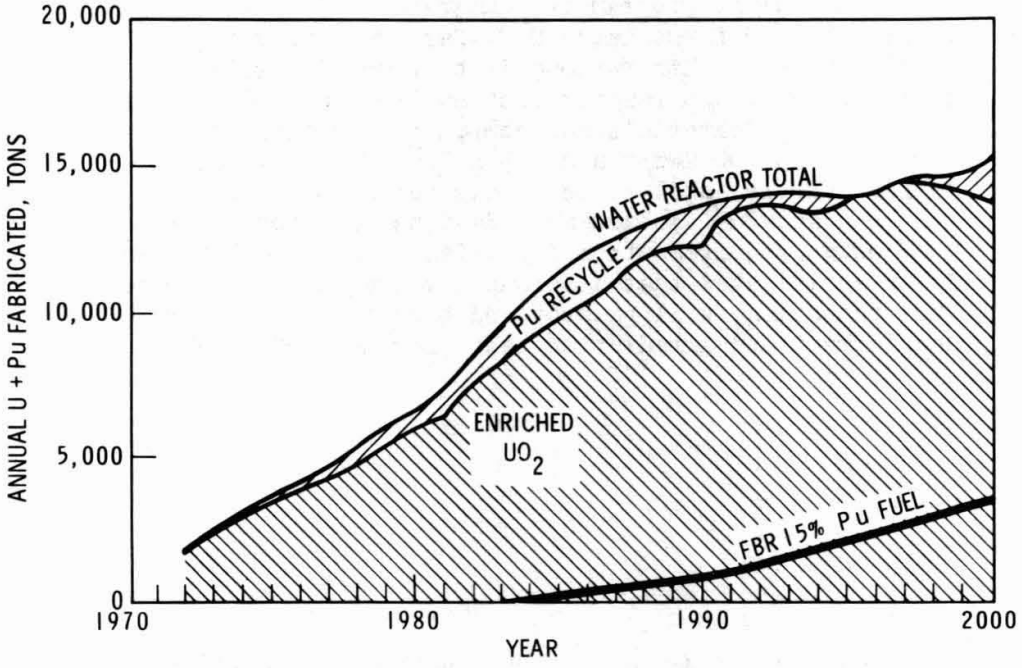

Figure 15. Annual Fabrication Volume

FFTF PLUTONIUM FUEL DEVELOPMENT

B. R. Hayward

Abstract

The Fast Flux Test Facility (FFTF) mixed oxide plutonium fuel development program is summarized. This test facility represents the first large U.S. fast reactor using plutonium fuel. Its purpose is to provide a well characterized fast reactor test environment. Only limited data exist on materials and components exposed to the goal burnup of 75,000 MWd/t and 1.3 x 10^{23} fluence. High performance reliability is emphasized in the program. The fuel pin and fuel subassembly designs are shown along with the design requirements and initial operating characteristics. It is anticipated that a strong advance in fast reactor fuel technology will be provided through this process development and irradiation test program for the FFTF.

B. R. Hayward is Manager, Fast Reactor Fuel Development with Battelle Northwest Laboratories, Richland, Washington.

The Fast Flux Test Facility or FFTF is the key facility construction program in the U. S. Liquid Metal Fast Breeder Reactor Program today. It will be constructed at the Pacific Northwest Laboratories in Richland, Washington with criticality currently planned for early 1973. The FFTF will include a Fast Test Reactor (FTR) and a Nuclear Proof Test Facility (NPTF). The FTR will be a sodium cooled, 400 MW fast reactor using ~700 kg Pu per year in mixed oxide fuel. The associated Nuclear Proof Test Facility or NPTF will use about 800 kg Pu total for physics measurements. The conceptual driver fuel subassembly for the Fast Test Reactor consists of a bundle of 217 one-quarter inch diameter 304 SS clad pins. Each seven foot long by .016" wall pin contains approximately 36" of high density sintered pellets. The fuel core average composition is approximately UO_2 + 25 wt% PuO_2 with an oxygen-to-metal ratio of 1.98. There are about 75 subassemblies in the core, the number depending on the complement of experiments in the core. The initial bulk sodium exit temperature is 900 °F with the plant to be designed for 1200 °F sodium.

This test facility is significant to the U. S. Program in that it represents the first large fast reactor using plutonium fuel technology. Its primary purpose is to provide a known and controlled environment for large scale fuel, materials, and fast reactor component tests in both open and closed loops. The initial series of mixed oxide cores with stainless steel clad are using conventional design and existing materials properties. The reliance on existing data requires some extrapolation for achievement of the peak burnup goal of 75,000 MWd/tonne on the fuel and 1.3 x 10^{23} n/cm^2 exposure to the clad. No data exist on materials and fuel configurations tested in full scale to these peak conditions. Through an extensive process and irradiation test development program at the Pacific Northwest Laboratories and similar AEC sponsored LMFBR development programs elsewhere, confirmation of the proposed design will be obtained well in advance of plant operation. This development program plus a continuing fuel surveillance program is expected to contribute to and advance the status of materials technology in such areas as nondestructive testing, quality assurance standards and methods, properties of irradiated fuel, statistical performance results, and in semi-remote and automated fabrication methods. The British and French fast reactor fuel work has significantly contributed to the FTR fuel technology and design.

A major goal in the development of the fuel subassembly is high reliability. Extensive efforts are in progress to assure the high performance goals. All detailed operations from the fuel and cladding material sources through to the final product are being thoroughly characterized and evaluated to assure that only high quality design materials and workmanship are used. The product specifications are stringent and each fuel and cladding supplier will be required to qualify by fabrication of prototypes with representative materials on representative scale equipment and to representative quality assurance standards. With this emphasis on reliability, the mixed oxide

specifications developed will probably represent the starting state of plutonium technology for the initial fast reactor demonstration power plants. Other ceramic fuels such as carbides and nitrides that show potential for increased performance will be tested in the FTR. Present plans anticipate an advanced core for FTR operation. This reactor will significantly contribute to all aspects of fast reactor development and plutonium technology.

The following three figures show the conceptual subassembly design, the fuel pin design, and the FTR test environment.

FTR FUEL SUBASSEMBLY DESIGN REQUIREMENTS AND OPERATING CHARACTERISTICS

Reactor	
Reactor Power, (MW):	
Thermal	400
Pin OD, (in.)	~0.250
Cladding ID, (in.)	~0.218
Sodium Coolant:	
Flow Direction	Up
Average Velocity, (ft/sec)	29
Core Pressure Drop, (psi)	60
Linear Power, (kW/ft):	
Average	9.2
Maximum	15.4
Heat Flux, (10^6 Btu/hr-ft^2)	
Average	0.485
Maximum	0.845
Coolant Inlet Temperature	500 ^oF
Coolant Outlet Temperature:	
Average	800-900 ^oF
Maximum (with hot channel)	1060 ^oF

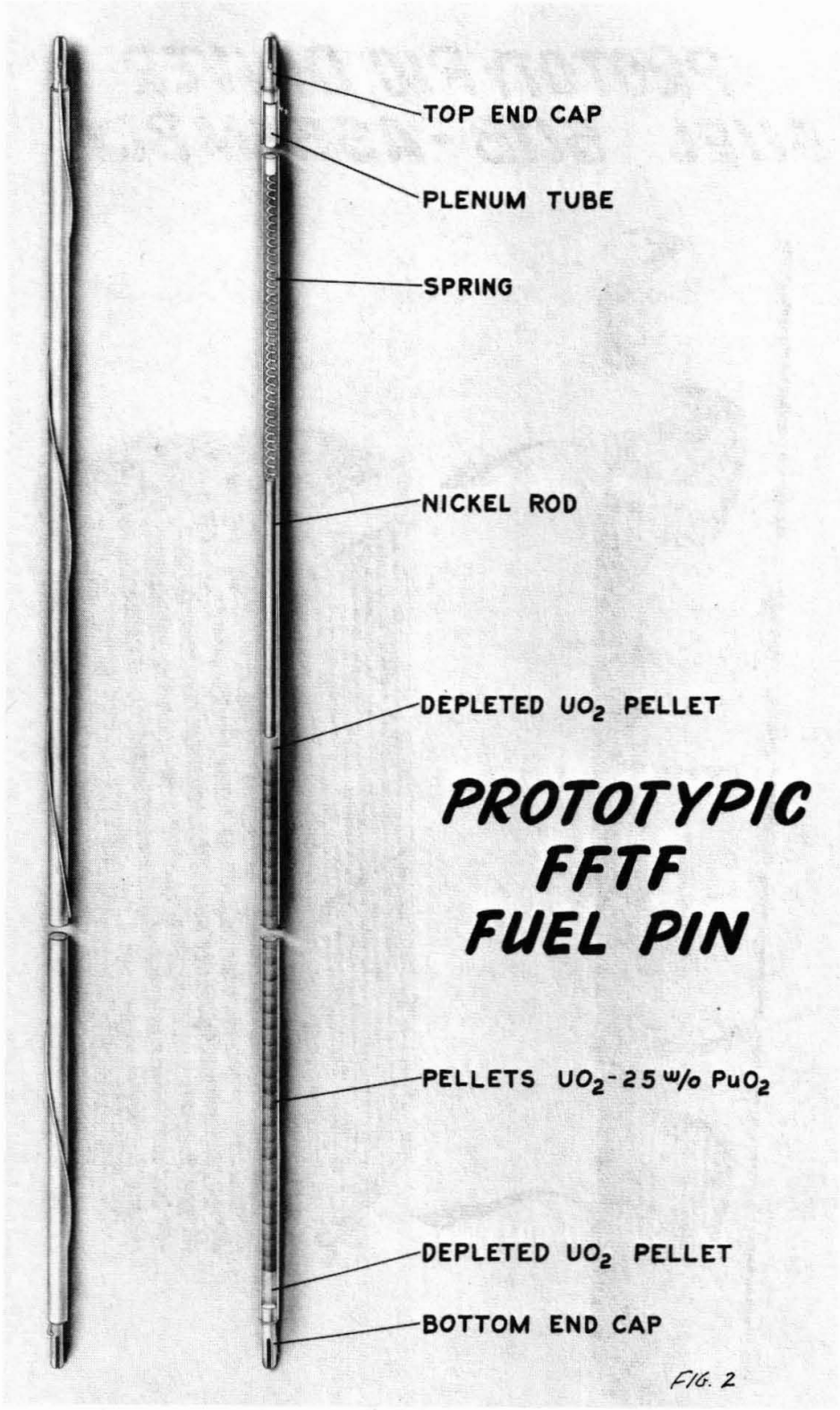
TOP END CAP
PLENUM TUBE
SPRING
NICKEL ROD
DEPLETED UO_2 PELLET
PROTOTYPIC
FFTF
FUEL PIN
PELLETS UO_2-25 w/o PuO_2
DEPLETED UO_2 PELLET
BOTTOM END CAP

FIG. 2

PROTOTYPIC DRIVER FUEL SUB-ASSEMBLY

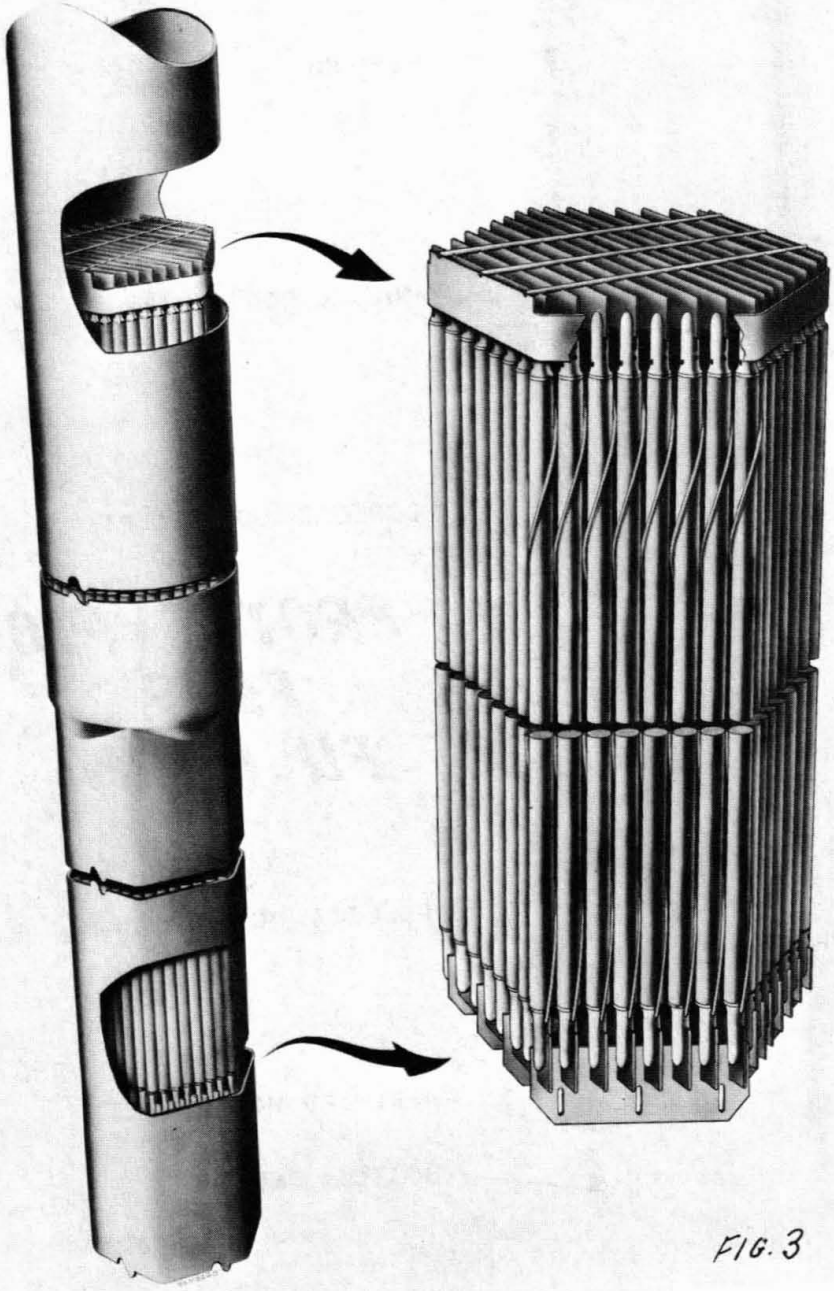

FIG. 3

CENTRAL STATION BREEDER REACTORS: PLUTONIUM FUEL REQUIREMENTS

United Kingdom Experience

B. R. T. Frost

Abstract

The United Kingdom programme for the installation of nuclear power stations envisages that the first commercial fast breeder station will start operation between 1976 and 1978. Since the P.F.R. is scheduled to reach full power in 1971 the fuel pin and sub-assembly designs for the first central stations must follow that of the P.F.R. quite closely. The core parameters of the P.F.R. and a published 1000 MWe design are compared; it is shown that the only essential difference is the larger number of sub-assemblies in the latter and hence a lower length : diameter ratio for the core. The key materials problems which need to be studied to improve fast reactor economics and safety are discussed.

B. R. T. Frost is leader of the Advanced Fuels Group in Metallurgy Division, Atomic Energy Research Establishment, Harwell, Berkshire.

Early Commercial Reactor Design

The United Kingdom has declared that it does not intend to recycle plutonium in its thermal reactors (1). It believes that greater economies can be achieved by developing fast breeder reactors, burning plutonium fuel, on as short a time-scale as possible. Construction of the 250 MWe prototype fast reactor (P.F.R.) began in 1966 with a target on-power date of 1971. Its main purposes are:

1. to gain engineering experience of the operation of a large sodium cooled fast reactor,
2. to develop fuel technology, and
3. to obtain physics data on a large core, including control and instrumentation.

This reactor project is supported by the Dounreay Fast Reactor (D.F.R.), which is now primarily a materials testing reactor, the ZEBRA fast zero energy assembly, numerous sodium loops and extensive plutonium laboratories and hot cells.

The rate of production of plutonium in thermal reactors in the United Kingdom will be sufficient to support the construction of the first commercial fast reactor ($\sim$ 1000 MWe) for an on-power date between 1976 and 1978 (2). In the absence of thermal recycle this early construction date is desirable. For it to be technically feasible there can be little deviation from the design principles already incorporated in the P.F.R. The basic 'building block' for the core must be the P.F.R. sub-assembly, the extra power output being obtained by increasing the core diameter, i.e. by adding more standard sub-assemblies to give a more pancake-shaped configuration.

The P.F.R. reference fuel pin design is shown in Figure 1. It is a type 316 stainless steel tube 0.200-inch I.D. and 0.230-inch O.D. containing a 36-inch length of fuel with $\sim$18-inch sections of axial breeder on either side and a plenum section 47-inches long which has a smaller diameter to reduce the coolant pressure drop. The fuel is 80% theoretically dense $(U,Pu)O_2$, the form being either annular pellets or vibrocompacted granules. The P.F.R. core has two enrichment zones for flux flattening (19% Pu in the inner zone, 25% Pu in the outer). Other important parameters are included in Table I.

325 pins are assembled inside a hexagonal sub-assembly wrapper and are spaced on a 0.290-inch pitch by means of metal grids (Figure 2) spaced at 4-inch intervals over the core length. The total length of each sub-assembly is 12-feet 6-inches. The P.F.R. core is made up of 78 of these sub-assemblies giving a core diameter of 5-feet surrounded by 42 radial breeder sub-assemblies containing natural or depleted UO_2 (Figure 3).

The 1000 MWe core design (3) uses 195 of the fuel sub-assemblies, giving a core still 3-feet long but 9-feet in diameter, i.e. with an $^{L}/_{D}$ ratio of 0.33 (Figs. 4 and 5). The parameters are summarized in Table II. This C.F.R. design involves a higher sodium outlet temperature (610°C cf. 580°C) and a higher maximum fuel rating (234 w/gm cf. 210 w/gm) but these differences are unlikely to have a marked effect on fuel element performance. The essential point is that the parameters of the early C.F.R.'s will resemble those of P.F.R. very closely.

Materials Problems: Current Status

A number of individual fuel pins and several 77 pin sub-assemblies containing $(U_{0.85}\ Pu_{0.15})O_2$ fuel in pellet and vibrocompacted form have been irradiated in the D.F.R. core. The fuel pins have incorporated the essential features of the P.F.R. design, particularly the correct radial dimensions, but have been shorter than the 36-inches of the P.F.R. core since the D.F.R. core is only 21-inches long. Nevertheless the tests were representative of P.F.R. temperatures and ratings. The incidence of cladding failure up to 7.5% burn-up was very low (4,5). It therefore appears that this is a reasonable target for the peak burn-up in P.F.R. The failure rate of single pins increases above this level, the cause being the strain induced by fuel swelling in cladding which has become embrittled by transmutation products. Improvements in burn-up will depend to a large extent on gaining a better understanding of these phenomena. It is already clear that clad failure occurs well before the initial 20% voidage is consumed by fuel swelling. A more efficient use of this voidage would be possible if the cooler regions of the fuel were more plastic and if the cladding afforded greater restraint; this suggests two lines of research which might lead to higher burn-ups.

The behaviour of the cladding is complex. It has been known for several years that the irradiation of stainless steels in a thermal flux produces a loss of ductility due to the production of helium from ^{10}B (6,7). Helium bubbles form in the grain boundaries and grow under a tensile stress until they weaken the grain boundaries (8). It has been observed that the embrittlement is greater for a given fast neutron dose than a thermal and the reason appears to be that not only are helium bubbles produced in a fast neutron flux but also voids which may be vacancy clusters containing some gas atoms (9). These can produce a nett swelling of the metal. The effect of fuel swelling strain on the density of void population is unknown but may be significant. Thus, fuel-clad interaction studies acquire an added significance in the quest for higher burn-ups.

Mixed oxide fuel technology has been built on the firm foundation of UO_2 technology and this has largely determined its choice for the P.F.R. first charge and for early C.F.R.'s. Other fuels, particularly mixed carbide, have been studied as possible replacements for oxide. Carbide has some of the attributes of a ceramic fuel (high melting point and isotropic structure) combined with some of those of metals

(particularly higher thermal conductivity and density). The basic problem is how to capitalize on these advantages. One way is to use the higher conductivity to use larger diameter pins without centre melting; this reduces the number to be made and may increase the fuel fraction in the core, provided sodium heat transfer limitations are not exceeded.

Alternatively the higher conductivity may be used, in conjunction with sodium bonding, to maintain the fuel at a low temperature thereby effectively immobilizing the fission products, minimizing the size of gas bubbles and the aggregation of solid fission products. Carbide already offers the attraction of better breeding. If this can be accompanied by a burn-up at least as high as that of oxide there is a strong economic incentive to introduce it into the C.F.R. programme at an early date.

Fuel cycle costs represent only a fraction of the fast reactor power costs. Significant cost reductions may also be achieved through engineering developments, e.g. improvements in heat exchanger design and ultimately through the use of alternative coolants. However, it is clear that the timescales discussed above do not permit much deviation from the established pattern and the concept embodying oxide fuel in sealed stainless steel pins cooled by sodium which uses two heat exchange circuits to generate steam is likely to dominate the scene until well into the 1980's. The longer term prospects in the United Kingdom, summarized in an earlier paper by Searby and Iliffe (10), are shown in Figures 6 and 7. These show the total national electricity capacity up to 1990 and the contributions of different reactors systems to this, making respectively pessimistic and optimistic assumptions on national needs. It shows a possible maximum installation of 49,000 MWe of fast reactors by 1990 with a potential cost advantage of ~£500 million or ~$1.2 billion. Thus there should be the economic incentive to pursue a large and vigorous programme of development and the capacity in which to introduce new concepts.

Acknowledgements: This paper has been written more from the viewpoint of fuel element development than of reactor economics, in which field the author freely acknowledges his ignorance. In consequence, free use has been made of published works of his colleagues in the U.K.A.E.A. and the United Kingdom nuclear industry.

REFERENCES

1. B. Kehoe and J. Williams, IAEA Conference on 'The Use of Plutonium as a Reactor Fuel', Paper SM88/23, Brussels, 1967.

2. P. J. Searby, 3rd Foratom Congress - Industrial Aspects of a Fast Breeder Reactor Programme - Paper I. London, 1967.

3. J. O. Tattersall, P. R. P. Bell and E. Emerson, London Conference on Fast Breeder Reactors, British Nuclear Energy Society, Paper 3/6 1966.

4. H. Lawton et al. ibid. paper 4B/4.

5. A. G. Frame, 'Status of the U.K.A.E.A.'s Prototype Fast Reactor', ANS Topical Meeting on Fast Reactors, San Francisco, 1967.

6. P. T. Nettley, I. P. Bell and K. Q. Bagley, London Conference on Fast Breeder Reactors, British Nuclear Energy Society, Paper 5B/3, 1966.

7. S. H. Bush, J. Moteff and J. Weir, Radiation Damage in Fast Reactor Components, ANS-100, 1965.

8. R. S. Barnes, Nature, 206, 1307, 1965.

9. C. Cawthorne and E. Fulton, Nature, 216, 575, 1967.

10. P. J. Searby and C. E. Iliffe, London Conference on Fast Breeder Reactors, British Nuclear Energy Society, Paper 1/1, 1966.

TABLE I

P.F.R. - List of Main Parameters

Thermal Output	559 MW Core	41 MW Breeder
Gross electrical output from generator	265 MW approx.	
Nett electrical output from station	248 MW approx.	
Coolant temperature at core inlet	400-430°C	752-806°F
Coolant temperature at core outlet	560-600°C	1040-1110°F
Secondary sodium temperature at steam generator inlet	530°C	986°F
Secondary sodium temperature at steam generator outlet	370°C	698°F
Primary flow through core	23.2×10^6 lbs/hr	70,500 l/min
Primary pump head	117 p.s.i.	8.23 kg/sq.cm
Secondary coolant flow	23.2×10^6 lbs/hr	70,000 l/min.
Secondary pump head	45 p.s.i.	3.15 kg/sq.in
No. of fuel pins per sub-assembly	325	
Outside diameter of fuel can	0.23 in	.585 cm
Fuel can thickness	0.015 in	.038 cm
No. of sub-assemblies in inner zone	30	
No. of sub-assemblies in outer zone	48	
No. of radial breeder sub-assemblies	42	
Length of fuel in pin	36 in	91.5 cm
Length of axial breeder	9 in	22.9 cm
Overall length of pin	103 in	262 cm
Weight of mixed oxide fuel in core	4.0 tonne	
Weight of PuO_2 in core	.902 tonne	
Diameter of primary vessel	40 ft.	1221 cm
Weight of sodium in primary vessel	900 tonne	
Steam temperature at T.S.V.	513-566°C	955-1050°F
Steam pressure at T.S.V.	2315 p.s.i.a.	163 kg/sq.cm
Reheat pressure inlet	495 p.s.i.a.	34.5 kg/sq.cm
Feed temperature	288°C	550°F

TABLE II

Fast Reactor Power Plant Design Parameters for Nominal 1000 MWe

Nett electrical output per reactor	1046 MW
Overall plant efficiency	44%
Core thermal power output (fuel cycle equilibrium)	2272 MW
Breeder and reflector thermal power output	107 MW
Total thermal power per reactor	2379 MW
Core and breeder size and performance	
Height of active core	91.5 cm
Axial breeder length at each end	23.0 cm
Diameter of active core	269.0 cm
Diameter over radial breeder	350.0 cm
Core volume	5210 litres
Number of sub-assemblies:	
Core fuel	195
Radial Breeder	150
Control	18
Reflector	66
Initial fuel loading (PuO_2 + UO_2)	15.1 tonnes
Initial Pu loading (metal)	2.4 tonnes
Mean rating of fuel	150.4 w/gm oxide
Average core density	436.0 kw/litre
Exponential fuel doubling time	10 years
Fuel and axial breeder sub-assembly	
Outside dimension across flat of hexagon	14.1 cm
Pitch	14.5 cm
Number of fuel pins	325
Pin pitch (triangular)	7.37 mm
Peak can temperature (mid wall)	670°C
Design maximum burn-up	10%
Weight of fuel in sub-assembly	51.3 kg
Weight of axial breeder per sub-assembly	28.1 kg
Primary Sodium	
Outlet temperature from core	610°C
Inlet temperature to core	380°C
Flow rate in core	29×10^6 kg/hr
Flow rate in breeder	0.52×10^6 kg/hr
Primary circuit pressure drop	4.2 kgf/cm^2
Primary circuit pumping power	6.2 MW
Secondary Sodium	
Inlet temperature to primary heat exchanger	340°C
Outlet temperature from primary heat exchanger	580°C
Flow rate	28.4×10^6 kg/hr
Secondary circuit drop	7 kgf/cm^2
Secondary circuit pumping power	9 MW

Table II (Continued

Steam Side Data	
TSV pressure	163 kgf/cm^2
TSV temperature	560°C
Number of reheat stages	one
Reheated steam inlet pressure	39 kgf/cm^2
Reheated steam inlet temperature	560°C
Superheated steam flow	3.16×10^5 kg/hr
Reheat steam flow	2.48×10^6 kg/hr
Feed temperature	252°C

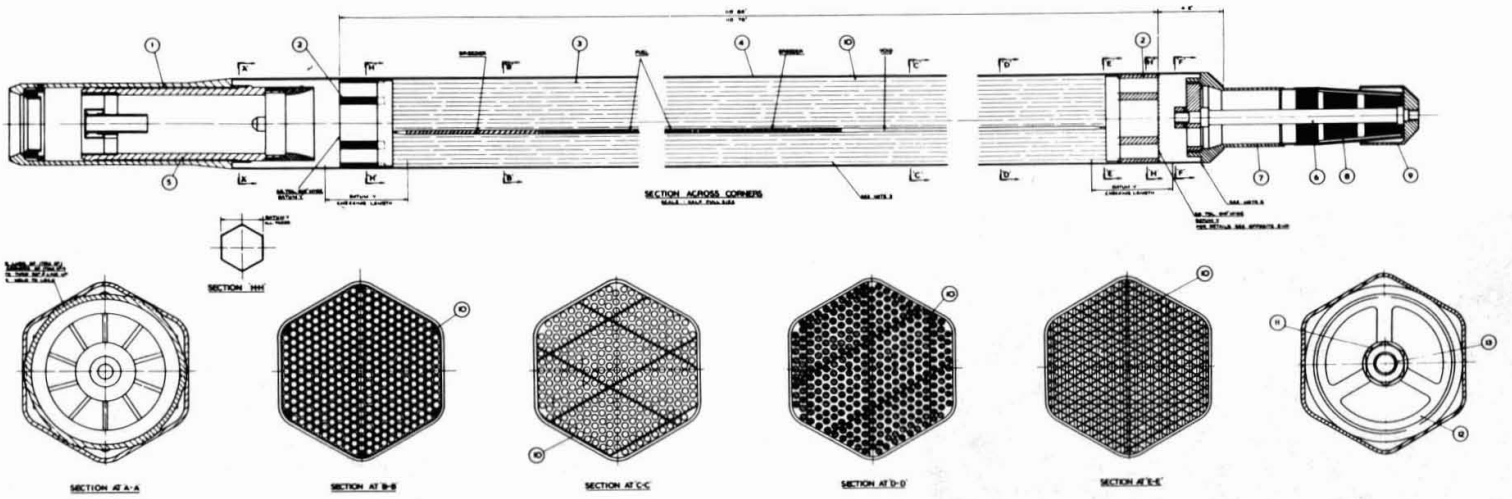
SECTION ACROSS CORNERS
SECTION AT A-A
SECTION AT B-B
SECTION AT C-C
SECTION AT D-D
SECTION AT E-E

FIG. 1

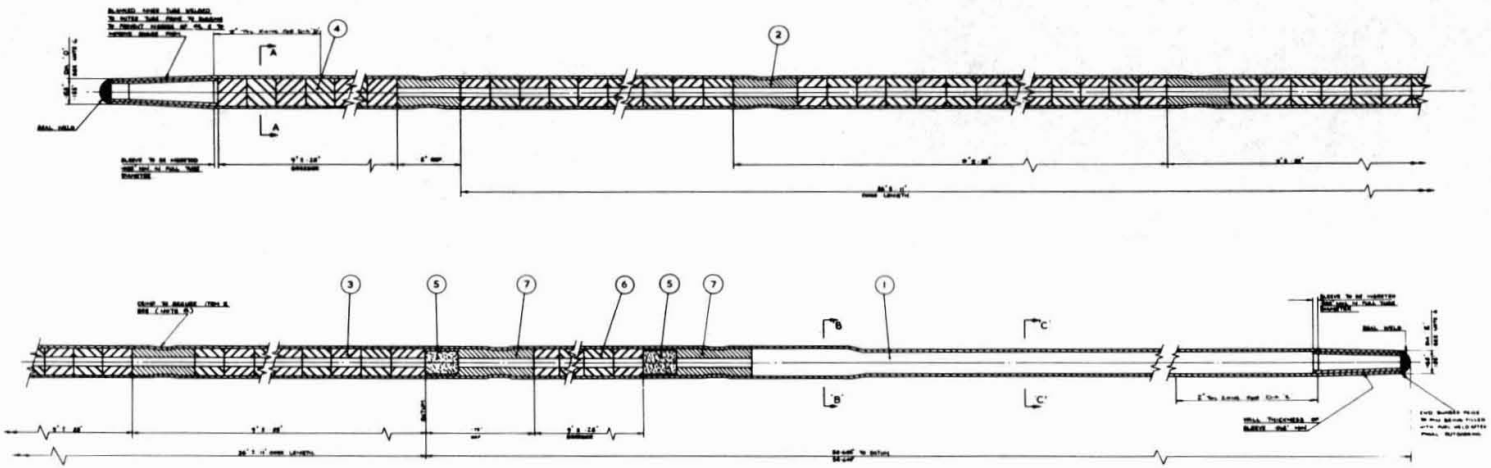

FIG. 2

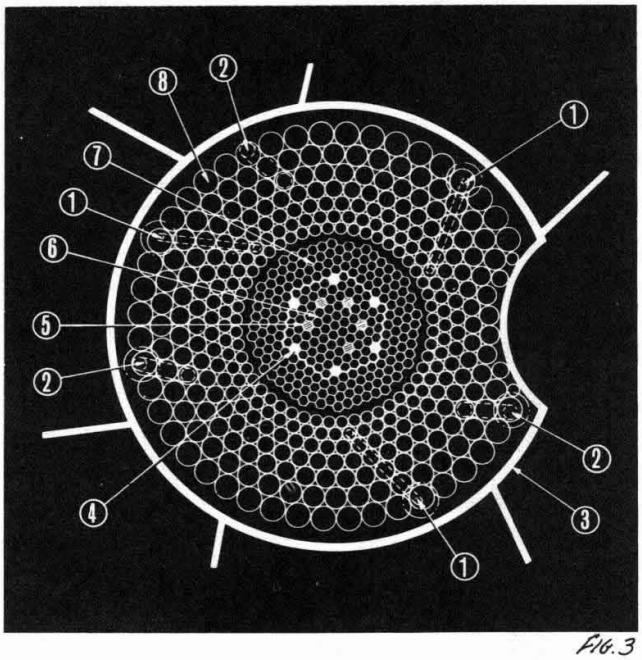

FIG. 3

Core of 250 MW(e) fast reactor

1 *Low Flux Instruments*
2 *High Flux Instruments*
3 *Stainless Steel Insulation to Reactor Jacket*
4 *Safety Rods*
5 *Control Rods*
6 *Core*
7 *Breeder*
8 *Neutron Shield*

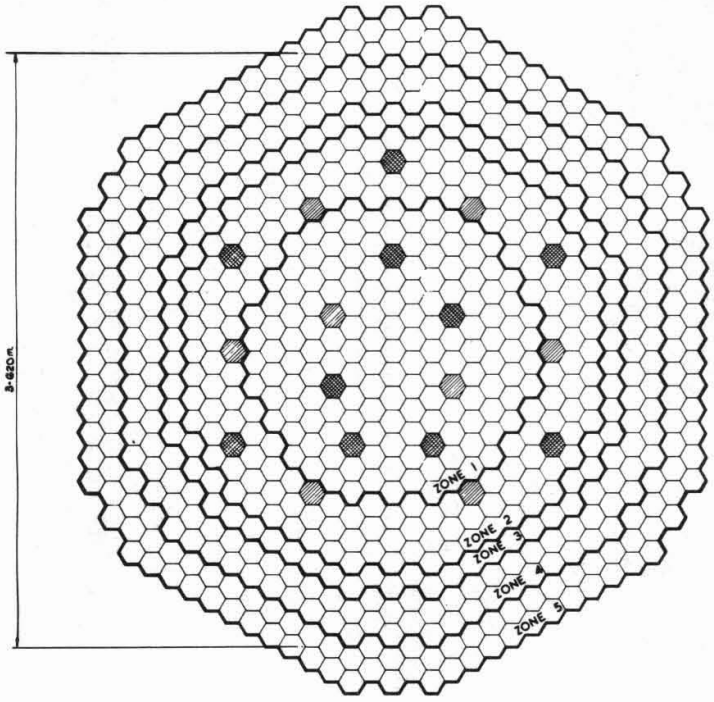

	DESCRIPTION	QUANTITY
	FUEL SUBASSEMBLIES IN ZONE 1.	144
	FUEL SUBASSEMBLIES IN ZONE 2.	151
	REFLECTORS IN ZONE 3	66
	BREEDER IN ZONE 4	150
	REFLECTOR AND SHIELD ASSEMBLIES IN ZONE 5	174
	BURN - UP AND CONTROL RODS	8
	START - UP RODS	10

FIG. 4

CORE UTILISATION DIAGRAM

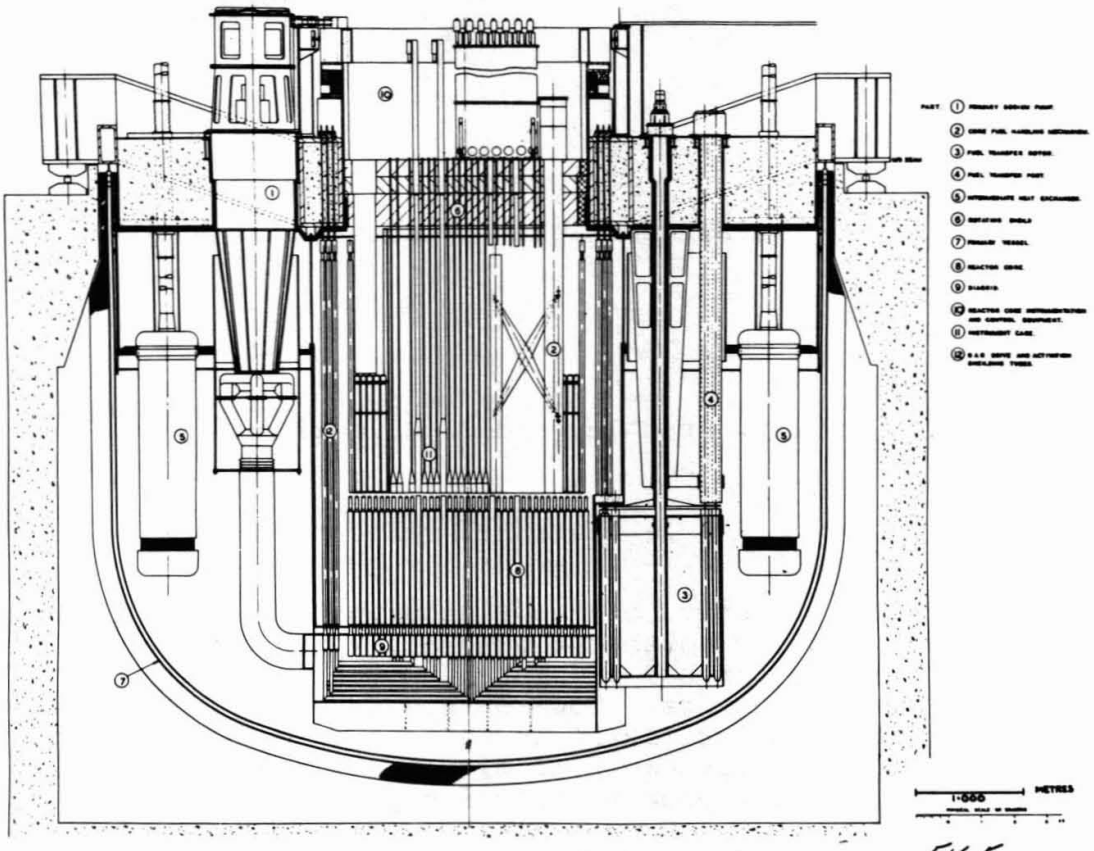

SECTIONAL ELEVATION THROUGH REACTOR & PRIMARY CIRCUIT

FIG 5

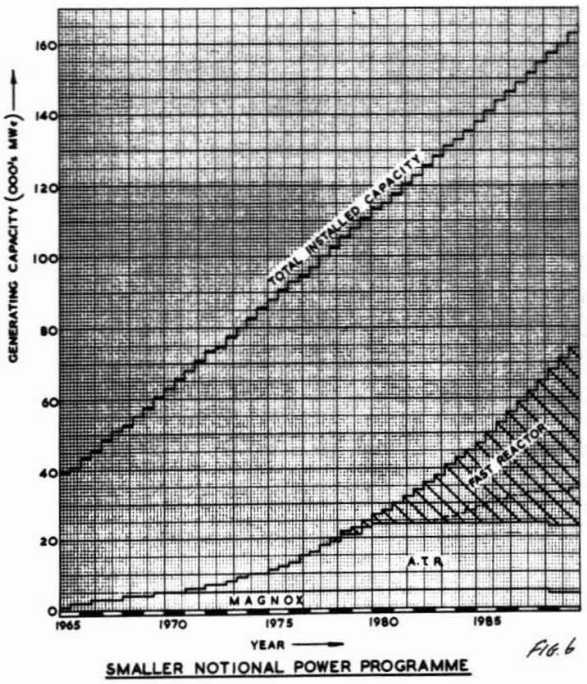

FIG. 6

SMALLER NOTIONAL POWER PROGRAMME

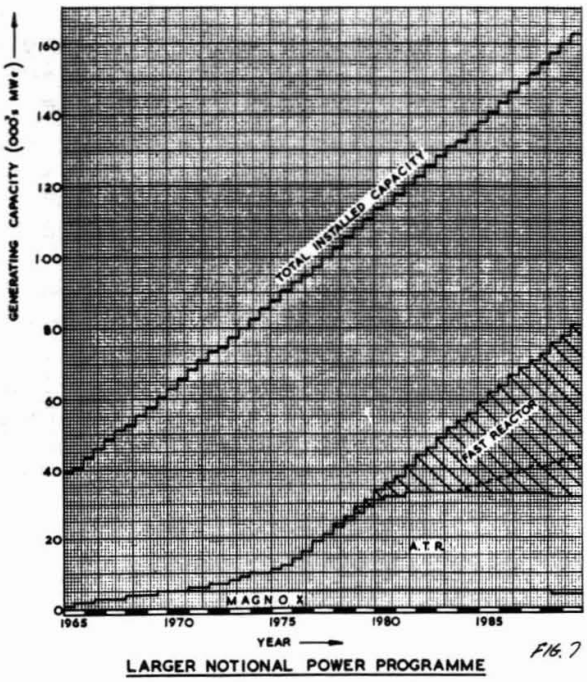

FIG. 7

LARGER NOTIONAL POWER PROGRAMME

OPERATING EXPERIENCE WITH PLUTONIUM FUELS IN PRTR

M. D. Freshley and S. Goldsmith

Abstract

A major objective of the Plutonium Utilization Program at Pacific Northwest Laboratory is to provide base technology for use of plutonium fuel in commercial thermal power reactors. Toward this end, the Plutonium Recycle Test Reactor (PRTR) in support of a diversified plutonium fuel development effort, has produced over 43,000 MWd of heat energy utilizing plutonium fuels.

To date, approximately 360 experimental fuel elements have been irradiation tested in the PRTR. Utilizing a basic 19-rod cluster fuel element design, such fuel materials as UO_2, Al-Pu, and UO_2-PuO_2 have been evaluated. Packed-particle oxide fuels fabricated by swaging or vibrational compaction have been emphasized. Over 10 tonnes of UO_2-PuO_2 packed-particle fuel has been irradiated in PRTR. Fuel material has been prepared by mechanically mixing discrete UO_2 and PuO_2 particles during loading or by pneumatic impaction. Plutonium compositions ranged from 0.5 to 4.0 wt% PuO_2 in UO_2. Maximum element burnups of over 11,000 MWd/tonne have been attained with prototypic UO_2-PuO_2 power reactor fuel assemblies. Maximum fuel temperatures have been above melting.

M. D. Freshley is a Research Associate and S. Goldsmith is Manager, Fuel Design and Evaluation Unit at Pacific Northwest Laboratory which is operated by Battelle Memorial Institute for the Atomic Energy Commission.

The Batch Core Experiment currently in progress in PRTR is providing statistically significant irradiation behavior data on High Power Density UO_2-PuO_2 fuel elements operated at power generations greater than those currently employed in commercial power reactors. Maximum linear rod power generations are 20 kW/ft with maximum fuel temperatures near melting. Goal burnups are over 13,000 MWd/tonne. The comparative performance of powder and pellet fuels is also being evaluated. Two vibrationally compacted UO_2-PuO_2 elements instrumented to measure plenum gas temperature and pressure are included in the Batch Core loading.

Results of the program to date indicate that for the low plutonium concentrations of interest in thermal reactor fuels the performance characteristics are not significantly different for UO_2 and UO_2-PuO_2 fuels. Experience with in-service failed and deliberately defected packed-particle fuels has been very encouraging. Deliberately defected irradiation tests with UO_2-PuO_2 fuels, some operating under molten core conditions, have been conducted in the Fuel Element Rupture Test Facility (FERTF), a pressurized water loop in the PRTR.

Concurrent with the Batch Core Experiment, irradiation tests of UO_2-PuO_2 fuel rods utilizing a special 8-rod test element are being conducted at higher power generations in the FERTF. Tests will be performed to evaluate the effects of fuel form (powder, pellet), power generation (20 to 28 kW/ft), and defect behavior on fuel performance.

Introduction

The objective of the Plutonium Utilization Program (PUP) at Pacific Northwest Laboratory has been to develop base technology to support the commercial application of plutonium recycle in thermal reactors (1). Included in this program is a major effort to (1) develop inexpensive and safe methods of fabricating plutonium fuels and (2) demonstrate through extensive irradiation testing the performance characteristics of such fuels.

The Plutonium Recycle Test Reactor (PRTR) (2), which began operation in July 1961, is the principal irradiation facility used in support of the PUP. It is a pressure tube reactor cooled and moderated with heavy water. The 70 MW(t) reactor is ideally suited for testing experimental fuel assemblies under power reactor conditions. Rod cluster fuel assemblies which are prototypic of power reactor designs can be tested in any of its 85 pressure tubes. The Batch Core Experiment*, which has been underway in PRTR since January 1967, uses High Power Density (HPD) fuel elements. Prior to this time the reactor was operated on a graded charge-discharge scheme utilizing fuel of various designs and compositions and fabricated by various processes.

The PRTR was originally loaded with 33 Al-Pu spike elements and 52 swage-compacted natural UO_2 elements. Starting in April 1962, the swaged and vibrationally compacted mixed-oxide elements containing mechanically mixed or incrementally loaded fuel were added to the core replacing the Al-Pu spike and UO_2 elements. The first recycled plutonium was returned to the core in May 1963. Irradiation of swaged and vibrationally compacted mixed-oxide elements fabricated from pneumatically impacted feed material began in October 1963. Irradiation of the first vibrationally compacted High Power Density elements containing pneumatically impacted UO_2-2 wt% PuO_2 fuel commenced in October 1964. The Batch Core Experiment utilizing a core loading of High Power Density fuel got underway in PRTR during the first part of 1967.

Basic PRTR Fuel Element Design

The basic PRTR fuel element design consists of 19 rods assembled into a 3-1/4 inch diameter cluster (Figure 1). The Zircaloy clad rods are 0.565 inches in diameter

---

* The High Power Density Program includes the Batch Core Experiment in PRTR to evaluate the physics parameters of a plutonium enriched fuel loading as a function of burnup under controlled conditions (3).

with a cladding thickness of nominally 0.030 inches. Twelve of the rods in the element are helically wrapped with an unbonded spacing wire (0.072 inch diameter) on a 10-inch pitch. PRTR fuel elements used prior to the current High Power Density fuel loading were 98 inches long with an active fuel length of 88 inches. Detailed descriptions of the principal pre-High Power Density fuels tested in the PRTR are given in References 4, 5, 6, 7, and 8.

The High Power Density fuel currently being used in the PRTR is 76 inches long with an active fuel length of 58 inches. A 7-inch long plenum was incorporated in the top of each fuel rod to accommodate the increased gas release at the higher fuel temperatures. Fuel rod diameter and cladding composition and thickness is the same as used in the pre-High Power Density fuel. A detailed description of the High Power Density fuel element is given in Reference 9.

More than 70 variations in fabrication techniques, fuel compositions, and cladding utilizing the basic Zircaloy clad 19-rod cluster have been tested in the PRTR (10). Included in the 361 elements irradiated in the PRTR are 75 aluminum-plutonium spike enrichment elements, 68 UO_2 elements, and 216 UO_2-PuO_2 elements. Both swaged and vibrationally compacted oxide fuels have been emphasized with most attention being given recently to vibrational compaction. A summary of the fuel elements irradiated in the PRTR is given in Table I.

Pre-High Power Density Fuel Irradiations

The spike enrichment elements used during initial operation of the PRTR contained non-segmented hot extruded, Al-2 wt% Ni-1.8 wt% Pu alloy cores inserted into Zircaloy cladding (4,5). A diametral gap of 4 to 8 mils between the fuel cores and the Zircaloy cladding was partially closed by differential thermal expansion during operation. These Al-Pu elements were irradiated at maximum rod powers of 15 kW/ft to burnups of 83% of the initial fissionable atoms (0.74×10^{20} fissions/cm^3). The most noticeable irradiation effect was progressive rod shortening upon repeated heating and cooling as a result of intermittent core-clad interaction. Fuel rod shortening caused the nonbonded spacer wires to appear loose after irradiation. Differential thermal expansion retightened the spacer wires during operation because no evidence of fretting or wear was observed.

The irradiation performance of UO_2 packed-particle elements fabricated by swaging and vibrational compaction has been excellent. A swage compacted UO_2 element which has reached a burnup of over 9400 MWd/tonne at maximum rod

powers of approximately 14 kW/ft is still being irradiated. One UO_2 element fabricated by hot swaging was irradiated to a burnup of approximately 1700 MWd/tonne.

The evaluation of irradiation performance of UO_2-PuO_2 elements fabricated by swaging (7) or vibrational compaction (8) is continuing. Several pellet rods are also being irradiated. PuO_2 concentrations include 0.50 wt%, 0.75 wt%, 1.0 wt%, 2.0 wt%, and 4 wt%. In the first mixed-oxide fuels, mechanical mixing or incremental loading of UO_2 and PuO_2 powders (11) was used to obtain a relatively uniform gross axial distribution of PuO_2 in both swage-compacted and vibrationally compacted elements. Moderate layering of the PuO_2 occurred within increments during loading and gamma scanning was used to assure that no hot spots caused by local concentrations of plutonium would exceed the maximum permissible point heat flux limit. In general, the irradiation performance of the mechanically mixed UO_2-PuO_2 elements in PRTR has been excellent (10). Maximum burnups of 11,000 MWd/tonne have been obtained at maximum rod powers of approximately 16 kW/ft. Localized regions of bulk sintering, grain growth, and central void formation were not detrimental to the fuel performance in PRTR.

High-density UO_2-PuO_2 feed material subsequently used in PRTR was prepared by high-energy-rate pneumatic impaction of blended powder mixtures (12). In this material, the -325 mesh PuO_2 particles are uniformly distributed in the UO_2 matrix. Pneumatically impacted UO_2-1 wt% PuO_2 fuel elements have achieved a maximum burnup of approximately 8500 MWd/tonne in PRTR (13). Pilot quantities of High Power Density elements containing UO_2-2 wt% PuO_2 fuel material have attained maximum burnups of approximately 5000 MWd/tonne (14).

Minor changes in the element design such as widening the end fixture bearing surfaces markedly improved resistance to fretting or wear corrosion between fuel elements and process tubes. During pre-High Power Density fuel operation PRTR fuel elements were manipulated more often than in most reactors because fuel management experiments were being performed. A total of 3500 fuel element movements were made (each element was moved an average of 12 times). Damage to some circumferential bands and spiral wire spacers resulted. Remote repair techniques have been developed which permit damaged elements to be returned to useful service.

Of nearly 5300 fuel rods irradiated in the PRTR prior to the start of High Power Density operation, only 38 failed in service (1 UO_2, 3 Al-Pu, and 34 UO_2-PuO_2). Even though severe localized embrittlement and loss of cladding fragments occurred in some instances, little or no fuel

loss into the coolant resulted and no severe reactor operating difficulties were experienced. Fuel washout resistance is improved as a result of in-reactor sintering which occurs during the early stages of irradiation. No water-logging occurred in in-service failed and intentionally defected elements. In many instances, the release of fission products was first detected during post-shutdown depressurization of the reactor system.

All of the UO_2-PuO_2 fuel element failures, with one exception, were attributed to three types of impurities in the fuel: (1) fluoride contamination in plutonium, (2) sorbed moisture, and (3) traces of hydrocarbons introduced by failure of mechanical processing equipment. These failures characteristically occurred at low burnups as a result of severe internal hydriding and embrittlement of the cladding caused by a gas phase hydriding mechanism. Typical PRTR vibrationally compacted UO_2-PuO_2 fuel rod failures caused by fuel contaminates are shown in Figure 2.

High Power Density Fuel Irradiations

The Batch Core Experiment is providing statistically significant irradiation behavior data on High Power Density UO_2-PuO_2 fuel elements operated at power generations greater than those currently employed in commercial power reactors. Maximum linear rod power generations are nearly 20 kW/ft with maximum fuel temperatures near melting. Goal element average burnups are over 13,000 MWd/tonne with peak burnups near 20,000 MWd/tonne (14,15). The present core loading status is summarized in Table II. Two vibrationally compacted UO_2-PuO_2 elements containing four rods instrumented to measure plenum gas temperature and pressure are included in the Batch Core loading. A similarly instrumented vibrationally compacted ThO_2-PuO_2 element will be charged into the reactor in the near future.

Vibrationally compacted UO_2-2 wt% PuO_2 elements in the Batch Core have reached an average burnup as high as 2100 MWd/tonne. Nondestructive and destructive examinations of selected fuel rods indicate that performance is satisfactory. No fuel failures have occurred thus far in the program. A transverse cross-section of a vibrationally compacted UO_2-2 wt% PuO_2 fuel rod irradiated in PRTR at approximately the maximum power expected during the Batch Core Experiment (20 kW/ft) is shown in Figure 3.

Irradiation of selected UO_2 and UO_2-PuO_2 fuel elements (pre-High Power Density vintage) containing 0.5, 1.0, 1.5, and 2.0 wt% PuO_2 is continuing in fringe positions of the PRTR during the Batch Core Experiment. These elements are being irradiated to determine their performance at higher

exposures. A listing of these elements and their current burnup status is given in Table II.

The fringe elements contain both pneumatically impacted and mechanically mixed (incrementally loaded) UO_2-PuO_2 fuel material. The highest burnup (over 11,000 MWd/tonne) is being obtained on one of the first mechanically mixed UO_2-PuO_2 elements charged into the PRTR. Periodic underwater examination of these elements indicates that their performance continues to be satisfactory. Irradiation of these elements will continue for the duration of the Batch Core Experiment.

Irradiations to Establish Reactor Power Limit

Among the first fuel irradiations to be performed in the PRTR during the Batch Core Experiment were tests to determine the maximum allowable reactor power level based on a maximum fuel temperature limit. The limiting PRTR power level is established by the linear rod power that produces fuel temperatures (~2790 °C) just below melting. Thirteen fuel rods were metallographically examined and maximum temperatures attained were deduced from the fuel structures formed during irradiation. These experiments indicated that under PRTR operating conditions the onset of melting in vibrationally compacted UO_2-2 wt% PuO_2 fuel rods occurs at a heat rating of 20.5 ± 0.5 kW/ft. This power to produce melting is equivalent to an $\int_0^{T_m} K dT$ of about 68 w/cm. Results of these examinations also show that:

(1) the temperature at which columnar grain growth apparently begins is approximately 2000 °C for irradiation times up to 80 hours;

(2) ceramographic evidence of typical once-molten fuel structures formed during irradiation are erased by time-temperature dependent diffusion phenomena in less than 72 hours irradiation under nonmolten, but high temperature conditions;

(3) fission product distribution patterns typical of molten fuel operation, as indicated on beta-gamma autoradiographs, are not completely eradicated during 72 hours of subsequent nonmolten irradiation;

(4) fuel structures formed in different rods irradiated under the same nonmolten conditions are comparable; and

(5) structural equilibrium is reached more rapidly at the higher power generations.

Fuel melting occurred in two of the vibrationally compacted rods examined. Fuel in one of the rods melted to approximately 10% of the radius (Figure 4) and to approximately 33% of the radius in the other. Both rods were presumably irradiated under the same conditions of approximately 21 kW/ft. The reason for the difference in the indicated melt radius is being investigated. Evidence of fuel melting at the time of shutdown is thought to be indicated by the formation of a subgrain structure in the thermal center of the fuel specimen (Figure 4). The extent of the central dark region on the beta-gamma autoradiograph corresponds with the subgrain region on the micrographs. Alpha autoradiographs of once-molten mixed-oxide fuel specimens show a centrally located dark region. The boundary of the dark area on the alpha autoradiograph extends beyond the high density grain region which surrounds the once-molten subgrain region. It is postulated that this dark region represents the molten fuel boundary at the start of the irradiation and recedes as the fuel sinters and the effective thermal conductivity improves.

In conjunction with the irradiation to establish the PRTR power level, autoradiographs were obtained of some irradiated UO_2-PuO_2 fuel specimens within 48 hours after shutdown of the reactor (Figure 5). The sample shown in Figure 5 was irradiated in PRTR for 48 hours at a linear rod power generation of approximately 18 kW/ft. In addition to the normal fission product distribution patterns, high concentrations were observed on the inner surfaces of cracks and large grain surfaces located equidistant from the thermal center. The fission product concentrated in these areas is apparently one with a high vapor pressure and a short half life. A second autoradiograph taken six weeks after fuel discharge showed no concentrations of fission products in these areas. Studies are underway to measure fission product concentrations in fuel as a function of time after shutdown.

Internal Gas Pressure Measuring Experiments

Pressure buildup in vibrationally compacted mixed-oxide fuel rods is being measured as part of the Batch Core Experiment in PRTR. Four instrumented fuel rods (Figure 6) presently operating in PRTR contain thermocouples to measure plenum gas temperatures and null-balance pressure transducers to measure internal gas pressures during irradiation. These measurements will be made to average rod burnups as high as 15,000 MWd/tonne.

Two of the instrumented rods have operated at a maximum linear rod power generation of nominally 9.5 kW/ft to approximately 1200 MWd/tonne and the other two rods have operated at a nominal maximum linear rod power of 16.5 kW/ft to a burnup of approximately 2400 MWd/tonne.

The pressure exerted by the sorbed gases and moisture in the fuel (the pressure at zero burnup) was less than calculated if 100% release of these gases is assumed. However, the rates of pressure increase are consistent with rates predicted from fission gas release measurements previously made for similar fuel (14). This comparison indicates that approximately 13% of the gases are being released from the low power fuel (volumetric averaged fuel temperature of 1250 °C). After about 1000 MWd/tonne exposure, the two high power fuel rods operated for a short time (∿5 hours) at a peak linear heat rating of 20 kW/ft and fuel temperatures above melting. No unusual gas release was noted. The rate of pressure increase in the high power fuel rods was lower during recent operation than during the first 1000 MWd/tonne because peak linear heat ratings, and hence fuel temperatures, were lower. The measured internal gas pressures during operation in the low and high power rods are presently about 20 and 55 psi, respectively.

Plenum temperatures have been measured in all of the instrumented fuel rods and are primarily a function of coolant outlet temperature; fuel temperatures have an insignificant effect on plenum temperatures. A one-half inch long depleted pellet at the end of the fuel column acts as an effective thermal insulator. At no time during operation (maximum fuel temperatures 200 °C to melting and maximum coolant temperatures of 270 °C) did the measured plenum temperatures exceed the coolant outlet temperatures by more than 13 °C.

Commercial Fuels Study

An important part of the Plutonium Utilization Program Fuel Development studies is to procure and test plutonium fuel rods designed and fabricated by commercial fuel vendors. A 19-rod cluster of commercially designed and fabricated fuel rods containing hot pressed UO_2-1.94 wt% PuO_2 pellets was irradiated in the Fuel Element Rupture Test Facility (FERTF) (16) at a linear rod power of 21.2 $\pm$ 1.0 kW/ft to an average element burnup of 1900 MWd/tonne.

Periodic examination of the element in the basin indicates that it is performing satisfactorily; no adverse effects of irradiation have been observed. Postirradiation examination of one of the rods indicates that incipient

fuel melting occurred and that structures typical of pellet fuel rods formed during irradiation (Figure 7). Incipient fuel melting is evidenced by the presence of a centrally located high fission product activity region on the β-γ autoradiograph. The fuel structure is characterized by an unaffected region adjacent to the cladding, an equiaxed grain growth region, a columnar grain growth region, and a central region composed of high density pore-free grains. Ceramographic examination and the beta-gamma autoradiograph indicate that molten fuel was extruded into radial cracks that apparently existed during irradiation. Irradiation of this pellet-containing element is to continue in the Batch Core. Another similar pellet element will also be irradiated in the Batch Core.

Three fuel rods containing cold pressed and sintered UO_2-PuO_2 fuel pellets have also been obtained from a commercial fuel fabricator. The performance of these fuel rods will be investigated and compared to that of the hot pressed pellet rods and to vibrationally compacted fuel rods designed and fabricated at BNW.

UO_2-PuO_2 Solubility Studies

The dissolution behavior of various unirradiated and irradiated mixed-oxide PRTR fuels in HNO_3 has been studied (17). The per cent of plutonium in mixed-oxide fuels which is soluble in HNO_3 was found to be a function of fabrication technique and irradiation history. The high-energy-rate pneumatic impaction process provides an oxide mixture that apparently dissolves more readily in HNO_3 than mixed-oxide fuel prepared by the mechanical mixing or incremental loading process. However, over 95% of the plutonium in fuel irradiated to 5000 MWd/tonne or higher is soluble in HNO_3 regardless of fuel fabrication process (Table III). Ceramography and autoradiography show that localized regions of high PuO_2 concentrations persist in the lower temperature peripheral fuel regions throughout the irradiation. These results indicate that the PuO_2 in the nonsintered lower temperature peripheral regions of the fuel rods becomes soluble in HNO_3 as a consequence of some as yet unidentified irradiation effect. The PuO_2 in the high temperature fuel regions forms solid solution with UO_2 during irradiation and becomes soluble in HNO_3.

Fuel Defect Behavior

The defect behavior of full-sized PRTR fuel elements operating under power reactor conditions is being investigated in the Fuel Element Rupture Test Facility (FERTF)(16). Irradiations of intentionally defected PRTR fuel rods have provided information on the relative fission product release rates from different types of defects. Defects have

been as holes and longitudinal slits up to six inches long through the cladding of swage-compacted as well as vibrationally compacted PRTR fuel rods. Release characteristics for the different types of defects were determined by analyzing the ratios of nuclides released to the coolant. Generally, the defect behavior of ceramic packed-particle elements has been excellent (14). No appreciable fuel washout, fuel rod deformation, water-logging effects, or hydriding of the Zircaloy cladding was observed in any of the packed-particle fuel element defect tests. The only exception was the rupture of a deliberately defected UO_2-PuO_2 rod operating with considerable fuel melting at the plane of the defect (18). A list of the defect tests performed in the FERTF is given in Table IV.

The current FERTF program is designed to study the effects of specific power and burnup on the defect behaviro of pellet and packed-powder fuel (19). An eight-rod element has been designed and built to provide the safety and ease of fuel rod manipulation required for defect testing in the FERTF. The FERTF Test Element illustrated in Figure 8 comprises a protective sleeve assembly surrounding the fuel rod rack that supports an eight-rod ring of fuel rods. The sleeve assembly provides protection for the surrounding Zircaloy pressure tube. The fuel rod rack assembly can be removed from the sleeve assembly as an integral unit to facilitate rod manipulations. The fuel rods are suspended from the top of the rack assembly and are free to expand or contract independently. Four circumferential strip bands secure the rods to the rack assembly. Power generation of fuel rods irradiated in the FERTF Test Element can be varied by using various sleeve and insert materials in the assembly.

Vibrationally compacted UO_2-PuO_2 fuel rods, pellet-containing UO_2-PuO_2 fuel rods, and vibrationally compacted enriched UO_2 fuel rods will be irradiated in the FERTF Test Element at linear heat ratings to 20 kW/ft. This test series will require approximately nine irradiation periods. Subsequent test series are planned for rod powers of 23 and 28 kW/ft with considerable fuel melting. Testing will include irradiation of both nondefected and deliberately defected fuel rods under these test conditions.

References

1. F. G. Dawson, BNWL-298, July 1966.

2. N. G. Wittenbrock, P. C. Walkup, and J. K. Anderson, HW-61236, Supp. 1, October 1959.

3. J. R. Worden, W. L. Purcell, and L. C. Schmid, BNWL-221, January 1966.

4. M. D. Freshley, HW-69200, Pt. 1, March 1961.

5. R. E. Sharp, HW-69200, Pt. 2, March 1961.

6. M. K. Millhollen, HW-64359, March 1960.

7. Staff of Ceramics Research and Development Operation, HW-79290, October 1963.

8. Staff of Ceramics Research and Development Operation, HW-79291, October 1963.

9. J. P. Keenan and R. E. Sharp, BNWL-349, January 1967.

10. M. D. Freshley and Staff, HW-SA-3642, Trans. Am. Nucl. Soc., Vol. 7, No. 2, (1964) pp. 388-389.

11. C. H. Bloomster, R. E. Bardsley, and W. T. Ross, Trans. Am. Nucl. Soc., Vol. 5, No. 2, (1962) p. 452.

12. D. W. Brite and C. A. Burgess, Trans. Am. Nucl. Soc., Vol. 7, No. 1, (1964) pp. 86-87.

13. W. J. Bailey and M. D. Freshley, BNWL-356, April 1967.

14. M. D. Freshley and F. E. Panisko, BNWL-366, March 1967.

15. M. D. Freshley, F. E. Panisko, and R. E. Skavdahl, Trans. Am. Nucl. Soc., Vol. 8, No. 2, (1965), pp. 365-366.

16. P. C. Walkup, BNWL-40, March 1965.

17. W. W. Schultz, Unpublished Data, February 1967.

18. M. D. Freshley, R. G. Wheeler, J. M. Batch, and G. M. Hesson, BNWL-272, May 1966.

19. M. D. Freshley, R. E. Sharp, and R. E. Skavdahl, BNWL-314, August 1966.

Table 1. - PRTR Fuel Element Irradiation Summary

Element Type	Number Of Elements (Sub-totals)		Maximum Linear Rod Power kW/ft	Element Average Burnup MWd/tonne)
Al-Pu	75		~15	(~80% of Pu)
UO_2	68			
Vipac		(1)	~10	2,200
Swaged				
(1 Hot Swaged)		(65)	~14	9,400
Vipac Tubular		(1)	--	1,500
Vipac Inverted Cluster		(1)	--	150
UO_2-PuO_2	216			
UO_2-0.5 wt% PuO_2	(81)			
Vipac		(20)	~16	11,000
Swaged		(61)	~13	10,200
UO_2-1.0 wt% PuO_2	(49)			
Vipac		(16)	~15	6,300
Swaged		(33)	~17	8,500
UO_2-2.0 wt% PuO_2	(84)			
Vipac		(79)	~20	5,400
Swaged		(2)	~20	3,200
Pellet (Hot Pressed)		(2)	~21.5	1,900
Vipac Salt Cycle		(1)	~17	1,600
UO_2-4.0 wt% PuO_2	(1)		~27	1,100
UO_2-1.5 wt% PuO_2	(1)		~ 6	3,000
MgO-2.1 wt% PuO_2 (Swaged)	1		~12	--
ThO_2-5 wt% PuO_2 (Vipac	1		~10	--

Table II. PRTR Core Loading Status (as of 9/1/67)

Element Type (a)	No. of Elements	Max. Rod Power Gen. (kW/ft)	Element Average Burnup (MWd/tonne)
Batch Core Experiment:			
Vipac PI (b) UO_2-2 wt% PuO_2 (Batch Core Experiment Elements)	65	∿ 20	2,100
Hot Pressed Pellet UO_2-1.94 wt% PuO_2	2	∿ 21.5	1,900
Fringe Position Tests:			
Vipac PI UO_2-2 wt% PuO_2 (Pilot HPD Elements)	6	∿ 20	5,400
Swaged PI UO_2-2 wt% PuO_2	1	∿ 20	3,200
Swaged PI UO_2-1 wt% PuO_2	1	∿ 17	8,500
Vipac PI UO_2-1 wt% PuO_2	2	∿ 15	6,300
Vipac MM (c) UO_2-0.5 wt% PuO_2	1	∿ 16	11,000
Swaged MM UO_2-0.5 wt% PuO_2	2	∿ 13	10,200
Swaged UO_2	1	∿ 14	9,400

(a) PRTR elements are 19-rod clusters of 0.565 OD Zircaloy-clad rods with active fuel lengths of 58.5 and 88.5 inches.
(b) PI = High-energy-rate pneumatically impacted fuel.
(c) MM = Mechanically mixed fuel.

Table III. Dissolution of UO_2-PuO_2 PRTR Fuels in HNO_3

Fabrication Process	Nominal Initial % PuO_2	Linear Rod Power, kW/ft	Approximate Burnup, MWd/tonne	Plutonium Soluble in HNO_3, %
MM (a) -Swaged	0.5	0	None	0.62
MM - Vipac	0.5	12	2,000	74.5
MM - Swaged	0.5	10	4,000	99.4
MM - Swaged	0.5	12	5,000	99.0
MM - Swaged	0.5	10	6,700	99.7
PI (b)-Swaged	1.0	0	None	6.2
PI - Vipac	2.0	0	None	5.3
PI - Vipac	4.0	27	1,100	95.2
PI - Vipac	2.0	19	3,700	94.6
PI - Vipac	2.0	19	5,100	93.4

(a) MM = Mechanically mixed or incrementally loaded fuel.

(b) PI = High-energy-rate pneumatically impacted fuel.

Table IV.- Coolant Activities From Defected PRTR Elements Irradiated in the FERTF

Test No.	Element Type	Cladding Defect	Maximum Rod Power, (kW/ft)	Loop Activity, (cpm) Steady State GM ($\beta\gamma$)	DN (Delayed Neutron)	Burst Activity GM ($\beta\gamma$)	Type of Release
A	Al-Pu FE-5008	6 in. Cracks	~7.0	15,000	13,000	------	Recoil[a]
B	Swaged UO_2 FE-1069	0.06 in. diam Hole	7.3	8,000	4,000	220,000	Equilibrium[b]
C	Swaged UO_2 FE-1039	0.62 in. long Longitudinal Slit	7.0	~23,000[c]	~13,000[c]	700,000	------
D	Swaged UO_2 FE-1039	3.2 in. long Longitudinal Slit	7.0	23,000	13,000	100,000	Diffusion[d]
E	Swaged UO_2 FE-1030	6.5 in. long Longitudinal Slit	6.1	68,000	38,000	150,000	Diffusion
F	Vibrationally Compacted UO_2 FE-1067	3.0 in. long Longitudinal Slit	7.3	47,000	26,000	170,000	Diffusion
G	Vibrationally Compacted UO_2 FE-1067	3,9 in. long Longitudinal Slit	7.3	60,000	31,000	------	Diffusion
H	Vibrationally Compacted UO_2-2 wt% PuO_2 FE-6004	0.06 in. diam Hole	24	80,000	4,000	660,000	Equilibrium
I	Vibrationally Compacted UO_2-4 wt% PuO_2 FE-6504	0.06 in. dia Hole	27	7.7×10^{6}[c]	1.6×10^{5}[c]	------	(Ruptured)

(a) Good communication between fuel and coolant - zero delay time.
(b) Poor communication between fuel and coolant - long delay time.
(c) Test was discontinued before stable form of release was established.
(d) Good communication between fuel and coolant - short delay time.

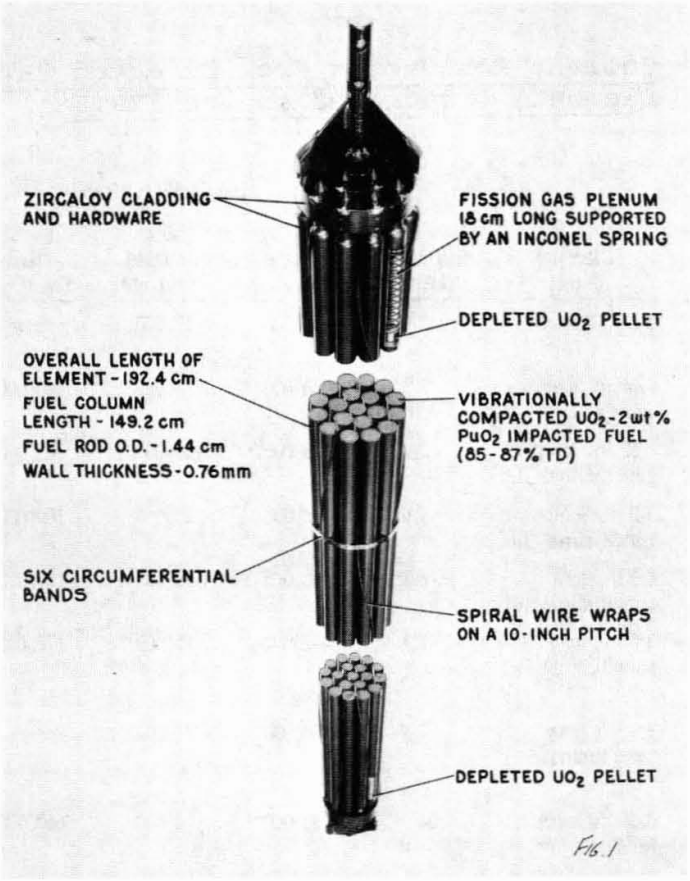
ZIRCALOY CLADDING AND HARDWARE
FISSION GAS PLENUM 18 cm LONG SUPPORTED BY AN INCONEL SPRING
DEPLETED UO_2 PELLET
OVERALL LENGTH OF ELEMENT - 192.4 cm
FUEL COLUMN LENGTH - 149.2 cm
FUEL ROD O.D. - 1.44 cm
WALL THICKNESS - 0.76 mm
VIBRATIONALLY COMPACTED UO_2 - 2 wt % PuO_2 IMPACTED FUEL (85 - 87 % TD)
SIX CIRCUMFERENTIAL BANDS
SPIRAL WIRE WRAPS ON A 10-INCH PITCH
DEPLETED UO_2 PELLET

FIG. 1

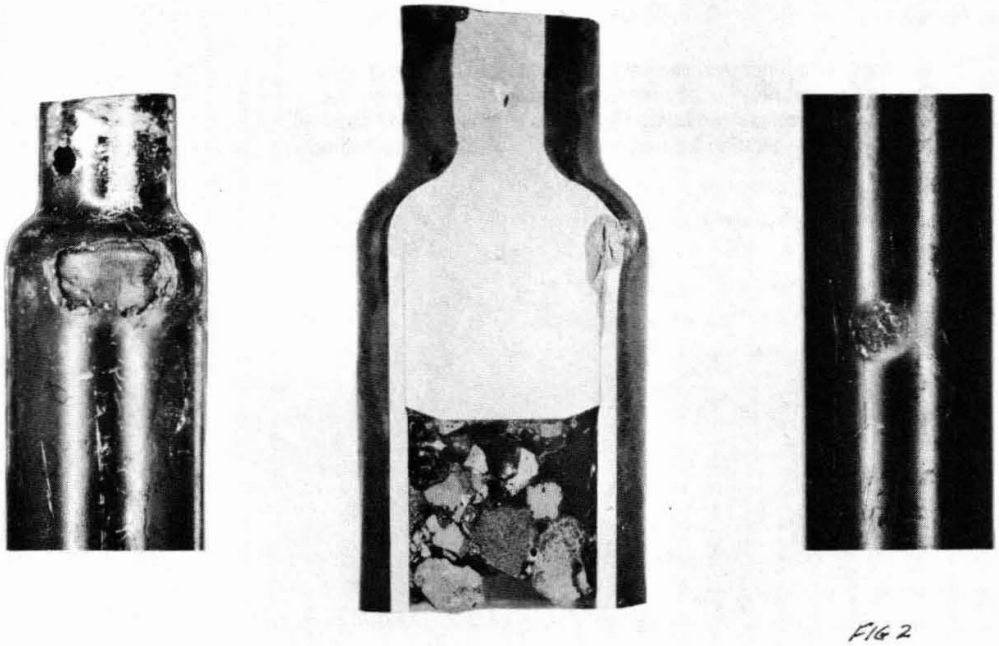

FIG 2

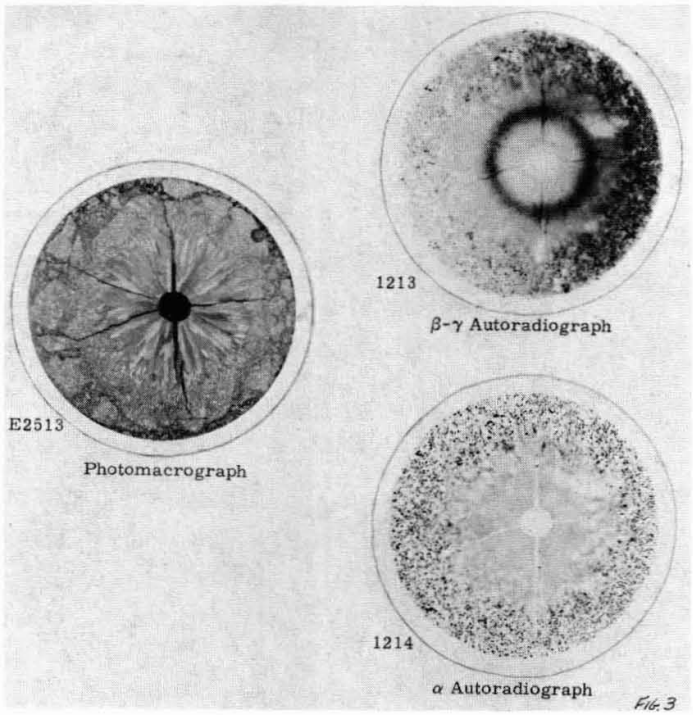
1213
β-γ Autoradiograph
E2513
Photomacrograph
1214
α Autoradiograph
Fig. 3

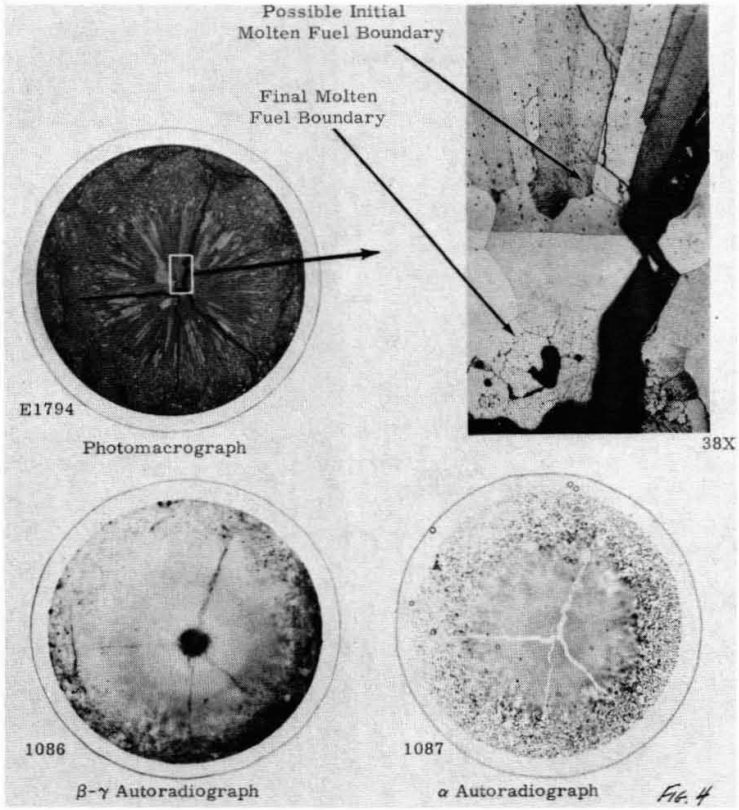
Possible Initial
Molten Fuel Boundary
Final Molten
Fuel Boundary
E1794
Photomacrograph
38X
1086
β-γ Autoradiograph
1087
α Autoradiograph
Fig. 4

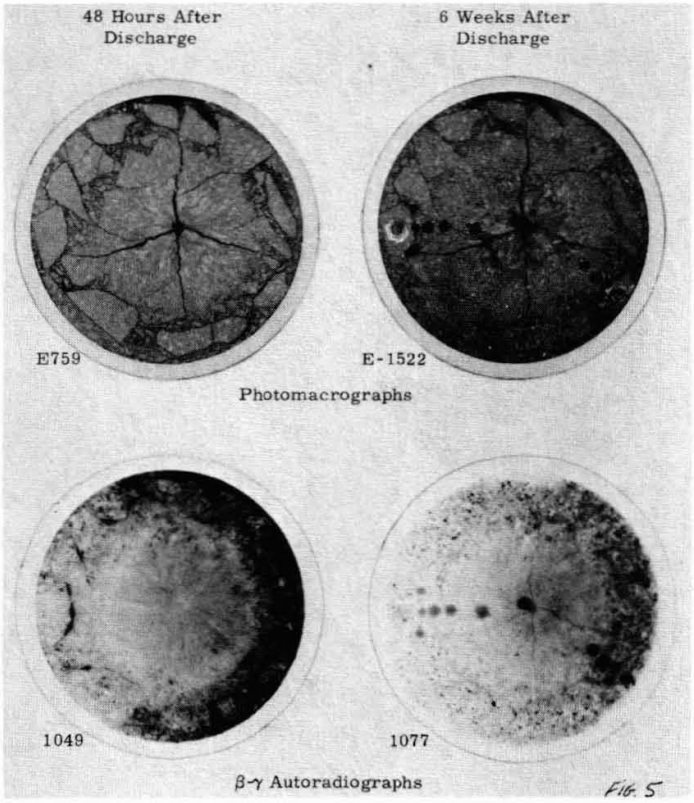
48 Hours After Discharge
6 Weeks After Discharge
E759
E-1522
Photomacrographs
1049
1077
β-γ Autoradiographs
FIG. 5

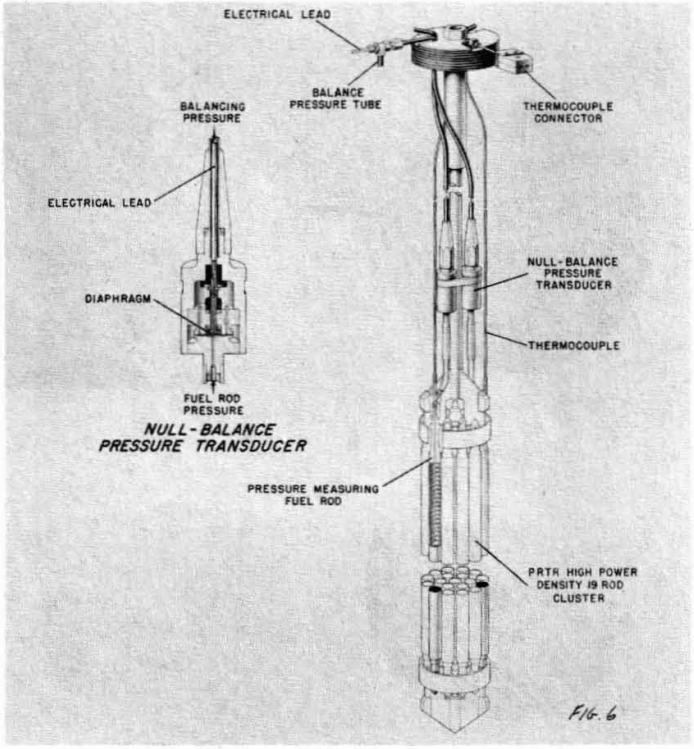
ELECTRICAL LEAD
BALANCE PRESSURE TUBE
THERMOCOUPLE CONNECTOR
BALANCING PRESSURE
ELECTRICAL LEAD
DIAPHRAGM
FUEL ROD PRESSURE
NULL-BALANCE PRESSURE TRANSDUCER
NULL-BALANCE PRESSURE TRANSDUCER
THERMOCOUPLE
PRESSURE MEASURING FUEL ROD
PRTR HIGH POWER DENSITY 19 ROD CLUSTER
FIG. 6

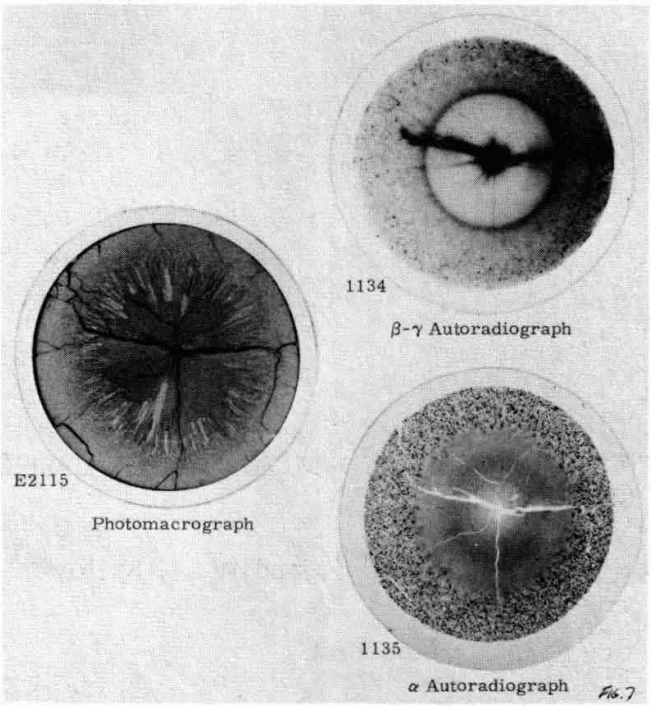
1134
β-γ Autoradiograph
E2115
Photomacrograph
1135
α Autoradiograph
Fig. 7

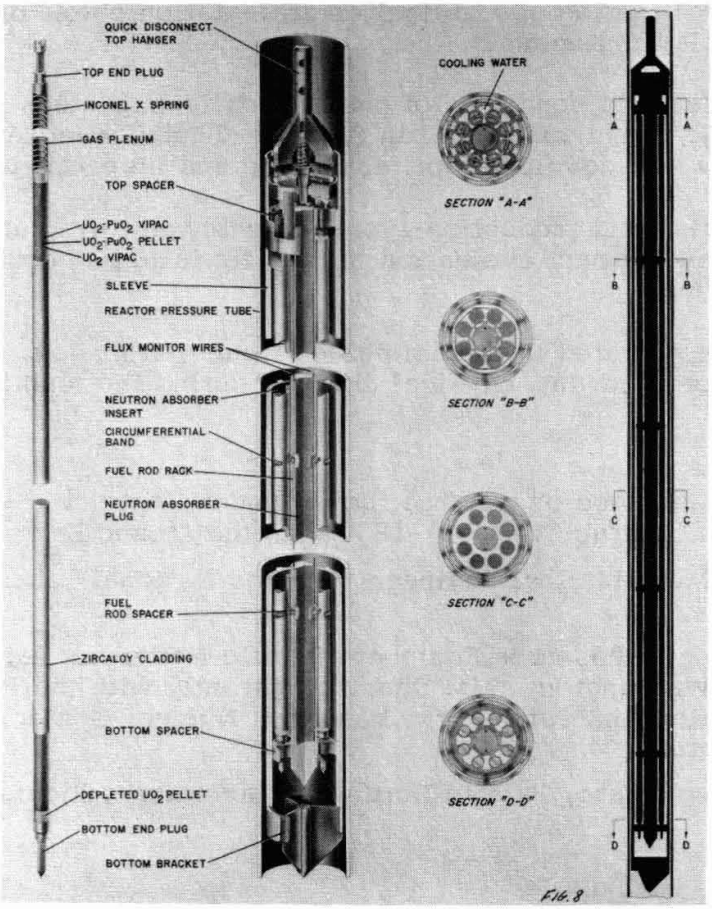
QUICK DISCONNECT TOP HANGER
TOP END PLUG
INCONEL X SPRING
GAS PLENUM
TOP SPACER
UO2-PuO2 VIPAC
UO2-PuO2 PELLET
UO2 VIPAC
SLEEVE
REACTOR PRESSURE TUBE
FLUX MONITOR WIRES
NEUTRON ABSORBER INSERT
CIRCUMFERENTIAL BAND
FUEL ROD RACK
NEUTRON ABSORBER PLUG
FUEL ROD SPACER
ZIRCALOY CLADDING
BOTTOM SPACER
DEPLETED UO2 PELLET
BOTTOM END PLUG
BOTTOM BRACKET
COOLING WATER
SECTION "A-A"
SECTION "B-B"
SECTION "C-C"
SECTION "D-D"
A
B
C
D
Fig. 8

THE EBWR PLUTONIUM RECYCLE DEMONSTRATION EXPERIMENT[a]

C. H. Bean[b], R. E. Sharp[c], and W. J. Bailey[d]

Abstract

The recycle of plutonium fuel was demonstrated in the Experimental Boiling Water Reactor at Argonne National Laboratory.[1,2] Engineering and physics data were obtained from this experiment for use in the design of future (or modification of existing) central-station power plants operated with recycled plutonium.

The fuel elements consisted of pneumatically-impacted, vibrationally-compacted, mixed-oxide fuel in Zircaloy-2 tubular jackets. A workable technology was developed for fabricating and inspecting the fuel.

Both capsules and production-type elements were irradiated in supporting fuels development evaluation tests. No failures occurred during evaluation testing.

The reactor operated in a predictable, trouble-free way, and the fuel elements did not show any physical changes during the length of the experiment.

(a) This paper is based on work performed under Contract W-31-109-eng-38 and Contract AT(45-1)-1830 with the Atomic Energy Commission.

(b) Associate Metallurgical Engineer, Argonne National Laboratory, Argonne, Illinois.

(c) Formerly Senior Research Engineer, Pacific Northwest Laboratory, Richland, Washington. Mr. Sharp is currently with the Plutonium Fuels Development Laboratory, Valecitos Nuclear Center, Pleasanton, California.

(d) Research Associate, Pacific Northwest Laboratory, Richland, Washington.

Introduction

Engineering-scale demonstration of the practicality of plutonium recycle in water reactors and pertinent physics design data were obtained from an AEC sponsored experiment consisting of a plutonium fuel loading in the Experimental Boiling Water Reactor (EBWR).[3] The EBWR, a prototype for a direct-cycle, natural-circulation, boiling-water-reactor, integrated power plant, is located at Argonne, Illinois.

This experiment was aimed at operating EBWR to obtain information useful for the utilization of plutonium as a fuel in light-water thermal systems. In particular, data were needed on the isotopic behavior of plutonium as it is irradiated in a thermal reactor. Plutonium fuel technology also would benefit if it could be shown that plutonium fuels could be fabricated that would operate reliably in a power reactor. It is this technology that is the subject of this paper.

The Plutonium Recycle Demonstration Experiment was a joint program conducted by Argonne National Laboratory (ANL) and Pacific Northwest Laboratory (PNL). The plutonium loading, the central part of the EBWR core, was fabricated at PNL. The Zircaloy-jacketed mechanically-mixed UO_2-1.5 w/o PuO_2 packed-powder fuel elements contained a total of 14.1 kg of Pu (8% Pu^{240}) and 1.9 kg of U^{235} in 1080 kg of UO_2-PuO_2.

EBWR Fuel Performance

EBWR, UO_2-PuO_2 Fuel Design

The central portion of the core loading consisted of 36 assemblies containing 1296 UO_2-1.5 w/o PuO_2 rod-type fuel elements. Fuel element and fuel assembly construction may be noted in Figure 1.

The vibrationally-compacted, Zircaloy-jacketed fuel elements were 1.07 cm OD by 148 cm long. These elements were jointly designed by PNL and ANL to be capable of achieving a burnup of 25,000 MWd/tonne. A 13.97 cm long plenum was located above the fuel. This plenum was adequate to accommodate 100% release of all fission gases. A single ZrO_2 pellet was inserted on top of the fuel column. A stainless steel spring loaded to 2.268 kg was positioned between this pellet and the top end plug to maintain the fission gas space and prevent shifting or dislocation of the fuel column during shipping, handling, and fuel loading at the reactor. The fuel assembly boxes held 36 rods. The assemblies were designed to allow individual elements, or rods, to be withdrawn and replaced. This essential feature permitted isotopic analysis studies, the main objective of the experiment, to be made as burnup proceeded without having to replace entire fuel assemblies. Thus the mixed oxide fuel loading, plus a few special elements of different fuel or isotopic Pu compositions, offered a great deal of flexibility for conducting an extensive set of experiments.

UO_2-PuO_2 Fuel Fabrication

The flow diagram for the fuel-element fabrication process[4,5] is shown in Figure 2. Specified requirements for materials and fuel elements[4-6] are shown in Tables I and II. The mixed-oxide feed material was prepared by mechanically blending depleted UO_2 (-65 mesh) with PuO_2 (-325 mesh), pneumatically impacting the mixture to >98% TD, crushing, and screening.

Two vibrational compaction techniques were used for this fabrication, a vertically-excited resonant-plate coupling and a transversely-excited resonant-beam coupling.[7,8] Up to 50 elements per 8-hour shift were vibrationally compacted with the pilot-scale units.

The total of 2250 fuel elements prepared by PNL included 1296 for the core, 750 for PNL physics tests, 25 special test elements and 179 spare elements for the core loading. Over two tons of mixed oxide were processed and loaded into more than two miles of fuel-jacket tubing. Cost data has been published[9] on the fabrication of these elements.

Fuel and Material Acceptance Controls

Fuel-Jacket Inspection. A newly developed ultrasonic test detected internal cracks in the jacket-to-end cap welds of a number of the UO_2-1.5 w/o PuO_2 fuel elements after they were fabricated. Ultrasonic techniques had been used to test the cladding of selected elements in previous studies and no defects were observed. However, near the completion of the fabrication, several elements broke during vibrational compaction. These failures prompted an intensive investigation in nondestructive examination. Existing techniques were unable to detect defects within about 0.64 cm (0.25 in.) of the tube ends because of background signals. Approximately 200 elements (10% of the total), representing all fabrication histories, were inspected by a modified procedure that permitted these regions to be scanned. Defects were found in the end cap region in more than half the elements. Metallographic examination of selected elements supported the ultrasonic evidence in every instance and showed typical fatigue-type cracks.

Finished elements were inspected by the modified procedure and many exhibited ultrasonic indications of internal cracks. Thermal-cycling tests were conducted by Lobsinger[10] to evaluate the potential, in-reactor propagation tendencies of defects in these elements. Eight elements with representative ultrasonic indications were heated to 400°C and 60 atm (1000 psig) in 1 hr, held at this temperature and pressure for 3 hr, and cooled to 100°C and 1 atm over an 8 hr period. In most cases the cracks propagated after 10 cycles. None of these elements failed in 52 cycles, at which time the test was terminated. Although the test conditions were more severe than any anticipated reactor service conditions, and the probability of elements failing in service was remote, it was decided that all welds showing indications of defects would be repaired.

A process for repairing fuel elements was developed. In this

repair process the tube was parted just below the defect, the end cap pulled from the tube, the weld area decontaminated, and a new end cap welded in place. The elements were successfully repaired in one month.

Plutonium Distribution in Impacted Fuel. The degree of uniformity of the PuO_2 distribution in impacted mixed oxide was analyzed.[11,12,13] The average PuO_2 particle size in the EBWR fuel was ~25 microns. The thermal time constant* for this fuel--slightly greater than 33 microseconds, the time constant for 22 micron particles--was more than satisfactory for a thermal reactor fuel.

Plutonium Distribution Along Fuel Rod Length. A gamma-scanning device, still under development, was used to investigate the plutonium distribution along the fuel element length. It essentially monitors gamma ray emissions only from the plutonium. Ninety production-run fuel elements--one or more from every lot of impacted mixed-oxide fuel--were scanned (100% coverage) while being rotated and translated in the device. The qualitative indication showed that the plutonium distribution was very uniform, as expected. Subsequently, all elements were scanned with this device to provide additional qualitative assurance of proper plutonium distribution. All fuel elements were accepted.

Linear Variation in Fuel-Rod Bulk Density. A gamma absorptiometer with a 10-curie Cs^{137} source provided data on the possible variation in fuel bulk density along the rod length. Based on determinations from 90 elements at roughly 0.318 cm (1/8-inch) intervals, the typical bulk density along the element length was within ± 1.0 to 1.5% of the overall bulk density of the element.

Irradiation Performance

Prototype Testing. Fuel development and evaluation for the mixed oxide loading for EBWR included prototype irradiation in other reactors of 32 capsules and 58 production-run elements. The irradiation tests were conducted to study fission gas release, sintering, plutonium and fission-product migration, isotopic changes, compatibility--e.g., jacket-coolant, fuel-jacket, spring-pellet-fuel--effect of fabrication variables and adequacy of design. Irradiation of all capsules and all but 21 of the rods is complete. Some of the results of these tests have been published.[14,15,16,17] Calculated burnups as high as 27,600 MWd/tonne (6.8×10^{20} fissions/cm^3) were attained. Specimens operated with linear powers of 1280 w/cm (39 kw/ft), well beyond those for EBWR.

Fission gas data are shown in Figure 3. The results[16,18] indicate a reasonably good correlation can be obtained if one assumes 100% release of the fission gas at fuel temperatures >1800°C and ~10 to 15% release below 1800°C.

*The thermal time constant is a measure of the rapidity with which heat is transferred from the PuO_2 to the surrounding UO_2, and is mainly a function of the PuO_2 particle size and PuO_2 concentration in the fuel.

The capsule in Figure 4 operated initially at ~460 w/cm (14 kw/ft) and attained a burnup of 18,300 MWd/tonne. In-reactor homogenization of the impacted fuel can be noted in the regions where grain growth and columnar grain formation have occurred. This is evidenced by the more uniform exposure on the beta-gamma and alpha autoradiographs for these regions. The dark areas on the autoradiographs correspond to regions of high radioactivity. The black dots on the autoradiographs are sites where the initial plutonium enrichment was located. Note the initial plutonium enrichment sites near the outer edge of the fuel and the metallic inclusions (fission products) at the specimen center.

Plutonium segregation studies were made by Freshley[15] on pneumatically-impacted mixed-oxide fuel operating under molten conditions. Segregation of alpha emitters was observed on intentionally defected specimens by autoradiography only.

Fission-product migration was noted in UO_2-1.5 w/o PuO_2 specimens which operated at high linear powers--e.g., 31 kw/ft. There was little migration of Zr^{95}-Nb^{95}, Sr^{90}, and Ce^{144}-Pr^{144}. Marked migration was observed for Cs^{137} and Ru^{106}. Little or no change was noted in the fission product distribution, except for Cs^{137}, at lower linear powers--e.g., 10-16 kw/ft.

Mass spectrographic data for irradiated EBWR test specimens are included in Table III. This is a more accurate determination of sample burnup and supplements the flux-monitoring-wire burnup data. Data were obtained on isotopes of interest for some of the higher burnup specimens because of handling problems--e.g., Pu^{238}, Pu^{236}, Pu^{240}--or as isotopic heat sources--e.g., Pu^{238}, Cm^{244}.

Fuel-Zircaloy reactions were observed in test specimens that operated at very high linear powers--e.g., >1150 w/cm or 35 kw/ft. Reactions were noted between the fuel and ZrO_2 pellets at the top of the fuel column in low burnup, <8000 MWd/tonne, capsules that ran at linear powers > 22 kw/ft. Fuel-ZrO_2 reactions that were time-temperature dependent also were noted in higher-burnup specimens, ~15,000 MWd/tonne at linear powers of ~590 w/cm (18 kw/ft).

Examination of full-size EBWR elements irradiated in the Plutonium Recycle Test Reactor, (PRTR), showed them to be in good condition, both externally and internally. No evidence of hydriding was detected. Plenum components were examined and autoradiographs bore no indications of fission-product or alpha-emitter migration into the ZrO_2 pellets.

Irradiation proof tests to date with capsules and production-run elements continue to indicate that the fuel elements are functionally adequate and capable of operating under EBWR conditions to the proposed burnup of 25,000 MWd/tonne.

Performance in EBWR. All plutonium fuel elements were available for service in EBWR by July, 1965. Fuel was loaded into the reactor in 1966 and used to obtain physics data before bringing the reactor to power. Zero power critical experiments; and subcritical, critical, and

low-power transfer-function measurements were obtained with the plutonium fuel.

The reactor was raised to power, 42 MW(t), in November, 1966. It operated at this level until March, 1967, at which time the power was raised to 70 MW(t). Except for scheduled interruptions for removal of test elements and for critical measurements prior to increasing power, the reactor operated continuously until the termination of the program on June 30, 1967.

Only 60% of the reactor power was produced in the plutonium fueled portion of the core. The remaining 40% was produced in the slightly enriched uranium-oxide driver fuel that surrounded the plutonium fuel in the core. Fuel burnup was concentrated in the lower 91 cm, (36"), of the 1296 plutonium fueled elements in the core during the 42 MW(t) operation. The average linear rod power was 210 w/cm, (6.5 kw/ft). The power was increased by further withdrawal of the control rods without increasing the linear rod power.

The first group of experimental elements was removed from the reactor in March, 1967, after 1300 MWd/tonne burnup. The second group was removed after 2200 MWd/tonne burnup. The surface of these elements was bright with no evidence of discoloration or other physical change. These elements were shipped to PNL for controlled reactivity measurements and fuel composition analysis.

The maximum burnup for the plutonium fuel at the termination of the program was 3,000 MWd/tonne. This is appreciably less than the maximum design burnup of 25,000 MWd/tonne. The plutonium fuel did perform reliably and complete integrity was maintained on all fuel elements at all times.

There are no plans for continued irradiation or destructive analysis of the irradiated fuel.

References

1. Nucleonics Week, Vol. 7, No. 47, p. 2, November 24, 1966.

2. Chemical Engineering, Vol. 73, p. 46, December 19, 1966.

3. F. G. Dawson, Program Analysis and Plans, Plutonium Utilization Program, FY-1967 through FY-1970, BNWL-298, July 1966.

4. R. E. Sharp, C. A. Burgess, J. R. Hague, and R. J. Lobsinger, UO_2-PuO_2 Fuel Elements for the Plutonium Recycle Demonstration Experiment, Trans. Am. Nucl. Soc., Vol. 7, No. 2, p. 403 (1964).

5. D. W. Brite and C. A. Burgess, High Energy Rate Pneumatically Impacted UO_2-PuO_2 Fuels, Trans. Am. Nucl. Soc., Vol. 7, No. 2, pp. 408-409 (1964).

6. H. J. Anderson and H. R. Wisely, Characterization of Impacted Mixed Oxides, Ceramics Research and Development Operation Quarterly Report, July-September, 1964, HW-81602, p.2.23.

7. J. R. Hague, EBWR Plutonium Fuel Elements, Ceramics Research and Development Operation Quarterly Report, January-March, 1964, HW-81600, p. 3.3.

8. J. J. Hauth, Process for the Fabrication of Nuclear Fuel Elements, U. S. Patent No. 3,141,911, July 21, 1964.

9. C. H. Bloomster, Fabrication Costs for Plutonium Fuel Elements, Part B: Variable Costs of Fabricating UO_2-PuO_2 Fuel Rods for the Experimental Boiling Water Reactor, BNWL-131B, September 1965.

10. R. J. Lobsinger, EBWR Plutonium Recycle Fuel, Ceramics Research and Development Operation Quarterly Report, October-December 1964, HW-81603, p. 5.2.

11. S. Goldsmith, M. D. Freshley, J. B. Burnham, and R. E. Skavdahl, A Physically Mixed and Impacted UO_2-PuO_2 Fast Reactor Fuel, Trans. Am. Nucl. Soc., Vol. 7, No. 2, p. 409 (1964).

12. R. E. Skavdahl, W. J. Bailey, M. D. Freshley, and S. Goldsmith, Irradiation Properties of High Energy Rate Pneumatically-Impacted UO_2-PuO_2 Fuels, BNWL-SA-223, presented at the Third International Conference on Plutonium, London, November 22-26, 1965, by The Institute of Metals.

13. V. W. Gustafson and R. E. Peterson, A. Computer Investigation of Doppler Delay in Mixed Oxide Fuels, Trans. Am. Nucl. Soc., Vol. 7, No. 2, pp. 275-276 (1964).

14. W. J. Bailey, Irradiation of Impacted, UO_2-PuO_2, Packed Powder Fuel, BNWL-SA-1065, presented at the Am. Nucl. Soc. Meeting, San Diego, California, June, 1967.

15. M. D. Freshley and W. J. Bailey, Irradiation Properties of High Energy Rate Pneumatically Impacted UO_2-PuO_2 Fuel, BNWL-356, April, 1967.

16. W. J. Bailey, Irradiation of Impacted UO_2-PuO_2, Trans. Am. Nucl. Soc., Vol. 8, No. 2, p. 424 (1965).

17. W. J. Bailey, Irradiation Testing in Support of the Plutonium-Recycle Demonstration Experiment in EBWR, Trans. Am. Nucl. Soc., Vol. 7, No. 2, p.389 (1964).

18. Personal Communication, G. Testa, CNEN, to W. J. Bailey, PNL, July 1965.

TABLE I - REQUIREMENTS FOR FUEL AND CLADDING MATERIALS FOR EBWR Pu RECYCLE FUEL

Fuel Material	
Fuel Composition	UO_2-1.5 w/o PuO_2
Pu^{240} Content in Pu	~8 a/o
U^{235} Content in U	~0.2 a/o
Fuel Particle Density (Min.)	10.76 g/cc (98% TD)
Size Fractions	55 w/o, -6 +10 Mesh
	25 w/o, -20+ 65 Mesh
	20 w/o, -200 Mesh
Moisture in Fuel, (Max.)	100 ppm
Cladding	
Material	Zircaloy 2 Tubing
Cladding Specification	ASTM-353-62T
Tubing Dimensions (As Purchased)	
Inside Diameter (Nominal)	0.945 cm (0.372 in.)
Wall Thickness (Nominal)	0.0685 cm (0.027 in.)
Tubing Dimensions (After Etching)	
Wall Thickness (Min.)	0.058 cm (0.023 in.)

TABLE II - SPECIFICATIONS FOR EBWR Pu RECYCLE FUEL ELEMENTS

Test Core Elements (Total of 2225)	
Overall Length	148 cm (58.3 in.)
Active Fuel Length	122 cm (48 in.)
Fuel Weight	825-830 g.
Plenum Length	14.6 cm (5.75 in.)
Stainless Steel Spring	Type 302
ZrO_2 Pellet Thickness	0.64 cm (0.25 in.)

Special Test Elements (Five Each)	
Fuel Core Composition	Pu^{240} Content in Pu, (w/o)
Al-3.35 Pu-2 Ni Alloy	8
Al-3.35 Pu-2 Ni Alloy	26
UO_2 (Normal)	--
UO_2-1.5 PuO_2	20
UO_2-1.5 PuO_2	26

TABLE III - BURNUP AND ISOTOPIC DATA FOR UO_2-1.5 w/o PuO_2 FUEL, IRRADIATED IN THE MATERIALS TESTING REACTOR (MTR)

MEASURED BURNUP MWd/tonne of fuel	MASS SPECTROGRAPHIC DATA[a] PLUTONIUM, (a/o) 236	238	239	240	241	242	URANIUM, (a/o) 234	235	236	238
0			91.53	7.75	0.69	0.03	<0.001	~0.22	<0.002	99.78
910			88.69	10.30	0.95	0.060	--	--	--	--
1,540			85.76	12.76	1.47	0.096	--	0.148	0.0055	99.846
2,750			85.22	13.08	1.48	0.22	--	--	--	--
4,290			72.94	22.90	3.67	0.484	0.0024	0.122	0.0095	99.868
4,950			69.66	24.93	4.74	0.670	--	0.113	0.0116	99.875
6,330			63.52	29.18	6.15	1.150	--	--	--	--
8,400	(b)	(b)	55.15	35.04	7.65	2.165	--	--	--	--
10,900	(b)	(b)	47.47	38.62	9.93	3.98	--	--	--	--
12,560	1.8×10^{-7}	0.23	47.28	37.22	9.24	6.03	ND[d]	0.0376	0.0214	99.941
13,650	(b)	0.32[c]	41.75	40.80	10.94	6.51	<0.001	0.042	0.023	99.935
16,930	2.2×10^{-7}	0.32	38.47	40.70	11.23	9.33	<5 ppm	0.0259	0.0228	99.9513
18,300	5.0×10^{-7}	0.42	38.87	38.22	11.74	10.76	ND	0.0234	0.0240	99.953

(a) Typical uncertainties (at the 95% confidence level) are: for Pu^{239} and Pu^{240} ± 0.1 to 0.2; for Pu^{241}, ± 0.02 to 0.1; for Pu^{242}, ± 0.002 to 0.08; for U^{234}, 5 ppm (detection limit) to ± 0.009; for U^{235}, ± 0.0008 to 0.002; for U^{236}, ± 0.0004 to 0.009; and for U^{238}, ± 0.0008 to 0.002.

(b) Analysis currently in progress.

(c) Value (0.32 ± 0.3) obtained by alpha energy analysis.

(d) ND = not detected.

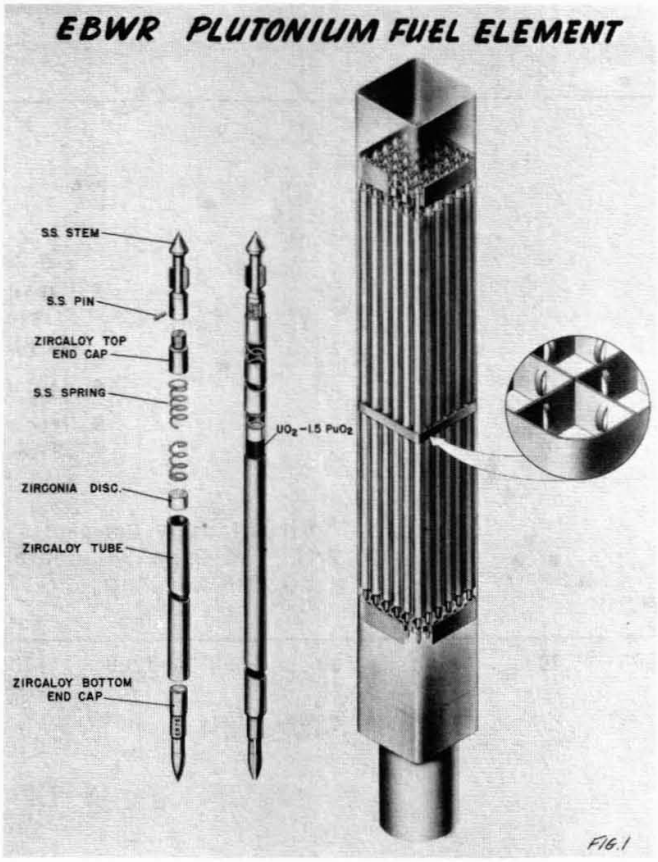
EBWR PLUTONIUM FUEL ELEMENT
S.S. STEM
S.S. PIN
ZIRCALOY TOP END CAP
S.S. SPRING
ZIRCONIA DISC.
ZIRCALOY TUBE
ZIRCALOY BOTTOM END CAP
UO_2-1.5 PuO_2
FIG. 1

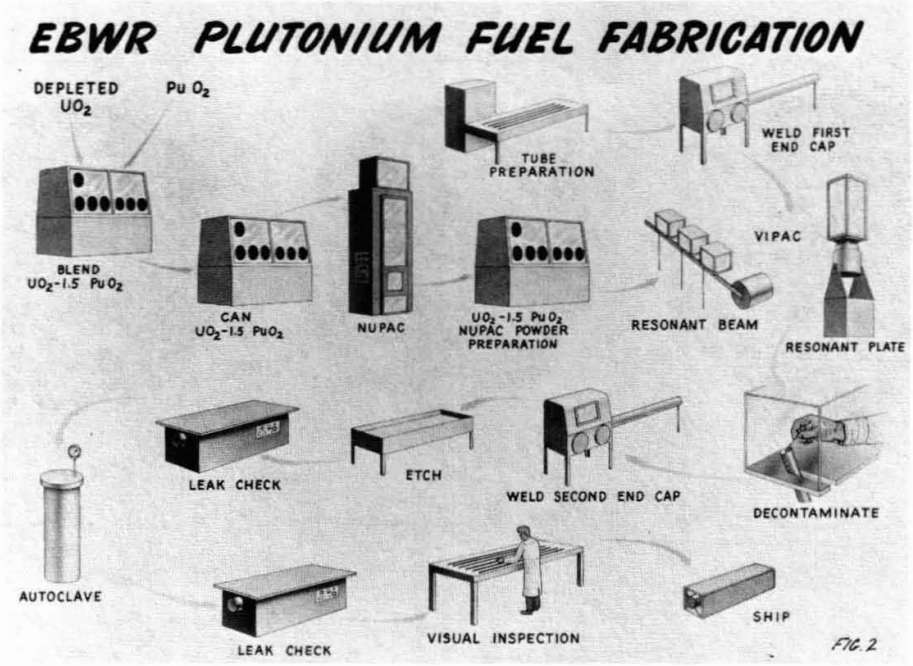
EBWR PLUTONIUM FUEL FABRICATION
DEPLETED UO_2
PuO_2
BLEND UO_2-1.5 PuO_2
CAN UO_2-1.5 PuO_2
NUPAC
TUBE PREPARATION
UO_2-1.5 PuO_2 NUPAC POWDER PREPARATION
WELD FIRST END CAP
VIPAC
RESONANT BEAM
RESONANT PLATE
AUTOCLAVE
LEAK CHECK
ETCH
WELD SECOND END CAP
DECONTAMINATE
LEAK CHECK
VISUAL INSPECTION
SHIP
FIG. 2

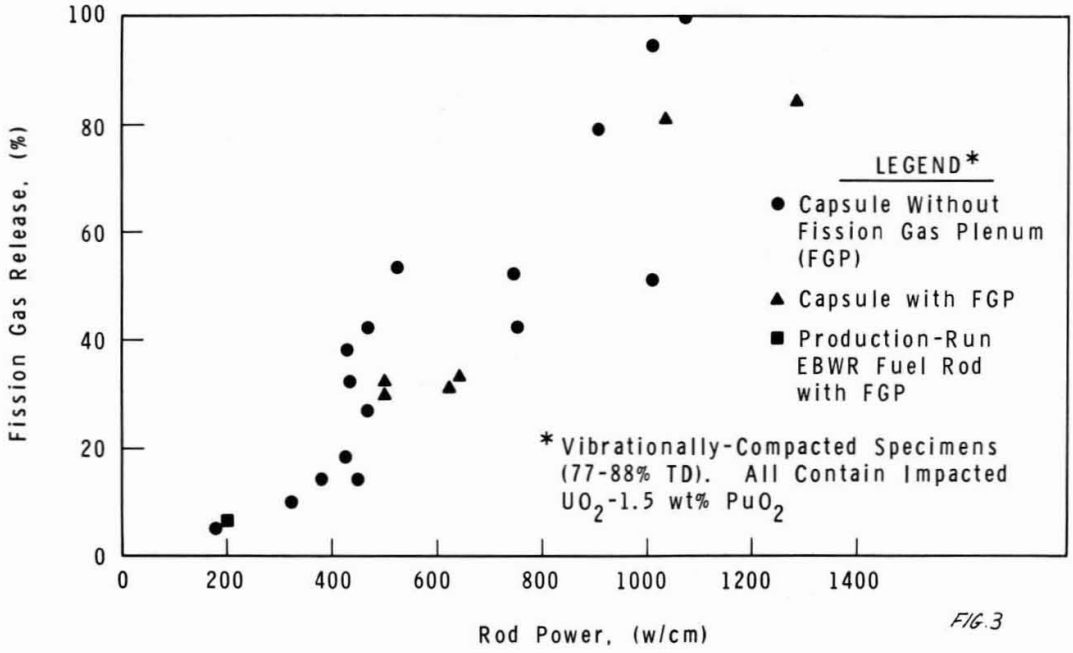

FIG. 3

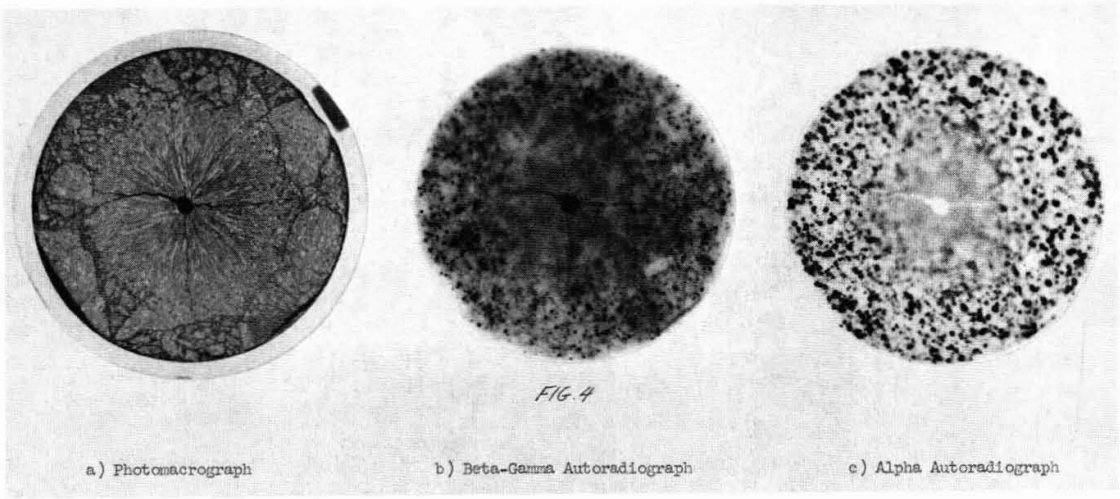

FIG. 4

a) Photomacrograph b) Beta-Gamma Autoradiograph c) Alpha Autoradiograph

OPERATING EXPERIENCE WITH THE SAXTON REACTOR PARTIAL PLUTONIUM CORE II*

R. S. Miller
J. B. Roll
K. R. Jordan
J. L. Rolin
C. J. Kubit

Abstract

Operation of the Saxton Reactor with nine central fuel assemblies containing 6.6 w/o PuO_2 in natural UO_2 and clad with Zircaloy-4 was begun in December, 1965 and continues through the present time. Observed nuclear, thermal-hydraulic, and fuel materials performance to date have agreed very well with the performance predicted during the design phase of the program. The results of the post-irradiation examination and evaluation of two pellet and two vipac fuel rods, removed from the central 3 x 3 subassembly at a peak burnup of 6100 MWD/MTM, are discussed.

*The Saxton Plutonium Project is conducted by the Westinghouse Electric Corporation in cooperation with the Saxton Nuclear Experimental Corporation (SNEC) under USAEC Contract AT(30-1)-3385.

The authors are with the Engineering Department of the Nuclear Fuel Division, Westinghouse Electric Corporation, Pittsburgh, Pennsylvania.

Introduction

The economic incentive for recycling plutonium in thermal reactors in the United States will be particularly strong in the mid-1970's to mid-1980's. This is the period when large quantities of plutonium will be discharged from operating water reactors and assurance of plutonium value by government purchase will have terminated. Furthermore, a significant demand for this material for use in fabricating fuel for fast reactor cores will not develop until late in the period.

If the plutonium were held until required for fast reactor use, the inventory cost could reduce the plutonium value considerably, thereby increasing fuel cycle costs for all operating water reactors. Although this situation has long been recognized by the nuclear industry, the rapid growth of water reactor sales in the past two years has re-emphasized the problem of plutonium value. The result has been a stimulated plutonium recycle activity in both government and industrial organizations. The nature, direction, and emphasis of the various plutonium recycle programs have been discussed at length at previous technical symposia.[1,2]

The basic objective of the Westinghouse recycle program is to achieve commercial recycle of plutonium in pressurized water reactors (PWRs) in the United States in the early 1970's. Since there are no questions of basic technical feasibility to be resolved, achievement of this objective is viewed as being an evolutionary process. However, in order to participate in the plutonium fuel business on a truly commercial basis, certain technical objectives have been identified:

1) Develop and evaluate plutonium core design technology and accumulate sufficient operating experience on plutonium - fueled reactors to ensure that the design and licensing of plutonium core regions can be accomplished in a period comparable to that required to perform the same function for a UO_2 replacement core region.

2) Demonstrate plutonium fuel manufacture on an engineering scale with processes which yield fuel cycle costs competitive with those for slightly enriched UO_2 fuel.

3) Successfully irradiate PuO_2-UO_2 fuel in operating PWRs at peak power levels and to peak exposure levels anticipated to be typical of core operating conditions in the mid-1970's.

A vital first step in this overall technical program is the Saxton Plutonium Project. This paper briefly describes this program and presents the results of a recently completed examination of low burnup fuel.

Saxton Plutonium Project

The Saxton Plutonium Project is the first AEC-Westinghouse plutonium recycle effort and constitutes the technological base upon which our overall program is being developed. This project is an integrated recycle program which includes core design, fuel fabrication, reactor operation and core operational follow, post-irradiation fuel examination, and post-operation evaluation of core materials performance as well as core design methods capability.

The Saxton Plutonium Project is part of the overall Saxton Reactor Program* for advancing PWR technology. The reactor involved is particularly well suited to conducting commercial bulk engineering tests of plutonium fuels because it is highly instrumented and core performance can be closely observed and continuously evaluated. The major objectives of the project are to:

1) Perform pilot-scale tests on PuO_2-UO_2 fuel in a PWR enrichment;

2) Provide a statistically valid performance comparison between two economically promising PuO_2-UO_2 fabrication techniques; and

3) Provide a preliminary basis for plutonium fuel selection and design for a large PWR.

To accomplish these objectives, nine assemblies (9 x 9 rod arrays) were inserted in the central region of the core in October, 1965, and will remain there for approximately two and one-half years. The central assembly contains a removable 3 x 3 subassembly constructed such that four of the fuel rods can be removed at exposure levels intermediate to those which will be achieved at the end of core life. Several of the rods within the 9 x 9 array are individually removable for intermediate examination or replacement. Seven of the assemblies contain pelletized fuel and two contain vibrationally-compacted fuel. Zircaloy-4 cladding was employed for the bulk of the fuel rods, with some Type 304 stainless steel cladding included for comparison. The post-irradiation examination scope includes physical, chemical and metallographic examination of several fuel samples at both intermediate and terminal burnup levels. In addition to providing statistical information relative to the two fabrication techniques, the program will enable evaluation of PuO_2-UO_2 performance limitations. It will thus furnish a basis for either partial or full-core loading of a large water reactor, as well as provide valuable preliminary design information.

*The Saxton Reactor is operated by the Saxton Nuclear Experimental Corporation in technical cooperation with Westinghouse.

The project was initiated in early 1964 and core design and fabrication activities were completed with delivery of the core at the reactor site in October 1965. Loading of the core and initial operation were accomplished by December 1965, and full power operation began in January 1966.

Plutonium Core Design

Nuclear Design

The nuclear design was conducted in three steps. Initially, parameter studies were carried out to determine the performance characteristics of the Saxton reactor containing a partial core of plutonium. Later, more specific nuclear design calculations were performed to set the enrichment specification and determine the available burnup for a core containing nine central plutonium fuel assemblies with twelve surrounding uranium assemblies. Finally, a series of critical experiments using the design fuel and a supporting program of analysis were used to confirm the specified nuclear design. Details of the nuclear design are described in Reference 3.

The Saxton Core II nuclear design predicted a lifetime capability of 9,300 MWD and an average burnup in the plutonium fuel of 15,350 megawatt days thermal per metric tonne heavy metal (MWD/MTM). The current estimates of Core II lifetime (overall, as well as plutonium region) show that these predictions will be essentially duplicated by actual operation to end of life.

The supporting critical experiment program[4] provided significant beginning-of-life physics information about the fuel and formed the basis for improving the correlation of analysis with experiment for plutonium-fueled systems. Critical experiments with water moderated, single region and multi-region PuO_2-UO_2 fueled cores were performed in the CRX reactor critical facility at the Westinghouse Reactor Evaluation Center (WREC) at Waltz Mill, Pennsylvania. Close agreement was thus found between predicted and measured beginning-of-life nuclear characteristics.

Mechanical, Thermal, and Hydraulic Design

The mechanical, thermal, and hydraulic design guidelines for the PuO_2-UO_2 portion of Saxton Core II included: a) 20,000 MWD/tonne peak rod average burnup; b) 16 kw/ft maximum heat rate in the rods; c) internal gas pressure at end of design life to be less than external reactor operating pressure; and d) fuel rod outside diameter, length and lattice spacing to be the same as for the UO_2 rods in Cores I and II. The details of this aspect of the program are reported in Reference 5.

In addition to the fuel rods, the basic components of each fuel assembly consist of four grids, two enclosure halves, and top and bottom nozzles. The grid assemblies are of brazed "egg crate" construction and are spaced axially on ten-inch centers to provide lateral support for the fuel rods. The enclosure halves are welded to the peripheral straps of the grid assemblies to support the grids and to tie the fuel assemblies together. The nozzles, which provide a means of handling the fuel assemblies and of positioning the assemblies in the reactor core, are welded to the top and bottom ends of the enclosure halves.

The fuel rods are arranged in a 9 x 9 square lattice with a 0.580-inch pitch in a typical main fuel assembly. Of the possible 81 lattice locations in this pattern, nine locations at one outer corner are eliminated from each fuel assembly to provide room for cruciform control rods positioned between the assemblies. In addition, two lattice locations in each fuel assembly were left vacant during fabrication to allow for insertion of flux wire thimbles, source rods, or removable fuel rods when the assembly was installed in the reactor.

The individual rods are 41 inches long; active fuel length being 36.6 inches. Rod outside diameter is 0.391 inches. Clad thickness is 23 mils for the Zircaloy clad and 15 mils for the stainless steel clad.

Materials Design

Materials design entailed selection of the cladding and fuel rod fabrication techniques employed for the project, development of fuel specifications, and provision of materials information to other design groups for establishing design parameters and safety criteria. The details of the materials design are given in Reference 6.

Oxide fuel was selected because it offers the best compatibility with present water reactor fuel cycles. In selecting the fabrication processes, the following factors were considered:

1) In-pile reliability of fuel fabrication by the method;

2) Projected economics of the process; and

3) State of development of the process.

Evaluation of the available evidence led to selection of vibrational compaction and pelletization of mechanically blended fuel. Fuel fabricated by both methods already had been tested in various short-term experiments. Testing of bulk quantities of vipac fuel in EBWR is reported in another paper in this conference.[7] Other fabrication methods, such as extrusion and swaging, were not considered

sufficiently advanced for proof-testing in commercial reactors.

Zircaloy-4 cladding was used for the bulk of the plutonium-bearing fuel rods because it was expected to be generally employed in future cores. Some Type 304 stainless steel cladding was included for comparison.

Table I summarizes the materials selection for the program. All fuel is natural UO_2 enriched to 6.6 w/o PuO_2. The plutonium contained 8.6 a/o Pu-240. Table II summarizes the reactor operating conditions for the program.

Reactor Operating Experience

Operation of the partial plutonium core at full design power levels has been completely satisfactory to date. A continuing program of nuclear operations analyses has shown no significant deviation from expected core operating characteristics. These analyses have included investigation, at power, of boron and control rod worths, temperature and power coefficients, core depletion rate, and core flux wire and detector maps. Core nuclear parameters have also been evaluated in two series of limited zero-power tests performed at approximately one-third and two-thirds of the expected core life. These latter tests included measurements of boron and control rod worths, temperature and pressure coefficients, minimum shutdown reactivity, and xenon decay. References 8 to 11 describe the plutonium core operations in detail.

Completion of operation with the partial plutonium core is scheduled for the first quarter of 1968. At the end of core life, the average exposure in the plutonium region will be 15,500 MWD/MTM; the average exposure in the peak power plutonium assembly will be 23,500 MWD/MTM; and the exposure in the peak plutonium pellet will be 31,800 MWD/MTM. The overall average core fuel exposure at the end of life will be 11,500 MWD/MTM. The reactor was shut down from January to August, 1967, to complete installation of an in-pile test loop. Estimated fuel exposure values at that time were 7,390 MWD/MTM average for the core; 12,210 MWD/MTM average for the plutonium-enriched region; and 21,500 MWD/MTM for the peak plutonium pellet.

The evaluation of materials performance will be accomplished in three distinct efforts:

1) The destructive examination of two rods removed from the core at relatively low burnup as described in the following section.

2) The end-of-life major post-irradiation examination and evaluation effort, planned for mid-1968, described later in the paper.

3) An examination of nine rods conducted during the recent extended shutdown as described below.

During the extended outage in the first half of 1967, five of the individually removable fuel rods were removed from the core, examined with an underwater periscope and remote profilometer, stored in the pool for use as reference rods, and replace with spare rods. Four other such rods were removed, examined and reinserted in the core. Typical grid contact marks were noted on all the rods. Further, the examination of these nine rods revealed no evidence of cladding deformation, strain or other evidence of anomalous performance. Thus, continued satisfactory performance of the plutonium fuel was indicated.

Examination of Low Burnup Fuel

In addition to the major post-irradiation examination and evaluation effort planned for plutonium rods removed from the fuel assemblies at the end of core life, two pelletized fuel rods and two vibrationally-compacted fuel rods were removed from the central 3 x 3 subassembly in April 1966. These rods had accumulated calculated average exposures of about 4500 MWD/MTM and calculated peak exposures of about 6100 MWD/MTM.

Visual and dimensional examination of the removed fuel rods revealed no anomalies or evidence of fretting corrosion at the area of contact between the support grid spring-clip fingers and the cladding tube. The diameter measurements obtained with a remote spiral trace profilometer showed no deviation from the original fabrication tolerances. Bambooing or unusual ovality was not observed. There was no difference observed in the dimensional performance between the vipac and pellet rods.

The rods were punctured to determine the volume of fission gases released from the PuO_2-UO_2 fuel and the contained gases were collected for mass spectrometer analyses. The results of the analyses are shown in Table III. Rods of the same kind yielded similar gas samples. The Xe/Kr ratios were similar for all rods. Observed differences in the composition of the vibrationally-compacted fuel and pelletized rod gas samples can be partly explained by the different gas atmosphere used in welding the rods. Further, the high nitrogen content of the vipac rods is believed due to release of pre-irradiation nitrogen impurity in the fuel at elevated temperatures. A release of 20 percent of this initial content would account for the 7 to 8 standard cubic centimeters observed.

The distribution of the various xenon and krypton isotopes was found to agree well with that which would be predicted using the fission yields reported by Katcoff.[12] The observed release of xenon and krypton corresponds to 2.1 percent and 10.8 percent for the pellet and vipac rods, respectively. Calculations [14] based upon the diffusion model and a realistic axial and radial temperature distribution predict

3.0 percent and 33.3 percent for the xenon and krypton release for the pellet and vipac rods, respectively. The calculation for the vipac rod used a model based upon pellet-type fuel and, further, assumed conservative[6] thermal parameters. However, the observed release for the vipac rods agrees well with that observed in irradiations of vipac fuel in the PRTR.[13] At the approximate average fuel temperatures for these low burnup rods ($\sim$700°C), a 14-15 percent release was observed in the PRTR rods.

A gamma scan was taken of each of the four rods. A typical result, rod D, is shown in Figure 1. Also shown is the location of the various samples taken for the destructive analyses. Graphical integration of the gamma scan curves confirms the axial peak-to-average power ratio of 1.37.

The burnup samples were analyzed for cesium-137, strontium-90, neodymium-148, and heavy-element isotopic ratios. The results of these chemical analyses were then used to infer a burnup for each sample.[14] These inferred burnups are shown in Table IV along with the burnup calculated based upon the reactor operating log and the average radial power factors for the particular fuel subassembly which contained these rods. Although the burnup inferred from the heavy element isotopic data was also calculated, some of the input data are suspect. Thus, the values are not reported. The discrepancy between the calculated and inferred values of burnup (average absolute percent difference $\sim$10) is due in part to the use of average subassembly radial power factors. The power skewing effects known to exist across the subassembly were not considered in obtaining the calculated burnup. The algebraic average percent difference is only 2.4 percent. This is consistent with the reported[16] estimated error in measurement of burnup by the fission product method of $\pm$2 percent at 1 σ.

Photomacrographs, taken in the as-polished condition, are shown in Figure 2 (left: Rod D, 12x; right: Rod, X-1, 8x). Etching revealed no substantial differences in structure from the as-polished sections. The microstructural features are essentially the same as those shown for unirradiated pellet[17] and vipac[18] PuO_2-UO_2 fuel.

Figures 3 and 4 show typical photomicrographs of the etched fuel surfaces. (All are 250x except 4a which is 100x.) The average grain size at the center of the pellet fuel (Figure 3a) is larger than that at the mid-radius (Figure 3b) or at the edge (Figure 3c). Further, there is a complete absence of columnar grains. Since equiaxed grain growth becomes apparent at about 1400°C, and columnar grains form at fuel temperatures between 1700°C and 1800°C, the microstructure suggests a maximum fuel temperature between 1400°C and 1700°C. This is consistent with a maximum observed power rating of the fuel of 10.6 kw/ft, which corresponds to a maximum center temperature of approximately 1500°C.

Figure 4a shows the vipac fuel at an r/a=0.6. Two anomalies were observed in the materials evaluation of the vipac rod, X-1:

1) The cladding from the vipac rod shows an average hydrogen content approximately 18 ppm higher than that from the pellet rod (Table V); and

2) The I.D. surface of the vipac rod has an 0.6-mil thick reaction layer (Figure 4b).

In each case, calculations were made to identify the sources and estimate the consequences of the observed effect.

In the first case above, fuel chemical analyses showed significantly higher moisture content in the vipac than in the pellet fuel, indicating that this extra moisture may be a possible source of the higher hydrogen content in the vipac cladding. Precise calculations are impossible because several batches of fuel, of varying moisture and hydrogen content, were used for both the vipac and pelletized rods.

Examination of the chemical analyses of the various fuel batches shows 25 ppm as a reasonable value for the difference in moisture content for the two fuel types. If all of this moisture reacted and released hydrogen which was subsequently absorbed by the cladding, the clad hydrogen content increase would be 15 ppm. It is therefore reasonable to hypothesize that the higher moisture content of the vipac fuel is the source of the higher hydrogen content of the vipac cladding.

The hydride distribution is shown in representative photomicrographs of the cladding in Figure 5 (left: from pellet rod; right: from vipac rod; both etched, 100x).

In investigating the second case noted above, the reaction layer was not identified positively. However, calculations based on fuel chemistry show that the extent of reaction cannot be explained on the basis of nitrogen or moisture impurities in the fuel. Reduction of the hyperstoichiometric fuel (O/M 2.01-2.02) to stoichiometric could account for the observed reaction layer. Also, this possible source is consistent with the absence of a similar reaction layer with the pellet fuel since the latter material was hypostoichiometric.

The possible consequences of this layer have been evaluated with respect to thermal performance. Considering possible further reaction of the fuel and clad to a fuel O/M ratio of 2.00, the resulting increase in the fuel center temperature at end-of-life has been estimated to be ~25°C. This small increase will not significantly influence fuel rod performance.

End of Life Examination

During the last quarter of 1967, the Saxton reactor power will be escalated to 35 MWt, resulting in a maximum calculated rod power of 19.1 kw/ft. Operation will continue at this higher power level until the end of operation of the Saxton partial plutonium core (Core II), presently expected in early 1968. At that time it is planned to subject fifteen rods to a more detailed non-destructive and destructive examination. It is expected that the maximum burnup of fuel to be examined will be about 31,000 MWD/MTM.

Elements of this examination program will include at least the following:

1) Physical examination of the intact assemblies and rods for twist, bow, wear, or other indications of undesirable mechanical performance.

2) Single channel and multi-channel gamma scans of the rods.

3) Fission gas analysis.

4) Burnup and isotopic analyses of selected fuel samples using cesium-137, strontium-90, neodymium-148, and heavy element isotopics as indicators.

5) Metallographic examination of selected fuel and cladding samples.

6) Autoradiographic examination of selected fuel samples.

7) Clad tensile and burst tests.

A final report will document the results of these examinations.

Conclusions

The Saxton Plutonium Project has been the vehicle for the design, fabrication, irradiation and evaluation of the first large-scale plutonium fuel demonstration. All evidence obtained thus far through post-irradiation examination of the fuel and by deduction from reactor operation data shows that, as expected, the plutonium-enriched mixed oxide fuel performs as well as the standard UO_2 fuel. It is also anticipated that excellent fuel performance will continue to be demonstrated throughout core life. By mid 1968, the ability to design, fabricate and operate plutonium-enriched mixed oxide fuel to peak exposure levels in excess of 30,000 MWD/MTM in a pressurized water reactor will have been successfully demonstrated.

REFERENCES

1. Commercial Plutonium Fuels Conference, Washington, D. C., March 1-2, 1966. Reported in CONF-660308.

2. Use of Plutonium as a Reactor Fuel, Brussels, March 13-17, 1967. Proceedings to be published by IAEA.

3. Orr, W. L., Sternberg, H. I., et al, WCAP-3385-51/EURAEC-1490 - Nuclear Design of the Saxton Partial Plutonium Core, December 1965.

4. Taylor, E. G., WCAP-3385-54/EURAEC-1493 - Critical Experiments for the Saxton Partial Plutonium Core, December 1965.

5. Bassler, E. A., Fischer, D. C., et al, WCAP-3385-52/EURAEC-1491 - Mechanical, Thermal and Hydraulic Design of Saxton Partial Plutonium Core, December 1965.

6. Biancheria, A., Stanutz, R. N., et al, WCAP-3385-53/EURAEC-1492 - Materials Design and Fabrication of the Saxton Partial Plutonium Core, December 1965.

7. Bean, C. H., Sharp, R. E., and Bailey, W. J., The EBWR Plutonium Recycle Demonstration Experiment.

8. Nelson, N. R., WCAP-3385-6/EURAEC-1435 - Quarterly Progress Report for the Period Ending December 31, 1965.

9. Nelson, N. R., WCAP-3385-8/EURAEC-1661 - Semi-Annual Progress Report for the Period Ending June 30, 1966.

10. Miller, R. S., WCAP-3385-10/EURAEC-1777 - Semi-Annual Progress Report for the Period Ending December 31, 1966.

11. Miller, R. S., WCAP-3385-12/EURAEC-1877 - Semi-Annual Progress Report for the Period Ending June 30, 1967.

12. Katcoff, S., Fission Product Yields from Neutron-Induced Fission, Nucleonics, 18, #11, November 1960.

13. Freshley, M. D., and Panisko, F. E., BNWL-366, The Irradiation Behavior of UO_2-PuO_2 Fuels in PRTR, March 1967.

14. Dean, R. A., et al, WCAP-2518, FIGHT - An IBM-7094 Code for Predicting Fission Gas Release, October 1963.

15. Nodvik, R. J., WCAP-6068, Evaluation of Mass Spectrometric and Radiochemical Analysis of Yankee Core I Spent Fuel, March 1966.

16. Aline, P. G., et al, Fuel Management and Isotopic Composition Prediction and Experiment in Light Water Power Reactors, Joint Conference on the Physics Problems in Thermal Reactor Design, June 1967.

17. Ross, W. J., et al, Post-Irradiation Examination of 5 w/o PuO_2-UO_2 Fuel, Trans. Am. Nuc. Soc., 9, #1. June 1966.

18. BNWL-225, Atlas of Irradiated Fuel Structures (1966).

TABLE I

MATERIALS SELECTION

Clad	Form	Powder Prep. Method	Fuel Density % T.D.**	No. Rods Inserted In Reactor
Zr-4	Pellets	Mechanical Mixing	94±2	470
Zr-4	Vipac	Mech. Mixing - Nupac*	87±1	138
304 SS	Pellets	Mechanical Mixing	94±2	20
304 SS	Vipac	Mech. Mixing - Nupac*	87±1	10

* Battelle Northwest Laboratories high energy impaction process.

** Percentage Theoretical Density.

TABLE II

SAXTON REACTOR OPERATING CONDITIONS

Maximum Power Level	23.5 Mw(t)
Maximum Linear Power Density	16 kw/ft
Maximum Heat Flux	531,400 Btu/hr-ft^2
Average Coolant Temperature	277°C (530°F)
System Pressure	2,000 psia
Maximum Clad Surface Temperature	339°C (642°F)
Average Clad Temperature at Hot Spot (SS)	356°C (674°F)
Average Clad Temperature at Hot Spot (Zr-4)	367°C (692°F)
Maximum Fuel Central Temperature	2200°C (3992°F)
Peak Burnup	>25,000 MWD/MTM
Chemical Shim, Beginning of Life	2,000 ppm Boron
Initial Loading - PuO_2-UO_2	345 Kg/9 assemblies
Initial Loading - UO_2	525 Kg/12 assemblies

TABLE III

POST-IRRADIATION GAS SAMPLE ANALYSIS RESULTS

	Gas Volume, cc at STP			
Gas	X-1	X-5	D	E
H_2	--	--	0.004	--
He	4.555	2.677	4.445	4.897
N_2	7.970	9.881	0.047	0.018
O_2	0.057	0.143	0.022	0.007
Ar	0.004	0.010	0.287	0.303
Kr	0.389	0.494	0.080	0.097
Xe	5.886	7.507	1.185	1.445
CH_4	--	0.037	--	0.001
Total Volume	18.86	20.75	6.07	6.77

TABLE IV

FUEL BURNUP

Sample	D-BU-1	D-BU-2	X-BU-1	X-BU-2
Inferred Burnup				
Cs	6146	5520	5207	4881
Sr	6445	6143	5277	4819
Nd	6223	5514	5246	4717
Avg.	6305	5725	5243	4805
Calculated Burnup	6015	5210	6240	5240
$\frac{\text{Calc-Inferred}}{\text{Calc}} \times 100$	-4.8	-9.9	16.0	8.3

TABLE V

HYDROGEN CONTENT OF IRRADIATED CLADDING

Rod No.	Sample No.	H_2 Content (ppm)
X-1	1	61
X-1	2	82
D	1	52
D	2	55

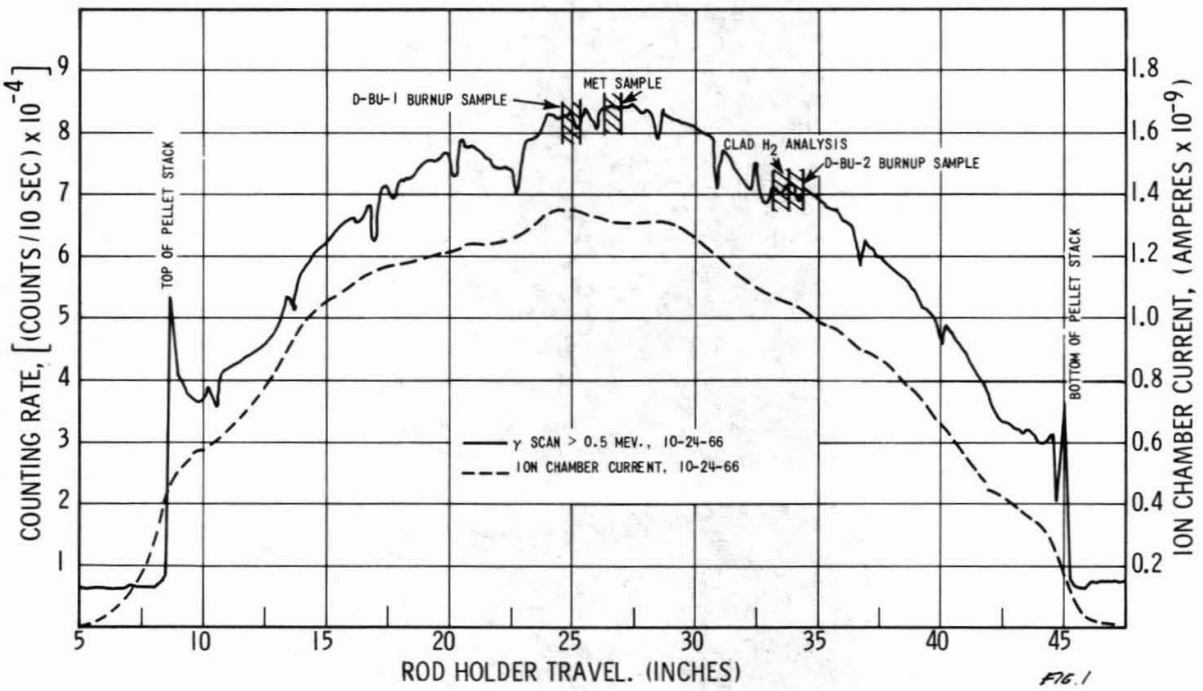
COUNTING RATE, [(COUNTS/10 SEC) x 10^{-4}]
ION CHAMBER CURRENT, (AMPERES x 10^{-9})
ROD HOLDER TRAVEL. (INCHES)
D-BU-1 BURNUP SAMPLE
MET SAMPLE
CLAD H_2 ANALYSIS
D-BU-2 BURNUP SAMPLE
TOP OF PELLET STACK
BOTTOM OF PELLET STACK
γ SCAN > 0.5 MEV., 10-24-66
ION CHAMBER CURRENT, 10-24-66

FIG. 1

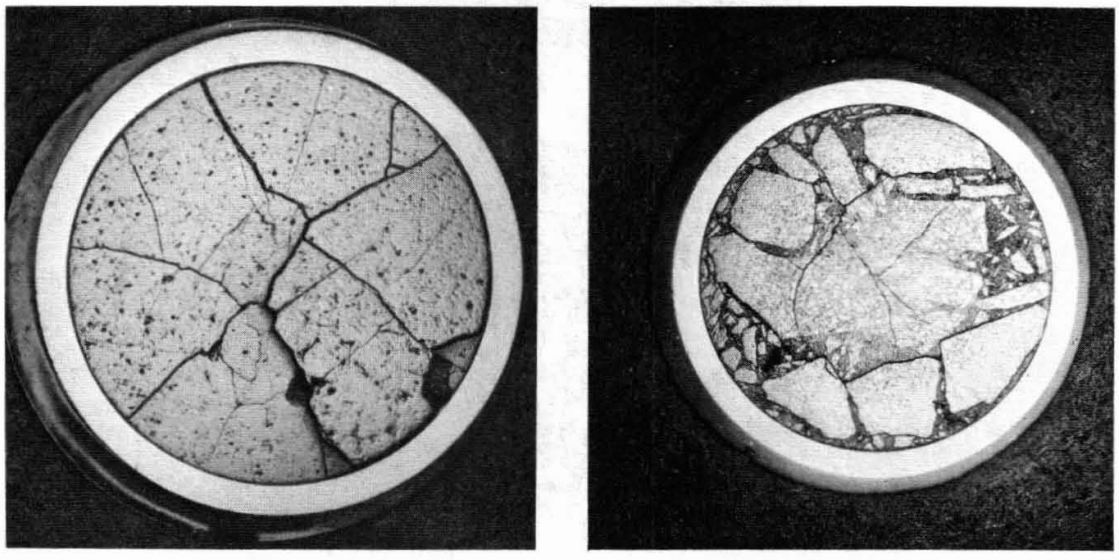

FIG. 2

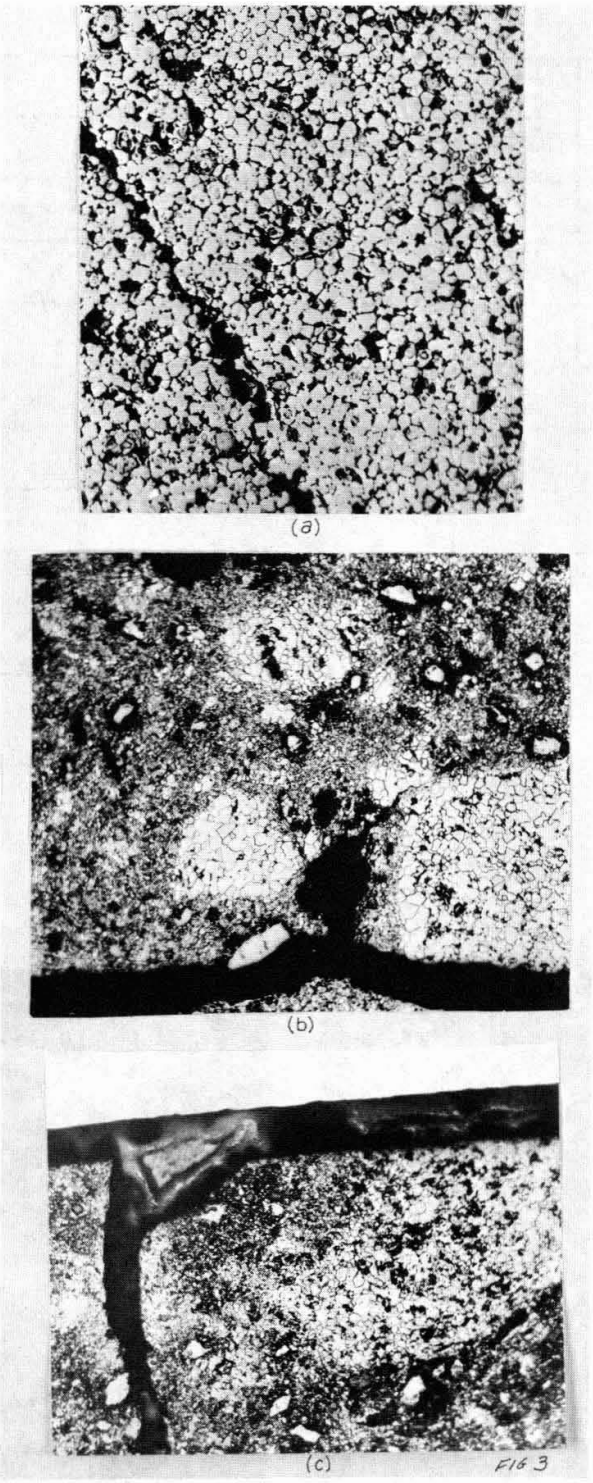

(a)

(b)

(c)

FIG 3

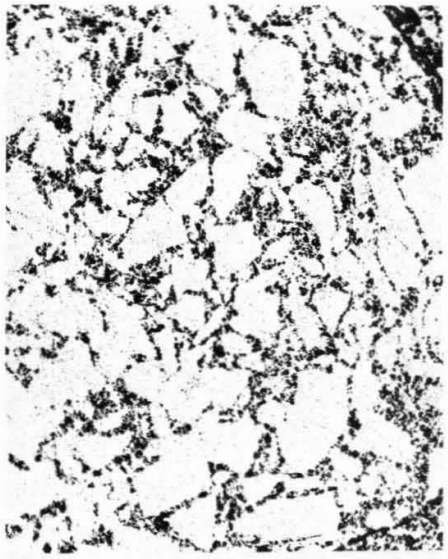

(a)

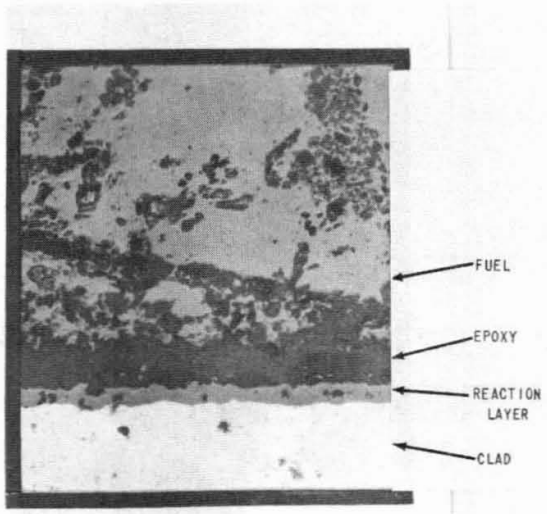

(b)

FIG. 4

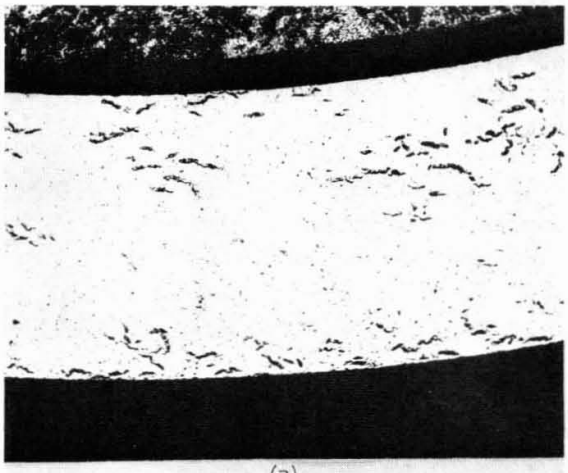

(a)

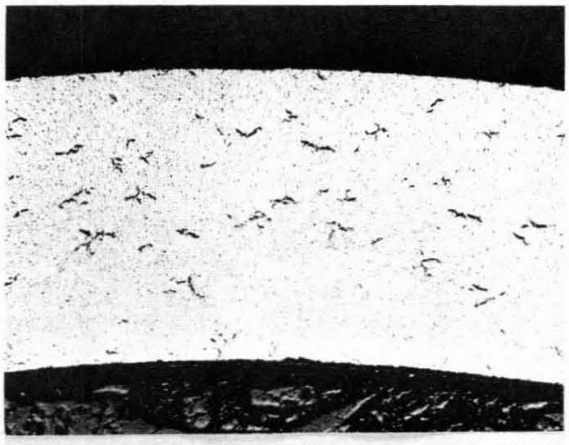

(b)

FIG. 5

IRRADIATION OF PLUTONIUM FUELS IN THE BR-3 *

H. Bairiot **
A. Lhost ***

Abstract

The paper describes schematically the different types of fuels which have been tested in the BR-3 reactor.

The first campaign enables to compare pelletized uranium fuel to vibratory compacted and to swaged plutonium fuels. Furthermore, different types of UO_2 have been utilized for the powders.

The burnup has been of the order of 5,000 MWd/t. The main result concerns the gas release of heterogeneous particulate fuels compared to pellets and the effect of the UO_2 powder used as starting material.

The BR-3/Vulcain experiment will enable to compare at high burnups (30,000 MWd/t) vibratory compacted and pelletized plutonium fuels. In this experiment, it has already been possible to evaluate some very important details concerning a simplified technique utilized for the manufacture of the plutonium fuels.

* Work performed in the frame of the Cooperation Agreement Euratom/United States Contrat Nr 001-64-1 TRUB, between the C.E.N. (Centre d'Etude de l'Energie Nucléaire) - BelgoNucléaire Association and Euratom.

** Ingénieur, Chef de Service at "BelgoNucléaire" (Société Belge pour l'Industrie Nucléaire, S.A.).

*** Ingénieur at "BelgoNucléaire".

1. INTRODUCTION.

The work presented in this paper has been performed by the Joint C.E.N. - BelgoNucléaire Plutonium Group, under contracts forwarded by the Euratom Commission within the Euratom/United States Joint Research and Development Program. It is part of the broad Belgian effort undertaken since 1958 to study the recycling of plutonium in thermal reactors.

The main fuel development effort has been devoted to assess the merits and disadvantages of a special fabrication technique based on powder packing processes (vibratory compaction or vibratory compaction followed by a small swaging step). The particularity of the investigated process consists of introducing the plutonium into the fine size fraction of the fuel only (1) ; this fabrication route has also been developed in the past at Hanford but has been superseded at the Richland site by the Dynapak process.

Among the main advantages (1), one should notice :

- a reduction of the fabrication steps involving the handling of plutonium,
- an enhanced heat transfer within the fuel rod (2, 3),
- the possibility of profiling the enrichment longitudinally.

Among the disadvantages, the two major ones are :

- the necessity of a long and tedious development effort,
- the occurrence of local plutonium concentration ; the local hot spots might impose a reduction of the fuel performances under certain circumstances (1, 4, 5).

The evaluation of this type of fuel is made primarily by comparative tests in the BR-2 reactor (2). Since "an evaluation of irradiation behaviour based upon a few specimens may be subject to considerable error" (6), these orientation tests are supported by a demonstration program performed in power reactors, which will be the subject of the present paper.

2. BR-3/PWR.

This experiment is the first step of the demonstration program. It is representative of the state of art prevailing in Belgium in 1962, when the fabrication technique was still in its infancy and a large uncertainty existed on the applicability of the core design codes to plutonium containing lattices. As a result, the fuel is of poor quality compared to our present standards and the power ratings to which the fuel was subject are very low.

2.1. Description of the fuel.

The fuel consists of three size fractions mixed together while loading the tube ; the coarse and the medium fractions are fused and ground UO_2 or Dynapak UO_2 (rods R 298 and R 307) ; the fine fraction is a blend of fused and ground UO_2 with sintered (U - 10 % Pu)O_2 or a blend of Dynapak UO_2 and sintered PuO_2 (rod R 307) or sintered (U - 5.65 % Pu)O_2 (rod R 298). In all cases, the uranium was natural and the total enrichment therefore 0.7 % U^{235} and 0.96 % Pu containing 5.7 % Pu^{240}, except for rods R 298 and R 307 (7.7 % Pu^{240}).

The fuel rod design is represented in figure 1. The vibrated rods have a fuel density of 86 % TD and a plenum partially filled with a hold down spring (0.7 cm^3 of the total 10 cm^3 voidage). The plutonium distribution along the rods may be characterized by maximum local 384 KeV gamma peaks of 27 to 40 % in the hot zone (1/3 to 1/2 of the fuel height) and up to 140 % at the upper end ; these values are measured with an uncertainty of $\pm$ 10 %. The swaged rods have a fuel density of 90.5 % TD and no plenum (total voidage : 7 cm^3). The plutonium distribution may be characterized by maximum local 384 keV peaks of 7 to 26 % in the hot zone and up to 210 % at the upper end.

The fuel rods are located in a now classical assembly made by "Métallurgie et Mécanique Nucléaires", in the positions indicated in figure 2. This figure also indicates the position of the assembly in the core.

2.2. Irradiation data.

The irradiation conditions are summarized in Table I.

It had been computed that for a core life of 4,000 EFP hours the burnup of the 12 plutonium rods would be between 3,500 and 4,800 MWd/t depending on their location in the assembly. The computed longitudinal and transversal power distributions are given in figures 5, 6 and 7.

The plant has been on power from December 1963 to July 1964 with a load factor indicated in figure 3. The reactor was shut down at 4,800 EFP hours because of the requirements of the Vulcain Program.

2.3. Post-irradiation tests.

1. Dimensional checks.

The visual examination revealed no deformations or defects of the cladding. The crud was uniform in color. Within the experimental errors (± 0.02 mm), no dimensional changes have been found ; a small decrease in diameter (0.01 mm, i.e. 0.1 %) might have occurred in the swaged rods. The hot spots did not show any departure from the average behavior of the rod, both for what crud deposition and dimensions are concerned.

2. Gammascannings.

Due to the late commissioning of the required hot cell equipment, the gamma activity was only sufficiently high at 0.1 MeV and 0.66 MeV to perform a gammascanning. The scannings at both energies are identical within the error limits (figure 5).

Figure 4 compares the gammascanning of rods fabricated by different methods. In the uranium rod utilized as standard, the location of the grids is noticeable. The plutonium rods show the effect of the heterogeneous distribution of the plutonium among the fuel. The "European Institute for Transuranic Elements" C.C.R.★ (Karlsruhe) has demonstrated that the fuel is still mobile by tapping a rod and comparing the gammascans taken before and after this test.

The swaged rods have maximum activity peaks of 0 to 16 % in the hot zone (for instance, figure 5) within the accuracy of the measurements (± 6 %).

★ Joint Nuclear Research Centre - Euratom

The vibrated rods have maximum local activity peaks of 9 to 25 % in the hot zone (for instance, figure 6). Assimilating these peaks to power peaks, it can be deduced from these figures that the 384 keV activity profile overestimates the longitudinal variations of the plutonium distribution by a factor 2 ; this conclusion is confirmed by the analysis of numerous other activation and irradiation tests. The comparison of the gammascans with the calculated longitudinal power distribution (figures 5 and 6) shows that the fuel assembly has still run at a high power at the end of life.

3. Radiochemical burnup determination.

One vibrated rod (V 41) has been chopped into 15 segments of 10 cm for the determination of the burnup profile along the rods. The burnup of other rods has been measured by sampling a specimen from the rod ; the average and maximum burnup data were deduced from the gammascanning profiles. The burnup of the other rods is calculated from the relative gamma intensities alone. The results described hereunder are based on the data obtained at Mol, which are nearly complete ; the work at Karlsruhe is still in progress.

V 41 rod. The rod has been chopped and the fuel dissolved at the LMA ★ in a HNO_3 10 M boiling solution, then in a HCl 5 M + HBr 5 M + HF 0.1 M boiling solution. An aliquot of each solution has been sent to the Radiochemistry Service of the C.E.N. ; some have also been sent to Eurochemic for isotopic composition determination ; some have finally been used at the LMA for Cs^{137} analysis.

The separation of Cs^{137} at the LMA is based on the precipitation of fission products carbonates other than caesium on an anionic exchange resin. The eluated solution is analyzed and measured spectrometically. The claimed accuracy of the method is ± 10 %. The results are given in Table II.

The separation of fission products at the Radiochemistry Service of the C.E.N. (7) is effected by determining the fission density of irradiated fuels by measurement of the concentration of Cs^{137}, Ce^{144} and Sr^{90}. This method is based on a separation on Dowex 50 resin with use of complexant products (7). From these different measurements, the burnup is determined by taking into account the uranium and plutonium isotopic composition after irradiation for estimation of fission yields, and the irradiation and cooling times.

★ LMA : Laboratoires de Moyenne Activité - GEX - C.E.N.-Mol

A third control was established by the BCMN [*], which determines directly the Cs^{137} content by mass spectrometry of the initial solution.

To the accuracies given by the authors should be added 10 % for the error in the fission yield of the different products. The total accuracy is then 20 %. The experimental data given in Table II do not support such a low figure for the accuracy. The comparison of the various experimental data is given graphically in figure 6.

Other rods. The only other experimental data concern two rods ; the average and peak burnups based on the data and on the gammascans are given in table III. These values confirm the data obtained by comparison with the rod V 41 on the gammascan basis, except for the average of R 289.

The average adopted burnup data are selected from the experimental data (radiochemical analysis, gammascanning, isotopic compositions) and predicted power distribution. These values are mapped in figure 7. In general, the agreement between experimental and predicted data is good in the case of plutonium rods.

4. Isotopic composition.

Table IV gives the result of 5 determinations of the isotopic composition performed at Eurochemic. From the results on three segments of rod V 41 the burnup was calculated , the values (Table II) are in agreement with the adopted values within the limit of accuracy. Likewise it may be seen that the isotopic composition varies continuously with the adopted burnup data within the limits of accuracy.

5. Fission gas release.

A few new fission gas release data have been obtained since the previous paper (4) , a summary is given in Table V.

The isotopic composition of the released xenon and krypton (Table VI) is similar for all plutonium rods, but slightly different for the uranium rods. The influence of the proximity of the control rod is noticeable, reflecting the difference in irradiation history.

---

[*] Central Office for Nuclear Measurements, Joint Nuclear Research Centre, Euratom, Geel, Belgium.

The efficiency of the gas collection during the post-irradiation test lies in the region 14 - 26 %, except for rod R 298. The high figure for this rod is surprising, taking into account the higher density and smaller grain size of the swaged fuel.

The free gases at room temperature represent a pressure of 4 - 9 atm. One should be careful in extrapolating this residual room temperature pressure to the gas pressure under operating conditions. It is noticeable that the highest pressures are for "dynapak" fuel, which should have the highest surface area for gas adsorption.

The hydrogen content of the gas corresponds to a hydrogen content of the fuel of 0.05 - 2.5 ppm or to a moisture content of the fuel of 0.4 - 22 ppm. Both contents are within the specification of the initial fuel. The lower value for "dynapak" fuel is probably due to the fact that it was carefully dried just before the fabrication of the rods.

The CO and CO_2 content of the rods with "dynapak" powder does not confirm the analyzed carbon content of the fuel (40 ppm C). It should be noted that the carbon content of the fused UO_2 was of the same order of magnitude (50 ppm C).

The fission gas release is more than one order of magnitude higher for the powder fuel than for the pelleted fuel (0.9 %). Since the central fuel temperature is estimated at 600°C in both cases (figures 8 and 9), the release rate for the powder fuel can only be explained by the heterogeneous nature of the fuel (plutonium in the fine size fraction only). It should be expected that small grains release more fission products ; the recoil distance is indeed of the same magnitude than the grain size. The comparison of results for rods R 307, R 289 and R 298, in which the plutonium was in solid solution in 1.10 and 18 % of the fuel respectively (Table V), suggests however that the saturation of the fuel lattice could be the main effect ; in Table V, the burnup and the release rate were computed for the plutonium containing part of the fuel, assuming 60 % of the power was generated by the initial plutonium and that all the release came from the fine size fraction of the fuel. It can be noticed that, on this basis, 20 % of the fission products enter the adjacent fuel by recoil, if one estimates that at 200,000 MWd/t and 300 - 600°C the fuel is completely saturated.

6. Structure.

Figures 8 and 9 present a macrography, an α - and a β - γ autoradiography of a cross-section of two representative rods. No major modification of the structure has occurred under irradiation, except an overall spike sintering phenomenon in the swaged fuel ; the strength of the sintered joints is such that circumferential cooling cracks are visible throughout the hottest specimens. This observation is not in contradiction with the assumed 600°C maximum central temperature since .

1) one of the authors found that swaged UO_2 sinters when subjecting the rod to 1,000°C (and even 900°C) for 1 h

2) it is well demonstrated that the fission process can lower the sintering temperature by 30 %. The 900 - 1,000°C range corresponds therefore to 550 - 600°C under irradiation.

The preferential plutonium and power distribution at the outer edge (4) is only slightly visible in the autoradiographs due to polishing effects. The flattened transversal distribution of temperature (2) is supported by the uniformity of the structure and by the pattern of cracks. These observations are only qualitative and even not conclusive by themselves.

3. BR-3/VN.

The program has been presented at the Brussels Symposium on the Use of Plutonium as a Reactor Fuel, March 13-17,1967 and its status will only be mentioned briefly hereafter. Characteristic data are given in Table I.

3.1. Description of the fuel.

A fuel assembly containing 18 pelleted rods and 19 vibrated rods has been made of plutonium enriched natural uranium. The vibrated rods were of the heterogeneous type.

The principal actual result was to show the great importance of the pessimistic hypotheses adopted for the interpretation of the control data and for the calculation of the burnout margin. The development program has been adapted consequently.

3.2. Irradiation data.

By the time of the present symposium, the plutonium fuel will have reached an average burnup of 9,000 MWd/t and a peak burnup of 12,000 MWd/t in the highest rated vibrated rod.

4. COMPARISON WITH RESULTS FROM IRRADIATION TESTS.

The past BR-3/PWR run is representative of the power rating of the lowest rated 40 % of the fuel charge of a modern water cooled power station. The present BR-3/VN run is representative of the power rating and the burnup of the lowest rated 60 % of such a fuel charge.

The present section will summarize the results of irradiation tests conducted under more extreme conditions. Those irradiations are realized in two facilities of the BR-2 ; a hydraulic rabbit (HR) and a "boiling water capsule" (CEB).

4.1. HR (Hydraulic Rabbit).

A research program to check the thermal behavior of plutonium enriched oxide fuel is performed in a hydraulic rabbit of the BR-2 at Mol in Belgium.

The tests include a series of specimens reaching full power after 15 min at linearly increasing power and a series of specimens reaching full power in 0.2 s. Each test also includes homogeneous and heterogeneous fuel.

Four irradiations have already been performed (2). The obtained powers are actually estimated in the 140 to 1,400 W/cm range (2). The most important results are a better determination of the factors of

$$q' = \frac{4\pi}{f} \int kdT \qquad \text{with} \qquad f = f_n f_g$$

where q' (W/cm) : power rating

f : correction for the heterogeneity in the transversal distribution of the power density (W/cm^3)

f_n : correction factor for a homogeneous fuel due to the neutron flux depression

f_g : correction factor for the heterogeneous distribution of the fissile material.

For vibratory compacted fuel at 85 % TD, the integral from 0 to 2,800°C is equal to 70 W/cm for specimens filled with argon and 70 - 80 W/cm for helium containing rods. The f_g factor is respectively 0.7 - 0.8 and 0.8.

This means that, under normal conditions of modern water reactors, the melting point should just be reached at 600 - 800 W/cm for homogeneous fuel and 900 - 1,000 W/cm for heterogeneous fuel.

On the basis of these data, it has been calculated that it would be possible to design and fabricate a fuel with a f_g down to 0.6.

4.2. Boiling water capsule.

The continuous monitoring system of the capsule (8) gives the evolution of the heat rating and the cladding temperature at various levels along the channel.

Only the first of the four irradiation capsules tested in the BR-2 is being examined presently in hot cells. The characteristics are given in Table I. The specimens were made by incremental loading; each increment of powder was a blend of the three size fractions. This produced a longitudinal segregation of plutonium to 4 levels corresponding to the interface between each of the four increments. The plutonium gamma activity of the rods presented 4 peaks up to 30 % (figure 11) ; the loading process avoided to a maximum extent any transversal heterogeneity of the plutonium distribution.

The irradiation history is given in figure 10. It can be noticed that the power rating was increased from 170 to 320 W/cm at 50 % of the fuel life ; this simulates power peaking that might arise from a reshuffling. The peak cladding temperature was 550°C. In a homogeneous fuel the central temperature would have been 1,600 - 1,700°C and the average fuel temperature 1,200°C. The total irradiation time was 2,400 h of which 200 h have been in high power rating after 1,200 h of irradiation. From the recorded data, the burnup has been estimated at 10,000 MWd/t.

The dimensional tests revealed no change due to the irradiation, which was a surprise considering the high cladding temperature.

The gammascanning (figure 11) indicates local power peaks equal (within the accuracy) to the plutonium activity peaks measured before irradiation. This is believed to confirm the good transversal distribution of the plutonium, although the effect of heterogeneities on the plutonium activity is much less in such small rods than in large ones.

The radiochemical burnup determination is still in progress at the moment of writing. From the neutron flux monitors, the burnup should be of the order of 16,000 MWd/t ; the peak power rating should then be 500 W/cm and the peak central temperature would have been 2,400 - 2,600°C in a homogeneous fuel.

The gas release data are given in Table V.

The structure of one of the specimens (V 62) is given in figure 12. The modifications are only a spike sintering from the cladding to a depth of 10 - 20 % of the radius in rod V 62 in a section at average power, 5 - 10 % of the radius in the same rod in a section at 120 % of average power and 50 % of the radius in rod V 59 at 90 % of the average power of rod V 62. In rod V 62, the plutonium has migrated to a 50 μ depth in the large UO_2 grains in the central portion ; such a phenomenon has not occurred in rod V 59. Since the metallographic examination is not completed, it can only be concluded that the central temperatures were respectively ranging from 1,500 to 1,600°C in rod V 62 and from 1,300 to 1,400°C in rod V 59. These figures lie in the present range of uncertainty of peak temperatures based on the available power data (continuous monitoring and neutron dosimetry) ; a conclusion will only be possible when the radiochemical analysis will have defined more precisely the burnups. It will then be possible to see to what extent the burnup influences the improved heat transfer properties of the fuel.

The fission gas release is given in Table V. The total of the collected gases from rod V 59 was only 20 % of that from rod V 62 and too small to enable an analysis to be performed. These rough values do not permit to draw a conclusion since they might be influenced less by the density than by the extraction efficiencies which can be as low as 20 % (Table V). The isotopic composition of the gaseous fission products is given in Table VI ; no major difference exists with the case BR-3/PWR. The hydrogen release is lower than in the BR-3 rods ; since the same powder and the same fabrication techniques have been used, it is probably an effect of the higher permeability of the cladding to hydrogen at high temperatures. The 70 % fission gas release can be influenced both by the higher temperature and the higher burnup. The comparison of

the release and the burnup reduced both to the plutonium bearing part of the fuel shows a good agreement with the BR-3/PWR results and tends to indicate that the temperature has not the major influence.

CONCLUSIONS.

The long term irradiations performed up to now have proved the beneficial effect of heterogeneous fuel on gas release. From the data available at the time of writing, the burnup influence on the improvement of heat transfer demonstrated in the rabbit experiment could not be deduced.

ACKNOWLEDGMENTS

The authors wish to thank the Management of the Centre d'Etude de l'Energie Nucléaire and the Syndicat Vulcain for having permitted the publication of this paper.

They are also grateful to the Euratom Commission for its financial aid and for the technical discussions they were able to have with its representative, Mr. P. Kruys.

Finally, they wish to mention also the important part taken by Mr. E. Vanden Bemden, Head of the Joint CEN-BelgoNucléaire Plutonium Group, in the supervision of the research, as well as the fine collaboration of the various departments ; among them should particularly be noted the fruitful collaboration of the Radiochemical Service of the CEN and the "Laboratoires de Moyenne Activité" of the GEX.

REFERENCES

1. Aerts, L., Bairiot, H., Mostin, N., Van Asbroeck, Ph., Van Lierde, W., "Manufacturing Processes of Vibratory Compacted Oxide Fuel", Paper presented at the Symposium on the Use of Plutonium as a Reactor Fuel (SM-88/13), Brussels, March 13 to 17, 1967.

2. Andriessen, H., Bairiot, H., Leblanc, J.M., Lhost, A., Van Asbroeck, Ph., "Influence of the Fabrication Technique on the Behaviour under Irradiation of Oxide Fuels", Paper presented at the Symposium on the Use of Plutonium as a Reactor Fuel (SM - 88/12), Brussels, March 13 to 17, 1967.

3. Kruys, P., "Euratom Program on Plutonium Recycle Fuels in Thermal Reactors", Paper presented at the 1967 AIME Nuclear Metallurgy Symposium, October 4 to 6, 1967, Phoenix, Arizona.

4. Bairiot, H., de Waegh, F., Leblanc, J.M., Lhost, A., Libotte, P., Motte, F., Van Asbroeck, Ph., "Irradiation d'éléments combustibles dans le réacteur belge BR-3", Paper presented at the Symposium on the Use of Plutonium as a Reactor Fuel (SM - 88/14), Brussels, March 13 to 17, 1967.

5. de Waegh, F., Demeulemeester, E., Guyette, M., Pilate, S., Vandenberg, C., "Assemblage plutonifère dans le coeur BR-3/ Vulcain", Paper presented at the Symposium on the Use of Plutonium as a Reactor Fuel (SM - 88/16), Brussels, March 13 to 17, 1967.

6. Freshley, M.D., and Panisko, F.E., "The Irradiation Behaviour of UO_2-PuO_2 Fuels in P R T R", BNWL 366, Battelle Pacific Northwest Lab., Richland (Wash), March 1967.

7. Cooperation Agreement Euratom - United States, Contract Nr. 001 - 64 - 1 TRUB, "Emploi du plutonium comme combustible dans les réacteurs nucléaires", Progress Report BN 6602-02 ; Period from October 1 to December 31, 1965, Commission de l'Euratom, C.E.N., BelgoNucléaire, Brussels, 1966.

8. Lhost, A., "La capsule à eau bouillante - Dispositif expérimental instrumenté et régulé dans la barrière thermique pour irradiation de combustibles nucléaires" - Topical Report BN-6704-03, Cooperation Agreement Euratom - United States, Commission de l'Euratom, C.E.N., BelgoNucléaire, Brussels, 1967.

TABLE I

IRRADIATION CONDITIONS

	Unit	BR-3/PWR	BR-3/VN	CEB-1
Date		1963 - 1964	1966 - 1968	1965 - 1966
Number of rods		12	19	3
Number of rods per assembly		108	37	1
Outer diameter	mm	8.7	8.5	6
Total length	cm	152	125	15
Cladding	SAE	348	304(L)	348
Thickness	mm	0.5* - 0.6**	0.5	0.5
Enrichment Pu	%	0.96	6.6	5
Density	% TD	86* - 90.5**	85	83 - 87
O/M ratio		2.01/2.02	2.00/2.01	2.00
Coolant		H_2O press.	H_2O - D_2O press.	NaK
Max. cladding temperature	°C	300	340	550
Max. power rating	W/cm	130	200	320
Max. heat flux	W/cm^2	50	70	180
Max. burnup	MWd/t	6,000	(25,000)	(10,000)

* Vibrated rod

** Swaged rod

TABLE II

BURNUP DETERMINATION OF ROD V 41 (MWd/t)

Operator	LMA	Radiochemistry Service C. E. N.				BCMN	Eurochemic	Adopted value
Method	Cs^{137}	Cs^{137}	Cs^{144} (1)	Sr^{90} (1)	Am^{241} (1)	Cs^{137}	Isotopic Composition	
Segment nr 15		660	530	700				650
Segment nr 14		950	800	1,000	1,100			950
Segment nr 13		1,840	1,500	2,000				1,800
Segment nr 12	2,470	2,620	2,200	2,600				2,500
Segment nr 11	2,640	3,550	2,900	3,450	3,400			3,100
Segment nr 10	3,220	4,040	3,300	3,650				3,500
Segment nr 9	3,010 and 3,250 (2)	4,920	4,100	4,000			3,800	3,800
Segment nr 8	3,930	5,300	4,350	4,900	5,000			4,600
Segment nr 7	4,010	5,680	4,600	5,100				4,900
Segment nr 6	4,300	6,210	5,100	5,200		4,350	4,200	5,000
Segment nr 5		6,510	5,300	5,200	5,300			5,400
Segment nr 4		4,875	4,000	4,500				4,400
Segment nr 3	2,900	4,640	3,800	4,200			3,800	3,900
Segment nr 2		3,080	2,550	2,700	2,400			2,900
Segment nr 1		2,130	1,800	1,800				1,900
Average burnup	(3,200)	3,700	3,400	3,400	3,400		(4,000)	(3,400)
Accuracy %	7	13	6	7	9		10	5
Peak burnup	(4,400)	6,500	5,100	5,200	5,000	(4,000)	(4,100)	5,400
Accuracy %	20	20	25	25	25	30	30	5

Note : ( ) indicates that the value is not deduced directly from measurement

(1) inaccurate results (cf. 2. 3. 2.) - Only the relative longitudinal figures were deduced from the experimental data

(2) results of two measurements on different aliquots of the solution

TABLE III

BURNUP (MWd/t) OF THE BR-3/PWR RODS

Rod	Average			Peak	
	From direct measurement (1)	From comparison with V 41 (± 10 %)	Adopted value (3)	From direct measurement (1)	From comparison with V 41 (± 10 %)
U 1		(3,300)	(3,700)		(5,000)
U 2		(3,300)	(3,500)		(4,300)
V 39		2,900	2,900		4,600
V 40		2,900	3,000		4,600
V 41	3,400 (± 5 %) (1)	3,400	3,300	5,400 (± 5 %) (1)	5,400
V 42	3,800 (± 20 %) (2)	3,500	3,600	7,100 (± 20 %) (2)	6,100
V 43		3,000	3,000		4,500
V 44		3,400	3,300		5,100
R 283		2,900	2,900		4,500
R 284		2,400	2,400		3,900
R 286		3,200	3,100		5,100
R 289	2,400 (± 20 %) (2)	4,000	3,200	3,900 (± 20 %) (2)	5,000
R 298		3,100	3,200		4,700
R 307		2,600	2,600		4,000

(1) see Table II
(2) from radiochemical determination of a segment and calculations based on gammascans
(3) from experimental determinations and theoretical data (see figure 7)

TABLE IV

ISOTOPIC COMPOSITIONS

Rod	Unit	Initial data	R 289	V 42	V 41		
Segment			17	16	9	3	6
Adopted burnup	MWd/t		3,200	3,200	3,800	3,900	5,000
U isot. compos.							
U^{234}	%		0.004	0.005	0.003	0.006	0.005
U^{235}	%	0.71	0.55	0.56	0.585	0.56	0.53
U^{236}	%		0.034	0.032	0.03	0.032	0.038
U^{238}	%	99.3	99.41	99.40	99.38	99.40	99.42
Pu content							
Pu/U + Pu	w/o	0.96	0.87	0.85	0.93	0.90	0.91
Pu isot. compos.							
Pu^{239}	%	93.7	74	74.9	75.8	75.0	71.6
Pu^{240}	%	5.7	18.5	18.1	17.8	18.5	20.0
Pu^{241}	%	0.6	6.8	6.3	5.8	5.9	7.4
Pu^{242}	%		0.77	0.68	0.59	0.635	0.96

TABLE V

FISSION GAS RELEASE

		BR-3/PWR							CEB-1
	Rod / Unit	U_1	U_2	V 41	V 42	R 289	R 298	R 307	V 62
Free space	cm^3	8		10	10	7	7	7	0.33
Average b. u.	MWd/t	(3,500)		3,300	3,600	3,200	3,200	2,600	(10,000)
Collected gases									
Ar + He + N_2 + O_2	cm^3	5.5	2.1	2.6	1.4	1.2	4.4	1.0	0.59
H_2	cm^3	7.2	4.7	2.3	2.5	0.8	0.25	0.5	0.01
CO + CO_2	cm^3	-	-	-	-	-	29.0	2.7	
Xe + Kr	cm^3	0.3	0.22	5.3	3.6	2.6	6.9	4.36	3.58
Total	cm^3	13	7.0	10.2	7.5	4.5	41	8.5	4.18
Efficiency of the gas collection	%	68	26	26	14	17	63	14	100
Gas pressure at room temperature	atm	2.4	3.4	4	5.3	4	9	9	13
H released	ppm/UO_2	1.5	2.4	1.2	2.5	0.65	0.05	0.5	0.05
C released	ppm/UO_2	-	-	-	-	-	40	17	
Fission gas released	%	0.7	0.9	32	39	27	19	55	70
Burnup in the (U, Pu)O_2	MWd/t			(22,000)	(23,000)	(20,000)	(11,000)	(200,000)	(180,000)
Fission gas released of the (U, Pu)O_2				(50)	(60)	(40)	(32)	(80)	(75)

Note : ( ) indicates that the values are estimated by calculations from experimental determinations

TABLE VI

ISOTOPIC COMPOSITION

OF THE RELEASED XENON AND KRYPTON (%)

			BR-3/PWR					CEB-1
Rod	V 41	V 42	V 289	R 298	R 307	U_1	U_2	V 62
Xenon								
131	12	12	12	12	11	14	10	12
132	20	19	19	18.5	19.5	21	15	18.5
134	28	27	27	29	27	29	30	26
136	40	41.5	42	40	43	36	45	43
Krypton								
83	18	17	17	17	12	15	20	12
84	28	28	29	29	27	30	35	31
85	7	7	6.5	7	4	6	-	7
86	47	48.5	48	48	58	49	45	50

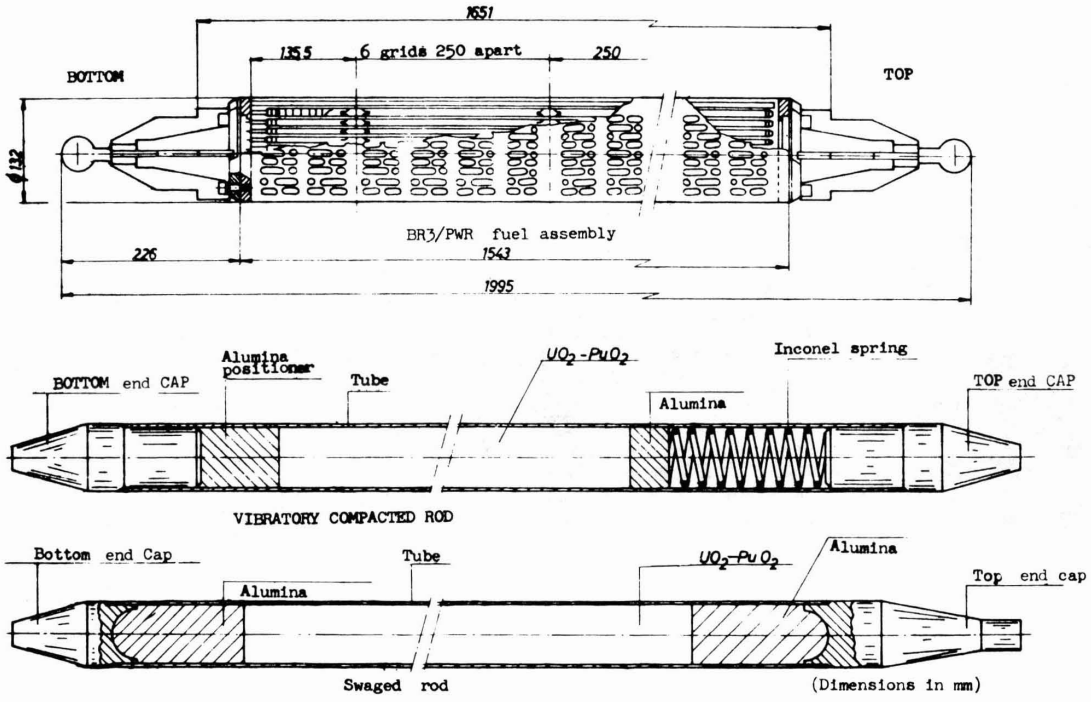
1651
1355
6 grids 250 apart
250
BOTTOM
TOP
Ø132
BR3/PWR fuel assembly
226
1543
1995
BOTTOM end CAP
Alumina positioner
Tube
UO_2-PuO_2
Alumina
Inconel spring
TOP end CAP
VIBRATORY COMPACTED ROD
Bottom end Cap
Tube
UO_2-PuO_2
Alumina
Alumina
Top end cap
Swaged rod
(Dimensions in mm)

FIGURE 1

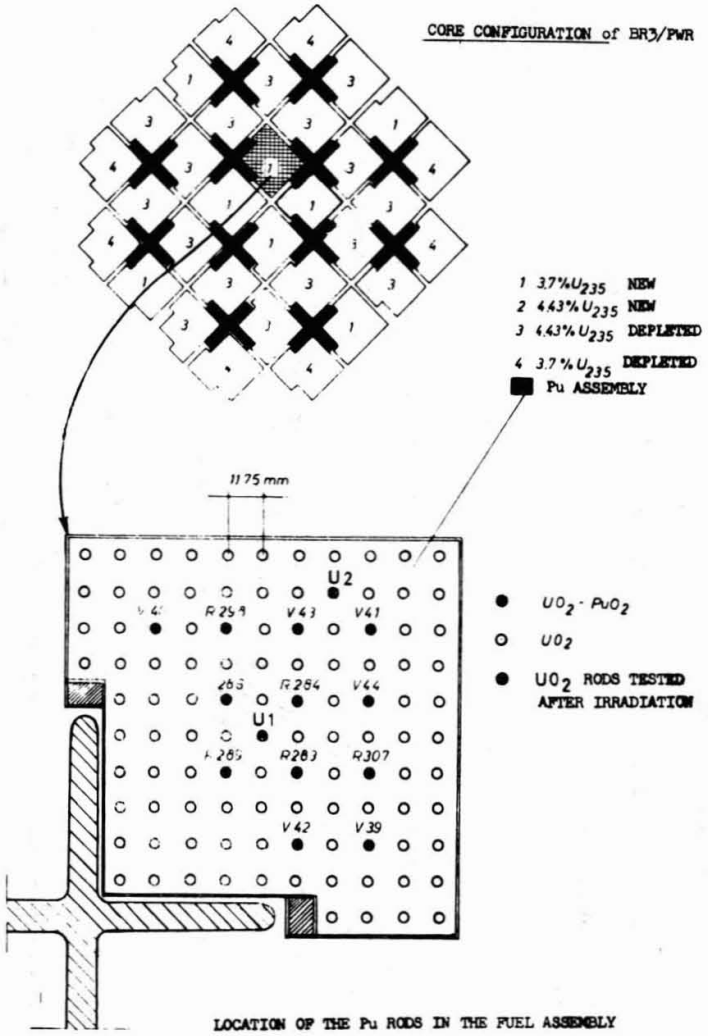

LOCATION OF THE Pu RODS IN THE FUEL ASSEMBLY

FIGURE 2

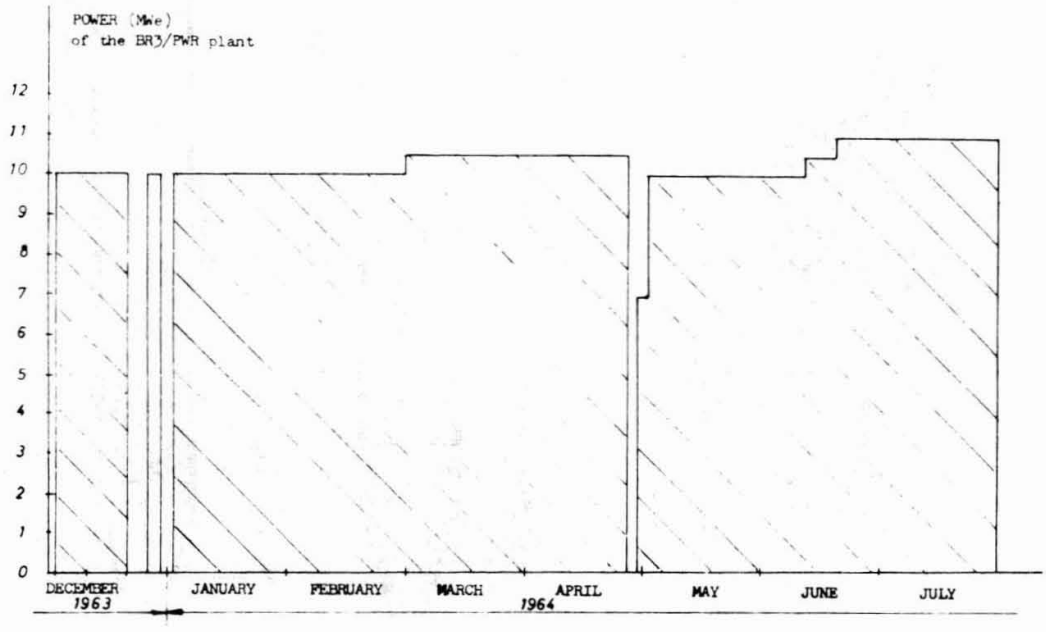

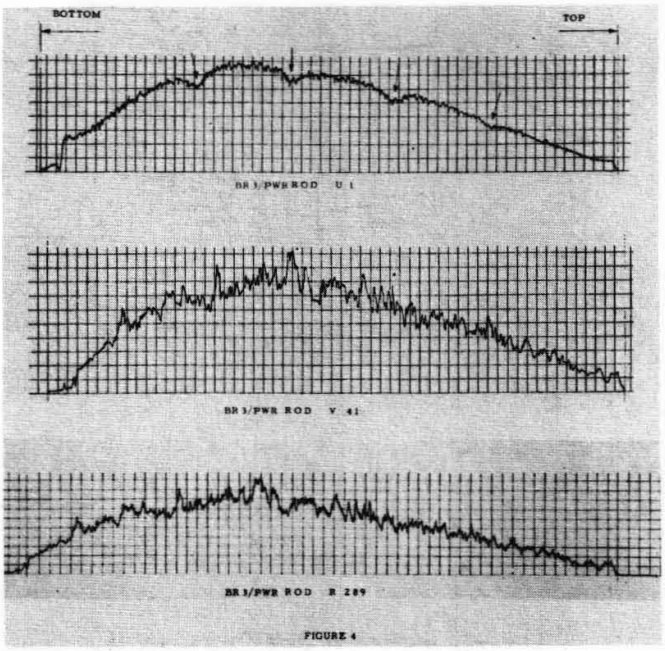

FIGURE 4

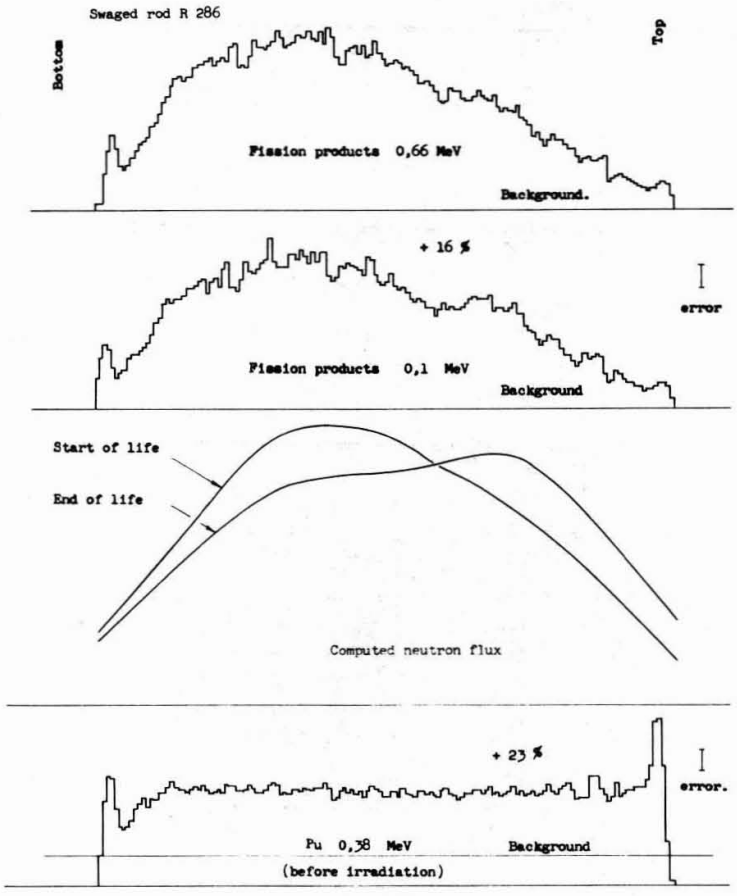

FIGURE 5

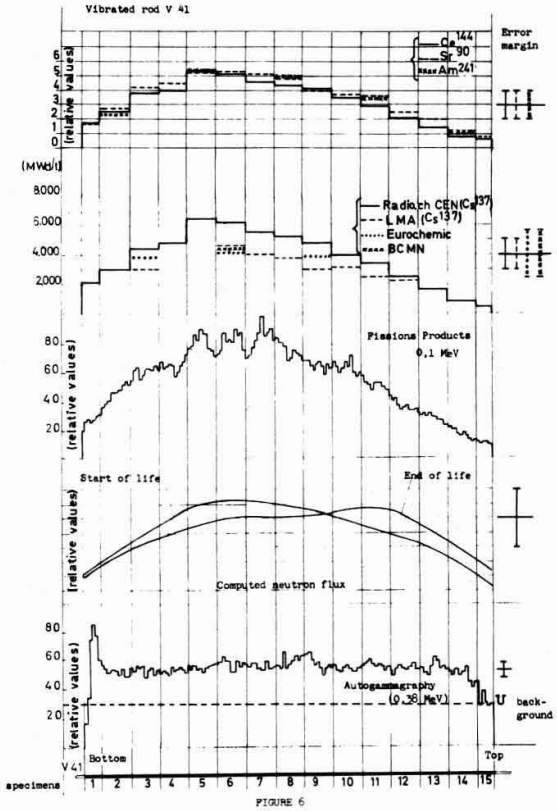

FIGURE 6

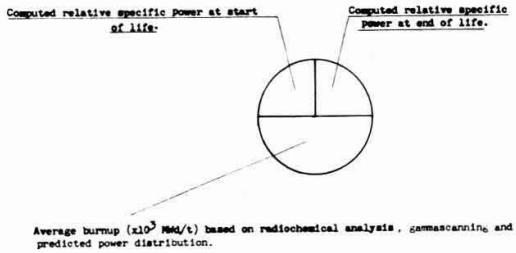

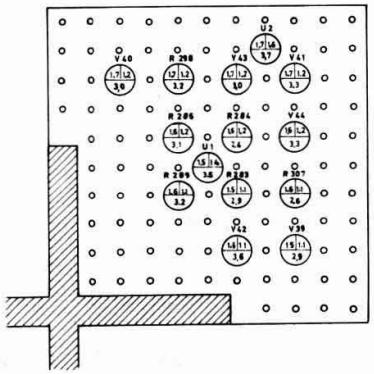

Map of the burnup in the Pu assembly of BR3/PM3

FIGURE 7

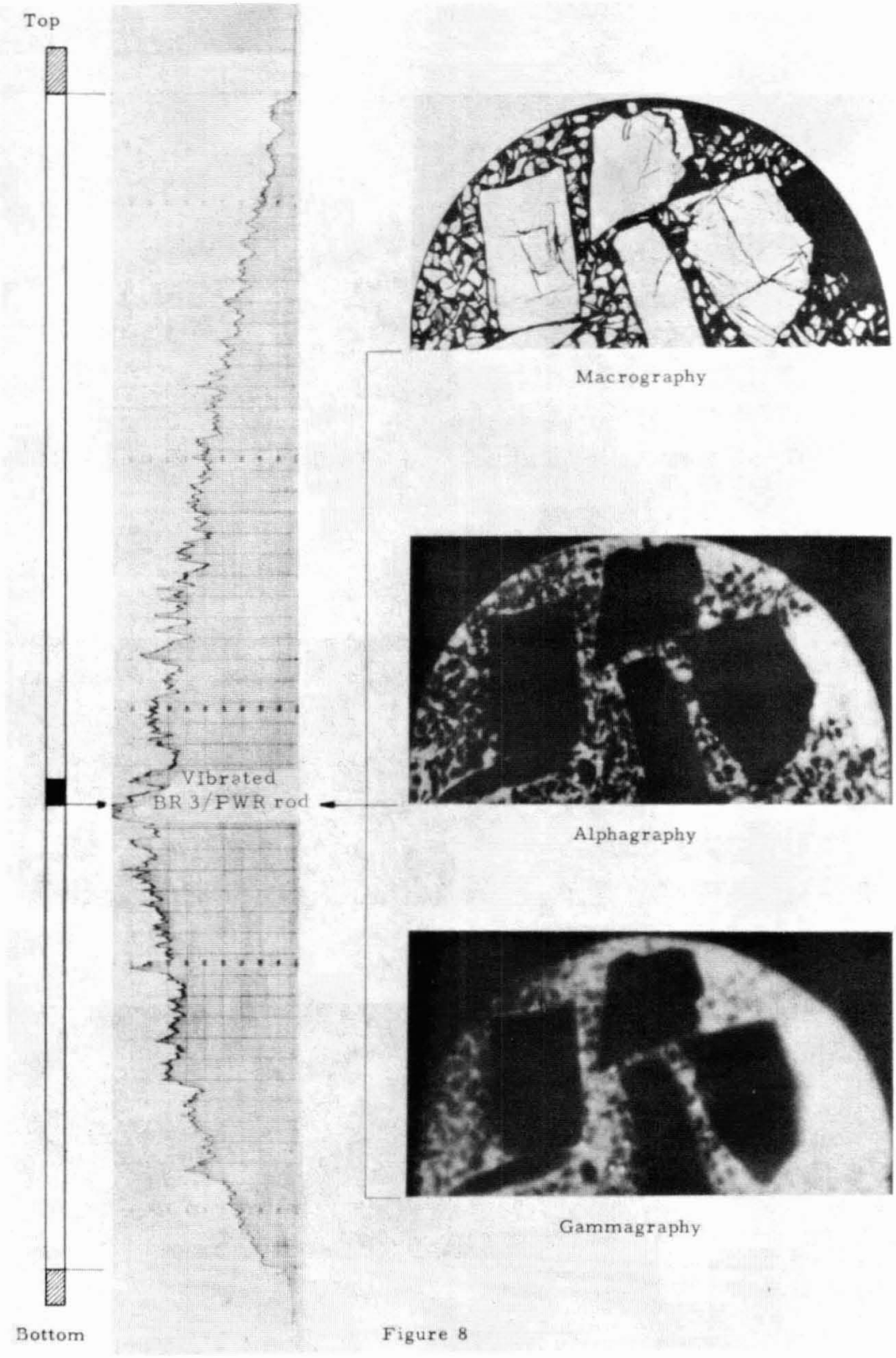
Top
VIbrated
BR 3/PWR rod
Bottom
Macrography
Alphagraphy
Gammagraphy

Figure 8

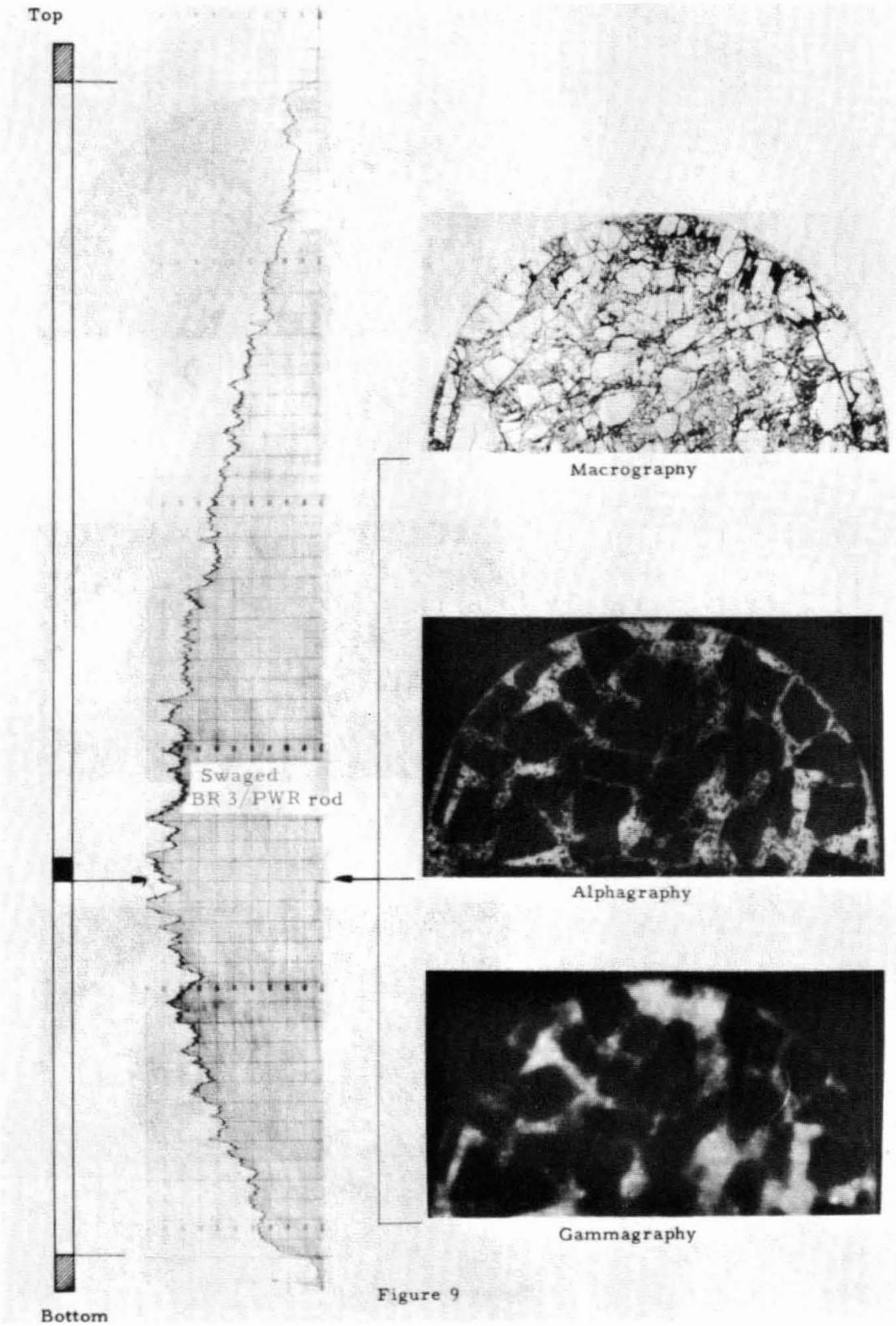
Top
Swaged
BR 3/PWR rod
Bottom
Macrography
Alphagraphy
Gammagraphy

Figure 9

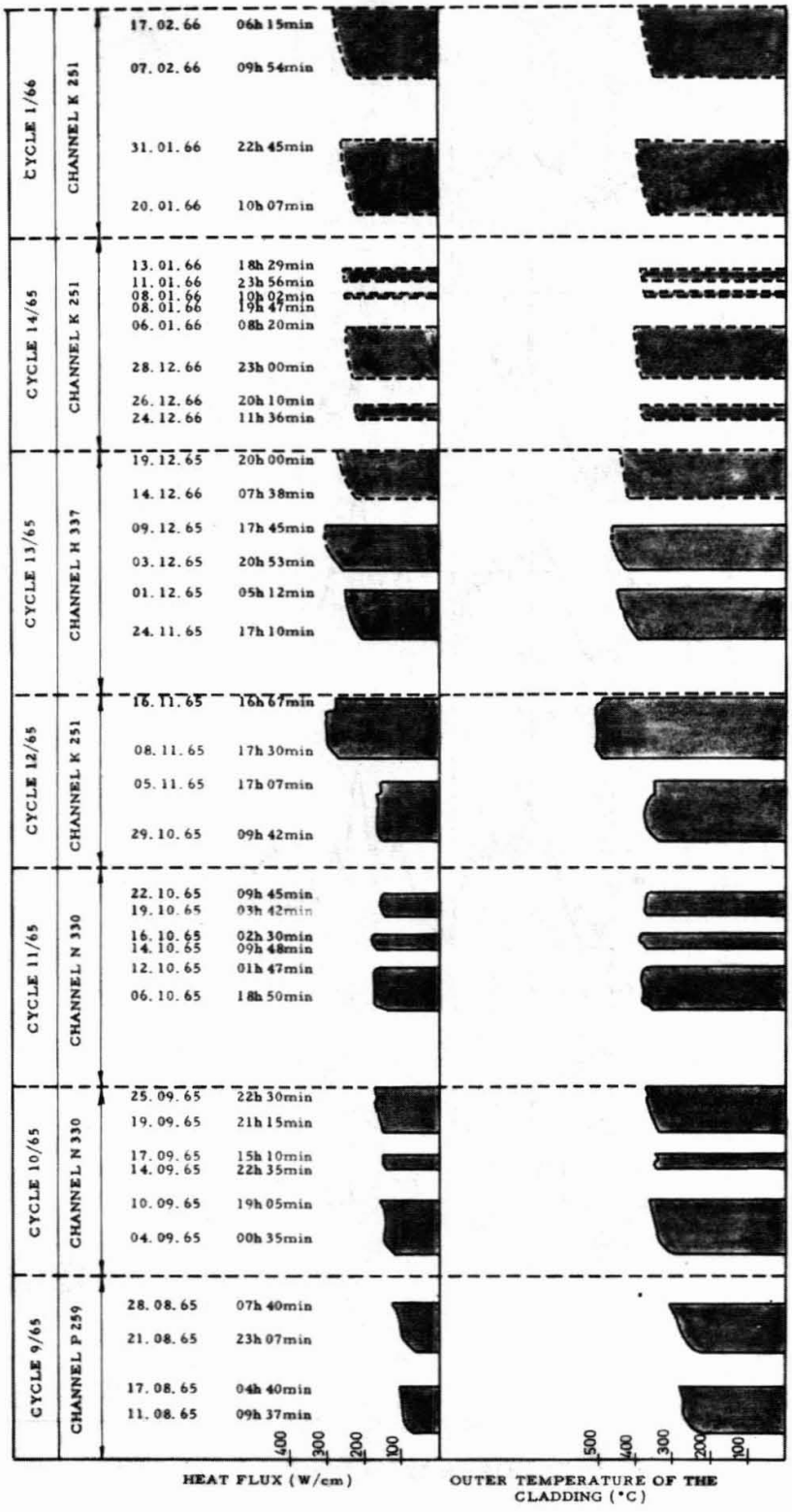
CYCLE 1/66
CHANNEL K 251
17.02.66 06h 15min
07.02.66 09h 54min
31.01.66 22h 45min
20.01.66 10h 07min
CYCLE 14/65
CHANNEL K 251
13.01.66 18h 29min
11.01.66 23h 56min
08.01.66 10h 02min
08.01.66 19h 47min
06.01.66 08h 20min
28.12.66 23h 00min
26.12.66 20h 10min
24.12.66 11h 36min
CYCLE 13/65
CHANNEL H 337
19.12.65 20h 00min
14.12.66 07h 38min
09.12.65 17h 45min
03.12.65 20h 53min
01.12.65 05h 12min
24.11.65 17h 10min
CYCLE 12/65
CHANNEL K 251
16.11.65 16h 07min
08.11.65 17h 30min
05.11.65 17h 07min
29.10.65 09h 42min
CYCLE 11/65
CHANNEL N 330
22.10.65 09h 45min
19.10.65 03h 42min
16.10.65 02h 30min
14.10.65 09h 48min
12.10.65 01h 47min
06.10.65 18h 50min
CYCLE 10/65
CHANNEL N 330
25.09.65 22h 30min
19.09.65 21h 15min
17.09.65 15h 10min
14.09.65 22h 35min
10.09.65 19h 05min
04.09.65 00h 35min
CYCLE 9/65
CHANNEL P 259
28.08.65 07h 40min
21.08.65 23h 07min
17.08.65 04h 40min
11.08.65 09h 37min
400 300 200 100
HEAT FLUX (W/cm)
500 400 300 200 100
OUTER TEMPERATURE OF THE CLADDING (°C)

FIGURE 10

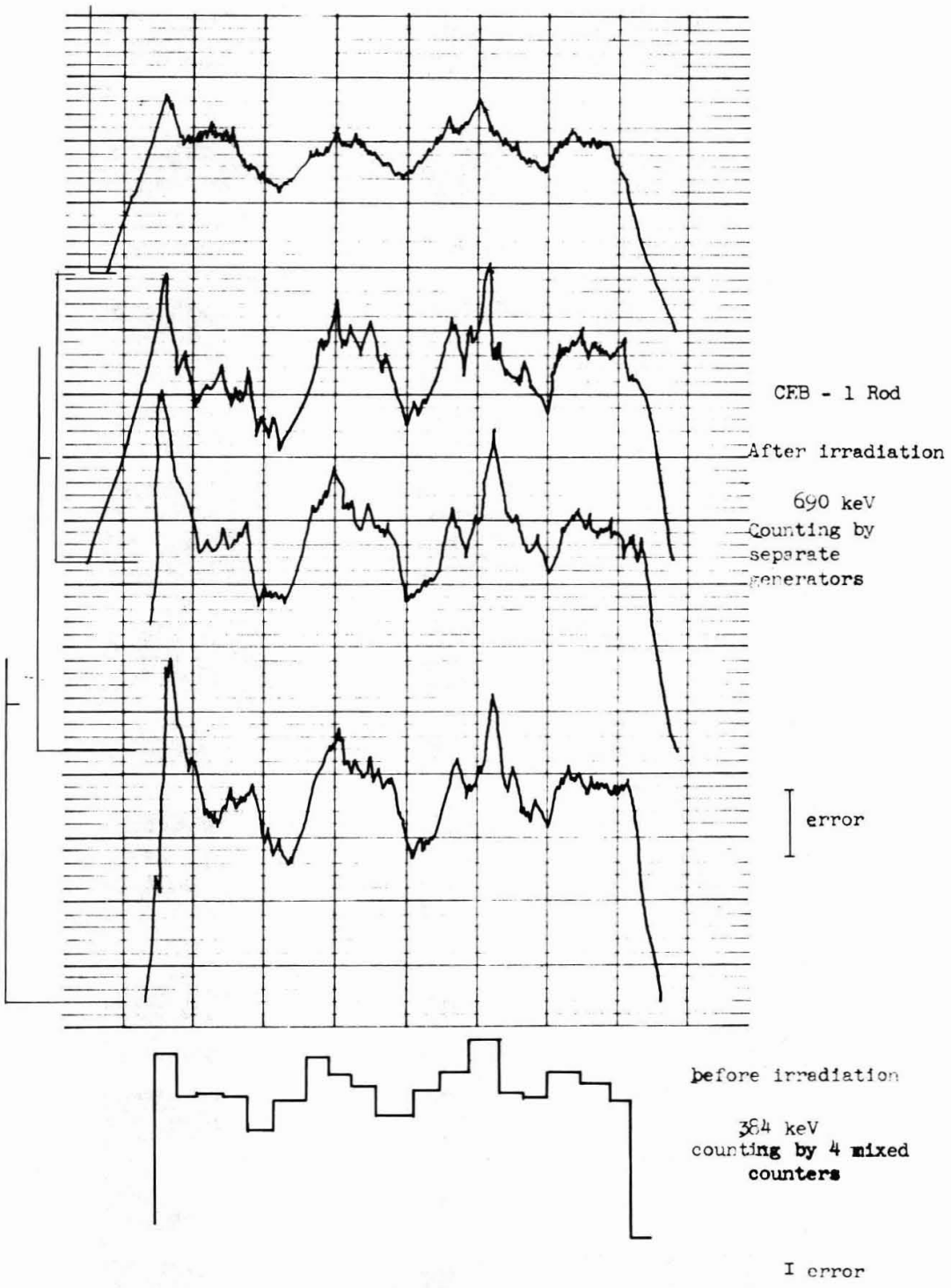
CEB - 1 Rod
After irradiation
690 keV
Counting by
separate
generators
error
before irradiation
384 keV
counting by 4 mixed
counters
I error

FIGURE 11

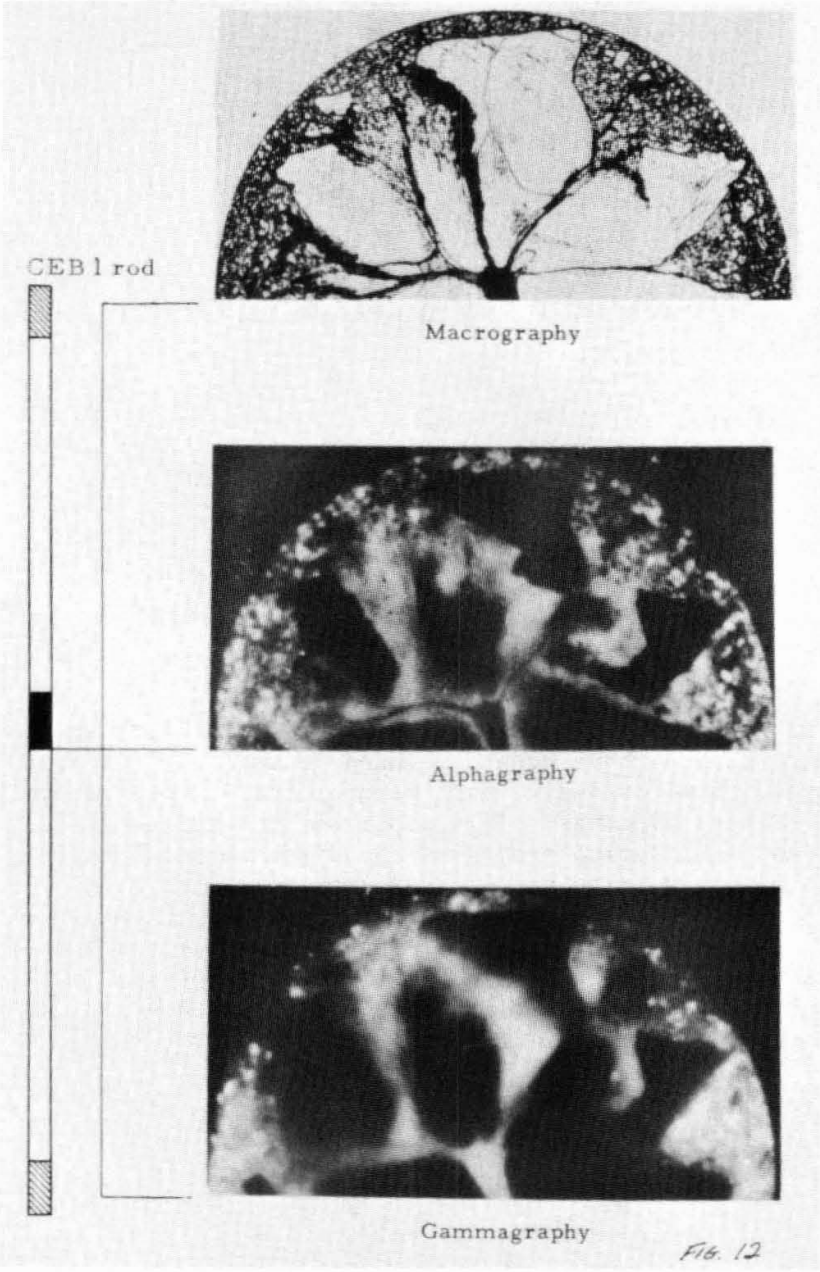

FIG. 12

PLUTONIUM-URANIUM DIOXIDE POWDER AND PELLET FUEL MANUFACTURE

C. S. Caldwell and K. H. Puechl

Plutonium-uranium dioxide powder preparation and pellet fuel manufacturing methods have been developed to meet increasing demands for critical assembly, test reactor and demonstration power reactor fuel elements. This paper reviews current conversion and fabrication processes and discusses techniques for control of mixed-oxide pellet characteristics including plutonium microhomogeneity and oxygen/metal ratio. Experience gained during fabrication of thermal recycle and fast breeder type PuO_2-UO_2 fuel materials in quantities up to 500 kg is presented. Product variability data are included.

Nuclear Materials and Equipment Corporation
Apollo, Pennsylvania

INTRODUCTION

Plutonium-uranium dioxide fuel manufacturing methods have been developed to meet increasing demands for critical assembly, test reactor, and demonstration power reactor fuel elements.[1] The most important areas which have been developed are (a) conversion of plutonium nitrate and metal to sinterable grade PuO_2 via four different process routes; (b) fabrication of PuO_2-UO_2 pellets from mechanically blended PuO_2-UO_2 powders; (c) fabrication of PuO_2-UO_2 fuel pellets from coprecipitated PuO_2-UO_2; (d) preparation of pellets of different oxygen-to-metal ratios over a wide range of plutonium concentrations to optimize the stoichiometry with regard to in-reactor performance; (e) control of pellet physical and mechanical properties such as density, dimension, and void distribution; (f) control of trace metallic impurities and other contaminants such as C, N, H, F, Cl, moisture, and total gas, having closely specified upper limits; (g) control of precise plutonium assay of fuel lots as well as microhomogeneity of individual pellets; (h) fuel rod loading, welding, leak checking, radiography, gamma scanning, and autoclaving; (i) supporting operations including materials receiving and product shipping, shipping container development and testing; accountability, criticality control, licensing, quality assurance, quality control, and radiological safety; (j) recycle and recovery technology for all process stages; (k) specialized equipment designs for all process stages.

During the first four year period between 1961 and 1965 the above stages of development progressed from a kilogram scale to contracts requiring over 500 kilograms of fuel. One multi-ton order for SEFOR is now being processed by a commercial supplier and additional large orders are expected to be fabricated by industrial suppliers during 1970 and beyond.[2]

The salient features of several alternate plutonium-uranium dioxide manufacturing processes now in use are described below.[3]

PROCESS DESCRIPTIONS

Preparation of Sinterable-Grade Plutonium Dioxide Powder

The Pu oxalate and peroxide routes, which have been used extensively for the conversion of plutonium nitrate into high reactivity intermediate compounds for subsequent hydrofluorination, are also well-suited for making PuO_2. Additional requirements for the resultant sinterable PuO_2 include closer control of impurity contents, physical properties, and assay. Comparative data on alternate routes have been obtained by processing and evaluating test batches prepared in safe geometry equipment. Direct conversion of metal to oxide is also described. Properties are summarized in Table I.

Continuous Precipitation and Calcination of Pu(IV) Oxalate

This is the current reference process for preparing nuclear grade PuO_2 with controllable physical properties and sinterability. Precipitation is easily controlled to yield a final sedimentation average powder size of 2-4 μ. Filtrate waste loss is less than 1 percent providing that the oxidation state of plutonium is pre-adjusted to Pu(IV) by the addition of H_2O_2. Plutonium recovery from the filtrate is required. Tap density, bulk density, B.E.T. surface area and residual carbon content are controlled by the time-temperature history during the thermal decomposition (calcination) step. Powder properties can also be adjusted by hammermilling and by dry ball milling. Purity of the product is higher than the nitrate feed solution. The PuO_2 powder thus produced has been used as a reference material to prepare (a) high density PuO_2-UO_2 pellets by mechanical blending and sintering; (b) high density PuO_2 pellets; (c) controlled density PuO_2 microspheres by powder agglomeration, sizing and sintering; (d) plutonium carbide by reaction with carbon at high temperatures under vacuum.

Continuous Precipitation and Calcination of Pu(III) Oxalate

In the recovery of plutonium from process scrap by nitric acid dissolution and anion exchange, the final elution step can be accelerated by establishing reducing conditions with hydroxylamine nitrate, for example. Oxalate precipitation from the resultant Pu(III) eluate solution is convenient, provides additional purification, and results in slightly lower filtrate losses than the Pu(IV) route. Calcination control provides the same function as previously described. The resultant PuO_2 has higher bulk and tap density, larger particle size, and slightly lower sinterability than the previous method, but these minor deficiencies can be improved by milling if required. Accordingly, this process is considered acceptable for cases where the feed solution is already available as Pu(III) nitrate.

Plutonium Peroxide Precipitation and Calcination

This route requires close control to obtain reproducible oxide properties due to the tendency to form varying amounts of cubic and hexagonal peroxide crystallites during precipitation. In addition, filter cake washing and drying control is more critical since the peroxide precipitates are less stable than the oxalates and generally contain more residual nitrate impurity. Physical properties of the final calcined PuO_2 are distinctly different from oxalate derived material, and in spite of a high surface area, the product has only marginal sinterability. With thorough calcination, combined with powder milling to reduce the size of agglomerates, an acceptable product can be obtained. Although the peroxide route produces the lowest total metallic impurity levels of the three methods, the process is considered sub-standard with respect to the others because of more difficult process control, poorer sinterability, and greater safety hazard associated with hydrogen peroxide.

Direct Conversion of Plutonium Metal to PuO_2

Plutonium metal buttons were oxidized directly to PuO_2 in a fixed-bed pan reactor under an atmosphere of moist air or oxygen. Halide impurities were removed during calcining, but total metallic impurities remained. To obtain reproducible sintering characteristics the powder was milled to an average particle size of 1-1.2 microns. Although the PuO_2 product was dense, when blended with sinterable-grade UO_2, good fabrication control was obtained for mixtures containing 1.5 to 20% PuO_2.

Mechanically Blended Fuel Pellet Fabrication

Powder Blending

In the mechanical blending process, individually prepared oxides of uranium and plutonium are intimately mixed together in the required proportion. Specialized equipment requirements are minimal since only the PuO_2 preparation, final blending, and pellet fabrication require alpha glove box containment. Sinterable-grade natural or depleted UO_2, usually the major component, is inspected, assayed, and pre-weighed for batch blending prior to transfer into the glove box system. In general practice, an attempt is made to match the particle size and surface area of the two components. Mechanical techniques which have been utilized for the mixing include (a) twin-shell pre-blending, (b) hammer-milling, (c) mix-mulling (wet), (d) paste blending (wet), and (e) ball-milling (wet or dry). Agglomerate "snow-balling" has been observed with simple dry twin-shell mixing, resulting in micro-segregation which is greater than fuel specifications allow. Dry pre-blending followed by hammer-milling and dry ball-milling, which imparts inter-particle shear forces to break down such agglomerates, results in good micro-homogeneity as shown by autoradiography of sintered pellets. Mix-mulling, wet ball-milling and paste blending produce uniform mixtures, but have the disadvantage of utilizing liquids which must be removed before pelletizing. Drying is a slow procedure even in a vacuum dryer, since the temperature must be kept below 80°C to prevent oxidation of the UO_2. Although acceptable for thermal recycle fuel compositions, the use of hydrogenous liquids in grinding, mixing, or granulation of fast fuels containing 20 to 25% PuO_2 is less satisfactory due to criticality limitations.

For example, the calculated safe mass limit for 25% PuO_2-UO_2 paste or slurry is 1 kg of contained Pu as compared with a dense powder dry limit of 22 kg contained Pu. Safe mass limits for typical material configurations are shown in Table II.

To control microhomogeneity, alpha autoradiographs of sintered test pellet transverse cross-sections are made and compared with visual standards. With the aid of electron microprobe verification, it has been shown that dry-milling and wet ball-milling of mechanically blended oxides will meet proposed microhomogeneity specifications for fast reactor fuels. To illustrate the relative degree of microhomogeneity attained with conventional ball-milling, an ARL-EMX electron microprobe was used to determine the microhomogeneity of UO_2-15% PuO_2 fuel pellets prepared by two alternate routes, coprecipitation + dry sintering and mechanical-blending + dry sintering.

The reference NUMEC R&D process was used for coprecipitation. Pu-IV oxalate derived PuO_2 and Eldorado Mining and Refining Company normal UO_2 were mechanically-blended by dry ball-milling for four hours. All pellets were sintered on a 4-4-4 schedule at 1650°C in a N_2-6% H_2 atmosphere in a 3 inch diameter molybdenum wound alumina muffle sintering furnace. Pellets were pressed without binders or lubricants in a double-acting hand press die set. "Dry" sintering denotes 100-200 ppm moisture content in the inlet gas to the furnace.

For purposes of visual comparison, the full pellet cross-sections as polished for microprobe examination were autoradiographed prior to platinum shadowing. The microprobe scanning target areas were selected at random and the local plutonium concentrations and uranium concentrations were examined using the Pu $L\alpha$ or Pu $M\alpha$ and U $L\alpha$ x-ray lines, respectively, using an accelerating voltage of 30 Kv and beam current of 0.2 μa. 11 inch LiF and 4 inch ADP analyzing crystals were used for the $L\alpha$ and $M\alpha$ lines, respectively. Step scanning at 1 micron intervals with a 1 micron spot was selected as the most sensitive procedure. Display scan x-ray and electron backscatter TV display prints were taken on most of the samples after quantitative scanning. These display prints illustrated general features over a 45 micron square area within which the step scans were made. Surface porosity was clearly shown in the backscatter displays.

Quantitative scan data were transferred from the strip charts to tabular form and analyzed for variance based on 95% confidence limit criteria.

Prior to ranking the product homogeneity, the data were tested first to:

1) determine that the CP data population variance was significant with respect to the variance due to instrument background variations;

2) determine that the population variances were the same for the duplicate sets of data for the CP (2 scans on same pellet) and the MB-dry (2 scans on the same pellet plus 1 scan on a duplicate pellet). The data were then tested to establish that the CP material was in fact more homogeneous than the MB-dry material.

The analysis showed that the point-to-point deviation of plutonium concentration of the mechanically-blended oxide was $\pm$ 3% which is only slightly greater than the value of $\pm$ 1.4% for coprecipitated material. The results are summarized in Table III.

The ability to control lot-to-lot macrohomogeneity during mechanically-blended fuel fabrication can best be illustrated by experience gained during manufacture of 530 kgs of 6.6% PuO_2-UO_2 pellet fuel. As shown in Table IV, product lot sample assays for plutonium varied from 5.75 wt % to 5.85 wt % Pu which represents a spread of only 0.1 wt % Pu. This result was achieved for 13 blend lots which were prepared in a twin-shell blender. The lot size was 35 kg.

After powder blending, the fabrication process follows a stepwise path which is similar to UO_2 pellet manufacturing practice, with modifications added to provide alpha containment. The process lends itself well to the stringent pellet inspection requirements which are necessary for reactor loadings. A typical dry process flowsheet suitable for PuO_2-UO_2 fast reactor fuel is shown in Figure 1. Each process step utilizes a separate glove box unit.

Pelletizing

Fuel shapes are continuously and automatically fabricated by mechanical compression of a powder possessing suitable physical characteristics. Such a powder must be free flowing for uniformity and duplication in the filling of the die and must impart to the compacted piece sufficient green strength to allow normal handling. Sinterable grade ceramic powders have an average particle size of about one micron, and as such are not free flowing. Therefore, the powder must be agglomerated either by dry pre-pressing at 4 to 8 TSI or by mixing with a solution of soluble wax and drying. A lubricant such as stearic acid is usually added to the granulated material to maintain the free flowing characteristics and to facilitate release from the die following compaction. Coprecipitated and mechanically-blended powders of PuO_2-UO_2 are generally compacted at 10 to 30 TSI to give a resultant green shape which has a density of 40 to 55 percent theoretical. Lower compaction pressures are insufficient to give suitable strength to the body and result in excessive shrinkage during sintering. Higher pressures cause conical end cracking unless a binder is utilized.

Sintering

Final densification of the compacted fuel shape is achieved by high temperature sintering. In this process the individual particles coalesce giving rise to grain growth, solid solution formation, and volumetric shrinkage. All of these effects are time, temperature, and atmosphere dependent. Furthermore, traces of chemically bound water or unconverted compounds will volatilize and thus may influence the pellet structure.

Sintering studies for PuO_2-UO_2 compositions have been carried out extensively. In general, the system can be described as one of complete solid solution between the component dioxides but complicated in the PuO_2-rich region by the formation of lower oxides, namely α-Pu_2O_3. This formation occurs in the reducing atmosphere which is necessary to maintain the stoichiometry of the UO_2 and at the temperatures required for sintering, 1500 to 1700°C. Various sintering atmospheres have been utilized; Ar, Ar-H_2, CO_2-CO, N_2-H_2, H_2, He, He-H_2. The non-explosive nature of Ar-H_2, N_2-H_2 and He-H_2 where the hydrogen content is below 8 percent is especially well-suited for venting into closed glove boxes. The reducing characteristics of such gases are less pronounced than pure hydrogen, but suitable oxygen/metal ratios are obtained during sintering. The behavior of molybdenum furnace heating elements in such atmospheres is also satisfactory.

The maximum practical charging rate of PuO_2-UO_2 in a continuous pusher furnace operating under a non-explosive N_2-6% H_2 atmosphere is limited by the in situ formation of large amounts of moisture from the reduction of super-stoichiometric oxide contained in the green pellets. If the charging rate is excessive, a high ratio of water partial pressure to hydrogen partial pressure can occur in the furnace atmosphere, resulting in cracked pellets, distorted pellet shape, or excessive "dishing". This condition can be corrected by increasing the gas flow rate, improving the countercurrent gas flow pattern or reducing the pellet charging rate. Decreasing the excess oxygen content of the green pellets by powder reduction or by presintering will also increase the sintering furnace capacity, in accordance with straight-forward stoichiometry considerations. Local temperature profiles and gas compositions in the discharge or cooling zone of the furnace are considered to be important factors in freezing the final pellet stoichiometry levels. Quantitative data on equilibrium oxygen partial pressure for mixed oxides[4] and the U-O and Pu-O systems are being used to set allowable ranges of gas compositions and to improve pellet stoichiometry control.

The lot-to-lot variability in pellet oxygen/metal ratio during production sintering of mechanically-blended 6.6% PuO_2-UO_2 is shown in Table IV. The oxygen/metal ratio of 13 production lots averaged 1.99 with a standard deviation of 0.01.

Density and size control of sintered pellets in the range 93-95% T.D. is achieved by the same techniques developed for UO_2, that is, by controlling pellet green density and size. Sintering temperature is adjusted initially within the range of 1550°C to 1650° $\pm$ 50°C. Final pellet density is maintained within $\pm$ 1 to $\pm$ 2% T.D. of the average.

Press feed properties, and sintering temperature are held constant. The die size is changed to compensate for different powder properties.

Recent results have shown that control of pellet density in the range of 91 to 93% T.D. is possible using a dry slugging-granulating process. Figure 2 shows typical fired density versus green density curves as a function of slugging pressure and granule particle size. The starting powder was 20% PuO_2-UO_2 having a surface area of 5 M^2/g and Fisher Subsieve size of 0.9 microns. In general, coarse particle sizes, high slugging pressures, and low pellet pressing pressures result in decreased density. The slugging-granulating method also offers a flexible means of controlling open and closed porosity. In general, high slugging pressures, an absence of "fines", and low pellet pressing pressure lead to open porosity. By decreasing slugging pressure, introducing "fines", or increasing pellet pressing pressure, the structure gradually changes to a higher ratio of closed to open pores. Porosity may be varied from 16% open/0.8% closed to 0.9% open/4% closed.

Density control in the region below 91% T.D. can be achieved by several approaches that offer the possibility of control with further development. These methods include the dry addition of organic (burnable) pore formers and the presintering of ceramic grade powders prior to pellet fabrication. Dry additions of 1.5 to 3% methylcellulose,

sucrose, dextrose and carbowax yield adequate control of density range, providing that the organic additive is removed prior to sintering by heat treatment in CO_2 at 880°C. The addition of powder presintered at 1400-1600°C in N_2-6% H_2 has also been used to obtain reduced pellet density. For example, a 25% addition of 1600°C presintered powder to virgin powder permits density control in the range of 88 to 91% T.D.

Pellet Grinding

Centerless grinders of two types have been used for obtaining close control of pellet diameter; belt centerless grinders and abrasive wheel grinders. These machines are capable of controlling diameters to ± 0.0005 - 0.001 inch on pellets of about 0.2 inch to one inch in diameter. Machines of both types ordinarily require a recirculating water spray for cooling and lubrication during grinding. Critical mass control is therefore a problem as the grinder sludge is entrained in the coolant. Control has been accomplished either by weighing pellets before and after grinding and limiting plutonium accumulation within the safe limit (250 grams) by accountability or by limiting the total liquid volume to less than 3 liters.

Tube Loading and Welding

Pellet loading and weld area decontamination represents the transition point in the process between complete glove box containment and secondary containment in an open-front hood. In general, all external cladding surfaces should be protected from contamination throughout the loading process. Usually the only area requiring decontamination is the internal surface of the tube in the end cap area. It is critical that this area be clean as contamination is otherwise trapped in the weld metal and can never be removed. Vinyl tape over the external tube end protects the surface and can easily be removed during decontamination. At least two techniques have been successfully utilized for attaching the tube end to the glove box while keeping the external tube surface outside the box. The most universally applicable technique is to attach a number of tubes to projections formed in a plastic pouch by means of tape and using the standard bagging procedure to connect to a bag port. After loading, the vinyl projection tubes are sealed off with a dielectric sealer and the bag remnant carefully removed from the tube end in an open front hood. The tube end is decontaminated with alcohol-dampened cloth patches and swabs. Clearance is needed between the fuel material and the tube end in order to thoroughly decontaminate the weld area. A plastic or rubber breather plug is then inserted in the tube to contain the fuel and control contamination during subsequent evacuation in the vacuum welding box. An alternative technique which can be used with relatively dust-free pellets is to insert the tube through a rubber grommet mounted in a wall between a glove box and a ventilated air lock or open front hood. Only the tape protected end of the tube is inserted for loadings. After loading, the end is withdrawn into the air lock, decontaminated, and closed with the previously described plastic plug. The second end cap is then inserted and the tube closed by conventional welding techniques. Welding is usually performed in an evacuable chamber backfilled with inert gas.

Coprecipitation Process for Mixed Oxide Fuel Pellet Fabrication

As an alternate to the mechanical blending process described above, mixed oxide pellets have also been fabricated from powder prepared by the coprecipitation process. The coprecipitation process provides slightly improved microhomogeneity and a greater assurance of solid solution in the final product. This process has been used for fabrication of fuel for physics tests and for reference materials which are used in irradiation testing and thermophysical property measurements.

The preferred chemical blending process is based on the coprecipitation of a plutonium hydroxide-ammonium diuranate intermediate compound from mixed uranium-plutonium nitrate solution, followed by filtration, washing, drying, thermal decomposition, and reduction in a N_2-6% H_2 atmosphere.

The corresponding mixed oxalate or mixed peroxide coprecipitation processes are unsatisfactory because of high solubility losses, incomplete solid solution, and sub-standard powder sinterability.

The following features led to the choice of the ammonium diuranate plutonium hydroxide conversion route as a final process.

1. The coprecipitation process was uniquely suited to the preparation of the required single-phase homogeneous mixed oxide ceramic fuel.

2. The continuous precipitation process took advantage of extensive large-scale experience with the closely-related ADU/UO_2 conversion route which minimized the cost of development and assured better control of product quality.

3. The process chemistry met requirements of close U/Pu composition control, flexibility in the choice of precipitants (i.e., gaseous ammonia or ammonium hydroxide), negligible corrosion contamination, and low plutonium waste losses.

4. Preliminary studies showed that the operational safety of the hydrogen atmosphere furnace reduction step could be maintained by using a dilute non-explosive mixture without sacrificing product quality.

Pre-assayed uranyl nitrate and plutonium nitrate solutions are blended to yield feed solution containing 0.4 - 0.6 mols (U+Pu) per liter and 1.0 mols free acid/liter. The feed solution and ammonia precipitant are contacted in an agitated precipitator at a temperature of 50-55°C. An average residence time of 25 $\pm$ 5 minutes is used to obtain satisfactory particle size and agglomerate structure. The slurry is continuously filtered and washed by reslurrying-filtration. After air-drying at 180-220°C, the solid material is thermally decomposed and reduced to uranium-plutonium dioxide in a nitrogen-6% hydrogen atmosphere at 850°C for 1-1/2 hours. The product is hammer-milled to eliminate agglomerates prior to use. A process flow diagram is shown

in Figure 3. The major process variable affecting final product sinterability is the time-temperature history during thermal decomposition and reduction. Precipitation transient conditions, ammonia concentration, pH, and the ammonium nitrate residue in the intermediate product after washing, were also variables which influenced the final oxide properties; however, these variables are easily controlled in practice.

The major control features underlying the successful use of this process for mixed oxide containing up to 35 percent PuO_2 are:

1. The basic powder properties required for pellet fabrication by cold-pressing and sintering to 93-96 percent density are controllable within acceptable limits. This includes homogeneity, purity, particle size, bulk density, tap density, surface area, and oxygen/metal ratio.

2. Key properties can be closely controlled to meet specific fabrication requirements, for example:

   a. The plutonium content can be controlled to a relative accuracy of $\pm$ 0.5 percent.

   b. Any desired surface area within the range 3-12 M^2/g can be obtained by controlling the reduction temperature, residence time, and gas atmosphere.

   c. Reduction time and temperature may both be used to control the final oxygen/metal ratio within the range of 2.10-2.30.

   d. Subsequent heat treatment in CO_2 can be used to adjust the oxygen/metal ratio downwards and to reduce surface area.

3. The basic precipitation process gives low aqueous Pu losses (0.01%). Clarified filtrate is decontaminated by an inexpensive standard water-treatment flocculation process prior to discharge to the environment.

Fabrication of pellets from coprecipitated PuO_2-UO_2 powder utilizes the same techniques described in the previous section, however, in order to guarantee reproducibility of powder fabrication characteristics additional precautions are required. Cross-blending is required for "levelling" of properties on a day-to-day basis during continuous operation. This requirement could be minimized by sophisticated process controls and by maintaining production at a steady rate; however, utilization of all material, including powder produced during transient operating conditions is an economic necessity and must be provided for by cross-blending. It should be pointed out that the coprecipitation process does not have the inherent size advantage of the established multi-ton batch ADU process used for the production of sinterable-grade normal or depleted UO_2 used in the mechanical blending process.

EQUIPMENT AND FACILITIES

Fuel Fabrication

The mixed-oxide ceramic fuel fabrication facility at NUMEC has been designed to fabricate full reactor core loadings, meeting a wide range of specific fuel parametric specifications. This degree of flexibility has been achieved by utilizing a unit process approach in the equipment design. The equipment to perform each unit process is installed within its own glove box and is complete. A fuel manufacturing line is then assembled by locating each unit process glove box in the proper sequence and then connecting boxes together with gloveport transfer tunnels to reduce handling and to allow continuous flow of product from one unit process to the next.

Utilizing this concept, we have fabricated and loaded 400 kilograms of 6.6% PuO_2-UO_2 fuel for the SAXTON reactor, involving 70,000 pellets which were produced from mechanically mixed PuO_2-UO_2. Then, by re-arrangement of the unit processes and substitution of a few process alternatives, 500 kilograms of 1.5% PuO_2-UO_2 fuel was produced for a critical assembly, involving 30,000 pellets made from mechanically-blended and coprecipitated powder. Another rearrangement allowed the fabrication of 30,000 20% PuO_2-UO_2 fast fuel pellets from mechanically-blended and coprecipitated powders. Irradiation testing of these pellets contained in encapsulated fuel rods is now underway in EBR-II. Performance data will provide feedback to determine the optimum process.

Greatly increased manufacturing capability can be obtained with the above approach, by duplicating unit process modules which limit the overall production capacity.

While this approach, at the present state of equipment development, does not result in a semi-automatic, low-hand contact, high capacity pellet production line and minimum projected fuel costs, the development of improved equipment for automating a few of the critical unit processes will be a major step toward such a line. Unfortunately, at the present time and for at least the next five years, the projected plutonium fuel fabrication business cannot justify much more commercial production capability than currently exists. Between the present two major commercial plutonium fuel fabricators (those who have produced over 50 kilograms of plutonium as mixed-oxide fuel), there is an existing mixed-oxide pellet fuel production capacity well in excess of three fast reactor cores per year and this capacity could easily be doubled within a short time.

Additional capacity can be gained by adding improved equipment for powder and press feed preparation for the mechanical blending process. Other equipment items designed specifically for plutonium, such as the continuous sintering furnace shown in Figure 5, have given reliable service and therefore require only improvements relating to gas atmosphere control in order to gain capacity.

Improved finishing and inspecting equipment including centerless grinders, pellet cleaning stations, pellet automatic gaging and plutonium compositional monitoring devices will be used to augment capacity up to the point of fuel rod loading. Adequate loading and welding equipment is already available and improvements now being made in the rapidly-growing UO_2 fuels manufacturing industry will be directly applicable to PuO_2-UO_2 fuel manufacture.

Recycle and Scrap Recovery

Recycle of fabrication scrap on a current basis and recovery of plutonium from end-of-job scrap, require facilities for dissolution, ion-exchange or solvent extraction partitioning of mixed actinide streams and plutonium product concentration. Experience has been gained during the operation of an ion-exchange pilot plant facility in which 30 kgs of plutonium was recovered from mixed-actinide scrap. Using this experience as background, improved facilities have been designed and are being installed for recovery and purification of plutonium as plutonium nitrate or plutonium oxide. Additional process and equipment development is needed to control plutonium losses in low-level raffinate streams and solid waste streams.

Since the current price of plutonium is $43,000 per kilogram, about four times higher than ^{235}U, the penalty for losses which occur during fabrication is extremely severe. The high material cost also results in lease charges and insurance charges which are four times higher than for ^{235}U processing. These considerations may require future plants to have higher throughput and lower holdup in order to minimize in-plant inventory. Rigidly controlled materials management and exploitation of high-yield processes are mandatory. The problem of reducing scrap generation and non-recoverable losses in plutonium processing is one of the most important economic challenges to be met during the growth of this industry.

Product Quality Assurance

Fast test reactor fuel and demonstration power reactor fuels will be purchased to rigid specifications designed to assure the quality and reliability needed for high-rating performance. Specifications are still under development, and feedback from manufacturing experience and performance tests will be used to establish limits. Confidence limits will be based on manufacturing experience and fuel designers' requirements. Resolving the details of product assurance for PuO_2-UO_2 fast fuels is a major task to the fuel manufacturer and to the designer, since the relationships between fuel performance, and product variability are not yet established. Although cost vs product variability relationships can be estimated from manufacturing experience with UO_2-based fuels, establishing the economic crossover point will remain a major challenge.

Acknowledgement

The authors wish to acknowledge the valuable contributions to this report provided by Dr. I. D. Thomas, Mr. Mario Zambernard, and Mr. Robert Seider. A portion of the development work was carried out under USAEC Contract AT(30-1)-3524.

References

1. D. G. Boyer and E. I. Goodman, "Civilian Uses and Production of Plutonium in the U. S.", Symposium on Plutonium as a Reactor Fuel, Brussels, March 1967.

2. C. A. Burgess, B. R. Hayward, W. E. Roake, "FFTF Fuel Suppliers' Meeting", BNWL-SA-1388, Richland, Washington, August 1967.

3. C. S. Caldwell and I. D. Thomas, "Plutonium-Uranium Mixed Oxide Preparation and Fabrication Experience", presented at A. I. Ch. E. National Meeting, San Francisco, 1965.

4. L. E. J. Roberts, et.al., A/Conf. 28/P/155; 11 464-71 3rd United National International Conference on Peaceful Uses of Atomic Energy, Geneva, 1965.

Table I

Typical Properties of Sinterable-Grade Oxide Powders

Material	Route	Furnace Conversion Temp°C	Milling	Bulk Density g/cc	Tap Density g/cc	Surface Area M^2/g	Fisher Sub-Sieve Size microns	Sedimentation Average Particle Size microns	Sintered Density 1 hour - 1650°C % of theoretical density Atmosphere: Air	Atmosphere: N_2-6% H_2
PuO_2	IV Oxalate	760	0	1.4-1.9	2.0-2.9	3.5-9.5	1.5-3.0	2.0-4.0	91.5-92.5	89.0-91.0
PuO_2	III Oxalate	760	0	1.2-1.5	1.7-1.9	1.6-4.8	1.5-5.0	3.0-4.0	90.0-91.5	85.0-89.0
PuO_2	IV Peroxide	490	HM	2.0-2.8	4.0-4.9	20.0-26.0	1.0-2.0	3.8-5.8	86.5-91.5	81.0-90.0
PuO_2	Direct Oxidation	760	DBM	4	5	3-4	--	1.0-1.5	--	--
$(U\text{-}20\%\ Pu)O_2$	ADU-$Pu(OH)_4$	840	HM	0.8-1.4	1.7-2.1	5.0-8.5	0.4-0.6	0.6-1.2	--	95.3-97.5
UO_2	ADU	500-600	HM	0.7-1.0	1.7-1.9	8.0-9.5	0.5-0.9	0.8-1.5	--	93.5-96.5

NOTE: Ranges illustrate typical upper and lower limits obtained during materials evaluation tests. Normal control bands are generally narrower.

HM: Hammer-Milling

DBM: Dry Ball-Milling

Table II

Safe Mass Limits for Water Reflected Systems Containing PuO_2

25 wt % PuO_2-UO_2 Systems	Safe Mass Limit[2] Kg Pu	Kg PuO_2-UO_2
Fuel in Solution	1.0	4.8
Fuel Pellets in Water	1.1	5.1
3 Ft. Fuel Pins in Water (Optimum Spacing)	2.0	9.1
High Density Pellets (Unmoderated)	22	100
3 Ft. Fuel Pins (Unmoderated)	47	215
Low Density Powder (Unmoderated)	59	270
100% Pu Systems		
Solution	0.25	
High Density PuO_2 Powder (Unmoderated)	4.6	
Low Density PuO_2 Powder (Unmoderated)	8.6	

Table III

Statistical Analysis of Microhomogeneity in 15% PuO_2-UO_2 Sintered Pellets

(Electron Microprobe Step Scan - 1 Miron Spot x 1 Micron Step)

		Plutonium Concentration	
		CP Dry	MB Dry
Sample Variance	s^2	0.08346	0.6570
Standard Deviation	s	0.289	0.811
Percent Deviation		1.4%	3.1%

		Uranium Concentration	
		CP Dry	MB Dry
Sample Variance	s^2	0.4076	1.3678
Standard Deviation	s^2	0.638	1.169
Percent Deviation		0.76%	1.4%

Table IV

Lot-to-Lot Variability during Manufacture of 6.6% PuO_2-UO_2 Pellet by Mechanical Blending Process

Lot Number	Pu Assay wt %	Oxygen/Metal Ratio
1	5.78	1.978
2	5.86	2.018
3	5.79	1.981
4	5.75	2.009
5	5.75	1.978
6	5.81	1.983
7	5.81	1.991
8	5.85	1.979
9	5.85	1.979
10	5.78	1.986
11	5.81	1.981
12	5.83	1.980
13	5.78	1.996
Average	5.80	1.988
Std. Deviation	0.04	0.012

MECHANICALLY BLENDED PuO_2-UO_2 PIN FABRICATION

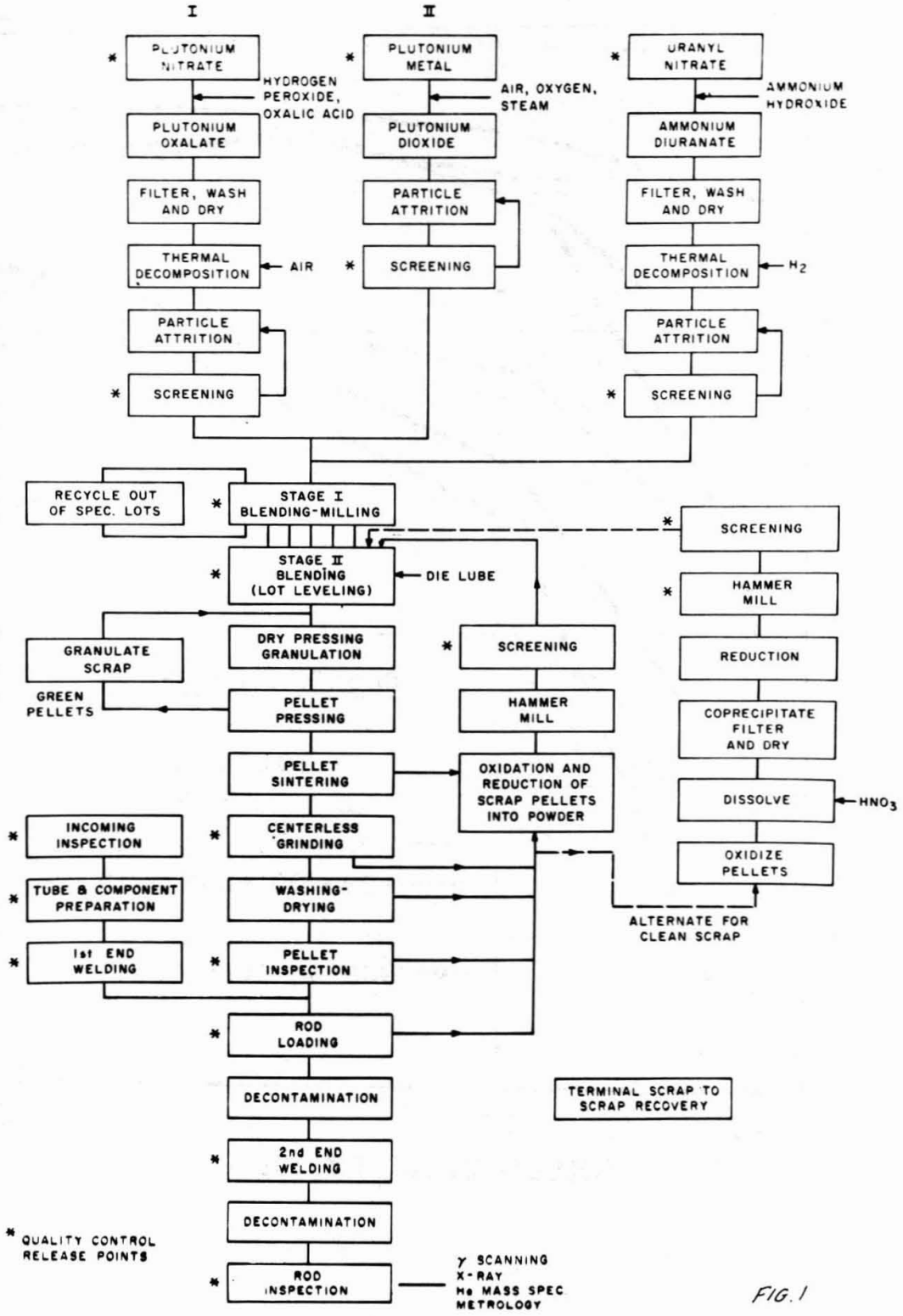

FIG. 1

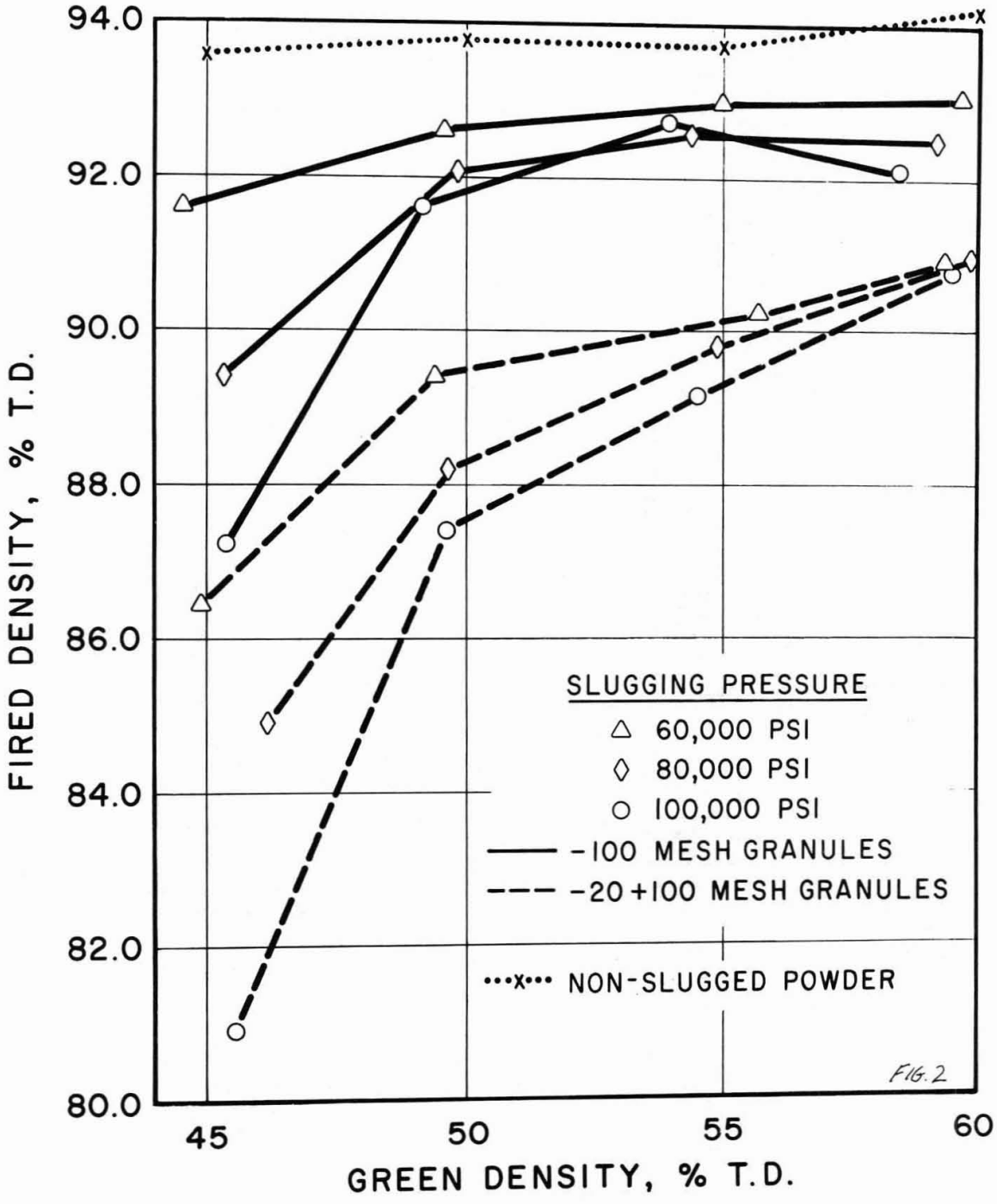
94.0
92.0
90.0
88.0
86.0
84.0
82.0
80.0
FIRED DENSITY, % T.D.
45
50
55
60
GREEN DENSITY, % T.D.
SLUGGING PRESSURE
△ 60,000 PSI
◇ 80,000 PSI
○ 100,000 PSI
—— -100 MESH GRANULES
– – – -20 +100 MESH GRANULES
···x··· NON-SLUGGED POWDER
FIG. 2

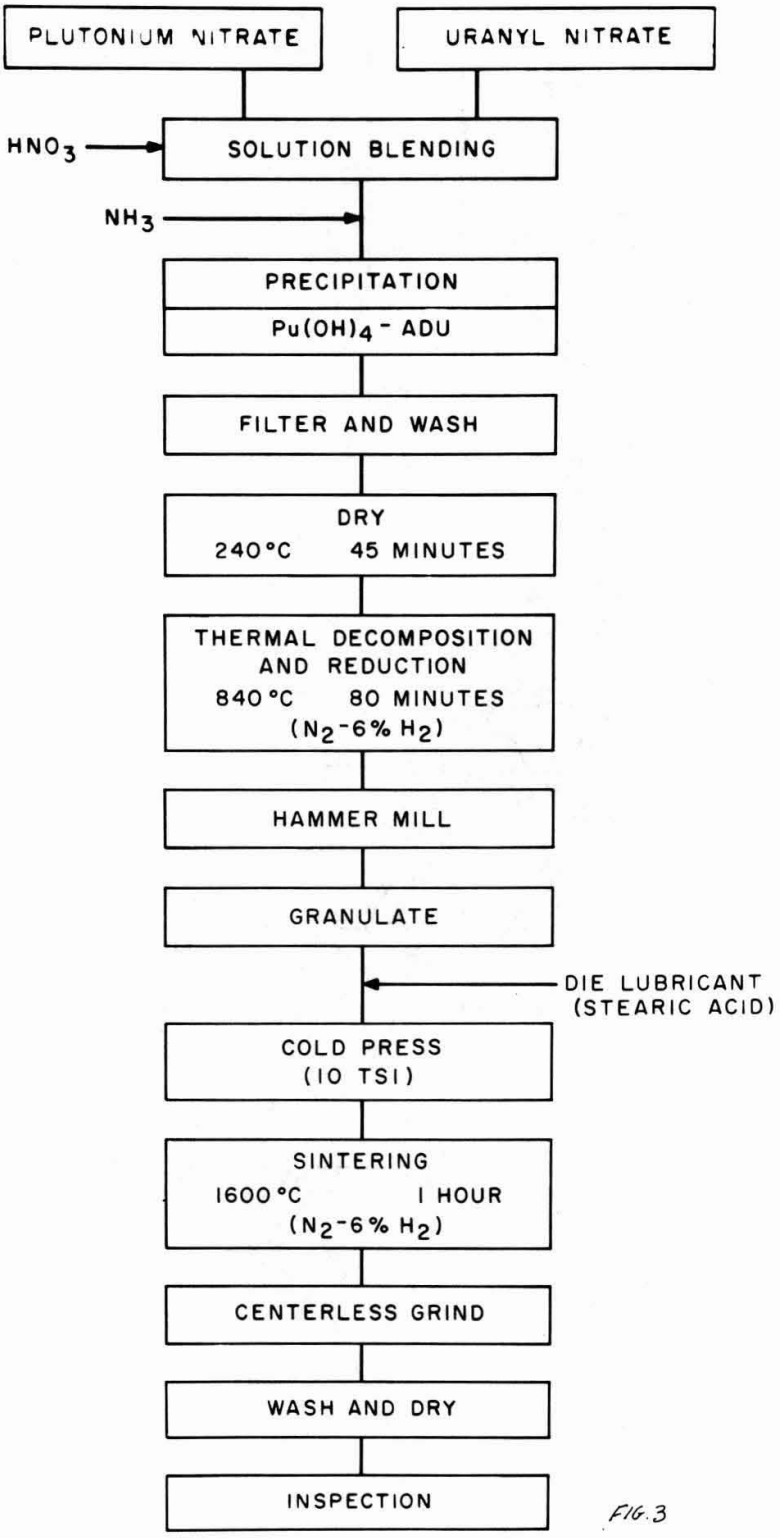
PLUTONIUM NITRATE
URANYL NITRATE
HNO_3
SOLUTION BLENDING
NH_3
PRECIPITATION
$Pu(OH)_4$ - ADU
FILTER AND WASH
DRY
240°C 45 MINUTES
THERMAL DECOMPOSITION AND REDUCTION
840°C 80 MINUTES
(N_2-6% H_2)
HAMMER MILL
GRANULATE
DIE LUBRICANT (STEARIC ACID)
COLD PRESS (10 TSI)
SINTERING
1600°C 1 HOUR
(N_2-6% H_2)
CENTERLESS GRIND
WASH AND DRY
INSPECTION

FIG. 3

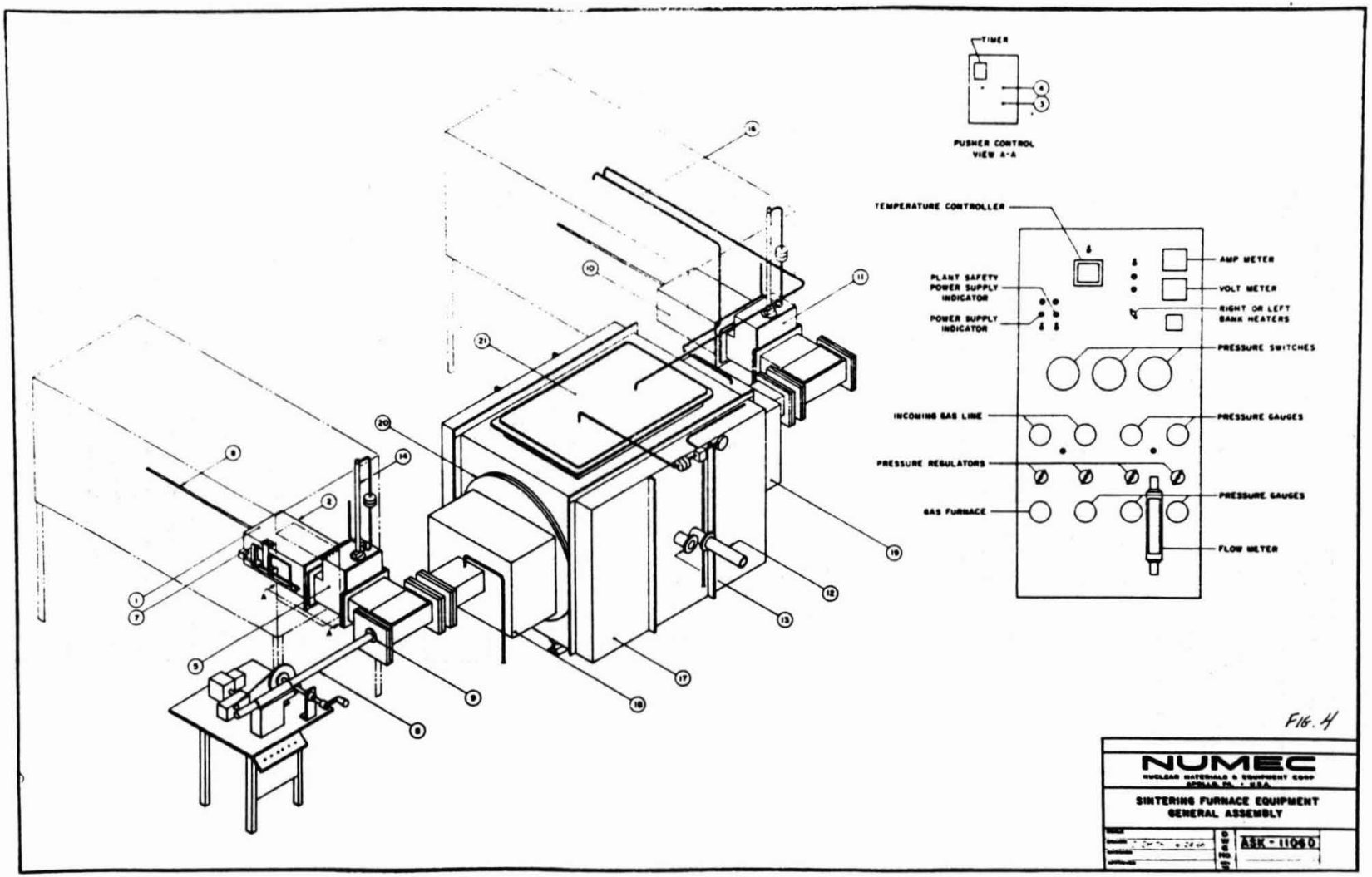
TIMER
PUSHER CONTROL
VIEW A-A
TEMPERATURE CONTROLLER
PLANT SAFETY
POWER SUPPLY
INDICATOR
POWER SUPPLY
INDICATOR
AMP METER
VOLT METER
RIGHT OR LEFT
BANK HEATERS
PRESSURE SWITCHES
INCOMING GAS LINE
PRESSURE GAUGES
PRESSURE REGULATORS
GAS FURNACE
PRESSURE GAUGES
FLOW METER
NUMEC
SINTERING FURNACE EQUIPMENT
GENERAL ASSEMBLY
ASK-11040

FIG. 4

SOL-GEL URANIA-PLUTONIA MICROSPHERE PREPARATION AND FABRICATION INTO FUEL RODS*

F. G. Kitts
Chemical Technology Division
R. B. Fitts and A. R. Olsen
Metals and Ceramics Division
Oak Ridge National Laboratory
Oak Ridge, Tennessee

Abstract

The sol-gel process, originally developed for thorium-base fuels, is currently being exploited to produce experimental quantities of urania-plutonia fuel material. This process provides an intimate mixture of fissile and fertile elements in an oxide of almost theoretical density. Although various fuel material preparation and fabrication processes are being studied at ORNL, this paper is limited to a discussion of the preparation of UO_2-PuO_2 microspheres and the development of a low-energy vibratory compaction technique (Sphere-Pac) for using these particles to prepare cylindrical fuel rods. Presently, mixed-oxide microspheres are prepared in ∿100-g batches in a facility consisting of three glove boxes: one for PuO_2 sol forming, one for sol mixing and microsphere forming and drying, and one for firing and classification. The test fuel rods are loaded and closure welded in two additional boxes.

Plutonia sol is formed by precipitation of the hydrous oxide from nitrate solution using excess NH_4OH, thorough washing of the precipitate, peptization at a NO_3^-/Pu mole ratio of 2, thermal denitration to a NO_3^-/Pu ratio of 0.1-0.2, and resuspension in water to a concentration of ∿300 g of Pu per liter. This material is mixed with urania sol[1] to obtain the desired composition. Microspheres are formed by dispersing the homogeneous mixture in 2-ethyl-1-hexanol, which dries the droplets to gel spheres. After separation of the gel from the alcohol and further drying, firing to 1100°C yields dense (≥95% of theoretical) microspheres.

The Sphere-Pac fabrication process, employing the sequential loading of two size fractions of these microspheres into vibrated tubes, yields a volume packing density approaching 85%. Laboratory experiments show that for our conditions the best Sphere-Pac results are obtained using ∿400 and <44-μ-diam spheres and 60-cps mixed axial and lateral vibration. The test fuel rods are closed by remote, automatic, Tungsten Inert Gas welding techniques.

Since nitrate solutions, the products of aqueous reprocessing, are the starting materials for both sols, the sol-gel approach to refabrication is consistent with established recycle technology. The adaptability of PuO_2 sol and UO_2-PuO_2 microsphere forming to semiremote techniques, necessitated by the accumulation of heavy-isotope radioactivity with recycle, will be demonstrated in a recently-completed facility with a nominal kilogram-per-day capacity. The Sphere-Pac technique appears to be well suited to remote fabrication. The irradiation performance of sol-gel-derived mixed-oxide microspheres fabricated by the Sphere-Pac technique is being determined by tests now in progress.

*Research sponsored by the U. S. Atomic Energy Commission under contract with the Union Carbide Corporation.

INTRODUCTION

The first ORNL sol-gel process was developed for the preparation of thoria sol, and was applied to the production of dense, irregularly shaped UO_2-ThO_2 fragments for vibratory compaction into tubes in the Kilorod Program.[2] The process was then adapted to the preparation of microspheres.[3] More recently it has been adapted to UO_2, PuO_2, and ZrO_2 and to mixtures of PuO_2-UO_2, PuO_2-ThO_2, and UO_2-ZrO_2. The sol-gel approach to all of these potentially useful reactor fuel materials is simple, yields a homogeneous product, and requires relatively low sintering temperatures (1100 to 1200°C) to produce the final dense, refractory fuel material. Development work at ORNL is presently concerned with the preparation of many types of fuel material based on the sol-gel process and with fuel element fabrication by a variety of methods. However, this paper is restricted to the discussions of preparing PuO_2 sol, mixing PuO_2 and UO_2 sols, forming, drying and firing microspheres, and the low-energy vibratory compaction of this dense product (Sphere-Pac) to prepare cylindrical fuel rods.

PREPARATION OF UO_2-PuO_2 MICROSPHERES

More than 4 kg of 15-20% PuO_2-UO_2 and 0.5 kg of 5% PuO_2-UO_2 microspheres have been produced, in batches of 50 to 150 g, in the ORNL development facility in the Chemical Technology Division Pilot Plant. Most of these spheres were 300-600 μ in diameter; however, enough fines (<44 μ in diameter) were produced to give a coarse material/fines ratio of approximately 3. Densities were generally $\geq$95% of theoretical. All this material was prepared by using the standard ORNL sol-gel process, which consists of sol forming, sol mixing, and sphere forming. Spheres $\geq$50 μ in diameter are formed in a tapered column, while fines (<44 μ in diameter) are made by the "stirred pot" method.[4] After drying, the spheres are fired to the dense oxide under controlled atmospheres at temperatures up to 1100°C. They are then classified with respect to size and roundness.

PLUTONIA SOL FORMING

Over forty plutonia sols (50-150 g of plutonium per batch) containing over 3 kg of plutonium have been prepared using the standard procedure of precipitation, washing, peptization, denitration, and resuspension. These preparations demonstrated the operability of equipment and the reproducibility of the standard flowsheet, and provided sol for the formation of mixed-oxide and plutonia microspheres.

The generalized flowsheet for the formation of plutonia sol is presented as Fig. 1. This is a flexible flowsheet as shown by the ranges of concentrations over which it has been demonstrated; the batch size shown is 150 g of plutonium. Prior to the use of this flowsheet, if necessary, NO gas is passed through the $Pu(NO_3)_4$ solution to convert both Pu^{6+} and Pu^{3+} to the desired Pu^{4+}. To date the $Pu(NO_3)_4$ solution that we have received has not required a plutonium valence adjustment. A minimum HNO_3 concentration of 1 M is maintained in the feed to prevent polymerization; successful sol preparation starting with free HNO_3 concentrations

as high as 3 M has been demonstrated. In the precipitation step, as little as 48% excess base has proved satisfactory as long as the molarity of the NH_4OH in the final solution is $\geq$1 M. The $Pu(NO_3)_4$ feed solution is added to the NH_4OH solution at rates up to 30 cc/min with moderate agitation to ensure rapid neutralization and precipitation of the $Pu(OH)_4$. The NH_4NO_3-excess NH_4OH solution is drawn off through a filter having 10-μ-diam openings. The precipitate is washed four times; the filter cake is resuspended in each wash. Filtration time is ∿40 min/wash, and four such washes give adequate NH_4^+ removal. Plutonium losses to the total filtrate have been less than 0.01%. After washing, the precipitate is digested for 2 hr in H_2O at 95-100°C; this treatment appears to stabilize the crystalline structure and prevents depolymerization in the subsequent denitration step. A high-nitrate sol is then formed by peptizing in dilute HNO_3 at a NO_3^-/Pu mole ratio of ∿2. All the steps to this point are carried out in a single precipitation-filtration vessel that is 8 in. in diameter with a porous stainless steel filter in the bottom. The high-nitrate sol passes out through the bottom of the vessel, leaving no solids on the filter.

A minimum NO_3^-/Pu ratio of 1 is necessary for sol formation. Ratios as high as 4 have been demonstrated, but a ratio of 2 is sufficient to produce a sol upon heating to ∿90°C. At this point a true sol (crystallite size ∿20 A) exists, but microspheres formed from this material have a low density and a low resistance to crushing. To form a desirable product, a sol must have a NO_3^-/Pu ratio in the range 0.1-0.2; this is accomplished by thermal denitration (baking). Several other methods of precipitation and denitration were tried, but none produced satisfactory results.[5]

The sol is first evaporated to dryness at 100°C, forming a thin, porous cake that remains intact through subsequent heating to ∿240°C. The higher the temperature, the shorter the time required for denitration. During the evaporation to dryness, excess HNO_3 is evolved, giving an initial NO_3^-/Pu ratio of 0.8-1.0 in the dry solid. Generally, after 1-2 hr at 240°C this ratio will have been reduced to 0.2-0.3; usually another 2-3 hr is required to attain a final NO_3^-/Pu ratio of 0.1-0.15. Progress of the denitration is followed by periodically resuspending a weighed sample of the dry material and titrating with NaOH to determine the NO_3^- content. It is important that the heating of the solid be uniform in order to produce a homogeneous product. If denitration is allowed to proceed until the NO_3^-/Pu ratio is appreciably <0.1, a form of PuO_2 that cannot be resuspended as a sol will result. A schematic of the denitration vessel, which allows independent control of temperatures of the top and bottom surfaces and limits radial gradients to ∿2°C, is shown as Fig. 2.

In addition to the decrease in NO_3^- concentration, crystallite growth and agglomeration also occur during the denitration step. After this step, the average size of the crystallites is ∿80 A; these form agglomerates on the order of 1000 A. Crystallite growth is apparently not detrimental, but the degree of agglomeration must be limited if a stable sol is to be obtained. Denitrated sol having a NO_3^-/Pu ratio in the range of 0.1-0.15 can be resuspended in water, by only mild agitation,

to form sols having plutonium concentrations approaching 2 M; more-concentrated sols may be produced by subsequent evaporation if desired.

FORMING OF PuO_2-UO_2 GEL MICROSPHERES

Sols droplets are converted to spherical gel particles by the extraction of water into an organic liquid such as 2-ethyl-1-hexanol, in a tapered column. To form wet gel microspheres of PuO_2-UO_2 it is necessary to:

1. Measure the separate sols to produce the desired composition, combine, and mix thoroughly.
2. Disperse the mixed sol into droplets of the proper size and suspend them in an immiscible liquid that will remove water to cause gelation.
3. Maintain the droplets as separate particles in the drying medium until they gel.
4. Maintain a constant drying condition in the solvent by removing water from it at approximately the same rate that it is extracting water from the sol.
5. Separate the gel spheres from excess solvent.

The first step, sol mixing, is very important since this is the point at which the final composition of the fuel particle is determined. In the work reported here, the urania sol concentration was 0.75 to 1.0 M and the plutonia sol concentration was 1.1-1.4 M. Mixed sols were made by measuring the required volumes of the analyzed sols and agitating. Simple sparging is not sufficient since it does not produce thorough mixing adjacent to vessel walls. Any system containing urania sol must be protected with an inert atmosphere at all times.

The Sphere Forming Column

Steps 2 through 4 listed above are accomplished in equipment similar to that shown schematically in Fig. 3. Sol is dispersed into droplets in a two-fluid nozzle at the top of a tapered drying column. This operation is important since the size of the ultimate particle is determined in this step. The rates of flow of the sol and the solvent through the nozzle are the principal determinants of droplet size, although sol concentration, viscosity, and nozzle configuration also play a part. The constancy of these flows, and nozzle dimensions affect the uniformity of the droplets. For diameters <800 μ a mathematical expression has been developed, assuming a varicose mechanism, which can be used as a first approximation in determining nozzle operating conditions to produce a given size range.[6] Final adjustments to obtain the desired product are based on experience with the particular system.

The sol droplets emerge in the top of a sphere forming or drying column where they are suspended by an upward flow of solvent. As water is extracted, the settling velocity of a sphere increases until ultimately it exceeds the solvent velocity in the throat (minimum diameter) of the column and it falls into the product receiver. The solvent entry, just below the throat, is tangetial, thus generating a vortex and flattening the normal parabolic velocity profile in the bottom section of the

column. This is necessary to keep spheres near the column wall from dropping out of the fluidizing zone prematurely. Our column is 5/8 in. at the throat, enlarging to 1-5/8 in. over 12 in. of height. For 350-500-μ-diam spheres the fluidizing flow is ∿1 liter/min. A sol flow of ∿1.2 cc/min and a normal residence time of ∿1/2 hr result in an average, steady-state column loading of ∿16%, based on sol volume.

In order to keep the droplets suspended as individual particles, the addition of surfactants to the 2-ethyl-1-hexanol is necessary. Although more than half of the PuO_2-UO_2 material was made with 0.3-0.6 vol % of both Ethomeen S/15 and Span 80,* 0.1 vol % Ethomeen S/15 and 0.4 vol % Span 80 was the most effective combination tried. Three common column malfunctions -coalescence, sticking, and clustering- can be caused by an improper surfactant system. Coalescence is the combination of two or more sol droplets to form an oversize droplet; this is usually most noticeable on startup. Sticking is the adherence of droplets to the wall of the column (usually smaller droplets, near the top) where they coalesce to form oversize droplets. Clustering is the adherence of spheres to each other while maintaining their original shape. This usually occurs when the spheres are partially dry and is not particularly detrimental unless the clusters drop out of the column prematurely.

One loop in the solvent recirculation system (Fig. 3) sends a stream of the drying solvent through a continuous still, which maintains a steady-state water content in the entire solvent system; this is represented schematically in Fig. 4. Saturated 2-ethyl-1-hexanol (2.5 wt % H_2O) boils at ∿100°C; dry solvent boils at ∿185°C. At a temperature of 170°C, effluent from the still contains ∿0.3 wt % water; the remainder of the water is vaporized overhead with ∿10 volumes of solvent. This stream separates into two phases upon condensation; the water (containing ∿0.1 wt % solvent) is disposed of as waste, while the relatively small volume of water-saturated solvent is returned to the still.

At the end of a period of column operation the gel microspheres are submerged in solvent in a small glass vessel with a fritted-glass bottom. This product receiver is disengaged from the bottom of the column, and the excess solvent is removed through the coarse (40-60μ) frit using vacuum.

DRYING AND FIRING

After removal of excess solvent the spheres are dried by passing argon up through the frit, with gradual heating to 150-170°C over a period of about 6 hr. This temperature is maintained for ∿16 hr, resulting in removal of most of the organic materials and residual water from the pores of the microspheres. In a few batches a steam-stripping step

*Proprietary products of Armour Industrial Chem. Co. and Allied Chem. Ind., respectively.

at 105-130°C was incorporated; this removed the 2-ethyl-1-hexanol more quickly but whether it has a beneficial effect on the final product has not yet been determined.

After the drying step the PuO_2-UO_2 gel spheres are fired at temperatures increasing to 1100°C at an average rate of ∿275°C/hr, using the following schedule of temperatures and atmospheres:

1. Heat to 450°C in argon-4% H_2.
2. Hold for 1/2 hr, then flush with argon for ∿5 min.
3. Heat to 850°C in CO_2.
4. Hold for 1-1/2 hr; then flush with argon for ∿5 min.
5. Heat to 1100°C in argon-4% H_2 and hold for 1/2 hr.
6. Cool to below 100°C in argon.

The total firing time is about 7 hr. A reducing atmosphere is maintained during heatup except for a period at intermediate temperatures when a mild oxidizing agent (CO_2) is used to burn out any carbon that may still be present as organic residues. Flushing with argon precludes the possibility of any reaction between H_2 and CO_2. After cooling, the dense spheres can be handled in air.

EVALUATION OF PRODUCT MICROSPHERES

After firing, the microspheres are sized using standard sieves, and the product fraction is passed over a roundometer to remove nonspherical particles. Table I shows the size ranges, total weights, number of batches, and physical properties of the three compositions of PuO_2-UO_2 microspheres produced in quantity to date. The properties of PuO_2-ThO_2 and PuO_2 spheres are also shown for comparison. Handling of the material containing enriched and normal urania was similar except that allowable inventories of the fissile material were much smaller. No significant differences in processing or properties were observed over the range of PuO_2 content (5-20%). The two size ranges of microspheres produced were roughly an order of magnitude apart as appears to be required for dense packing in tubes.

Densities of microspheres of all compositions were $\geq$95% except for the fines fraction. The fines, when compacted with the coarse fraction, gave composite densities consistent with their high-pressure densities (Table I) rather than with their bulk densities. Possibly the extremely small voids between the smaller spheres in the fines fraction appear as porosity in the analytical method used (Hg porosimetry), thereby causing the low bulk densities shown. Surface areas of the coarse materials were $\leq$0.06 m^2/g, and carbon levels were less than 100 ppm in all cases. Gas release on heating from room temperature to 1200°C was usually $\leq$0.05 cm^3/g. An average crushing strength of 600 g/sphere was measured for 300-μ-diam spheres of the 15% PuO_2-$^{238}UO_2$ material. Good reproducibility in crushing strengths was obtained; thirteen determinations gave a range of 475 to 725 g/sphere.

Electron microprobe techniques were used to measure the homogeneity of the 20% PuO_2-UO_2 material. Two cross-sectioned microspheres (∿400 μ

in diameter) were traversed at 10-μ intervals near the centers of the spheres and at 2-μ intervals near the edges. No significant differences in composition were observed. The maximum deviations from the calculated mean compositions were 1.9 and 1.5 wt % uranium.

REMOTE FACILITY

We have recently completed the installation, in Building 3019, of an alpha-contained, remote facility; it is capable of handling batches of PuO_2 sol containing 200 g of Pu and producing mixed-oxide microspheres at a rate of 1 kg per day. A schematic equipment flowsheet of this facility is presented in Fig. 5. The sol-forming equipment will utilize the chemical flowsheet in Fig. 1; the two principal pieces of equipment were described earlier. Operation in this facility should have several advantages over that in glove boxes. Manual operations have been minimized; those remaining will be performed with manipulators. All solution transfers will be made using gravity or vacuum techniques; solids will be conveyed hydraulically or pneumatically. Heat will be provided by steam rather than by electrical resistance elements; thus, heat-transfer surfaces will operate at lower temperatures without the possibility of severe overheating or element burnout. This feature should be especially beneficial in the solvent still, resulting in longer surfactant life, with less makeup required, and a slower buildup of decomposition products in the recirculating solvent.

REACTOR FUEL PREPARATION BY SPHERE-PAC

The high-density spheres produced in the sol-gel process are ideally suited for fabrication into reactor fuels rods by a low-energy vibratory loading process. In this technique, which we call Sphere-Pac, low-energy vibration of the cladding tube is employed to impart energy to the microspheres; this allows them to assume the preferred, closely-packed, high-density configuration. The use of Sphere-Pac with sol-gel microspheres offers a fabrication technique employing a minimum number of operations and items of equipment. The elimination of powder processes and their attendant dust problems would appear to be beneficial with regard to both equipment maintenance and inventory control. These factors are particularly important for remote fabrication operations. The need for a two-step loading procedure and the limit on attainable densities are possible objections to this technique. Uncertainty about in-reactor performance characteristics, particularly the thermal conductivity of the packed bed, is to be resolved by irradiation testing.

LABORATORY EXPERIMENTS

We have conducted laboratory experiments, using sol-gel microspheres, to investigate loading procedures, equipment requirements, time cycles, and attainable packing densities. These experiments were based on the reported work of others[7,8] and were directed toward providing practical experience with the technique and producing fuel rods for irradiation testing of performance characteristics.

Two size fractions of microspheres were used in the initial tests. The coarse fraction, 420-500 μ in diameter, was produced by the column-forming technique, while the fine fraction, <44-μ-diam microspheres, was made by the sol-gel "stirred pot" method.[4] As found by others, all attempts at mechanical blending or simultaneous separate feeding resulted in gross segregation of the two sizes of spheres and, consequently, low packing densities. Sequential loading, in which the coarse fraction is loaded into the tube first and the fine fraction is then infiltrated from the top, produces the most uniform packing and the highest density.

We tested a variety of vibrational frequencies and modes of input. Frequency had little effect on density; however, a frequency of about 60 cps provided the best loading rate. Vibration methods that included a lateral component gave faster packing and higher densities than did pure axial vibration. We have obtained 84% volume packings in 9 min using 0.230-in.-ID tubing with a fuel column height of 2 ft. The effects of sphere size variation within the size fractions appear to be minimal (e.g., we have found no variation in loading characteristics using spheres from 14 different batches). The optimum coarse/fine particle volume ratio is approximately 2.7 for these particular size ranges.

A light follower rod on top of the fine-particle bed prevents expansion of the coarse-particle bed during infiltration and increases the packing density. For fabrication involving plutonia, where a low contamination of the upper part of the tube is desirable, we have used a funnel with a screen in the bottom, as suggested by Ayer,[8] to restrain the coarse bed during the infiltration of the fine spheres.

We have not attempted to optimize all of the variables. Utilizing the available sol-gel products, a ternary loading appears impractical because the ratios of tube diameter/largest microspheres and largest microspheres/fines fraction are about 10:1. A ternary loading with a smallest size fraction of about 20 μ (the practical minimum) would require a primary-size microsphere about 2000 μ in diameter, or about four times the maximum diameter now practical. Densities of 82 to 84% are readily attained with two size fractions. Since this is the density range required for high-burnup Liquid Metal Fast Breeder Reactor fuels, we have concentrated our efforts in this area.

TEST FUEL ROD FABRICATION

Twenty-four fuel rods have been fabricated from plutonium-bearing microspheres using Sphere-Pac. The results of these test rod loadings are shown in Table II; UO_2-bearing rods are included for comparison. They consist of 3-in. fuel columns in 7-1/2-in. long, 0.250-in.-OD by 0.010-in.-wall stainless steel tubes, or 6-3/4-in.-long fuel columns in 9-1/2-in.-long, 0.5-in.-OD by 0.035-in.-wall Zircaloy-2 tubes. The fuel column heights, densities, and density variations are quite consistent. The lower-density rods, which are the result of low-density microspheres, still exhibit the 84% volume packing that is expected. Most of these are presently being irradiated in the Engineering Test Reactor.

The principal items of equipment employed in the fabrication of these rods were a Syntron vibratory feeder, which was tilted 45° to obtain mixed lateral and axial vibration, and a C-clamp modified slightly to hold the cladding tubes and the screened-end funnel during vibration. These are located inside a 6-ft glove box. A vacuum glove box is also employed in which end plugs are welded into the top ends of the tubes under a helium atmosphere.

The assembly of a rod is begun by introducing into the fuel loading box a plastic-covered stainless steel or Zircaloy tube, with its bottom end plug and extruded-thoria[9] bottom insulator already in place. A plastic bag is taped to the top end of the cladding; this keeps it clean during handling in the box. Other non-fuel portions of the fuel rod are inspected, weighed, checked dimensionally, and placed in the box in marked bottles.

In the loading box the large microspheres are poured into the cladding tube. The screened-end funnel is inserted into the tube, and this assembly is placed in the holder on the vibrator, clamped in place, and vibrated for approximately 20 sec. The small microspheres are then poured into the funnel, a follower rod is inserted, and this assembly is vibrated for 2 min. The follower rod and the funnel are removed, and the top thoria spacer is pushed down to contact the top of the fuel column. Out-gassed Fiberfrax* (30% dense) is placed on top of the thoria spacer to prevent movement of the fuel bed during subsequent handling.

The assembly is then ready for installation of the top end cap and closure welding. It is bagged out of the loading box and into the welding box. During this transfer the contaminated protective bag on the cladding is stripped off so that only the uncontaminated rod is introduced into the welding box.

After Tungsten Inert Gas closure welding is accomplished, the finished rods are inspected. In particular, variations in density are measured by gamma scanning, using a technique that was developed for the Kilorod operation;[2] this technique has proved to be satisfactory for detecting variations of $\pm$1% of the average density.

SUMMARY

We have demonstrated, in laboratory and semi-engineering equipment, a reliable sol-gel process for the production of uniform-composition, high-density microspheres of UO_2-PuO_2 containing 5 to 20% plutonium. Equipment has been designed and installed in an existing semiremote facility to produce batches of PuO_2 sol containing 200 g of plutonium, and 1 kg per day of sol-gel mixed-oxide microspheres.

Using two size fractions of these microspheres ($\sim$420 μ and $<$44 μ in diameter) with a sequential loading procedure and a low-energy vibratory

*Fiberfrax is a product of the Carborundum Co. It is composed of equal quantities of Al_2O_3 and SiO_2 plus about 4% ZrO_2.

compaction method, we have fabricated 24 irradiation test rods having uniform 84% volume packings. These rods are now undergoing irradiation testing.

ACKNOWLEDGEMENT

Grateful acknowledgement is made of the advice of M. H. Lloyd and R. G. Haire in the forming of plutonia sols, S. D. Clinton and P. A. Haas in microsphere forming and drying, and W. D. Bond and the late A. T. Kleinsteuber in firing schedules. We also recognize the assistance of R. E. Purkey and S. E. Shell in all phases of Pu sol forming and microsphere production, of R. A. Bowman in the laboratory development of the Sphere-Pac procedures, and of J. E. Eve, R. A. Buhl and H. G. Moore in the fabrication of test fuel rods.

REFERENCES

1. P. A. Haas, S. D. Clinton and A. T. Kleinsteuber, "Preparation of Urania and Urania-Zirconia Microspheres by a Sol-Gel Process," Canadian J. Chem. Engr., 1966, 44 (6), 348-53.

2. C. C. Haws, J. L. Matherne, F. W. Miles and J. E. Van Cleve, "Summary of the Kilorod Project — A Semiremote 10 kg/Day Demonstration of $^{233}UO_2$-ThO_2 Fuel-Element Fabrication by the ORNL Sol-Gel Vibratory-Compaction Method," TID-4500 (42nd ed) and ORNL-3681.

3. Paul A. Haas and S. D. Clinton, "Preparation of Thoria and Mixed Oxide Microspheres," I and EC Product Res. Dev., 1966, 5 (3), 236-244.

4. M. E. Whatley, et al., Unit Op. Sec. Quarterly Progress Report, July-Sept. 1965, ORNL-3916, 43-50.

5. R. G. Haire and M. H. Lloyd, "Development of a Sol-Gel Process for the Preparation of Dense Oxide Forms of PuO_2," presented at the 12th Annual Meeting ANS, June 19-23, 1966; to be submitted for publication in Nuclear Applications.

6. P. A. Haas, F. G. Kitts, and H. Beutler, "Preparation of Reactor Fuels by Sol-Gel Processes," presented at AIChE Nat. Meet, Salt Lake City, Utah, May 21-24, 1967; to be published in Nuclear Engineering Series.

7. R. K. McGlary, J. Am. Ceram. Soc. 1961, 44 (10), 513-22.

8. J. E. Ayer and F. E. Soppet, J. Am. Ceram. Soc. 1965, 48 (4), 180-3.

9. R. B. Fitts, J. D. Sease and A. L. Lotts, "Preparation of Ceramic Nuclear Fuels by Sol-Gel Extrusion," presented at AIChE Meeting, May 1967, to be published in "Nuclear Engineering Series."

Table I. PuO_2-Containing Microspheres Prepared in Glove Box Facility, Building 3019

Type of Material	Size Range (μ)	Total Wt. (g)	No. of Batches	Density by Hg Porosimetry			Carbon (ppm)	Surface Area	
				Bulk (g/cc)	10,000 psi (g/cc)	10,000 psi Theoretical (%)		Gas Adsorption (m^2/g)	Calculation (m^2/g)
20% PuO_2-$^{235}UO_2$	300-600	1900	23	10.3	10.5	95	<10	0.02	—
	<44	340	5	∿6	9.0	82	<10	0.04	0.08
15% PuO_2-$^{238}UO_2$	300-600	970	11	10.5	10.6	97	<90	—	0.06
	<44	234	4	5.6	∿9.2	∿84	<100	—	0.5
5% PuO_2-$^{238}UO_2$	300-600	496	3	—	—	—	—	—	—
5% PuO_2-ThO_2	300-600	1148	5	9.48	9.84	97	<10	0.02	—
	<44	403	4	∿6	∿9.5	∿94	—	0.17	—
PuO_2	250-600	251	4	11.13	11.22	98	<30	0.02	0.03
	50-250	571	7	11.06	11.19	98	<70	0.01	0.02
	<44	43	1	—	—	—	—	—	—

Table II. Sphere-Pac Fuel Rods

Rod[c] No.	Fuel Material	Microsphere Density (% of Theo.)	Fuel Column (% Theo. Oxide Density)[a]	Max. Density Variation (%, ±)[b]	Volume Packing (%)	Fuel Column Height (in.)
IV-1	$(Th+5\% Pu)O_2$	99.8	84.8	2	85.0	6.67
IV-2	$(Th+5\% Pu)O_2$	99.8	84.7	1.5	84.9	6.70
IV-3	$(Th+5\% Pu)O_2$	99.8	83.5	2	83.7	6.69
IV-4	$(Th+5\% Pu)O_2$	99.8	84.0	1	84.2	6.74
IV-5	$(Th+5\% Pu)O_2$	99.8	83.3	1	83.5	6.69
IV-7	$(Th+5\% Pu)O_2$	99.8	83.3	1	83.5	6.73
2	$(Th+5\% Pu)O_2$	99.8	84.0	2	84.2	3.15
3	$(Th+5\% Pu)O_2$	99.8	83.8	1	84.0	3.16
4	$(Th+5\% Pu)O_2$	99.8	84.5	1	84.7	3.13
5	$(Th+5\% Pu)O_2$	99.8	83.9	1.5	84.1	3.15
7	$(U+20\% Pu)O_2$	91.5	75.8	1	82.8	3.14
8	$(U+20\% Pu)O_2$	91.5	76.0	4	83.1	3.13
9	$(U+20\% Pu)O_2$	91.5	75.9	1	83.0	3.14
10	$(U+20\% Pu)O_2$	91.5	75.9	1	83.0	3.13
12	UO_2	87.7	73.2	2.5	83.5	3.12
13	UO_2	87.7	73.8	2	84.2	3.09
14	UO_2	87.7	73.5	2	83.8	3.10
16	UO_2	87.7	74.1	3	84.5	3.07
26	UO_2	87.7	73.6	2	83.9	3.00
28	UO_2	87.7	73.2	2.5	83.5	3.01
22	$(U+15\% Pu)O_2$	95.0	80.3	2	84.5	3.17
23	$(U+15\% Pu)O_2$	95.0	80.3	2.5	84.5	3.12
24	$(U+15\% Pu)O_2$	95.0	78.9	2	83.1	3.04
25	$(U+15\% Pu)O_2$	95.0	81.2	2	85.5	3.01
27	$(U+15\% Pu)O_2$	95.0	81.7	2	86.0	2.99
32	$(U+15\% Pu)O_2$	95.0	81.4	2	85.7	2.99
38	$(U+15\% Pu)O_2$	95.0	80.5	2	86.0	2.99
39	$(U+15\% Pu)O_2$	95.0	80.7	3	84.9	3.02
40	$(U+15\% Pu)O_2$	95.0	79.8	2	84.0	3.02
41	$(U+15\% Pu)O_2$	95.0	79.0	2.5	83.2	3.04

[a] Calculated from height, weight, and inside diameter.

[b] Determined by transmission gamma scan along rod.

[c] ETR-IV group rods were 1/2 in. in diameter; all others were 1/4 in. in diameter.

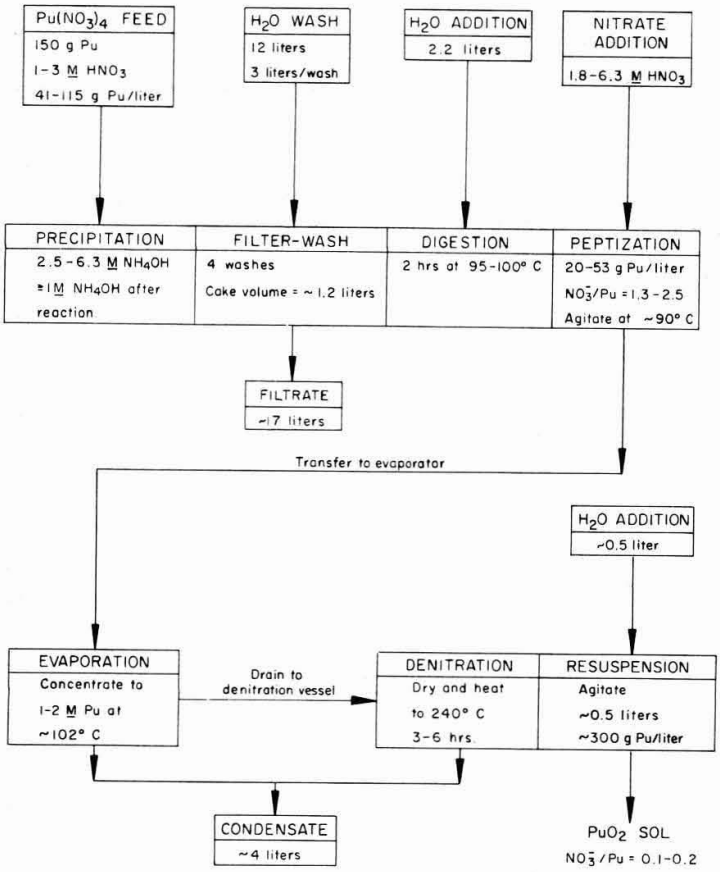

Fig. 1. Typical Flowsheet for Plutonia Sol Preparation

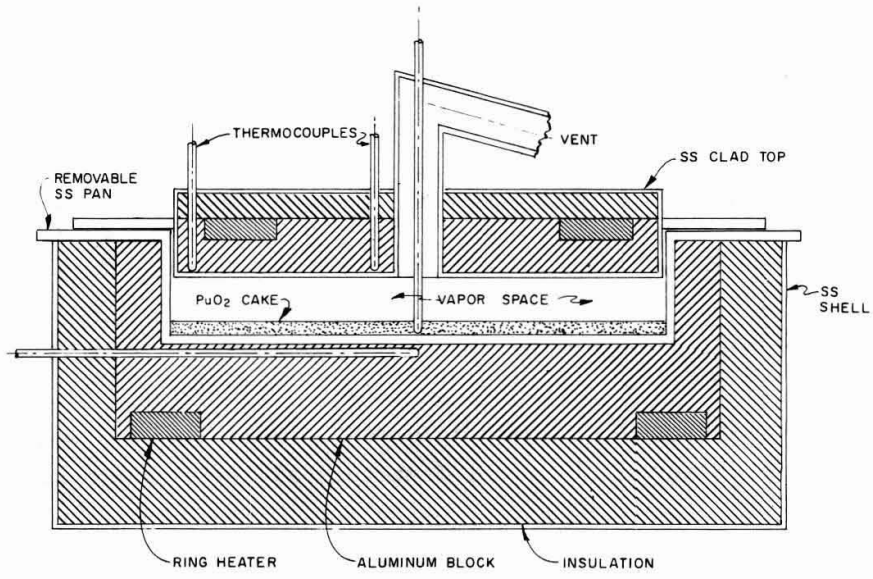

Fig. 2. VESSEL FOR THE THERMAL DENITRATION OF PuO_2 SOL

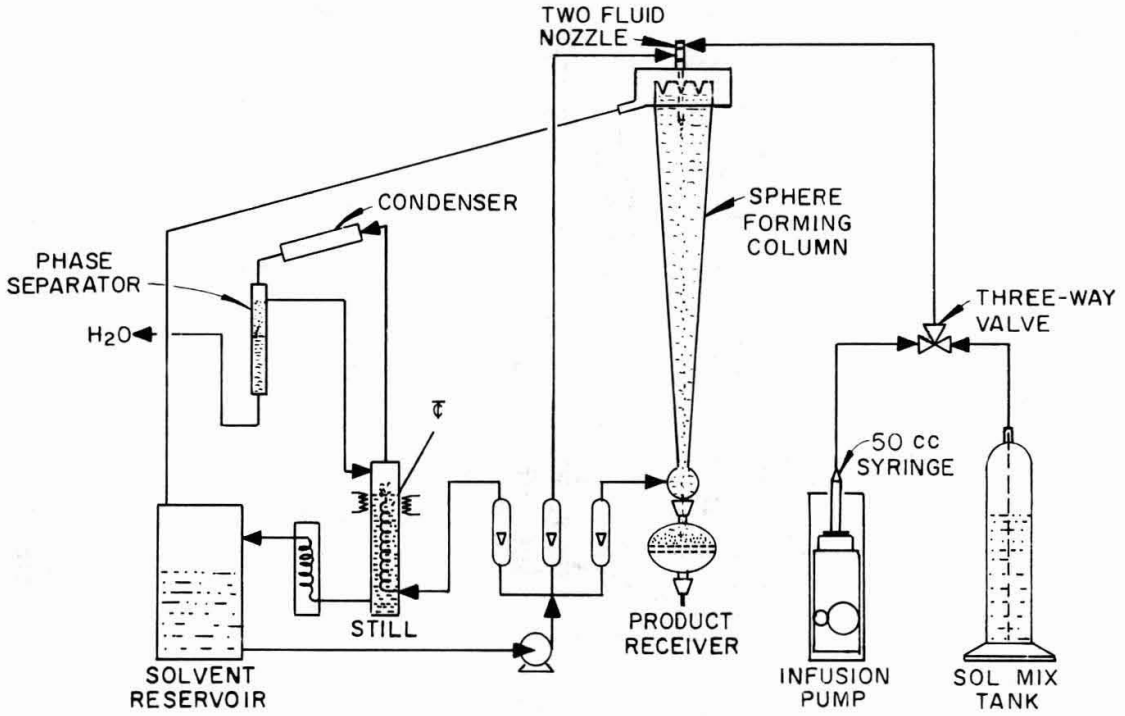

Fig. 3. Apparatus for Forming Gel Microspheres.

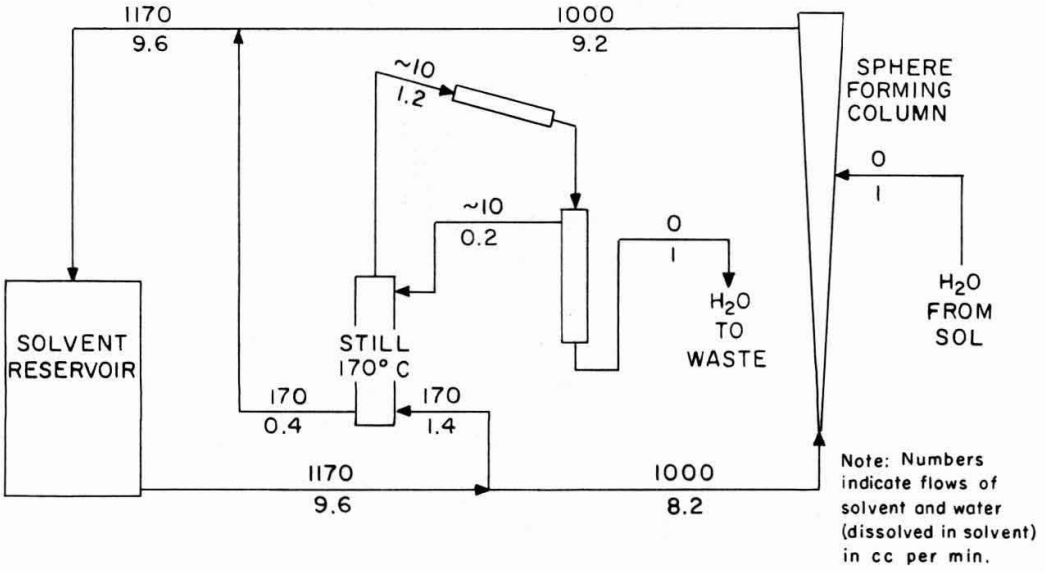

Fig. 4. Schematic Showing Water Contents in Recirculating Solvent System at Steady State.

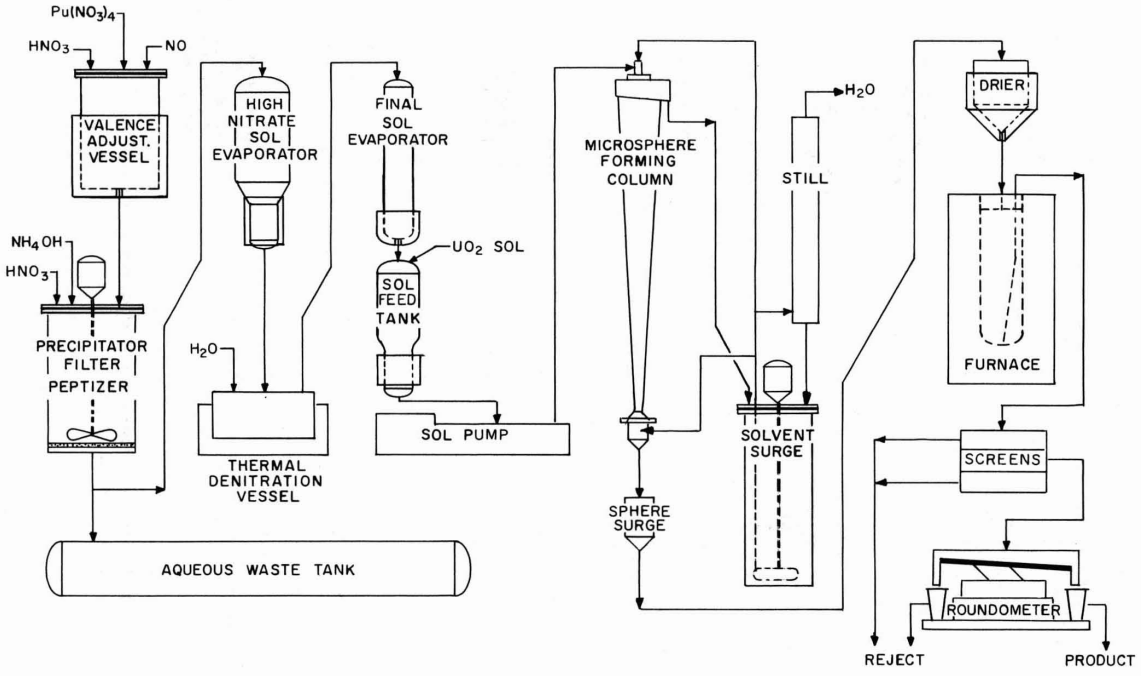

Fig. 5. Schematic Flowsheet of Pu Sol and Mixed-Oxide Microsphere Forming Equipment, Cell IV, Bldg 3019

A SIMPLIFIED SOL - GEL METHOD FOR MIXED OXIDE FUELS

G. Cogliati and G. Schileo

SUMMARY

Microparticles of plutonium, uranium-plutonium and thorium-plutonium oxides of a controlled size (up to 600 microns), nearly theoretical density, low surface area and good crushing strength, were produced. The starting materials were colloidal urania or thoria sols, as those used for the previous urania sol-gel process developed by CNEN, and plutonia sols with a relatively high nitrate content. Plutonia sols with NO_3^-/Pu mole ratios between 1 and 1,5 were prepared from plutonium nitrate solutions by extraction of nitrate by strong-base amines and evaporation to the desired plutonium concentration.

The sols then are dispersed as uniform droplets in an organic liquid by use of two-fluid nozzles. The droplets are suspended and converted to gel spheres by extraction of the residual nitrate by an amine dissolved in the solvent. The spheres are separated from the organic liquid, washed, dried and calcined to 1200° C.

The ability to produce dense plutonia, as well as homogeneous urania-plutonia or thoria-plutonia microparticles at any desired ratio has been demonstrated on a laboratory scale. The first specimen loaded with UO_2-16% PuO_2 is awaiting irradiation in the Avogadro test reactor of SoRIN in Saluggia, Italy.

Comitato Nazionale per l'Energia Nucleare -Via Belisario,15
Rome, Italy

INTRODUCTION

Plutonium is attracting a growing interest as nuclear fuel material. The Italian output of bred plutonium from the three existing power stations has been estimated at about a third of a metric ton of metal per year. However the production rate is expected to grow significantly in the coming years.

Substantial programs for plutonium utilization have been therefore undertaken both by Enel (Ente Nazionale per l'Energia Elettrica), the Italian Government power agency, and by C.N.E.N. (Comitato Nazionale per l'Energia Nucleare), the Italian Government nuclear agency.

Enel program was undertaken in cooperation with Euratom and it is aimed at the practical and immediate goal of thermal utilization. Such program covers comprehensively all aspects of the problem, from the neutron design to the technological specifications, and has as a main goal the irradiation testing of a rather large number of full-size plutonium-base fuel elements in one of Enel's power stations.

C.N.E.N. program covers a wider scope of research and development, spanning from thermal to fast utilization. Such program is an eight-million-dollar undertaking started in 1966 with funds allocated through 1969.

CNEN PLUTONIUM PROGRAM

The major objective of this program is to provide CNEN in the shortest possible time with a plutonium capability - both in personnel and facilities - in the area of ceramic fuels. While the program is intended to include research

work on non-oxide compounds, such as carbides or nitrides, by far the main emphasis is now being put on oxide fuels. The fabrication methods considered are: (a) the pelletization technique, either by mechanical mixing or coprecipitation routes, where a choice between the two will be made at a later date, and (b) the vibrocompaction technique of micro-particles, produced by modified sol-gel methods, two of which are now under investigation. One of these is the subject of the present paper; the other is a proprietary method developed at the laboratories of the SNAM-PROGETTI, in Milano, Italy.

To fasten the development of said methods, the decision was made to build at CNEN La Casaccia Center near Rome, Italy a 21,000 -sq.ft. facility, approximately half of which consists of alpha laboratories. The building has been finished and completion works are now underway.

While awaiting for the plutonium laboratory to be ready for use in Italy, it was decided to push the program by renting some alpha laboratory space where available, and therefore gain time by starting the comparison between the two considered sol-gel methods without any further delay.

To this purpose a contract was signed early in 1966 with the Centre d'Etude de l'Energie Nucléaire (C.E.N.) and the Société Belge pour l'Industrie Nucléaire (Belgonucléaire) for renting in Mol, Belgium an empty 600 - sq.ft. alpha laboratory plus cold laboratory space and offices for about ten people. Contractual previsions were also made to have ancillary services performed, such as health physics surveillance, analyses, etc. The laboratory was then equipped with ten glove-boxes in two parallel lines to perform

plutonium chemistry (precipitation, filtration, liquid-liquid extraction, centrifugation, etc.), thermal treatments (in air, Ar-H_2, Co_2, Ar) and some basic characterizations, chemical analyses, etc.

CNEN SOL-GEL METHODS

CNEN's previous experience in the field of nitrate extraction with strong-base amine led to the development of modified sol-gel processes capable of yielding micro-particles of thorium and uranium oxide or carbide with satisfactory nuclear characteristics. The general results and findings are reported here concerning the extension of such experience and methods to the preparation of microparticles of plutonia, urania-plutonia, or thoria-plutonia. For detailed data, reference is made to the papers that have been presented a few days ago at the Turin Sol-Gel Symposium (2).

It might be remembered that all known sol-gel methods for the production of heavy metal oxide microparticles include: (a) the preparation of a colloidal solution (sol)carring the heavy metal ions, (b) the dispersion of said solution into droplets of the desired diameter, (c) the drying of said droplets into solid (gel) microparticles, and finally (d) the appropriate thermal treatment of said microparticles to convert them into small and compact oxide bodies.

A substantial difference between the sol-gel methods developed by CNEN and those developed at other laboratories, as in the United States or United Kingdom (3,4), lies in the NO_3^-/ metal ratio of the starting colloidal solution. The ratio is at a relatively high value (NO_3^-/ metal = 1.0 +

1.5) with the CNEN method, while with the other methods every effort must be made to reduce it as much as possible (down to a value of NO_3^-/ metal = 0.1 ÷ 0.3).

Thorium colloidal solutions with a low NO_3^-/Th ratio are relatively easy to prepare, almost independently of the methods used: (a) by steam denitration (5), (b) by peptizing the hydroxide in nitric acid (6), or (c) by denitration of thorium nitrate solution by liquid-liquid anionic exchange (7); all these methods yielding a low-ratio thorium colloidal solution with satisfactory characteristics.

Greater difficulties are encountered in the preparation of the colloidal solutions of uranium-thorium. The difficulties increase by increasing the U/Th ratio until instability or an excessive viscosity might be obtained.

Colloidal solutions of U(IV) with a low NO_3^-/U(IV) ratio are obtained with relative ease by peptizing uranous hydroxide; however,when trying to obtain a colloidal solution of U(IV) with the lowest possible content of either NO_3^- or U(VI). much greater care is required, as an inert gas atmosphere, and much larger washing - and then waste - volumes are needed (2).

Lastly, plutonium colloidal solutions with a low NO_3^-/Pu ratio are particularly difficult and tedious to prepare (8).

Direct denitration of plutonium solutions do not yield colloidal solutions with a NO_3^-/Pu molar ratio less than one. On the other handpeptizing plutonium hydroxide leads to a product with a high NO_3^-/Pu ratio and the excess nitrate must then be disposed of by cautious baking of the plutonium polymer produced by peptization.

The need for low - NO_3^-/metal - ratio colloidal solutions stems from the particular type of gelation process used. In

fact with sol-gel processes using such solutions, the change of a sol into a gel is generally accomplished by removal of water. After syneresis,the shrunk microparticles cannot therefore be washed in any aqueous medium, so that essentially all the nitrate contained in the colloidal solution is still in the solid microparticles undergoing the thermal treatments. It is universally accepted that one of the main reasons for rupturing during the thermal treatments is actually the presence of too high a nitrate content, and particularly of ammonium nitrate.

A process was then sought by CNEN in which the gelation would be performed by extracting directly the nitrate from the colloidal solution. In such a way the need for a low - NO_3^-/ metal - ratio colloidal solution is eliminated. As indicated, in the sol-gel methods developed by CNEN, the starting colloidal solution has a NO_3^-/metal ratio between 1.0 and 1.5. The gelation of a sol then is accomplished by raising the pH value of the solution that had been previously dispersed into droplets of the desired size, by means of a liquid anionic exchange agent dissolved in the dispersing medium. In such a fashion, the resulting process is tremendously simplified and shortened, with clear economic implications. In the uranium case, for instance, the colloidal U (IV) solution can be directly obtained during the reduction of U (VI) to U(IV) from a starting solution of uranyl nitrate having a NO_3^-/U(VI) ratio of about 1.5. In 1962 CNEN developed a process for the hydrogen catalytic reduction of uranyl nitrate solutions by means of a platinum-alumina bed under pressure (9). Dilute acid solutions containing up to 1 mole/liter of uranyl nitrate can be reduced continuously over a fixed catalytic bed in an

autoclave; while concentrated acid-deficient solutions containing up to 4 mole/liter of uranium can be reduced discontinuously by mechanically agitating in an autoclave batches of a dispersion of catalytic powder in the same solution. Naturally, the operating conditions during the reduction of U (VI), and hydrolisis and polimerization of U(IV) should be set to avoid any precipitation that would inhibit the catalyzer from being further contacted by the solution. As mentioned before, colloidal solutions of U(IV) obtained by reduction of acid-deficient solutions of uranyl nitrate have a much higher NO_3^-/U(IV) ratio than those prepared by peptizing uranous hydroxide in nitric acid. Furthermore the direct reduction method permits to work on solutions much more concentrated in uranium than would be otherwise permissible, with negligible contents of U (VI). This is an important advantage when preparing microparticles with a diameter, after calcination, greater than 500 microns.

CNEN SOL-GEL METHOD FOR PLUTONIUM FUELS

Plutonium colloidal solutions with a NO_3^-/Pu ratio between 1.0 and 1.5 can be easily obtained either by peptization of the hydroxide or direct nitrate extraction from a solution of Pu(IV) nitrate. On the basis of CNEN experience the latter is by far the simplest method, since tedious operations, such as washing - with the resulting large volumes of waste solutions - or plutonium hydroxide recovery, are avoided altogether. Moreover the direct extraction technique is more amenable to continuous operations.

On a small-scale laboratory line (with a capacity of ten to twenty grams of material per batch) the solution of

Pu(IV) nitrate is contacted in a separatory funnel with a long-carbon-chain primary amine (Primene JMT) in an aliphatic solution. The Pu(IV)/amine ratio is established in order to obtain a final NO_3^-/Pu(IV) ratio in the aqueous phase between 1.0 and 1.5. Since generally the Pu(IV) nitrate solution comes from an ion-exchange column with a plutonium concentration of 0.2-0.3 mole/liter, the diluite aqueous phase is evaporated at 80°C to a final plutonium concentration of 1 ÷ 2 mole/liter. The residual plutonium content in the organic phase does not exceed a few milligrams per liter and can be recovered as usual by conventional means.

A high number of batches have been processed discontinuously through the line;while a mixer-settler extractor for continuous operation is under design.

The Pu(IV) colloidal solutions obtained as described show a low viscosity even at a high plutonium concentration and can be safely stored for months without showing any alteration whatsoever. Such a colloidal solution can be used as prepared for producing plutonia microparticles or can be properly mixed with other colloidal solutions of heavy metals, such as tetravalent uranium or thorium, to produce mixed urania-plutonia or thoria-plutonia.

The dispersion of colloidal solutions into small droplets is easily performed by conventional techniques by either mechanical stirring or spraying two immiscible fluids: one, the aqueous colloidal solution and the other, an organic fluid with which the first is immiscible. The latter contains in solution the denitration agent to produce gelation.

The choice between the two systems, stirring or

spraying, is essentially determined by the desired size of the microparticles. The gelation of small diameter microparticles (less than 100 microns after thermal treatment) is performed in a beaker with diaphragms. The gelation of microparticles of a larger diameter is made in a Plexiglas column with a conical section in which the sprayed droplets are lifted and kept in a suspension by an ascending current of the organic phase containing in solution the denitrating agent.The column is very similar to that originally developed by ORNL (5).

A low-cost commercial product "Alphanol 79", that essentially consists of a mixture of high-carbon-number alcohols, is used as the organic dispersing medium. In order to keep microparticle coalescence to a minimum, 0.5 volumetric percent of a tensionactive agent (SPAN-85) is added.

Finally the denitrating extractant, 1 or 2 volumetric percent of an amine mixture, commercially known as Primene JMT, is also added to the organic phase. The amines of Primene JMT show also a tensioactive action. The solubility of water in the Alphanol-79 is 3 or 4 percent in volume; if used in the anhydrous state the Alphanol-79 would therefore extract water from the sol droplets. Incidentally, this process of water extraction is precisely the cause of gelation in the mentioned sol-gel processes developed by others while in CNEN modified sol-gel process the water extraction must be strictly avoided since it would form a nitrate-impervious thin layer at the surface of the microparticles with the resulting difficulty to complete the gelation of the innermost parts of the microparticles. Therefore, before using it, the organic phase needs to be

saturated with water at the operation temperature. Among the many factors that affect the duration of complete gelation, the most important ones are certainly the amount of nitrate to be extracted and the microparticle diameter.

It has to be borne in mind, though, that the nitrate extraction must be strictly controlled not to exceed a limiting rate, otherwise too rapid a gelation of the outer skirt of the microparticles occurs that would cause gelation inequalities. However, the nitrate migration is not stopped altogether by gelation, but simply slowed down.

Gelation is assumed to be completed when a limit between 0.1 and 0.2 of the NO_3^-/metal ratio is reached. Such a nitrate content has been shown not to have any harmful effect on the characteristics of the microparticles after the thermal treatment.

It has been routine practice in the reported experiments to discharge completely the gelation column after every run. After rinsing the gelled microparticle with an organic volatile solvent to free it of the Alphanol-79 excess, the product is ready to undergo the thermal treatments.

The plutonia, urania-plutonia and thoria-plutonia specimens referred to in this paper,have been all fired under an argon - 5% hydrogen atmosphere in resistence tubular ovens for four hours to reach the soaking temperature of 1,200°C at which they were held for two hours.

The oxide microparticles so produced showed a satisfactory spherical form in all batches with different diameters: from a few microns up to a maximum of about 600 microns. The carbon content of the calcined product is tipically less than 100 parts per million. The individual

microparticle crushing strength values for 300-micron (U-16%Pu)O_2 microparticles showed a variance between 6 and 10 kilograms. This value is very difficult to keep constant from particle to particle within a single batch and to reproduce from batch to batch. X-ray analyses showed that the urania-plutonia microparticles have a solid solution (U, Pu)O_2 structure. The microparticle densities ranged from 98%, of theoretical density for urania -16% plutonia, to consistently higher than 99.5% of theoretical density for mixed oxide of urania or thoria with only a few units percents of plutonia (up to 5 or 6% Pu).

The appearance and cross-section of urania - 5% plutonia, urania -16% plutonia and thoria -5% plutonia microparticles produced by the modified sol-gel process here described are given in the figures.

Preliminary vibratory compaction tests of such microparticles in typical fuels sheets indicated that smeared densities around 81-82% of theoretical using a binary size mixture and around 85-86% of theoretical using a ternary mixture can be achieved.

The first specimen loaded with UO_2-16%PuO_2 is awaiting irradiation in the Avogadro test reactor of SoRIN in Saluggia, Italy. A comprehensive irradiation program is being now started, for which use of the HBWR reactor in Halden, Norway and the R-2 reactor in Studsvik, Sweden, is planned.

FUTURE ACTIVITY

The optimization of the single steps of the described process will be continued up to a point where a comparison can be made with the other modified method under investigation

at CNEN laboratories. The latter method, that has been developed by SNAM-PROGETTI, avoids altogether the use of colloids and yields almost identical microparticles. This work will be performed at the rented laboratory in Mol, Belgium. As soon as the 21,000-sq.ft. plutonium facility is ready for use at the outskirts of Rome, Italy (scheduled for 1968) a similar comparison work will begin between coprecipitated and mixed pelletization techniques on one side and between the most promising pelletization technique and (sol-gel + vibratory compaction) technique on the other side.

The irradiation experiments with such materials will be continued and expanded.

ACKNOWLEDGMENTS

The authors are indebted to A. Recrosio, V. Lupparelli, R. Lanz, P. Capuzzo and R. Chiarizia who performed the actual experimental work and to M. Zifferero and G. Calleri whose aid was determinant for the successful implementation of CNEN Plutonium Program.

Last, but not least,the cohoperative help constantly given by the "Groupe Mixte Plutonium CEN-Belgonucléaire" of the Belgian center in Mol, Belgium is gratefully acknowledged.

BIBLIOGRAPHY

1. Cogliati G., De Leone R., Guidotti G.R., Lanz R., Lorenzini L., Mezi E., Scibona G., "The Preparation of Dense Particles of Thorium and Uranium Oxide", III Geneva Conference on the Peaceful Uses of Atomic Energy, A (Conf. 28) P 555, 1964.

2. Cogliati G., Collenza F., Lanz R., Lupparelli V., Maltzeff P., Mezi E., Recrosio A., "Sol-gel processes for ceramic fuel microparticles developed at CNEN laboratories", Sol-Gel Processes for the Production of Ceramic Fuels - Turin, Italy - October 2-3, 1967.

3. Mc Bride L.P., "Preparation of UO_2 Microspheres by Sol-Gel Technique" ORNL-3874 (1966).

4. Lane E.S., Fletcher J.M., Fox A.C., Holdoway M.J., Hyde K.R., Lyon C.E., Woodhead J.L., "Sol-gel studies. Part I. Urania Preparation of sols, aggregate and spheres". AER-R-5241, 1966.

5. Ferguson D.E., Dean O.C.,Douglas D.A., "The Sol-Gel Process for the Remote Preparation and Fabrication of Recycle Fuels", Geneva Conference A (Conf. 28) P.237, 1964.

6. Hermans M.E., Slooten H.S.G., "Preparation of UO_2-ThO_2 Powders in the Subsieve Range" - Geneva Conference A

(Conf.28) P. 634, 1964

7. Cogliati G., Lanz R., Mezi E., "Preparation of Uranium Dioxide and Carbide Particles by Sol-Gel Methods" RT/CHI (65) 30, 1965.

8. Haas P.A., Dean O.C., Kleinsteuber A.T., Snider J.W., Haws C.C., "Sol-Gel Development and Microsphere Preparation" Second International Thorium Fuel Cycle Symposium - Gatlinburg, 1966.

9. Cogliati G., De Leone R., Lanz R., Lorenzini L., "Studies of uranium (IV) nitrate" p. 307-319 - TID - 7641 (1962).

FIG.1

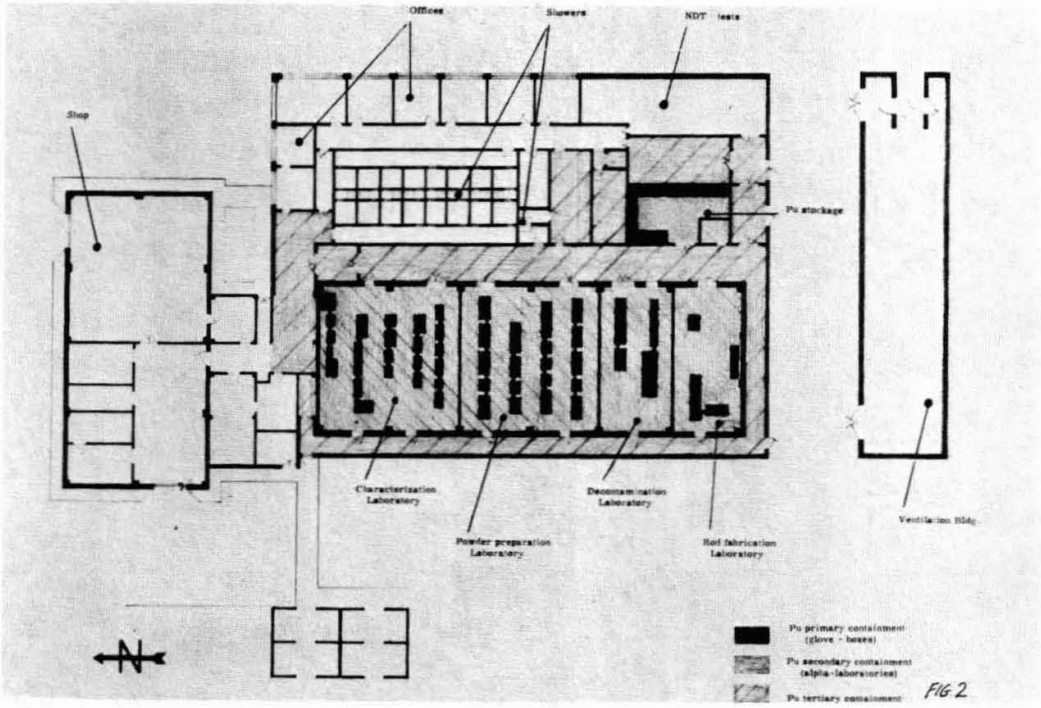
Offices
Showers
NDT tests
Shop
Pu stockage
Characterization Laboratory
Decontamination Laboratory
Powder preparation Laboratory
Rod fabrication Laboratory
Ventilation Bldg
Pu primary containment (glove - boxes)
Pu secondary containment (alpha-laboratories)
Pu tertiary containment

FIG. 2

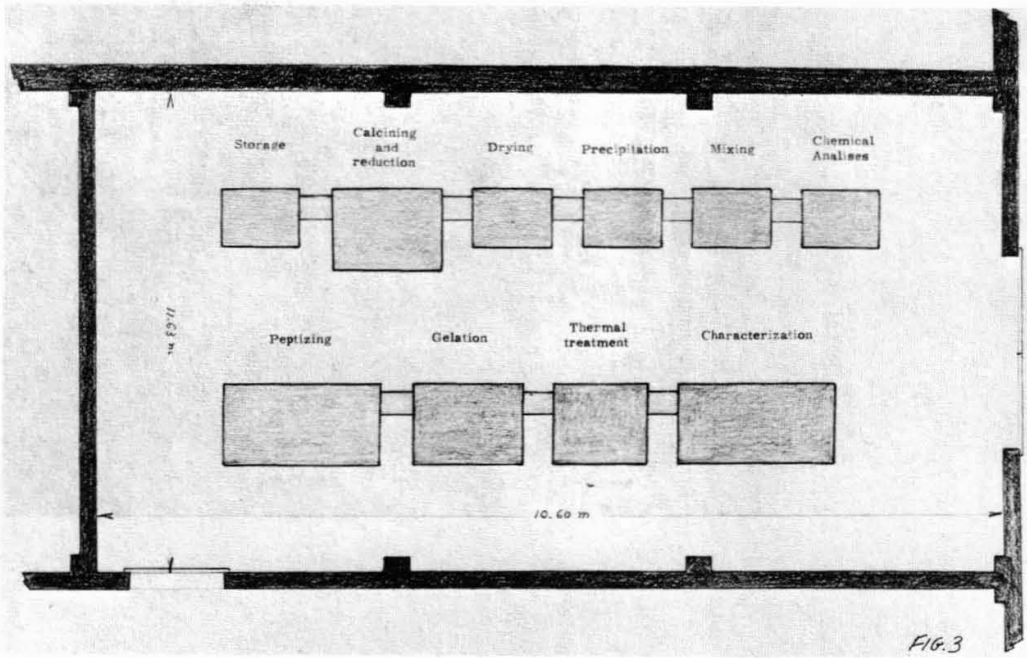
Storage
Calcining and reduction
Drying
Precipitation
Mixing
Chemical Analises
Peptizing
Gelation
Thermal treatment
Characterization
10.60 m

FIG. 3

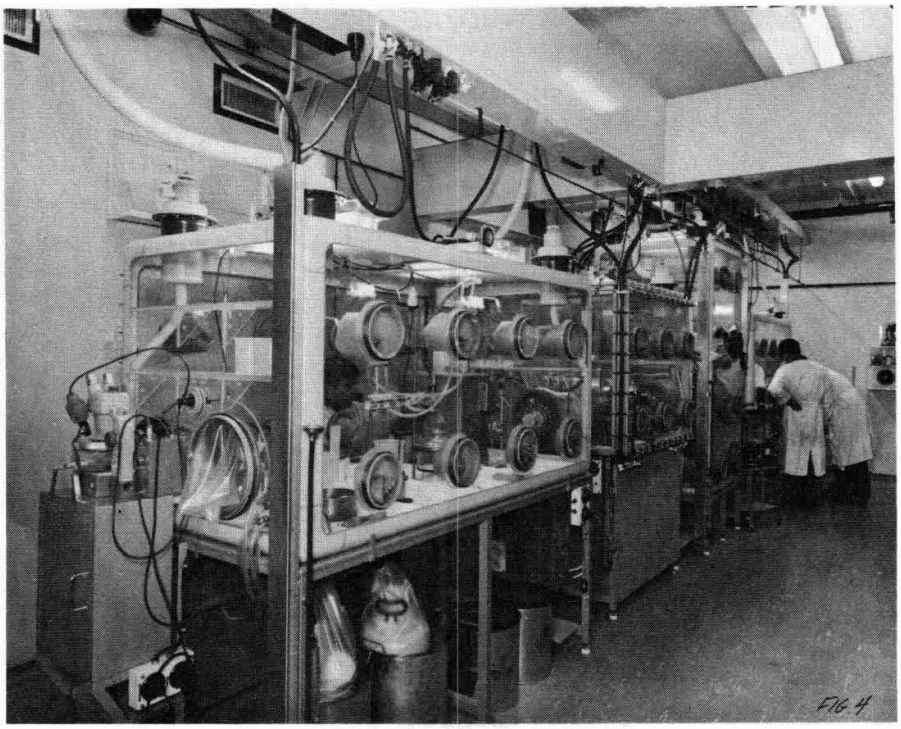

FIG. 4

FIG. 5

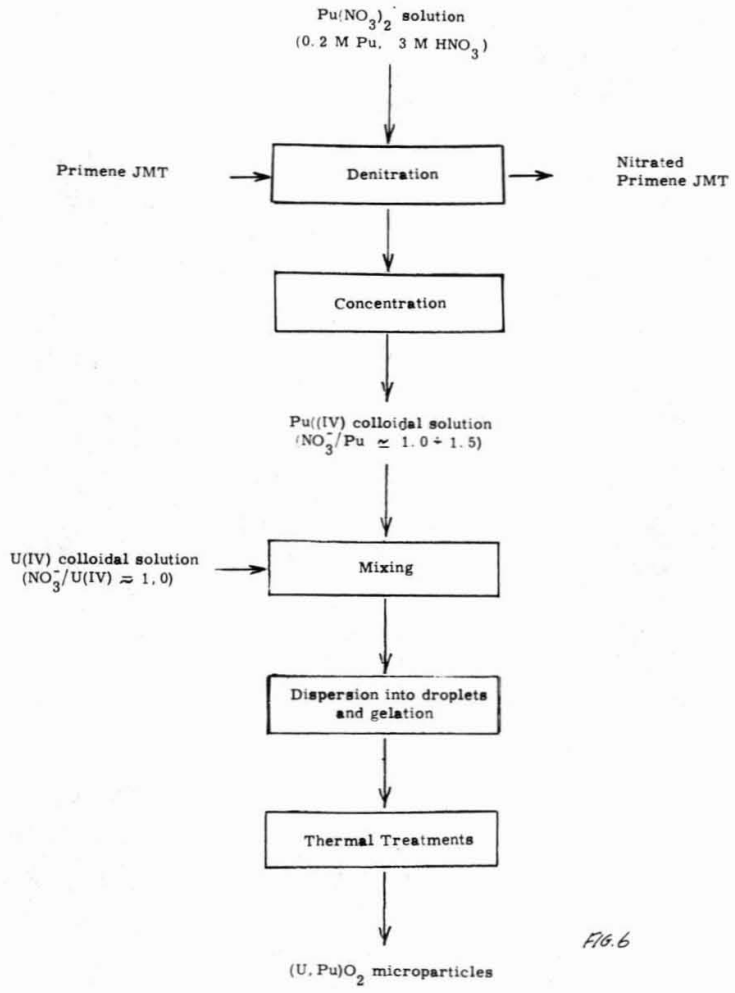
Pu(NO3)2 solution
(0.2 M Pu, 3 M HNO3)
Primene JMT
Denitration
Nitrated
Primene JMT
Concentration
Pu(IV) colloidal solution
(NO3-/Pu ≃ 1.0 ÷ 1.5)
U(IV) colloidal solution
(NO3-/U(IV) ≃ 1.0)
Mixing
Dispersion into droplets
and gelation
Thermal Treatments
(U, Pu)O2 microparticles

FIG. 6

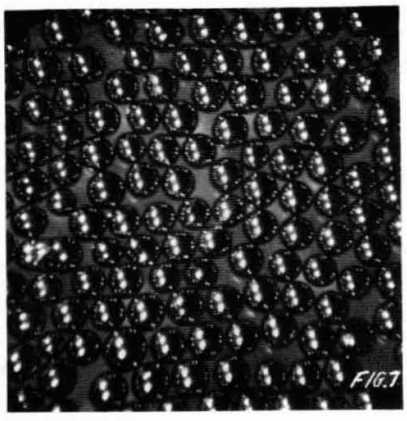

FIG. 7

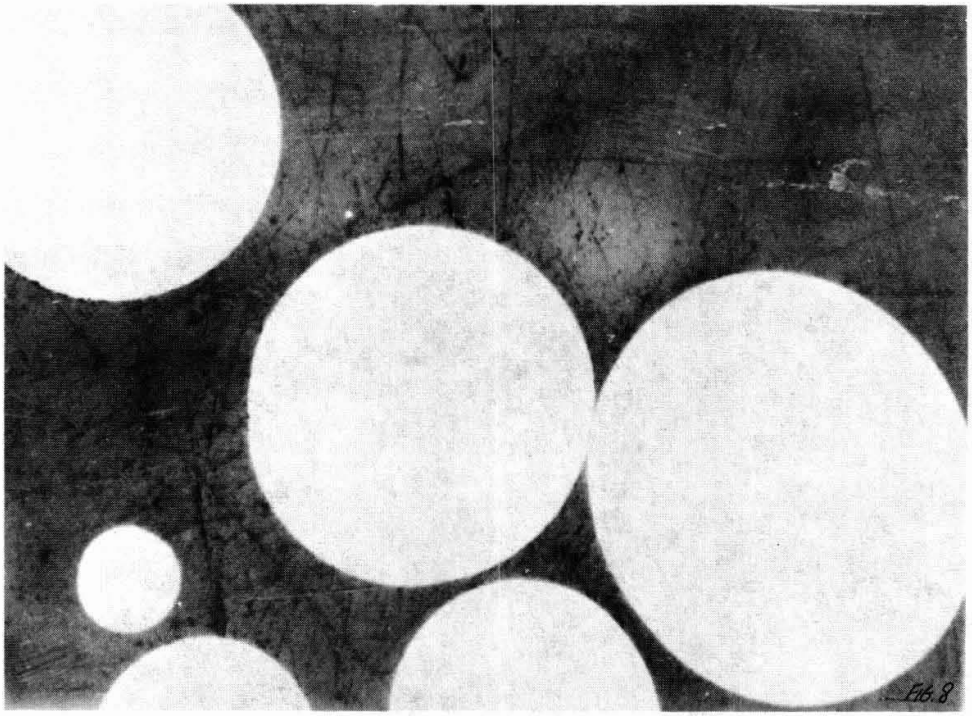

FIG. 8

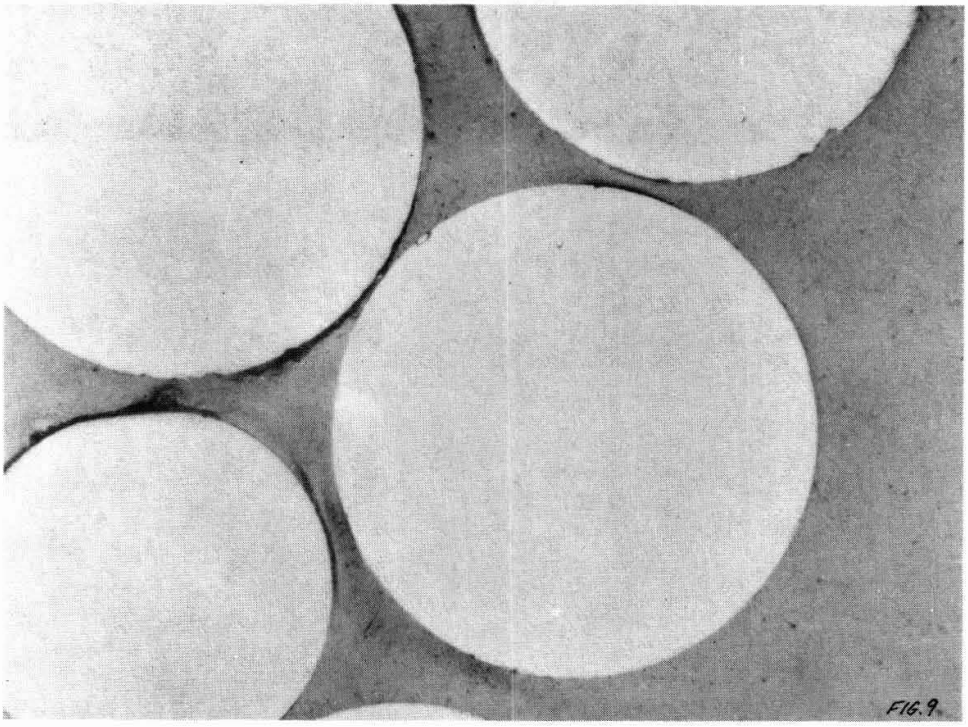

FIG. 9

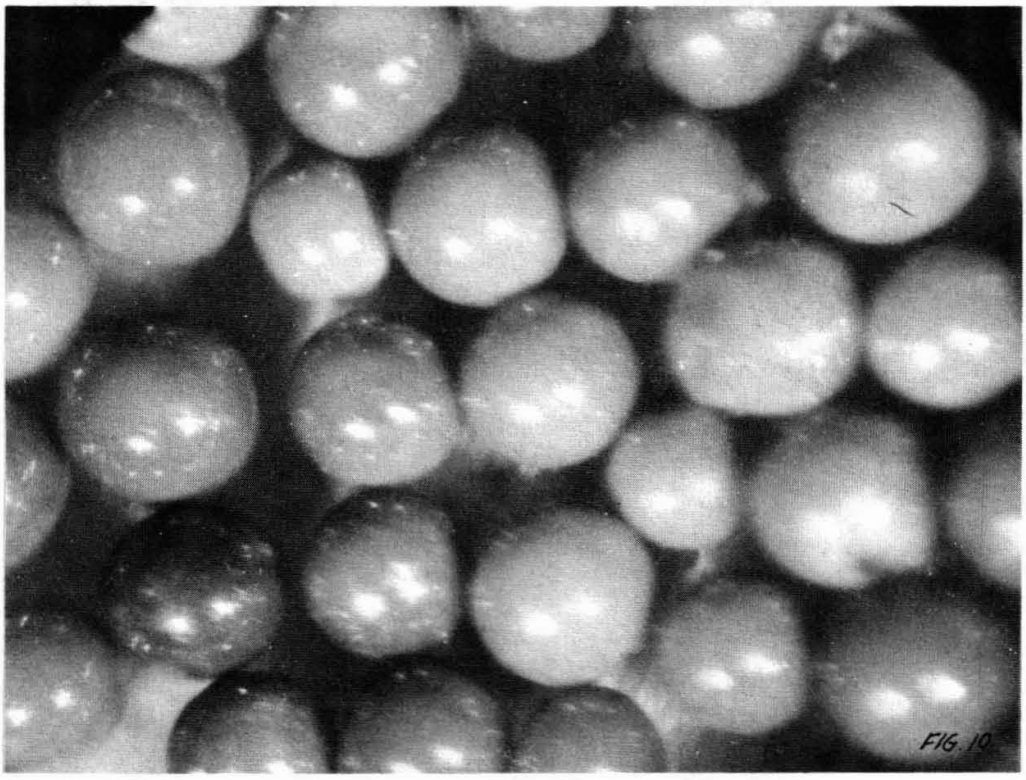

FIG. 10

MIXED URANIUM-PLUTONIUM OXIDE FUEL FABRICATION FOR RAPSODIE

S. BATALLER, M. GANIVET, H. GUILLET
Y. MASSELOT, A. ROBILLARD, F. STOSSKOPF

Abstract

The fabrication of the 96 first elements for the Rapsodie reactor has been carried out at the Atelier de Technologie du Plutonium in 1965-1966. It represents the use of 320 kg of mixed oxide $(U,Pu)O_2$ containing about 70 kg of plutonium. First, we examine the fabrication itself, the total evaluation of the fabrication and the yield of the different stages are detailed. Then, we study the problems and difficulties raised by the fabrication. At last, we summarise, as an extension, the studies devoted to the adjustments of the procedure for the fabrication of low density oxide for Rapsodie. In the end, we give the specifications considered just now for the first charge pellets of the Phenix reactor.

Commissariat à l'Energie Atomique (France),
Direction des Matériaux et Combustibles Nucléaires,
SECPER, Service des Techniques Appliquées au
Plutonium (Centre d'Etudes Nucléaires de Cadarache)

Introduction

Up to now, ninety six fissile assemblies for the Rapsodie Reactor have been manufactured at the Atelier de Technologie du Plutonium in CADARACHE. A first series of pins for seven assemblies was made between April and October 1964, in order to adjust the manufacturing process and settle the specifications. The pins for seventy-nine standard and three special assemblies were then made between November 19th 1964 and October 20th 1965. The corresponding assemblies were fitted up during the first months of 1966. The further standard assemblies were made at the end of the same year.

A report[1] has described in detail this production and a communication was presented in BRUSSELS in March 1967[2], in which we showed the evolution of the process and its extrapolation to the fuel for the Phenix Fast Reactor Project. It also gave indications on the economical aspect of these fabrications.

In this paper, we shall deal with the production of mixed (U, Pu) O_2 oxide pellets during the first and second campaigns and we shall consider the problems connected with it.

Fabrication of mixed oxide pellets

Manufacturing process and specifications.

The production flow line is shown on Figure 1. It was settled at the end of the first series, which also showed the good quality of the pellets and allowed us to determine the following limits for the specifications :

Pu O_2 content : $\frac{\text{Weight Pu } O_2 \times 100}{\text{Weight mixed oxide}} = 25{,}91 \pm 0{,}25$

or $\frac{\text{Weight Pu} \times 100}{\text{Weight mixed oxide}} = 22{,}84 \pm 0{,}25$

Stoichiometry : $\frac{O}{U + Pu} = 2{,}00 \begin{matrix} +\,0 \\ -\,0{,}05 \end{matrix}$

Diameter of the pellets..... = 5,57 $\pm$ 0,05 mm

Geometrical density..... = 95,5 $\pm$ 2 % of the theoretical density
(measured on unrectified pellets)

External aspect of the pellets : no chip of more than 1 mm.

Quantitative results. The results of the measurements carried out on the pellets are shown as histograms on the subjoined figures. They call on the following remarks :

- Plutonium content : Chemical analysis is carried out on five sintered pellets per half-batch. One batch is made of all the pellets containing uranium from one reduction step, one half-batch being made of all the pellets coming out of the same sintering furnace (one half-batch contains 480 to 550 pellets).

Figure 2 shows that the histogram of the first campaign is centered slightly higher than the nominal value. Although all the batches are good, the mean value given by chemical analysis is 22.95 %, whereas the value aimed at by weighing is 22.84 %.

This difference is lower for the second campaign, but the number of batches is ten times less.

- Stoichiometry : $\frac{O}{M}$ ratios are determined on one pellet per half-batch by X ray diffraction measurement of the lattice parameter. This can be done accurately only on single phase oxides[3]. The last third of the first campaign and all the second campaign were double-phased so that the histogram on Figure 3 does not show all the fabrication.

It is however noticeable that all the single phase batches are substoichiometric, the mean value being 1.985.

- Diameters. The diameters are determined as the mean value between two measurements near the ends of each pellet on 10 % of each half-batch. The histogram on Figure 4 shows that the specifications have easily been maintained. The average value is slightly higher than the nominal value, because of the adjustement of the process. The reason is that if the diameter is too large, pellets can easily be rectified. Only 2 % of the batches fell in that case.

- Density. Density is determined by geometrical measurements and weighing on 4 % of the pellets for each half-batch. Figure 5 shows that the histogram is centered on high values. A certain number of batches of the first campaign were even out of the specifications (they were however accepted with derogation).

- Longitudinal mass. Longitudinal mass is calculated from the diameter and the density. Figure 6 gives the distribution of the half-batches of the first campaign that were not rectified with respect to the lines of equal longitudinal mass. Figure 7 shows the histograms of longitudinal mass for the first and second campaigns.

Material balance. The total plutonium balance for the 86 standard assemblies and the three special ones, first series included, is the following :

Total quantity of plutonium used		
- estimed by weighing	69.488 kg	
- profit after chemical analysis	.252 kg	
- total quantity taken into account	69.740 kg	100 %
Plutonium delivered in the 89 fissile assemblies and in the additional accepted pins	67.889 kg	97.34 %
Plutonium recoverable by chemical means		
- analysis and destructive controls	1.353 kg	1.94 %
- fabrication scraps	.458 kg	.66 %
- total	1.811 kg	2.60 %
Unrecoverable losses	.040 kg	.06 %

About this balance, a significant decrease of the oxide mass (0.35 weight per cent) during sintering, lubricant excepted, was shown on the overall first run. Chemical analysis of the utilized UO_2 powder led to an $\frac{O}{M}$ ratio equal to 2.06. We assume that the PuO_2 $\frac{O}{M}$ ratio is equal to 2.00. The oxides being manipulated in a purified argon atmosphere, we assume that UO_2 does not undergo reoxidation, and that the observed weight loss is due essentially to an oxygen loss during sintering. In this case, calculations of the average $\frac{O}{M}$ ratio of the sintered oxide lead to the value 1.986.

This value is to be compared with the average value 1.985 obtained by X-ray diffraction on single phased batches. Therefore, it is reasonable to assume that the $\frac{O}{M}$ ratio for double phases batches is also close to this value.

Problems raised by the fabrication

After this rapid survey of the results, it is interesting to emphasize some important aspects of this fabrication.

The options. The fabrication was directed from the start by some leading ideas on the oxide and the technology of the process.

The burnup estimated for the first charge was not higher than 35,000 M W D / T, so that the choice of densities near the theoretical value had the following advantages : neutron economy, good mechanical strength owing to the lack of cracks and porosity, low dispersion of characteristics of the manufactured pellets.

Consequently we tried to optimize the fabrication parameters, by studying mainly the influence of the A D U calcination temperature, of the milling time and of the organic additions. Thus we were obliged to eliminate the camphor process and to replace wet granulation by double compacting.

We decided secondly to pilot the fabrication by measuring the density of the pellets in the green state and varying the pelleting pressure (this shows the advantage of a hydraulic press). This method and the choice of the matrix allow a good reproducibility of the sintered pellets and avoid, as much as possible, rectification which may cause difficulties with the future behaviour of the pellets and with criticality. Figure 8 gives as an example two parts of the diameter control curve corresponding to two fabrication periods.

The third choice is the use of sintering furnaces with molybdenum resistors, which need a reducing atmosphere (non explosive mixture of hydrogen and argon in 10/90 proportion). Sintering under these conditions leads to substoichiometric oxide which seemed to be a good guarantee against the appearance of U_3O_8 in the case of slow reoxidation (stocking atmosphere) which could embrittle the pellets. It was shown later that substoichiometric despite a lower thermal conductivity gave an advantage for the resistance of the oxide to swelling under irradiation. Moreover, it was found that hyperstoichiometric pellets crumble to powder after a few hundred hours in sodium at 600° C, probably because of the presence of U_3O_8 at the grain boundaries. On the contrary substoichiometric pellets have a good resistance under these conditions and this is a guarantee in the case of can failing.

Lessons drawn from the fabrication. A first fact is the satisfactory external aspect of all the pellets. Even after rectification no crack can be seen in the oxide, the mechanical strength is good and the number of pellets discarded because of chips before cladding is very small.

The second observation is the following :

Because of the need to minimize the number of density measurements, which long time require, it appeared more interesting to caracterize the pellets by their linear mass, which is easier to obtain through measures and computations.

Moreover, this parameter is of greater interest than density for the physicist, in order to evaluate the linear power within a pin.

Figure 9 shows the results of density vs. diameter measurements for 3 half batches covering the whole range of linear masses.

It can be seen that a linearized relationship betwen diameter and density is quite valid within the range of variations of these parameters.

Furthermore is should be recolled that the rate of change of density versus diameter depends upon each particular half batch : this explains the slight variations of slope of the fitted straight lines on these diagrams.

It was checked that the experimental relationships were quite close to the ideal density vs. diameter relationship for constant linear mass (see figure 6).

Since people are very interested in keeping a linear mass as constant as possible, they should avoid centerless grinding wich, while reducing the diameter dispersion does not keep the linear mass constant since there is a mass loss at constant length.

A third fact is the importance of the specifications on raw materials. Without talking of the second phase, which we shall see later, we have observed that is was necessary to carry out new adjustements on the pelleting pressure or on the diameter of the matrix when we used a new batch of A D U.

If we suppose that the physico-chemical properties of raw materials guarantee a certain quality of mixed oxide, it is very important for the manufacturer that the fluctuations of these properties be as small as possible. That is to say, these products must be as homogeneous as possible.

This desire is not easy to translate into specifications ; but it would lead to the use of batches as large as possible, taking however, criticality into account.

Difficulties encountered. Two main difficulties were encountered during the production : one is the slight difference between the Plutonium content aimed at by weighing and the value determined by chemical analysis ; and the other is the appearance of a second phase in some batches, which makes the determination of stoichiometry difficult.

For the first point, the results are given in table I.

The relative difference is $5^{0}/_{00}$ which is small and very near the error on chemical analysis. However the difference was systematic batch after batch and not a mean value, so that this is a problem.

Various hypothesis have been suggested :

. Methods of analysis to be improved
. Partial reduction of oxides during sintering
. Presence of americium
. Initial hyperstoichiometry of UO_2.

Finally, the retained explanation is the following : a theoretical value of 22.84 was desired while assuming that the mixed oxide was exactly stoichiometric. Taking into account an $\frac{O}{M}$ ratio equal to 1.98_5 leads to the new

value 22.89. Furthermore, is was assumed that UO_2 was exactly stoichiometric in the initial coumpound, but further chemical analysis showed the formula to be $UO_{2.06}$. By adding the corresponding correction to the previous one, one finds a Pu percentage equal to 22.94, which is remarkably close to the analytical average.

The second difficulty is the existence in the mixed oxide of a second phase corresponding to the use of a certain batch of A D U, covering the last third of the 1st campaign and all the second campaign.

This phase was first revealed by X-ray diffraction and micrography (Fig. 10 and 11). It is made of clusters, 20 to 50 microns in size composed of small grains of .5 to 5 microns. Microprobe recordings of the U and Pu contents have shown this phase to be richer in uranium and poorer in plutonium than the matrix, its composition being UO_2, as could be predicted from X-ray diffraction measurements. Electron microscopic studies by a two stage replica method showed that the UO_2 grains were surrounded by a fine edging which was supposed to be the $(U,Pu)O_2$ matrix, for plutonium was detected in these clusters by autoradiography.

Although the second phase has been well investigated its origin is still undetermined. The processing conditions did not vary and it seems that the properties of the A D U could account for it. A different behaviour during the milling or the existence of an impurity which could slow down the diffusion have been considered. High temperature annealings should have made this second phase disappear, but did not, and thus eliminates the first assumption (in fact, the highest temperature used was 1800° C, and the diffusivity of plutonium in UO_2 is still very low [4]). As regards the second assumption, we should have been able to detect this impurity that did not appear in the other batches of A D U, but none was to be found. So that the question is still unanswered.

Because of this second phase, it was impossible to measure accurately the stoichiometry of the corresponding batches. Because stoichiometry is determined by X-ray diffraction measurements of the lattice parameter, it is necessary to know accurately the percentage of the second phase, and it is not the case. However if we take the utmost estimated value, 4 % (1.6 % being the mean value determined by micrographic counting) we have verified that the oxide is still substoichiometric, and this is confirmed by the good resistance to sodium that was observed for double-phase pellets.

It is interesting to note that X-ray diffraction evaluations give a higher percentage for the second phase, 15 % being the maximum. This could be due to the preponderance of very small isolated particles which are not counted by micrographic examination.

Studies of future development of oxide fuels

The burnup aimed for the future cores of Rapsodie and Phenix are near 100,000 M W D/T and it is necessary to study oxides having a good resistance to swelling under irradiation. For that, we are trying to obtain densities between 75 and 90 % of the theoretical density.

Preliminary studies

A - During the trials that were made before the fabrication we have just described, we were able to see the influence of sintering temperature on the final density of the oxide.

Therefore we have studied systematically the behaviour of UO_2 pellets having a green state density of 65 % of the theoretical value, under sintering temperatures varying from 1150° C to 1650° C. We can see on the corresponding curve of Figure 12 that the densities obtained vary from 68 % for the lowest temperature (1200° C) to 97 % for the maximum temperature (1650° C).

There are two disadvantages to this method : risk of bad diffusion in a mixed oxide and lack of stability of the density for temperatures higher than the sintering temperature. Once in the pile, the zone of low density oxide could be reduced to a fine annular layer near the can.

B - We have therefore searched for a method allowing sintering temperatures of at least 1500° C :

a) with this object we reduced the specific area of the powders by high temperature treatment. A trial on UO_2 heated in a reducing atmosphere at 1350° C for 4 hours, gave after sintering at 1500° C for 3 hours a density of 90 % to 92 % of the theoretical value for a green state density of 70 %. This result was still inadequate.

b) we decided to increase the quantity of zinc behenate which was initially .2 wt % and added around the oxide granules after the first compacting.

By adding 1 wt % behenate in a mixed oxide that had been calcined at 1100° C for 4 hours we obtained after sintering for 3 hours at 1500° C a density of 88 % of the theoretical value. The porosity was heterogenous and mainly made of cracks due to the accumulation of behenate around the granules. It seemed therefore impossible to increase the quantity of zinc behenate introduced in this manner.

c) we were thus lead to the method now used which consist in the incorporation of behenate to the milled mixed oxide powder before the first compacting[5]. Thus, behenate is distributed much more regularly in the oxide and we verify that its capacity to slow down the densification is highly

increased. We can avoid a high temperature initial treatment of the oxide and still have densities near 80 % of the theoretical value after sintering for 3 hours at 1700° C (Figure 12).

Spectrographic analysis of the pellets show that the zinc content is below the detection limit (50 ppm) and carbon analysis give results lower than 50 ppm.

Fabrications for irradiation tests

A - Irradiation of mixed oxide in Enrico Fermi reactor.

This new method was first applied to the fabrication of low density (85 % of the theoretical density) mixed $(U_{.8}, Pu_{.2})\ O_2$ oxide for irradiation in the Enrico Fermi reactor which should have started in 1966 (Figure 13).

In this manner 15 pins, containing 2.5 kg of mixed oxide in conformity with the specifications were made in June and July 1966.

For the same irradiation programme 15 other pins, containing the same quantity of mixed oxide were filled with annular pellets. These pellets have a density of 95 % of the theoretical value and a central hole made directly during pelleting, bringing the apparent density down to 85 %.

B - Irradiation of mixed oxide in the Dounray Fast reactor.

A second fabrication, to be irradiated in the D F R, took place in December 1966. Six pins filled with about .5 kg of low density (85 %) $(U_{.8}, Pu_{.2})\ O_2$ oxide were made.

C - Irradiation of mixed oxide in Rapsodie.

The fabrication of the pins for 4 experimental fissile assemblies has started in April 1967, filled of $(U_{.8}, Pu_{.2})O_2$ pellets. They will be irradiated in Rapsodie in July 1967. They contain 5.5 kg of full pellets with a density of 80 % and 5.5 kg of full pellets with a density of 85 % of the theoretical value.

Four further assemblies containing a similar fuel (partly with annular pellets) will be manufacturel in the second half of 1967).

Specifications considered for the Phenix reactor fuel.

The fabrications we have just mentionned show that low density oxide falls in the domain of practical application. They have also been used as a base for the specifications considered for the fuel for Phenix reactor and which we hope to confirm by the irradiations in progress.

These specifications are the following :

PuO_2 content : $\dfrac{\text{weight Pu} \times 100}{\text{weight mixed oxide}} = \begin{cases} \text{central zone} & 20 \\ \text{external zone} & 25 \end{cases}$

Stoichiometry : $\dfrac{O}{U + Pu}$ 2.00 (desired : 1.96)

Diameter of the pellets : 5.5 mm

Longitudinal mass on unrectified pellets (full pellets of density equal to 85 % of the theoretical value)	central zone	2.23 g cm^{-1}
	external zone	2.24 g cm^{-1}

External aspect of the pellets :	maximum of 5 chips	1 mm
	or 1 chip	2 mm

Conclusion

The fabrication of the first charge of Rapsodie and the studies of low density mixed oxide in an extended irradiation programme has enabled us to collect a large information as well on the fabrication and control processes as on the physico-chemical properties of the oxides. This knowledge is now used for the definition of the fuel for the Phenix reactor and for the survey of the manufacturing plant, capable of producing every day 30 kg of oxide, which will be equipped in 1968.

Acknowledgements

We would like to thank the Section d'Etude des Céramiques à base de Plutonium for its help in the study of the problems raised by the fabrication of the first charge for Rapsodie and of the low density oxides.

We also thank the Section du Plutonium Irradié for their suggestions in the general trend of the studies devoted to low density oxide fabrication.

REFERENCES

1. Y. Masselot, Report CEA to be published later on "Fabrication du premier coeur de Rapsodie".

2. S. Bataller, M. Ganivet, H. Guillet, Y. Masselot and F. Stosskopf, Brussels, March 1967, Symposium on plutonium used as nuclear fuel. "Quelques enseignements tirés de la fabrication du premier coeur de Rapsodie".

3. G. Dean, C. Pelou and D. Beugnies, Report CEA R. 2737, "Fabrication de pastilles d'oxydes mixtes d'uranium et de plutonium", 1965.

4. F. Schwitz and R. Lindner, Radiochimica Acta 1 - 218 - 220, Diffusion of Pu in UO_2, 1963.

5. Y. Masselot, French patent n°PV 97 722 of february 13th 1967.

Table 1. Weight Percentage of plutonium in mixed oxide

	Aimed at by weighing Pu O_2 calcined in air at 700° C	Determined by chemical analysis	
		1st campaign mean value on 220 half-batches	2nd campaign mean value on 26 half-batches
$\frac{\text{Weight Pu} \times 100}{\text{Weight mixed oxide}}$	22,84	$22,95_5$	$22,93_7$

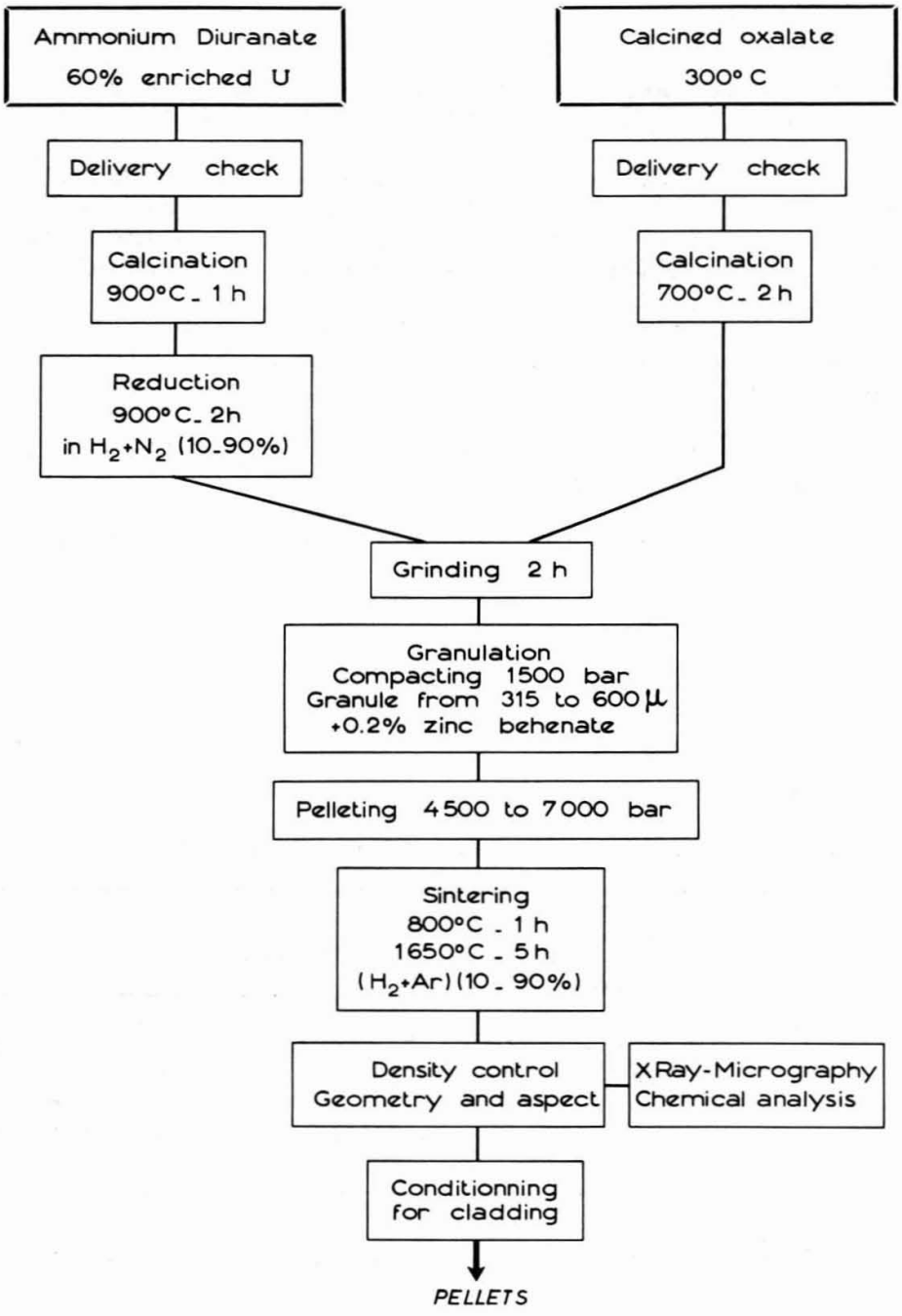

Fig. 1 - Processing diagram of the pellets.

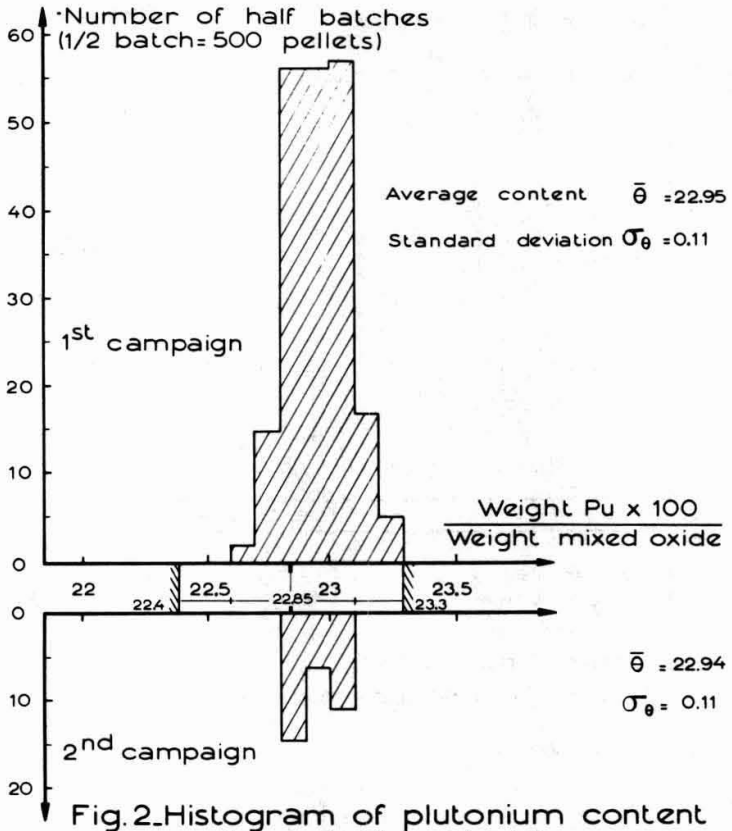

Fig. 2_Histogram of plutonium content (chemical analysis)

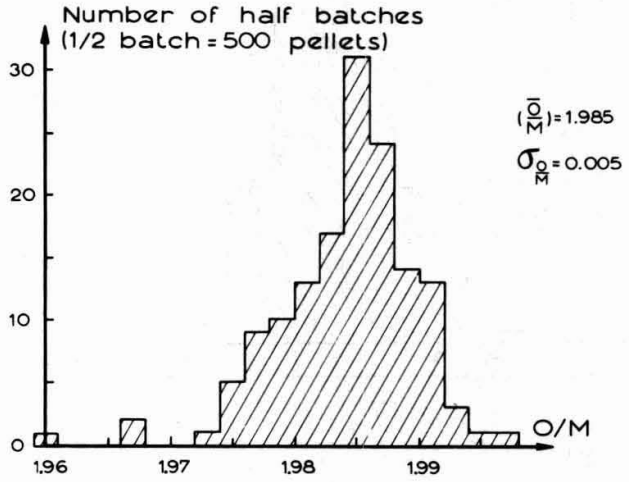

Fig. 3_Histogram of O/M Ratio for single phase batches of the first campaign

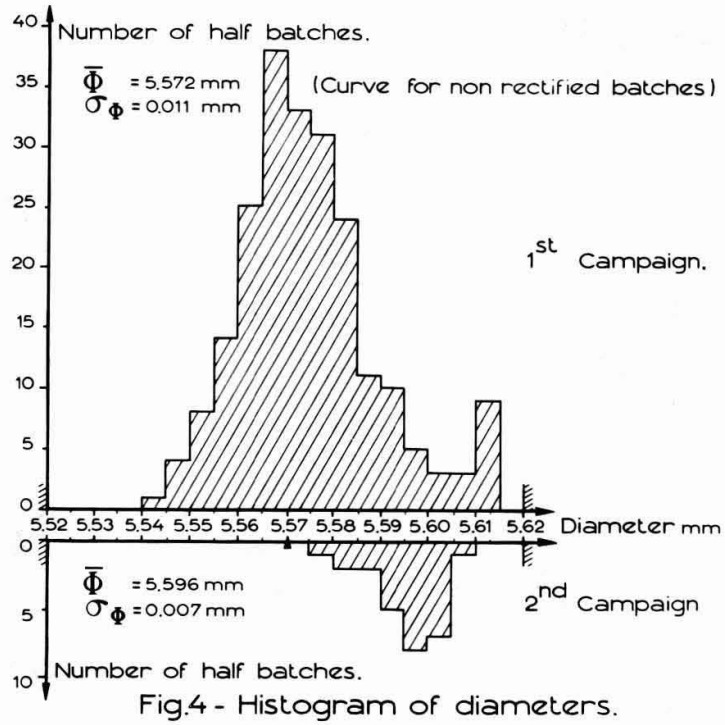

Fig.4 - Histogram of diameters.

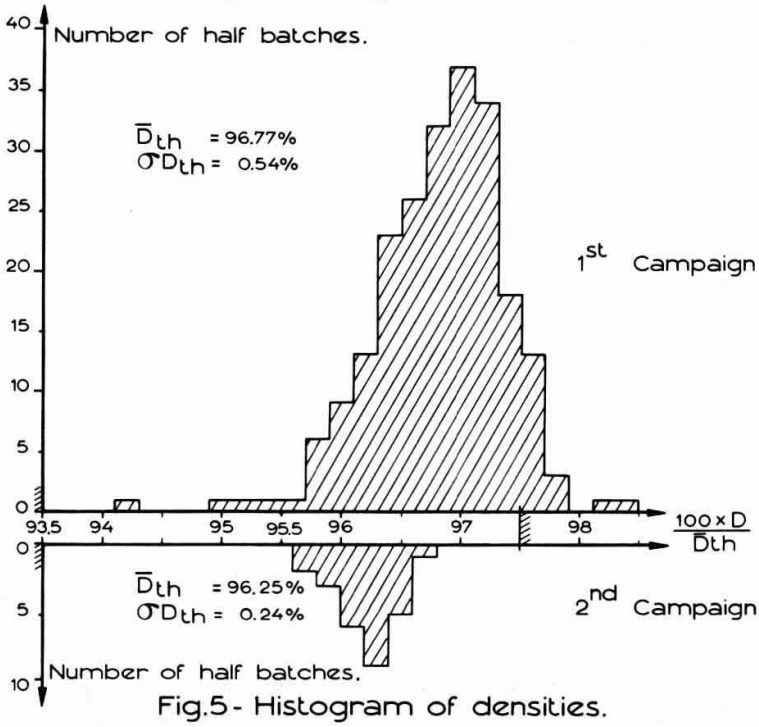

Fig.5 - Histogram of densities.

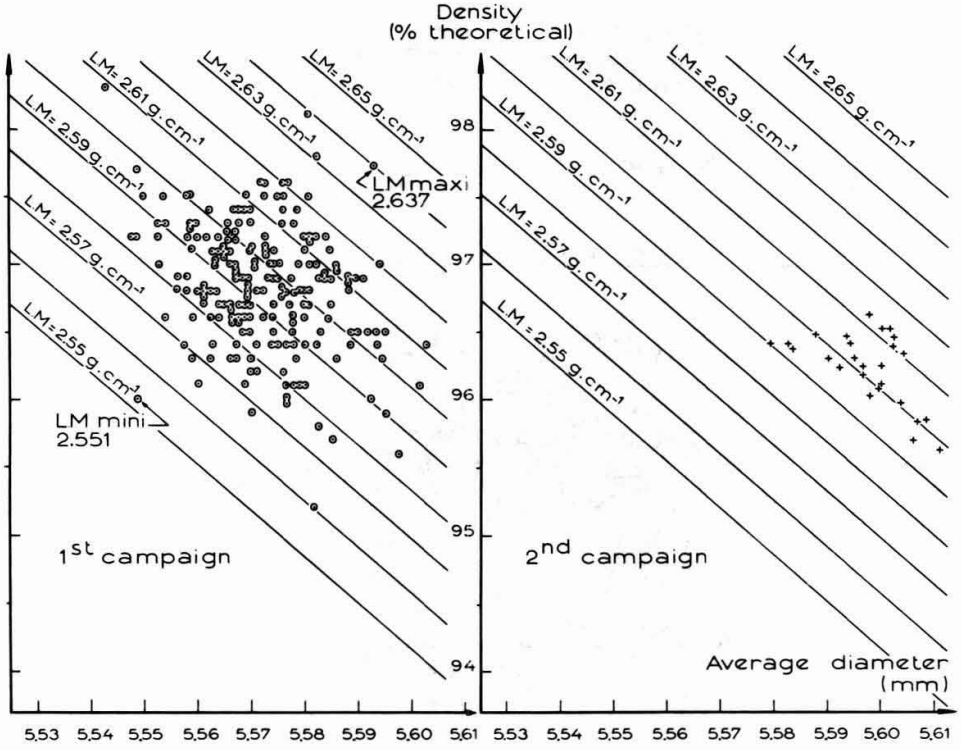

Fig.6. Diameter density distribution and longitudinal mass curve system for the whole of the batches of the 1st and 2nd campaign.

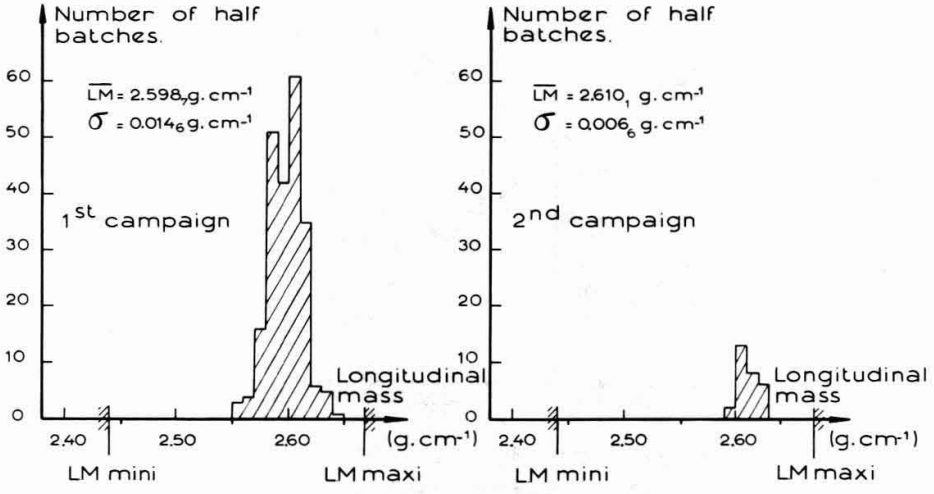

Fig.7. Histogram of longitudinal mass.

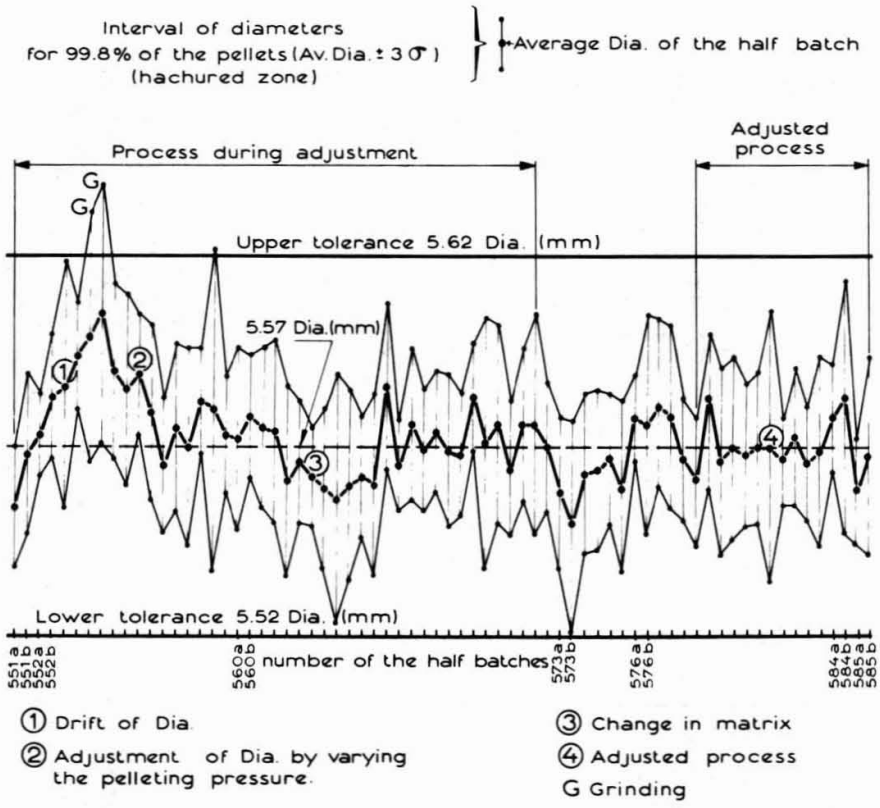

Fig.8 - Diameter variation of sintered pellets.

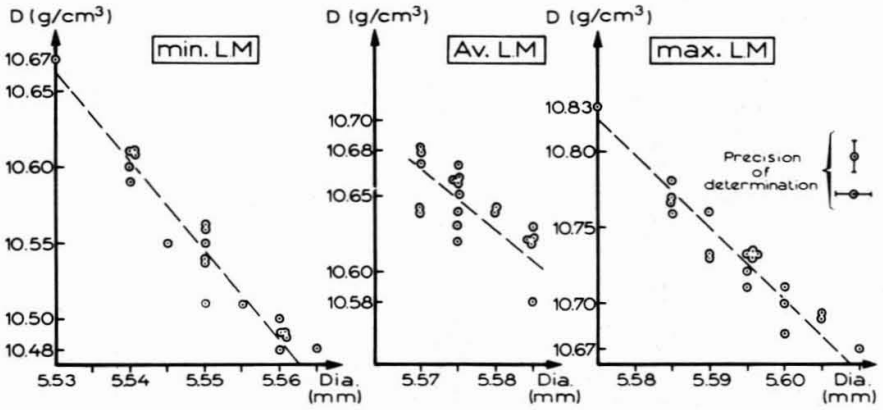

Fig.9 - Diameter density relationship in a same batch.

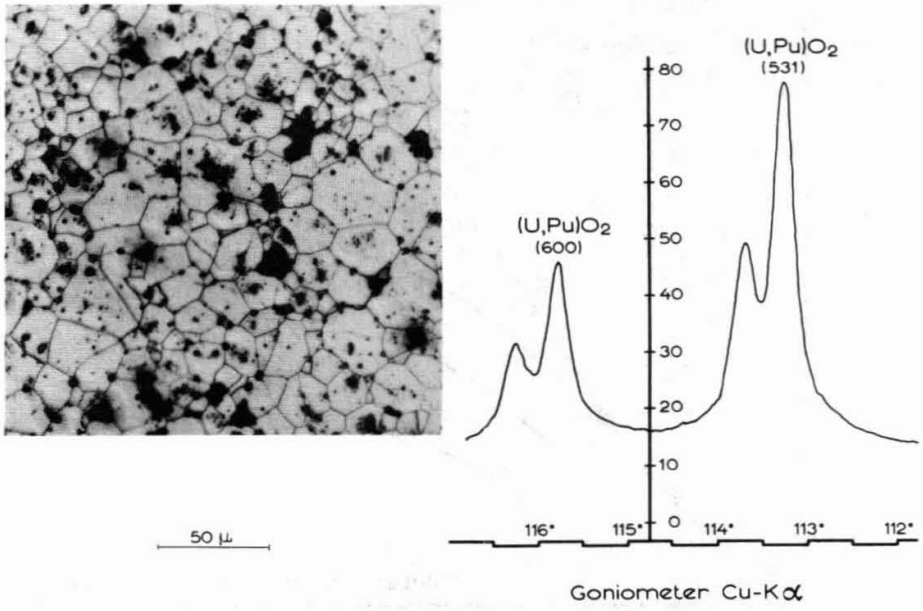

Fig.10- Micrography and X Ray diffraction analysis of a single-phase pellet.

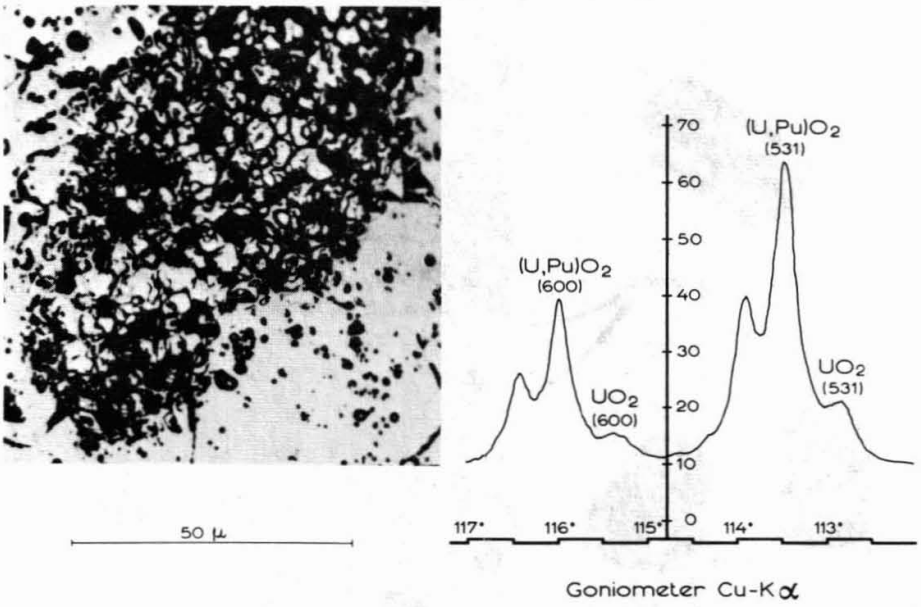

Fig.11- Micrography and X Ray diffraction analysis of a two-phase pellet.

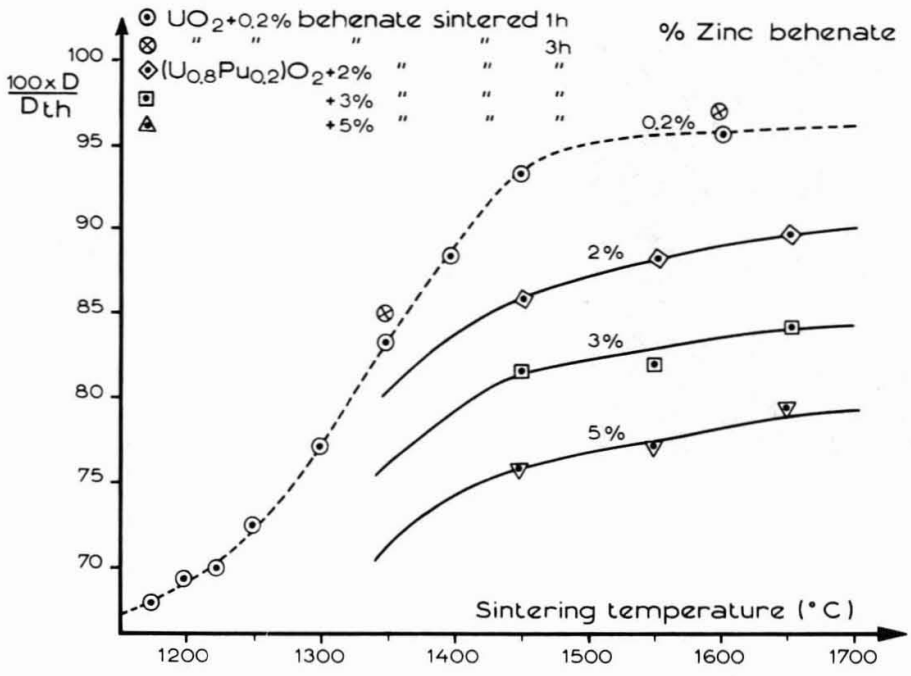

Fig.12-Influence of zinc behenate content and of sintering temperature on the density of the sintered pellets.

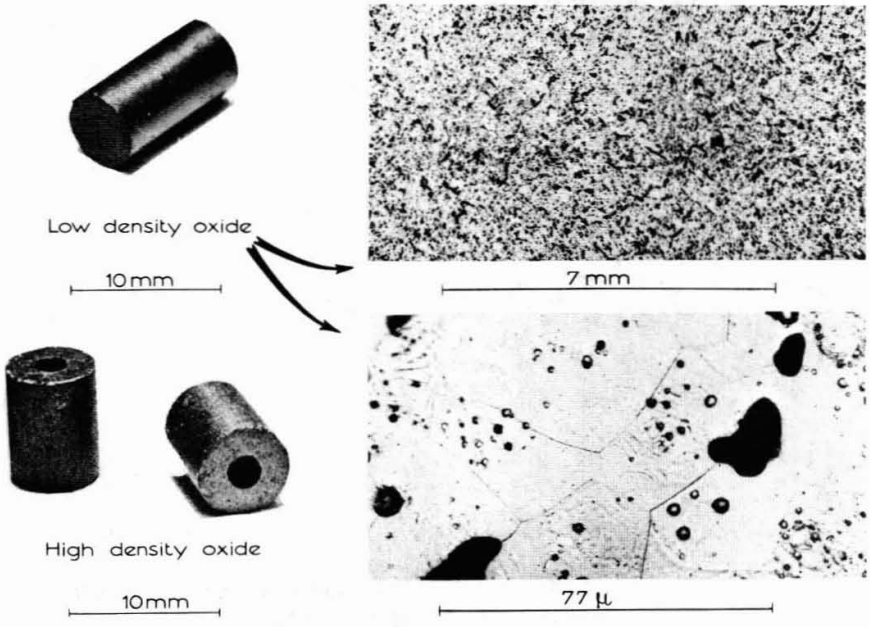

Fig. 13 - Aspect and micrography of low density pellets

(U-Pu)C PARTICULATE FUEL FABRICATION

J. E. Ayer

Abstract

A series of uranium-plutonium carbide elements were fabricated for fuel element performance studies. The fuel consisted of mixed uranium and plutonium carbides and solid-solution uranium-plutonium carbide. The fuel elements were manufactured by vibratory compaction employing an infiltration technique. The loading process parameters were determined on the basis of model studies carried out on non-fissile materials.

Eleven rods containing 80% uranium carbide and 20 plutonium carbide and five rods containing solid-solution carbides were fabricated. The mixed carbide fuel elements were all loaded to "smear" densities of 80% of theoretical with the exception of one which was compacted to 83.8% theoretical density. The solid-solution rods were formed to fuel densities of 84.2 $\pm$ 1.3% of theoretical.

Fabrication revealed that the packing characteristics of carbides deviated from the model studies due to attrition of the fuel material. In some cases 20 percent of the first component addition was reduced to finer screen sizes during loading. Uniformity of density is promoted by infiltration, although angular particles are conducive to low infiltration rates.

J. E. Ayer is the Leader of the Plutonium-Materials Fabrication Group, Metallurgy Division, Argonne National Laboratory, Argonne, Illinois.

Carbide fuel fabrication development at Argonne National Laboratory is motivated by two stimuli. One is the desirability of developing improved fabrication techniques and the second is the need of the carbide fuels performance program which exercises a continuing demand for fabricated elements. Both facets of the development program are incorporated in the results described in this paper.

Generally ceramic fuels are presented to the jacket in one of two forms; pellets or granules. Because a fuel body density between 80 and 85% of theoretical is desired for our fuels evaluation program, particulate fuel columns formed by vibratory compaction are of interest. The interest in particulate fuel columns derives from the void space that must accompany fuels of this low density. The voids offer paths for the accumulation and release of fission gases and provide space into which swelling may be accommodated. Small particle size promotes fission gas release by limiting the distance that the gas must travel in order to diffuse to the particle surface.

The attainment of capability to fabricate ceramic fuel bodies by vibratory compaction was preceded by considerable development. Studies were carried out on model systems to determine the effect of particle geometry and vibratory mode on packing characteristics. The initial studies were conducted with spherical particles in single and multi-component systems. The results of experiments with malleable steel shot have been published in the Journal of the American Ceramic Society (1) and are shown in Fig. 1. This is a plot of the void packing efficiency versus diameter ratios of container to first component spheres and spheres to spheres. The void packing efficiency is defined as the fraction of available void volume that is occupied by the entering component. The equations given on the figure are least-squares fits to data points determined from experimentation. The standard deviation of data from the mathematical expression was found to be 0.01 for over 200 individual data points determined on single component systems. In the case of binary systems 60 data points showed a standard deviation of 0.013 from the curve fit. These findings permit one to predict achievable density by mathematical calculation (2). These data were gathered by employing an infiltration technique, thereby the lower curve in Fig. 1 represents the void packing efficiency of the second component in the first component matrix spheres. The lower curve is universal in the sense that it represents the packing efficiency of any size sphere in a matrix of spheres.

The above work has been extended to the compaction of angular shapes. In this study the infiltration technique was used to find the influence of particle dimension and shape upon void packing efficiency. The results of this study, which have also been published in the Journal of the American Ceramic Society (3), are shown in Fig. 2. Figure 2 like Fig. 1 is a plot of void packing efficiency versus the diameter ratios of container and matrix particle to entering particle dimension. Particle dimension was determined by

sieving and is the average between screen openings through which the particles pass and on which they are collected. The least-squares fit of the packing efficiency data is shown as the mathematical expression on the figure. The standard deviation of packing efficiency of angular particles from the curve fit found on over 100 data points was 0.009 for a single component system of particle dimension less than 300 microns. The mathematical expression generated for spherical and angular particle packing are of similar form. The expression for the angular system, however, has an added term. This middle term is a function of reciprocal of particle dimension and is dependent upon the surface-to-volume ratio of the particles being packed.

The experiments in spherical and angular packing are sufficient to define the spatial characteristics and limitations of the systems studied. They do not, however, reflect the influence of attrition of particles or permit one to infer rate of infiltration. Preliminary studies to determine the influence of factors effecting the infiltration rate have been conducted. Results indicate that infiltration rate is a function of frequency and acceleration of vibration and particle shape. Generally, infiltration time for both spherical and angular particles varies inversely with acceleration to about 15 g's. Little difference in the infiltrating rate was observed between 15 and 20 g's. This finding suggests that a plateau is reached in the rate of infiltration between these two values. The rate of infiltration was a maximum between 40 and 80 cycles per second for all accelerations to 20 g's. At driving frequencies between 100 and 400 cycles per second, infiltration time increased with increasing frequency. This finding prompted the use of 60 cycle vibration for all fabrication work. The influence of particle shape on infiltration time can be illustrated through one experiment in which comparable sized spheres and angular particles were loaded. In this instance, a 22-inch long, 1/4-inch diameter column was loaded at 60 cycles per second and 15 g's. The infiltration time for the angular particles was about 25 minutes. About 7 minutes was necessary to complete the infiltration of spherical particles.

Translation of information from the development studies into fabrication was accomplished through the fabrication of 16 elements for fuel evaluation studies (4). The fuel specimens consisted of cylindrical metal jackets with welded end plugs, a fuel column, and a retainer. The over-all length of fuel elements was 25-1/4". The fuel occupied the lower 14" of the element and a plenum for the accommodation of fission gases occupied the upper 9" of the element between the top plug and the retainer. The inside diameter of all elements was 0.256". Pertinent data on the fuel-jacket combinations and the fuel composition are shown in Table 1 and Table 2. Two types of elements were fabricated: one was a uniform column of solid solution (U·Pu)C at 85% theoretical density; the other consisted of a UC matrix into which PuC was infiltrated to achieve an over-all density of 80% of theoretical. In both cases the uranium-plutonium ratio was to be 4:1.

Previously described development work conducted with malleable, non-fissile material indicated that the maximum packing fraction for a two-component system of angular particles in small diameter tubes would be about 80%. Because the density of fuel carbides was about 97-1/2% of theoretical a two component system would yield a fuel density of only 78% of theoretical. One method by which the packing density may be increased is to use a three-component system. This method has been successful in model systems using spherical shapes. However, efforts to produce uniform density by an infiltration technique on three component systems of angular particles has been unsuccessful. Another alternative is to blend three components of predetermined size and quantity and introduce them to jackets while vibrating. This approach was rejected because we have found that in unconstrained columns the fine fraction will settle, levitate the coarse particles, and result in non-uniform axial density distribution. The problem of achieving "smear" density greater than 80% of theoretical was resolved as a compromise between these two solutions. Two size components were selected such that the smaller component would be small enough to fit into the voids in the coarse component matrix and large enough to be retained in these voids. The finely divided third component was infiltrated through this mixture. The coarse fraction size was calculated to give the maximum packing efficiency determined by the use of the angular particle packing efficiency curve previously shown in Fig. 2. The mathematics necessary to determine the maximum packing efficiency is as follows:

$$P\varepsilon_1 = 0.635 - \frac{32.0}{d_1} - 0.072\, e^{-0.207D/d_1}$$

$$\frac{\Delta P\varepsilon_1}{\Delta d_1} = \frac{32.0}{d_1^2} - \frac{(0.072)(e^{-0.207D/d_1})(0.207D)}{d_1^2} = 0$$

$$0.0149D\, e^{-0.207D/d_1} = 32.0$$

when, $D = 6.50 \times 10^3\ \mu$ (0.256 in.)

$$e^{-0.207D/d_1} = 0.330$$

$$0.207D/d_1 = 1.11$$

$$D/d_1 = 5.36$$

$$d_1 = 1.22 \times 10^3\ \mu \text{ (0.048 in.)}$$

$$P\varepsilon_{1(Max)} = 0.635 - \frac{32.0}{1220} - 0.072\, e^{-(0.207)(5.36)}$$

$$P\varepsilon_{1(Max)} = 0.635 - 0.026 - 0.072\, e^{-1.11}$$

$$P\varepsilon_{1(Max)} = 0.635 - 0.026 - (0.072)(0.33)$$

$$P\varepsilon_{1(Max)} = 0.609 - 0.024 = 0.586$$

The optimum size for the coarse fraction is found by setting the derivative of $P\varepsilon_1$ with respect to d_1 equal to 0 and solving for d_1. The maximum packing efficiency of this component was found to be 58.6%. The size of the coarse component to achieve this maximum packing efficiency was determined to be 0.048". The size and quantity of the second component to raise the packing fraction to above 66% was determined by making model runs with angular blast cleaning grit. By this method we determined that the second component size should be about 1/2 of the first component size. The model conditions required to yield a fuel body of 80% coarse material, 20% finely divided material and 82% packing fraction were thus determined. In terms of percentages, the carbide fuel charges were as follows: 62.4% of 12/14 mesh material blended with 17.6% of 30/35 mesh material into which was infiltrated 20% of -325 mesh powder. Similar calculations were made to determine the quantities and sizes of components to achieve 85% TD bodies of solid-solution carbides.

The fabrication procedure is outlined in Fig. 3. All jacket material was inspected, measured for volume, and cleaned before entering the process. Massive chunks of fuel material were reduced to desired mesh sizes by hand using a Plattner mortar. The product was screened to obtain the coarse fractions and the unacceptably small sizes were passed through a micro-pulverizer to generate fines for infiltration. Fuel charges were weighed out according to calculation, placed in plastic bottles, and stored in a desiccator under vacuum until ready for use. Once in the gloveboxes the jackets were attached to a vibrator platen by a stud that was threaded into the bottom plug. A rattle cage was dropped over the tube and a funnel inserted into the open end. Figure 4 shows such an element ready for loading. Pre-weighed coarse and intermediate sized fractions were blended and the mixed charge was poured into the jacket through a long funnel. During the introduction of the blended fuel charge the 60 cycle vibrator was operating at about 5 g's determined by an accelerometer attached to the bottom side of the vibrator platen.

After complete introduction of the large component the funnel was carefully removed to prevent contaminating the upper portion of the inside wall of the jacket with plutonium. The funnel was replaced by a thimble and a shorter funnel as shown in Fig. 5. The thimble is a brass tube soldered to a standard Swage-lok reducer. The bottom of the thimble contains a screen with a mesh larger than the most finely divided fuel fraction and smaller than the coarser fractions. The O-rings at the bottom prevent the infiltrating fraction from being conveyed up the fuel tube wall and contaminating the fuel rod hardware. The thimble was seated against the fuel jacket top by downward pressure on the reducer while the fuel tube is driven at 60 cycles per second and 15 g's. When the thimble is seated, vibration is stopped and the Swage-lok fitting tightened against the top of the fuel tube. The funnel is then inserted and the fine fraction is introduced. Introduction of the coarse fraction took from 30 to 40 seconds and the fuel level was invariable within 1/8" of the final calculated depth.

Five specimens of solid-solution (U·Pu)C were fabricated for the carbide fuels evaluation program. The densities attained were 84.2 ± 1.5% of theoretical employing 97.1% TD particles. This is equivalent to an average void packing efficiency of 86.7%. An indication of the uniformity of the solid-solution columns may be seen in Fig. 6. The two elements on the left of this figure are the solid-solution-containing columns. The rod on the extreme left is quite uniform and packed to a density of 82.9% of theoretical. The rod on its right is packed to a density of 85.5% of TD and exhibits isolated low density regions at the top half of the rod. Low density regions are acceptable from the standpoint of irradiation behavior since they form cold rather than hot spots. They are, however, deviations that may not yield to control and are thereby objectionable. This kind of structure is not typical of vibratorily compacted rods but it does illustrate one of the anomolies that may occur during this type fabrication. Ten specimens of mixed UC-PuC were assembled by the described process. Five of these specimens are shown on the right hand side of Fig. 6. All elements show a low density region at the top that is caused by the absence of fine fraction. The extent of this low density region varies from 1/2 to 1-3/4". The low density at the top of the fuel column was brought about by the deviation of the carbide system from the model system previously discussed. The model system was made up of angular particles of malleable material. The carbides, which are brittle, undergo attrition during the loading process due to the vibration. We have determined that attrition will bring about a change in particle surface-to-volume ratio and a consequent change in particle packing efficiency. This characteristic was confirmed when some elements, which behaved in an unpredictable manner during loading, were emptied of fuel material and the material was screened. We found that 20% of the fuel fraction could be reduced to a smaller size during loading of the matrix material alone. It is interesting to note that the "smear" density of the fabricated rods would increase only one to two and one-half percent by the complete filling of the void, which appears at the top of the rod, with the infiltrating fine fraction.

The results of development work, and this fabrication effort, tend to support a number of conclusions. First, model studies can be used to determine, mathematically, the sizes and weight of first component fuel charges to attain desired density. This conclusion is supported by our success at achieving desired column height in the matrix component. Secondly, prediction of fuel density from model behavior is possible to within one to two percent; a part of this deviation is due to attrition of the matrix particles during vibration. This conclusion is supported by the absence of the finely divided component at the top of the UC-PuC rods. Finally, the low density regions that occur unpredictably when loading irregular particles can be avoided and fabrication rates can be markedly improved by using spherical particles. To support this conclusion, I submit Fig. 7. Figure 7 is a model of an integrated fuel rod containing simulated fuel and upper and lower blanket without mechanical separation between

the fuel and the blanket sections other than the particles themselves (5). This rod, whose "smear" density is 80% TD was loaded at 60 cycles per second and 15 g's in a glass tube. The total loading time for this model rod, which is four feet long, was about one hour. Here again it is possible to load a number of such rods on a single vibrator platen. The charges of simulated fuel and blanket were determined using the mathematical expression shown on Fig. 1 and the degree of intermixing of blanket and fuel sections is shown in Fig. 8.

REFERENCES

1. J. E. Ayer and F. E. Soppet, Vibratory Compaction - Part I, The Compaction of Spherical Shapes, Journal of the American Ceramic Society, 48, (4), 1965, pp. 180-183.

2. James E. Ayer and Frederick E. Soppet, Method and Apparatus for Vibratory Compaction, U.S. Patent No. 3,261,378.

3. J. E. Ayer and F. E. Soppet, Vibratory Compaction - Part II, The Compaction of Angular Shapes, Journal of the American Ceramic Society, 49, (4), 1966, pp. 207-210.

4. J. E. Ayer, F. E. Soppet, G. J. Talaber, and B. H. Bieler, Nuclear-Fuel-Element Loading by Vibratory Compaction -- Uranium-Plutonium Carbide Specimens for EBR-II Irradiation, ANL-7076, February 1966.

5. J. E. Ayer, Method of Making Combination Fuel Rods, Patent Application S-33,888, Filed 28 April 1967, U.S. Patent Office.

Table 1. Average Composition of Fuel Carbides for Performance Studies

		Fuel Material		
		UC	PuC	(U·Pu)C
I.	Chemical Composition in w/o			
	A. Uranium	95.12	--	76.33
	B. Plutonium	--	95.02	19.07
	C. Carbon	4.59	4.85	5.11
	D. Oxygen	0.47	0.044	0.0066
II.	Isotopic Analysis in w/o			
	A. U^{234}	1.00	--	0.76
	B. U^{235}	88.60	--	71.32
	C. U^{236}	0.24	--	0.18
	D. U^{238}	5.29	--	4.08
	E. Pu^{239}	--	90.26	17.43
	F. Pu^{240}	--	4.38	1.50
	G. Pu^{241}	--	0.37	0.13
	H. Pu^{242}	--	0.02	0.01
III.	Density Measurement			
	A. Absolute Density g/cc	13.28	13.24	13.21
	B. Theoretical Density in %	97.1	97.4	97.1
IV.	Carbon + Oxygen/Metal Ratio	1.02	1.02	1.05

Table 2. Specifications for Carbide Irradiation Specimens

Number of Specimens	Jacket Material	Wall in in.	Fuel Form	Density % T.D.
4	Hastelloy-X	0.015	UC-PuC	80
3	Nb-1w/o Zr	0.012	UC-PuC	80
2	Ta-10w/o W	0.020	UC-PuC	80
1	316-SS	0.020	UC-PuC	80
1	304-SS	0.020	UC-PuC	80
2	Nb-1w/o Zr	0.012	(U·Pu)C	85
1	V-20w/o Ti	0.020	(U·Pu)C	85
1	V	0.020	(U·Pu)C	85
1	W-coated Hastelloy-X	0.005 0.015	(U·Pu)C	85

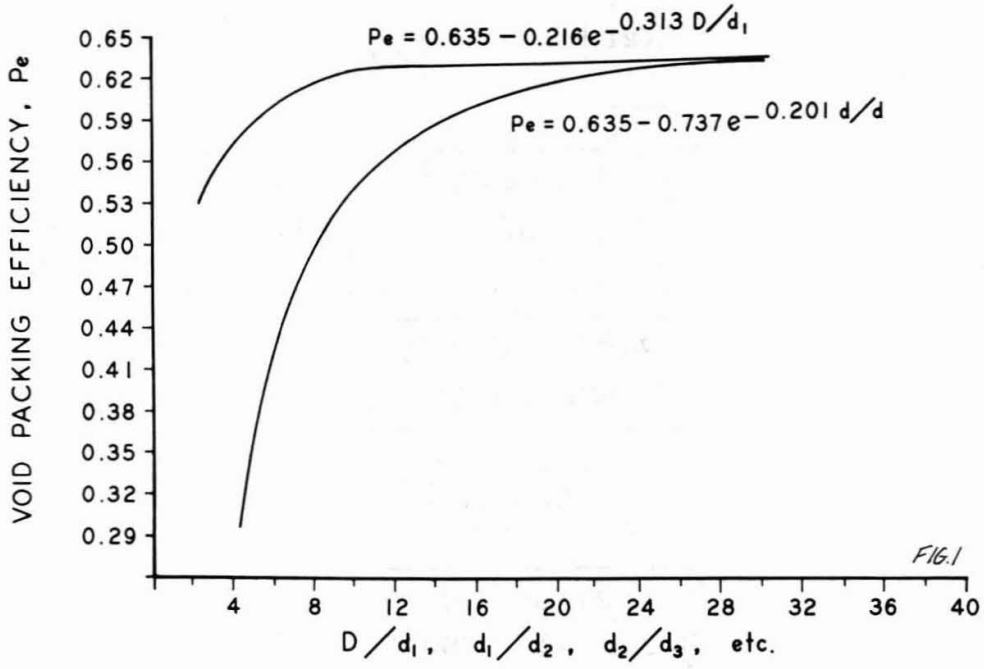

VOID PACKING EFFICIENCY VS RATIO OF DIAMETERS

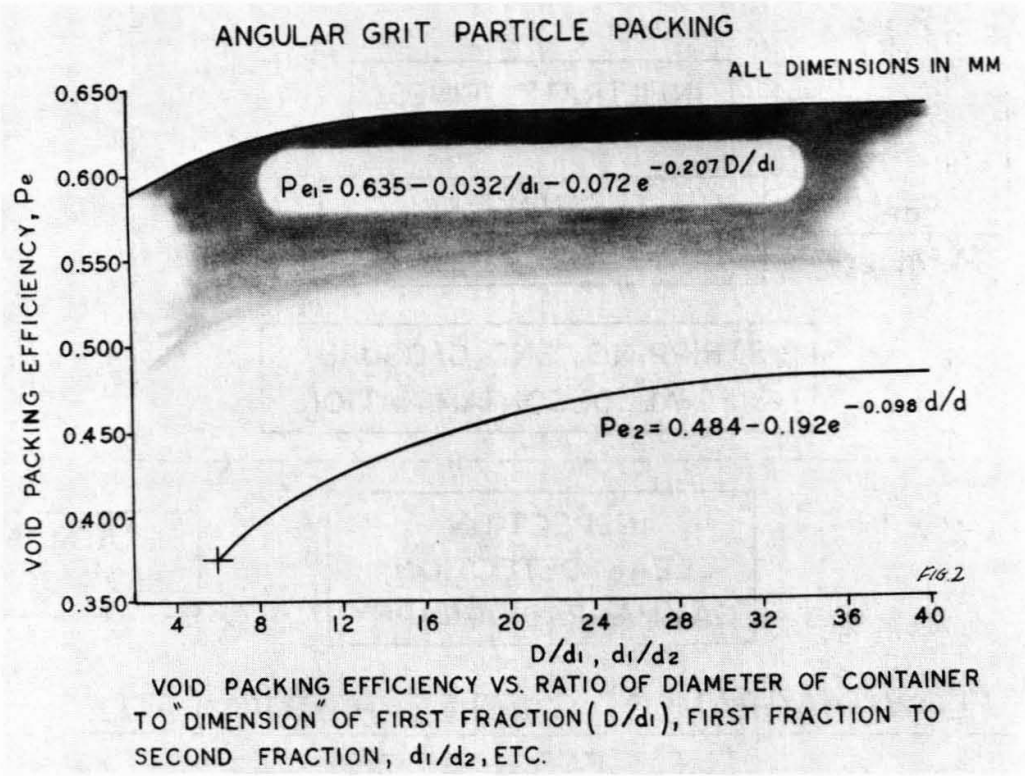

VOID PACKING EFFICIENCY VS. RATIO OF DIAMETER OF CONTAINER TO "DIMENSION" OF FIRST FRACTION (D/d_1), FIRST FRACTION TO SECOND FRACTION, d_1/d_2, ETC.

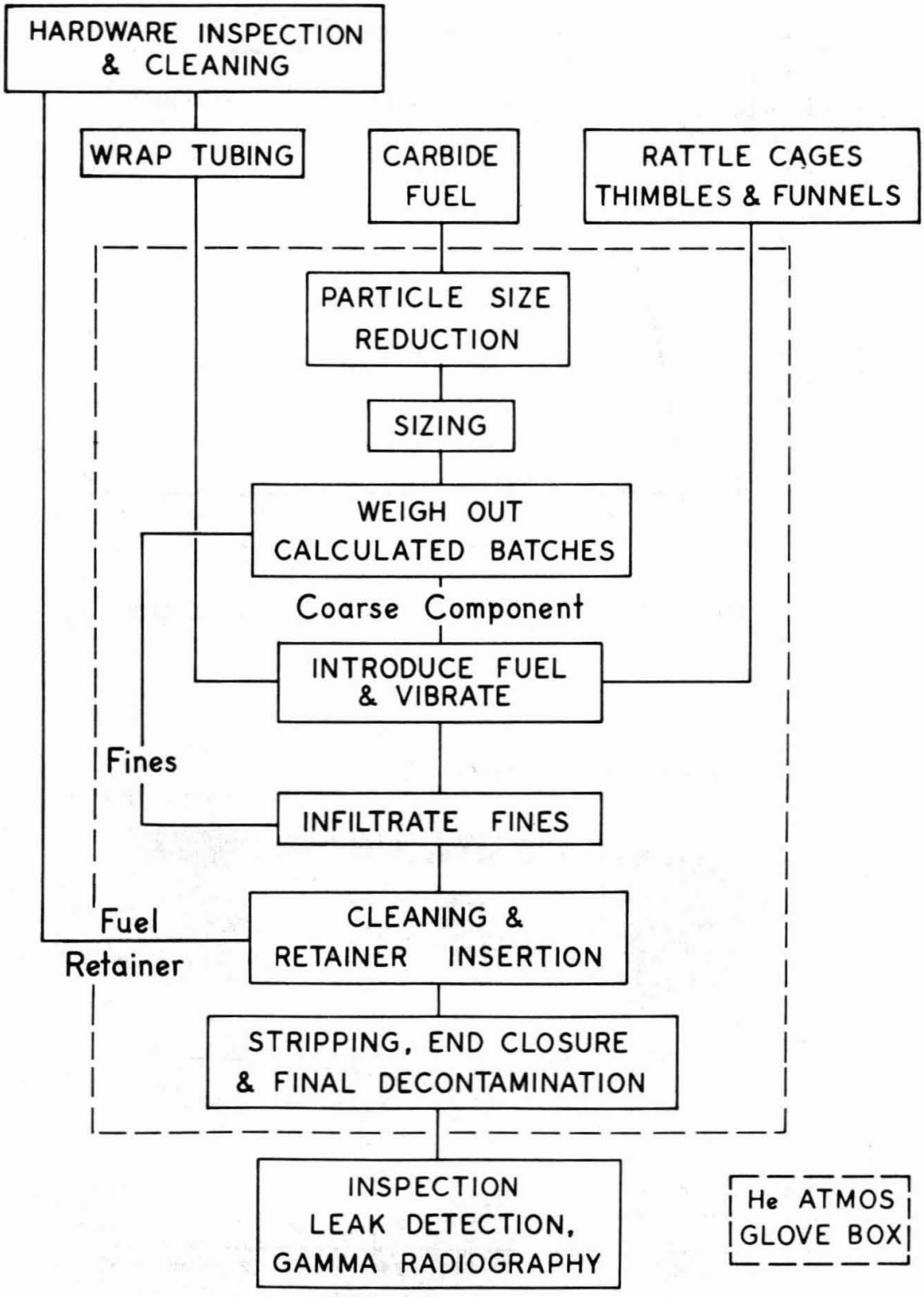

FLOW DIAGRAM OF CARBIDE PARTICULATE FUEL FABRICATION

FIG. 3

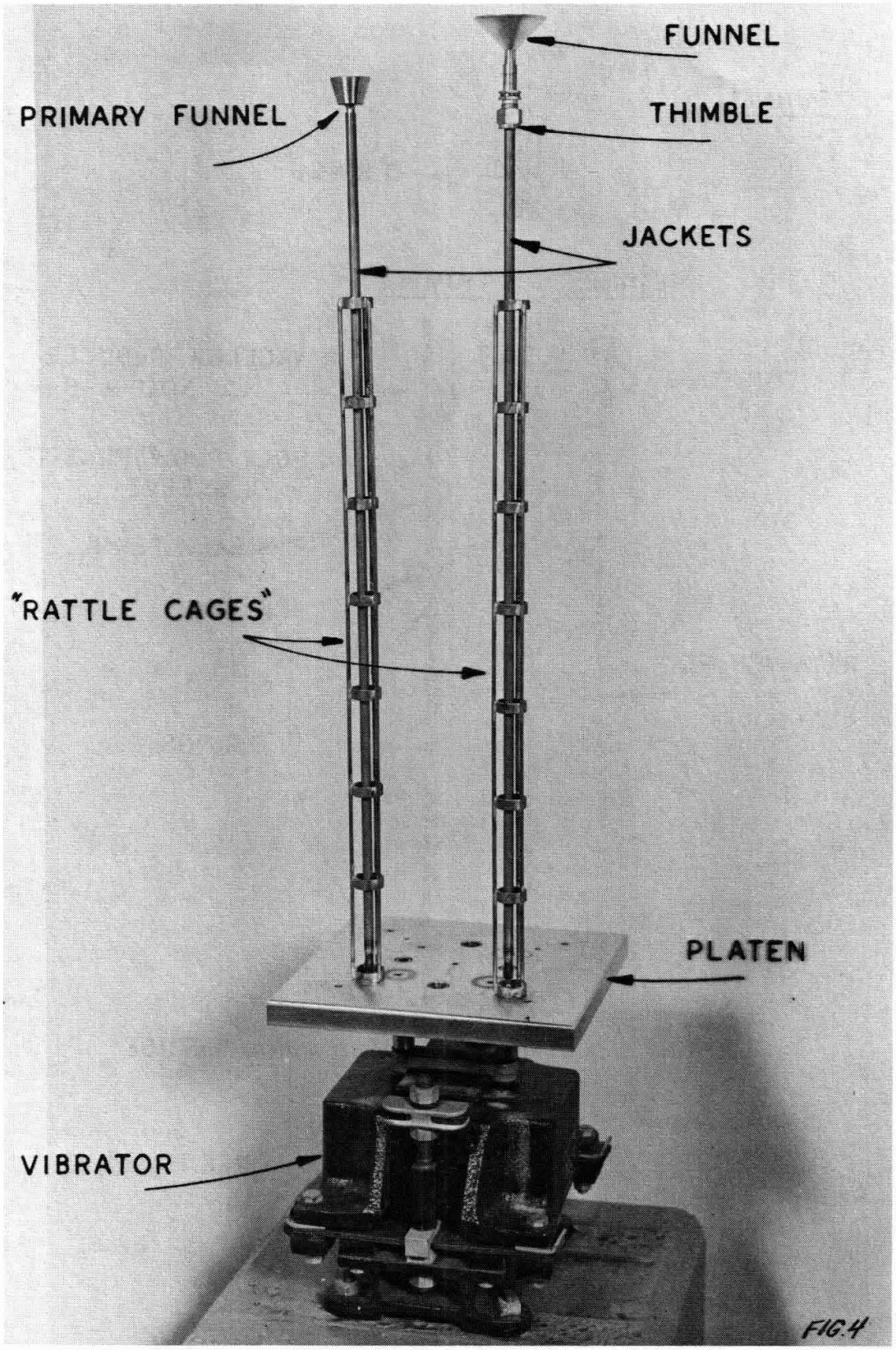
FUNNEL
PRIMARY FUNNEL
THIMBLE
JACKETS
"RATTLE CAGES"
PLATEN
VIBRATOR
FIG.4

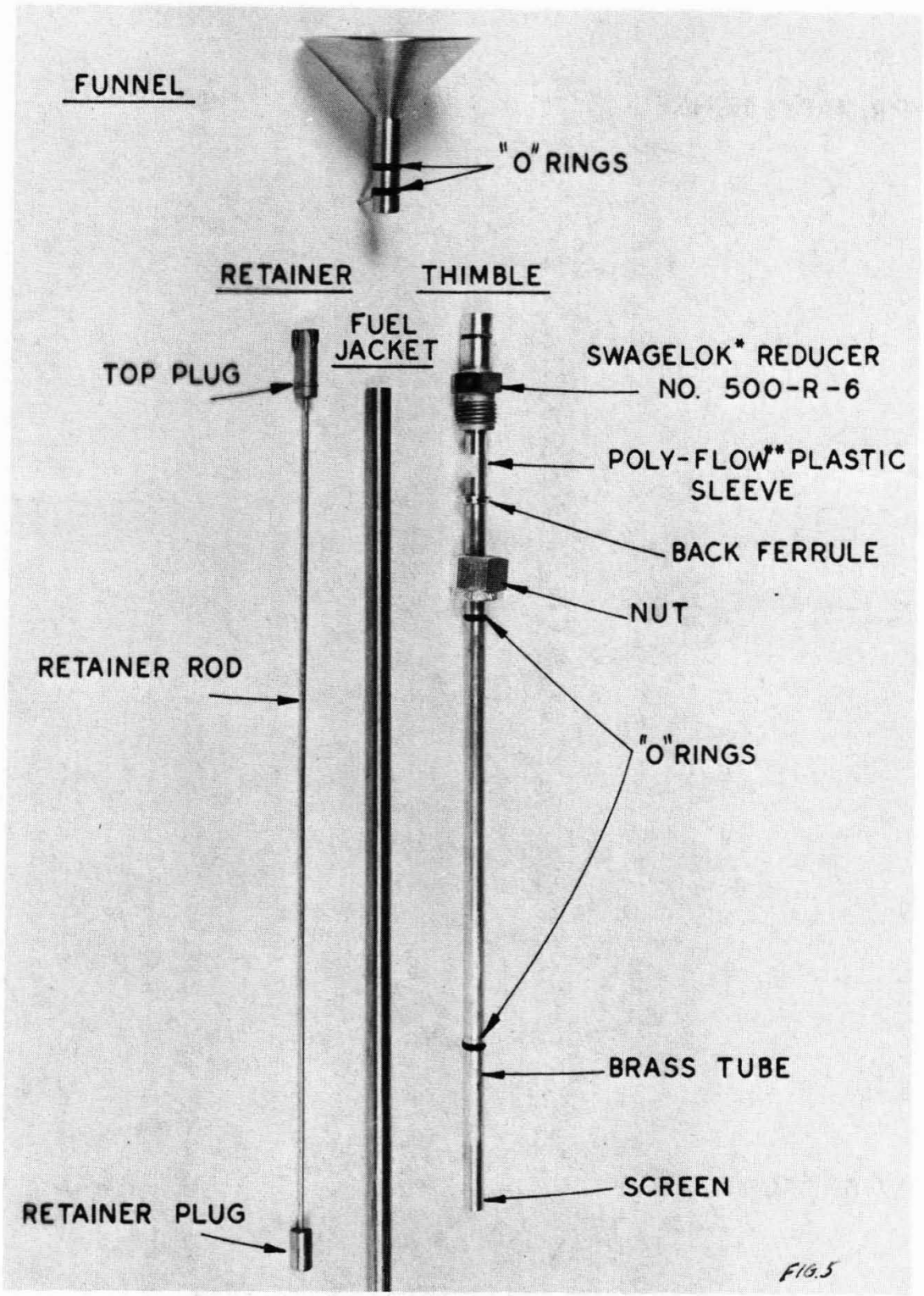
FUNNEL
"O" RINGS
RETAINER
THIMBLE
FUEL JACKET
TOP PLUG
SWAGELOK* REDUCER NO. 500-R-6
POLY-FLOW** PLASTIC SLEEVE
BACK FERRULE
NUT
RETAINER ROD
"O" RINGS
BRASS TUBE
SCREEN
RETAINER PLUG
FIG.5

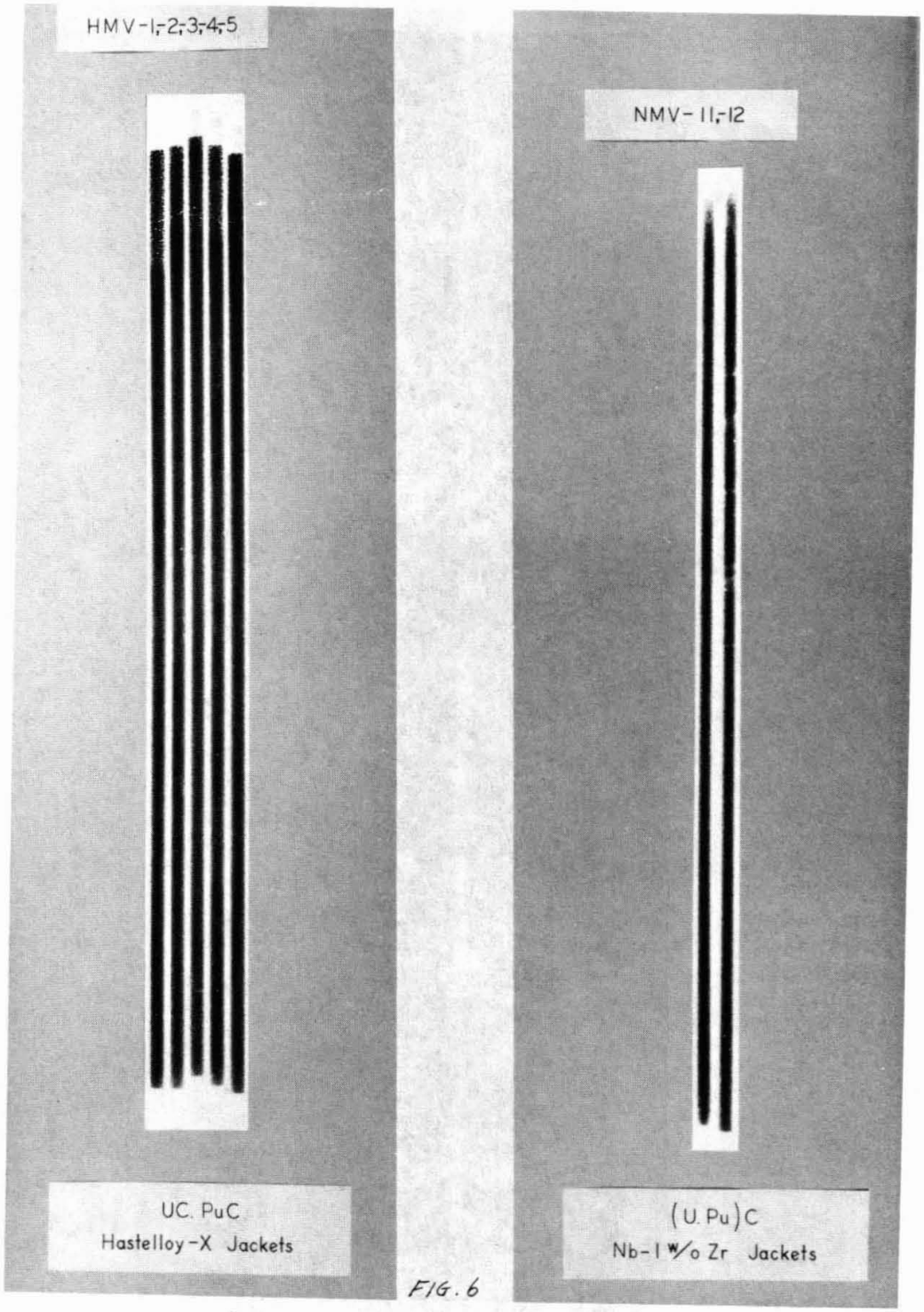
HMV-1,-2,-3,-4,-5
UC. PuC
Hastelloy-X Jackets
NMV-11,-12
(U. Pu)C
Nb-1 w/o Zr Jackets

FIG. 6


ONE FOOT

FIG. 7

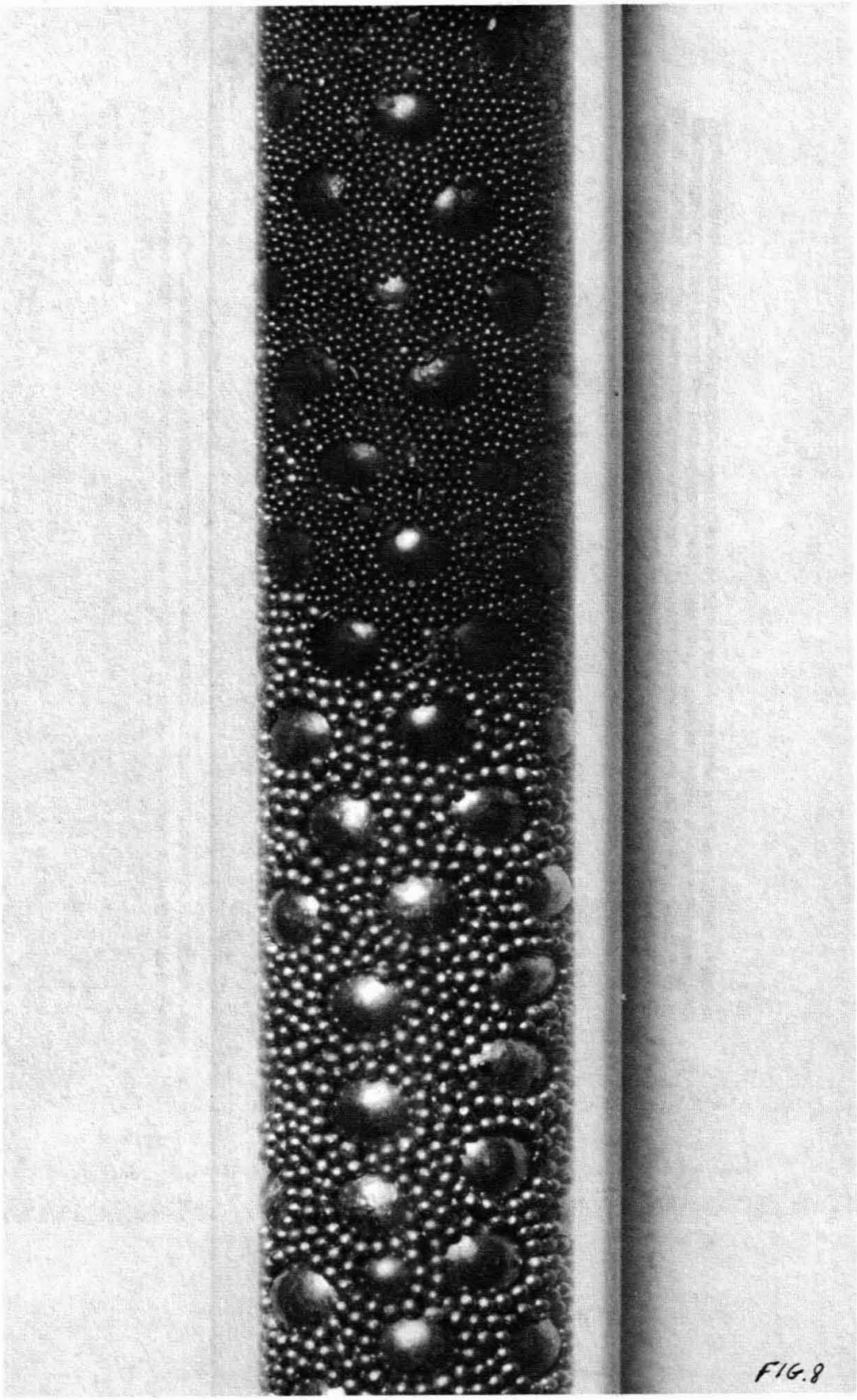

FIG. 8

URANIUM-PLUTONIUM ALLOY FUEL FABRICATION*

Arthur B. Shuck

Abstract

The uranium-plutonium alloys have been used principally in zero-power and fast-reactor experiments where a high density of fissile atoms, good thermal conductivity and high thermal expansion are required. The binary uranium-plutonium alloys have very poor mechanical properties and oxidation resistance, except in low plutonium concentrations. Modifying elements, such as molybdenum, zirconium, or titanium, have been added to improve the mechanical properties with some measure of success. These alloys have been fabricated into reactor fuel elements.

The largest single requirement, to date, for uranium-plutonium alloy fuels has been for the fast zero-power physics experiments. Approximately 11,000 kilograms of U-28.3w/oPu-2.5w/oMo alloy is being fabricated into 15,500 plate-type elements for the Zero Power Plutonium Reactor. The elements consist of rectangular plates of the fuel alloy in tight-fitting stainless steel jackets. Conventional hot-working methods of fabrication required temperatures in excess of 500°C to avoid billet cracking and a high-purity inert atmosphere to prevent oxidation. Jacket- and pack-rolling techniques were not promising because of the tendency of the alloy to react with most of the commonly used jacket materials.

Vacuum melting and casting the U-28.3w/oPu-2.5w/oMo alloy into reuseable, multiple-cavity molds was found to be a practical method for making rectangular-section bars from which the element plates were machined. Directional solidification of the castings from the bottom and continuous feeding of molten metal into the hot-topped molds was necessary to prevent internal shrinkages. The cast bars were parted into the individual plates, which were machined to the specified weights and dimensions.

The stainless steel jackets were stretch formed from welded-and-drawn, Type-304L tubing. As with all plutonium fuel elements, loading the alloy cores into the jackets must be done by methods that do not contaminate the weld joints and jacket exterior with plutonium. The jackets were enclosed in a protective fixture and the cores were loaded through a funnel that prevented contact of the core with the jacket lip. Close-fitting end plugs were inserted in the jacket sleeves and forced tightly against the cores. The seal welds between the jacket sleeves and end plugs were made at less than one-half atmosphere pressure of inert gas. The reduced internal pressure prevented inflation of the fuel element at operating conditions.

Arthur B. Shuck is a Senior Metallurgical Engineer with Argonne National Laboratory, Argonne, Illinois.

---

*Work performed under the auspices of the United States Atomic Energy Commission.

INTRODUCTION

The uranium-plutonium alloys have the advantages of high density of fissile atoms, good thermal conductivity, large thermal expansivity, and minimal neutron moderation. These advantages are such that there has been a continued interest in metallic fuels for fast reactors in spite of operating temperature and burnup limitations. Several thousands of uranium-plutonium alloy fuel pins have been fabricated by injection casting methods[1] for experimental use in EBR II. These have been alloyed with fissium (a synthetic fission product composition), zirconium, titanium, or molybdenum to improve the properties and irradiation resistance[2] of the binary alloy.

The greatest application for uranium-plutonium alloy fuels to date, however, has been for zero-power reactors. Approximately 11,000 kilograms of U-28.3w/oPu-2.5w/oMo alloy is presently being fabricated into 1/4-inch thick by 2-inch wide, stainless steel jacketed plate elements for use in the Zero Power Plutonium Reactor, ZPR-3, ZPR-6, and ZPR-9. These zero-power reactors at Argonne, Illinois and the National Reactor Test Station are large separable tables, each with a three-dimensional framework in which one-half a reactor may be assembled. The fuel, structural materials, coolants, and parasitic neutron absorbers may be mocked up, building block fashion, for any given reactor design. Control and safety mechanisms are also incorporated and the reactors are highly instrumented. When the two one-half reactors are brought together, the assembly may be made to approach and become critical, and to display the nuclear characteristics of the full-scale reactor of which the design is being studied. The principal advantage of the zero-power reactors (ZPRs) is the ease and economy with which the building-block arrangement of fuel and nonfissile materials can be changed. Even greater economy and flexibility can be achieved by zone assemblies, where smaller, highly instrumented zones are built within the core of a larger reactor assembly to study the fine-scale neutronic effects of fuel variability or composition.

ZERO POWER REACTOR FUEL REQUIREMENTS

The zero-power reactors require fuel elements with the following characteristics:

(1) Each fuel element of a given size must be of known and uniform weight and composition.

(2) The fuel elements must have a prompt, positive expansion in the longitudinal direction when heated by a nuclear power excursion.

(3) The core plates must not burn if exposed to air.

(4) The outside of the jackets must remain free of plutonium contamination.

(5) The fuel elements must withstand shipment, normal wear, and repeated use without core breakup, distortion or jacket leakage.

(6) The fuel elements must be practical to manufacture.

In order to meet these requirements, the core alloy should have a high coefficient of thermal expansion, sufficient strength to stretch the jacket and resistance to oxidation and ignition. The jacket must fit the core tightly in the longitudinal direction, and have flat ends to transmit thermal expansion to the adjacent elements in the reactor. If the jacket is gas bonded to the fuel element core, the pressure of the gas should be sufficiently low that the jacket does not inflate at reduced barometric pressure and increased operating temperature.

The zero-power reactor fuel element should be of as simple a design as possible. Figure 1 shows the evolution of the plutonium zero-power reactor fuel element. The first elements were Pu-1.2w/oAl, rolled plates in loose fitting jackets. A spring held the core against one end of the jacket so that expansion was always against the spring. The first of these elements was made in Illinois and the jackets sealed at 600 feet altitude pressure. When the elements were taken to Idaho, at 6,000 feet altitude, all of them inflated so that they would not pass the thickness gages. Subsequent elements were welded in a reduced pressure chamber and had an internal pressure of about 1/2 an atmosphere. The sides of the jackets now pressed so tightly against the cores that the spring action was largely defeated.

The second design, Figure 1-b, was developed for the SEFOR critical experiment in ZPR-3. The cores were precision cast from U-20w/oPu-2.5w/oMo alloy. The jackets were two drawn half panels with turned-out rims that enclosed the core plates and were sealed by a peripheral fusion weld that joined the rims. A heavy weld bead was cast at each end of the jacket, which was machined to form a shoe to transmit expansion. The jacket was easily assembled and fit the core quite tightly as the result of contraction of the weld. Precision individual castings, and jackets were required with separate tooling for each size. The welds were easily damaged and the shoes tended to become bent out of shape. Production costs were high.

The present ZPPR fuel element is shown by Figure 1-c. The cores consist of rectangular fuel alloy plates, which may be cut from precision-section bars. The jacket consists of a rectangular sleeve, which may be cut from formed tubing, and two end plugs. The core is loaded through the sleeve opening and the final weld is made under reduced pressure while the end plug is loaded against the core.

FABRICATION PROPERTIES OF URANIUM-PLUTONIUM ALLOYS

The uranium-plutonium alloys, in the 15 to 40 percent plutonium range, are not satisfactory for fuel-element fabrication. The zeta-phase field occurs in this composition range, and the zeta-phase-containing binary alloys tend to fragment in the casting molds and to disintegrate at room temperature, probably as a result of microfissuring and oxidation of the zeta phase. These binary alloys are decidedly pyrophoric. Heating in air showed that ignition would occur at temperatures as low as 150°C[3]. Spontaneous ignition has been experienced in air-filled gloveboxes on several occasions. The addition of 2.5 weight percent of molybdenum to the binary alloy modifies and largely eliminates the microfissuring and

oxidizing tendencies of the binary alloy. The ignition temperature of a U-28.3w/oPu-2.5w/oMo alloy was above 500°C and is similar to that of unalloyed uranium. Fairly good oxidation resistance was observed with an alloy of U-37.0w/oPu-2.5w/oMo.

The U-28.3w/oPu-2.5w/oMo alloy solidifies over a range of 1020 to 920°C and the as-cast microstructures show the coring and microsegregation that might be expected. The as-cast hardness is influenced by gamma-uranium phase retention. Castings that were made in molds at 600 to 900°C and very slowly cooled had a Rockwell C hardness of 45 to 54, and were quite difficult to machine. Castings that were made in molds at about 400°C, and more rapidly cooled, were of Rockwell C hardness 35 to 40 and were machinable with carbide-edged tools. The alloy has very little ductility at room temperature. Compressive strength at room temperature was between 140,000 and 170,000 psi. Very little compressive plasticity occurs until the alloy is heated above 450°C. It is highly plastic at 550°C.

The alloy, when cast into coated carbon molds, shows a very good fluidity and replicates the mold surface precisely. About 300°C of superheat was needed to eliminate laps and flow marks. The liquid volumetric thermal contraction is several times that of the solid metal, and good foundry practices, directional solidification of the castings and continuous feeding of the solidifying interface, are required to prevent internal macro- and microshrinkage. The alloy is highly plastic between 600 and 900°C and gas pressure on the casting surfaces will cause them to dimple in as the metal freezes. This is prevented by vacuum casting or by casting against a chilled surface. Internal fracturing may occur if the mold draft is insufficient. All of these potential defects may be corrected by proper mold design and selection of casting parameters.

There was an interest in metalworking as a possible means of fabricating the ZPPR fuel. Rolling was tried on a number of cast billets. Rolling at billet temperatures below 500°C resulted in extensive damage to the billets at less than five percent reduction as shown by Figure 2-a. The metal became quite soft at 550°C and could be rolled by rolls heated to 250°C, as shown by Figure 2-b. Surface cracking occurred when the 550°C billets were rolled between rolls at room temperature. A very good inert atmosphere was required to prevent excessive oxidation. Oxidation was excessive in an atmosphere that contained about 0.1 percent oxygen and 30 ppm of moisture. Jacket rolling was not successful because the fuel alloyed with the metals that were tried for jacketing, making it very difficult to strip the jackets from the cores. Similar problems were experienced with sticking of the metal in steel extrusion dies. Metal working was abandoned as a means of fabricating the cores because of these difficulties.

DEVELOPMENT OF FABRICATION METHODS

The method developed at Argonne National Laboratory for the fabrication of the zero-power reactor fuel elements consisted of the following operations:

1. Plutonium from various sources was melt-blended to produce a composition containing 11.5±0.5w/o ^{240}Pu. The blended plutonium was cast as ingots that weighed about one kilogram each.

2. A uranium-molybdenum binary alloy was prepared and cast into ingots of suitable size for remelting.

3. After analysis of the plutonium and the binary alloy, they were alloyed together to produce a ternary alloy containing 25.0w/o(^{239}Pu+^{241}Pu) and 2.5w/o molybdenum. The composition of the resulting alloy was approximately U-28.3w/oPu-2.5w/oMo. This alloy was cast into bars of finish thickness and of sufficient width to allow machining. The length should be selected to allow two or more core plates 4, 5, 6, 7, or 8 inches long to be machined from each casting. The experimental molds were 10-1/2 inches long. Twelve or fifteen inch molds may be more efficient for production of elements.

4. One edge of the bar was machined full length.

5. Core plates were parted from the cast bars by means of carbide-tipped milling saws. More than one milling cut was made by mounting more than one saw on a common arbor.

6. The edges of the core plates were chamfered and the ends machined to finished length. The width was cut to the top of the tolerance range.

7. The core plate was weighed, and, if too heavy, the width was remachined to bring the core plate weight to within the weight tolerance range.

8. Jackets were fabricated by stretch forming 1.35-inch diameter by 0.016-inch wall, Type-304L, stainless steel tubing into a box die by means of an expanding mandrel. End plugs were machined and one end was TIG welded to the jacket sleeve.

9. The jackets were protected against plutonium contamination during core-plate loading by enclosing them in a protective fixture, and the core plates were loaded through disposable aluminum-foil funnels.

10. After removal of the funnel, the second end plug was inserted and the fixture was closed to exert a clamping force of 40 pounds on the two ends of the element. The loading and welding fixture was provided with the copper chill pads that were necessary to control the contour and penetration of the welds.

11. The ends and one side of the plug was welded to the sleeve with the welding chamber at atmospheric pressure. The final weld was made after the chamber had been evacuated and back filled with argon-helium mixture to six psia.

12. Final inspection consisted of alpha count, neutron count, leak detection, visual inspection, gaging and radiography.

Plutonium Ingot Preparation

The available plutonium varied in isotopic composition. The ^{240}Pu content ranged from eight to fifteen percent and there were similar variations in other isotopes. From many analyses it was determined that an approximately uniform composition could be achieved by blending low and high ^{240}Pu material to produce a composition that contained 11.5w/o^{240}Pu. The plutonium was then added to the ternary alloy in an amount that would yield 25w/o of fissile $^{239}Pu+^{241}Pu$ in the core plates. An order was given at Hanford to produce the 11.5 percent ^{240}Pu to Argonne specification as one kilogram ingots.

Preparation of Binary Alloy

It was found that much lower losses of plutonium and better control of composition could be achieved if the alloy were prepared in two steps. The first step was the preparation of a U-3.54w/oMo binary alloy. Uranium and molybdenum compacts were melted in yttria-washed MgO crucibles. The molybdenum compacts were obtained commercially. They were made from hydrogen-reduced molybdenum, which was pressed into 3/4-inch diameter tablets that were low fired to produce an outgassed, somewhat porous, and easily dissolved tablet. About 1470°C was found to be necessary to dissolve about 360 grams of molybdenum in ten kilograms of uranium. A 40-minute melting cycle gave complete dissolution. The resulting alloy was made up to be slightly uranium-poor, so that a small amount of uranium could be added for adjustment of the ternary composition. The binary alloy was cast in yttria-coated carbon bar molds of the same type as used for ternary alloy casting. In production it would be advisable to cast into molds of a different shape.

Alloying and Casting the Ternary Alloy

Ternary alloy preparation and casting the bars for core-plate manufacture was carried out in a single operation. Casting is shown in Figure 3. All operations involving unjacketed plutonium alloys were carried out in helium-filled gloveboxes. The furnace glovebox line is shown in Figure 3-a. The furnaces were of the bell-jar, lift-coil type, shown schematically by Figure 3-b. Solid tungsten coils, powered by a 10,000 Hz, 220-volt generator, were used to heat tantalum susceptors around the crucibles and the top of the carbon molds. Bottom pouring magnesia crucibles with 3/4-inch pouring holes, stopper rods, and crucible covers were coated with alcohol suspended yttria on all melt contacting surfaces and dried. Broken pieces of the binary alloy were placed in the bottom of the crucible with the plutonium on top, so that maximum contact would be achieved as the plutonium melted down through the binary fragments.

Multiple-cavity, book molds of high-density carbon were used to cast bars of finished thickness. Various refractory coatings were tried including milled calcium and magnesium zirconate, thoria, and zirconia. Yttria of minus six-micron particle size suspended in ethanol seemed to give the best surfaces, although this material may cause some problems in the plutonium recovery operation.

The molds are shown, in exploded view, in Figure 3-c. The separators between mold cavities were made quite thin in order to reduce the heat capacity of the sections on the two-inch wide surfaces. This prevented freeze-off across the 0.205-inch width of the casting. Solidification from the bottom of the casting was promoted by removing heat through a conductive stool, which rested on the water-cooled furnace bottom. Molten metal feeding of the solidifying casting was provided by extending the top of the mold into the furnace coil, while the sides of the mold were insulated with porous-alumina tiles. This arrangement caused a thermal gradient of from about 300°C at the bottom of the molds to about 900°C at the top of the mold before pouring. The castings produced by pouring 1325°C molten alloy into these molds from the crucible described above were solid and essentially free of surface defects. A typical casting is shown in Figure 3-d. The casting parameters and optimum conditions for binary and ternary alloy casting are shown by Table I.

Core Plate Machining

The castings had a Rockwell-C hardness of 35 to 45 depending upon the amount of retained gamma-phase material in the structure. Machining with high-speed steel cutters was found to be quite difficult at room temperature, but machinability was improved when the alloy was heated. An electrically heated fixture was designed to test the feasibility of hot machining core plates with high-speed tools, but the method lacked the precision required unless time was allowed for the workpieces, fixtures and the milling machine to come to thermal equilibrium before start of machining. The hour or more required for this was too long for the method to have practical application. Burns to operators were an ever present hazard and oxidation of the core plates was greatly increased.

Room-temperature machining of the core plates by means of carbide milling cutters was found to be practical. Solid carbide milling saws of 0.040-and 0.060-inch thickness were first tried. These were so easily broken that 0.090-inch carbide-tipped, side-cutting saws were substituted. These lasted for 40 to 50 cuts before dulling, if the sharp corners were radiused slightly to prevent breakdown. Clamping was a problem because the as-cast surfaces were slightly irregular and the brittle plates were easily broken. Breakage and chipping of the edges were greatly reduced when an 0.030-inch-thick soft-aluminum shim was placed between the fixture and the core plate. Some work was done to determine whether the core plates might be sawed directly to length, but the results were somewhat imprecise, possibly because of difficulties in keeping a zero end play in the milling machine arbor. Better precision was obtained by a second milling operation to finish the ends. The edge chamfers were machined by means of two 45° cutters that were mounted on the same arbor.

The machining sequence is shown by Figure 4. One edge of the casting was milled first as a fixturing base line. Several castings were clamped on the sawing fixture and core plates were parted as shown by Figure 4-a. The ends and second edge of the core plates were milled by a side cutter in a vertical milling machine, as shown by Figure 4-b. At this point the cores were machined to the maximum width allowed. They were weighed and if too heavy, a calculated amount was removed from the width to bring them within the specified weight. Chamfering of the edges, Figure 4-c,

was the final operation of machining followed by weighing. Machining of the two-inch wide surfaces was not normally done unless required to salvage a rough or warped casting.

Jacket Manufacture

Initially the jacket sleeves were made from stainless steel sheets that were folded around a mandrel and welded at one corner. The method was imprecise and the corner welds on the thin metal leaked and caused trouble in loading the cores. Commercially-formed rectangular tubes did not meet the dimensional requirements, and attempts to draw form the tubes resulted in overworked and thinned corners.

A method was developed at ANL by which commercially welded and drawn tubing was flattened over a mandrel and then stretch formed into a rectangular box die by means of a wedge-actuated expanding mandrel. This method distributed the deformation over the flat surfaces of the sleeve and did not cause corner thinning. The cold working of the flat sides of the sleeves added greatly to their rigidity. The dimensional requirements were easily met.

The end plugs were manufactured from Turk's-head-formed stainless steel wire. It was originally felt that except for machining of the ends, very little machining would be required, but this was not true. It was necessary to flatten and die size the wires, and then to produce the end form and radii by means of a shaving die operation. This produced end plugs of good quality.

Fuel Element Assembly and Welding

The tungsten-electrode, inert-gas shielded, (TIG) method was used to fusion weld the end plugs into the jacket sleeve. By enclosing the sleeve in chills and a chill against the end plug it was possible to fuse the joint between the end plug and sleeve producing a contour of controlled radius. One end plug was welded before the core was loaded.

Contamination of the exterior surfaces of the jackets by the plutonium has always been a problem in loading plutonium elements. Contaminated welds usually cannot be cleaned to the required alpha radiation levels and the element must be rejacketed. Careful cleaning of the core plates to remove all loose particles is the first step of the loading operation. The subsequent steps of assembly and final welding are shown by Figure 5. The jacket-sleeve surfaces were protected by enclosing the jacket in the protective welding fixture. Strippable tape was used to protect the exposed surfaces of the fixture. Loading of the cores was done through a formed-aluminum funnel that was inserted in the top of the jacket sleeve. The funnels were disposable and used only once. The loading operation is shown in Figure 5-a.

The end plugs were inserted and forced down against the core plates. The open chill fixture is shown by Figure 5-b. It is designed so that when it is closed a forty-pound load is exerted against the two ends to hold the plugs in contact with the core. The ends of the plugs were first tack welded as shown by Figure 5-c. This was a hand operation that

required considerable skill, which could be mechanized for production. After welding the ends of the plugs the chill was transferred to the welding chamber, where the first of the two-inch long welds were made at atmospheric pressure as shown by Figure 5-d. The welding chamber was then closed, evacuated and backfilled to six psia with 40v/o argon-60v/o helium mixture. The final weld was made at this reduced pressure with a flow of gas through the electrode shroud. Chamber pressure was controlled by means of a regulating valve between the vacuum pump and chamber. The weld parameters are shown by Table II.

Inspection

Inspection of the core plates, jacket components, and finished fuel elements was established on a go, no-go gaging basis where practical. Measurements and analytical information were required as follows: (1) total weight of element to 0.01-gram accuracy, (2) total weight of core to 0.01 gram, (3) length and parallelism of core ends to nearest 0.001 in., (4) length and parallelism of element ends to nearest 0.001 in., (5) alpha total surface count rate, and (6) neutron emission rate.

Leak detection was done by helium leak detectors and bubble test. The bubble test was needed for very large leaks, which were pumped out and missed by the helium leak detector. The test elements were radiographed to determine gap between the core and end plugs. In production this will be determined from the length and end parallelism measurements. All welds were inspected visually and by binocular microscope at 15 or 20 X. Weld sectioning and metallography was required at the start of each operator shift on an element loaded with a stainless steel core before fuel cores were loaded. This allowed the operator's loading and welding practices to be checked by the supervisor on the dummy element.

Analytical Requirements

Complete charge-in data were maintained on all melts from which the uranium, plutonium, and molybdenum composition of each batch were calculated. This information was verified by analysis of samples taken from one casting from each melt. Isotopic analyses were made by mass spectrometer and metallic impurities were obtained by arc-source spectrograph. Oxygen, nitrogen, and carbon analyses were made by fusion and gas train methods. Radiochemistry was used to analyze ^{238}U and ^{241}Am. Impurities were easily held to below the 4200 ppm maximum of the specification. Elements that would yield α,n neutrons were kept to a minimum. Total neutron emission was well within the 140% of spontaneous fission neutron level allowable. The isotopic, chemical, and major impurities analyses were converted to core-plate composition and a data card was designed upon which all information pertinent to that element was punched and printed. These data cards will be furnished to the experimentalists and will also be used in development of accountability records.

CONCLUSION

The objective of the zero-power reactor fuel development was to write a realistic product specification, backed up by well-developed methods for the manufacture of the fuel elements. These objectives were met with a specification[4] furnished for quotation and a process development report[5] furnished for information. Two organizations, Dow Chemical Company at Rocky Flats, Colorado and Nuclear Materials and Equipment Corporation at Apollo, Pennsylvania, have contracts for the furnishing of the fuel in accordance with the specification. The processes differ in detail only from those described in this paper.

ACKNOWLEDGMENT

Many persons at ANL contributed to the design and development of zero-power reactor fuels. F. W. Thalgott and W. Y. Kato and other members of the Idaho and Reactor Physics Divisions helped to develop the requirements. H. F. Jelinek and D. A. Kraft developed the casting methods. N. J. Carson, Jr., and D. Rabe worked out machining techniques. A. A. Denst of Central Shops was primarily responsible for development of jacket-forming methods. D. C. Carpenter, A. G. Hins, and J. R. Summers worked out the assembly and welding techniques. Tom Steele and members of the Industrial Hygiene and Safety Division developed α and neutron counting methods. It would have been impossible to characterize the process and develop realistic specifications without the services of many members of the ANL Chemistry Division from which the help of H. B. Evans is particularly acknowledged.

REFERENCES

1. Shuck, A. B. *Apparatus and Method for Injection Casting,* U. S. Patent No. 2,952,056, September 13, 1960.

2. Beck, W. N., Brown, F. L., Koprowski, B. J., and Kittel, J. H. *Irradiation Performance of Fast Reactor Fuels, Uranium-Plutonium Metal Fuels, 1967 Nuclear Metallurgy Symposium on Plutonium Fuels Technology,* 4-6 October, 1967. (To be published.)

3. Kelman, L. R., Rhude, H. V., Schnizlein, J. G., Jr., and H. Savage "Metallic Plutonium Alloys for Fast Critical Experiment" *Plutonium 1965, Proceedings of the Third International Conference on Plutonium,* Chapman and Hall (London) 1967.

4. ANL Specification PF-1600, *Uranium-Plutonium-Molybdenum Alloy ZPPR Fuel Elements,* Revision 3, May 29, 1967, Argonne National Laboratory.

5. Shuck, A. B., Jelinek, H. F., Hins, A. G., Carson, N. J., Jr., Denst, A. A., and Steele, T. A., *The Development of a Design and Fabrication Method for Plutonium Bearing Zero-Power Reactor Fuel Elements,* ANL-7313, 1967.

TABLE I. CASTING PARAMETERS

	Binary Alloy		Ternary Alloy	
Variable	Range Tested	Selected Datum	Range Tested	Selected Datum
Heating Cycle				
Min. to melt	40-75	60	40-100	50
Min. above 1200°C	-----	--	8-40	30
Min. above 1275°C	8-60	40		
Mold Temp.*				
Top, °C	400-700	500	400-1050	900
Center, °C	150-300	200	200-600	450
Bottom, °C	80-300	100	100-400	300
Max. Melt Temp. °C	1350-1500	1470	1300-1480	1380
Casting Temp. °C	1335-1445	1400	1270-1390	1280

*Mold temperature was a function of melt cycle and temperature.

TABLE II. OPTIMIZED WELDING PARAMETERS

Arc Voltage	12 ± 1.0
Arc Current, amperes	36 ± 2.0
Shroud Gas Flow	
argon, cfh	10 - 12
helium, cfh	15 - 18
Electrode	thoriated tungsten
Electrode diameter, in.	0.060, 30° point
Arc gap, in.	0.025 ± 0.003
Torch traverse rate	3.2 in. per min.
Pressure first weld	one atmosphere
Pressure final weld	6 - 7 psia

LIST OF FIGURES

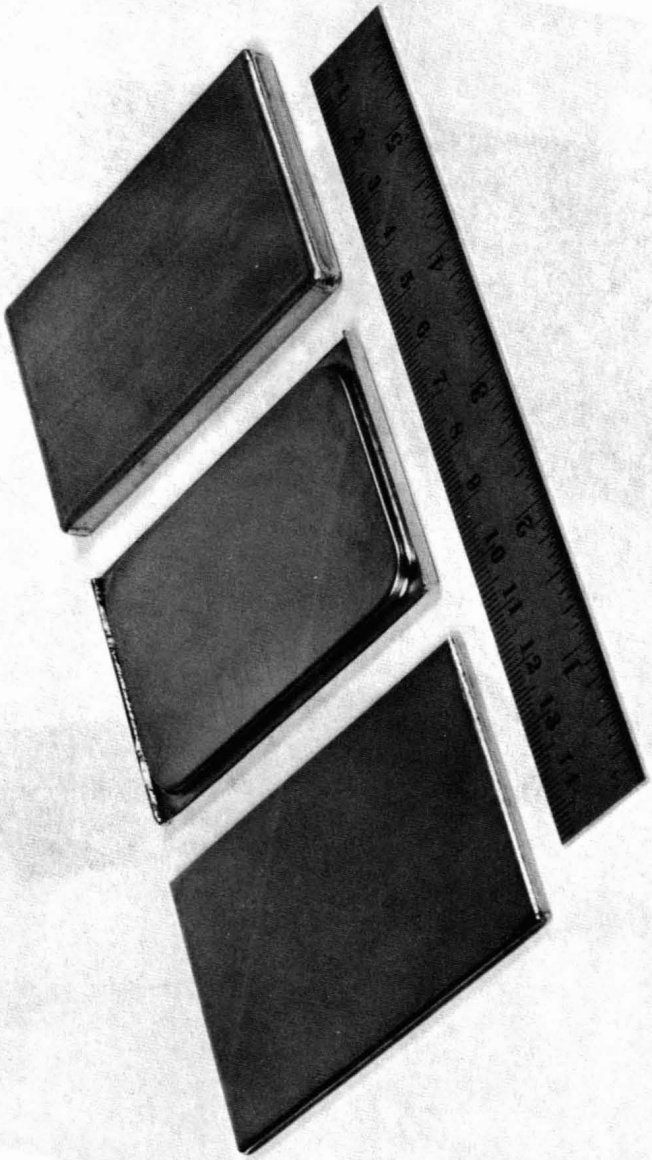

FIG. 1

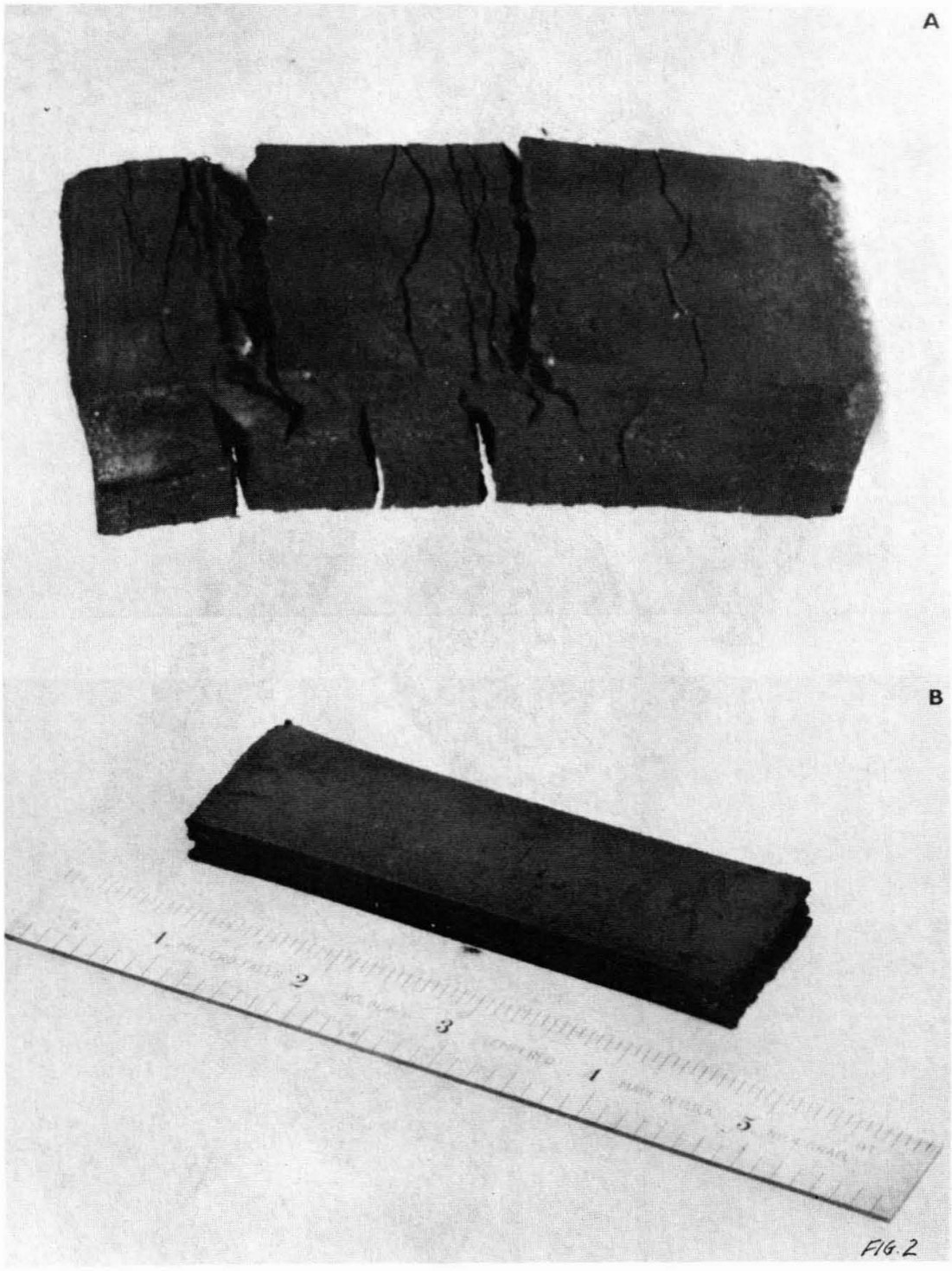

FIG. 2

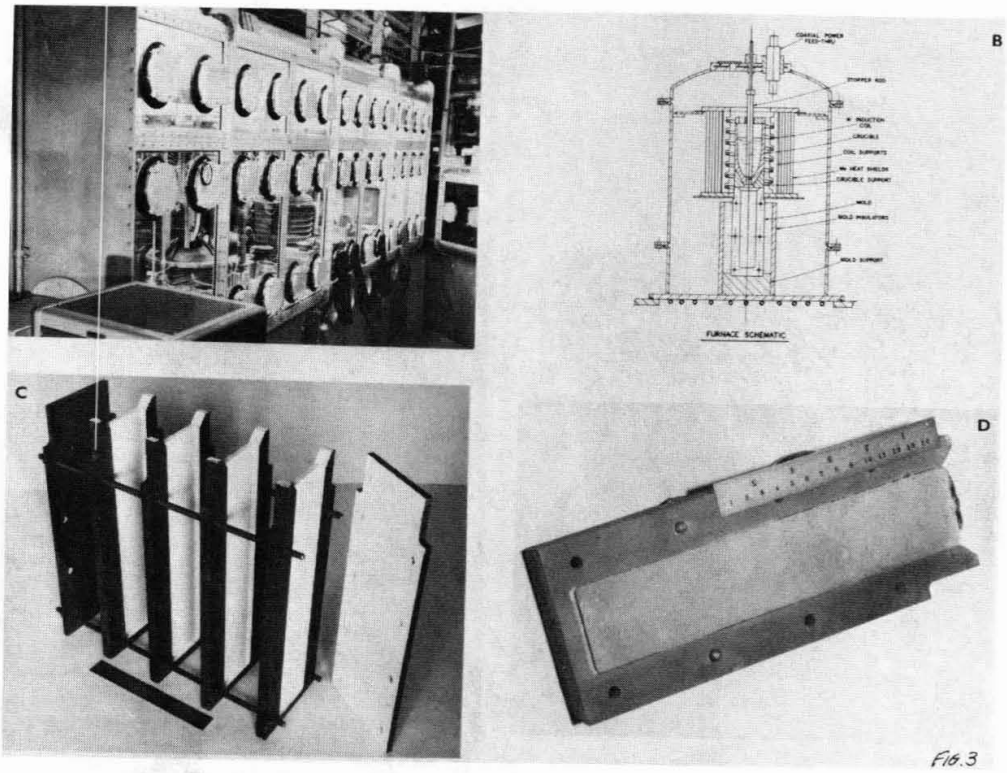

FIG. 3

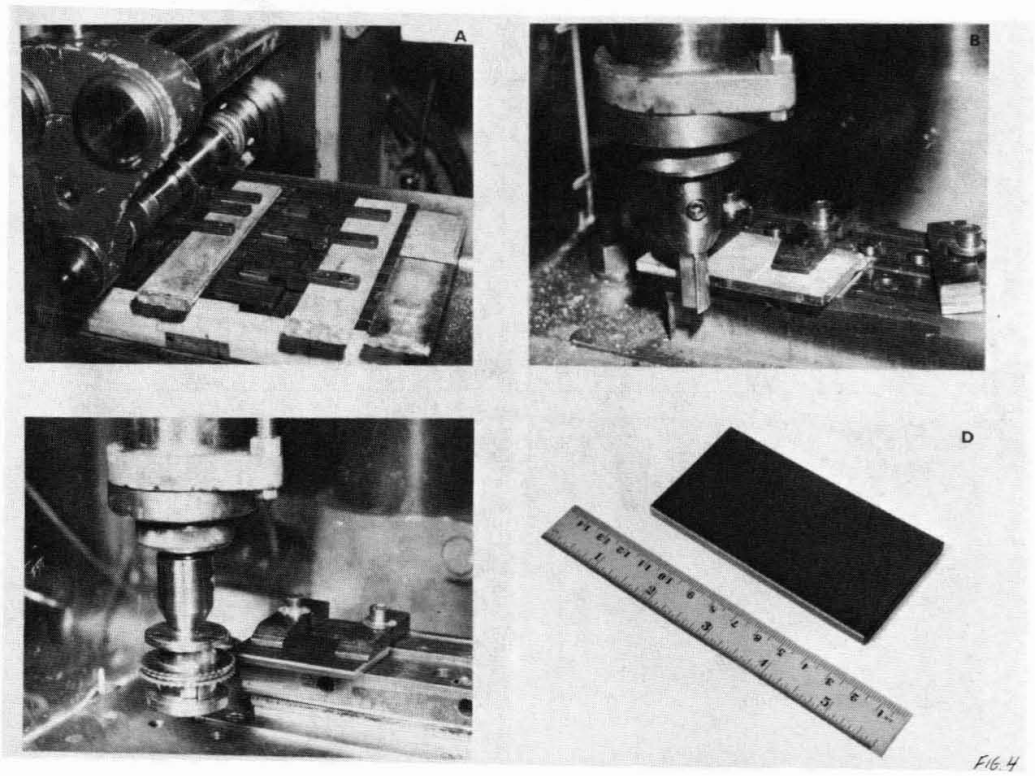

FIG. 4

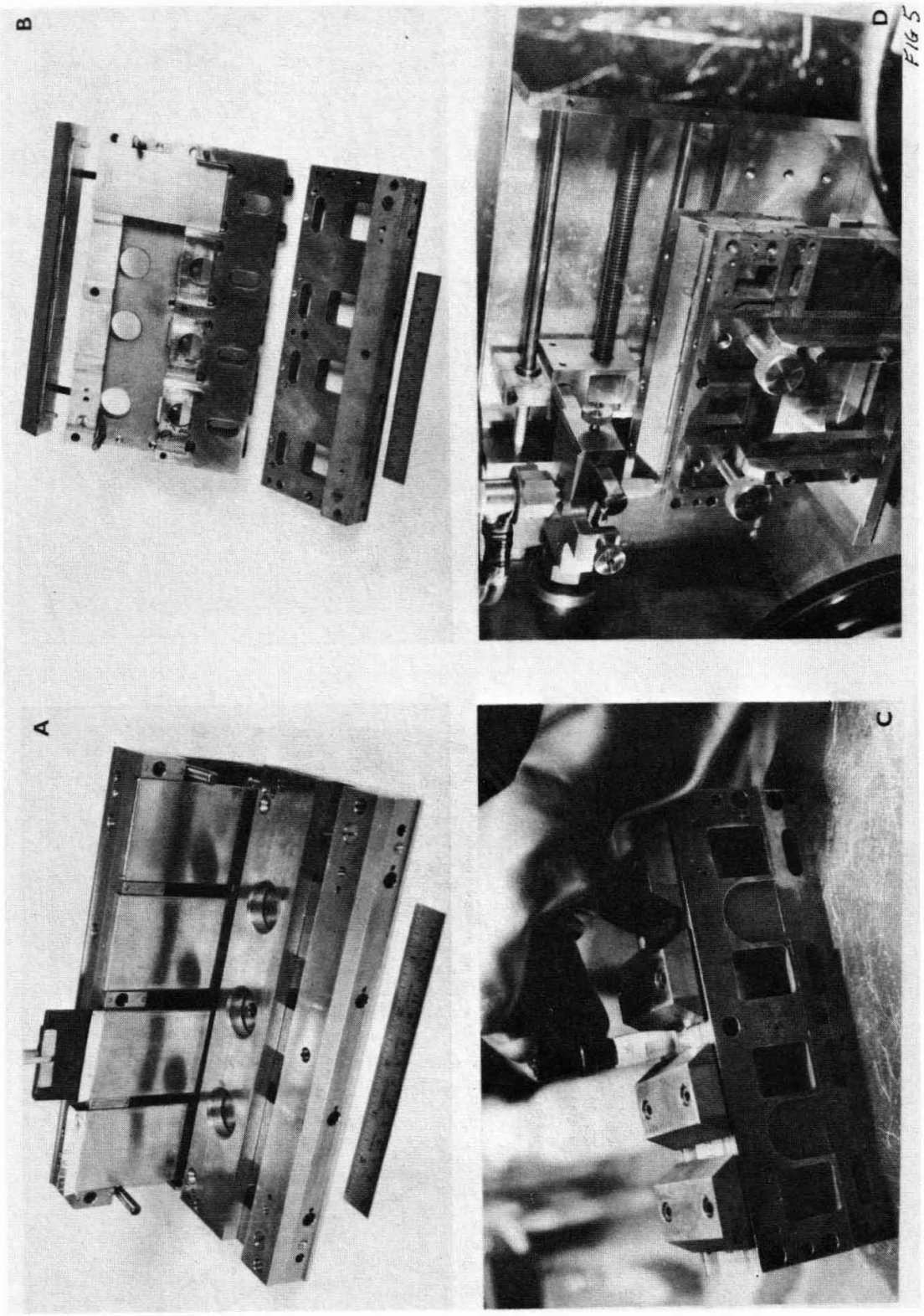

FIG 5

PLUTONIUM METALLIC AND CERAMIC FUEL FABRICATION AND DEVELOPMENT AT THE EUROPEAN INSTITUTE FOR TRANSURANIUM ELEMENTS

H.M. MATTYS

Abstract

Some aspects of our work in the field of plutonium fuel fabrication and development are reported.

- 2,100 uranium - plutonium-iron alloy fuel rods have been produced for the critical experiment MASURCA by a centrifugal casting method. The total amount of plutonium contained in this loading was 175 kg.
- 7,000 uranium - plutonium oxide pellets have been sintered for our fast reactor irradiation program. Dry powder blending was preferred to coprecipitation. No centerless grinding was necessary to obtain reproducible pellet diameter (5.40 mm $\pm$ 0.03 mm). The stoichiometry of our pellets was adjusted by sintering atmosphere control.
- Spherical particles of $PuO_{1.62}$ have been produced to be irradiated as graphite coated particles.

H.M. Mattys - Assistant Manager - European Institute for Transuranium Elements - EURATOM - Karlsruhe, Germany.

INTRODUCTION

The European Institute for Transuranium Elements is located at Karlsruhe, Germany, and is an Establishment of the Common Research Center of Euratom.

The Institute, specialized in the field of high activity alpha emitters, has been built in 1963 - 1964. Scientific work started in the beginning 1965.

At present, 220 people, including administration, maintenance and health physics, are working in the Institute.

Most of our activity is presently devoted to plutonium and deals with fundamental research on fuel materials, fuel fabrication development, and post irradiation examination.

In this paper we will report some aspects of our work in the field of fuel fabrication and development.

METALLIC FUEL FOR THE FAST CRITICAL EXPERIMENT MASURCA

In 1966, the Metallurgy group of the Institute for Transuranium Elements fabricated a plutonium bearing metallic fuel loading for the MASURCA fast critical assembly, which is operated by the CEA-EURATOM Association in Cadarache, France.

This fuel loading consisted of 2100 fuel elements containing a total amount of 175 kg plutonium. The fuel material was an alloy of 74% uranium, 25% plutonium and 1% iron.

The maximal length of an element is 101.6 mm (4") or 202.2 mm (8"). The external diameter is 12.7 mm (0.5"). The thickness of the cladding is 0.25 mm (0.010").

The fabrication process (see flow sheet fig. 1) was composed of the following steps:

1) The alloy components are melted together in an induction furnace (shown in fig. 2) under vacuum to obtain a homogeneous ingot of 10 kg, a photograph of which is given in fig. 3.
2) The ingot is re-melted in a centrifugal casting furnace, where the metal is distributed and injected into 22 stainless steel tubes set in a steel rotary mould. The stainless steel tubes are of the same internal diameter as the ultimate claddings and are lined with a 5 microns thick silicon dioxide layer. Fig. 4 shows the open rotary mould of the furnace after a casting.
3) The alloy core is removed from the stainless steel tube, (see fig. 5) polished to discard the outer silicon dioxide layer and cut to provide a required weight of fissile plutonium. In fig.

6a and 6b a fuel rod is shown before and after polishing and cutting.

4) The rods are then inserted into a cladding tube closed at one end. The second end plug is put into place after decontamination and is then welded by electron bombardment.

5) The element is brought to its specified length by grinding the end caps. Fig. 7 shows a finished fuel element.

6) After a helium leak test, the weight of Pu-240 contained in the element is determined by counting the spontaneous fission neutrons. This enables the total weight of fissile material in the element to be determined on the basis of the isotope analysis.

7) The elements undergo a check for dimensions and a final test for non-contamination.

To obtain 2115 fuel elements, corresponding to the specifications, 2376 fuel rods were cast. This means that 11% of our material was reintroduced into the first casting operation. The final product had the characteristics reported in table I. Table II gives the plutonium balance of the fabrication.

The production started on February 1, 1966 and ended in October 1966. A team of 17 people was involved in this task. This number does not include the persons belonging to the analytical chemistry and health physics groups.

PRODUCTION OF FAST REACTOR UO_2 - PuO_2 FUEL PELLETS

About 7000 fully enriched UO_2 - PuO_2 pellets have been produced to cover the needs of our fast reactor irradiation program. Part of the fuel will be irradiated in Enrico Fermi Reactor as soon as this will be possible. Another part is already under irradiation in Dounreay Fast Reactor.

In this part of the paper we will deal with three problems we had to solve to produce the specified material: homogeneity control, dimension control and stoichiometry control. The flow sheet of our production process is given in fig. 8.

1. Homogeneity Control : coprecipitation versus powder blending

Fast reactor mixed uranium - plutonium oxides have to be homogeneous in order to ensure a sufficient contribution of the Doppler coefficient to the reactor safety.

From this point of view a sufficient homogeneity is achieved when the PuO_2 is statistically dispersed in the UO_2 matrix as particles which do not exceed 100 microns.

It is evident that pellets made from coprecipitated powders, will meet this minimum requirement. Their production is not difficult:

6 fuel rods which are, or have been, irradiated in Dounreay Fast Reactor to study the influence of stoichiometry on irradiation behaviour have been loaded with pellets we produced from a coprecipitate.

It is, however, most unprobable that a fast power reactor fuel loading will be made from coprecipitaded powders. A fuel which obeys the minimum homogeneity requirements can be produced at lower cost from mechanical blends of UO_2 and PuO_2. Since the UO_2 is by far the major constituant of the fuel material, its sintering behaviour will control the sintering behaviour of the mixed powders. PuO_2 does not need to be a high quality ceramic grade material. It can be produced in any rapid process and this will allow to simplify the problems of criticality control.

Therefore, most of the mixed fuel we produced was prepared from dry blends of UO_2 and PuO_2. An efficient and rapid dry blending process has been developed by our ceramists: the well dried starting materials, UO_2 and PuO_2, are first sieved on a 125 or 250 mesh screen and then mixed in a paddle mixer. We observed that in pellets made from these blends and sintered for three hours at 1520°C in hydrogen, more than 65% of the PuO_2 had diffused in the UO_2. The rest of the plutonium oxide was statistically dispersed as particles smaller than 100 microns.

A longer sintering time, a higher sintering temperature or a previous ball milling of the blended powders improve the micro-homogeneity. However, a cost increment has then to be taken into account.

2. Dimension Control

In plutonium ceramics technology, centerless grinding is a very obnoxious operation, because it has to be performed in glove boxes and because of the criticality problem involved in slurry handling.

Therefore, we tried to define the conditions which would allow us to produce sintered pellets with high dimensional precision. The diameter of the pellets was specified as 5.40 ± 0.03mm. A density variation of $\pm$ 1.5% was considered to be acceptable.

The precision sintering of high density pellets (90 to 95% of the crystallographic density) was quite easy. Once the sintering behaviour of a batch of powder is known, the only problem is to press green pellets with a satisfactory dimension reproducibility, and this is easily achieved by pressing to saturation with a good hydraulic press. Provided sintering time is long enough to compensate for temperature inhomogeneities in the sintering furnace, all the pellets will reach the same final density which depends on the precipitation conditions. Twelve per cent of the sintered high density pellets were out of tolerances and were reintroduced into the starting powder mixture, after a heat treatment under air. Our pellets had a length to diameter ratio of about 2. Even with this

rather high ratio the diameter in each part of the pellet was constant within ± 10 microns.

Production of low density pellets (80 to 90% of the crystallographic density) is more difficult if centerless grinding has to be avoided.

We tried, without success, three different procedures:
- uncomplete sintering of high density green pellets,
- complete sintering of low density pellets (uncomplete pressing),
- complete sintering of pellets which contain large amounts of organic material.

The problem of low density pellets production was solved by a preliminary heat treatment of the UO_2 powders or of the UO_2 + PuO_2 mixtures. In this way, we obtained without centerless grinding the 3000 low density pellets needed for our irradiation program. 15% of the pellets which were out of tolerances had to be reintroduced in the starting material, after a heat treatment under air. Nevertheless, the production of low density material with a high dimensional precision was much more time consuming than the production of high density pellets, because the suitable preliminary heat treatment conditions had to be carefully determined for each powder batch.

It is not clear that such a high precision on pellet dimensions is really needed. The important specification of a fuel rod is the smeared density of the fuel it contains. In Dounreay Fast Reactor an irradiation program is under way in which we study the effect of the radial repartition of the fuel density. We compare the behaviour of low density pellets, high density pellets with a very large diametral gap and high density cored pellets. If it appears that the original fuel density repartition has no influence on the irradiation behaviour, the production of low density fuel rods will be much easier because pressing will be the only critical step of the fabrication.

If not, it is possible that vibration compaction will be considered as the only practical way to produce those low smear density fuels.

3. Stoichiometry Control

The most suitable oxygen to metal ratio of a fast reactor mixed oxide fuel has not yet been established.

Out of pile measurements performed in our Institute have shown that heat conductivity of uranium- 15% plutonium oxide is a maximum when the O/U + Pu ratio is 2,000.

Nevertheless, as thermal conductivity is not the only important property of a fuel, we felt that influence of stoichiometry on the behaviour under irradiation had to be checked by a careful fast reactor irradiation experiment. This is the aim of some of the irradiations we perform at present in Dounreay.

The oxygen to metal ratio of the pellets for the Dounreay stoichiometry experiments were adjusted by a careful control of the oxygen partial pressure in the atmosphere of the sintering furnace. O/U + Pu ratios of 1.97 and 1.92 have been obtained by heat treatment in nearly dry hydrogen at 1550 and 1650°C, respectively. Nearly stoichiometric oxides were obtained by sintering in a H_2 - N_2 atmosphere containing about 4000 ppm of water.

PRODUCTION OF SPHERICAL PARTICLES OF PLUTONIUM OXIDE

Pure plutonium dioxide spherical particles, 250 microns in diameter, have been produced in our Institute by a sol gel process, in view of an irradiation experiment for a High Temperature Gas Cooled Reactor project.

The preparation of a concentrated sol, with a low NO_3/Pu ratio, was a necessity to obtain sound large microspheres. We established suitable conditions to prepare such a sol: the plutonium in nitrate solution is first hydrolised at a pH of about 1.2 and, after about one hour, is precipitated at a pH of 6. The precipitate after filtration and washing can be dispersed in diluted HNO_3 and gives a 2 M plutonium sol with a NO_3/Pu ratio lower than 0.2. No intermediate baking step is involved in this procedure.

The formation of the microspheres was obtained by gellation in Ethylhexanol.

After sintering in dry hydrogen we obtain microspheres of $PuO_{1.62}$. Substoichiometric plutonium oxide was preferred to stoichiometric PuO_2 to avoid any reaction with graphite during the graphite coating process.

Table I

Fuel rod	long	short
Diameter mm	12.10 ± 0.03	
Length mm	196.10 ± 0.05	99.6 ± 0.05
Weight g	400 ± 1	200 ± 1
Fissile Pu content g	91 ± 0.90	45.75 ± 0.45
Clad fuel element		
Outer diameter mm	12.67 ± 0.03	
Length	203.23 ± 0.03	101.63 ± 0.03

Table II

	Pu weight kg	%
- Masurca rods delivered at Cadarache	175.10	93.47
- Oxyde on received ingots	0.50	0.27
- Analytical samples	0.68	0.36
- Scraps, waste and losses	11.04	5.90
Total received	187.32	100.00

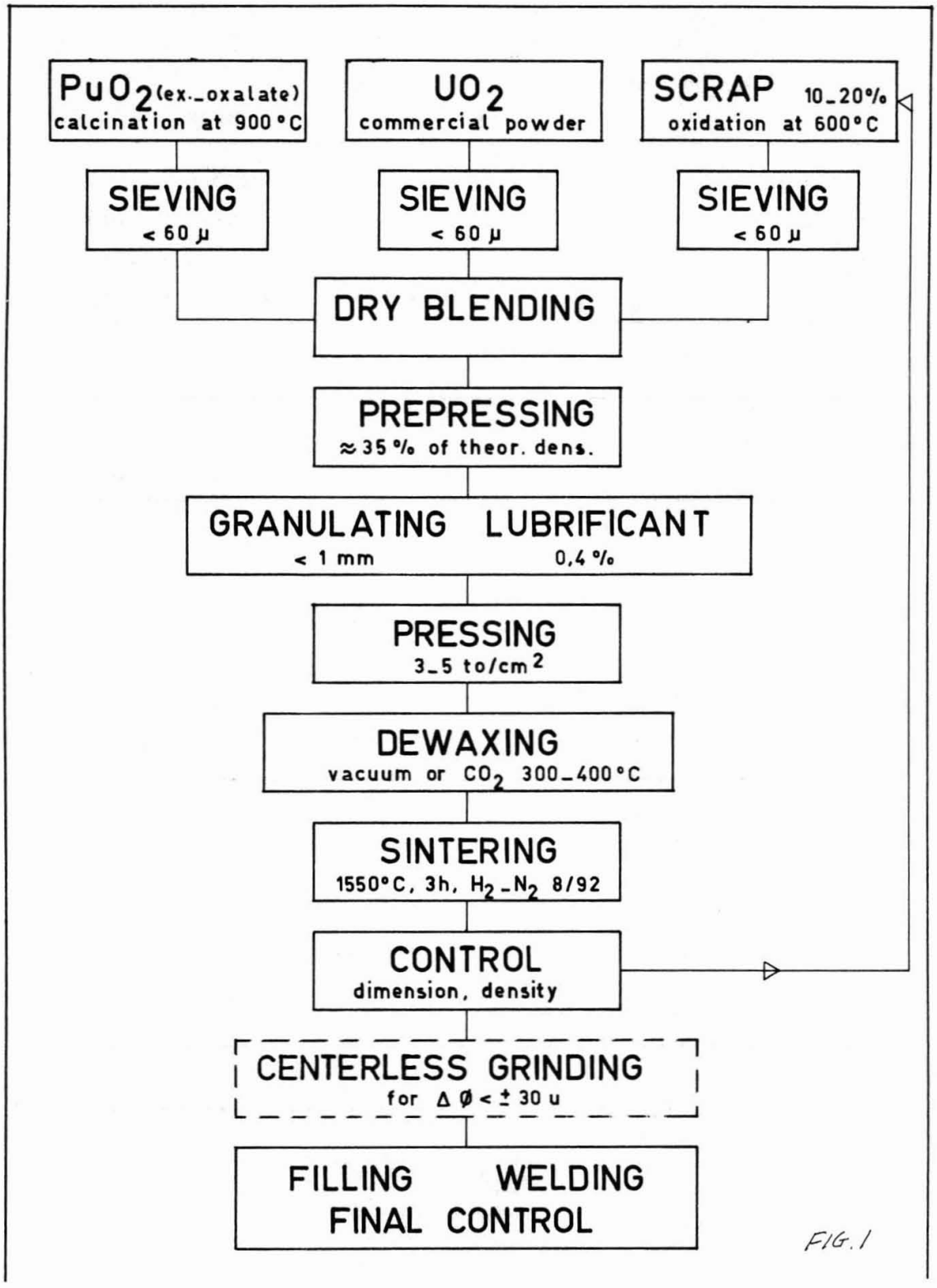
PuO2 (ex._oxalate)
calcination at 900 °C
UO2
commercial powder
SCRAP 10_20%
oxidation at 600 °C
SIEVING
< 60 µ
SIEVING
< 60 µ
SIEVING
< 60 µ
DRY BLENDING
PREPRESSING
≈ 35 % of theor. dens.
GRANULATING LUBRIFICANT
< 1 mm 0,4 %
PRESSING
3_5 to/cm2
DEWAXING
vacuum or CO2 300_400 °C
SINTERING
1550°C, 3h, H2_N2 8/92
CONTROL
dimension, density
CENTERLESS GRINDING
for Δ Ø < ± 30 u
FILLING WELDING
FINAL CONTROL

FIG. 1

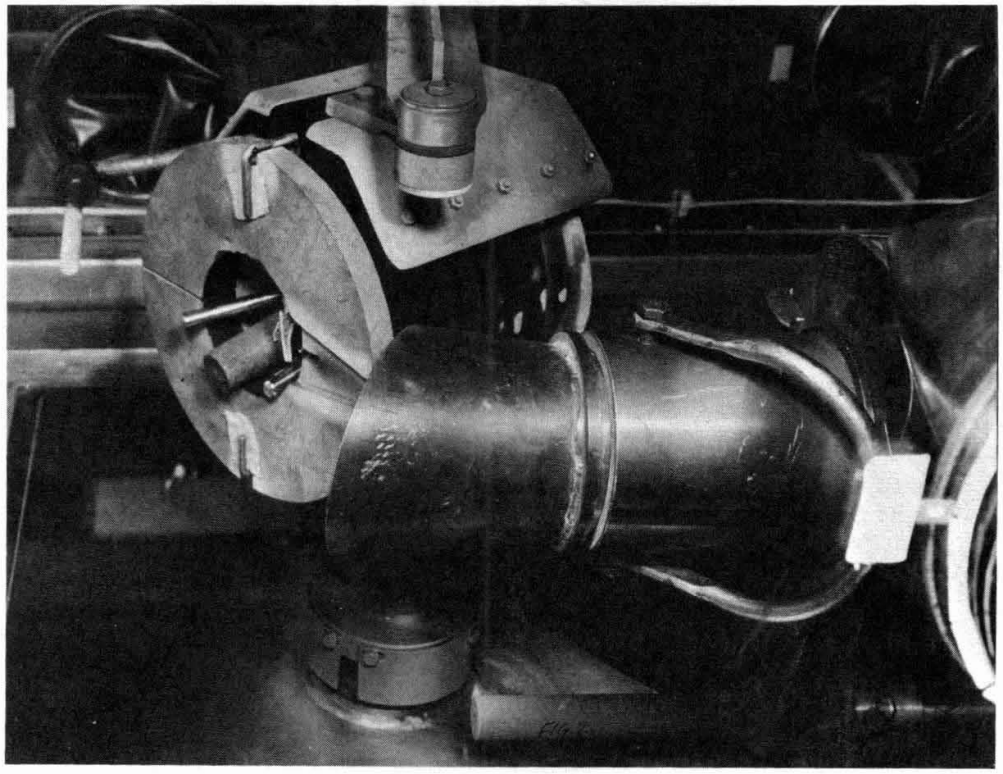

FIG. 3

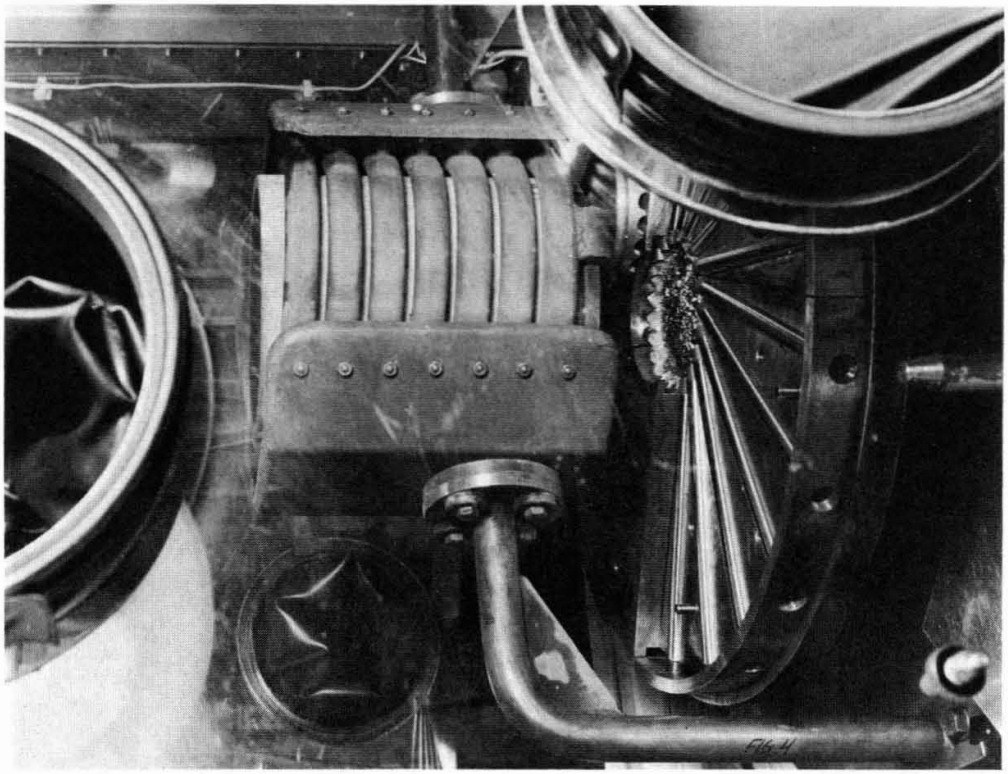
FIG. 4


FIG. 5

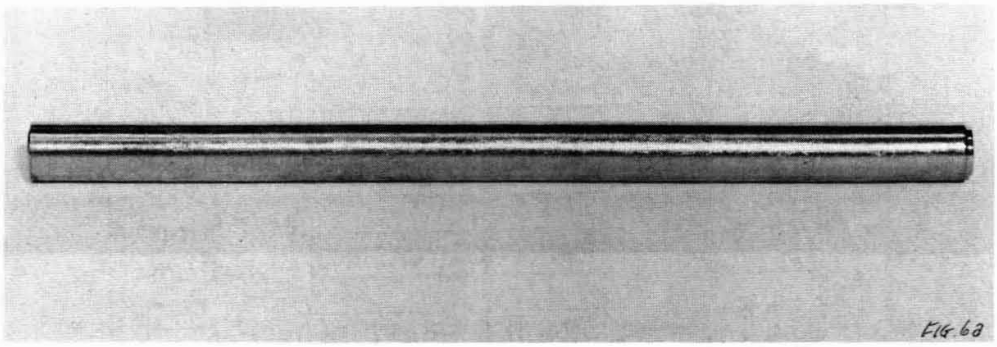

FIG. 6a

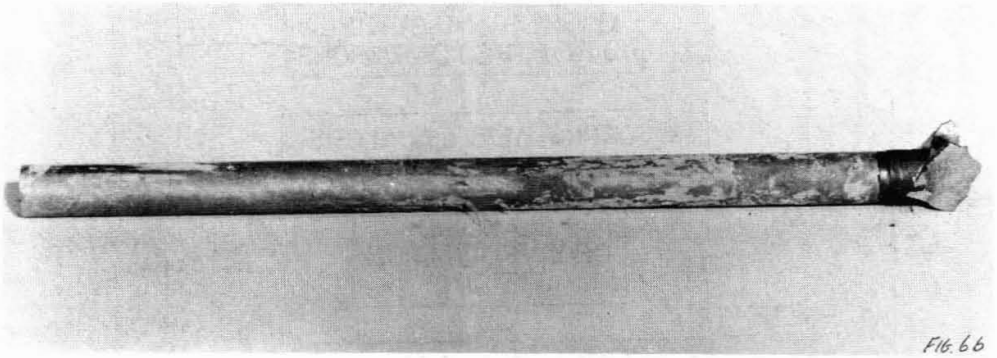

FIG. 6b

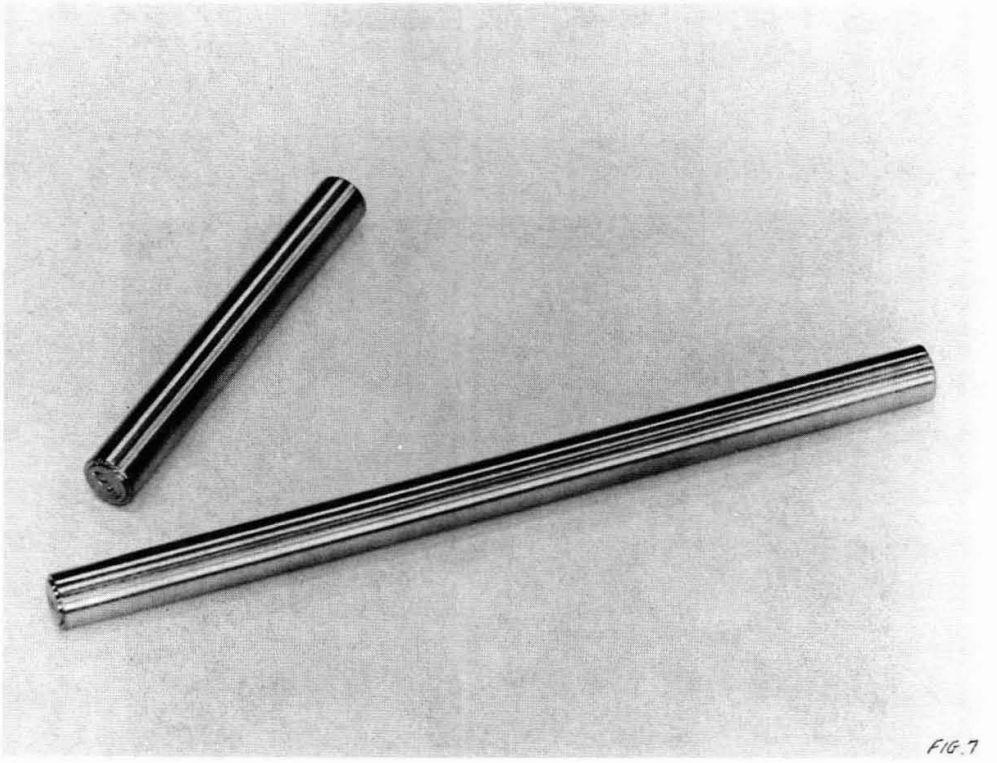

FIG. 7

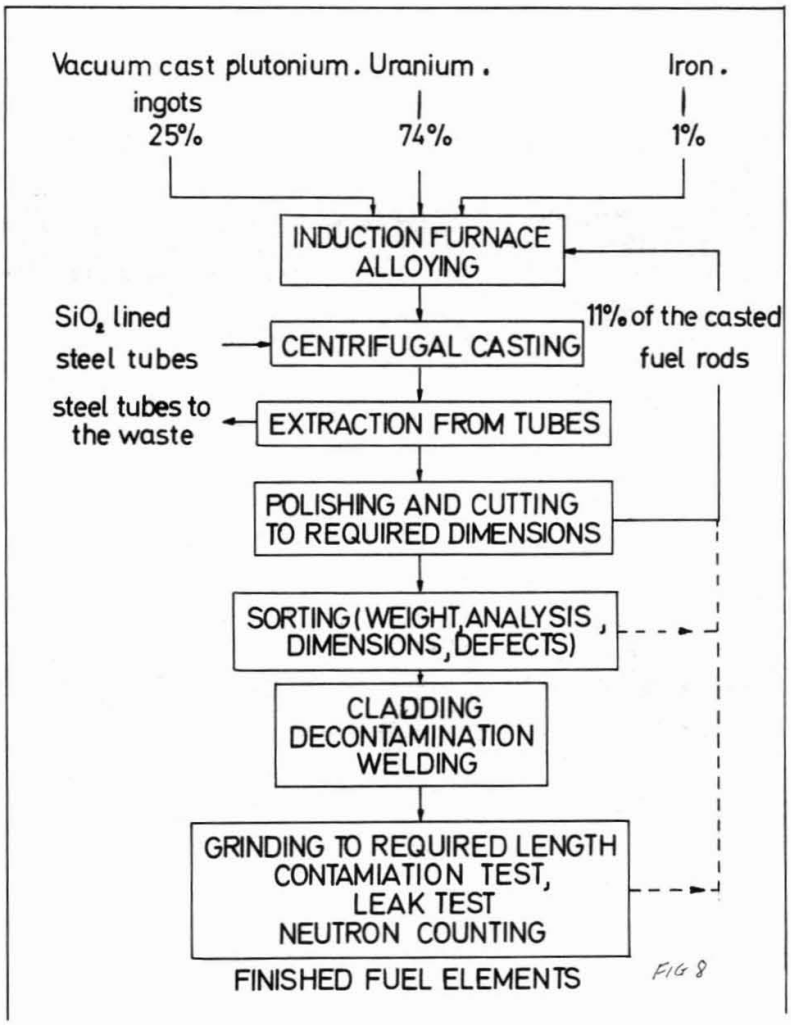
Vacuum cast plutonium. Uranium. Iron.
ingots
25%
74%
1%
INDUCTION FURNACE ALLOYING
SiO2 lined steel tubes
CENTRIFUGAL CASTING
11% of the casted fuel rods
steel tubes to the waste
EXTRACTION FROM TUBES
POLISHING AND CUTTING TO REQUIRED DIMENSIONS
SORTING (WEIGHT, ANALYSIS, DIMENSIONS, DEFECTS)
CLADDING DECONTAMINATION WELDING
GRINDING TO REQUIRED LENGTH CONTAMIATION TEST, LEAK TEST NEUTRON COUNTING
FINISHED FUEL ELEMENTS
FIG 8

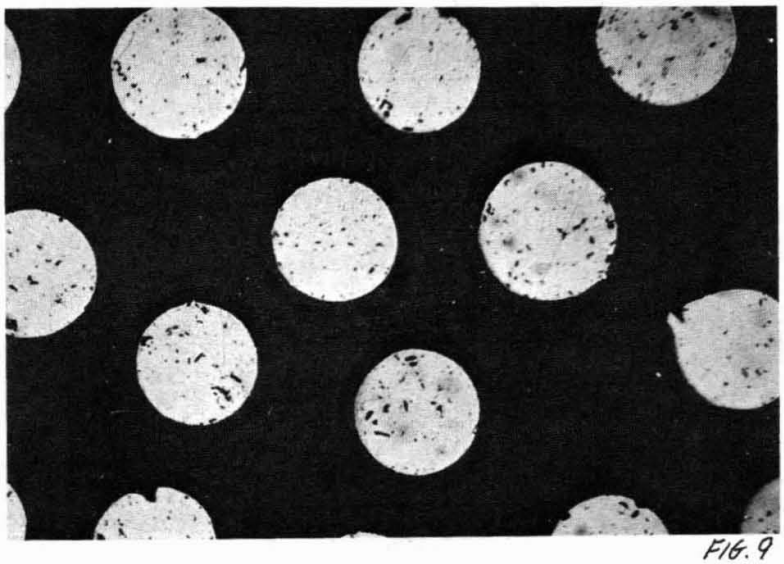
FIG. 9

The heat conductivity of Uranium Plutonium mixed oxides

H.M. Mattys

Mr. H.E. Schmidt of the Institute for Transuranium Elements, has measured the thermal conductivity and the thermal diffusivity of uranium-plutonium mixed oxide pellets with different oxygen contents All specimens had a density very close to 94% of the crystallographic value. Stoichiometry changes were introduced by appropriate heat treatment of the samples under reducing or slightly oxidizing atmosphere.

Mean value curves of the results of conductivity measurements - obtained with a stationary, absolute, longitudinal heat flow method - are given in fig. 1. It is clearly seen, that stoichiometric samples (with O/M-ratios between 1,997 and 2,000) exhibit the highest conductivities within the observed temperature range.

Above 200°C and up to 800°C, the results may be represented analytically by $K = (A + Bt)^{-1}$, where the stoichiometry dependance of A can be related to the variation of the phonon mean free path due to the presence of excess oxygen atoms or oxygen vacancies.

The diffusivity of mixed uranium-plutonium oxide, measured between 800°C and 1700°C on two hypostoichiometric samples varies with oxygen concentration (see fig. 2) in the same manner as the conductivity at lower temperature.

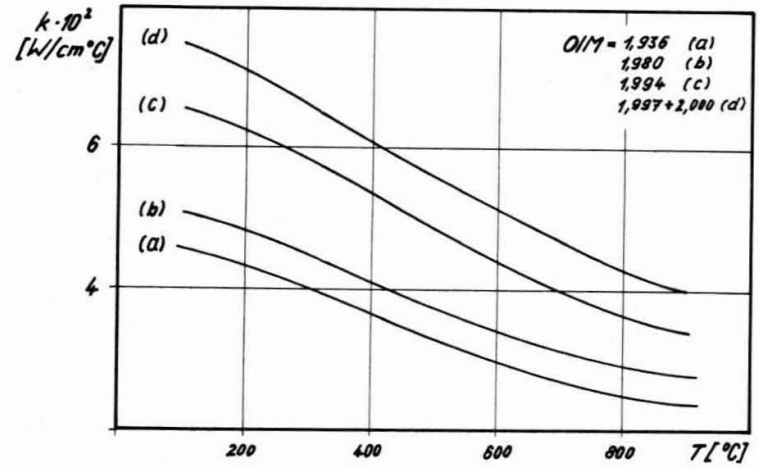
k·10²
[W/cm°C]
(d)
(c)
(b)
(a)
6
4
O/M = 1,936 (a)
1,980 (b)
1,994 (c)
1,997÷2,000 (d)
200
400
600
800
T[°C]

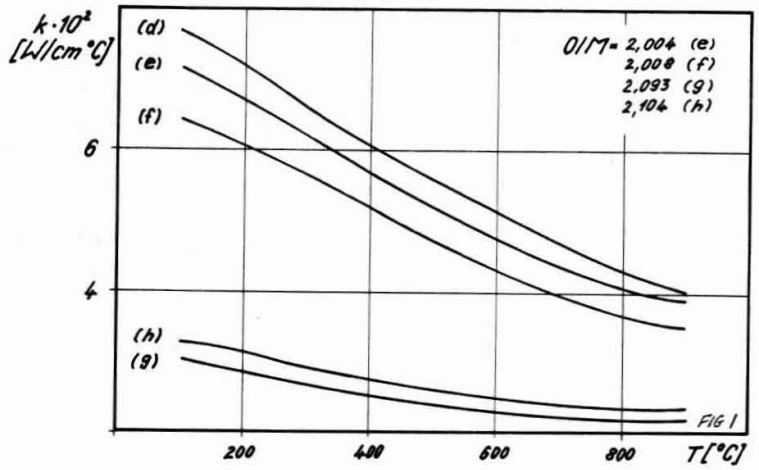
k·10²
[W/cm°C]
(d)
(e)
(f)
(h)
(g)
6
4
O/M = 2,004 (e)
2,008 (f)
2,093 (g)
2,104 (h)
200
400
600
800
T[°C]

FIG 1

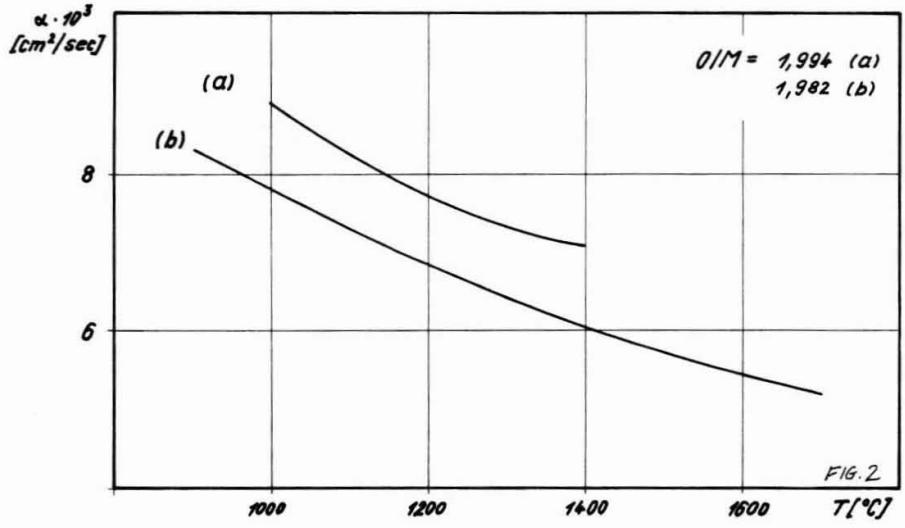
α·10³
[cm²/sec]
(a)
(b)
8
6
O/M = 1,994 (a)
1,982 (b)
1000
1200
1400
1600
T[°C]

FIG. 2

THERMAL CONDUCTIVITY OF URANIUM-PLUTONIUM OXIDE FUELS

W.E. Baily*
E.A. Aitken**
R.R. Asamoto***
C.N. Craig***

Abstract

Thermal conductivity measurements from both in- and out-of-pile experiments are summarized and indicate that stoichiometric mixed oxide fuels at near the 20 wt/% PuO_2 composition exhibit an integral to melting value of 86 watts/cm. Hypostoichiometric compositions indicate a higher value at 89 watts/cm. The results of these measurements also indicate that the mixed oxide fuel has a slightly lower conductivity than UO_2.

A new model, derived experimentally, has been developed for correcting thermal conductivity for density. This model indicates that the standard Loeb correction is not valid, and that the density correction is a function of temperature. Experiments to measure the effect of burnup on the conductivity of mixed oxide fuel indicate that there is no gross change in the integrated conductivity to melting.

Worked Performed Under Contract AT (04-3)-189, Project Agreement 10, Between the US Atomic Energy Commission and the General Electric Company, Advanced Products Operation, Sunnyvale, California

*Manager. Fast Reactor Ceramic Fuels, General Electric Co, NED Advanced Products Operation, 310 DeGuigne Dr, Sunnyvale, California.

**Manager. Plutonium Research, General Electric Co., NED Vallecitos Nuclear Center, P.O. Box 846, Pleasanton, California

***Engineer. General Electric Co. Advanced Products Operation, NED 310 DeGuigne Dr, Sunnyvale, California.

INTRODUCTION

At present, the preferred fuel for power producing, fast reactors is the oxide of plutonium and uranium. Its demonstrated ability to remain single phase throughout its operating lifetime and its relatively high melting point and fissile density makes it an ideal choice for fast reactor application. In addition, recent thermal and fast flux irradiation results at high burnups indicate that no burnup limitation has been observed in the mixed oxide fuel.[1] The one obvious disadvantage of oxide fuel is its low thermal conductivity. This disadvantage however is partially balanced by its high melting point and its ability to retain heat during a transient. This results in an increased Doppler effect and delayed heat transfer to cladding.

There are two primary processes by which heat is conducted in solids. These include energy transferred by coupling between lattice vibrations or by electronic movement and collision with atoms, or both. For most metal-oxides with the fluorite structure, the electrons are not free to move through the structure in appreciable concentrations, and heat is transferred primarily by lattice vibrations. If the lattice vibrations are completely harmonic there is little resistance to heat flow. In a practical sense, however, the anharmonic nature of the vibrations leads to attenuation of the thermoelastic waves and a lowered conductivity. This anharmonicity is particularly affected by the relative atomic weights of the ions present. For example, the higher the atomic weight of the cations, such as plutonium in UO_2, the lower the thermal conductivity. Conduction processes in solids indicate that conductivity is directly proportional to the mean free path between collisions. At temperatures above the Debye temperature, the mean free path for thermal scattering is inversely proportional to temperature. This mean free path is also decreased by the addition of a second cation to the structure, such as the replacement of a uranium site with a plutonium cation. Consequently the thermal conductivity of $(Pu_xU_{1-x})O_2$ can theoretically be expected to be slightly lower than that of UO_2.

The application of thermal conductivity values for temperature calculations of ceramic oxide fuels under irradiation is complicated by structural changes insitu such as grain size and orientation, fuel movement, radial fuel densification, burnup, gap conductance and compositional changes. This paper will attempt to correlate the existing out-of-pile and in-pile thermal conductivity data and associated structural and chemistry changes that occur insitu in mixed oxide fuels, to develope a means for predicting fuel temperature profiles.

OUT-OF-PILE THERMAL CONDUCTIVITY MEASUREMENTS

Detailed information is readily available on UO_2 conductivity from both in- and out-of-pile experiments.[2,3,4,5] Detailed information on the conductivity of PuO_2, however, is limited to one study which was performed by thermal diffusivity techniques.[6*] Available data on the conductivity

*Thermal conductivity is related to thermal diffusivity by the expression $K = k\rho C_p$ where k is the thermal diffusivity, ρ density and C_p is the specific heat of the material.

of PuO_2-UO_2 solid solutions is limited to the work of Hetzler, et al and Schmidt, et.al.[7,8] A comparison of the existing PuO_2 and UO_2 data shown in Figure 1, indicates that the thermal conductivity of PuO_2 is, as expected, lower than UO_2, based on a comparison of results by two different measuring techniques. Unfortunately, the results on PuO_2 are partially clouded by the possibility of (1) the reduction of the PuO_2 to a hypostoichiometric composition, and (2) uncertainty in the specific heat of PuO_2 which is required for the conversion of thermal diffusivity measurements to thermal conductivity data.

Mixed oxide conductivity measurements have in general been limited to compositions of interest to fast ceramic reactors (i.e., 15 to 30 wt/% PuO_2.) The results of these studies comparing stoichiometric compositions of 15 and 20 wt/% PuO_2 are shown in Figure 2. The studies by Schmidt, et al were by the longitudinal heat flow method to a temperature of 900°C. Remarkably good agreement at 900°C is observed between this data and that of Hetzler, which was measured using the radial heat flow technique. Because the majority of the conductivity data on UO_2, UO_2-PuO_2 and PuO_2 have been corrected for density by the Loeb equation, it is difficult to compare results from various sites because of uncertainties in this correction factor.[5] (Specimens in the 92 to 95% density range, however, are reasonably correct using the Loeb factor at temperatures between room temperature and 1000°C.) Specimen fabrication technique is not known to cause a major difference in conductivity, but it should be noted that specimens of Schmidt were fabricated by the physically mixed technique while those of Hetzler were made by coprecipitation.

The effect of stoichiometry on the thermal conductivity of $(Pu_{0.2}U_{0.8})O_{2\pm x}$ specimens was determined by Hetzler using the radial heat flow technique. Direct relative measurements were made in this study which eliminated any error in heat flux and gave good relative but not absolute values for the effect of stoichiometry on mixed oxide conductivity.[7,9] These data are shown in Figure 3. The results of this study indicate that the stoichiometric composition exhibits the highest effective conductivity with both the hyper- and hypo-stoichiometric compositions being lower with the maximum difference occurring in the low temperature region. The lower conductivity of the nonstoichiometric compositions may be accounted for in part by their defect structures. The absence or presence of excess oxygen atoms might be expected to lead to increased anharmonic disturbances and phonon scattering. Calculations have been made for UO_2, however, which suggest that enhancement in thermal conduction of hypostoichiometric fuel may be realized from electronic conduction In-pile results to date have indicated that hypostoichiometric fuel does have a higher conductivity (see Figure 5 and discussion).

EFFECTS OF RESTRUCTURING

During reactor operation at fuel center line temperatures in excess of 2000°C, the oxide fuel changes its appearance from a solid ceramic body with a uniform density to a body with a very marked density and structure distribution. The formation of the center void for example is the result of the movement of fuel porosity and some of the gap from the cooler region to the center void. The columnar grains are the product of lense shaped pores sweeping up the thermal gradient. The large massive grains occasionally observed in irradiated fuel however, are the product of grain boundary migration rather than lenticular pore sweeping. For

example, pore sweeping will occur under thermal gradients greater than 2000°C/cm. At lower thermal gradients, boundary migration can be expected. Whichever mechanism occurs, there is a large shift in porosity. In a typical fuel pin, regions greater than 1400 to 1500°C will increase in density to values between 96 to 100%. This change has a marked effect on thermal conductivity, and in fuels where porosity in amounts up to 15% are required to contain fuel swelling, a correction must be made for this changing density condition.

As noted earlier, density has been routinely corrected by the use of the Loeb Equation.[10]

$$\frac{K_{1-P}}{K_{100}} = 1 - P, \tag{1}$$

where

K_{100} = conductivity of solid at 100% P, and
P = fractional pore volume.

Recent investigators measuring the thermal conductivity of UO_2 in-pile have proposed the following modifications of the Loeb Equation.[11]

$$\frac{K_{1-P}}{K_{100}} = 1 - \alpha P, \tag{2}$$

where α is a proportionality constant of 2.5 ± 1.5.

Other modifications, Equations (3) and (4), such as the Maxwell-Eucken expression or modifications thereof, have been suggested.[12,13]

$$\frac{K_{1-P}}{K_{100}} = \frac{1 - P}{1 + \beta P}, \tag{3}$$

where β is related to the pore shape.

$$\frac{K_{1-P}}{K_{100}} = \frac{1 - P}{1 + P(\alpha - 1)}, \tag{4}$$

where α is a shape factor.

Asamoto's recent studies on the effect of density on conductivity with a radial heat flow apparatus have indicated that the above expressions are not valid for predicting temperature profiles of irradiated fuel.[5] His measurements, summarized in Figure 4, indicate that density corrections must be applied as a function of temperature and that a nonlinear density correction factor with temperature must be applied. For example, Asamoto's recommended conductivity expression for UO_2 as a function of density and temperature is:

$$K = 0.0130 + \frac{1}{T\,(0.4848 - 0.4465D)} \quad \text{(watts/cm°C)}, \qquad (5)$$

where $800°C \leq T \leq 2200°C$ and $0.80 \leq D \leq 0.95$.

The effect of grain size, grain orientation, and stoichiometry has been suggested by various investigators as a means whereby the electronic and internal radiations contribution to thermal conductivity can greatly be increased. No detailed information on mixed oxides has been developed at this time to suggest a further improvement in conductivity at elevated temperatures. Some out-of-pile studies on UO_2 suggests that these additional contributions will increase the effective conductivity. Most in-pile conductivity results on UO_2 as well as mixed oxide test results suggest that the density correction is a much larger factor than the increased electronic phonon contribution.

IN-PILE THERMAL CONDUCTIVITY MEASUREMENTS

Effect of Stoichiometry

With one or two notable exceptions, in-pile measurements* on smeared thermal conductivity of mixed oxide fuel agree reasonably well with lower temperature out-of-pile studies. The effect of stoichiometry on the in-pile performance of mixed oxide fuels is shown in Figure 5.[14] The microstructures shown are from three fuel pins with stoichiometries of 2.03, 2.00, and 1.98 which received a burnup of approximately 2000 MWD/Te in EBR-II. A further comparison of these pins is noted in Table I.

TABLE I

COMPARISON OF THREE STOICHIOMETRIES IRRADIATED IN EBR-II

$(Pu_{0.2}U_{0.8})O_{2 \pm x}$

Pin Number	O/M	Radii of Structural Change (mils) EA GG	C GG	CV	$\int_{T_s*}^{T} cgg_{kdT}$	$\int_{T_s}^{T} c_{kdT}$
F1D	1.98	80	40	0	34.0	39.2
F1B	2.00	82	50	0.5	30.9	38.9
F1C	2.03	110	75	8.5	20.9	38.9

*Based on a T_s of $\sim 900°C$

Heat transfer calculations with these values based on a fuel surface temperature of 900°C indicate that the temperature for columnar

*In-pile measurements refer to $\int_{T_s}^{T_{melting}} kd\theta$ values where the effective smeared thermal conductivity of a given fuel element is based on (1) linear power (Q), (2) molten boundary, and (3) flux depression. While these measurements are the most useful to fuel designers they do have the largest uncertainty because of difficulties in measuring Q and the molten boundary accurately.

grain growth in the 1.98, 2.0 and 2.03 O/M fuel are 2400, 2200 and 1900°C respectively. This inconsistency implies that a common conductivity curve for the three stoichiometries is not valid, and suggests that the conductivity of $(Pu_{0.2}U_{0.8})O_{2\pm x}$ fuel increases with stoichiometry from 1.98 through 2.03. (As noted earlier this is inconsistent with the out-of-pile data.) Another possible reason for this apparent difference is that the mass transport mechanism and grain growth kinetics are altered significantly by stoichiometry. Similar observations on the effect of stoichiometry on fuel movement in $(Pu_{0.05}U_{0.95})O_2$ have been reported by NUMEC.[15]

Because most applications of thermal conductivity are used for calculating the linear power level to melting, it is necessary to know the melting limits of the particular composition or stoichiometry, or both, under concern. The phase diagram determined by Lyon and Baily should be applicable for all studies associated with stoichiometric mixed oxide compositions.[16] Information on the effect of stoichiometry on the melting point of mixed oxides is limited to the 20 wt/% PuO_2 composition range with O/M varying between 1.93 and 2.00. These studies conducted under the FCR (Fast Ceramic Reactor) program indicate a maximum in the melting point at approximately 1.97 stoichiometry for the 20 wt/% PuO_2 compositions. This is shown in Figure 6. In addition, it was observed by X-ray studies that this region is a single phase area.

In-pile smeared thermal conductivity measurements on the effect of stoichiometry by Craig indicate an approximately 7% higher $\int_{T_s}^{T_m} k d\theta$ value (based on a fuel surface temperature of 900°C) for 1.98 O/M fuel compared to 2.00 O/M compositions.[17] Structures of 1.98 and 2.00 O/M fuel irradiated for 5 hours at 36 kW/ft are shown in Figure 7. Based on a porosity limit as a molten boundary,* the corresponding $\int_{900}^{T_m} k d\theta$ of these stoichiometries are 45.8 and 43.2 watts/cm, respectively. Thus, these measurements also tend to disagree with the out-of-pile measurements and suggest that a higher effective conductivity can be obtained from the 1.98 O/M fuel compared to the 2.00 at low burnups. Comparison of hypo- and stoichiometric mixed oxide fuels at 50,000 MWD/Te, however, show little difference in the structure, which suggests that the low burnup benefit of stoichiometry may be lost at higher burnups. (See section on stoichiometry change.)

The effect of fuel density on the in-pile thermal conductivity of mixed oxide fuels is significant. For example, significantly more melting can be expected in specimen at 85% density compared to specimens at 95%, operating at comparable power levels. A slightly lower effective conductivity of powder versus pellet fuel at near identical smeared densities has been observed in thermal and fast flux irradiations of mixed oxide fuel.[14, 18] Figure 8 shows a comparison of three stoichiometric mixed oxide specimens irradiated in EBR-II, at near identical conditions, which indicate the amount of fuel restructuring that has occurred insitu in these specimens because of the reduced thermal conductivity in low density fuel.

*The molten boundary used in this study was the porosity limit. The utilization of the substructure as the boundary would not significantly change the difference between these two values.

Comparison tests of $(Pu_{0.2}U_{0.8})O_{1.98}$ to $UO_{2.0}$ measured by both smeared conductivity techniques as well as direct (in-fuel thermocouple and gas bulb thermometry) indicate that the mixed oxide fuel has a slightly lower conductivity than UO_2.[17,19] In-fuel thermocouple measurements indicate that this lower conductivity is more pronounced at temperatures below 1200°C which is reasonable because any defect in the lattice would be more pronounced at lower temperatures.

Effect of Diametral Gap

A significant factor in fuel center temperature calculation is the thermal resistance offered by the diametral gap. In-pile experiments to establish the effect of diametral gap on fuel centerline temperature indicate that cold diametral gap sizes of 2,4 and 10 mils result in initial h (gap conductance) values of 2000,1100 and 600 Btu/h-ft^2 respectively.[20] Measurements of diametral gap size change with burnup indicate that the gap decreases in size with burnup and thermal cycling. For example, the 2, 4 and 10 mil gap specimens, referred to above, decreased to 2, 2.5 and 5 mils respectively after approximately 500 MWD/Te (42 hours at 20 kW/ft with 2 thermal cycles). Similar tests in EBR-II indicated that after a burnup of 2000 MWD/Te the diametral gap had decreased by a factor of 2.[14] Fast flux irradiations to 50,000 MWD/Te indicate that the diametral gap is essentially gone.[21] Based on these observations, the effect of diametral gap on fuel center line temperature in fuels operating at power levels of > 15 kW/ft can be noted to be extremely important in the early period of irradiation. After time periods of 7 days or less, the diametral gap size is known to decrease by a factor of 2 and the large Δt originally present across the gap will be significantly lower than the initial size. Figure 9 shows measured and projected h values that may be expected in mixed oxide fuel pins operating at power levels greater than 15 kW/ft at the start of irradiation and approximately 7 days later. At some burnup below 50,000 MWD/Te for fuels operating at comparable linear power levels, h values of 2000 or greater can be expected. One byproduct of this changing gap is that $\int_{T_s}^{T_c} k d\theta$ experiments that are performed by rapid reactor insertion (i.e. hydraulic rabbit) will result in integral to melting values that represent early-in-life values and may present an overly pessimistic value for conductivity. A more satisfactory experimental procedure is one where approximately 10 hours are taken to reach peak power and sintering insitu takes place prior to melting.

Effect of Burnup on Conductivity

The preceding section outlined the general increase that can be expected in gap conductance values with burnup. Other parameters which have been reported to change with burnup are melting point and thermal conductivity. Detailed data on the effect of burnup on the melting point of mixed oxides are lacking, and the 150°C decrease in the UO_2 melting point at 100,000 MWD/Te is presently accepted as an estimate for mixed oxides.[22]

No data exist for the effect of burnup on mixed oxide conductivity. Information developed at BAPD for UO_2 suggests that at low temperatures (below 1000°C) the conductivity is severely depressed with burnup.[12,23] Most of the justification for these data is from in-fuel Pt - Pt 10 Rh thermocouples. Based on thermocouple decalibration caused by transmutation of the rhodium to palladium it is difficult to evaluate this data.[24]

Observations on high burnup (> 100,000 MWD/Te) thermal flux irradiations of mixed oxide fuels indicate there is, at most, a small depression in conductivity with burnup.[25,26]

Effect of Stoichiometry Change

In an earlier section the effect of stoichiometry on the in-pile performance of mixed oxide was discussed. It was indicated that at low burnup the hypostoichiometric fuel had a high $\int_{T_s}^{T_m} kdT$ value presumably because of the higher melting point. Because of the large thermal gradient across the fuel radius (6000°C/cm) and compositional changes from burnup, it is possible that the stoichiometry will not remain at a fixed value. For example, stoichiometry changes have been observed in mixed oxide fuel irradiated to 1500 MWD/Te. This study indicated that a stoichiometric fuel became hypostoichiometric in the central region as noted in Figure 10. In addition, out-of-pile studies indicate that a stoichiometry gradient can be expected in initially hypostoichiometric fuel if there is a significant temperature gradient. Experiments in which a stack of mixed oxide pellets were sealed in a molybdenum capsule and heated in a temperature gradient indicated that oxygen migrated preferentially to the cold end.

In the absence of a clear cut understanding of the stoichiometry gradient and the stoichiometry change during irradiation, the effect on thermal conductivity is difficult to assess. If oxygen migrates to the cold region which is maintained near the stoichiometric composition, the difference in overall thermal conductivity as a function of initial stoichiometry may be eliminated.

UTILIZATION OF INTEGRAL CONDUCTIVITY VALUES

The integral form is the most useful form of fuel thermal conductivity data for reactor design and irradiated fuel evaluation purposes. At present $\int kdT$ curves for fuel of a given density are generated by utilizing both in- and out-of-pile data. Specifically, the integral conductivity from room temperature to approximately 2000°C is calculated from out-of-pile data. This method of determining $\int kdT$ curves can and has lead to erroneous interpretations of the true effective conductivity that exists in-pile. This method for generating $\int kdT$ curves has often led to a conductivity upswing in the high temperature regions. Differentiation of these curves results in a corresponding increase in the thermal conductivity curve to unusually high values in the high temperature regions. By utilizing a density-conductivity relationship recently developed, it is possible to develop out-of-pile integral values corrected for density which can more realistically be related to integral to melting values measured in-pile. By correcting for fuel densification, all or

most of the apparent upswing in the conductivity curve is eliminated.

After a given irradiation period, three distinct regions can be assumed to exist across the radius of the fuel: (1) a region which maintains the original density of the fuel, (2) a sintered or grain growth region, or both, and (3) a columnar grain growth region. The corresponding temperature of these regions are: (1) fuel surface to 1400°C, (2) 1400°C to 1900°C, and (3) 1900°C to the melting point. The density in this first region is the initial fuel density; the second, between 96 and 98% T.D.; and in the third between 98 and 100% T.D.* For example, for a 95% dense mixed oxide fuel, the integral to melting across the radius can be defined as:

$$\int_{T_o}^{T_m} k\,dT = \int_{T_o}^{T_s} k_{95}\,dT + \int_{T_s}^{T_{1400}} k_{95}\,dT + \int_{1400}^{T_{1900}} k_{97}\,dT + \int_{T_{1900}}^{T_m} k_{99}\,dT; \quad (6)$$

where

T_o = room temperature,
T_s = fuel surface temperature,
T_{1400} = temperature of equiaxed grain growth,
T_{1900} = temperature of columnar grain growth, and
T_m = temperature of fuel melting.

Although the above description is generally accepted, the lack of a reliable density-thermal conductivity relationship has prevented the use of corrections to account for the densification changes. Based on recent results developed by Asamoto, a thermal conductivity-density relationship has been established for stoichiometric mixed oxide fuel. This relationship is expressed by the following equation:

$$K = 0.0110 + \frac{1}{T\,(0.4848 - 0.4465D)} \quad \text{(watts/cm °C)}, \quad (7)$$

where

T = temperature (°C), and
D = fractional theoretical pellet density.

*Microstructural changes are dependent on the time, temperature gradient, and initial density of the fuel. Temperature and density values selected here are nominal values. Other values for these parameters may be used in the analysis to obtain more precise results.

This expression is plotted in Figure 11 which shows corresponding integral and thermal conductivity values for 95% dense stoichiometric $(Pu_{0.2}U_{0.8})O_2$ fuel under a thermal gradient typical of what might be expected in a FCR. As noted in Figure 11 identical conductivity curves are recommended for both hypo- and stoichiometric mixed oxides with a 3 watts/cm higher value for the 1.98 O/M fuel based on the observed higher melting point.

CONCLUSION

Thermal conductivity measurements from both in- and out-of-pile experiments indicate that stoichiometric mixed oxide fuels at near the 20 wt/% PuO_2 composition exhibit an integral to melting value of 86 watts/cm. Hypostoichiometric compositions indicate a higher value at 89 watts/cm. These values are slightly lower than those previously published and are considered accurate to within ± 15%. The results of these measurements indicate that the mixed oxide fuel has a slightly lower conductivity than UO_2.

A new model, derived experimentally, has been developed for correcting thermal conductivity for density. This model indicates that the standard Loeb correction is not valid, and that the density correction is a function of temperatures as expressed by the equation

$$K = 0.0110 + \frac{1}{T\,(0.4848 - 0.4465\,D)} \quad \text{(watts/cm °C)} \qquad (7)$$

Experiments to measure the effect of burnup on the conductivity of mixed oxide fuel indicate that there is no gross change in the integrated conductivity to melting. While these data are not conclusive, they do imply that the depression in the integral conductivity, if any, is less than 15 watts/cm at 120,000 MWD/Te.

REFERENCES

1. Skavdahl, R.E., Spalaris, C.N. and Zebroski, E.L., "U.S. Experience on Irradiation Performance of UO_2-PuO_2 Fast Reactor Fuel", Presented at the AIME Nuclear Metallurgy Symposium; Phoenix, Arizona, October 4-6, 1967.

2. de Halas, D.R., and Horn, G.R., "Evolution of Uranium Dioxide Structure During Irradiation of Fuel Rods" Jour. of Nuc. Matls, (1963) 8, No 2, 207-220.

3. de Halas, D.R., "Understanding UO_2 Thermal Conductivity", Nucleonics, October, 1963.

4. Lyon, M.F., Straley, R.L., Coplin, D.H., Weidenbaum, B., and Pashos, T.J., "UO_2 Thermal Conductivity at Elevated Temperatures", Trans. ANS, June 1963, Vol 6 No.1, Salt Lake City, Utah.

5. Asamoto, R.R., Anselin, F., and Conti, A.E., "The Effect of Density on the Thermal Conductivity of Uranium Dioxide", GEAP-5493.

6. Legedrost, J.F., Askey, D.F., Storhok, V.W., and Gates, J.E., "Thermal Conductivity of PuO_2 as Determined from Thermal Diffusivity Measurements", to be published in "Nuclear Applications".

7. Hetzler, F.J., Lannin, T.J., Perry, K.J., and Zebroski, E.L., "Thermal Conductivity of 20:80 $(Pu,U)O_2$", Trans, ANS, June, 1965, Vol 8, No.1.

8. M. Mattys, Private Communications.

9. FCR Development Program, Twenty-First Quarterly Report, November to January 1967. GEAP-5433, February, 1967.

10. Loeb, A.L., "Thermal Conductivity: VIII A Theory of Thermal Conductivity of Porous Materials", J. Am. Cer. Soc, 37, (1954) (2) Part II, 96-99.

11. Ross, A.M., "The Dependence of the Thermal Conductivity of Uranium Dioxide on Density, Microstructure; Stoichiometry and Thermal-Neutron Irradiation" AECL-1096 (September 1960).

12. Belle, J., Berman, R.M. , Bourgeois, W.F., Cohen, I., and Daniel,R.C., "Thermal Conductivity of Bulk Oxide Fuels" WAPD-TM-586 (Revised) April 1967.

13. Biancheria, A., "The Effect of Porosity on Thermal Conductivity of Ceramic Bodies", ANS Trans. (June 1966) 9, (1) p. 15.

14. Rabin, S.A., Kendall, W.W., and Baily, W.E., "Short Term Fast Flux (EBR-II) Irradiation of PuO_2-UO_2 Fuel Pins", GEAP-4473 (to be issued).

15. NUMEC Quarterly Progress Report, "Irradiation Testing of PuO_2-UO_2 Fuels", Jan. 1966 through March 1966. NUMEC-3432, May 1966.

16. Lyon, W.L., and Baily, W.E., "The Solid Liquid Phase Diagram for the UO_2-PuO_2 System", Journal of Nuc. Mat. (1967) 22, No. 3.

17. Craig, C.N., and Baily, W.E., "In-Pile Comparison of Effective Thermal Conductivity of PuO_2-UO_2 Mixed Oxides" (To be published September, 1967).

18. Perry, K.J. and Anselin, F., "The Short Term Performance of VI-Packed Powder and Low Density Pellet Mixed Oxide Fuels under Condition of Gross Fuel Melting", GEAP to be issued in Sept. 1967.

19. Baily, W.E., Hines, D.P. and Zebroski, E.L., "In-Pile Thermal Conductivity of UO_2 and 20:80 $(Pu:U)O_2$ Specimens", Trans ANS, June 1967, Vol 8, No.1.

20. Baily, W.E., Craig, C.N. and Zebroski, E.L., "Effect of Diametral Gap Size on the In-Pile Performance of Fast Ceramic Reactor Mixed Oxide Fuel", Trans ANS, June 1966, Vol 9, No.1.

21. Nelson, R.C., Rubin, B.F., Kendall,W.W. and Baily W.E., "Performance of Mixed Oxide Fuel Pins Irradiated in a Fast Reactor to 50,000 MWD/Te" to be presented at Chicago, ANS Meeting, November 1967.

22. Christensen, J.A., "Irradiation Effects on Uranium Dioxide Melting" HW-69234 (March 1962).

23. Daniel, R.C., and Cohen, I., "In-Pile Effective Conductivity of Oxide Fuel Elements to High Fission Depletion", WAPD-246, April 1964.

24. Asamoto, R.R., and Novak, P.E.,"A Survey for a High Temperature Sensor for SEFOR", GEAP-4903, July, 1965.

25. Rubin, B.F., Nelson, R.C., and Perry, K.J., "The Irradiation of Stoichiometric and Hypostoichiometric UO_2-PuO_2 Fuels to Exposures of 125,000 MWD/Te", Trans ANS, June 1967, Vol 10, No.1.

26. Perry, K.J., Rubin, B.F., Nelson, R.C., "High Burnup Performance of Mixed Oxide Fuel to 100,000 MWD/Te" to be presented at Chicago, ANS Meeting, November 1967.

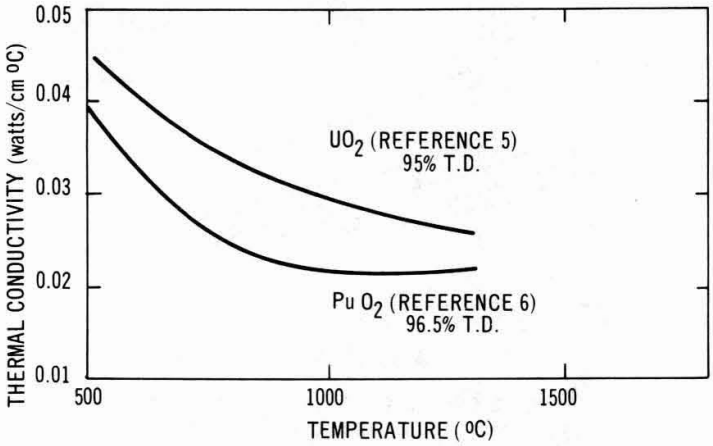

FIGURE 1. COMPARISON OF UO_2 AND $Pu\ O_2$ CONDUCTIVITY

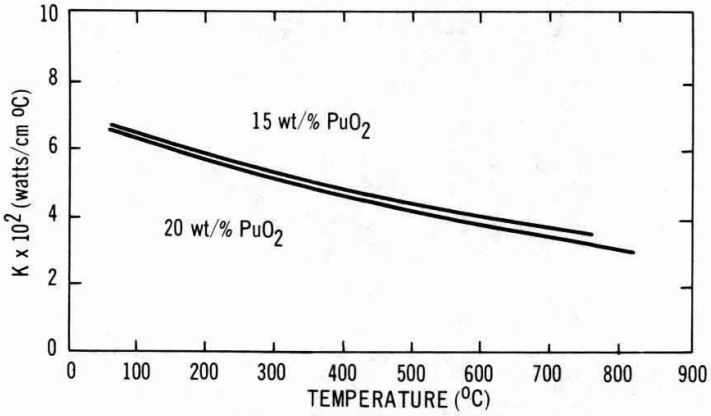

FIGURE 2. COMPARISON OF 15 AND 20 wt/% PuO_2 STOICHIOMETRIC MIXED OXIDE CONDUCTIVITY

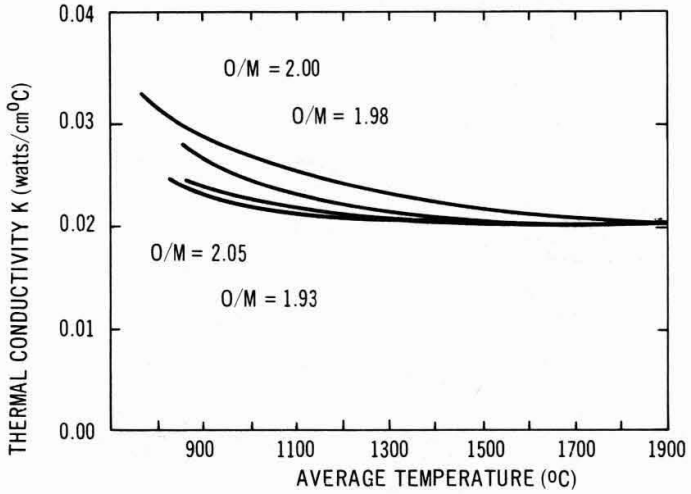

FIGURE 3. EFFECT OF STOICHIOMETRY ON THE THERMAL CONDUCTIVITY OF $(Pu_{0.2}\ U_{0.8})\ O_{2.00}$

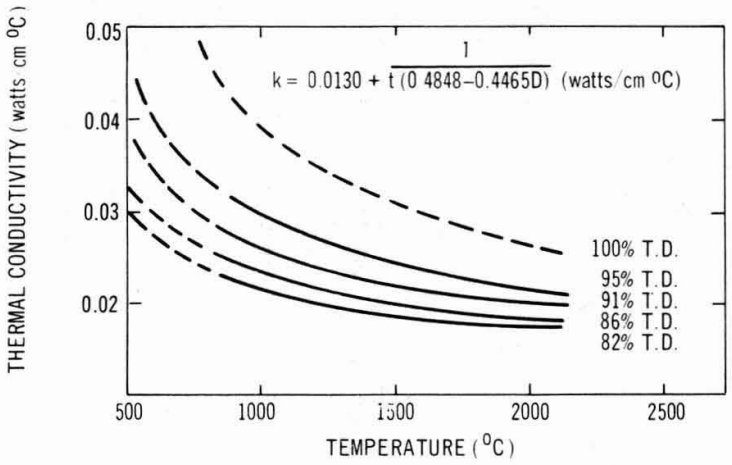

FIGURE 4. THERMAL CONDUCTIVITY OF UO_2 AS A FUNCTION OF TEMPERATURE AND DENSITY

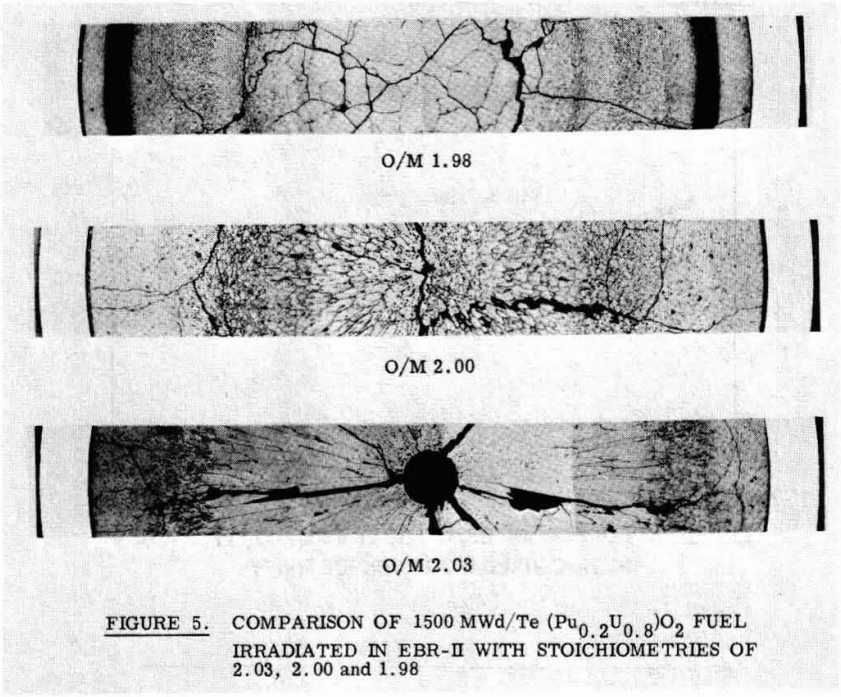

FIGURE 5. COMPARISON OF 1500 MWd/Te $(Pu_{0.2}U_{0.8})O_2$ FUEL IRRADIATED IN EBR-II WITH STOICHIOMETRIES OF 2.03, 2.00 and 1.98

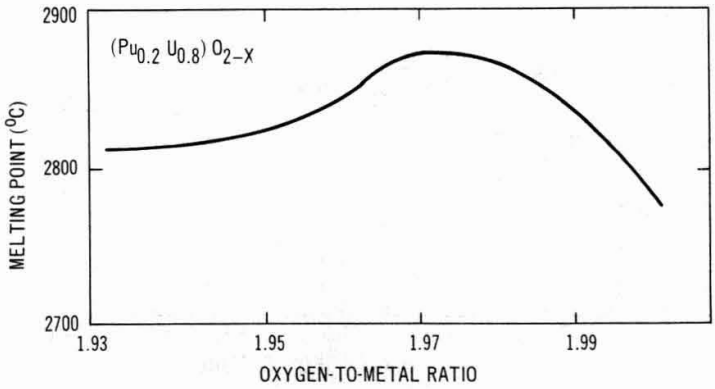

FIGURE 6. MELTING TEMPERATURE VERSUS O/M FOR (Pu,U) O_2

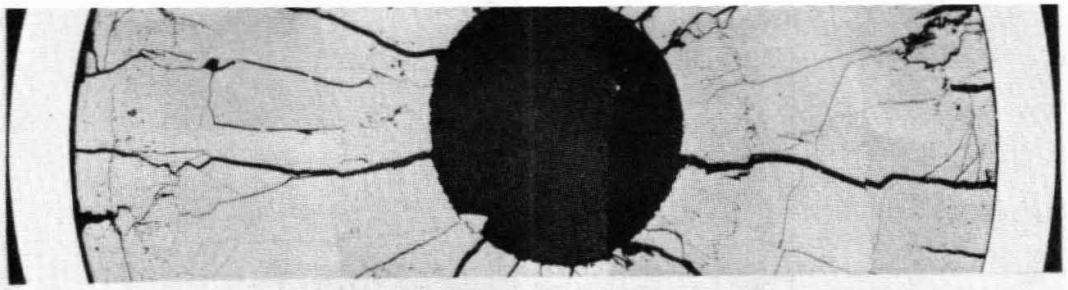

2.00

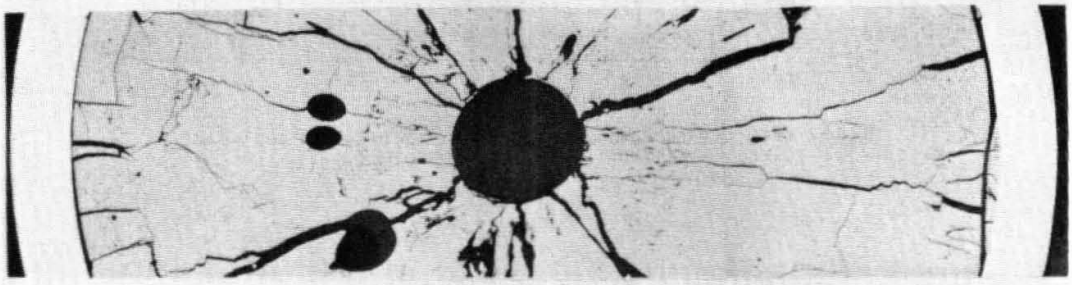

1.98

FIGURE 7. COMPARISON OF $(Pu_{0.2}U_{0.8})O_{2.00}$ AND $(Pu_{0.2}U_{0.8})O_{1.98}$ FUEL IRRADIATED UNDER IDENTICAL TEST CONDITIONS

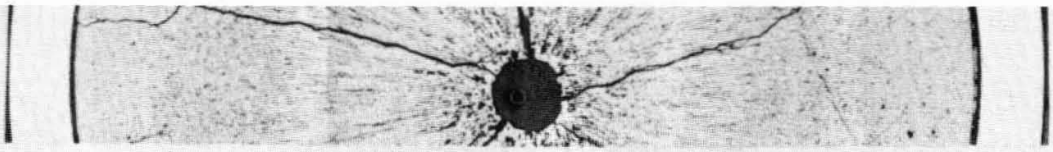

95% Dense Pellet 3 mil Diametral Gap

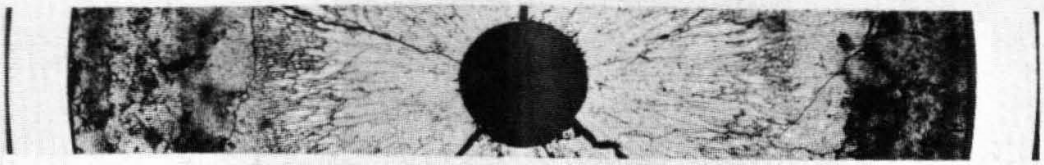

85% Dense Pellet 3 mil Diametral Gap

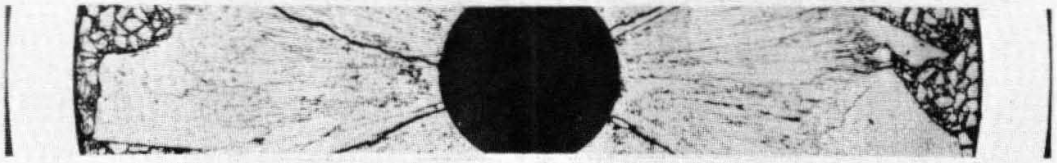

83% Dense Powder

FIGURE 8. EFFECT OF DENSITY ON FUEL STRUCTURE

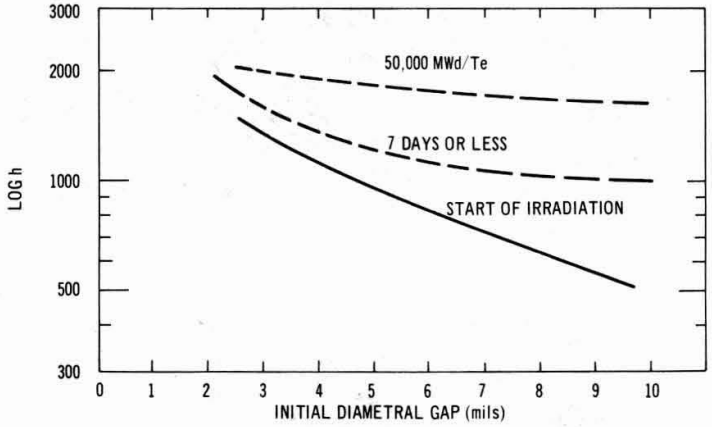

FIGURE 9. EFFECTIVE GAP CONDUCTIVITY AS A FUNCTION OF BURNUP AND INITIAL GAP SIZE (NEGLECTING FISSION GAS CONTRIBUTION)

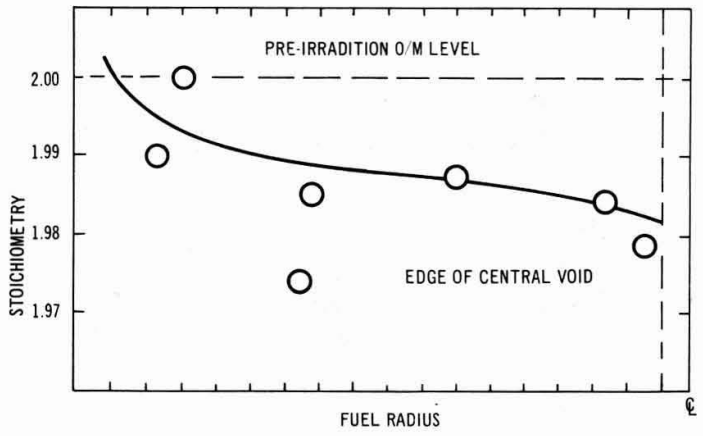

FIGURE 10. OBSERVED STOICHIOMETRY SHIFT IN IRRADIATED MIXED OXIDE FUEL

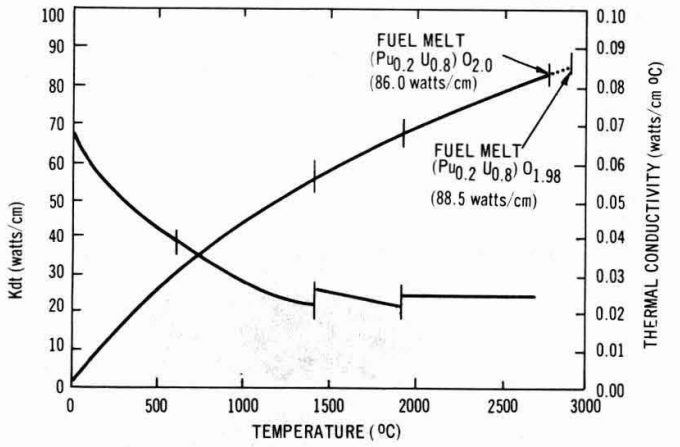

FIGURE 11. THERMAL CONDUCTIVITY AND INTEGRAL CONDUCTIVITY OF INITIALLY 95% T.D. $(Pu_{0.2}\ U_{0.8})\ O_{2\pm X}$ AFTER MICROSTRUCTURAL CHANGES HAVE OCCURRED

THERMAL CONDUCTIVITY OF URANIUM-PLUTONIUM CARBIDE FUELS

J. A. Leary and K. W. R. Johnson

Abstract

The thermal conductivity and thermal diffusivity of uranium monocarbide, plutonium monocarbide, and uranium-plutonium monocarbide, solid solutions are reviewed. Effects of sample porosity, stoichiometry, temperature, impurities, and solid solution formation are discussed.

Los Alamos Scientific Laboratory, University of California
Los Alamos, New Mexico 87544 USA

This work was sponsored by the United States Atomic Energy Commission.

INTRODUCTION

Thermal conduction in a solid phase involves three processes, 1. radiation or photon scattering, 2. electronic scattering by thermal vibrations of the lattice, and 3. anharmonic lattice vibrations, or phonon scattering. In opaque conductors the first process can be disregarded. Electronic scattering becomes of increasing importance as temperature increases, while phonon scattering generally decreases as temperature is increased above the Debye temperature. Introduction of "impurity" constituents into the lattice tends to reduce the thermal conductivity in the temperature ranges of interest, as these provide additional scattering sites. In this regard, porosity, grain boundary solid inclusions, and solid constituents can all be considered as "impurities".

The thermal conductivity of uranium-plutonium monocarbide solid solution fuels is of great technical importance. However, almost nothing is known about this property under the thermal, the radiation, and the compositional conditions that typify reactor fuel operation. Moreover, very little is known in regard to the thermal conduction in solid solution carbide fuels under "ex-reactor" conditions. Although some experimental work has been reported on the conductivity of these carbides, much of it is difficult to reconcile.

In order to anticipate what might be expected in fast reactor carbide fuels, it is helpful to review what is known about the thermal conductivity of uranium monocarbide. In view of the fact that fast reactor carbides are about 80 percent uranium monocarbide, some of the trends observed in UC should be relatable.

URANIUM MONOCARBIDE

The variation of thermal conductivity with temperature for 100% dense, stoichiometric uranium monocarbide is shown in Fig. 1. Low temperature measurements were made under steady state conditions (1-4) whereas higher temperature values were based on thermal diffusivity measurements (5, 6). It is unlikely that the slope of curve 1 between 500°C and 1000°C is truly representative of the specimen thermal conductivity. An increase of this magnitude is more customarily associated with photon conduction of elevated temperatures. Such an increase is also typical of data from comparative thermal conductivity assemblies in which the specimen and standard differ more than 10% (7). When the thermal conductivities represented by curve 5 were initially calculated they were necessarily based on an estimated specific heat of 0.05 cal./g.°K (8). It was subsequently determined that the specific heat of UC was considerably higher (9), hence curve 5A represents a recalculation of the original data incorporating this new information.

Essentially all of the results fall within a range of values of 0.05 ± 0.01

cal./sec. cm. °C. The average is approximately equal to the 0.22 watts/cm. °C previously suggested (10). Large as this deviation may seem, it compares favorably with the span of data on more common materials as BeO, Al_2O_3, and TiO_2 (11). Undoubtedly the precision of individual thermal conductivity measurements is much better than the absolute accuracy.

The thermal conductivity of UC depends on the porosity; an increase in porosity causes a decrease in thermal conductivity. Various methods have been proposed to correlate porosity and thermal conductivity of dense materials (10, 12, 13). The most commonly used expression is the simplified Loeb equation (12):

$$K_T = \frac{K_P}{1 - P}$$

where K_T = thermal conductivity of 100 percent dense material

K_P = thermal conductivity porous material

P = pore fraction

As shown in Fig. 2 , this equation does not always provide a sufficient correction for porosity. In this illustration, the conductivities of essentially 100 percent dense UC have been determined by the same investigators that determined the conductivities of less dense carbide. If a similar correction is applied to the data of Hayes and DeCrescente (10), the thermal conductivity estimated for 100 percent dense UC is again too low. However, the (1 - P) relationship gives excellent agreement between their corrected thermal conductivities for 91 percent dense and 95 percent dense carbides. Therefore this relationship might be more useful in referring the conductivities of porous materials to a reference porosity, rather than to full density. The importance of pore shape in correcting for porosity has been emphasized (13). Unfortunately, pore shape is rarely characterized in thermal conductivity specimens.

The effects of variations in the stoichiometry of UC have been reported by several investigators. Russell (3) has studied the thermal conductivity at 70° C over the carbon range of from 4.55 to 5.50 percent by weight. As shown in Fig. 3 , a maximum thermal conductivity of 0.0645 cal./sec. cm. °C was observed at 4.9 percent carbon, which is in the hyperstoichiometric region. A decrease in thermal conductivity in the 500-1000° C temperature range also was reported by BMI as carbon was increased from 4.9 to 5.3 percent (2). In the temperature range 1000-2000° C, Wheeler also reported decreasing conductivity as the carbon content was increased above 4.8 percent (5). The decrease in high temperature thermal conductivity of UC as the carbon concentration is decreased in the hypostoichiometric range also has been observed by Carniglia (14). On the other hand, Crane and Gordon (1) generally observed minimum

thermal conductivities at near-stoichiometric compositions in the 500-1000°C range for cast UC.

The temperature dependence of the thermal conductivity of UC in the 500-1000° C temperature range is not well defined. However, most investigators have reported either a slight positive increase or no increase with temperature up to about 1400° C. Above this temperature, scattering is principally by the electronic process, and estimations based on the Wiedemann-Franz rule apply (10).

The effects of common anion impurities on the thermal and electrical properties are not well known. There is evidence to support the generalization that high levels (>0.2 percent by weight) of oxygen and nitrogen cause a significant reduction in the thermal conductivity of UC (10).

URANIUM-PLUTONIUM CARBIDES

The thermal conductivity of uranium-plutonium monocarbide solid solutions has not been investigated in detail. Some work has been reported by workers at Harwell (3), at Los Alamos (4), and the Mounds Laboratory (15). Intercomparison of these results is difficult, as the measurements were done on various types of carbide and entirely different experimental methods were used.

The thermal conductivity of PuC_{1-x} is about one-fourth that of UC at low temperature, as shown in Table I. Therefore, one can expect a decrease in conductivity with the addition of about 20 percent PuC that is required for fast neutron breeder reactor fuels. Moreover, a decrease in thermal conductivity is expected when uranium is replaced by plutonium in the carbide lattice, as the second atom in solid solution provides additional scattering centers. Examples of this can be found in the UO_2 - ThO_2 (17) and the UC-ZrC (18) solid solution systems.

Thermal conductivities at 70° C of $U_{0.85}Pu_{0.15}C$ and PuC_{1-x} have been reported by Russell (3) using an apparatus of the type described by Schröder (19). The conductivity of slightly hyperstoichiometric arc cast UC (5.06 w/o C) was decreased from 0.0645 to 0.0405 cal./sec. cm. °C for the slightly hyperstoichiometric (5.03 w/o C) solid solution carbide. The effect of carbon concentration was similar to that reported for UC, as shown in Fig. 3. Maximum conductivity was found at 4.95 percent by weight carbon. The decrease in conductivity in going to higher carbon concentrations is expected. The similar decrease in conductivity that resulted from free metal in the grain boundaries might be attributable to the lower thermal conductivity of plutonium metal. However, the same effect was noted for free uranium metal in hypostoichiometric UC even though the conductivity of uranium metal is about the

same as that for UC. Free actinide metal is intolerable in a fuel because of clad incompatibility, but it is important to know the effect of free fission product metal on the thermal conductivity of carbide fuels after significant burnup.

Workers at Los Alamos, using a cut bar method in the 200-400° C temperature range have reported on the thermal conductivities of arc cast single phase UC, (U, Pu)C solid solutions, and $PuC_{0.87}$. The electrical resistivity also was determined in the temperature range 25-800°C.

The results, shown in (Fig. 4 and 5) indicate that:

1. The thermal conductivity of UC is decreased rather markedly when uranium is replaced by plutonium in the stoichiometric solid solution lattice. This decrease amounts to 0.006 cal./sec. cm.° C per 10 percent PuC in the 0-30 percent PuC range.

2. Thermal conductivity increases with increasing temperature. Greater rates of increase are associated with larger plutonium concentrations in the concentration range 10-30 percent PuC.

3. The electrical conductivity is decreased markedly when uranium is replaced by plutonium, as has also been observed by Pascard (20).

4. If the thermal conductivity of $U_{0.80}Pu_{0.20}C$ is extrapolated to 70° C, good agreement is obtained with that reported by Russell for $U_{0.85}Pu_{0.15}C$.

Hayes and DeCrescente (21) have reported that the electronic scattering contribution of UC varies from 80 percent of the total thermal conductivity at 1000°C to about 100 percent at 1300° C; above this temperature conduction is determined by the electronic scattering process. The Los Alamos work indicates that the electronic contribution at 400° C is about 70 percent of the total conductivity for $U_{0.80}Pu_{0.20}C$, and about 50 percent for $PuC_{0.87}$.

The thermal diffusivity of pressed and sintered carbides in the temperature range 250-1000° C has been reported by Mounds Laboratory (15). These carbides were prepared by carbothermic reduction of the corresponding oxides, and had the general formula $MC_{0.95}$. The oxygen concentration was greater than 2000 ppm. The results shown in Fig. 6 indicate that:

1. Substitution of plutonium for uranium in UC decreases the diffusivity substantially, and hence, decreases the

conductivity. A decrease of from 24 to 45 percent of the diffusivity of UC was observed for 20 percent PuC solid solution carbide in the temperature range 600-900°C. For the 95 percent dense carbides sintered with 0.1 percent by weight nickel, this decrease was approximately 50 percent.

2. The diffusivity of 91 percent dense $U_{0.80}Pu_{0.20}C_{0.95}$ without nickel was 0.039 cm^2/sec. in the range 250-1000°C, while the diffusivity of 95 percent dense $U_{0.80}Pu_{0.20}C_{0.95}$ with nickel was 0.028 cm^2/sec. This corresponds to a decrease of 28 percent. If the 91 percent dense material is corrected to 95 percent density, the reduction amounts to 32 percent.

3. The diffusivity and conductivity of UC with nickel decreases rapidly from 250 to 600°C, then increases slowly. However, the solid solution carbide diffusivities were independent of temperature. Thermal conductivities of the solid solution carbides would therefore increase with increasing temperature.

CONCLUSIONS

1. The thermal conductivity data for UC generally fall within ± 20% in the temperature range 200-2000°C. Over this range the conductivity is approximately constant at 0.05 cal./sec. cm. °C.

2. Replacement of uranium by plutonium in UC causes a significant decrease in thermal conductivity and diffusivity in the temperature range 250-1000°C.

3. Maximum thermal conductivity is observed in the near-stoichiometric composition range for UC and $U_{0.85}Pu_{0.15}C$.

4. Nickel sintering aid, even in the 0.1 percent by weight concentration range, lowers the thermal conductivity and diffusivity of UC and $U_{0.80}Pu_{0.20}C_{0.95}$.

5. Apparently excessive amounts of oxygen and nitrogen lower the thermal conductivity of carbides.

6. There does not appear to be a satisfactory quantitative method for adjusting for effects of porosity on thermal conductivity of carbides.

7. As fission products are generated in carbide fuels, it is unlikely that they will improve thermal conductivity. It seems more probable that the thermal

conductivity will be reduced.

8. More experimental work must be done on the thermal conductivity of fully characterized carbides. Future work on thermal conductivity should be related to measurement of the electrical resistivity on the same materials.

REFERENCES

1. J. Crane and E. Gordon, "The Development of Uranium Carbide as a Nuclear Fuel," Report UNC-5080 (1964).

2. R. W. Dayton and C. R. Tipton, Jr., "Progress Relating to Civilian Applications During August, 1959," Report BMI-1377.

3. L. E. Russell, "New Nuclear Materials Including Non-Metallic Fuels," Proceedings of the Conference on New Nuclear Materials Technology, Including Non-Metallic Fuel Elements, Prague, July 1-5, 1963, p. 423.

4. J. A. Leary, R. L. Thomas, A. E. Ogard and G. C. Wonn: Thermal conductivity and Electrical Resistivity of UC, (U, Pu)C and PuC, "Symposium on Carbides in Nuclear Energy," Vol. 1, L. E. Russell, et. al, Ed., Macmillan Co., London (1964) p. 365.

5. M. J. Wheeler: Thermal Conductivity of Uranium Monocarbide, ibid., p. 358.

6. G. Mustacchi and S. Guiliani, "Development of Methods for the Determination of the High Temperature Thermal Diffusivity of UC," Report EUR-337e (1963).

7. P. Mahmoodi, "An Improved Comparative Type Thermal Conductivity Apparatus," Proc. 3rd Conference on Thermal Conductivity, ORNL, Vol. 1, p. 194 (1963).

8. W. Chubb and E. A. Rough, "An Evaluation of Data on Nuclear Carbides," Report BMI-1441 (1960).

9. J. M. Leitnaker and T. G. Godfrey, "Thermodynamic Properties of Uranium Carbides," J. Nucl. Mater., 21 175 (1967).

10. B. A. Hayes and M. A. DeCrescente, "Thermal Conductivity and Electrical Resistivity of Uranium Monocarbide," Report PWAC-480 (1965).

11. R. W. Powell, C.Y. Ho and P. E. Liley, "Thermal Conductivity of Selected Materials," Report NSRDS-NBS-8, Washington, D. C. (1966).

12. A. L. Loeb, "Thermal Conductivity: VIII, A Theory of Thermal Conductivity of Porous Materials," J. Am. Chem. Soc., 37 (No. 2 Part II), 96 (1954).

13. H. S. Carslaw and J. C. Jaeger, "Conduction of Heat in Solids," 2nd Ed., Oxford University Press, London (1959) p. 425.

14. S. C. Carniglia: Single Crystal and Dense Polycrystal Uranium Carbide: Thermal, Mechanical, and Chemical Properties," Symposium on Carbides in Nuclear Energy," Vol. 1, L. E. Russell, et. al, Ed., Macmillan Co., London (1964) p. 403.

15. L. J. Wittenberg and G. R. Grove, "Reactor Fuels and Development Plutonium Research: 1964 Annual Report," Report MLM-1244.

16. A. V. Crewe and S. Lawroski, "Reactor Development Program Progress Report, February, 1967," Report ANL-7308, p. 57.

17. W. D. Kingery, "Introduction to Ceramics," John Wiley and Sons, Inc., New York (1960).

18. L. N. Grossman, "Electrical Conductivity, Thermal Conductivity, and Thermal Expansion for Fuel-Bearing Carbides: UC_2, UC, $U_{0.5}Zr_{0.5}C$, and ThC_2, L. E. Russell, et. al, Ed., Report GEST-2015 (1963).

19. J. Schröder, "A Simple Method for Determining the Thermal Conductivity of Solids," Phillips Technical Review, 21 (No. 11) 307 (1959/60).

20. R. Pascard, "Preliminary Studies of the Plutonium Carbide System and the Solid Solutions of the Carbides of Plutonium and Uranium," Report CEA-235 (1961).

21. B. A. Hayes and M. A. DeCrescente, "Thermal Conductivity and Electrical Resistivity of Uranium Mononitride," Report PWAC-381 (1965).

22. A. C. Secrest, E. L. Foster and R. F. Dickerson, "Preparation and Properties of Uranium Monocarbide Castings, "Report BMI-1309 (1959).

Table I

Thermal Conductivity of PuC_{1-x} at Low Temperature

Fabrication Method	Density % Theo.	Temperature, °C	k Cal./sec. cm.°C	Ref
Arc cast	100	200	0.0232	4
Pressed and sintered	93	200	0.015	16
	(100)*	200	(0.016)	16
	93	70	0.011	16
	(100)	(70)	(0.012)	
Pressed and sintered	89	70	0.013	3
	(100)	(70)	(0.015)	
Arc cast	100	(70)	(0.018)	4

Note (*) Numbers in parentheses are extrapolated

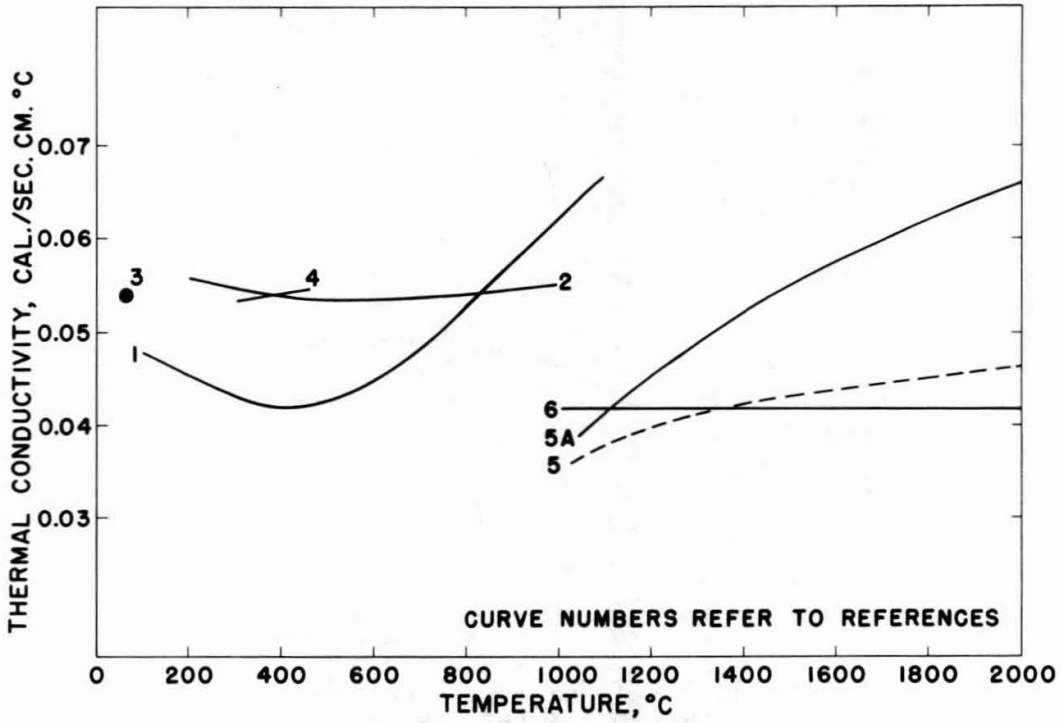

FIG. 1. THERMAL CONDUCTIVITY OF 100% DENSE STOICHIOMETRIC $UC_{1.00\pm0.01}$

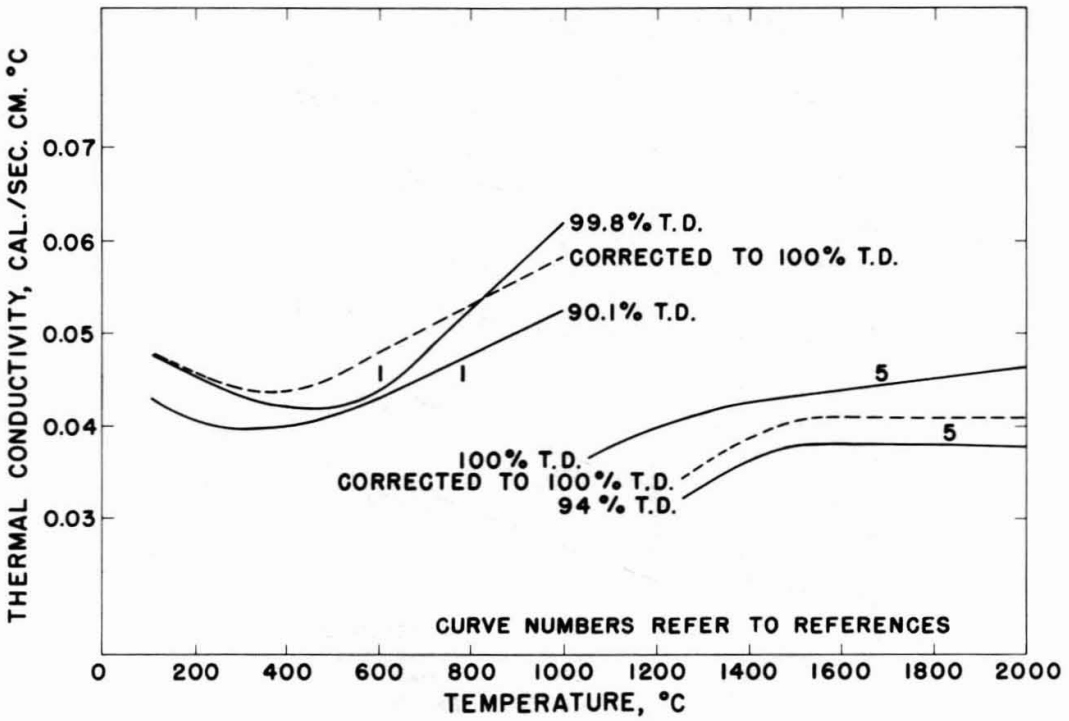

FIG. 2. POROSITY EFFECT ON THERMAL CONDUCTIVITY OF STOICHIOMETRIC UC

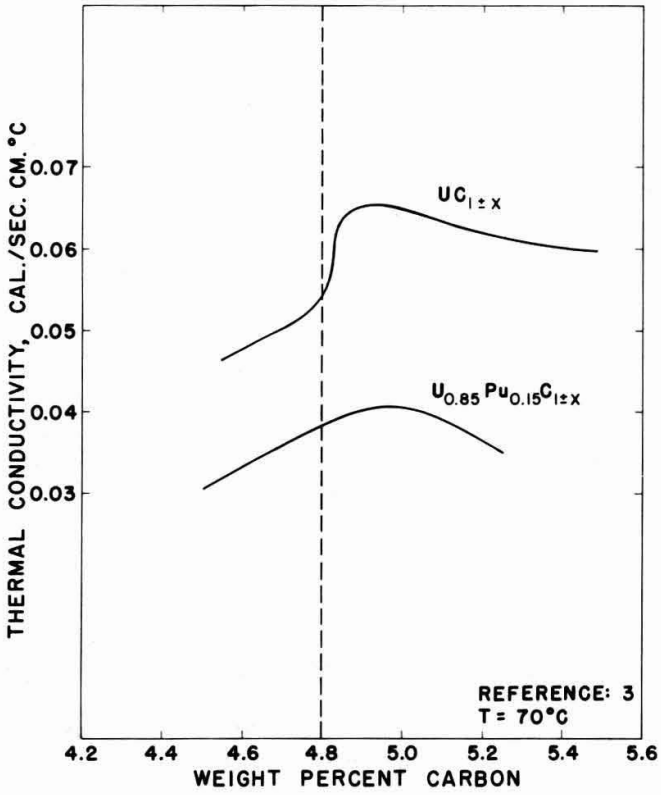

FIG. 3. STOICHIOMETRIC EFFECT ON THERMAL CONDUCTIVITY OF ARC CAST UC

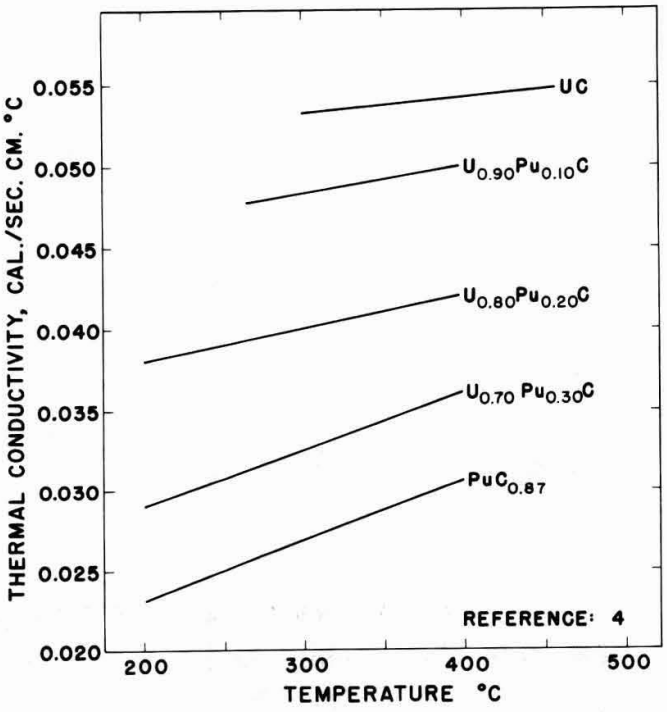

FIG. 4. VARIATION OF THERMAL CONDUCTIVITY OF (UPu)C ALLOYS WITH TEMPERATURE

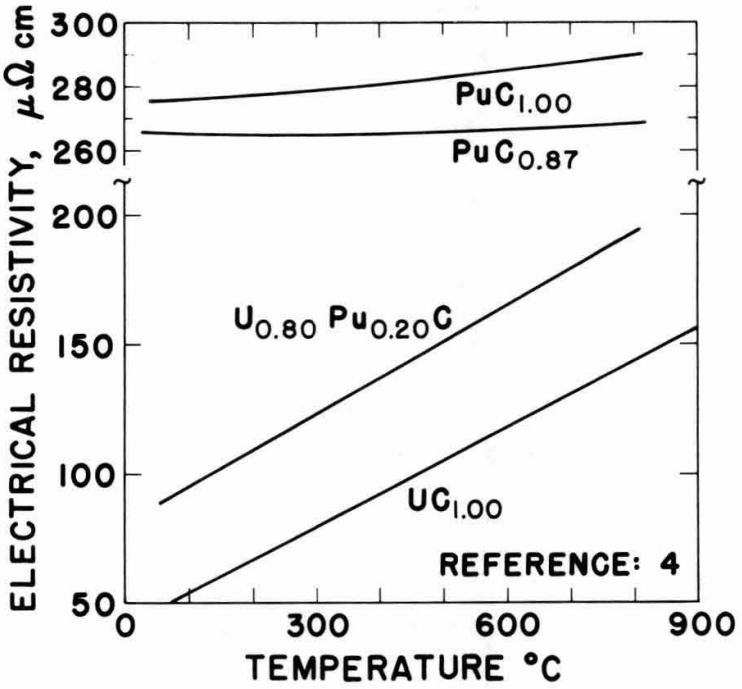

FIG. 5. VARIATION OF ELECTRICAL RESISTIVITY WITH TEMPERATURE ON UC, $U_{0.80}Pu_{0.20}C$, $Pu_{0.87}$ AND $PuC_{1.00}$

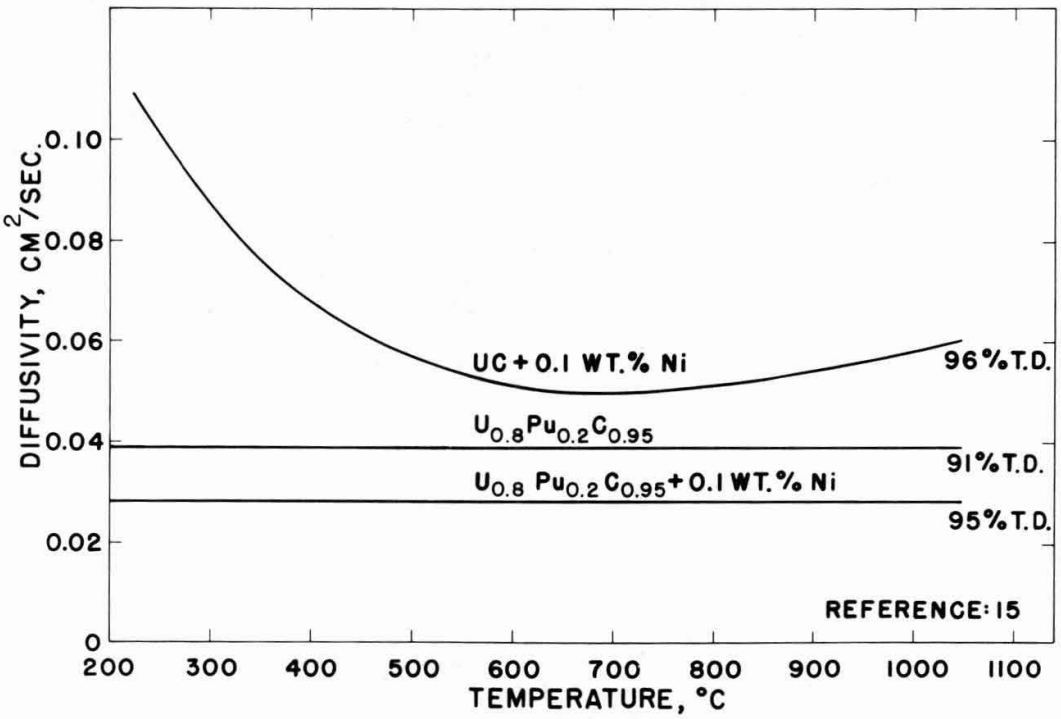

FIG. 6. THERMAL DIFFUSIVITY OF UC AND TWO (U,Pu)C COMPOSITIONS

COMPATIBILITY OF (U,Pu) CARBIDES WITH POTENTIAL JACKETING MATERIALS

T. W. Latimer and W. R. Jacoby*

ABSTRACT

Observations were made of the extent and type of reaction of several iron-, nickel-, and vanadium-base alloys in contact with uranium-plutonium carbide compositions in the temperature range 700-1100°C. Reaction zones were analyzed by means of metallography and an electron microprobe. Bands in which fine precipitates were found to a depth of approximately 25 microns were observed in some iron-base alloys after contact with (U,Pu)C for 1000 hours at 800°C. Reaction of (U,Pu)C with nickel-base alloys was characterized by the formation of $(U,Pu)Ni_5$ in the fuel, and the formation of a layer, having a relatively high chromium and carbon content, in the jacketing alloy.

Addition of iron was shown to eliminate free uranium and plutonium from hypostoichiometric (U,Pu)C. $(U,Pu)Fe_2$ was found to have excellent compatibility with stainless steel at 800°C.

*Assistant ceramist, Argonne National Laboratory, Argonne, Illinois, and Manager, Ceramic Materials Development, Westinghouse Advanced Reactor Division, Cheswick, Pennsylvania, respectively.

Introduction

The selection of jacketing materials for uranium-plutonium carbide nuclear fuels must be based on many criteria. One critical property of the materials must be their ability to be essentially unaffected by prolonged contact with the carbide fuel. The formation of new phases at the fuel-jacketing interface or other changes in the alloy chemistry of the jacketing material can significantly affect the load-bearing capacity of the jacketing. An analysis of these changes occurring at the fuel-jacketing interface can be used as a guide in the development of potential jacketing materials, as well as in the selection of available materials prior to irradiation testing.

From a fuels standpoint, stoichiometric (U,Pu)C appears to be a very promising fuel material, but large-scale production of single-phase material has not yet been developed. Very close control of the carbon content is necessary to produce material containing only the monocarbide phase. Furthermore, maintaining a single-phase structure is complicated by: (1) contamination of finely-divided (U,Pu)C powder by oxygen and nitrogen during fabrication procedures, and (2) the relative ease by which oxygen and nitrogen can substitute for carbon in the monocarbide lattice. Since single-phase monocarbide is produced only when the nonmetal atom (C + O + N) content totals 50 at.%, material containing free metal (hypostoichiometric monocarbide) or higher carbides (hyperstoichiometric monocarbide) is frequently the end product. Therefore, in order to investigate the potential usefulness of these materials, the compatibility of $(U,Pu)_2C_3$ was included, as well as the possibility of eliminating the free metal phase by combination with additives during fabrication. This paper summarizes compatibility work involving (U,Pu) carbides done at Argonne National Laboratory.

Materials

Jacketing Materials

All iron- and nickel-base alloys were purchased from vendors. Nominal compositions of these alloys are given in Table 1. The vanadium alloys were prepared by the ANL Fabrication Technology Group.

Preparation of (U,Pu) Carbide Specimens

Three carbide compositions, each having an overall uranium-to-plutonium ratio of 4 to 1, were tested: 4.83 wt.% equivalent carbon (single-phase (U,Pu)C), 5.25 wt.% equivalent carbon (approximately 20% $(U,Pu)_2C_3$), and 6.75 wt.% equivalent carbon (approximately 90% $(U,Pu)_2C_3$). It should be noted that, although both compositions containing the sesquicarbide phase had the same uranium-to-plutonium ratio, the plutonium content of this phase in the two compositions was not equal. The plutonium content of the sesquicarbide phase in the 5.25 wt.% C composition was found to be over 1-1/2 times that of the monocarbide matrix.

Arc-melted buttons of the desired composition were crushed to -44 micron powder in glove boxes that contained an inert atmosphere of nitrogen with impurities of oxygen and water vapor of about 0.005 and 0.01 wt.%, respectively. The powder was coated with 0.5 wt.% Carbowax binder and pressed into pellets at a pressure of about 4200 kg/cm^2 (60,000 psi). The as-pressed pellets were 6.94 mm in diameter by approximately 5.1 mm long. The pellets were sintered in a tantalum-element resistance furnace under a flowing argon atmosphere (approximately one liter/minute) and were held at the sintering temperatures for three hours. The sintering temperatures and densities of each of the three compositions are listed in Table 2.

Experimental Procedure

Preparation of Compatibility Specimens

Each compatibility assembly consisted of a pellet of the carbide fuel between two disks of jacketing material held in contact by means of a molybdenum frame. In addition, a third metal disk was added to the assembly to make the total length of pellets in the assembly 1.7 cm.

Approximately 0.5 mm was ground off each end of the carbide pellets to minimize the chance of surface impurity phases. The fuel-jacketing contact surfaces were then polished flat by use of 4/0 emery paper on a glass plate and a special specimen holder. Immediately after polishing, the specimens were assembled and pressure applied by a screw in one end of the molybdenum holder. The assembly was then placed in a capsule, evacuated, backfilled with 1/3 atmosphere of helium, and sealed. Quartz capsules were used for the majority of the tests although stainless steel capsules were used for the 4000 hour tests.

Evaluation of Compatibility Specimens

The couples were mounted in a polyester resin after removal from their capsules. Longitudinal sections were then prepared by grinding through series 120- to 600-grit grinding paper. Polishing was done with 6-micron diamond paste on AB Texmet paper, and 1-micron diamond paste on AB microcloth. HYPREZ lubricant was used throughout the grinding and polishing procedure.

The iron- and nickel-base alloys were etched electrolytically using either: (1) 10 wt.% oxalic acid in water, or (2) 32 vol.% H_3PO_4 (concentrated, commercial), 59 vol.% diethoxyethanol, and 9 vol.% water. The vanadium-base alloys were chemically etched with a solution of 5 wt.% $AgNO_3$ plus 2 vol.% HF in water.

Results and Discussion

Compatibility of Stoichiometric and Hyperstoichiometric (U,Pu)C with Various Jacketing Materials

Type 304 Stainless Steel. In 1000 hour tests at 800°C a band brought out by etching was observed in the specimen that was in contact with the hyperstoichiometric carbide (see Figure 1). A similar, but

smaller, band was also observed after 1000 hours at 700°C. The size of these bands are given in Table 3. However, compatibility couples containing both the stoichiometric and hyperstoichiometric compositions and heat-treated at 800°C for 4000 hours indicated no correlation between this band and the presence of $(U,Pu)_2C_3$. The band was present in both samples to a depth of 15 to 30 microns, comparable to the depth after 1000 hours. The boundary between the band and the unaffected steel was less distinct in the case of the 4000-hour specimens. An electron microprobe analysis of this band revealed a decrease in chromium content of about 3 wt.% and an increase in iron content of about 3 wt.% compared to the unaffected steel; the nickel content was unchanged. In addition, a number of small carbide precipitates consisting primarily of chromium (estimated to be at least 60 wt.%) and iron were found in the band (see Figure 1). There was no evidence of uranium or plutonium in the band.

At 1100°C, melting of the Type 304 stainless steel occurred between 400 and 1000 hours when in contact with (U,Pu)C. Particles of relatively high uranium and plutonium contents were found by microprobe analysis to a depth of 125 microns in a specimen heat-treated for 168 hours at this temperature.

16-25-6 and 16-15-6 Alloys. The compatibilities of the 16-25-6 and 16-15-6 alloys appear to be quite similar. A typical photomicrograph of the effect on these alloys after heat-treatment at 800°C in contact with (U,Pu) carbides is shown in Figure 2. Although the affected zone was somewhat larger in the case of the hyperstoichiometric composition (containing approximately 20% $(U,Pu)_2C_3$) than for the stoichiometric one (see Table 3), no increase was found in the case of the composition containing approximately 90% $(U,Pu)_2C_3$. It is not known whether this result is related to the difference in plutonium content of the $(U,Pu)_2C_3$ or to some other variable in the fuel compositions.

The affected zones of these alloys, when etched, appear to contain a large number of very small precipitates. An electron microprobe study of a specimen containing 16-25-6 and heat-treated for 1000 hours at 800°C indicated that among the major elements in the alloy, the distribution of molybdenum had been most significantly affected. The matrix of the unaffected material was found to contain about 3.5 wt.% molybdenum while the grain boundaries and spots within grains, although small in size, registered peaks indicating 14-19 wt.% molybdenum. The very fine particles in the affected zone, believed to be molybdenum-rich, were too small for even semi-quantitative results. A transverse across the affected zone with a beam size of 1-2 microns showed relatively small differences in molybdenum content from 5-7 wt.%.

Haynes 56. No compatibility effects have been observed after testing this alloy at 800°C with the 4.83 and 5.25 wt.% C compositions for 1000 and 4000 hours. Likewise, no effect was observed in tests of this material with the 6.75 wt.% C composition after 1000 hours at 800°C or with the 4.83 and 5.25 wt.% C compositions after 1000 hours at 900°C. This material is significantly stronger than Types 304 or 316 stainless steels but is not presently commercially available.

Inconel 625. The formation of three separate zones was observed after 1000-hour tests with this alloy in contact with the 4.83 and 5.25 wt.% C compositions (see Figure 3). The size of these zones after 1000-hour heat treatments at 700 and 800°C are compared in Table 4. One of these zones was in the direction of the fuel and has been identified as $(U,Pu)Ni_5$. This compound could be expected in high-nickel alloys since UNi_5 has been shown to be the principal product formed in a diffusion couple of UC versus Ni heat-treated at 800°C for 950 hours.(1) Using arc-cast hyperstoichiometric (U,Pu)C, French and Hodkin (2) noted localized reaction at 650°C and a continuous reaction zone at 800°C with Nimonic 80A (70 wt.% Ni). A continuous network of $(U,Pu)Ni_5$ surrounding (U,Pu)C grains was formed in the hyperstoichiometric (U,Pu)C in contrast to the solid $(U,Pu)Ni_5$ band formed in the single-phase (U,Pu)C. Evidence that the (U,Pu)C grains within the $(U,Pu)Ni_5$ network were formed by reduction of the $(U,Pu)_2C_3$ grains in the initial material will be given later in this section.

The dark, mottled, zone on the jacketing side of the interface appeared to be composed of two bands of rather complex composition containing high percentages of chromium. The composition of these bands was not well established but approximate values are given in Table 5. Percentages of carbon (5.25 wt.% in the fuel) and niobium and tantalum (4 wt.% in the jacketing) were not determined. Although no uranium was found on the jacketing side of the interface, an average of 5 wt.% plutonium was observed in this area. Beyond the two main reaction zones, chromium-rich precipitates were observed. In the area containing these precipitates, three observations were made: (1) a 12-micron band immediately adjacent to the mottled zone was richer in iron than any other portion of the jacketing material, (2) nickel and iron contents continuously decreased throughout this area from the iron-enriched band to the unaffected jacketing matrix, while the chromium and molybdenum contents continuously increased, and (3) the precipitates, which were numerous and very small in size close to the original interface, became less frequent but larger in size as the distance from the interface increased.

Although the reaction with the hyperstoichiometric carbide composition containing 20% $(U,Pu)_2C_3$ was somewhat greater than that with the single-phase (U,Pu)C, a couple containing the 6.75 wt.% C composition indicated that the sesquicarbide phase is actually more compatible at 800°C than the monocarbide phase. Only the precipitates were observed on the jacketing side of the interface, while the dark, mottled, band was absent, and less $(U,Pu)Ni_5$ was formed. However, two other bands were observed on the fuel side of the interface. Beyond the $(U,Pu)Ni_5$ band, there was a 4-micron gray layer and beyond this, a 9-micron zone which appeared to be monocarbide resulting from reduction of the sesquicarbide phase. The gray layer was probably a uranium-plutonium oxide. The cladding itself was undoubtedly the source of the oxygen since no other surface of the fuel pellet exhibited any oxide formation. The formation of a visible oxide layer as part of the overall interaction in the case of the sesquicarbide phase can be related to the insolubility of oxygen in U_2C_3.(3)

Hastelloy X. The same general type of reaction, but to a lesser extent, occurred with Hastelloy X at 700 and 800°C as occurred with Inconel 625. However, Hastelloy X was found to be less compatible with $(U,Pu)_2C_3$ than (U,Pu)C (see Table 4).

No reaction was observed between Hastelloy X and (U,Pu)C after heat-treatment at 700°C for times up to 4000 hours. Intermittant reaction along the interface was observed in the case of the hyperstoichiometric (5.25 wt.% C) composition at this temperature, but no increase in the size of the reaction zone after 1000 hours. A test with the 6.75 wt.% C composition at 700°C for 1000 hours revealed a 4-micron reaction zone (equivalent to that found with the 5.25 wt.% C composition) and also an adjacent 8-micron zone in the fuel that had been reduced from $(U,Pu)_2C_3$ to (U,Pu)C. This observation explained the absence of sesquicarbide grains at the jacketing interface in the test with the 5.25 wt.% C composition, since these grains were all less than 10 microns in diameter.

At 800°C, both (U,Pu)C and $(U,Pu)_2C_3$ reacted with Hastelloy X to form $(U,Pu)Ni_5$ and a chromium-rich zone in the jacketing. Figure 4 illustrates, in the case of the 5.25 wt.% C composition, the comparatively greater extent of reaction at those points in contact with $(U,Pu)_2C_3$. Reaction with the 6.75 wt.% C composition, revealed, as with Inconel 625, a gray layer of about 5 microns, and a 25-micron layer of (U,Pu)C resulting from the reduction of $(U,Pu)_2C_3$. In addition, extensive precipitation was observed in the Hastelloy X after heat-treatment at 800°C with this composition (see Figure 5).

After 1000 hours at 950°C, (U,Pu)C had reacted with Hastelloy X to form a zone of $(U,Pu)Ni_5$ averaging 64 microns in depth.

Vanadium Alloys. Vanadium-base alloys appear promising as jacketing materials for (U,Pu) carbide fuels because of their superior creep strength at 650°C compared to stainless steels and their satisfactory compatibility with liquid sodium. These alloys were developed originally because of their good compatibility with uranium-plutonium-bearing metallic fuels.

Compatibility tests with two vanadium alloys, V-20 wt.% Ti and V-15 wt.% Ti - 7.5 wt.% Cr, have indicated incompatibility with (U,Pu) carbides in the 700-800°C range. In addition to the main reaction zone, there appeared to be some grain-boundary penetration into the jacketing materials. The extent of these reactions are shown in Table 6; a characteristic photomicrograph of this effect is shown in Figure 6. In contrast, there was no evidence of reaction with a more-recently developed alloy, V-15 wt.% Cr - 5 wt.% Ti, with either the stoichiometric or hyperstoichiometric carbide compositions when tested at 800°C for 1000 hours.

Compatibility of Modified Hypostoichiometric (U,Pu)C with Type 304 SS

Hypostoichiometric (U,Pu)C fuel compositions contain free uranium and plutonium which will react with iron- and nickel-base jacketing materials at relatively low temperatures. The use of iron to react with

the free metal phase to form (U,Pu)Fe_2 or of chromium carbide ($Cr_{23}C_6$) to form Cr and (U,Pu)C has been proposed.(4,5) These additions react to form more refractory and less reactive secondary phase products and can be justified provided neutron economy and irradiation stability are not unduly sacrified. The results obtained by Jordan, et al,(5) of compatibility tests with Fe- and $Cr_{23}C_6$-stabilized UC versus Type 316 stainless steel showed essentially no reactions. Concurrently, their results with similar tests of unstabilized hypostoichiometric UC showed localized reactions up to 175 microns in depth.

Hypostoichiometric (U,Pu)C pellets were made as described previously; the Fe or $Cr_{23}C_6$ powders were added just prior to the binder addition. Sintering temperatures and sintered densities are given in Table 7. Typical microstructures of the pellets containing the Fe and $Cr_{23}C_6$ additions are shown in Figures 7 and 8, respectively.

Microprobe studies of the Fe-modified pellets indicated the composition of the minor phase areas to be 20-42 wt.% U, 8-22 wt.% Pu, and 32-70 wt.% Fe. This compositional range lies between (U,Pu)Fe_2 and Fe. Microprobe studies of the $Cr_{23}C_6$ modified pellets showed no free uranium or plutonium, nor the existence of free Cr. The only minor phases found were identified qualitatively as chromium carbides.

Compatibility capsules containing both unmodified and Fe-modified pellets in contact with Type 304 stainless steel were tested for 1000 hours at 650 and 800°C. No observable reactions were found in any of the specimens. The discrepancy between these findings and those of Jordan, et al, in the case of the unmodified pellets can be explained by the differences in microstructure in the fuel specimens. The microstructures of Jordon, et al, show areas of considerable concentration of free metal which correlates with their findings of one or two spots at which the stainless steel was attacked. The finely-dispersed metal phase found in the authors' specimens would not be expected to lead to such a result.

The compatibility of (U,Pu)Fe_2 with Type 304 stainless steel was also determined. Essentially single-phase $(U_{0.8}Pu_{0.2})Fe_2$ (containing 0.4 wt.% excess Fe over that required for stoichiometry) pellets were produced by powder metallurgy techniques. A test of this material with Type 304 stainless steel at 800°C for 1000 hours produced a 2-micron layer at the interface.

In addition to the contact compatibility tests, the unmodified and the Fe- and $Cr_{23}C_6$-modified compositions were tested with Type 304 stainless steel in liquid sodium at 800°C. The container for the test was an Inconel capsule into which a stainless steel sleeve (closed at one end), containing the fuel pellets, was placed. The capsule was evacuated, loaded with liquid Reagent-grade sodium, back-filled with helium, and sealed. After a 60-day test period, there was no metallographic evidence of carburization of the stainless steel sleeves for any of the three fuel compositions.

Acknowledgment

The authors wish to thank Messrs D. C. O'Rourke and J. A. Lahti for their help in preparing the compatibility specimens and J. E. Sanecki for the microprobe data. This work was performed under the auspices of the U. S. Atomic Energy Commission.

References

1. F. Anselin et al, Etude du Diagramme Ternaire Uranium-Carbon-Nickel, CEA-R 2845 (August 1965).

2. P. M. French and D. J. Hodkin, Mechanical Properties and Compatibility of Uranium-Plutonium Carbides, Plutonium 1965, Chapman and Hill, London (1967) p. 718.

3. E. K. Storms, A Critical Review of Refractories, LA-2942 (March 1964), p. 185.

4. Westinghouse Atomic Power Division Staff, Liquid Metal Fast Breeder Reactor Design Study, WCAP-3251-1 (January 1964).

5. K. R. Jordon et al, Compatibility of Modified Carbide Fuels with Stainless Steel, Proceedings of the Conference on Safety, Fuels, and Core Design in Large Fast Power Reactors, ANL-7120 (October 1965), pp. 301-313.

TABLE 1

COMPOSITION AND CREEP-RUPTURE DATA OF POTENTIAL JACKETING ALLOYS

Alloy	Creep-Rupture Stress*, psi x 10^{-3} for Failure in 10^4 hrs at 700°C	Composition (wt.%)						
		Fe	Ni	Cr	Mo	Mn	Co	Other
304 SS	9	67	10	19	--	2	--	2
16-15-6	15	55	15	16	6	7.5	--	0.5
16-25-6	14	50	25	16	6	1.3	--	1.7
Haynes 56	22	45	13	21	4.5	1.5	11.5	3.5
Hastelloy X	15	18	48	22	9	1	1.5	0.5
Inconel 625	30	3	61	22	9	0.15	--	4.8

*Extrapolated and estimated where adequate data do not exist.

TABLE 2

COMPOSITIONS AND SINTERED DENSITIES OF (U,Pu) CARBIDE PELLETS USED FOR COMPATIBILITY TESTS

Equivalent Carbon (wt.%)	C (wt.%)	O_2 (ppm)	N_2 (ppm)	Sintering Temp. (°C)	Density (g/ml)	Percent Theoretical Density
4.83	4.74	900	300	1900	11.67	86
5.25	5.10	800	1000	1850	11.28	84
6.75	6.73	80	100	1800	11.90	92

TABLE 3

EXTENT OF ZONES OBSERVED METALLOGRAPHICALLY IN IRON-BASE ALLOYS AFTER CONTACT WITH (U,Pu) CARBIDES FOR 1000 HOURS

Alloy	Temp. (°C)	Stoichiometric (U,Pu)C (4.83 wt.% Equivalent C)		Hyperstoichiometric (U,Pu)C (5.25 wt.% Equivalent C)	
		Average (μ)	Maximum (μ)	Average (μ)	Maximum (μ)
304 SS	700	Nil	--	4	6
	800	Nil	--	24	29
16-25-6	800	26	30	32	36
16-15-6	800	28	34	35	38
Haynes 56	800	Nil	--	Nil	--
	900	Nil	--	Nil	--

TABLE 4

EXTENT OF ZONES OBSERVED METALLOGRAPHICALLY IN NICKEL-BASE ALLOYS AFTER CONTACT WITH (U,Pu) CARBIDES FOR 1000 HOURS

Alloy	Temp. (°C)	Carbide Composition (wt.% Equivalent Carbon)	$(U,Pu)Ni_5$ Zone (μ, into Fuel)		Cr-Rich Zone (μ, into Jacketing)		Precipitates (μ, from Interface)	
			Average	Maximum	Average	Maximum	Average	Maximum
Inconel 625	700	4.83	18	30	20	25	45	55
		5.25	18	30	20	25	45	55
		6.75	Nil	--	Nil	--	20	30
Inconel 625	800	**4.83**	25	**37**	23	30	130	160
		5.25	36	**44**	26	36	145	180
		6.75	7	10	Nil	--	65	80
Hastelloy X	700	4.83	Nil	--	Nil	--	Nil	--
		5.25	--	4	--	2	Nil	--
		6.72	2	4	2	2	Nil	--
Hastelloy X	800	4.83	5	8	3	5	Nil	--
		5.25	--	8	--	7	Nil	--
		6.75	8	10	6	12	125	175

TABLE 5

COMPOSITION OF REACTION ZONES HYPERSTOICHIOMETRIC* (U,Pu)C vs INCONEL 625-800°C FOR 1000 HOURS

Element	(U,Pu)C (wt.%)	Zones Identified Metallographically						Unaffected Inconel 625 (wt.%)
		$(U,Pu)Ni_5$ Zone in Direction of Fuel (36 μ)	Mottled Reaction Zone in Direction of Cladding (26 μ)		Inconel 625 Containing Precipitates (120 μ)			
		Average Size of Zones Identified with Microprobe						
		36 μ	8 μ	18 μ	12 μ	Precipitates	108 μ	
U	76	34	-	-	-	-	-	-
Pu	19	12	1	5	-	-	-	-
Ni	-	54	10	21	61	24	70 → 61	61
Cr	-	-	52	43	20	61	15 → 22	22
Mo	-	-	13	16	7	14	7 → 9	9
Fe	-	-	1	0.5	8	1	4 → 3	3

*5.25 wt.% Equivalent Carbon

TABLE 6

EXTENT OF ZONES OBSERVED METALLOGRAPHICALLY IN VANADIUM-BASE ALLOYS AFTER CONTACT WITH (U,Pu) CARBIDES FOR 1000 HOURS

Carbon Equivalent of (U,Pu) Carbide	Alloy (wt.%)	Temp. (°C)	Reaction Zone (Ave., μ)	Grain Boundary Penetration (Average Distance from Interface, μ)
4.83	V-20Ti	700	10	50
5.25	V-20Ti	700	18	65
4.83	V-15Ti-7.5Cr	800	65	95
5.25	V-15Ti-7.5Cr	800	65	95
4.83	V-5Ti-15Cr	800	Nil	Nil
5.25	V-5Ti-15Cr	800	Nil	Nil

TABLE 7

COMPOSITIONS AND SINTERED DENSITIES OF MODIFIED HYPOSTOICHIOMETRIC (U,Pu)C PELLETS

Modifier (wt.%)	Carbon (wt.%)	Oxygen (ppm)	N_2 (ppm)	Sintering Temp. °C	Density (g/cm^3)
None	4.36	1100	540	1600	11.47
3.89 Fe	4.36	1100	540	1500	11.29
7.32 $Cr_{23}C_6$	4.40	300	580	1500	10.13

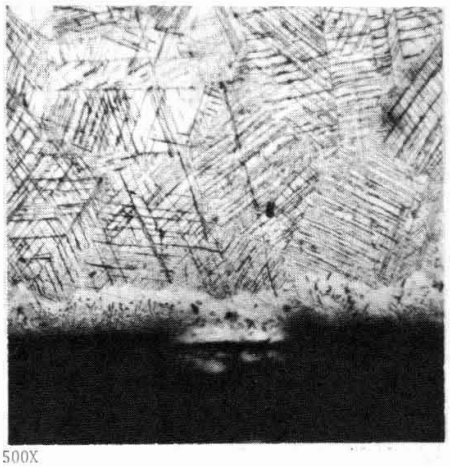

500X

Figure 1. Type 304 Stainless Steel vs. Hyperstoichiometric (U,Pu)C, 800°C for 1000 Hours.

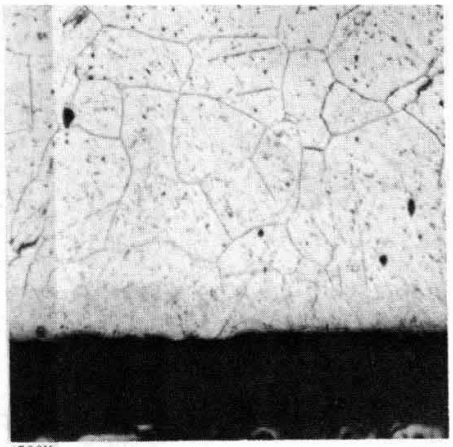

500X

Figure 2. 16-25-6 vs. (U,Pu)C, 800°C for 1000 Hours.

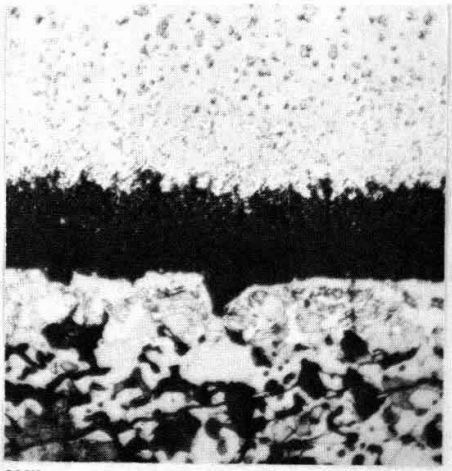

500X

Figure 3. Inconel 625 vs. Hyperstoichiometric (U,Pu)C, 800°C for 1000 Hours.

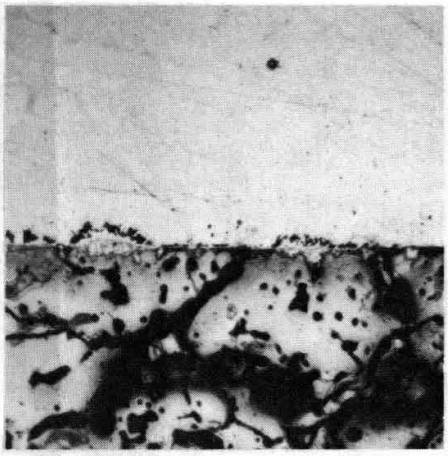

500X

Figure 4. Hastelloy X vs. Hyperstoichiometric (U,Pu)C, 800°C for 1000 Hours.

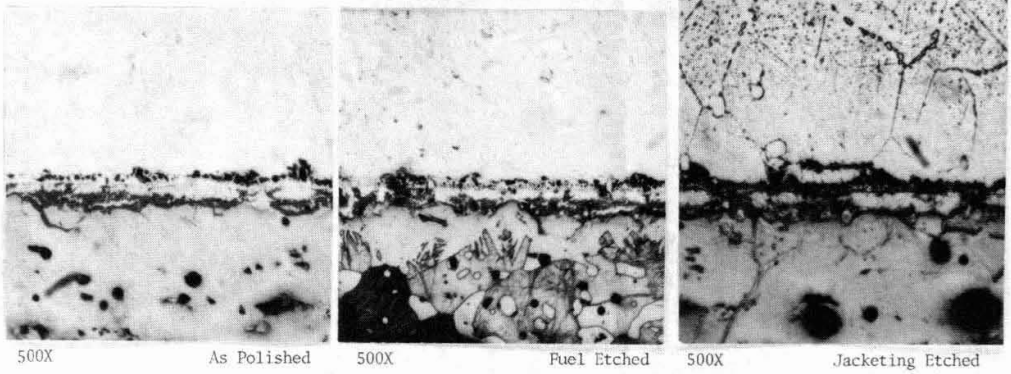

500X As Polished 500X Fuel Etched 500X Jacketing Etched

Figure 5. Hastelloy X vs. Hypostoichiometric $(U,Pu)_2C_3$, 800°C for 1000 Hours.

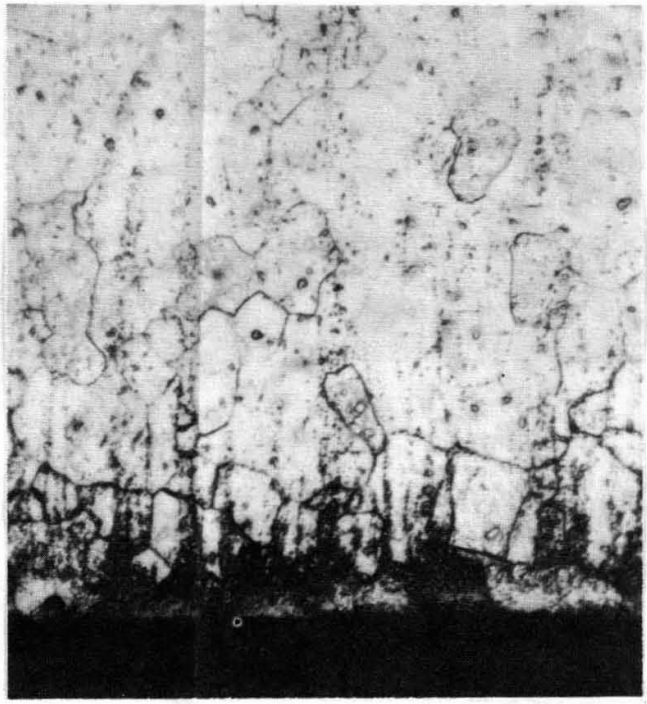

500X

Figure 6. Vanadium -20wt.% Titanium vs. Hyperstoichiometric (U,Pu)C, 700°C for 1000 Hours.

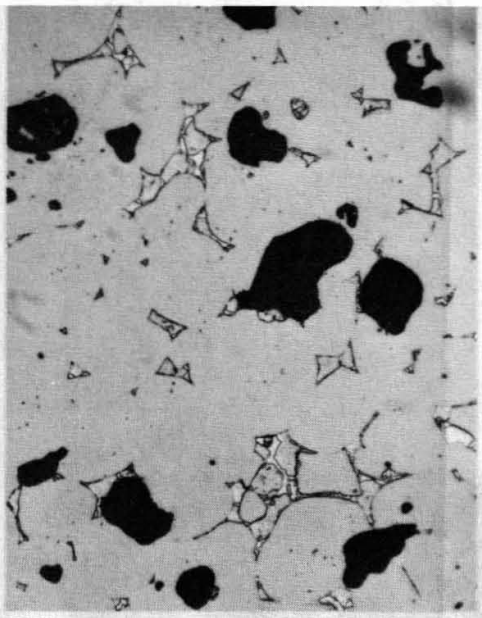

500X

Figure 7. Fe-Modified Hypostoichiometric (U,Pu)C.

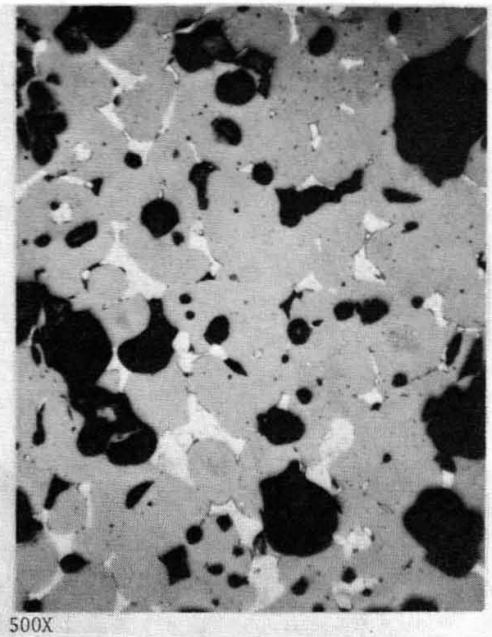

500X

Figure 8. $Cr_{23}C_6$-Modified Hypostoichiometric (U,Pu)C.

COMPATIBILITY BETWEEN METALLIC U-Pu-BASE FUELS AND POTENTIAL CLADDING MATERIALS

S. T. Zegler and C. M. Walter

Abstract

The compatibility of U-Pu-base fuel alloys with a variety of jacket materials has been investigated in connection with a program aimed at developing improved metallic fuels.

The most recent work has resulted in the development of U-Pu-Zr alloys that have much improved compatibility with 304 stainless steel and other iron-base cladding materials. Specifically, U-15%Pu-10%Zr and U-18%Pu-14.1%Zr have good compatibility with 304 stainless steel at temperatures up to 800°C.

S. T. Zegler is an associate metallurgist and C. M. Walter is an assistant metallurgical engineer with the Metallurgy Division, Argonne National Laboratory, Argonne, Illinois. Work performed under the auspices of the U. S. Atomic Energy Commission.

Introduction

The extent to which fuel and cladding materials interact in a nuclear reactor is a primary consideration in their selection. Clearly, combinations that interact to affect either melting of the fuel or marked degradation of the mechanical properties of the cladding material should be avoided. In a previous paper (1) we discussed the out-of-reactor compatibility of a variety of Fe-, Ni-, and V-base alloys with certain U-Pu-Fz* alloys. The present paper describes a similar compatibility survey of U-Pu-Zr and U-Pu-Ti alloys with a number of cladding alloys including some of those investigated in the previous study.

Experimental Procedure

Materials. The U-Pu-Zr and U-Pu-Ti alloys contained from 15 to 22%** Pu, from 6 to 14% of Zr or Ti, and were prepared from 99.8% pure U and Pu and crystal bar Zr or Ti. The alloys were melted in vacuum at 1 x 10^{-5} torr in induction-heated yttria-coated zirconia crucibles and were injection cast in an inert gas atmosphere in yttria-coated quartz molds. The data obtained from chemical analyses at the top and bottom ends of the ingots are given in Table 1.

Alloys of U-10%Zr and U-10%Ti, prepared from 99.9% pure U and crystal bar Zr and Ti, also were included in the survey. These alloys were prepared by arc-melting on a water-cooled hearth in an inert gas atmosphere. The major impurities in the alloys were 132 to 190 ppm oxygen, 104 to 122 ppm nitrogen, and 9 to 53 ppm carbon.

The nominal compositions of the cladding materials are given in Table 1 together with the chemical analyses for oxygen. All of the alloys were procured from commercial sources except the V-base alloys, which were prepared by electron beam melting at Argonne National Laboratory.

Diffusion-Couple Assembly. For the construction of diffusion couple assemblies, discs (approximately 10 mm in diameter by 10 mm in length) were machined from the described materials and the faces of the discs were polished, flat and parallel, with 4/0 emery paper. Immediately after polishing the discs were assembled in molybdenum holders and inserted in evacuated stainless steel capsules as described previously (1). The assemblies were annealed for times up to 5,000 hours in furnaces (controlled to within $\pm$ 3°C) at temperatures from 600 to 850°C.

*Fizzium (Fz) is an aggregate of fission-product elements that are not removed in the pyrometallurgical reprocessing cycle designed for Argonne Experimental Breeder Reactor II. The major components of the aggregate are zirconium, molybdenum, palladium, ruthenium, and rhodium.

**All material compositions are reported in weight percent.

Metallography and Microprobe Analyses. The widths of the diffusion layers were determined by scaler measurements on etched microstructures. Electron microprobe analyses were made on some of the couples to corroborate the penetration depths. Diffusion layers in the fuel alloys generally were most clearly defined by electrolytic etching in H_3PO_4 solutions containing ethylene glycol and ethyl alcohol. Several etchants were used to reveal diffusion zones in the cladding materials (1).

Results and Discussion

The fuel-cladding combinations that were studied are given in Table 2 together with measured penetrations into the claddings after specific annealing treatments at 700, 750, and 800°C. Also listed in Table 2 are values of T_m, the temperature at which a liquid phase is formed in the diffusion layer. The compatibility of the U-Pu-Zr alloys with the Fe-base alloys (Type 304 SS, 16-15-6, 16-25-6, and Haynes 56) depends upon the zirconium concentration in the ternary alloys. With 6.3% or less zirconium, the formation of liquid phases precludes the use of Type 304 stainless steel at temperatures above 700°C. In contrast, with 10% and 14.1% Zr, T_m values for the Fe-base alloys are above 800°C. With all the U-Pu-Zr alloys, T_m values for the Ni-base alloys (N-155, Incoloy 800, and Hastelloy-X) are significantly lower than for the Fe-base alloys and cladding penetrations are higher at all temperatures. Thus, increasing the nickel content in the cladding materials results in a degradation of compatibility. With the U-Pu-Zr alloys containing 10% and 14.1% Zr, T_m was determined, in the present work, to be below 800°C for pure nickel but above 800°C for pure iron. Both T_m and cladding penetration for the U-10%Zr alloy with Type 304 stainless steel are nearly the same as for the U-Pu-Zr alloys containing 10% and 14% Zr.

The U-Pu-Ti alloys have markedly poorer compatibility with Type 304 stainless steel than the U-Pu-Zr alloys. This is clearly evidenced by their significantly lower T_m values.

The log of penetration distance into the cladding vs log annealing time for some of the fuel-cladding combinations are plotted in Figs. 1 to 4. Maximum cladding penetrations are plotted as points and estimated possible errors are indicated by vertical bars. In drawing the curves, greater weight has been placed on long time data and, because of the relatively large possible errors, it has been necessary to assume the parabolic rate law normally found in volume diffusion $X^2 = Kt$*. With the U-10%Zr, U-15%Pu-10%Zr, and U-18%Pu-14.1%Zr alloys, penetration of Type 304 stainless steel is very limited, less than 10^{-3} cm in 1000 hours, at all temperatures up to 750°C. In Fig. 5, these results are compared with those obtained for the V-base alloys and with results previously reported for U-10%Pu-10%Fz (1) and U-5%Fs (2) alloys. The penetration coefficients K for

*X is the cladding penetration as seen metallographically in centimeters; t is the annealing time in seconds; and K is the penetration coefficient in cm^2/sec.

the U-Pu-Zr alloys vs Type 304 stainless steel and the V-base alloys are given in Table 3 together with the coefficients previously determined (1) for the U-Pu-Fz alloys.

Uranium forms eutectics with Fe and Ni at 725 and 740°C, respectively. Therefore, the use of Fe- and Ni-base alloys as claddings for uranium-bearing fuels generally has been restricted to temperatures well below 700°C. The compatibility of U-Zr and U-Pu-Zr alloys with Type 304 stainless steel at temperatures to 800°C requires explanation. Electron microprobe analyses made on certain of the annealed diffusion couples indicate that the enhanced compatibility results from the formation in the fuels of diffusion layers that consist of one or more zirconium-rich phases stabilized by oxygen. The phases include 1. alpha zirconium, 2. a body-centered cubic gamma uranium solid solution based on the γ_2 phase in the U-Zr system (3), and 3. a phase based on the ternary γ phase in the Zr-Ni-O system (4). These phases restrict the transport of Fe and Ni into the fuels, as well as diffusion of U and Pu into the steel. The presence of oxygen in the steel and fuel alloys in concentrations greater than 100 ppm is a beneficial, if not necessary, factor for affecting enhanced compatibility.

The use of the V-Ti and V-Ti-Cr alloys as claddings for the U-Pu-base alloys at temperatures to 800°C is limited solely by the extent to which U and Pu penetrate the claddings and form brittle phases. The V-20%Ti alloy is highly compatible with the U-Pu-Zr and U-Pu-Fz alloys up to approximately 650°C. Above 650°C its use is limited because of pronounced cladding penetration. Substitution of chromium for some of the titanium in the alloy has little, if any, effect on the compatibility.

REFERENCES

1. C. M. Walter and J. A. Lahti, Nucl. Appl., 1966, Vol. 2, pp. 308-319.

2. C. M. Walter, Rept. No. ANL-6816, Argonne National Laboratory, 1964.

3. S. T. Zegler, Rept. No. ANL-6055, Argonne National Laboratory, 1962.

4. M. V. Nevitt, Trans. A.I.M.E., 1961, Vol. 221, pp. 1014-1017.

Table 1. Compositions of Survey Materials
(wt% except where noted otherwise)

Injection Cast Fuel Alloys Nominal Composition (wt%)	Oxygen (ppm)	Nitrogen (ppm)	Hydrogen (ppm)	Carbon (ppm)
U-16.6Pu-6.3Zr	430 to 500	125 to 147	< 1	360
U-15Pu-10Zr	206 to 400	17 to 82	< 1	410
U-18.5Pu-14.1Zr	920 to 1300	17 to 21	3 to 4	236
U-15Pu-10Ti	224 to 510	18 to 360	5 to 7	870
U-22Pu-11.8Ti	189 to 400	21 to 37	< 1	196

Cladding Alloys	Oxygen (ppm)	Fe	Ni	Cr	Mo	Co	W	Mn	C
Type 304 Stainless Steel	160 to 420	70.7	8.8	18.5				1.14	0.05
Haynes 56	62								
Timken 16-15-6	109	55	15	16	6			7.5	
Timken 16-25-6	43	50	25	16	6			1.3	
N-155	39	30	20	21	3	20	3	1.5	
Incoloy 800	11	46	32	21				0.75	
Hastelloy-X		18	48	22	9	1.5	0.6	1.0	
V-20Ti									
V-15Ti-7.5Cr									

Table 2. Fuel Penetration into Fe-, Ni-, and V-Base Alloys

Fuel Alloy	Cladding	Penetration ($cm \times 10^4$)			T_m (°C)
		5000 hr at 700°C	1000 hr at 750°C	168 hr at 800°C	
U-16.6Pu-6.3Zr	Type 304 SS	12 (400 hours)	Melted	Melted	725 ± 25
	Hastelloy-X	50 (400 hours)	Melted	Melted	725 ± 25
U-15Pu-10Zr	16-15-6	2	< 5	< 5	825 ± 25
	16-25-6	4	-	-	< 850
	304 SS	10	12	30	825 ± 25
	Haynes 56	-	15	8	825 ± 25
	Incoloy 800	-	27	Melted	775 ± 25
	N-155	30	> 40	-	< 850
	Hastelloy-X	70	Melted	Melted	725 ± 25
U-18.5Pu-14.1Zr	16-15-6	< 3	< 6	< 6	835 ± 15
	Haynes 56	-	5	4	825 ± 25
	304 SS	4	9	12	825 ± 25
	16-25-6	2	15	-	< 850
	V-15Ti-7.5Cr	17	-	17	
	V-20Ti	23	-	-	
	N-155	80	20	20	825 ± 25
	Incoloy 800	-	> 40	70	825 ± 25
	Hastelloy-X	30 (1000 hours)	Melted	Melted	725 ± 25
U-15Pu-10Ti	304 SS	Melted	-	-	< 700
U-22Pu-11.8Ti	304 SS	Melted at 650°C	-	-	< 650
U-10Zr	304 SS	3 (1000 hours)	9	28	835 ± 15
U-10Ti	304 SS	-	12 (168 hr)	Melted	775 ± 25

Table 3. Cladding Penetration Coefficients (K) in cm^2/sec (except where noted)

Combination (wt%)	Temperature (°C) 550	600	650
V/U-10Pu-10Fz	[a] 7.5×10^{-14}	[a] 1.5×10^{-13}	[a] 4.0×10^{-13}
V-20Ti/U-10Pu-10Fz	[b] 2.3×10^{-15}	1.3×10^{-14}	6.4×10^{-14}
V-20Ti/U-15Pu-10Fz		[b] 1.3×10^{-14}	8.1×10^{-14}
V-10Ti/U-10Pu-10Fz	4.7×10^{-15}	2.3×10^{-14}	1.1×10^{-13}
Mo/U-10Pu-10Fz		4.5×10^{-14}	1.2×10^{-13}
Mo/U-15Pu-10Fz		[b] 7.5×10^{-14}	[b] 2.0×10^{-13}
304SS/U-10Pu-10Fz	6.9×10^{-14}	2.2×10^{-13}	1.1×10^{-12}
304SS/U-15Pu-10Fz			[b] 3.4×10^{-12}
Hast-X/U-10Pu-10Fz	1.8×10^{-13}	8.0×10^{-13}	3.6×10^{-12}
Hast-X/U-15Pu-10Fz			[b] 1.1×10^{-11}
Nb/U-10Pu-10Fz	1.3×10^{-13}	6.3×10^{-13}	[c] 2.2×10^{-9} cm/sec
Nb/U-20Pu-10Fz	2.3×10^{-13}	1.8×10^{-12}	[c] 4.2×10^{-9} cm/sec
Nb-1Zr/U-10Pu-10Fz	1.6×10^{-13}	4.0×10^{-13}	[c] 1.9×10^{-9} cm/sec
304SS/V			[d] 3.4×10^{-13}
304SS/V-20Ti			[d] 2.3×10^{-13}
V-20Ti/U-18Pu-14Zr		1.5×10^{-14}	
V-15Ti-7.5Cr/U-18Pu-14Zr		8.0×10^{-15}	

Combination (wt%)	Temperature (°C) 700	750	800
V-20Ti/U-10Pu-10Fz	3.1×10^{-13}	[b] 1.7×10^{-12}	
V-20Ti/U-15Pu-10Fz	[b] 8.0×10^{-13}	[b] 3.0×10^{-12}	
Cr/U-10Pu-10Fz	[b] 3.5×10^{-13}		
Mo/U-10Pu-10Fz	1.9×10^{-13}		
Mo/U-15Pu-10Fz	[b] 4.0×10^{-13}		
V-20Ti/U-18Pu-14Zr	3.5×10^{-13}		
V-15Ti-7.5Cr/U-18Pu-14Zr	1.8×10^{-13}		
304SS/U-10Zr	1.5×10^{-14}	2.0×10^{-13}	6.0×10^{-12}
304SS/U-15Pu-10Zr	8×10^{-14}	3.8×10^{-13}	
304SS/U-18Pu-14Zr	3.6×10^{-14}	1.6×10^{-13}	9.8×10^{-13}

a. No cladding penetration. K's represent band on the fuel side believed to be $(U,Pu)O_2$. Vanadium contained 1300 ppm O_2.
b. Calculated from only one datum point assuming an $X^2 = Kt$ law.
c. Obeyed the $X = Kt$ rather than $X^2 = Kt$ rate law.
d. Total band width. Also calculated from only one datum point assuming an $X^2 = Kt$ law.

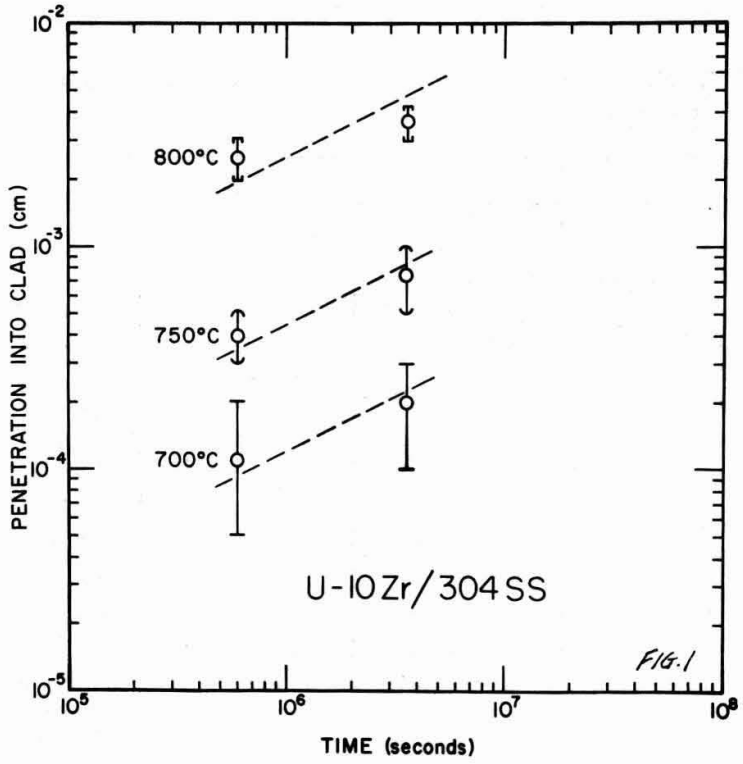
PENETRATION INTO CLAD (cm)
TIME (seconds)
800°C
750°C
700°C
U-10Zr/304SS

FIG. 1

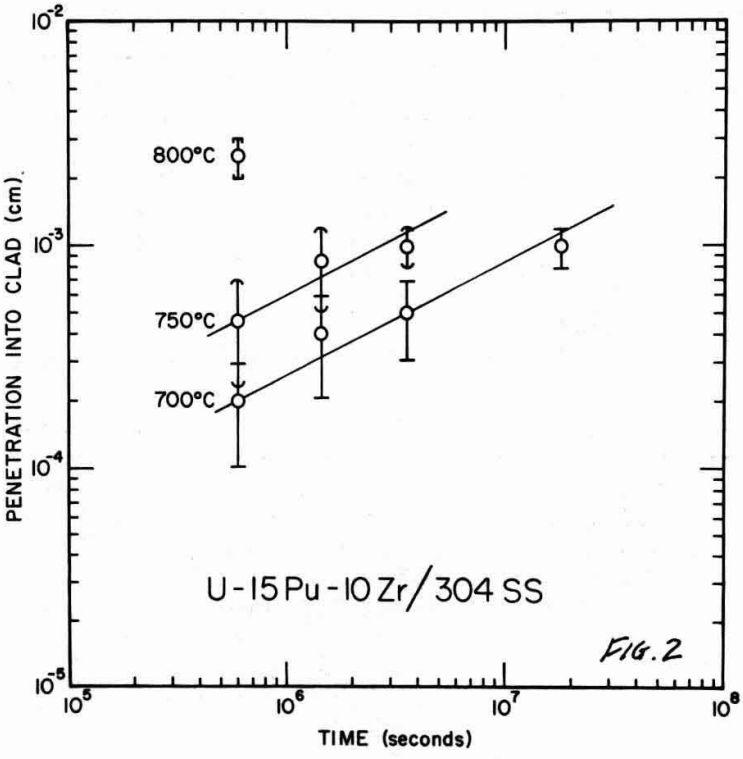
PENETRATION INTO CLAD (cm)
TIME (seconds)
800°C
750°C
700°C
U-15Pu-10Zr/304SS

FIG. 2

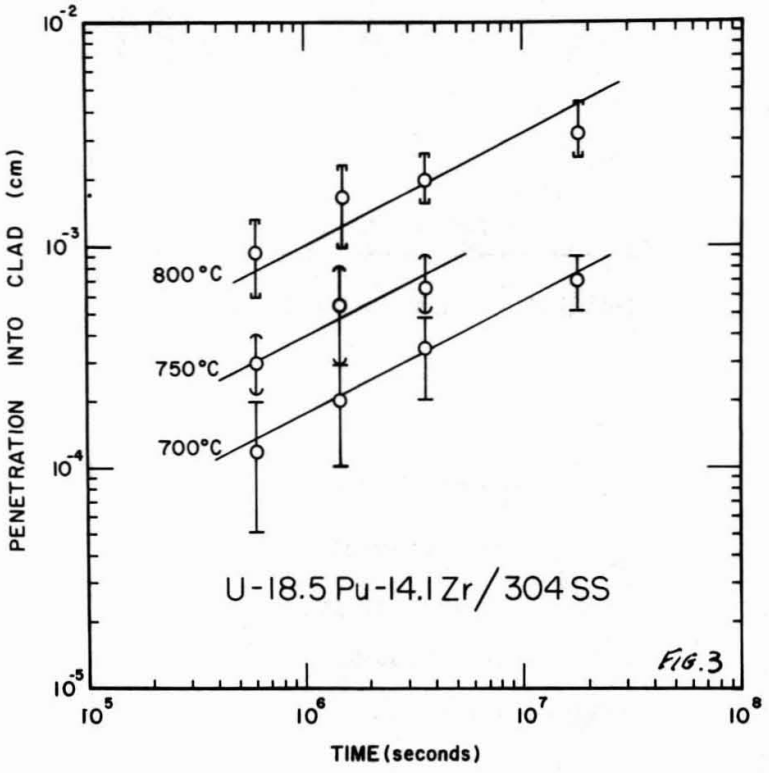
PENETRATION INTO CLAD (cm)
TIME (seconds)
800°C
750°C
700°C
U-18.5 Pu-14.1 Zr / 304 SS
FIG. 3

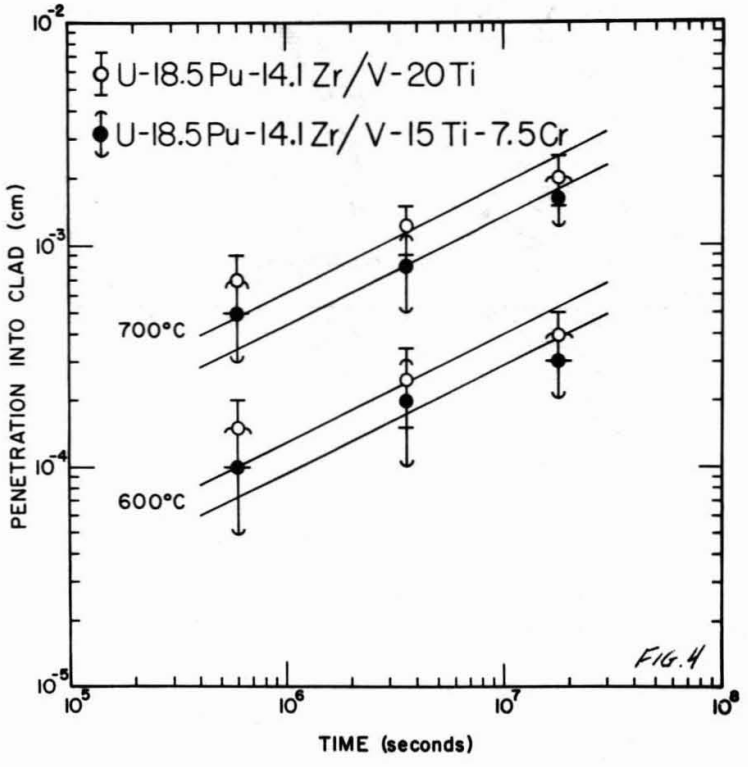
PENETRATION INTO CLAD (cm)
TIME (seconds)
U-18.5 Pu-14.1 Zr / V-20 Ti
U-18.5 Pu-14.1 Zr / V-15 Ti-7.5 Cr
700°C
600°C
FIG. 4

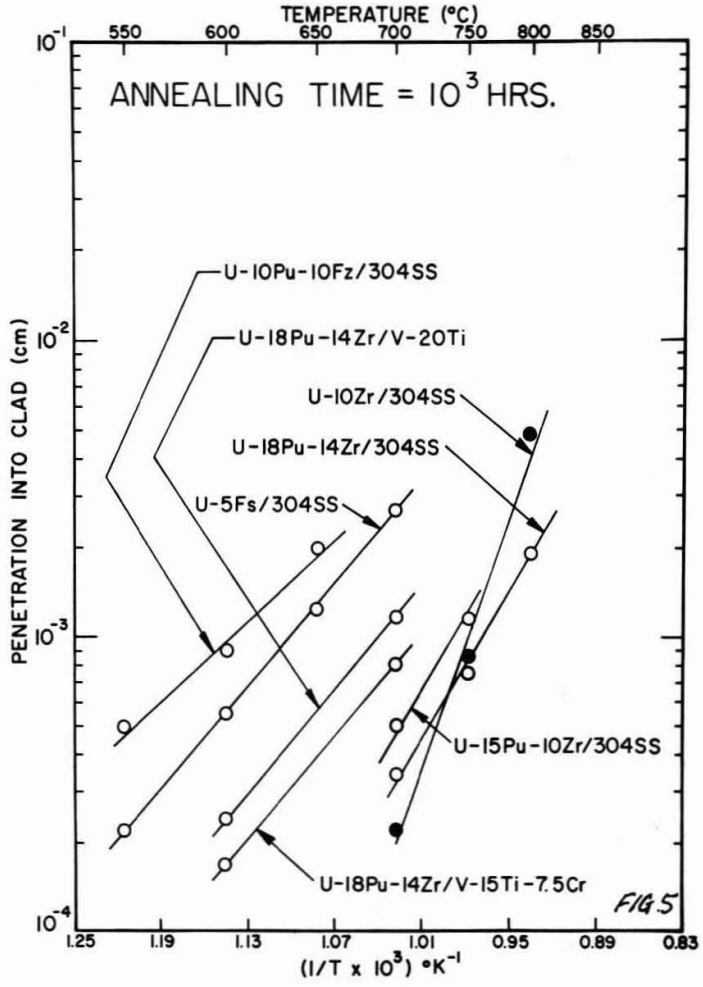
TEMPERATURE (°C)
550
600
650
700
750
800
850
ANNEALING TIME = 10^3 HRS.
U-10Pu-10Fz/304SS
U-18Pu-14Zr/V-20Ti
U-10Zr/304SS
U-18Pu-14Zr/304SS
U-5Fs/304SS
U-15Pu-10Zr/304SS
U-18Pu-14Zr/V-15Ti-7.5Cr
FIG.5
PENETRATION INTO CLAD (cm)
10^-1
10^-2
10^-3
10^-4
1.25
1.19
1.13
1.07
1.01
0.95
0.89
0.83
(1/T x 10^3) °K^-1

PROPERTIES of CARBIDES and CARBONITRIDES

R. PASCARD

Abstract

We have studied the system (U,Pu)(CNO) in order to have a basis to select the best composition for a fast reactor fuel.

The studies are the following :

a) Diagram studies
b) Compatibility tests with stainless steel in sodium
c) Thermal diffusivity measurements

It is difficult to weight a priori the relative importance of the results and there is a strong feeling that decision, if any, must come from extensive irradiation experiments.

R. PASCARD is head of the ceramics section at the Centre d'Etudes Nucléaires de Fontenay-aux-Roses France.

Introduction

In previous papers (1) (2), we have suggested to enlarge the concept of pure carbide fuels to carbide-type fuels, by deliberate total or partial substitution of carbon by nitrogen and / or oxygen. Such fuels are represented by points in the ternary diagramm MC-MN-MO (fig. I) (Where M stands for U and Pu). The most obvious advantage of the M (CNO) or more precisely M (C, N) fuels is that they can be prepared routinely as strictly single phased compounds is contrast with pure monocarbides. The impurity M_2C_3, thougt to be dangerous for clad compatibility, is in fact specific of the carbide part of the ternary diagramm (part I, fig. I).

Work has been pursued along the general ideas expressed in a previous paper (2) in order to check the most important properties of the M (CN) fuels. In this paper, after a brief survey of preparation methods, prelimary results of compatibility experiments and thermal conductivity measurements will be given. Irradiation properties are dealt with in an other paper (3). The work done on arc-casted carbides, where additions of Ti and Mo have been made in order to improve the properties of pure carbides has been described in other publications (14, 15).

II - FABRICATIONS STUDIES

II. 1/ The general process developped at Fontenay-aux-Roses uses the metals or their hydrides as the starting materials, according to the reactions :

$$MH_x + C \longrightarrow MC + \frac{x}{2} H_2 \qquad (a)$$

$$M + \frac{x}{2} N_2 \longrightarrow MN_x \qquad \begin{matrix} M = U\,,\ x \simeq 1{,}75 \\ M = Pu,\ x = 1{,}00 \end{matrix} \qquad (b)$$

$$MH_x + MO_2 \longrightarrow 2\,MO + \frac{x}{2} H_2 \qquad (c)$$

Details concerning these reactions have been given in previous paper (1) (4) (5). Pure nitrides are prepared through reaction b, and by proper blending of the nitrides so obtained and other constituants according to reactions a and c, any compound of intended composition M (CNO) can be easily prepared at a temperature not exceeding 1.400°C. The resulting ingots, consisting in well-diffused solid solutions, are crushed and finally ballmilled to give the appropriate powder for final sintering. Cold-pressed pellets are sintered at temperatures ranging from 1.400 to 1.650°C, depending on the composition and the presence of a sintering aid (0,2 w % Ni powder for carbides). The general trend towards low density fuels has prompted us recently to abandon Ni as a sintering aid for carbides. A "smoothed" sintering process has resulted, at temperature near 1.600°C, independent of the nature of the fuel. Maximum densities achieved vary from roughly 95 % theoretical density for pure carbides to 92 % for pure nitrides. Lower densities are easily obtained by reducing the sintering temperature.

II. 2/ In contrast with carbides containing nickel, nickel free carbides generally do not exhibit any trace of higher carbides M_2C_3 and MC_2. Starting with the same powder, nickel addition can result in the presence of more than 10 % M_2C_3 even at 1.600°C : this demonstrates that Ni containing carbides are not in thermodynamic equilibrium, the high density associated with Ni preventing CO outgassing. Due to this last result, it is fair to say that the strongest a priori motivation for discarding carbides to the benefit of nitrides seems to disappear.

II. 3/ In connection with carbonitrides work, some diagramm studies in the system U-C-N and Pu-C-N have been completed.

Mixtures of UN or PuN and varying quantities of graphite powder were heated at 1.400°C and 1.600°C under vacuum and theresulting phases determined at room temperature by X ray and metallography.
The corresponding ternary diagrams are represented on fig. II a, b.

From these diagrams, it can be seen that uranium carbonitrides prepared under vacuum are necessarily single-phased, provided that $\frac{N}{C + N} > 0{,}20$: any slight excess of C + N with respect to M escarping under the form of free nitrogen (point B in II a). With Pu, the limit for single phased carbonitride is drastically shifted to the nitride side, 75 % nitrogen being required in the carbonitride phase to suppress the possibility of existence of Pu_2C_3 (point A in II b).

The corresponding diagram for U-15 % Pu mixed carbonitrides is very similar to that of pure uranium. The composition of the limit carbonitride is still very close to U, Pu $(C_{0,8}\ N_{0,2})$, but the MC_2 phase is now suppressed with a corresponding simplification of the diagram near the carbide side.

III - COMPATIBILITY STUDIES

III. 1/ A simple compatibility test in the ternary system carbide-type fuel, sodium, stainless steel has been devised : fuel samples, massive or in powder, are sealed in a stainless steel pot with a weighted 316 L S.S. plaquette in presence of a large excess of sodium. The plaquette, 1 mm thick, is cut to fit exactly in the sample holder of a Phillips X ray goniometer. After heating at 700°C during about 1.000 h., the containers are opened and the excess sodium removed by filtration. The fuel sample and the plaquette are thoroughly washed with butyl alcohol. The plaquette

is weigthed again and immediately submitted to X ray analysis. Control analysis is also performed by metallography for the plaquette and by X ray and metallography for the fuel sample. No mechanical measurement being available for the plaquette, a very trivial bending test has been used in order to display any gross change in mechanical properties of the stainless steel. Finally, after these non destructive tests, the carbon content of the plaquette has been determined, in most of the cases by chemical analysis.

III. 2/ Before going to carbonitrides, preliminary tests were performed in order to check current ideas concerning the compatibility of UC fuels. These were blank tests (no fuel sample) and runs with graphite powder, pure massive UC_2, pure massive U_2C_3 and UC containing a small quantity of U_2C_3 or UC_2. In the last case, the carbide was of the same overall composition, one of the samples being quenched from 1.900°C (practically all excess carbon being present as UC_2) and the second thoroughly annealed at 1.300°C (all excess phase U_2C_3 with no UC_2). The excess carbon was about 5 %.

Fortunately, the blank tests gave repeatedely no detectable change in the plaquette for all kinds of controls, except may be metallography. At the other end of the scale, graphite produce a strong carburisation visible to naked-eye. The plaquette has become tamished and increased in weight 2,8 mg/cm^2 ; the X ray pattern displayed, aside the austenite lines, all the lines characteristic of the $Cr_{23}C_6$ phase. Furthermore, the plaquette has become brittle.

UC_2 and U_2C_3 exhibit a drastically different behaviour. The UC_2 pellet is destroyed whereas U_2C_3 pellet is still integer (see X ray radiography fig. III). X ray analysis shows that UC_2 has completely reversed to monocarbide. The accompanying plaquette displays all the features of

the one heated with graphite powder. From the intensity of the $Cr_{23}C_6$ lines a carburization equal to 70 % of that given by free carbon can be inferred. In contrast, no change can be evidenced in the U_2C_3 pelled and the corresponding plaquette is identical to the blank one. In particular, no $Cr_{23}C_6$ lines can be detected, despite the fact that this test, as it will be seen further, is a rather sensitive one.

Finally, the UC containing UC_2 and U_2C_3 pellets gave apparently classical results. Metallography reveals that UC_2 is progressively leached out from the UC matrix, while UC containing U_2C_3 pellet remains unchanged. This could be be due to the fact that UC_2 is easily semi-quantitatively estimated ; nevertheless no diminution of the U_2C_3 content, even at the edge of the pellet, is noted (fig. VI). In both cases, carburization evidenced by the presence of faint but complete pattern of $Cr_{23}C_6$ is roughly the same.

III. 3/ After these first experiments giving rather expected results, (except may be the complete inertness of uranium sesquicarbides) a complete set of carbonitrides with N content varying from 0 to 100 %, with and without Pu and sesquicarbide phase, were subjected to compatibility tests. All the fuel samples were in powder form, in order to accelerate the carburization process. The conditions were 700°C, 1.000 h. Results are given in table I. Some plaquette X Ray patterns corresponding to typical cases are shown on fig. IV.

In these experiments, the plutonium content of the fuels studied was 15 %.

The ratio of the intensities of the X ray line 440 of $Cr_{23}C_6$ and 200 of austenite in taken as a measure of the

	M_2C_3 content %	Weight change in mg/cm^2	Carburization extent	Increase in carbon content (ppm)
graphite		+ 2,8	1.000	11.450 ± 1.500
UC	no	+ 0,8	168	1.140 ± 250
(UPu)C	10	+ 0,05	176	
(UPu)C	no	- 0,7	174	
$(UPu)C_{85}N_{15}$	4	+ 0,12	180	
$(UPu)C_{85}N_{15}$	no	+ 0,14	230	770 ± 150
$UC_{75}N_{25}$	no	- 0,05	136	840 ± 150
$(UPu)C_{70}N_{30}$	no	+ 0,62	170	1.620 ± 300
$(UPu)C_{65}N_{35}$	no	- 0,04	120	
$UC_{50}N_{50}$	no	+ 0,22	124	1.080 ± 250
$UC_{20}N_{80}$	no	- 0,10	152	270 ± 100
UN			0	
(UPu)N		- 0,28	0	170 ± 100

TABLE I - Carburization of stainless steel 316 L after 1.000 h at 700°C, in sodium, by different fuel samples.

carburization extent. This ratio has been normalised to 1.000 for graphite carburization, and is given in the last column of table I.

The weight changes are probably not significant, due to a possible small erosion during washing; carburization extent, as given by X ray, is in general qualitative agreement with analytical results. Quantitatively, the agreement is rather poor, X rays results being obviously more sensitive to surface carburization and for this reason analytical results are considered to be more representative of true carburization and they are reported on fig. V.

These results are rather puzzling. They show that, except for pure nitrides, a slight definite carburization is observed, roughly the same for all compounds. Most surprisingly, this carburization does not depend on the sesquicarbide content. Correspondingly, the presence of nitrogen changes nothing to the compatibility problem, except of course for pure nitrides. In this last case, the plaquette X ray pattern is that of pure austenite (no trace of lines of any knownchromium nitride compound).

In all cases, the bending properties of all the plaquettes, except in the graphite case, being the same as those of plaquettes of the blank run.

The lattice parameters of all the samples remain unchanged, but sometimes small traces of oxide appear. A straightforward explanation of the observed results would be that carbon transfer takes place from the monocarbide-type phase itself. If this was true, it would be likely to observe a decrease in carburization with increasing nitrogen content, as carbon activity decreases. This is not found.

A more probable explanation involves a possible role of oxygen contamination of the sodium. Traces of oxygen would oxide the fuel, giving free carbon as actual source of carburization. In this hypothesis, slight oxydation of highly nitrogen charged carbonitrides would give free carbon instead of free nitrogen. Experiments are currently carried on to check this hypothesis.

As a provisory conclusion, we may state that strictly speaking, only pure nitrides are compatible with stainless steel, sodium being present. For other compounds, the presence of U_2C_3 as an impurity does not play any role in compatibility.

IV - THERMAL DIFFUSIVITY MEASUREMENTS

IV. 1/ Although not as decisive as compatibility or swelling properties for fuel selection, thermal conductibility must be known for proper fuel designing. A programm has been set up for measurement of thermal conductibilities in the binary system MC - MN.

Two different apparatus, both using transient methods, have been set up :

a) a "low" temperature apparatus, from room temperature to about 1.000°C using samples in the form of pellets as they are routinely fabricated (about 12 mm long, 6 mm in diameter). Through two thermocouples about 6 mm apart, fitted in small holes radially drilled along a sample generatrice, the attenuation a and the phase shift $\bar{b}$ of a heat sine wave are recorded. It can be shown that a $\bar{b} = \frac{\omega}{2D}$, where ω is the pulsation of the sine wave and D the diffusivity, provided that the sine wave is completely attenuated at the free end of the sample and that a and $\bar{b}$ are not too much different. (See for ex. ABELES and CODY (6)).

The apparatus has been found to work satisfactorily with pure iron and nickel standards, despite the unusually short length of the samples.

b) a high temperature apparatus, from about 1.000°C to melting or decomposition temperature. Thin slices, cut in normal pellets by spark-erosion, are heated by a sinusoïdally modulated electron beam. The diffusivity D can be deduced from the temperature phase shift between both faces of the slice. Thorough mathematical treatment has been given by COWAN (7).
The rather complicated relation between the phase shift and the diffusivity can be dealt with easily by working in such condition that : $\Delta\varphi > \frac{\pi}{2}$ so that it reduces to a fairly linear relationship between the phase shift $\Delta\varphi$ and the square root of the frequency f

$$\frac{\Delta\varphi}{\pi} \cong \frac{l}{\pi}\left(\frac{\pi f}{D}\right)^{1/2}$$

with actual samples, the condition $\frac{\Delta\varphi}{\pi} > \frac{1}{2}$ is fulfilled for sample thickness of the order of 1 mm. The measurements were performed at varying frequencies between one and five herz and D deduced from the slope p of the curve $\frac{\Delta\varphi}{\pi}$ versus f 1/2.
From the relation (a) we get :

$$D = \frac{l^2}{\pi} \times \frac{1}{p^2}$$

This plot provides a useful chek for internal consistency as the curve should be a straight line passing through the origin when the heat losses are negligible.
In both cases, the accuracy is estimated at ± 10 %. This is probably lower than the steady-state measurements accuracy but the transient methods have invaluable advantages : use of small samples and rapidity of measurement.

IV. 2/ First measurements were made with pure uranium carbonitrides in order to determine the general shape of the conductibility curve with increasing nitrogen content. An immediate difficulty is encountered in transforming diffusivity data in conductibility data, using the formula : $k = D\rho c$, where ρ and c are the density and the specific heat of the sample respectively. Specific heat is reasonably known for carbides

but a wide discrepancy exists for UN data, as they are found in ONRL (8) and BMI (9) reports. Data given in the BMI report have been preferred, because the corresponding specific heat-temperature curve has a classical shape (the ONRL curve is very unusual).

Finally, the relevant molar specific heat data are quoted in the table II.

TABLE II

T°c	50	200	500	1.000	1.500	2.000
UN	11,5	12,8	13,9	14,7	(15,4)	(16,1)
UC	12,4	13,95	14,8	15,22	15,44	

corresponding identical values have been assigned to PuN and PuC and the specific heat of any M (CN) compound deduced from linear combination. Such procedure is certainly justified in connection with the UN data uncertainty. Mean results found for pure[/] UN and UC are compared on figure VII. In accordance with previous results (10), the UN conductibility is found to be lower than that of UC at lower temperature. The situation is reversed beyond about 900 °C, instead of 700°C after BMI results. The conductivity gain for UN at high temperature remains small, a definite positive slope being found for monocarbide also.

Results in the UC-UN binary system are reported on fig. VIII for four temperatures. Despite some experimental scattering, the general shape of the conductivity curves against composition is clearly outlined. All these curves pass through a minimum near 30 % nitrogen, whatever is the temperature. This minimum is deeper, the lower is the temperature.

[/] UC : 800 ppm oxygen, 1.300 ppm nitrogen - d = 95 % d_{th}
UN : 800 ppm - d = 92 % d_{th}

IV. 3/ The same kind of measurements have been repeated in the MC-MN binary, the Pu content being fixed at 15 %. Since generally any kind of lattice defect diminished the thermal conductivity, k is expected to decrease with plutonium introduction. This is found to be the case. In figure IX are compared the conductibility curves against temperature, for UC, (UPu)C and UN, (UPu)N. Dotted curves correspond to available result in the litterature. In contrast with pure uranium compounds, the (UPu)N conductivity remains slightly lower than that of (UPu)C even at higher temperature. The conductivity loss, with respect to uranium compound is about 15 % for (UPu)C and 20 % for (UPu)N, at 1.400°C.

Fig. X represents the conductibility variation against nitrogen content in the pseudo-binary MC-MN at fixed Pu concentration equal to 15 %. These preliminary results indicate a smooth variation of k beetween MC and MN with a flat minimum. At 1.500°C, the conductivity appears to be practically constant from MC to MN.

V - SUMMARY AND CONCLUSIONS

Compatibility and thermal conductivity measurements have been made in the binary system MC-MN. Although far to be complete they are nevertheless sufficient to get a general idea about the fuel behaviour with respect to these main properties : From compativility results superiority of nitride fuels emerges. Nevertheless, it would be prematurate to base a choice on this apparently clear advantage, as long as the compatibility behaviour of monocarbide fuels is not better understood. In particular, bad results experienced in the early days of uranium carbides, could be not extrapolated to plutonium fuels, as far as UC_2 alone may be taken as responible of compatibility lack.

On the other hand, thermal conductivity data are slightly in favor of pure monocarbides fuels. It then appears that not one of the properties studied does offer a decisive criteria for selecting a given carbide-type fuel. The same balance would be met if secondary properties like corrosion resistance or thermal stability were taken into consideration. It would be difficult to weight a priori the relative importance of all these properties and there is now a strong feeling that decision, if any, must come from extensive irradiation experiments. Such experiments are now currently in progress, where representative fuels, pure carbides, pure nitrides and carbonitrides with 30 % nitrogen are irradiated in conditions as severe as possible.

BIBLIOGRAPHIE

1 F.ANSELIN, G. DEAN, R. LORENZELLI et R. PASCARD
Carbides in Nuclear Energy
Macmillan and Co, London (1964) p. 113

2 R. PASCARD
Bulletin d'informations scientifiques et techniques du C.E.A.
n° 100 - Janvier 1966

3 H. MIKAILOFF, J.P. MUSTELIER, J. BLOCH, J. LECLERE et L. HAYET
Rapport CEA-R 3223 (1967)

4 F. ANSELIN
J. Nucl. Mat. 10, 4 (1963), 301

5 F. ANSELIN
Rapport CEA-R 2988 (1966)

6 B. ABELES, G.D. CODY et D.S. BEERS
J. Appl. Phys. 31 (1960), 1585

7 R.D. COWAN
J. Appl. Phys. 32 (1961), 1363 ; Rapport LA-2460

8 Rapport ORNL 1596 (1966)

9 Rapport BMI 1692 (EUR AEC 1210) (1964)

10 E.O. SPEIDEL et D.L. KELLER
Rapport BMI 1633 (1963)

11 L.A. Report LA 3431 MS (1965)

12 J.A. LEARY, R.L. THOMAS, A.E. OGARD et G.C. WONN
Carbides in nuclear energy
Macmillan and Co, London (1964), p. 365

13 R.L. GIBBY
Private communication

14 R. BOUCHER et P. BARTHELEMY
Rapport CEA R.3229 (1967)

15 C. MILET
Rapport CEA R.3201 (1967)

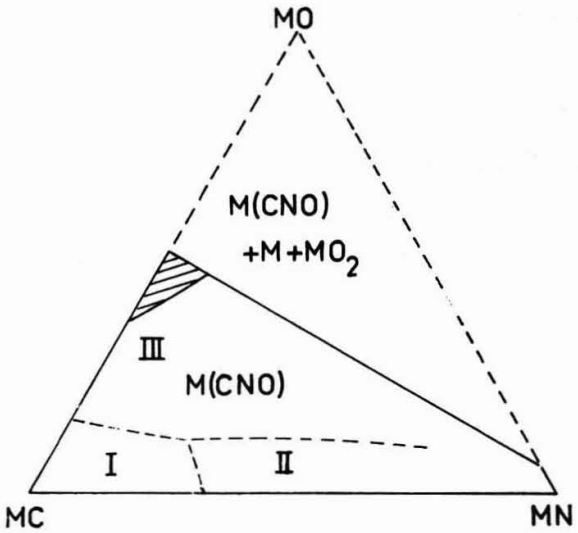

FIG. 1

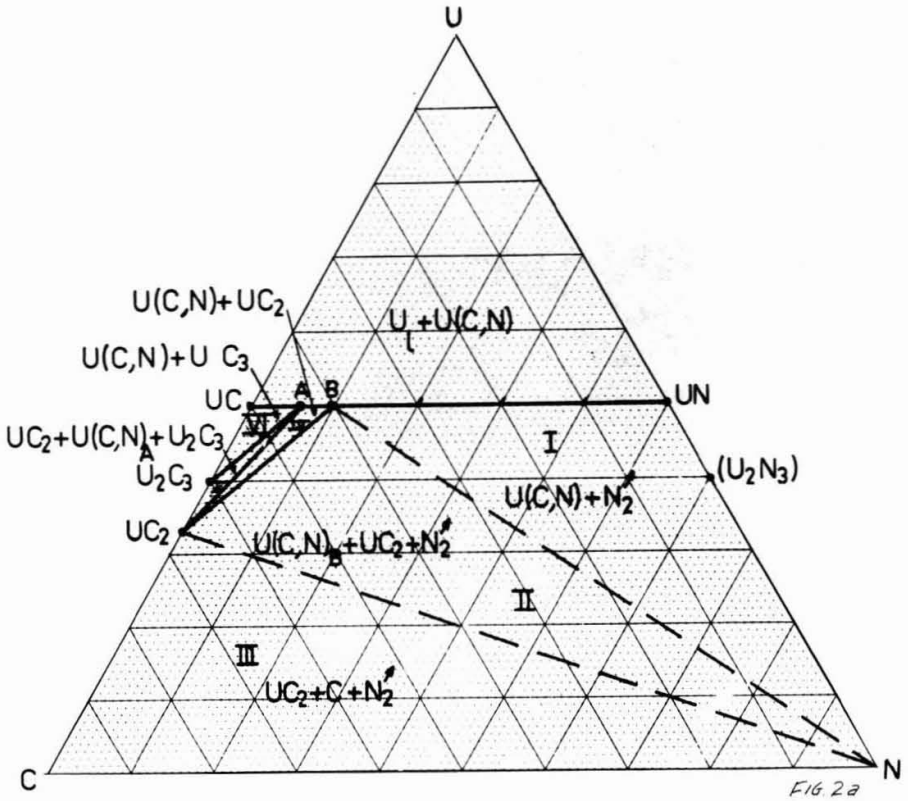
U
U(C,N)+UC2
Ul+U(C,N)
U(C,N)+U C3
UC
A
B
UN
UC2+U(C,N)A+U2C3
U2C3
(U2N3)
I
U(C,N)+N2
UC2
U(C,N)B+UC2+N2
II
III
UC2+C+N2
C
N

FIG. 2a

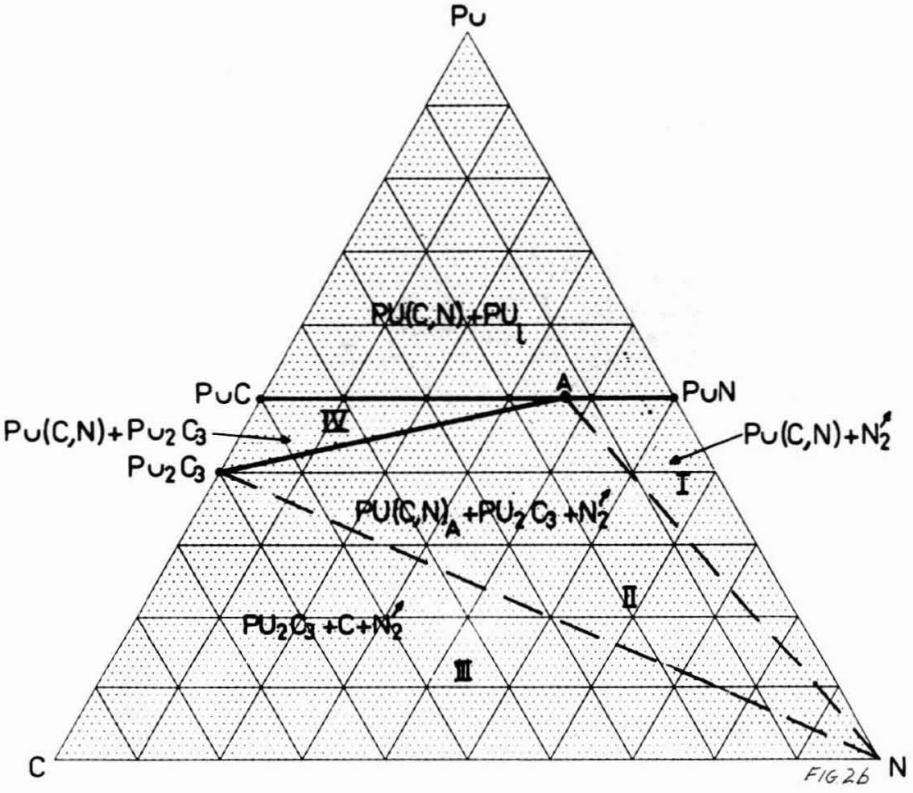
Pu
PU(C,N)+PUl
PuC
A
PuN
Pu(C,N)+Pu2C3
IV
Pu(C,N)+N2
Pu2C3
I
PU(C,N)A+PU2C3+N2
II
PU2C3+C+N2
III
C
N

FIG. 2b

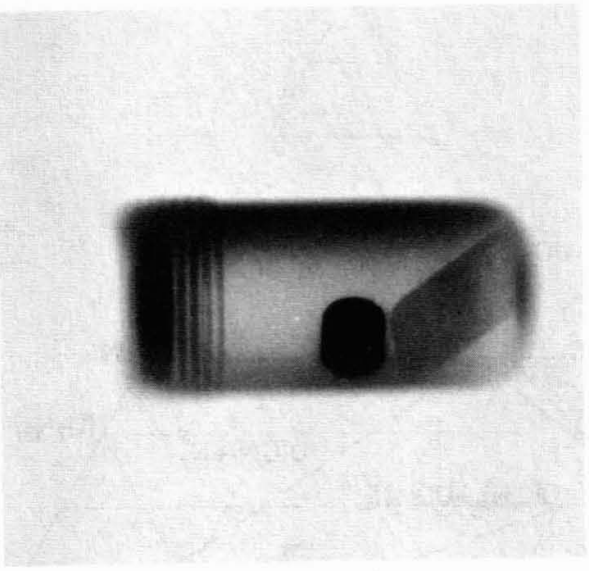

U_2C_3

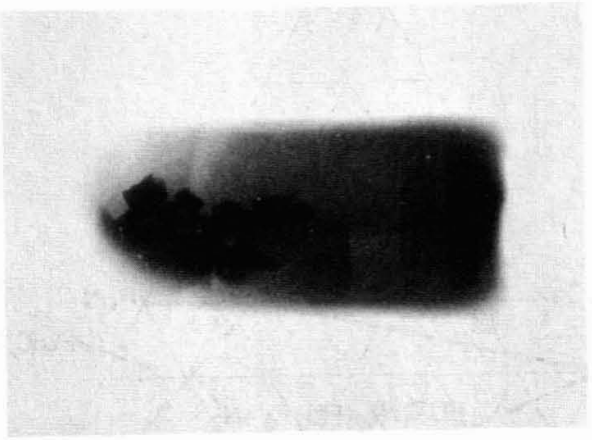

UC_2

FIG. 3

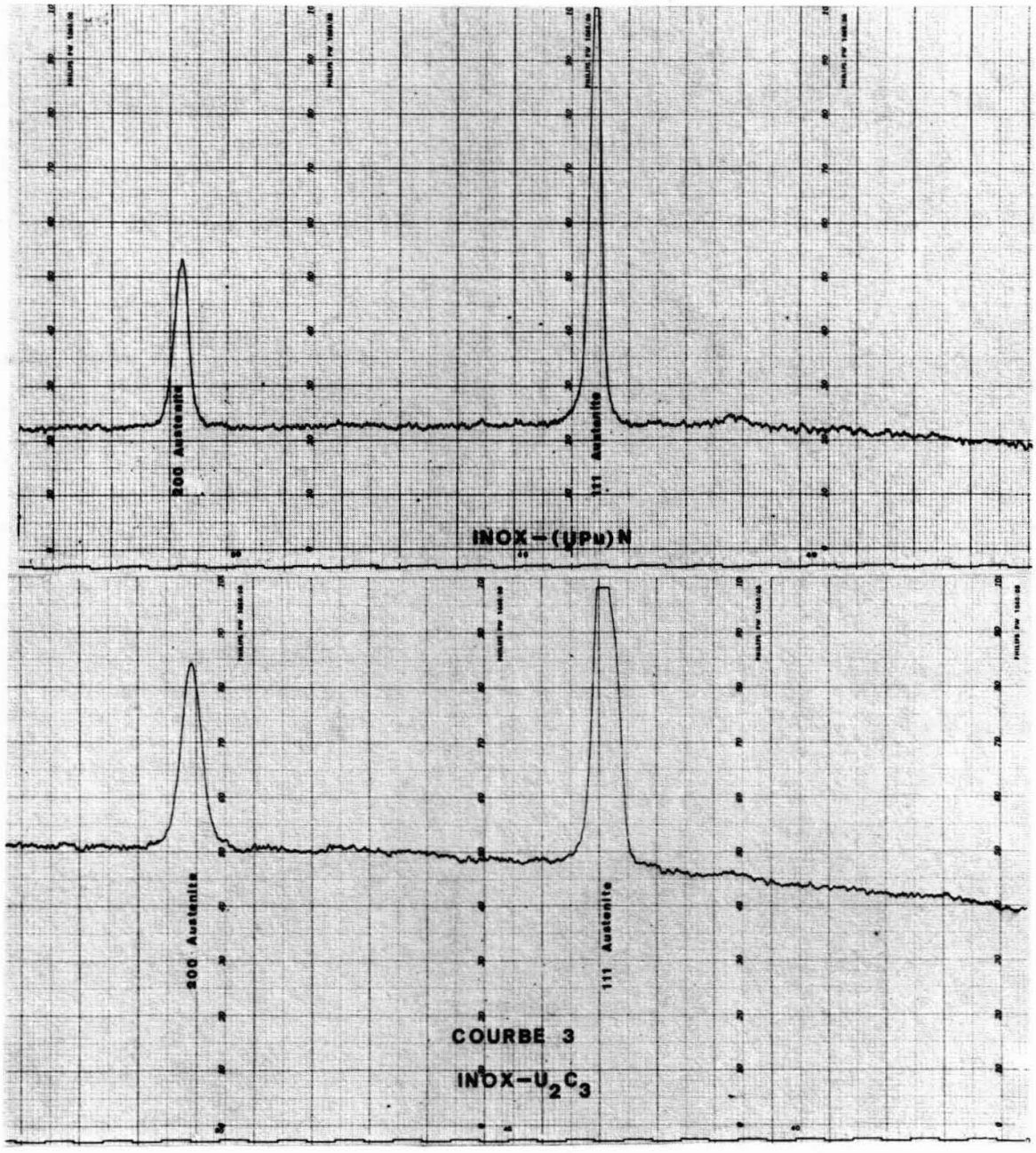
200 Austenite
111 Austenite
INOX–(UPu)N
200 Austenite
111 Austenite
COURBE 3
INOX–U_2C_3

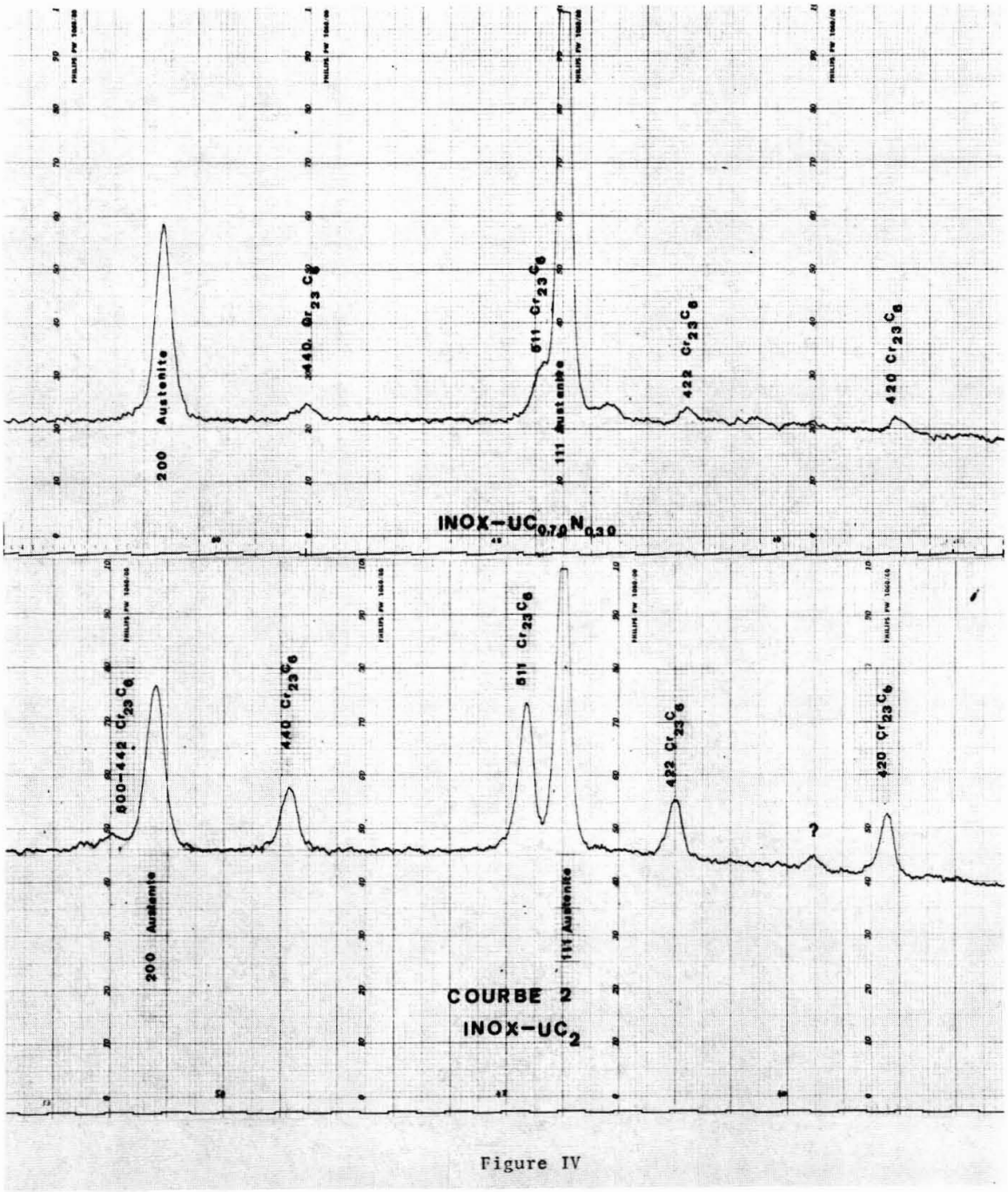
Austenite
200
440 $Cr_{23}C_6$
511 $Cr_{23}C_6$
111 Austenite
422 $Cr_{23}C_6$
420 $Cr_{23}C_6$
INOX–$UC_{0,7}N_{0,3}$
800–442 $Cr_{23}C_6$
440 $Cr_{23}C_6$
511 $Cr_{23}C_6$
422 $Cr_{23}C_6$
?
420 $Cr_{23}C_6$
200 Austenite
111 Austenite
COURBE 2
INOX–UC_2

Figure IV

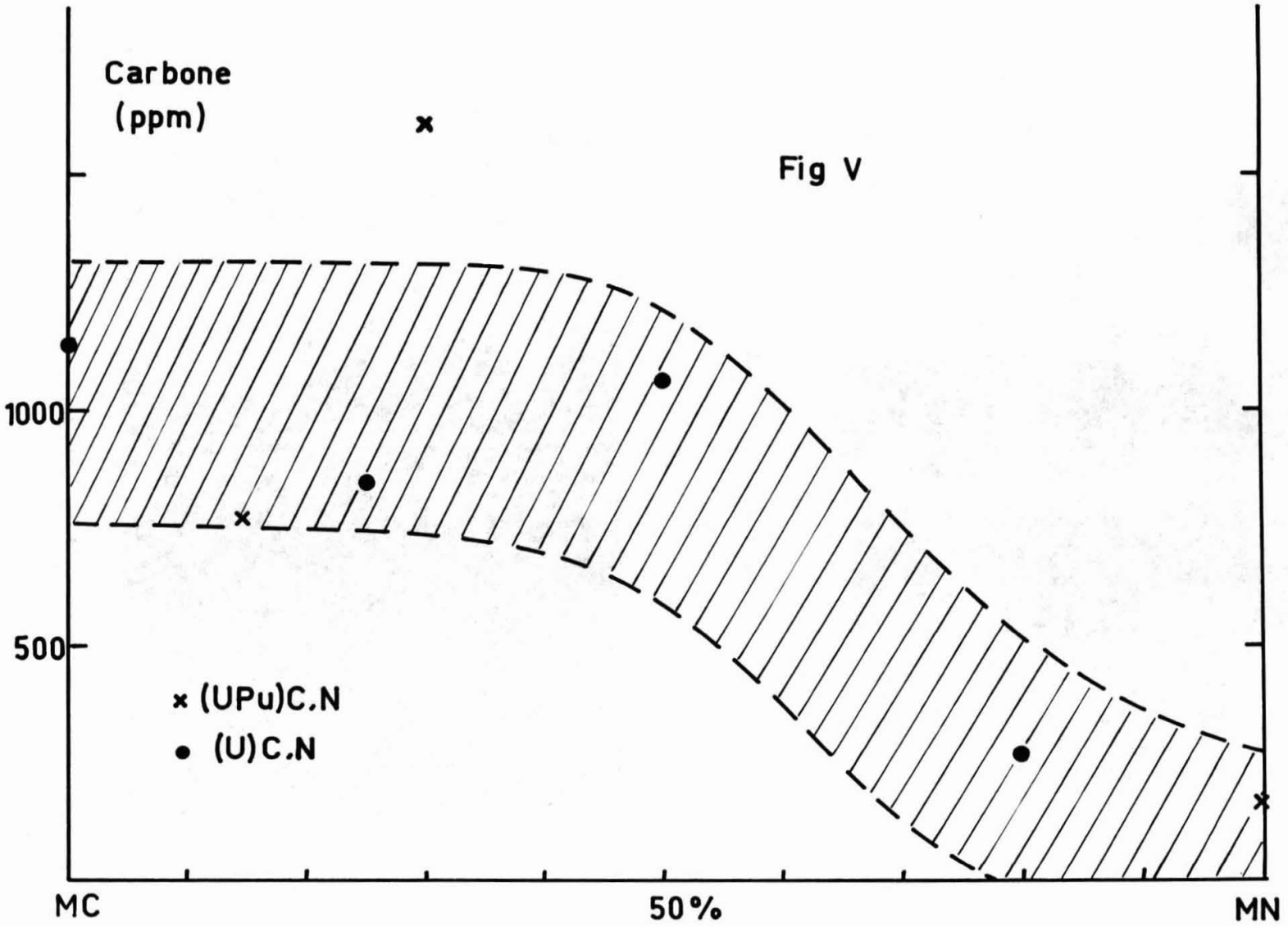
Carbone
(ppm)
Fig V
1000
500
× (UPu)C.N
• (U)C.N
MC
50 %
MN

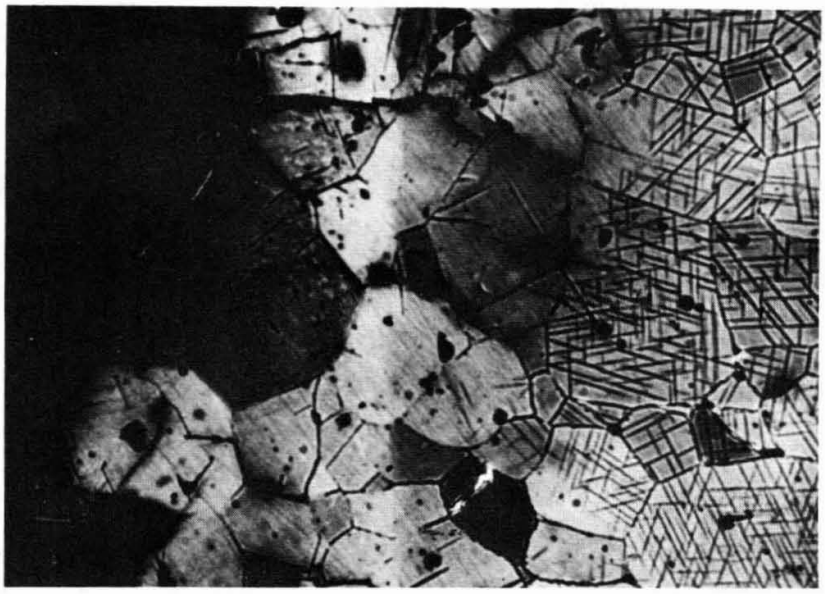

UC containing U C_2

note that UC_2 is leached out on the edge side

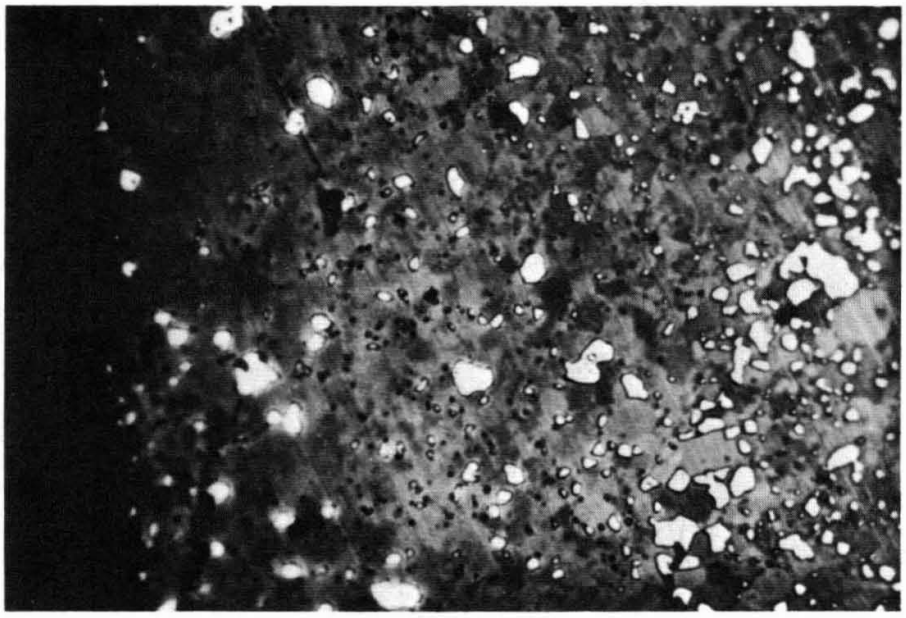

UC containing U_2C_3

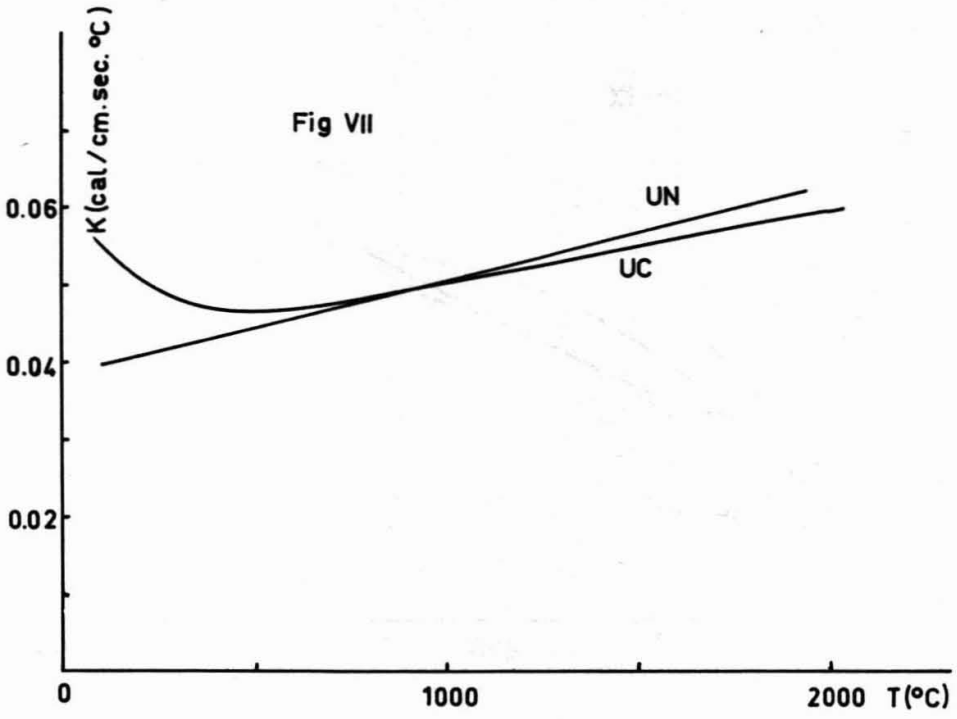
K (cal / cm. sec. °C)
Fig VII
UN
UC
0.06
0.04
0.02
0
1000
2000 T(°C)

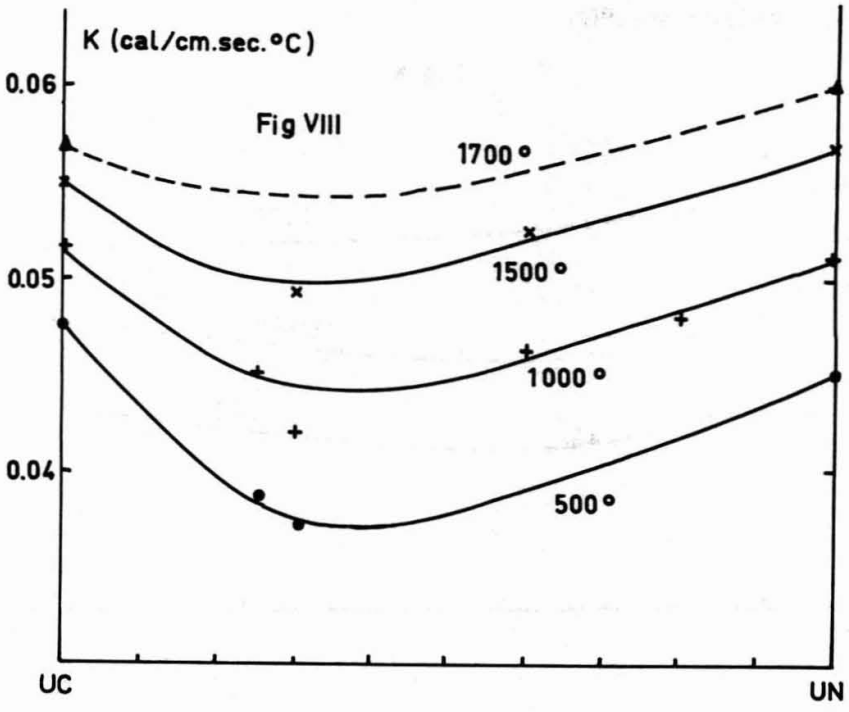
K (cal/cm.sec.°C)
0.06
Fig VIII
1700°
1500°
0.05
1000°
0.04
500°
UC
UN

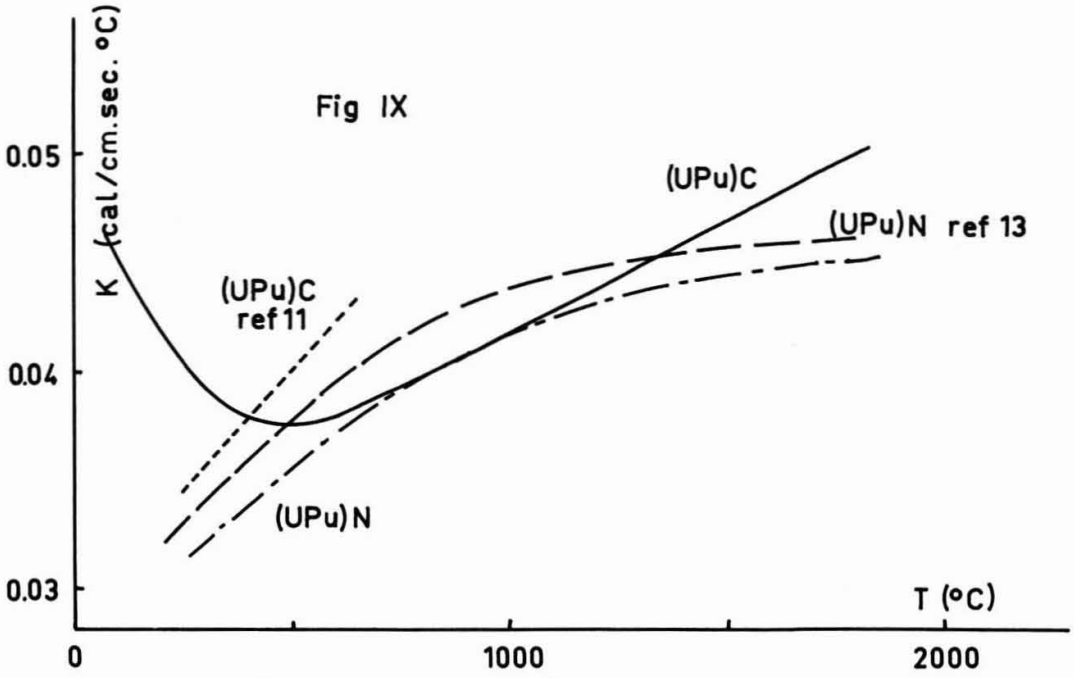
K (cal/cm.sec. °C)
0.05
0.04
0.03
0
1000
2000
T (°C)
(UPu)C
(UPu)N ref 13
(UPu)C
ref 11
(UPu) N

Fig IX

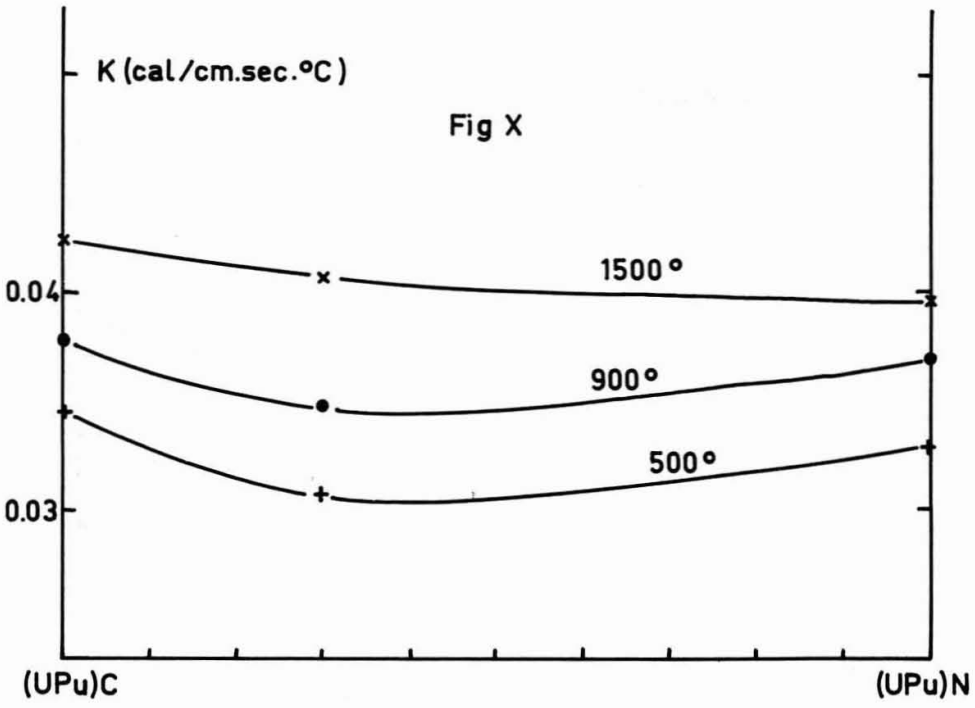
K (cal/cm.sec.°C)
0.04
0.03
1500 °
900 °
500 °
(UPu)C
(UPu)N

Fig X

URANIUM-PLUTONIUM NITRIDES: FABRICATION AND PROPERTIES

W. M. Pardue, F. A. Rough, and R. A. Smith

Abstract

Synthesis of nitride powders has been accomplished by a successive hydride-nitride-vacuum outgas treatment of the metallic elements. Densification of these powders into useful pellet or rod form can be accomplished by hot pressing or sintering. Properties of importance for reactor design have been measured and include volatilization tendencies relating to vapor-phase transport under thermal influences, thermal conductivity, and chemical stability of the fuels in contact with potential LMFBR (liquid metal fast breeder reactor) cladding and coolant materials. Grain-growth behavior of high-density specimens also has been determined.

William M. Pardue, Frank A. Rough, Roy A. Smith, Division Chief, Research Fellow, Project Leader; respectively, with Battelle Memorial Institute, Columbus Laboratories, 505 King Avenue, Columbus, Ohio.

Introduction

Those known or conjectured physical and chemical properties of (U,Pu)N indicate a strong potential for LMFBR-fuel applications. The fuel composition of primary interest is a solid-solution alloy of UN-20 w/o PuN. Those data reported herein were obtained on a Battelle-Columbus program that has the objective of establishing the potential of (U,Pu)N LMFBR fuels.* While other sites are engaged in similar research, the brevity of this paper precludes detailed discussion of data from those efforts.

Powder Synthesis

The majority of UN-PuN powders have been prepared either by the mechanical mixing of separately prepared PuN and UN powders or by direct gas-solid reactions on arc-cast uranium-plutonium buttons. To date, the mechanical mixing approach has received major attention at Battelle-Northwest (1) and Los Alamos (2), while arc-cast uranium-plutonium buttons have been used as feed material in most of the powder synthesis at Battelle-Columbus. Since the synthesis of both UN and PuN using a metal-hydride-nitride approach (a final U_2N_3 vacuum-decomposition heat treatment is required in UN synthesis[3]) has received rather widespread reporting, the description of powder synthesis will be restricted herein to the use of uranium-20 w/o plutonium feed material.

In the as-cast condition, uranium-20 w/o plutonium buttons appear metallographically as a severely microcracked metastable solid solution. In this condition the alloy is quite susceptible to oxidation and requires either protective storage or immediate processing after casting. The buttons are not amenable to direct nitriding and require an intermediate hydride step before subsequent reaction with nitrogen. Hydriding temperatures range from 200 to 400 C, while reaction of the hydride preparation with nitrogen proceeds quite rapidly at 650 C.

The rate of reaction is critical during the initial hydriding and nitriding stages. Both of these reactions are exothermic and, if they proceed too rapidly, will result in overheating and localized melting, an occurrence which usually results in a final powder product containing some particles that are deficient in nitrogen. The use of reduced (below 1 atm) hydrogen or nitrogen pressures combined with low furnace heating rates effectively circumvents this problem of overheating during initial hydriding and nitriding.

In the as-nitrided condition, the powders contain appreciable amounts of uranium sesquinitride (U_2N_3). Nitrogen contents of 6.0 w/o or above are typical (as opposed to a stoichiometric value of 5.55 w/o). While the formation of higher nitrides somewhat reduces powder homogeneity, lattice parameters indicate considerable alloying of UN and PuN. A 5-hr vacuum treatment at 1400 C has been effective in elimination of sesquinitride.

* Work performed under AEC Contract W-7405-eng-92.

Powder Densification

In general, UN, PuN, and UN-PuN alloys show similar densification characteristics during sintering and hot pressing. There is some indication that PuN may be slightly more amenable to sintering and hot-pressing densification than either UN or the mixed nitride alloys.

Hot Pressing

Both uniaxial and isostatic hot-pressing techniques are suitable for preparing bodies of good purity with densities approximately theoretical. The more efficient application of pressure in the isostatic hot pressing enables the densification of complex shaped specimens or specimens having high length-to-diameter ratios. Table 1 includes characterization data for material from a 3-in.-long by 0.5-in.-diameter $(U_{0.8}Pu_{0.2})N$ specimen that was isostatically hot pressed for 4 hr at 1600 C and 10,000 psi.

Table 2 includes densities and uniaxial hot-pressing parameters for several $(U_{0.8}Pu_{0.2})N$ specimens. The use of a barrier layer of tantalum foil for prevention of carbon diffusion from the graphite dies into the specimens is required when the hot-pressing temperature exceeds approximately 1600 C. Figure 1 shows a typical uniaxially hot pressed $(U_{0.8}Pu_{0.2})N$ microstructure containing some fine, secondary oxide inclusions.

There is one potential problem when nominal UN-20 w/o PuN powders prepared using a hydride-nitride-vacuum degas cycle on arc-cast buttons are then used as feed material for specimen fabrication by hot pressing. As prepared, these powders have a wide range in particle sizes with the different-size particles varying in both grain size and purity. If segregation of the different particle sizes occurs during handling, specimens hot pressed from the same powder batch may have markedly different microstructures.

Sintering

Sintering is of interest as a potentially economical approach for the densification of fuel pellets on a production scale. The difficulty posed here, however, is that UN, PuN, or mixtures of these two compounds are generally quite resistant to sintering. In the absence of any developed sintering aid for these materials, the approach of using an extremely fine powder has been required to obtain sufficient surface activity for sintering.

Table 3 includes results for ball-milled UN powders sintered for 3 hr under various conditions of time and temperature. The powders were wet ball milled for 16, 32, or 64 hr in a stainless steel mill containing tungsten carbide-cobalt balls and nanograde hexane. The results show that densities in the range of 95 percent of theoretical can be obtained by nitrogen or argon sintering at 1900 C. At 1500 C, vacuum sintering is more effective than argon or nitrogen sintering. Also, ball milling in excess of 32 hr apparently provides negligible improvement in densification.

Figure 2 shows a microstructure of Specimen 9 which was sintered to 93.5 percent of theoretical density at 1900 C in argon. The dark spherical pores have been slightly enlarged during metallographic etching.

Properties of Nitride Fuel Materials

A wide range of properties is of interest in the development of nitride fuel materials. Powder handleability, or oxidation resistance, and grain-growth characteristics are of importance in the fabrication of specimens of controlled purity and microstructure. In addition, fuel volatility, thermal conductivity, and compatibility with cladding and coolant materials are factors which are of prime importance in determining in-pile fuel performance.

Thermal Conductivity

The thermal conductivities of UN, PuN, and solid-solution $(U_{0.8}Pu_{0.2})N$ have been determined over the range of 300 to 1000 C. Thermal conductivities of these materials were determined by measuring the thermal diffusivity across disk-shaped specimens using a flash-laser heat-pulse technique and then calculating thermal conductivity values from the relationship

$$k = \alpha C_p \rho , \qquad (1)$$

where α is the thermal diffusivity in cm^2/sec, C_p is the specific heat in cal/(gm)(C), ρ is the density in gm/cm^3, and k is the thermal conductivity. In the absence of experimentally measured specific heats for PuN or (U,Pu)N solutions, the specific heat of UN was used in calculating the respective thermal conductivities. Specimen densities were corrected for volumetric thermal expansion using linear thermal expansion coefficients of 9.7, 11.2, and 9.8 ($\times 10^{-6}$ in./in./C) for UN, PuN, and $(U_{0.8}Pu_{0.2})N$, respectively. The thermal expansion value for $(U_{0.8}Pu_{0.2})N$ was that actually obtained for a $(U_{0.85}Pu_{0.15})N$ specimen.

The thermal conductivities calculated from thermal-diffusivity data and corrected to 100 percent of theoretical density are presented graphically as a function of temperature in Figure 3. As can be seen, the thermal conductivity of PuN is lower than that of UN with both materials showing a general increase in thermal conductivity with increased temperature. The reason for the discontinuity in the PuN curve at approximately 560 C is uncertain and may be indicative of a hypostoichiometric material (a similar discontinuity was noted for a specimen containing a slight trace of free plutonium metal) or of some more fundamental behavior of PuN.

Thermal-conductivity curves for two different $(U_{0.8}Pu_{0.2})N$ specimens are included in Figure 3. The lower curve was obtained for hyperstoichiometric material containing a slight amount of U_2N_3 and shows a leveling off in conductivity at 700 C. The upper curve was obtained for material containing only slight oxide inclusions

as a metallographically distinguishable secondary phase. The curve shows a discontinuity at approximately the same temperature as that noted for PuN and shows a leveling off in conductivity at 1000 C. Additional work is required before the difference in shape and magnitude of the two $(U_{0.8}Pu_{0.2})N$ thermal-conductivity curves can be explained.

Grain Growth

Grain growth in high-density solid-solution $(U_{0.8}Pu_{0.2})N$ specimens becomes rapid as the temperature exceeds approximately 1700 C. This is shown in Figure 4, which also includes, for comparison, grain-growth data for high-purity (300 ppm by weight oxygen) powder-metallurgy UN. While the temperature at which grain growth becomes appreciable is the same for both curves, the $(U_{0.8}Pu_{0.2})N$ appears more resistant to grain growth. It is not known whether this greater resistance is related to the secondary oxide inclusions present in the mixed nitride material or to some other factor.

Figure 5 shows a photomicrograph of a $(U_{0.8}Pu_{0.2})N$ specimen which received a 50-hr treatment at 1800 C. The as-fabricated microstructure of this material was previously shown in Figure 1. It is evident in comparing Figures 1 and 5 that the 1800 C heat treatment resulted not only in appreciable grain growth but also in apparently complete solution of secondary oxide inclusions.

Initial grain sizes for the UN and $(U_{0.8}Pu_{0.2})N$ specimens were 30 and 44 μ, respectively, while specimen densities were 99 percent of theoretical.

Volatility of PuN and (U,Pu)N

Effusion determinations have been made for PuN in a tungsten effusion cell with an orifice 1.1 mm in diameter. In addition, free evaporation experiments have been conducted on PuN and (U,Pu)N in the temperature range of 1523 to 1823 K. Effusion experiments have been performed at 1985, 2090, 2195, and 2300 K. No indication of a time-dependent transport was observed, and examination of the charge material after the experiments indicated that the overall composition had not markedly changed from the original single-phase PuN material. Using the assumption that the PuN vaporizes as elemental plutonium and nitrogen, an assumption which is somewhat supported by the observation that the condensate collected was metallic, the pressures of plutonium determined at the above temperatures are 6.1×10^{-6}, 2.3×10^{-5}, 8.0×10^{-5}, and 2.2×10^{-4} atm, respectively. Should the assumption of congruent vaporization be made, these values are high by approximately 3 percent. The above data were fitted to the following expression:

$$\log P_{Pu(atm)} = -22{,}900/T^{\circ}K + 6.30. \qquad (2)$$

Vacuum-fusion analysis of the PuN used in the vaporization studies indicated that the material contained nearly 2.8 mole percent PuO; however, this oxygen appeared to be in solid solution with the PuN based upon metallographic evaluation.

The solid-solution alloys of UN and PuN show lower volatiliities than unalloyed PuN. This is evident in Table 4 which includes results of free-evaporation weight-loss experiments on cylindrical PuN, UN, $(U_{0.85}Pu_{0.15})N$ and $(U_{0.8}Pu_{0.2})N$ specimens. In comparing the data at 1550 C, it is noted that weight losses for the $(U_{0.85}Pu_{0.15})N$ and $(U_{0.80}Pu_{0.20})$ alloys approximate one-fifth and one-fourth, respectively, of that for unalloyed PuN.

Again, assuming that PuN vaporizes as elemental plutonium and nitrogen, the vapor pressure of PuN calculated from these data at 1985 K is 3×10^{-6} atm and is in good agreement with the value of 6.1×10^{-6} atm determined by effusion techniques.

Compatibility

The objective of the compatibility effort has been to establish the reactivity of solid-solution $(U_{0.8}Pu_{0.2})N$ toward potential LMFBR cladding materials and sodium. Compatibility heat treatments between 700 and 1000 C have been performed using specimens with the fuel and cladding either separated by a 30-mil layer of sodium or in direct contact. Claddings investigated include Type 304 stainless steel, Type 316 stainless steel, ORNL modified stainless steel (essentially an 18-8 stainless steel with 0.155 w/o Ti), Incoloy Alloy 800, Inconel 625, and Nb-1 w/o Zr. Compatibility heat treatments utilizing UN and PuN with some of these same cladding materials were conducted, as were thermodynamic calculations to ascertain those claddings which might show the greatest tendency to react with UN or $(U_{0.8}Pu_{0.2})N$.

Included in Table 5 are some results of various compatibility heat treatments. The oxide layer noted on several of the fuel pellets in the sodium-bonded specimens is believed to reflect a gettering of oxygen from the sodium. Where Types 304 and 316 stainless steel have been investigated with UN, PuN, or $(U_{0.8}Pu_{0.2})N$ in the pressure-contacted or sodium-bonded capsules, compatibility has been excellent at 1000 C. Those claddings which show some tendency to react or form nonoxide layers on the fuel are the nickel-base Inconel 625 alloy, Incoloy Alloy 800, and the ORNL modified stainless steel.

Those reaction products noted between the nitride specimens and the above cited cladding materials have not been identified and, therefore, reaction mechanisms cannot be conclusively put forth. It is considered likely that the slight reaction between UN and ORNL modified stainless is related to reaction between excess nitrogen (U_2N_3) in the UN and titanium in the cladding alloy.

Summary

The synthesis of mixed nitride powders using a hydride-nitride-vacuum outgas approach on arc-cast uranium-20 w/o plutonium is readily accomplished. In the as-synthesized condition, these powders are partially alloyed and thus can be fabricated into chemically homogeneous bodies using relatively short times and moderate temperature for densification. Both uniaxial and isostatic hot pressing have been demonstrated as excellent approaches for fabricating high-density nitride bodies of good purity.

Of major significance toward improved economy in mixed-nitride fuel fabrication are the indications that high-density bodies can be attained by sintering of fine powders. With the application of this approach, the intimate mixing attainable during powder comminution enables the use of separately prepared PuN and UN powders.

The combination of high thermal conductivity and good compatibility with sodium and potential LMFBR cladding materials are particularly advantageous features of (U,Pu)N fuels. Grain-growth and volatility measurements indicate that thermally induced compositional or microstructural changes will be negligible at typical LMFBR operating temperatures of 800 to 1000 C.

REFERENCES

1. Weber, E. T., Personal Communication.

2. Leary, J. A., "Preparation and Properties of Plutonium Mononitride and Uranium Mononitride-Plutonium Mononitrides Solid Solutions", Paper presented at the 19th Pacific Coast Regional American Ceramic Society Meeting, October 26-28, 1966, Portland, Oregon.

Table 1. Results from X-Ray Diffraction, Chemical, and Metallographic Studies on Isostatically Hot Pressed $(U_{0.8}Pu_{0.2})N$[a]

Density, percent of theoretical	99.4
Microhardness, DPH (1000-g load)	622
Nitrogen Content, w/o	5.29
Oxygen Content, ppm	2261±184
Hydrogen Content, ppm	29±23
Lattice Parameter, Å	4.8920±0.0002
Oxide Inclusion, v/o	1.4
Oxygen Present as Oxide Inclusions, ppm	1200
Oxygen Present in Solid Solution, ppm	1060

(a) Hot pressed for 4 hr at 1600 C and 10,000 psi.

Table 2. Uniaxial Hot-Pressing Data for $(U_{0.8}Pu_{0.2})N$

Time, min	Temperature, C	Pressure, psi	Length:Diameter Ratio of Hot-Pressed Specimen	Hot-Pressed Density, percent of theoretical[a]
5	1850	18,000	2.54	98.6
5	1850	12,000	1.52	93.5
5	1850	18,000	3.05	97.1
5	1850	18,000	2.80	94.4
5	1900	23,000	3.05	99.8
5	1850	21,000	3.05	97.1
5	1850	18,000	2.72	99.5

(a) Measured and weighed densities after hot-pressed specimens were machined to shape.

Table 3. Sintering Results for Ball-Milled UN Powders

Specimen	Ball-Milling Time[a], hr	Sintering Parameters			Sintered Density, percent of theoretical
		Atmosphere	Temperature, C	Time, hr	
1	16	Vacuum	1500	3	77.8
2	32	Vacuum	1500	3	88.3
3	64	Vacuum	1500	3	88.1
4	16	Argon	1500	3	73.1
5	32	Argon	1500	3	67.6
6	64	Argon	1500	3	68.9
7	16	Argon	1900	3	92.0
8	32	Argon	1900	3	94.4
9	64	Argon	1900	3	93.5
10	16	Nitrogen	1500	3	75.0
11	32	Nitrogen	1500	3	76.0
12	64	Nitrogen	1500	3	76.2
13	16	Nitrogen	1900	3	93.4
14	32	Nitrogen	1900	3	94.8
15	64	Nitrogen	1900	3	96.5

(a) Particle size less than 4.5-μ diameter.

Table 4. Data for PuN, UN, and UN-PuN Volatility

Material	Temperature of 5-Hr Vacuum Treatment, C	Nitrogen Content, w/o		Weight Loss g/cm^2
		Before Heat Treatment	After Heat Treatment	
PuN	1550	5.24	5.20	0.0924
PuN	1450	5.33	5.31	0.0207
PuN	1350	5.33	5.30	0.0031
PuN	1250	5.33	5.34	0.0005
$(U_{0.85}Pu_{0.15})N$	1550	5.34	5.42	0.0148
$(U_{0.8}Pu_{0.2})N$	1550	--	--	0.0213
$(U_{0.8}Pu_{0.2})N$	1450	--	--	0.0013
$(U_{0.8}Pu_{0.2})N$	1400	--	--	0.0008
UN	1600	--	--	0.0045

Table 5. Compatibility of Nitride Fuels With Claddings

Fuel	Cladding	Time, hr	Temperature, C	Results
$(U_{0.8}Pu_{0.2})N$[a,b]	Type 304 stainless	1000	1000	No reaction
	Nb-1 w/o Zr	1000	1000	No reaction
	Sodium-bonded Type 304 stainless	3000	1000	Less than 5 μ of oxide on fuel
	Sodium-bonded Nb-1 w/o Zr	1000	1000	Less than 5 μ of oxide on fuel
	Sodium-bonded molybdenum	100	1200	Less than 5 μ of oxide on fuel
PuN[a]	Type 316 stainless	1000	1000	No reaction
	Incoloy Alloy 800	1000	1000	No reaction
	Inconel 625	1000	1000	Less than 5 μ of nonoxide on fuel
	Sodium-bonded molybdenum	100	1200	Less than 5 μ of oxide on fuel
UN[b,c]	ORNL modified stainless	1000	1000	Less than 5 μ of nonoxide on fuel
	Incoloy Alloy 800	1000	1000	Spotty 5 μ of nonoxide on fuel
	Inconel 625	1000	1000	Spotty 5 μ of nonoxide on fuel
	Sodium-bonded molybdenum	5	1400	No reaction
	Sodium-bonded 304 stainless	1000	1000	No reaction
	Sodium-bonded 316 stainless	1000	1000	No reaction
	Sodium-bonded ORNL stainless	1000	1000	Less than 5 μ of nonoxide on fuel
	Sodium-bonded Incoloy Alloy 800	1000	1000	10 μ of nonoxide on fuel
	Sodium-bonded Inconel 625	1000	1000	5 μ of nonoxide on fuel

(a) Contained approximately 2000 ppm oxygen.
(b) Slightly hyperstoichiometric, second-phase nitride.
(c) Contained less than 200 ppm oxygen.

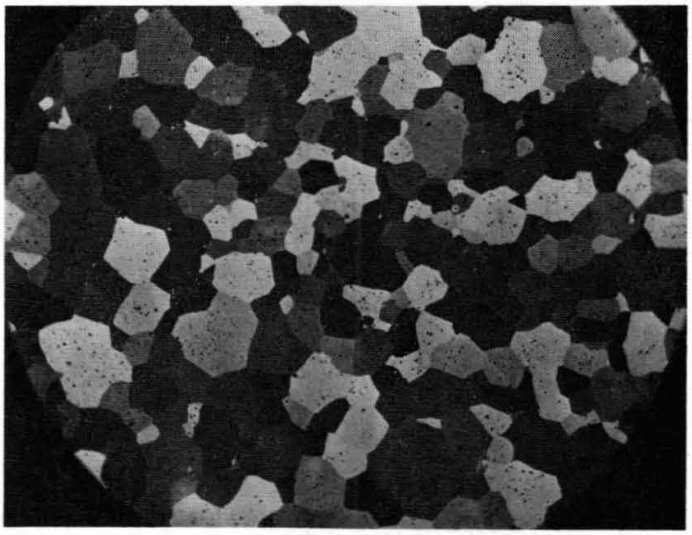

125X Etched PL2758

FIGURE 1. MICROSTRUCTURE OF $(U_{0.8}Pu_{0.2})N$ DENSIFIED BY UNIAXIAL HOT PRESSING FOR 8 MIN AT 1800 C AND 18,000 PSI IN 1 ATM OF NITROGEN

Average grain diameter is 44.0 μ. Fine oxide inclusions are noted in the microstructure. Oxygen, hydrogen, and nitrogen analyzed at 1142 ppm by weight, 27 ppm by weight, and 5.20 w/o, respectively.

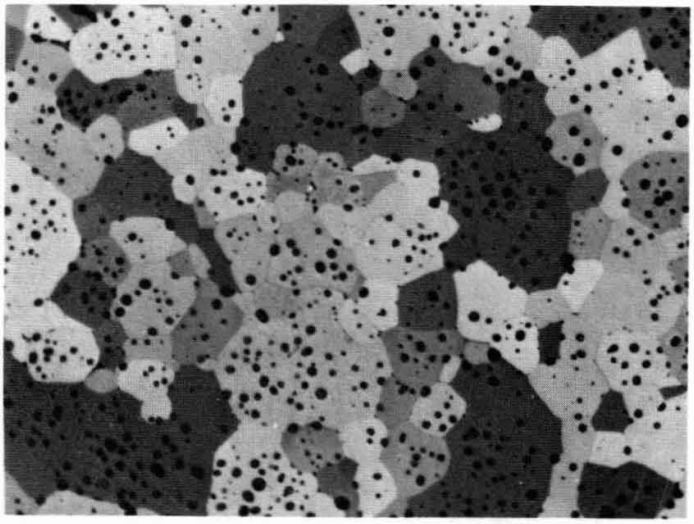

750X Etched 7B804

FIGURE 2. MICROSTRUCTURE OF UN SINTERED FOR 3 HR AT 1900 C IN ARGON TO 93.5 PERCENT OF THEORETICAL DENSITY

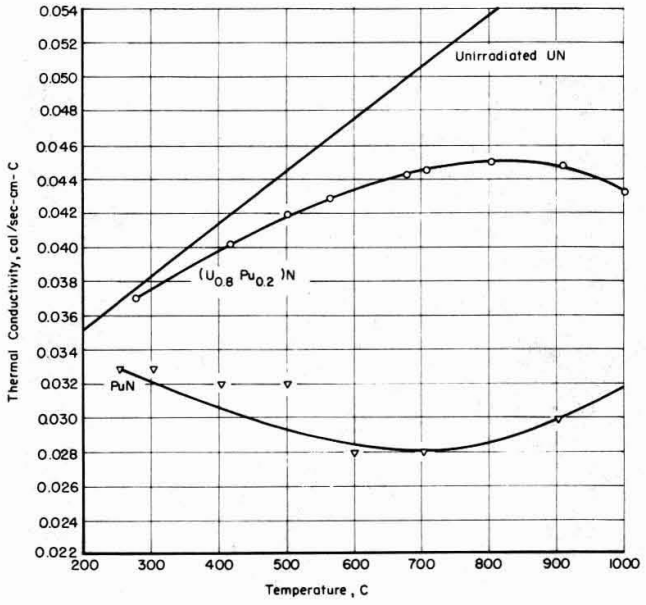

FIGURE 3. THERMAL CONDUCTIVITIES OF UNIRRADIATED UN, PuN, AND $(U_{0.8}Pu_{0.2})N$

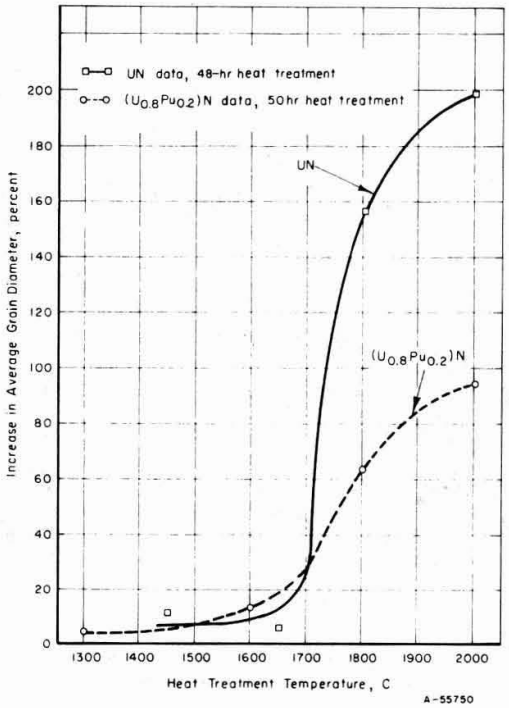

FIGURE 4. GRAIN GROWTH VERSUS HEAT-TREATMENT TEMPERATURE FOR UN AND $(U_{0.8}Pu_{0.2})N$

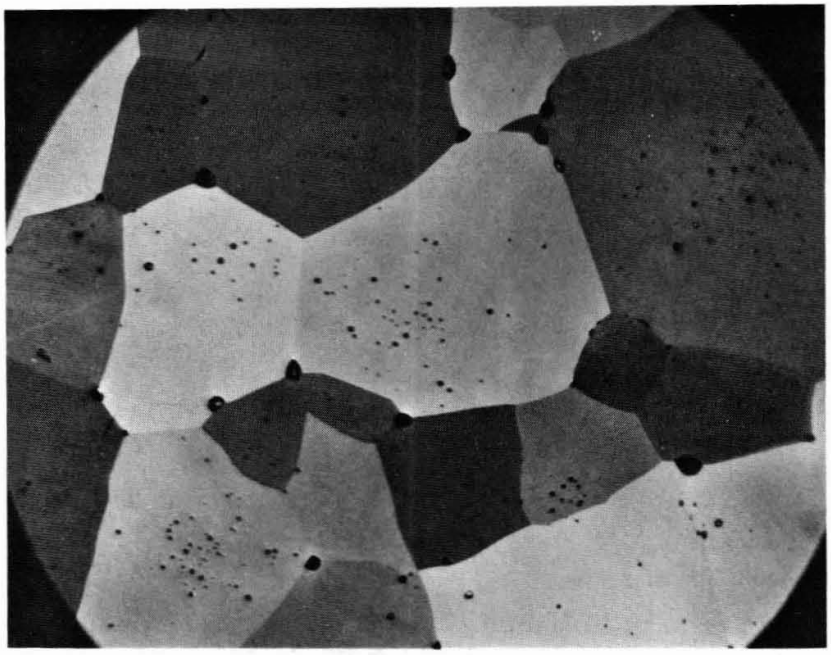

250X Etched PL2830

FIGURE 5. MICROSTRUCTURE OF $(U_{0.8}Pu_{0.2})N$ AFTER A 50-HR HEAT TREATMENT AT 1800 C IN A SEALED TUNGSTEN CAN

See Figure 1 for the as-fabricated microstructure. The heat treatment has effected essentially complete solution of the secondary oxide particles and increased the average grain diameter from 44.0 to 72.2 μ.

FRENCH IRRADIATION EXPERIENCE WITH MIXED OXIDE FUELS FOR FAST-REACTOR APPLICATION

J. P. Mustelier

Abstract

An irradiation program of UO_2 PuO_2 mixed oxides has been performed from 1962 to 1966 in the thermal reactor EL 3 in order to design the Rapsodie fuel element. Post-irradiation examinations have shown that the design of the fuel element was realistic.
The reactor Rapsodie was raised to nominal power in April 1967 and an examination program on complete subassemblies was initiated in May 1967. To design and test the reference fuel of the power fast reactor Phenix, an irradiation program in both fast and thermal flux was initiated in the beginning of 1966.

J. P. Mustelier Chef de la Section du Plutonium Irradié
Association EURATOM-CEA Neutrons Rapides, Centre d'Etudes Nucléaires de Fontenay-aux-Roses, B.P. n° 6
Fontenay-aux-Roses - 92 - France.

Introduction

At the Commissariat à l'Energie Atomique, the behaviour under irradiation of UO_2 PuO_2 mixed oxides, is studied from the angle of their utilization as fast reactor fuel. The main purpose of the first series of experiments was to develop and check the performance of the fuel of the first core of Rapsodie (1). The experiments have now ended, the reactor was raised to full power in April 1967 and an initial irradiated fuel assembly is currently being examined.

To develop the fuel for Phenix, which is a 250 MW electric fast reactor project, a much more extensive program of irradiation tests than the last one has been prepared and is now being executed.

Behaviour under irradiation of Rapsodie's fuel elements

Originally two fuels were envisaged for Rapsodie ; a metallic fuel (U-Pu-Mo alloy) and an oxide fuel UO_2-PuO_2. As a result of the fabrication trials, the study of the metallurgical and physical properties, and of the irradiation trials, the U-Pu-Mo alloy, was finally abandoned because of incompatibility with stainless steel (forming of a liquid phase when 600° C was reached) and excessive fuel swelling. In 1963 a fuel element was chosen for Rapsodie composed of sintered UO_2-PuO_2 mixed oxide pellets in stainless cladding. The design and dimensions of the assembly and of the fuel pin were fixed. In order to analyse the behaviour of full scale pins under conditions similar to those foreseen in Rapsodie, a thermal neutron irradiation program was carried out in the EL 3 reactor. Fig. 1 shows the design of the Rapsodie pin which has the following characteristics :

Fuel : Sintered UO_2-PuO_2 with a 25.91 % PuO_2 content
- Diameter of pellets : 5.57 mm
- Density : 96 % of theoretical density
- Oxide-Clad diametral gap : 230 $\pm$ 80 μ
- Stoichiometry : $1.96 < \frac{O}{M} < 1.99$

Cladding : Type 316 L stainless steel with integral helicoïdal fin
- Filler gas : Helium
- Column of pellets : spring retained

Nominal operating conditions at 20 MW are the following :
- maximal specific power : 1310 w/cm^3
- maximal conductivity integral : 26 w/cm
- sodium inlet temperature : 410° C
- sodium outlet temperature : 500° C
- hot spot temperature of cladding : 650° C

The preceding data served as a reference to fix the thermal

neutrons irradiation parameters. Eighteen prototype pins were irradiated in the EL 3 reactor from 1963 to 1967. These pins were composed of sintered mixed oxide UO_2-PuO_2 pellets with various PuO_2 contents : 11 %, 20 % and 25.91 % by weight. The cladding was either 304 L or 316 L stainless steel. Design characteristics were varied from one pin to an other.

- oxide density : 84 to 97 % of theoretical density
- clad thickness: 0.2 to 0.45 mm
- diametral gap between oxide and clad : 30 μ to 290 μ
- clad filler gas : Helium or Argon
- capsule column retaining system : blocking by rigid tube or flexibly by spring

The stoichiometry of the oxide varied from 1.97 to 2.01 according to the case.

During irradiation each pin is enclosed in a leak proof capsule filled with sodium. The temperature of the sodium is measured by one or more thermocouples. The stainless steel capsule is in turn placed in a Zircalloy tube forming a sufficiently adequate heat barrier to obtain a temperature of 500° C to 650° C on the clad at the linear powers foreseen. Burn up rates are computed from the activity of 1 % Co. Co-Al alloy flux monitors fitted round the pins and the average conductivity integrals are deducted from preceding irradiations.

The results of the post irradiation examination of these pins are given below together with the results obtained on a first Rapsodie irradiated subassembly.

Stability of The Pellet Column

Axial Stability

The pins were examined radiographically after irradiation. In every case the overall pin length is unchanged wether the column of pellets is rigidly or spring secured.

If spring secured, the oxide columns elongate slightly by irradiation and this varies haphazardly, pin to pin from 0.5 mm to about 5 mm. It seems possible to distinguish the two following cases.

Low Conductivity Integral (central oxide temperature under 1700° C), Short Irradiation Time, Little Heat Cycling.

This is particulary so in the case of the 37 pins from the first Rapsodie subassembly which was examined after irradiation to 150 MWD/t at a central temperature of 1700° C max. Elongation of the oxide columns ranged from 0.2 to 0.8 mm and was to be found mainly in the gaps between the flat sides of the pellets. This effect is shown in the radiograph of Fig. 2a.

Higher Conductivity Integral, Appreciable Irradiation Time, Much Heat Cycling.

The elongation varies by 1 to 5 mm from one pin to the next, but fuel column do not grow any more when the burn up is raised from 3, 000 to 22, 000 MWD/t.

With increased irradiation, the gaps between the pellets tend to disappear and no longer provides a guide as to the elongation of the column and the pellets are welded to each other through the central zone. Fig. 2b is a radiograph of the upper part of pin n° 7. The central temperature is 1750° C, the burn up 4000 MWD/t and an increase in length of the fuel column of 4 mm has been measured. Al_2O_3 markers placed in some columns made it possible to see that the elongation rate of the column increases the closer one gets to the positioning spring.

The elongation of the pellet columns is therefore a phenomenon that appears as soon as irradiation begins and then saturates out. It is closely related to the phenomenona of thermal expansion of the column, fragmentation of the pellets and the inter-welding of pellets. In none of the cases was very great inter-pellet gap observed. It would seem, on the contrary, that such gaps tend to disappear at high burn up.

Evolution Of Initial Oxide-Clad Gap - Distribution of voidage in the Oxide.

The nominal diametral gap of Rapsodie's fuel pin is 230 μ +80 μ and contains helium. The initial gap of the pins irradiated by thermal neutrons was between 30 and 290 μ according to the case. After irradiation micrograph cross-sectional measurements of the gaps between the oxide and the cladding were made after vacuum loading with araldite, a polymerisable resin.

In every case it was observed that the initial gap diminishes down to 30 to 40 μ in all the pins that have been irradiated for a sufficient length of time. The two following cases may be distinguished.

Pins With a Central Temperature Under 1700° C.

From the start of irradiation the pellets crack, thus reducing the gap. In the Rapsodie subassembly, after an irradiation of six hours at core temperatures of 1650 to 1700° C, the diametral gap drops from 190 μ to 140 μ. Fig. 3 shows a micrographic section of an irradiated Rapsodie pin (central temperature 1650° C - τ = 150 MWD/t - I = 26 w/cm). The radial gap between oxide and cladding is of the order of 70 μ. With increasing irradiation as well as thermal heat cycling, the gap continues to decrease to a minimum value of about 40 μ.

When irradiation continues for a sufficient length of time, the cracks were found to disappear in the grain growth area. Fig. 4a shows the micrographic structure of the central zone of pin n° 8

(central temperature 1650° C - τ = 21, 500 MWD/t - I = 20, 6 w/cm). A very great grain boundary porosity is noticeable. Fig. 4 b shows the formation of this porosity by sintering of a crack, leaving holes at grain boundaries. The disappearance of the gap, through the crack and crack disappearance mechanics, gradually provokes very great grain boundary porosity in the equiaxed grain growth zone and the zone of columnar small grains. Therefore considerable de densification of the oxide is noticed in the central region with porosity increasing as the center is approached. In the case of Fig. 4 for example, the average density of the oxide of this pin dropped from 98 % to 92. 5 % of the theoretical, and in the central zone the density of the oxide is only 75 % to 80 % of the theoretical.

Pins With a Central Temperature Exceeding 1750° C

Here also the gap disappears by oxide cracking. However, these cracks are very unstable except in the peripheral zone. The porosities migrate to the center of the oxide by an evaporation condensation process ; columnar grains form and a central void that appears to increase with the increase in linear power. This effect can be seen in the macrographic sections of Fig. 5. The average density of the oxide increases instead of dimishing.

It should be noted, however, that even when the linear power is very high, the gap between oxide and cladding does not disappear very quickly. This is what may be observed on pin n° 27, which was irradiated for 4 1/2 hours with an initial Argon filling of 190 μ at a maximum linear power of 670 W/cm (maximum conductivity integral = 45.8). The oxide melted, slumping to the lower part of the pin. Fig. 6 shows two macrographic sections of this pin, one of the upper part of the pin with a central hole, and the other one of the lower part of the pin, entirely filled with melted oxide. Fig. 7 shows the corresponding micrographic aspect of the two sections. In both cases the diametral gap is still 150 μ at the end of irradiation.

Heat Performance Of The Fuel - Evolution Of the Oxide's Structure

The main novelty of Rapsodie's fuel lies in the use of dense non rectified sintered pellets with a large gap of up to 310 μ between oxide and cladding. The question was posed as to the value of the heat exchange coefficients between oxide and cladding as well as the conductivity of the oxide during de densification. None of the experiments were carried out with thermo couples in the oxide. The temperatures were evaluated by the following hypotheses :

a) It is assumed ; in the manner of Bates (2) that the outside limit of the small columnar grains in irradiation extending over more than a few days, corresponds to 1650° C in temperature.

b) This value is checked against a temperature reference mark obtained by comparing the equiaxed grain growth with the published kinetics (3), (4), (5). This temperature reference mark is used mostly for short time irradiation extending from a few hours to a few days.

c) The temperatures are calculated by using the conductivity integral = f (Θ) curve plotted for UO_2 - 20 % PuO_2 by G.E. (6).

d) If the density of the oxide strays from the 95 % value, a porosity correction of the shape $k = k_{th} (1 - 2p)$ is applied to the heat conductivity (7).

e) The conductivity integral is corrected of the flux depression and of the forming of the central void.

These hypotheses are open to question, of course. In particular, the exchange coefficient obtained by this process may possibly represent the minimum value reached during irradiation.

Several cases were considered.

High Density Oxide - Large Gap Between Oxide and Cladding.

Fig. 5 shows a number of pins of increasing central temperatures. Table I indicates the characteristics of some of them as an example.

As will be noticed from Fig. 3 and especially from the micrograph studies, the oxide of the Rapsodie pins irradiated for about six hours did not undergo any change in structure, nor was there any grain growth, and pins 7 and 8 underwent significant de densification. Pin 7 shows a small central void surrounded by a crown of small columnar grains. Pin 8 has no central void and only a few small columnar grains (Fig. 4). Pin 9 has a large central void (Fig. 5) surrounded by a large crown of columnar grains. The central void contributes to lowering the conductivity integral.

On the basis of the hypotheses explained above, the in fuel temperatures were evaluated as well as the exchange coefficients between the oxide and the can. The results are given in Table II.

Relatively good concordance is observed, particularly between pins 7, 8 and the Rapsodie pin, the oxide clad gap of which has not yet disappeared. It would seem that the temperature drop provoked by the decrease of the oxide clad gap is offset by the rise due to the helium becoming polluted by the Xe and the Kr and to oxide de densification.

Low Density Oxide - Large Gap Between Oxide and Clad

Two pins (n° 5 and 6) containing sintered pellets, density 86 % of the theoretical and an initial gap of 270 μ were irradiated at linear powers of 385 and 460 W/cm. Fig. 5 shows that in pin 6

there was considerable densification in the fuel, gap disappearance, large central void formation. Using the hypotheses put forward earlier, the exchange coefficients were calculated equal to 0.25 and 0.4 W/° C. cm^2. From the detailed analysis of the relative offsetting of the crown of columnar grains and of the central void, it may be assumed that the heat exchange coefficient thus calculated improves rapidly when irradiation continues and the gap disappears.

The poor heat exchange coefficient at the beginning of irradiation has been attributed to degassing of the porous pellets when the reactor was raised to full power. These pellets had been stored for a fairly long time in glove box atmosphere before canning.

High Density Oxide - Argon Filler Gas

Three pins (n° 2 - 27 and 28) were irradiated at different powers (Table III).

The examination of the three pins produced the above coefficient. The oxide of pin 27 melted and slumped, thereby completely filling the lower part of the pin, leaving a central void in the upper part (Fig. 6). Fig. 7 shows a micrograph view of the top of this pin where the liquid oxide has disappeared and one of the lower half where the oxide has solidified in the shape of a porous central zone. It has been observed that the oxide-clad gap diminished but little during the fusion experiment which lasted several hours.

High Density Oxide, Small Gap, Helium Gas Filler

The oxides temperatures obtained by micrographic examination of pins irradiated for more than a month differ very little from those of large gap pins of which the initial filler gas is helium. This clearly shows that from a heat exchange stand point the gap disappearance, which increases heat transfer, is offset by fission gas pollution of the helium, which lowers conductivity.

Release Of Fission Gases

The gases contained in the gas plenum of some pins were recovered. Data are contained in table IV.

These data indicate that :

a) The higher the conductivity integral and the burn up, the greater are the amounts of gas released.

b) In point of fact, the study of sections through these pins enables the conductivity integral to be corrected of the central void and it observed (assuming that cladding temperatures are identical, which is an approximation) that the central temperatures of the various pins vary little from one to the next. However, the greater the central void, the greater the amount of high temperature fuel (above 1650° C) where gas release is total.

c) The cladding temperature of pin 30 is 100° C higher than the

other pins. This temperature increases appreciably the volume of the oxide above 1650° C. There is a correspondingly great fission gas release.

d) The cladding of pin 29 and pin 31 ruptured (hot spot in the capsule). The sodium in the capsule entered the pin. The fission gas release was measured by puncturing the capsule. The effect of the sodium in the pin is complex and not entirely clear, but the micrograph studies seem to show that the following damage is caused (1) :

1 - Inter-granular attack of the oxide of the periphery of the pellets (which probably provokes the release of gases trapped on the grain boundaries).

2 - During heat recycling (from ambiant temperature), ejection outside the pin of fuel from the periphery of the pellets.

3 - Deterioration of heat exchanges and general temperature increase of the oxide.

All these effects bring about an almost total release of fission gases as well as the shifting of some fission products (Ru^{106}).

Conclusions

The Rapsodie Fuel Element

The purpose of the preceding experiments was limited to testing the fuel element of Rapsodie up to 30,000 MWD/t. To a certain extent they were upset by cooling faults in the capsule. The successful tests however enabled a fairly detailed analysis of the behaviour of the fuel. It was observed that the column of pellets elongates slightly leaving gaps between them. At the same time one observes a gradual disappearance of the gap between the oxide and the cladding and the pellets becoming wedged against the cladding. When the central temperature does not exceed 1650° C to 1700° C, the disappearance of the gap can be associated with de densification in the oxide particularly in the grain growth zone. The release of fission gases is very sensitive to linear power and particularly to the volume of the zone exceeding 1650° C. In the Rapsodie pins, the volume of this zone is not very great if the reactor operate at 20 MW. Therefore, from the results obtained one may consequently foresee moderate gas release up to 25,000 MWD/t, if irradiation continues of the present power level.

All these facts go to show that the fuel of Rapsodie is assured of operating correctly up to 25,000 MWD/t.

Limitations Of The Rapsodie Fuel

On studying the published results (8), (9) a first limitation of

the Rapsodie fuel element may come from the release of fission gases. If the fact that the fission gases release rate increases with burn up is taken into account, a calculation of clad creep at a 60 % fission gas release and a cladding hot spot of 650° C can be made. If can then be observed that the maximum burn up causing creep distortion of 0.1 to 0.2 % is equal to 45,000 MWD/t. Consequently one may expect a limitation to be on the hotest of these fuel elements.

The second problem concerns swelling at high burn up about which we have no experience. The Rapsodie fuel element has a high smeared density (89 %) a factor which at first sight seems unfavourable to accommodate the swelling. From the results presently published on this problem, (8), (10) one may assume that the power level of Rapsodie's fuel elements are unfavourable for swelling, ie, core temperature not enough to release much gas and large oxide zone volume between 1400 and 1700° C. However, no model exists at the moment to clearly anticipate the behaviour of the Rapsodie pin under swelling.

In the coming years, the study of many Rapsodie irradiated fuel pins should make it possible to provide clear answers to these questions of primary interest.

Study Of The Phenix Fuel Element

The C.E.A. is presently studying Phenix, a fast demonstration reactor of 250 MWE (11). The reference fuel element has points in common with that of Rapsodie, particularly :

a) a sintered UO_2-PuO_2
b) a 316 stainless steel clad

Some characteristics have been foreseen with higher values :

a) maximal linear power : 430 W/cm
b) sodium outlet temperature: 560° C
c) clad hot spot temperature : 700° C
d) burn up : 50,000 MWD/t

To reach these objectives, three essential modifications are proposed :

a) lowering of the "smeared density" to 80 % of the theoretical density
b) increase in the volume of "gas plenum"
c) improvement in the high temperature mechanical properties of the steel.

An irradiation program of fuel elements and of samples is being prepared. To conclude we give below some indications on the experiments that have been planned.

High Burn-up Irradiation Experiments With Thermal Neutrons

Twenty samples are currently being irradiated in EL 3 and Siloe. Smeared densities of 89 %, 80 % and 70 % are studied at

two linear powers (240 and 440 W/cm). Burn up reached in June 1967 amounted to 40, 000 MWD/t and irradiation is to continue up to 100, 000 MWD/t.

A second batch of 24 samples is to be placed in pile during the first half of 1968.

Short Time Irradiation Experiments

A thermal performance study program of the low density oxide fuel elements in a power zone bracketing the reference value, is currently being undertaken. It comprises irradiation extending from a few hours to several months of 48 sintered oxide samples of various densities, with and without central voids, and of vibration compacted oxides. Various gaps between oxide and cladding and various stoichiometry (1.92 to 2.02) are being tested. Some samples are sodium filled ; and 8 samples have a thermocouple in the center of the oxide.

Irradiation Experiments in Rapsodie

Four special assemblies comprising 27 fuel pins each, have been placed in Rapsodie in July 1967.

The main characteristics of these fuel elements are :

a) pellets : two densities - 80 and 85 % of theoretical density, obtained either by spread lowering of the density of the pellets or by central void.
b) diameter of the pellets : 6.05 mm
c) diametral gap between oxide and clad : 0.2 mm
d) filler gas : Helium
e) stoichiometry : O/M = 1.96
f) cladding : stainless steel and Hastelloy X, thickness : 0.45 mm
g) maximal linear power : 400 W/cm
h) maximal nominal outlet temperature of Na : 600° C
j) burn up : 30, 000 50, 000 and 70, 000 MWD/t.

Other experimental subassemblies are being designed and will be inserted in Rapsodie in the coming year. The results of this irradiation program, and particularly of the statistical experiments in Rapsodie, shoud enable the essential specifications of the fuel element of Phenix to be fixed by the end of 1969.

REFERENCES

1. H. Mikailoff, J. P. Mustelier, J. Bloch, L. Ezran, L. Hayet, Résultats d'irradiation d'éléments combustibles en oxyde mixte UO_2-PuO_2. Rapport C.E.A. - R. 3066 - Septembre 1966

2. J. L. Bates, Thermal conductivity of UO_2 improves at high temperatures Nucleonics Vol. 19, n° 6, June 1961, p. 83

3. J. R. Mac Ewan - V. B. Lawson, Grain Growth in Sintered UO_2, J. Am. Ceram. Soc. Vol. 45, n° 1, p. 42

4. H. Hausner, "Grain Growth of UO_2" Part. I - August 1963 - GEAP 4315

5. H. Stehle, Korn Wachstrum von UO_2 Keram. Werstoffe in Reaktorbau. Baden Baden Nov. 1962

6. General Electric, Liquid metal fast Breeder reactor design study GEAP 4418

7. M. J. F. Notley - J. R. Mac Ewan, "The effect of UO_2 density on fission product gas release and sheath expansion" March 1965 - AECL 2.230

8. H. Lawton, K.G. Bagley, E. Edmonds, H. E. Tilbe, The irradiation behaviour of Plutonium bearing ceramic fuel pins. London Conference on fast Breeder Reactors - BNES May 1966

9. K. G. Bagley and D.M. Donaldson, Fission gas release from mixed oxide fuels. Third International Conference on Plutonium London 1965 - London - Chapman and Hall - p. 1063

10. Geap 5198, 19th Quaterly Report - May - July 1966

11. L. Vautrey - J. Faure, Le réacteur prototype Phénix 3è Congrès de Foratom 1967 - Bulletin d'information de l'ATEN 1967, n° 65, p. 5 à 18.

Table 1. Characteristics of some Irradiated Pins

	Pin 7	Pin 8	Pin 9	Pin - 1 st Rapsodie Assembly
Oxide density (th. dens. %)	98 %	98 %	96 %	95 %
Oxide density after irradiation	92.5 %	92.5 %	97 %	94 %
Initial diametral gap (μ)	240 ± 40	220 ± 40	200 ± 40	190 ± 60
Final diametral gap (μ)	45	35	35	150
Filler gas	He	He	He	He
Linear power (W/cm)	350	300	554	335
Conductivity integral (W/cm)	24	20, 6	40	26, 7
Internal °C temperature of clad	500	530 to 610	460	440
Burn up (MWD/t)	4000	21, 500	5, 400	150

Table 2. Heat Exchange Coefficient Evaluations

	Pin 7	Pin 8	Pin 9	Pin - 1 st Rapsodie Assembly
Central temperature (° C)	1760	1650	2100	1720
Oxide surface temperature (° C)	800	835	940	710
Heat transfer coefficient (W/° C. cm^2)	0.65	0.55 / 0.75	0.74	0.66

Table 3. Heat Exchange Coefficient Evaluation

	Pin 2	Pin 27	Pin 28
Initial diametral gap (μ)	variable	190 ± 50	160 ± 50
Burn up (MWD/t	2750	51	6900
Linear power (W/cm)	345	670 (max)	550
Conductivity integral (W/cm)	24	45.8 (max)	35.8
Internal clad temperature (° C)	470	677	630
Oxide clad exchange coefficient (W/°C.cm^2)	0.28 to 0.4	0.4	0.5

Table 4. Fission Gas Release of some Pins

Pin	MWD/t	$Kd\Theta^{*}$ (W/cm)	$Kd\Theta^{**}$ corrected (W/cm)	% of gas released	Kr/Xe	Notes
Rapsodie	150	28	28	1	10 - 20	
7	4,000	24	24	12.6	-	
35	5,700	25.1	24.5	17.3	6	
8	21,500	20.6	20.6	23.3	5.62	
6	19,000	32	23	26.5		oxide 85 % th. dens.
33	6,600	28.8	26.1	31.4	5.9	
30	13,800	29.6	27.7	60	6.37	high clad temperature
31	16,800	32.6	27.7	100	6.3	broken pin
29	26,400	32	27	100	6.3	broken pin

* Conductivity integral corrected by flux depression

** Conductivity integral corrected by flux depression and central void.

Figures for this paper were not submitted in time for publication

IRRADIATION PERFORMANCE OF FAST REACTOR FUELS *)

D. Geithoff, G. Karsten and K. Kummerer

Abstract

The requirements for uranium-plutonium dioxide fuels are the basis for a program of irradiation tests. Some hypothetical considerations supply a rational background for the design of specimens and the chosen operation conditions. The experimental facilities and irradiation devices are shortly described and discussed with respect to the irradiation characteristics.
One group of experiments refers to the short term behaviour of the oxide type fuel. In another group the long time behaviour of oxide fuel pins is studied. The present results indicate, that the basic assumptions for the pin design are principally confirmed. Finally the status of knowledge and experimental experience is composed in a set of conclusive remarks.

Institut für Angewandte Reaktorphysik
Kernforschungszentrum Karlsruhe
Federal Republic of Germany

*) Work performed within the association in the field of fast reactors between the European Atomic Energy Community and Gesellschaft für Kernforschung m.b.H., Karlsruhe

INTRODUCTION

The operational requirements for oxide type fuel, which are described in full details in the related paper (1) in the first session of this symposium, are the principal guidelines for all irradiation test work in the Karlsruhe fast breeder project. The most important technical features are the proper irradiation conditions with respect to linear rod power, to cladding temperature and to the expected total burnup performance. The typical external and internal geometry is characterized by a small fuel diameter (compared to thermal reactor fuel) and a length distribution which includes an active fuel zone, at least one axial blanket region and a fission gas plenum. The typical ranges of requirements both for sodium and steam cooled pins are compiled in Table I.

The whole irradiation program is oriented towards these target data. As in the first period only a thermal reactor with a limited neutron flux, the Karlsruhe research reactor FR2, was available, significantly larger fuel diameters were necessary in order to reach the linear rod power wanted. Above the intention of a mere performance test up to high burnups - a goal which will be achieved by tests currently underway - the here described work refers partly to parameter studies. The short term tests try to evaluate a systematic scheme of parameter variations. The quoted long term tests are only a first step, which has to demonstrate the feasibility of the irradiation equipment and furthermore to experience the post irradiation examination routine. The next step with much higher target burnups and parameter constellations more similar to fast reactor conditions are already in operation, on the one side with improved irradiation devices in the FR2 again, on the other side with fast flux irradiations in the Dounreay Fast Reactor.

The present paper describes the status of our experimental potential and experience and also some introductory theoretical considerations. We feel it necessary, to establish simple model assumptions concerning the expected irradiation behaviour as a rough guide.

IRRADIATION HYPOTHESES

The target burnup for a fast breeder fuel pin is 100 000 MWd/t. In order to make predictions about the pin behaviour within an equivalent irradiation time, the pin design is based on a theoretical fuel pin behaviour analysis. In this context two limitating assumptions are made, namely

- the fuel operation time will come to an end, after the available void volume of the most critical fuel cross section has been filled by fission-induced fuel swelling to the highest possible extent,

- the fuel operation might end earlier by mechanical contacts between cladding and non-plastic fuel.

As a consequence of these assumptions three separate questions can be discussed with theoretical methods:

1. What is the maximum achievable burnup locally, if only the volume swelling due to fission products is considered?
2. Applying the answer of question 1, where is the most critical fuel cross section along the fuel pin located?
3. Does a socalled "non-plastic" fuel behaviour arise under the planned operation conditions, leading to a mechanical attack on the cladding?

In order to produce an answer to the first question a burnup model is established using some schematic considerations:

- The internal volume of the pin consists of the fuel volume V_F, the (hot) gap volume between fuel and cladding V_G, and the dishing volume (if applicable) V_D.
- The fuel volume itself can be divided into a plastic zone V_{pl} with temperatures above 1700°C, a creep zone V_{cr} with temperatures between 1300 and 1700°C, where creep and diffusion are of remarkable velocity, and a low temperature zone V_{lt} below 1300°C with visco-elastic behaviour mainly (2,3,4).
- Furthermore there are defined availability factors ℓ, m and n in the 3 fuel zones, which give the volume portions of the porosity being actually available for volume expansion due to swelling processes. The porous volume should be available (5) to any expansion with about 80 v/o above 1700°C, with 50 v/o at 1300-1700°C and - according to a numerical evaluation - with not more than 30 v/o below 1300°C. The last figure may rise somewhat during long time operation as the fuel becomes more plastic at low temperatures. Hence we apply for numerical evaluations $\ell = 0.8$, $m = 0.5$, $n = 0.3$.
- Finally two swelling processes are envisaged which need a continuously increasing amount of space with burnup. The basic swelling effect is defined here to be caused by solid fission products and a contribution of fission gases, working in all three zones. According to a literature evaluation (5) this basic swelling rate h_s seems to be 1.6 % volume change in 100 % dense oxide per 10 MWd/kg heavy metal burnup. That means a figure $h_s = 1.6 \times 10^{-3}$ kg/MWd. An additional swelling effect caused by fission gases mainly is added for the creepzone. Its rate is assumed to be $h_g = 0.4 \times 10^{-3}$ kg/MWd.

With these explanations the maximum possible burnup B (in MWd per kg heavy metal content), after which all available volume is used up by the swelling fuel, is:

$$B = \frac{(1-\varrho_F)\,(\ell V_{pl} + m\,V_{cr} + n\,V_{lt}) + V_G + V_D}{\rho_F\,h_s\;V_F + h_g\;V_{cr}} \qquad (1)$$

where ρ_F means the fuel density in the pellet fuel. A graphic evaluation of this burnup formula is given in Fig.1 for a linear rod power of 500 W/cm.

The second question for the most critical cross section is handled by applying the burnup formula, which represents the fuel swelling capacity. Hence locally the maximum allowable burnup can be evaluated for the axial power distribution of a pin. These local maximum burnup figures have to be compared with the really arising burnup at each axial part of a pin in equal times. For certain parts of a pin, which are not necessarily the absolute maximum burnup ranges, the capacity for burnup is implemented firstly. These constitute the critical fuel cross sections. Such an analysis can be expanded of course on a total reactor core by application of specific thermal design data. Generally the critical zones are in the half of the core with the coolant inlet.

To deal with the third question for the existence of non-plastic fuel, the expansion rate of the fuel, which is given by the swelling rate, is compared to a compression rate, which is produced by an evaluation of fuel-cladding interaction, Fig.2. Here irradiation damages and thermal stresses with the cladding are taken into account by a pessimistic assumption for the 0.2 %-creep stress for 10 000 hours of the considered stainless steel. Furthermore, by application of mechanical oxide data (2,3,4) the force of the cladding on the swelling fuel ring with the volume V_{1t} is calculated. The result is, that, under the assumption of 950°C average ring temperature, only those parts of the fuel with linear rod powers lower than 250 W/cm behave non-plastic. They are situated beyond the critical zones mentioned above and hence do not represent limitations for operation time in such designs.

EXPERIMENTAL FACILITIES

The irradiation program in the Karlsruhe research reactor FR2 - a heavy water-moderated reactor with 44 MW thermal power - is performed with two types of irradiation equipment. There is a helium loop operating in the central channel and furthermore, there can be introduced irradiation capsules into normal fuel subassembly positions. The helium loop can be loaded with two different irradiation inserts. For long term irradiation an insert is used containing 4 fuel pin specimens in a cluster. The maximum achievable linear rod power is about 800 W/cm cladding temperatures up to 600°C. The second loop insert is movable in axial direction, also during reactor operation. Only one specimen can be irradiated at the same time. Here the maximum linear rod power can be up to 1000 W/cm, and both central temperatures and specimen inside pressure can be measured. This "short term loop insert" is primarily provided for irradiations in the time scale between a few minutes and a few days.

The irradiation capsules for fuel specimens use liquid metal layers consisting of lead-bismuth and sodium as heat transfer

media. There are three variants available, two with lead-bismuth of eutectic composition - 26 and 19 mm in diameter - for specimens of 12 and 10 mm diameter. The third one has two separate layers of lead-bismuth and sodium at 26 mm capsules diameter, the specimen diameter being 7.4 mm in this case. The maximum linear rod power which may be produced is 400, 500 and 800 W/cm in these three designs. Each capsule can be loaded with four specimens some thermocouples being welded to the can or - in the third design - fixed in the sodium gap.

The post-irradiation examination of fuel test specimen is carried out in a group of hot cells. This group consists of five cells with heavy concrete shielding and an attached ceramographic line with 15 cm lead protection. With the shielding installed, it is possible to handle up to 10^7 MeV Curie of γ-rays in the cells and some 50 MeV Curie in the ceramographic line. All the facilities are completely α-tight and are operated by master slave manipulators.

POST IRRADIATION EXAMINATION METHODS

The majority of irradiated specimens is examined according to a standard procedure, which has been developed and exercised during the past years with only a few samples subjected to a more detailed examination. The most important examination steps are shortly described in the following paragraphs.

Isolation of specimens. Post irradiation examination starts with the isolation of a specimen. This means a simple disassembling procedure for the helium loop specimens, but is of a more complex nature for the capsule specimens. The complete removal of the lead-bismuth alloy, adhering to the can is accomplished by a combination of chemical and mechanical methods. Care must be taken not to do any sort of damage to the cladding, as this would impair precise dimensional measurements.

Visual examination. All fuel specimens are visually examined through the lead-glass windows in front of the cells, since no appropriate periscope is available at the present time. Slight magnification of the inspection zone is achieved by using a monocular. In the same way photographs are taken, which nevertheless show a remarkably good quality.

The leak testing method accepted for the fuel specimens is considered to be severe and has the virtue of simplicity. The procedure is to dip a specimen into liquid nitrogen until the thermal equilibrium is reached. When the specimen thereafter is quickly transferred to a transparent container filled with alcohol, any nitrogen trapped inside the can expands and produces a stream of bubbles thus showing location and size of a defect. In a few cases helium leak testing has been tried to check the reliability of the nitrogen method. Both results are in good agreement.

Metrology. Profile readings are made with the help of an automatic profilometer. From each specimen three circumferential

profiles and four profiles along the axis are recorded. The same readings are made before the irradiation. To avoid the difficulties of contamination of the unirradiated specimens, duplicate equipment has been installed for getting the preirradiation data.

γ-Scanning. γ-scans of the test specimens are taken with a collimator slit having the dimensions 0.5 mm x 20 mm x 700 mm. The specimen is rotating during the scan. Two energy regions are investigated, one being characteristic for Zr 95 - Nb 95 (700-800 keV), the other comprising Ce 144 and Xe 133 (100-150 keV). For short term irradiations the low-energy scan gives a good indication of the release of fission gas into the gas plenum, Fig.3.

X-Raying the specimens is considered to be one of the most important points in the post irradiation examination. The X-ray source is a betatron, emitting X-rays with a maximum energy of 18 MeV and having a focus of less than 1 mm^2. Details like dishing dimensions, cracks and central holes can easily be seen on the pictures. A quantitative evaluation of the X-ray photos concerning dimensional measurements shall be developed.

Fission Gas Release. After puncturing the can, the released gas is collected and analysed for krypton and xenon by means of gas chromatography. Gas volumes down to 0.5 mm^3 can be measured in this way. For double control, the activity of each fission gas fraction is determined in an ionisation chamber and the specific activity thus obtained is checked against the calculated value.

Sectioning of the Specimen. After the evaluation of γ-scans and X-ray-photos an individual sectioning plan is set up for each test specimen. Irregular zones of the fuel are picked out for ceramographic preparation, while samples for fission gas analysis and burnup analysis are taken from unaffected normal zones.

Burnup Analysis. The radiochemical method using Cs 137, Sr 90 and Ce 144 as burnup indicator has been applied in the past, when U 235 was the only fissionable isotope in the fuel. It is intended to turn to other methods like determination of fuel isotopic composition or of stable fission products.

Ceramographic Preparation. Cut sections of fuel pins are impregnated with epoxy resin under vacuum for ceramographic preparation. The solidified samples are mounted into bakelite holders and polished in the conventional manner. Grain structure is made visible by etching with HNO_3 and H_2O_2.

Autoradiography. Contact α- and β-γ-autoradiographs will be taken from samples which have been mounted for ceramographic examination. This point of examination is still in development.

Fission Gas Trapped in Pores. For determining fission gas, that is trapped in larger pores, fuel samples are ground to small size grains and the released fission gases are quantitatively determined by gas chromatography. The grinding process is controlled by intermittent determinations of the free surface of the powder using the BET-method.

Fission Gas Trapped in Fuel and Small Pores. Ultimatively the ground fuel samples are dissolved in nitric acid and the released fission gas is determined in the manner mentioned before. With all the fission gas data a balance is made, which shows how much of the gas is released at each step.

SHORT TERM IRRADIATION PERFORMANCE

Short term irradiations are being performed with the movable insert in the helium loop of the FR2. Different fuel variants are tested in order to study the parameter dependent behaviour of the fuel on operation after short duration, that is shortly after a reactor startup or on short power excursions. The parameters which are varied are the linear rod power, the density, the fuel form and the gap width at pellet type fuel. Furthermore central temperature measurements are carried out. Vibrocompacted fuel is irradiated as sintered and molten oxide, including pressure-buildup measurements in both cases. The Table II gives a survey of a detailed program.

Meanwhile most of the specimens were irradiated with the given parameter constellation. After some cooling time an examination routine comprising X-raying by a betatron device, γ-canning and ceramography was performed. The details of the results are presently compiled.

LONG TERM IRRADIATION PERFORMANCE

The long term irradiation program was started with the aim of making selection of the fuel type and form. It is being continued in order to study the long time behaviour of fuel pins, which are produced with respect to some hypothetical deliberations. Thus in the first group, which is described in Table III, UO_2 and UO_2-Mo were irradiated for fuel selection. As to the pellet form a choice of ground and unground condition and also dished and undished shape was investigated. The vibrational compacted powder was included in a sintered and a molten form. Furthermore, by application of advanced capsule types the fuel diameter could be reduced to 6.4 mm. Though very high burnups were the target, the start of the program was accompanied by pin failures mainly due to capsule failures. Thus the maximum burnup, which was achieved in the first run of experiments did not exceed 20 000 MWd/t. Meanwhile the irradiation performance has been improved very much by improvements in the capsule design. The introduction of sodium as a heat transfer medium restricted the corrosion and void formation at reactor shut down.

Up to now all capsules of the first part (up to KVE 7) are post irradiation examined. As all the different specimens of this part were operated with 360 W/cm, the results can reasonably be compared. The specimens had a fuel diameter of 10 mm, an active

fuel length between 225 and 228 mm and were canned in stainless steel. In the following some remarkable features are illustrated and discussed for vibrated powder as well as for pellet fuel.

Vibratory Compacted Powder Fuel. All specimens with vibro-fuel have a uniform fuel density of 85 % of theoretical density. They were irradiated up to burnups of about 8 000 MWd/t. Although some of the pins achieved a considerably lower burnup, their behaviour concerning gas release and their appearance were very similar to the higher burnup specimens.

Fig.4 and Fig.5 show two length sections of the same pin (KVE 3 / Specimen 3). The central hole is formed as expected with enlarged ends on both sides. The lower end of the central hole is filled with fuel debris up to a height of 1 cm. As close-up views show, the debris is mainly originating from the fuel zone adjoining the can with only a few particles coming from the surface of the central hole. Radial cracks might be the pathway by which the transport is made. The hole was filled at a rather early date after the end of irradiation as X-ray photos already show the filling. The cross sectional area of the central void covers 2.5 % of the internal pin cross section or 5 % of the densified central zone.

The fission gas data for the vibrated specimens are as follows:

52 - 56 % released on puncturing the can
14 - 20 % released on grinding fuel sample
30 - 34 % released on dissolving fuel sample

The combined fission gas data were precise enough as to be the basis for burnup calculations, which within ± 20 % agreed well with the radiochemical values.

Fig.6 (KVE 7 / Specimen 8, UO_2-Powder Fuel) shows a cross sectional view with a central hole apparently located excentric. Higher porosity on one side (smaller powder particles) causing lower thermal conductivity of the fuel in this region has drawn the central void closer to the can.

Powder fuel with molybdenum as additive, a fuel type considered promising at an earlier date, was tested in a few specimens in KVE 7. The idea that the addition of 10 % molybdenum will increase the thermal conductivity considerably, thus lowering the central temperature, is visibly confirmed by Fig.7 (KVE 7 / Specimen M7). The compacted particles have been molybdenum coated. No grain growth is observed throughout the whole fuel area which means that central temperatures remained below 1500°C in the center. Fission gas release was reduced to less than 5 % with only an additional 10 % release found on grinding the fuel. More than 80 % of the gas was strongly trapped in the fuel itself.

Pellet Fuel. The fuel specimens referred to in this chapter contained pellets with fuel density of 91 % th.d. They were dished on one side with a dishing volume of 2.7 - 2.8 %. Cladding and fuel were separated by a gap of 60 µm diametral. With this type of fuel specimen burnups up to 8 600 MWd/t were achieved.

The influence of the gap width on the formation of the cen-

tral hole can be discerned in a X-ray photo, although the gap width was not included as parameter in the study. A stepwise dislocation of the central hole in two neighbouring pellets, see Fig.8 (KVE 4 / Specimen B) can be reasonably interpreted only as a result of different gap widths which are caused by filling the pellets in such a way into the canning that one side touches the canning while the other leaves a gap of the whole 60 µm.

A dislocated central hole and an additional cavity having the shape of a half moon is shown in Fig.9 (KVE 4 / Specimen B). The cavity lies on the borderline between uneffected UO_2 and visible grain growth. From the shape of the cavity it can be concluded that this is what has been left over from a pellet dishing.

To study the function of the dishing in pellets was one of the objects of the irradiation test. Fig.10 (KVE 4 / Specimen D) shows how the dishing was consumed by the expanding fuel. (The oblong inclusion in the middle pellet is an impurity introduced in the manufacturing process.) The pellets have protruded, apparently from both sides, and nothing is left of the dishing volume in the central zone. Only a doughnutlike ring in the cooler fuel zone marks the position of the former cavity. The consumption seems to be irreversible but there is not indication where the void volume has vanished.

In a stage where the central hole has been formed, the dishing volume becomes visible again, Fig.11 (KVE 4 / Specimen D). At pellet interfaces the central channel is widening to form the diamond shaped void. This form of the central void may be smoothed to constant diameter at longer irradiation times but with the burnups we achieved so far it was always discernable.

What can happen to a dishing void at low rod power is demonstrated in Fig.12 (KVE 4 / Specimen A). Due to thermal cracking in a test specimen with a linear rod power of only 250 W/cm (marginal position in KVE 4) the dishing void is filled with a large piece of the upper pellet, thus transferring the void to another position. This phenomenon has only been observed once. So it will not be the cause for smearing the dishing void volume uniformly along the whole fuel length. That this is only a single case can be documented by Fig.13. The shifted void can be easily detected in the X-ray photo.

IRRADIATION PROGRAM CONTINUED

The irradiation performance tests are being continued in thermal and fast reactor environments. Presently a new series of UO_2-PuO_2-specimens for irradiation both in capsules and in the helium loop of the FR2 is prepared. Fast neutron irradiations are carried out in the Dounreay Fast Reactor for our program, where at present a trefoil rig with UO_2-PuO_2 pins is in operation and a bundle irradiation is being prepared. Also irradiation space in the hard spectrum of the BR2 reactor in Belgium is now available and will shortly be used for testing fast reactor fuel pins.

CONCLUSIONS

In view of the still rather limited experimental experience concerning the irradiation performance of fast reactor fuels the following conclusions are established:

1. With mixed oxide fuel a linear rod power of up to 500 W/cm maximum - as required for present fast reactor prototype designs - can be achieved without central melting. Also the burnup range of up to 100 000 MWd/t is a reasonable target; it needs, however, a careful adjustment of the internal fuel geometry.

2. An additive to the fuel like molybdenum improves the thermal conductivity to some extent. This improvement - being lower than originally expected - is, according to the recently established hypotheses, not only not necessary, but also harmful to the radial swelling problem, as a reduced average fuel temperature lowers the availability of porous volume to fission products.

3. According to the present state of fabrication technology the pellet type oxide fuel has some preference compared to vibrocompacted powder fuel. But the irradiation results do not demonstrate any advantageous features for one of both "competitors".

4. The short term behaviour of the fuel (at startup or at power level changes of the reactor) seems to be quite smooth and normal, without any indication of undesired internal fuel movement.

5. The applied internal geometry parameters (low smeared density, gap width and dishing or non-dishing at pellets) are experimentally confirmed within the now evaluated limited burnup range.

ACKNOWLEDGEMENT

The authors would like to express appreciation to W. Stegmaier for his help in performing the experimental program and to K. Scheeder, who is responsible for the operation of the hot cells. The efforts of Dr. H. Gräbner, in charge of the fission gas analysis, and of K. Ritzka for the preparation of the ceramographic samples are also gratefully acknowledged.

REFERENCES

1. K. Kummerer, Central Station Fast Breeder Reactor Plutonium Fuel Requirements, This Symposium, Session A, KFK-661

2. W.H. Armstrong et al., Creep Deformation of Stoichiometric Uranium Dioxide, J. Nucl. Mat. 7 (1962) 133-141

3. L.G. Wisnyi et al., In-Pile Mechanical Properties of Nuclear Fuels, Trans. ANS 9, 2 (1966) 393/4

4. R. Scott et al., The Plastic Deformation of Uranium Oxides above 800°C, J. Nucl. Mat. 1 (1959) 39-48

5. G. Karsten, Th. Dippel, H.J. Laue, Fabrication of Fast Reactor Fuel Pins for Test Irradiations, IAEA Symposium on the Use of Plutonium as a Reactor Fuel, Brussels, March 13-17, 1967, KFK-577

Tab. I Typical Requirements for Irradiation Performance Tests

		Sodium Cooled Version	Steam Cooled Version
Max. Linear Rod Power, nominal	(W/cm)	400 - 500	300 - 400
Max. Can Midwall Temperature, hot spot	(°C)	650 - 700	700 - 750
Max. Burnup	(MWd/t of U + Pu)	~ 90 000	~ 50 000
Fuel Diameter	(mm)	5.0 - 5.5	6.0 - 6.5
Fuel Length	(mm)	~ 1 000	~ 1 500

Tab. II Short Term Irradiations

Specimen Identification for the Different Parameter Constellations

Linear Rod Power (W/cm)				500			750			1000			400
Irradiation Time				10 min.	2 h	24 h	10 min.	2 h	24 h	10 min.	2 h	24 h	24 h
Fuel Form	Diam. Gap (µm)	Fuel Density (% th. d.)	Smear Density (% th. d.)										
Pellet	100	93	90	L1	L2z		L1x	L2		L1z	L2x		L3••
		88	85	L4	L5	L6	L7	L8	L9	L10	L11	L12	L13••
		93 (5 % dish)	85	-	L14	L17	-	L15	-	-	L16	-	-
	250	90	85	-	-	-	L18	L19	-	-	L21	L20	L22••
		90 (5 % dish)	80	-	-	L23	L24	L25	L26	-	-	-	L27••
Vibro Powder	Sintered Particles		85	-	L28	L29•	L30	L31	L32•	L33	L34	-	-
	Molten Particles		85	-	L35	-	L36	L37	L38•	-	L39	-	-

• Specimens with inside pressure measurement
•• Specimens with central temperature measurement

Tab. III Long Term Irradiation

Capsule No.	Number of Specimens	Fuel	Fuel Form	Fuel Density (% th. d.)	Fuel Diameter (mm)	Irradiat. Time (days)	Linear Rod Power (W/cm)	Max. Burnup (MWd/t)
KVE 3	4	UO_2	Sintered Particles, Vibrated	85	10	13	360	690
KVE 4	4	UO_2	Ground Pellets with Dishing	91	10	22	360	730
KVE 5	2	UO_2	Ground Pellets with Dishing	91	10	147	360	7770
	2		Sintered Partikles, Vibrated	85				
KVE 7	1	UO_2	Sintered Particles, Vibrated	85	10	86	360	4545
	1	UO_2-Mo	Sintered Particles, Vibrated	85				
	1	UO_2-Mo	Ground Pellets with Dishing	90				
	1	UO_2	Ground Pellets with Dishing	91				
KVE 10	4	UO_2	Molten Particles, Vibrated	86	10	36	450	1300
KVE 11	4	UO_2	Unground Pellets without Dishing	90	10	58	450	2600
KVE 12	4	UO_2	Sintered Particles, Vibrated	86	8.6	+	500	16000
KVE 13	3	UO_2	Ground Pellets with Dishing	90	10	145	450	5000
KVE 17	1	UO_2	Sintered Particles, Vibrated	86	8.6	+	500	>8000
	1		Molten Partikles, Vibrated					
KVE 20	1	UO_2	Ground Pellets without Dishing	93	6.4	30	650	5000
	2		Unground Pellets without Dishing					
KVE 21	2	UO_2	Unground Pellets without Dishing	93	6.4	+	650	

+ = in operation

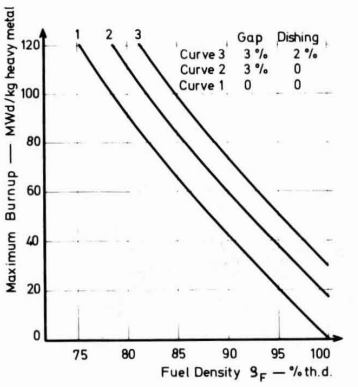

Linear Rod Power 500 W/cm
Fuel Surface Temperature 900 °C
Average Thermal Conductivity 0,022 W/cm °C

Fig.1 Maximum Burnup Evaluation

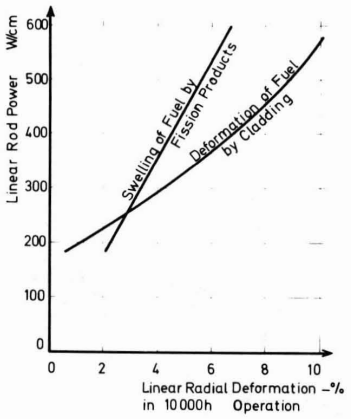

Cladding Temperature 550-650 °C
Temperature in the Swelling Fuel Ring 950-1000 °C

Fig.2 Fuel-Clad Interaction

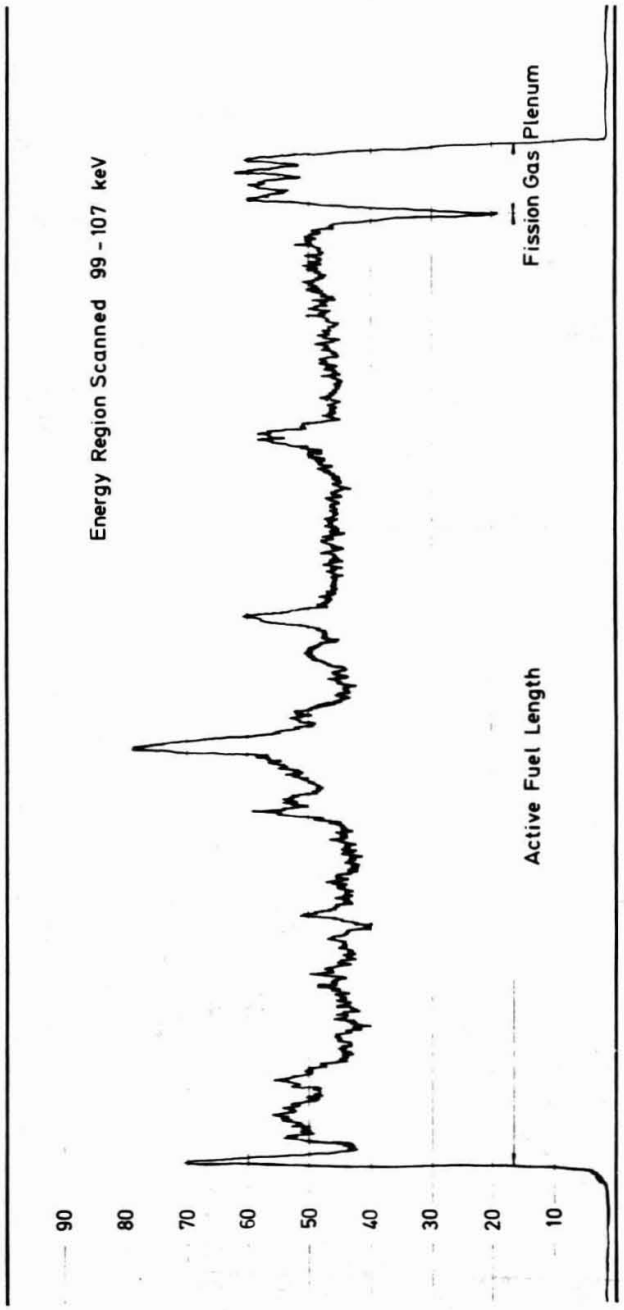

Fig.3 γ - Scan of Specimen L 9

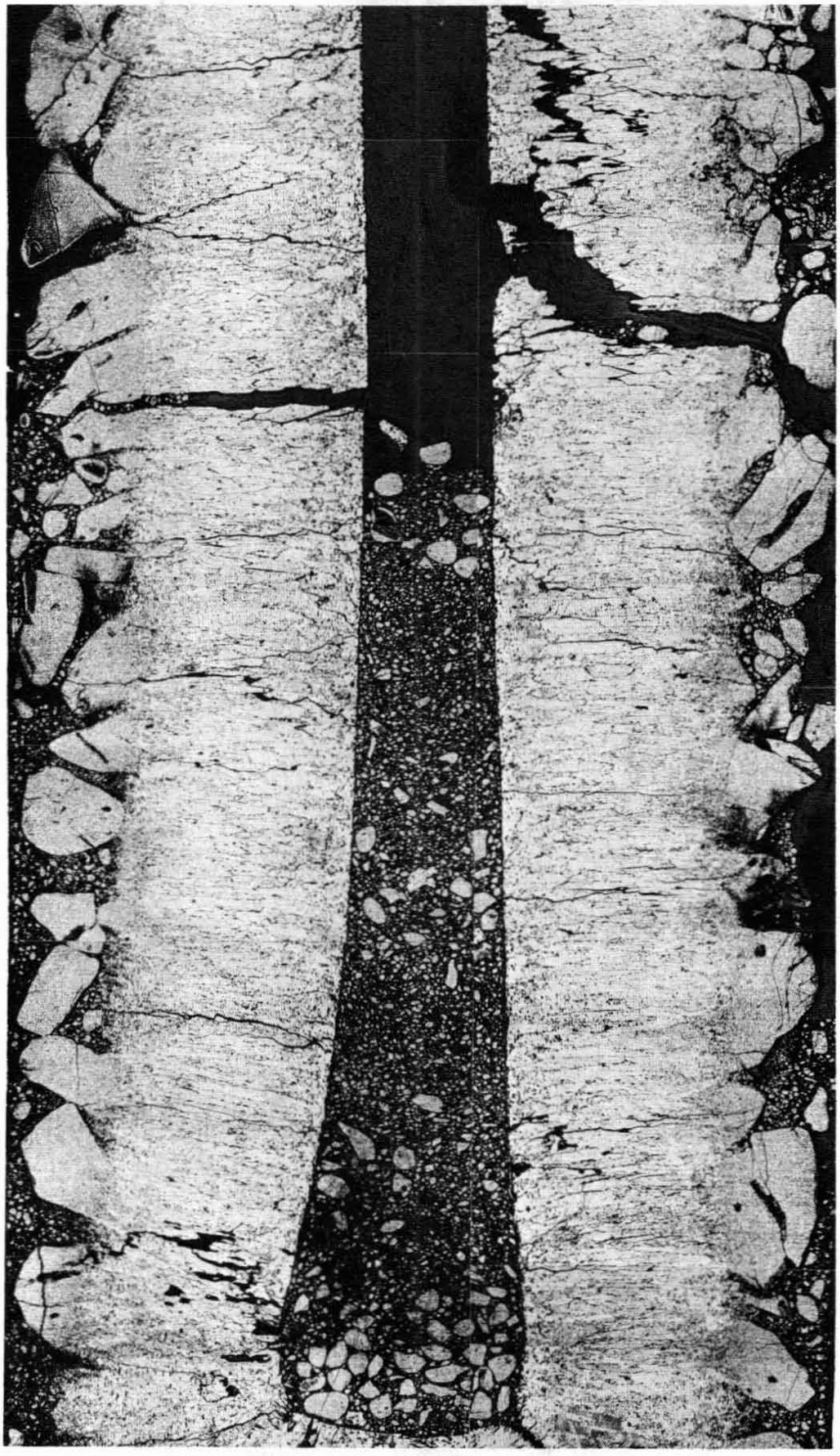

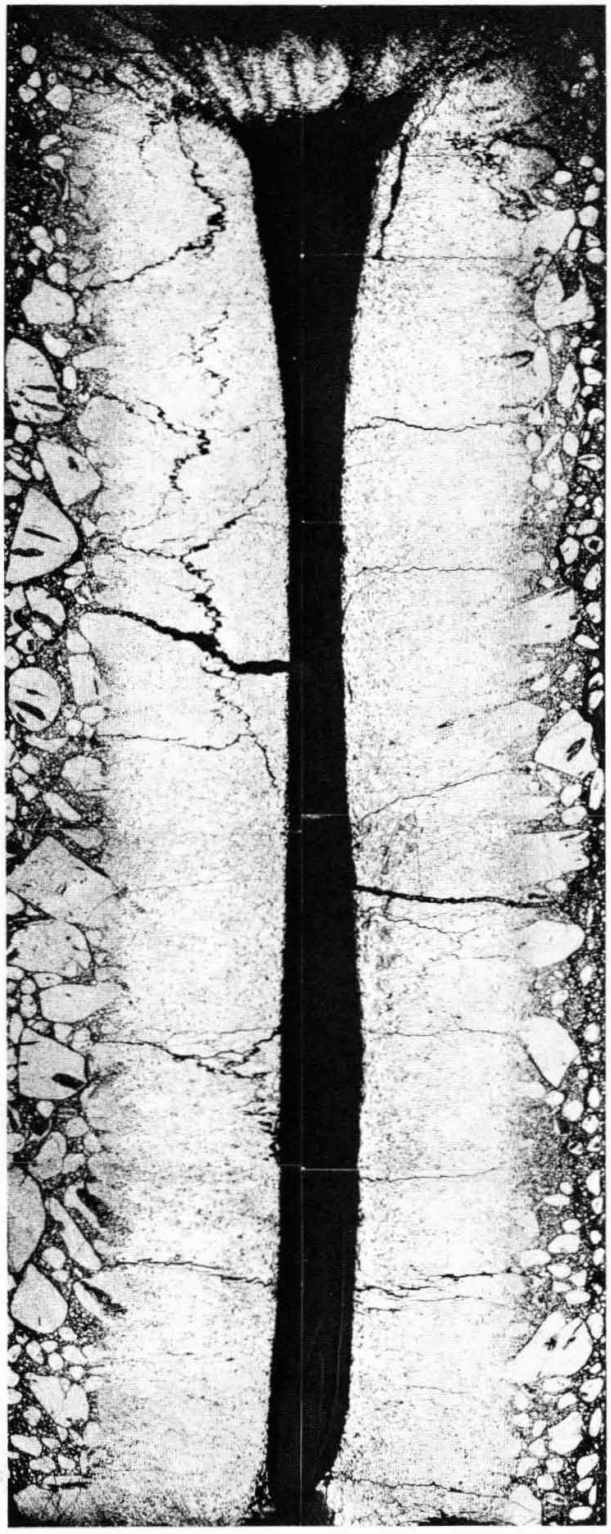

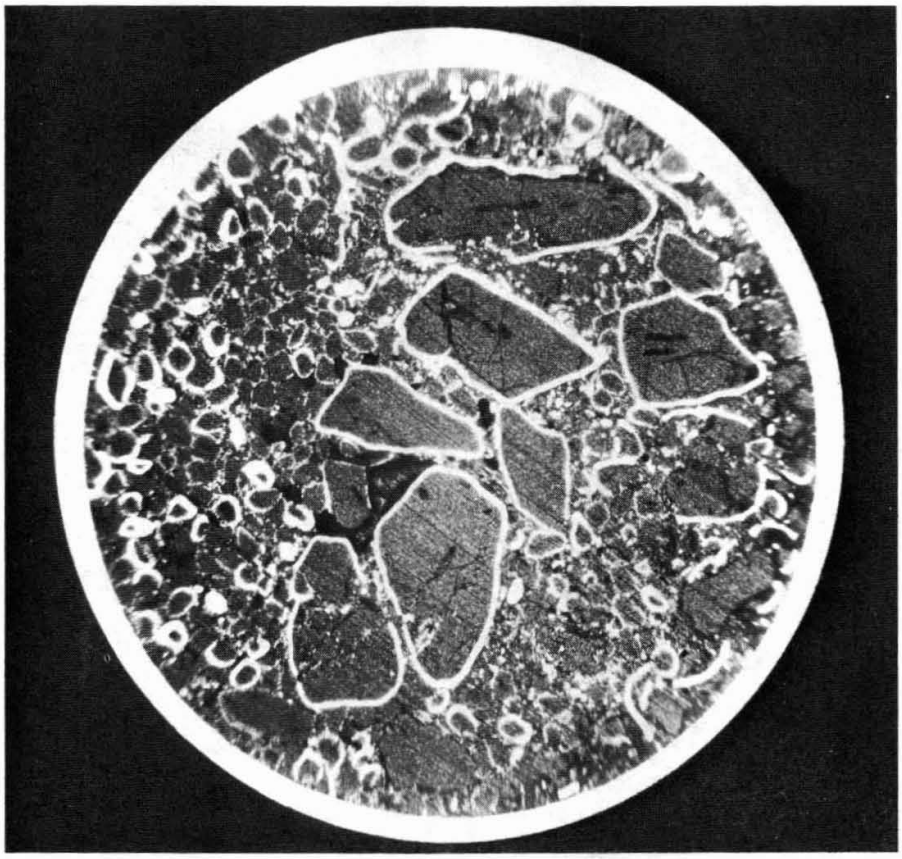

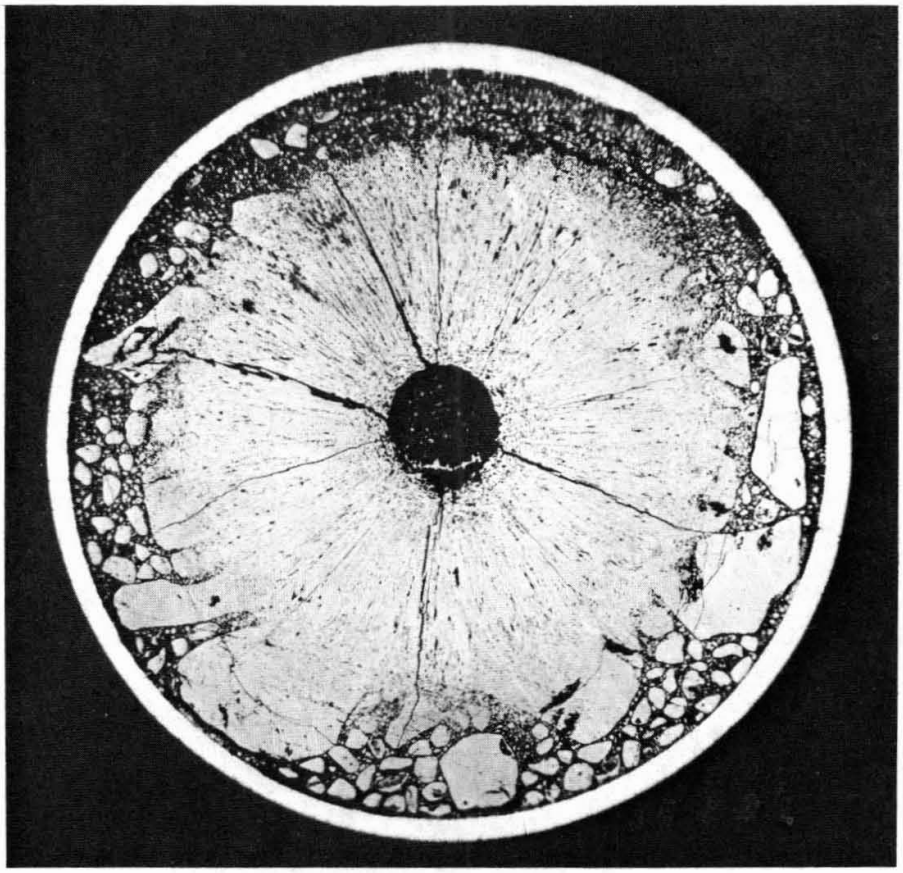

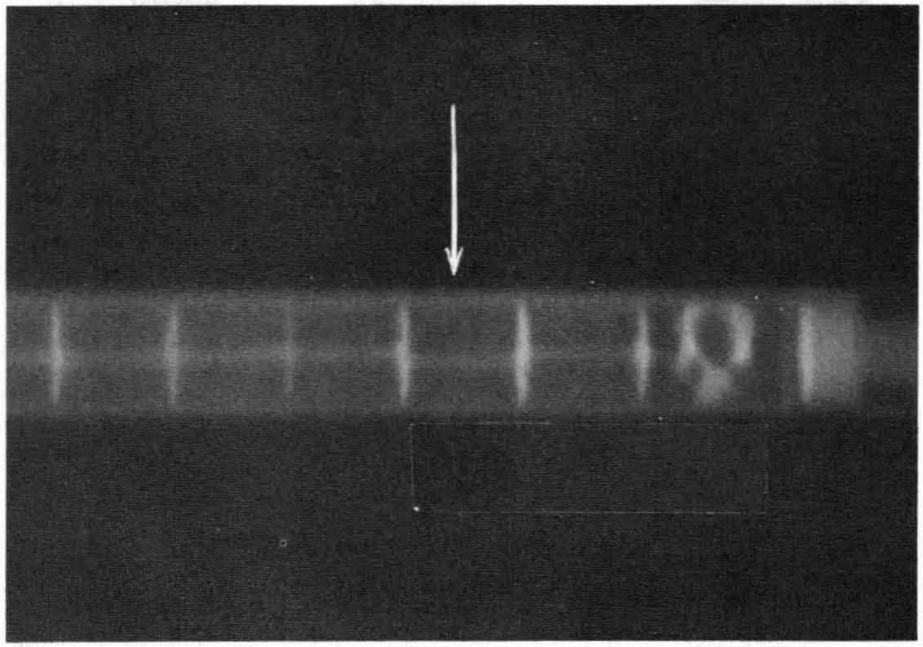

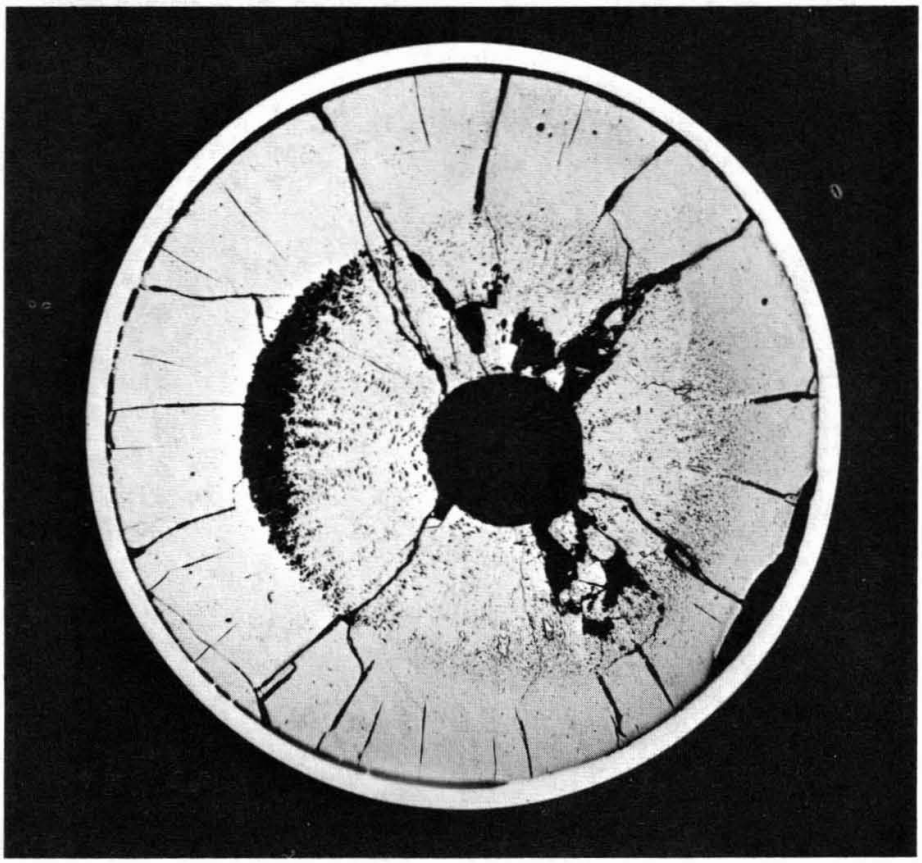

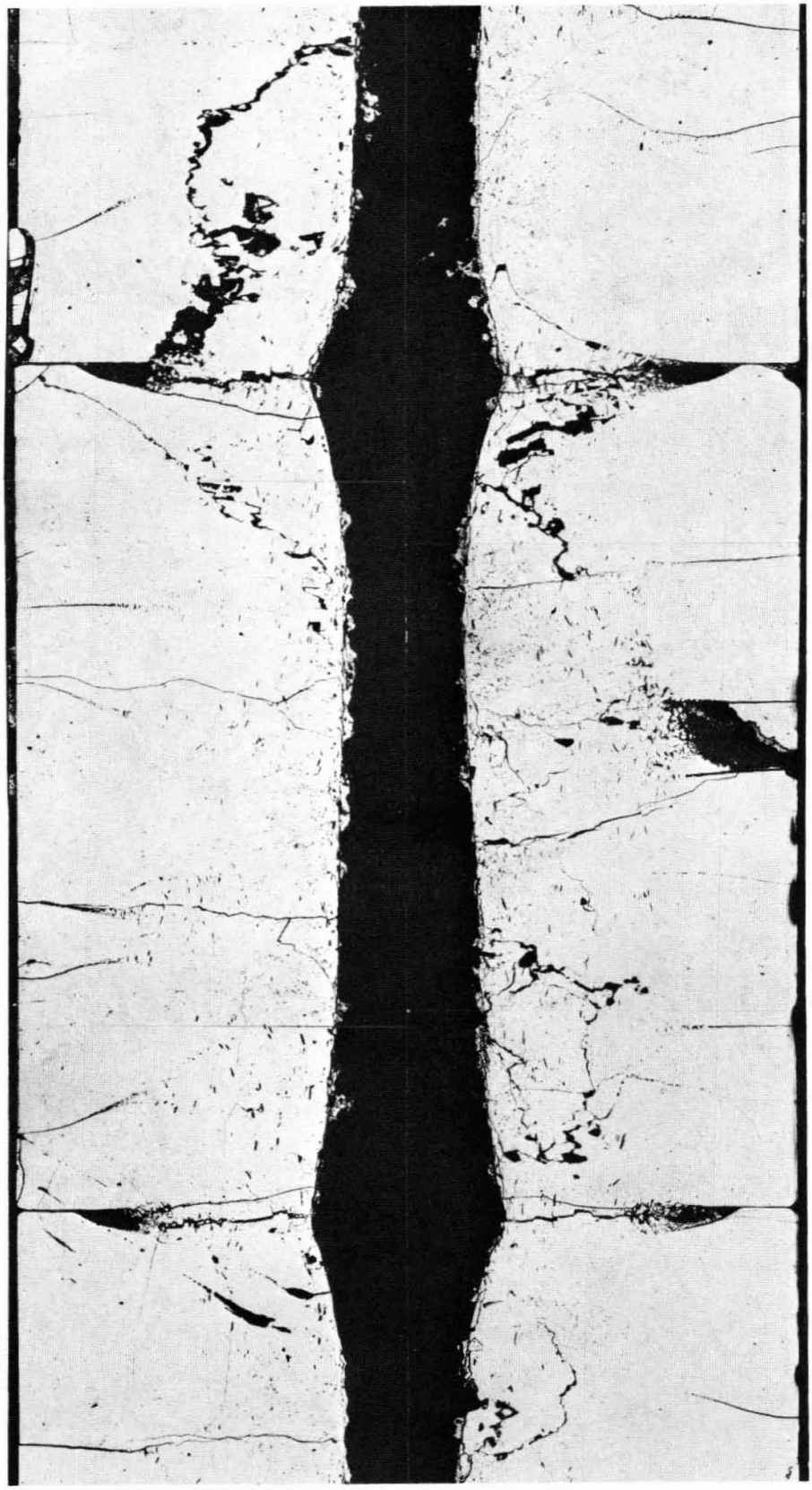

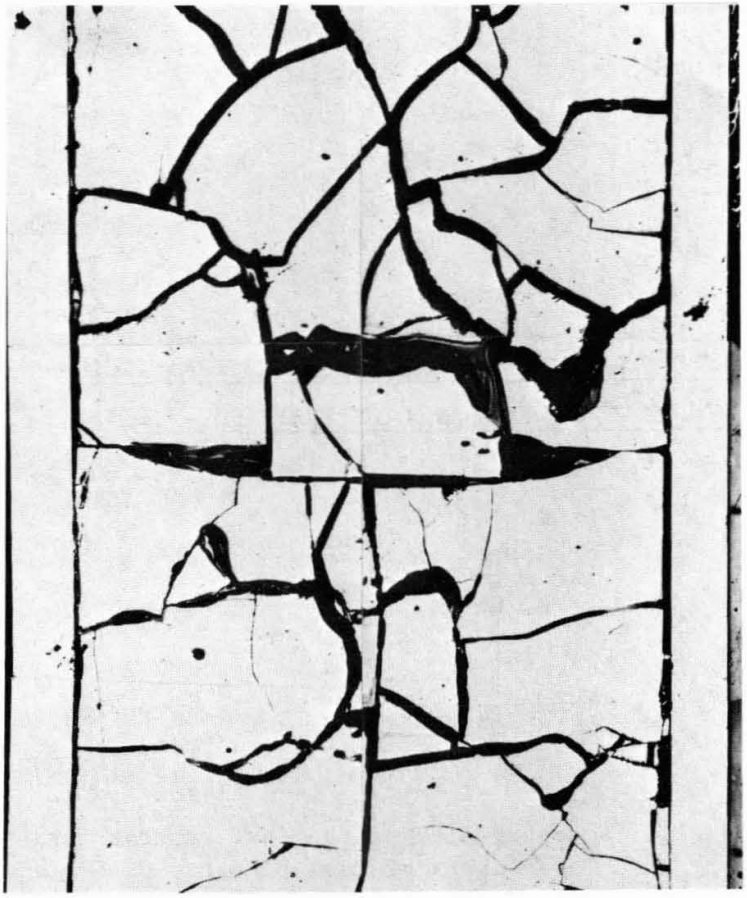

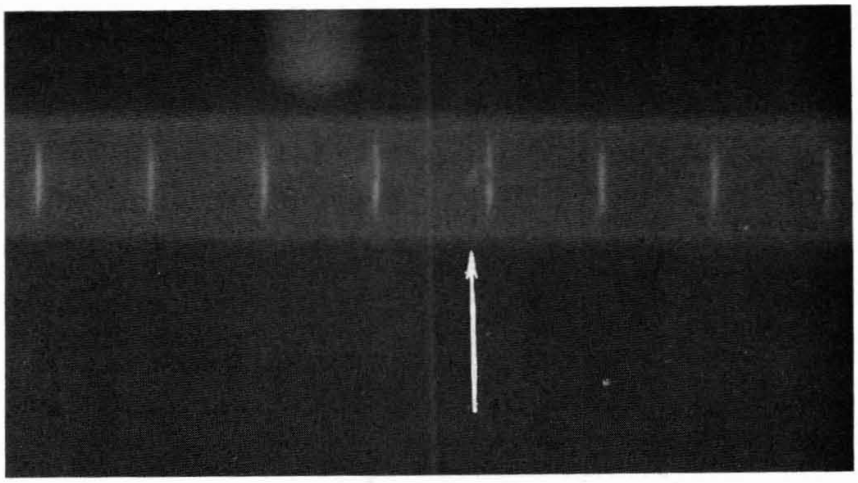

BELGIAN EXPERIENCE IN FABRICATION AND IRRADIATION PERFORMANCE OF FAST REACTOR FUEL (UO_2-PuO_2) *

J.M. Leblanc **
R. Horne ***

Abstract

The paper gives a description of the fast reactor fuel development program. Three types of fuel pins are developed : conventional pelleted fuel pins, collapsed clad fuel pins and vibratory compacted fuel pins. The specifications of the three types of fuel pins and the fabrication flowsheets are given. Parameters related to low density fabrication are discussed.

Irradiation tests on fast reactor fuel pins will be achieved in the Enrico Fermi fast reactor, the Dounreay fast reactor and the BR2 reactor. The paper gives the irradiation parameters which have to be evaluated.

* Work performed in the frame of the C.E.N. (Centre d'Etude de l'Energie Nucléaire) - BelgoNucléaire Association for Plutonium Fuel Development

** Chemical Engineer at "BelgoNucléaire" (Société Belge pour l'Industrie Nucléaire)

*** Engineer at A.P.D.A. (Atomic Power Development Associates, Inc.)

INTRODUCTION

In the frame of the Association contract between the European Community and the Belgian Government concerning the development of fast reactors, the Joint C.E.N.-BelgoNucléaire Plutonium Group investigates the fabrication possibilities of mixed uranium and plutonium oxide fuel pins.

The C.E.N.-BelgoNucléaire Fast Reactor Fuel Program enters into the plan of the Atomic Power Development Associates, Inc.(APDA) for demonstrating a plutonium fuel in a large fast reactor.

This latter program involves the design and development of an UO_2-PuO_2 core and subsequent manufacture and operation of this core in the Enrico Fermi Fast Breeder Reactor.

The work which is carried out is mainly related to the first phase of the program whose objective is to evaluate various oxide fuel preparation techniques and to fabricate various representative prototype fuel pins for irradiation in the Enrico Fermi Reactor.

FUEL PIN TYPE FOR FAST REACTOR

Three types of fuel rods have been developed to be used for irradiation tests :

a. low density dished pellets in conventional cladding (nominal diametral gap : 120 mm)

b. low density dished pellets in collapsed cladding

c. vibratory compacted fuel pins.

Figure 1 illustrates the design concept of each fuel pin type whose preliminary specifications are reported on Table I. In all cases the clad outside diameter (316 and 347 AISI strainless steel) is 6.35 mm and its thickness 0.40 mm, the fuel length is 775 mm (to correspond to the height of the Enrico Fermi core A) without the depleted UO_2 insulator pellets and the hold down device at both ends. A split fission gas plenum is used, the lower one and the upper one being respectively 190 and 251 mm. In all cases the smeared fuel density is 83 ± 2 % TD. In both cladding designs, the tight and the conventional one, dished pellets are utilized to minimize fuel movement relative to the cladding. The dished ends of such pellets provide built-in space to accomodate most of the fuel thermal expansion. The pellets are 5.415 mm in diameter for the conventional clad and 5.540 mm for the tight clad. The pellet density for the tight clad is 86.5 TD while that for the conventional clad is 89.5 TD.

The tight clad design is aimed at the solution of two fuel compaction problems :

a. axial cracks developed in the fuel during power operation, which may subsequently compact under mechanical or thermal shocks,

b. the center hole which is formed under irradiation and into which molten fuel may slump under accidental conditions.

One approach to solve these potential safety problems is to use collapsed cladding in which the diametral clearance between fuel and cladding is reduced almost to zero. This could limit the amount of fuel ratcheting when cracks are present and therefore the amount of compaction. It would also promote heat transfer between the fuel and cladding and consequently tends to reduce the diameter of the center hole. Reduced slumping potential of molten fuel would thereby be achieved.

COLLAPSED CLAD FUEL PIN FABRICATION

The aim of the experiments which were made to fit the cladding against the fuel pellets was to reduce to a minimum the gap between pellets and cladding, while holding the increase in length of the fuel column to a minimum. Experiments have been conducted utilizing different techniques. Two of these gave good results : flexible swaging and isostatic creep.

For the flexible swaging, the pelleted fuel pins are first surrounded by discontinuous plastic tubes which are themselves surrounded by a thin metallic tube and then run through a conventional rotary swaging machine. An inner spring exerts a force on the fuel column during swaging and therefore reduces to a minimum the lengthening of the pellet stack (less than 0.2 %). With initial diametral gap of 100 to 150 microns, the maximum remaining diametral gap is less than 40 microns.

According to the isostatic creep technique, the pelleted fuel pins are collapsed by autoclaving during eight hours at 850°C using pressures of 150 - 200 atmospheres. No fuel column elongation occurs and the maximum remaining diametral gap is less than 25 microns. Figure 2 shows a fuel pin fabricated utilizing the isostatic creep technique.

LOW DENSITY UO_2-PuO_2 PELLETS PREPARATION

Different routes can be followed to prepare low density pellets [1]. The technique which is now applied and developed is illustrated in Figure 3. The reasons why this process is used to prepare low density pellets and comments concerning the different steps are given hereunder.

Mechanical Mixing or Coprecipitation

From the examination of both preparation routes, it appears that the coprecipitation process presents several disadvantages, which would impair the fuel fabrication cost. The most important disadvantages are :

a. the starting material : The plutonium as sinterable or even stoichiometric (high fired) PuO_2 is more easily and accurately sampled and analyzed for Pu content than any other plutonium salt. Furthermore,

criteria for controlled transportation of large quantities of PuO_2 are less severe than for the plutonium solid compounds or solutions, such as hydroxide, oxalate, nitrate, etc.

b. the quantity of material to be handled safely in glove boxes : When processing PuO_2 powder, the use of mechanical mixing allows a larger amount of plutonium material to be safely handled than when using the coprecipitation method.

c. the liquid wastes : The coprecipitation route leads to the handling of large quantities of plutonium liquid wastes, affecting the fuel fabrication cost.

Plutonium Oxide ex-Hydroxide or ex-Oxalate.

It is obvious that the characteristics of the PuO_2 powder from hydroxide or oxalate are affected by the precipitation and calcination conditions and therefore it should be possible to prepare sinterable or disactivated PuO_2 powder from hydroxide or oxalate calcination. However, it has to be pointed out that :

a. the hydroxide precipitation gives less plutonium losses than the oxalate precipitation,

b. to avoid the expensive separation of plutonium from uranium, the recycling of the rejected pellets has to be achieved according to the hydroxide coprecipitation,

c. utilizing disactivated or sinterable UO_2 powder, the highest densities for UO_2-PuO_2 pellets are obtained with PuO_2 ex-oxalate. Lower densities with PuO_2 ex-hydroxide may be due to the $NH_4\ NO_3$ which can only be removed after repeated washing or to the powder morphology. For the above reasons both PuO_2 starting materials are now utilized to allow economical and technical comparison for well specified UO_2-PuO_2 low density pellets fabrication.

Sinterable or Disactivated Uranium Oxide and Plutonium Oxide Powders

The route followed to prepare pellets has to lead to :

a. UO_2-PuO_2 pellets with reproducible low densities and diameters without centerless grinding,

b. UO_2-PuO_2 pellets thermally stable and having the required homogeneity,

c. pellets with good porosity distribution.

In order to promote the thermal stability and the interdiffusion of mechanically mixed, high sintering temperatures have to be used (1 550°C - 1 650°C). When using sinterable powders, low green density pellets obtained by means of binders must be prepared to achieve low density sintered pellets. However the lower the green densities, the lower the reproducibility of the sintered densities is (fig. 4 shows

the reproducibility of the sintered density for 2 different kinds of UO_2 powders). Disactivated powders are now used to get high green densities which allow reproducible low sintered densities and which reduce the shrinkage during sintering and therefore reduce the variation of the diameter of the sintered pellets. Furthermore these disactivated powders give a better porosity distribution and pellet shape.

Granulation and Pelletizing

No binder is used. The lubricant has been added according to the wet process, however development work is being done to allow the use of dry lubricants in order to promote the criticality safety. The granulation is done by the pelletizing-crushing process. This technique limits the stress gradients during subsequent small pellet pressing and therefore leads to sintered pellets having more a cylindrical shape.

Either mechanical or pneumatic presses may be utilized. Even though the pneumatic press produces pellets with reproducible green densities, its production capacity is less than that of the mechanical press which requires reproducible powder weights in the die to give green pellets with reproducible densities. Such reproducible weights are obtained using granules within well defined sizes. An apparatus is now under development to produce these granules with 100 % efficiency. Both pelletizing processes are being developed to allow technical and economical comparisons.

Sintering Atmospheres

When using the reported pellet preparation process, the pellet characteristics will depend on the UO_2 and PuO_2 powder characteristics, the PuO_2 content, the pellet green density and the sintering conditions. The fabrication of pellets with well defined specifications will therefore depend on the adjustment of one or several of those parameters.

Concerning the fast reactor safety related to the Doppler reactivity coefficient, the mechanically mixed UO_2-PuO_2 fuel has to be homogeneous and the PuO_2 particle size has to be limited in order to promote heat transfer from the fissile fuel (PuO_2) to the fertile material (UO_2). Applying the mixing-milling sequence the average size of the PuO_2 particles inside the UO_2 matrix can be limited to the acceptable size of 25 microns. Another step which could enhance the fuel homogeneity is the sintering operation.

UO_2-PuO_2 pellets (18, 20, 30 and 40 w/o PuO_2) have been sintered during 2 heat 1600°C with different sintering atmospheres : Argon + 5 % H_2, Argon + 5 % H_2 + 2500 ppm H_2O, Argon + 2500 ppm H_2O, Argon + 3 % air. From these sintering experiments it appears that the percentage of $(U - Pu)O_2$ solid solution increases when increasing the oxygen partial pressure in the sintering atmosphere (10 % solid solution for Argon + 5 % H_2, 100 % solid solution for Argon + 3 % air [2]. Figures 5 and 6 show the results of electron microprobe scans and ceramographies of UO_2 - 18 w/o PuO_2 pellets respectively sintered under

reducing atmosphere (Argon + 5 % H_2) and oxidizing atmosphere (Argon + 3 % air). The sintering atmosphere will be chosen on the basis of UO_2-PuO_2 pellets specifications and the reproducibilities of the pellet characteristics on a statistical basis.

UO_2-PuO_2 DENSE PARTICLES PREPARATION AND VIPAC FUEL FABRICATION

The choice between vibratory compacted fuel pins and pelleted fuel pins as fuel for fast reactors will be based on :

a. fuel pin fabrication cost,

b. irradiation behaviour.

First of all the cheapest process for Vipac fuel pin fabrication has to be compared with the cheapest way to fabricate pelleted fuel pins.

Three main routes can be followed for the fabrication of dense UO_2-PuO_2 particles for the vibratory compacted fuel pins :

a. sintering of small pellets (nodules) and granules coming from green pellets crushing,

b. sieving after crushing of fused UO_2-PuO_2 ingots,

c. sintering of UO_2-PuO_2 spheres prepared by a Sol - Gel process.

The two first techniques are now developed for comparison.

Sintering Process (Nodules)

Figure 7 gives the flow sheet for UO_2 - PuO_2 dense particle preparation according to the sintering process [3, 4]. Conformably to this technique, homogeneous UO_2-PuO_2 green pellets prepared by mechanical mixing are crushed to get granules of different sizes which can be used, after sintering and subsequent milling, as the fine and medium fraction or to prepare small pellets (nodules) for the coarse fraction of the powder to be vibratory compacted. The main advantage of this process is that it avoids any recycling. The PuO_2 particle size in the UO_2 matrix depends on the technique applied to prepare the sinterable mixed UO_2-PuO_2 powder and the sintering process. Taking advantage of the particle shape factor of the small pellets used on the coarse fraction of the dense powder (Fig. 8) fuel pins with a smeared density of the order of 84 - 85 % TD can be easily obtained with 97 % TD particles using the electromagnetic vibration.

Fusion Process

Figure 9 gives the flow sheet for UO_2 - PuO_2 dense particle preparation according to the fusion process[5]. The high density UO_2-PuO_2 powders are obtained by crushing UO_2-PuO_2 ingots coming from the melting of mechanically mixed UO_2-PuO_2 powders in an induction furnace. Near theoritical density and homogeneous (solid solution) UO_2-PuO_2 particles can be produced using this self containing ingot fusion process (Fig. 10 shows a UO_2 - 18 w/o PuO_2 fused ingot). The main disadvantages of this technique is the necessity of recycling a large fraction of the crushed powder ($\simeq$ 60 %) and the angular shape of the

dense particles (on Fig. 11 we can see UO_2 - 18 w/o PuO_2 fused particles coming from crushed fused ingot). With this dense powder, fuel pins with a smeared density of the order of 86 % TD can be easily fabricated using electromagnetic vibrations.

IRRADIATION PROGRAMME

Fast reactor fuel irradiation tests are planned in the Enrico Fermi Fast Breeder Reactor and in the Dounreay Fast Reactor.

Irradiation Experiments in Enrico Fermi

The irradiation programme is devided into two overlapping series : a preliminary fuel evaluation series and a fuel performance evaluation series.

The purpose of the preliminary fuel evaluation series is twofold : first, to provide low burnup fuel pins on which post-irradiation tests will be conducted to demonstrate freedom from axial fuel movement and second, to determine the power level that can be achieved without the formation of a significant central hole. This series are thus part of the experimental effort on safety problems. Assuming that the results show that oxide fuel movement is not a problem, the objective of the fuel performance evaluation series will be to evaluate the behaviour of the fuel pins at high burnup and high specific power.

The three fuel pin designs previously reported will be tested :

a. low density dished pellets in conventional cladding,

b. low density dished in collapsed cladding,

c. vibratory compacted fuel pins.

If preliminary fuel evaluation series indicates that the axial compaction of fuel is not a realistic safety problem the tight clad design may be dropped in favor of the other two.

The fuel for the pelletized or vibratory compacted designs will be PuO_2 - enriched UO_2 or enriched UO_2 alone. The plutonium concentration of the former will be 32 w/o to correspond to the initial UO_2-PuO_2 Enrico Fermi core design, while the uranium enrichment will be either 60 or 93 % depending on the desired heat generation. Both UO_2-PuO_2 pins and UO_2 pins will be tested for all three designs (Fig.1) at maximum values of linear power generation ranging from about 320 W/cm to about 560 W/cm. A total of about 150 pins will be irradiated at burnups ranging from 20000 to 90000 MWd/t.

The test subassembly which will be used for irradiation experiments has four independent coolant channels or thimbles in which bundles of fuel specimens will be tested. Each thimble will be individually orified and thus the coolant flow to produce any desired coolant temperature up to a design limit of 650°C.

Irradiation Experiments in D F R

The irradiation experiments which are planned in the Dounreay Fast Reactor are burnup tests. These irradiation tests will begin in 1967 and will continue during the next years. The three first fuel pins which will be irradiated (1967) will be low density dished pellets in conventional cladding (Fig. 12) with the following specifications :

Cladding Tube (316 AISI)

Inner diameter : 5.555 ± 0.010 mm

Wall thickness : 0.420 ± 0.030 mm

Outer diameter : 6.395 ± 0.015 mm

Fuel Pellets (mixed oxide)

Diameter : 5.430 ± 0.050 mm

Height : 6.0 ± 1.0 mm

Plutonium content : 20 w/o

Uranium enrichment : 93 w/o

Density : smeared : 83 ± 2 % TD

bulk : 89.5 ± 1.5 % TD

Fuel Pin (Fig. 12)

Total pin length : 710 ± 1 mm

Fuel length : 340 ± 3 mm

UO_2 bottom blanket : 50 ± 3 mm

UO_2 upper blanket : 105 ± 3 mm

The irradiation experiment will be done at a maximum specific power of 220 W/g (488 W/cm) and is expected to reach a maximum burnup of 60.000 - 65.000 MWd/t. The maximum nominal mid wall clad temperature will be 650°C at the beginning of the irradiation.

REFERENCES

1. J.M. Leblanc.
   Euratom - Belgium Fast Reactor Association
   Contract n° 015 - 65 - 1 R A P B
   Fast Reactor Fuel Development Programme
   Progress Report 1965, June 1 to Dec. 31 - N° BN - 6512 - 01.

2. H. Andriessen, R. Horne, J.M. Leblanc, M. Stiévenart, W. Van Lierde
   "Fabrication de combustibles à oxydes mixtes UO_2 - PuO_2 pour réacteurs à neutrons rapides".
   Paper presented at the Symposium on the Use of Plutonium as a Reactor Fuel, Brussels, March 13 to March 17, 1967. SM - 88/19

3. Belgian Patent Application Nr 29.130 filed June 7, 1966.
   "Combustible pour réacteurs nucléaires", Inv. J. Draulans and E. Jonckheere.

4. A.J. Flipot, G. Mestdagh.
   "Uranium Oxide Dense Sintered Nodules and Granules Preparation for Vibratory Compacted Fuel Pin Fabrication".
   Euratom - Belgium Fast Reactor Association.
   Brussels, May 1967 - n° BN - 6705 - 03

5. Belgian Patent Nr 689.476 filed November 9, 1966
   "Matériaux céramiques", Inv. H. Bairiot, and P. Papeleux.

TABLE I

PRELIMINARY SPECIFICATIONS OF FAST REACTOR FUEL PINS

TO BE IRRADIATED IN ENRICO FERMI

	Collapsed clad pelleted fuel pin	Conventional pelleted fuel pin	Vibratory compacted fuel pin
Cladding tube (316 and 347 AISI SS)			
Wall thickness	0.40 mm	0.40 mm	0.40 mm
Outer diameter	6.35 mm	6.35 mm	6.35 mm
UO_2-PuO_2 fuel			
Fuel type	Dished pellets	Dished pellets	Fused or sintered powder
Height	6 mm	6 mm	
Diameter	5.540 + 0.050 mm	5.415 + 0.050 mm	
Bulk density	86.5 $\pm$ 1.5 % TD	89.5 $\pm$ 1.5 % TD	> 98 % TD
O/M ratio	1.98	1.98	1.98
Pu content	32 w/o	32 w/o	32 w/o
Fuel pin			
Smeared density	83 + 2 % TD	83 + 2 % TD	83 + 2 % TD
Total length	1.286 mm	1.286 mm	1.286 mm
Fuel length	775 mm	775 mm	775 mm
Bottom FG plenum	190 mm	190 mm	190 mm
Top FG plenum	251 mm	251 mm	251 mm

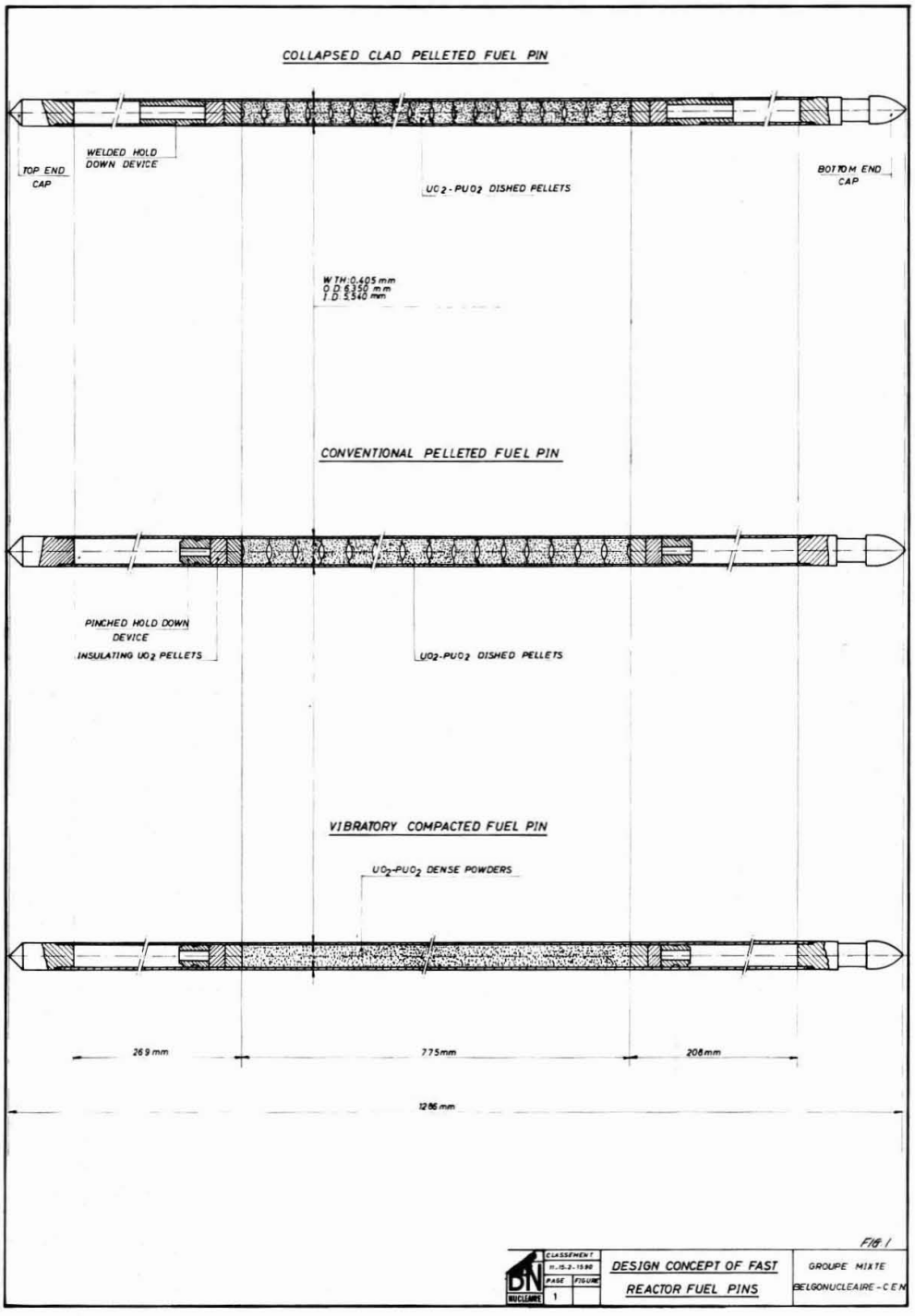
COLLAPSED CLAD PELLETED FUEL PIN
TOP END CAP
WELDED HOLD DOWN DEVICE
UC2-PUO2 DISHED PELLETS
BOTTOM END CAP
WTH:0.405 mm
O.D 6.350 mm
I.D. 5.540 mm
CONVENTIONAL PELLETED FUEL PIN
PINCHED HOLD DOWN DEVICE
INSULATING UO2 PELLETS
UO2-PUO2 DISHED PELLETS
VIBRATORY COMPACTED FUEL PIN
UO2-PUO2 DENSE POWDERS
269 mm
775mm
208mm
1286 mm
FIG 1
CLASSEMENT
11-15-2-1590
PAGE
FIGURE
1
DESIGN CONCEPT OF FAST REACTOR FUEL PINS
GROUPE MIXTE
BELGONUCLEAIRE - C E N

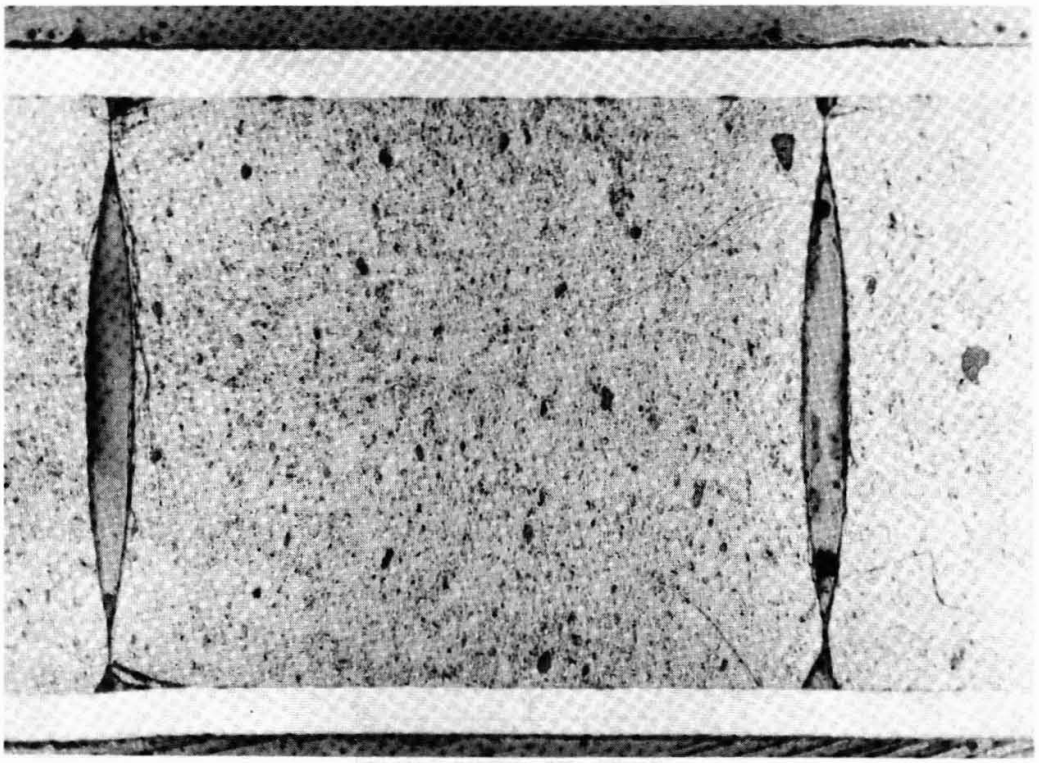

(x 12)

Figure 2

Sample of fuel pin fabricated
utilizing the isostatic creep technique

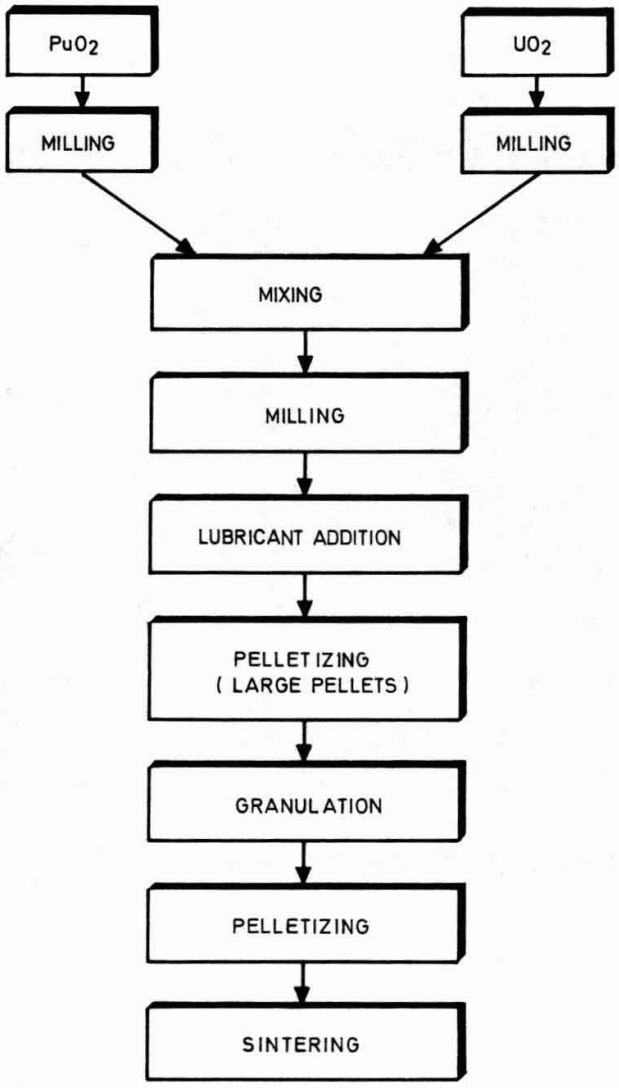

FIGURE.3: FLOW SHEET FOR LOW DENSITY PELLET FABRICATION

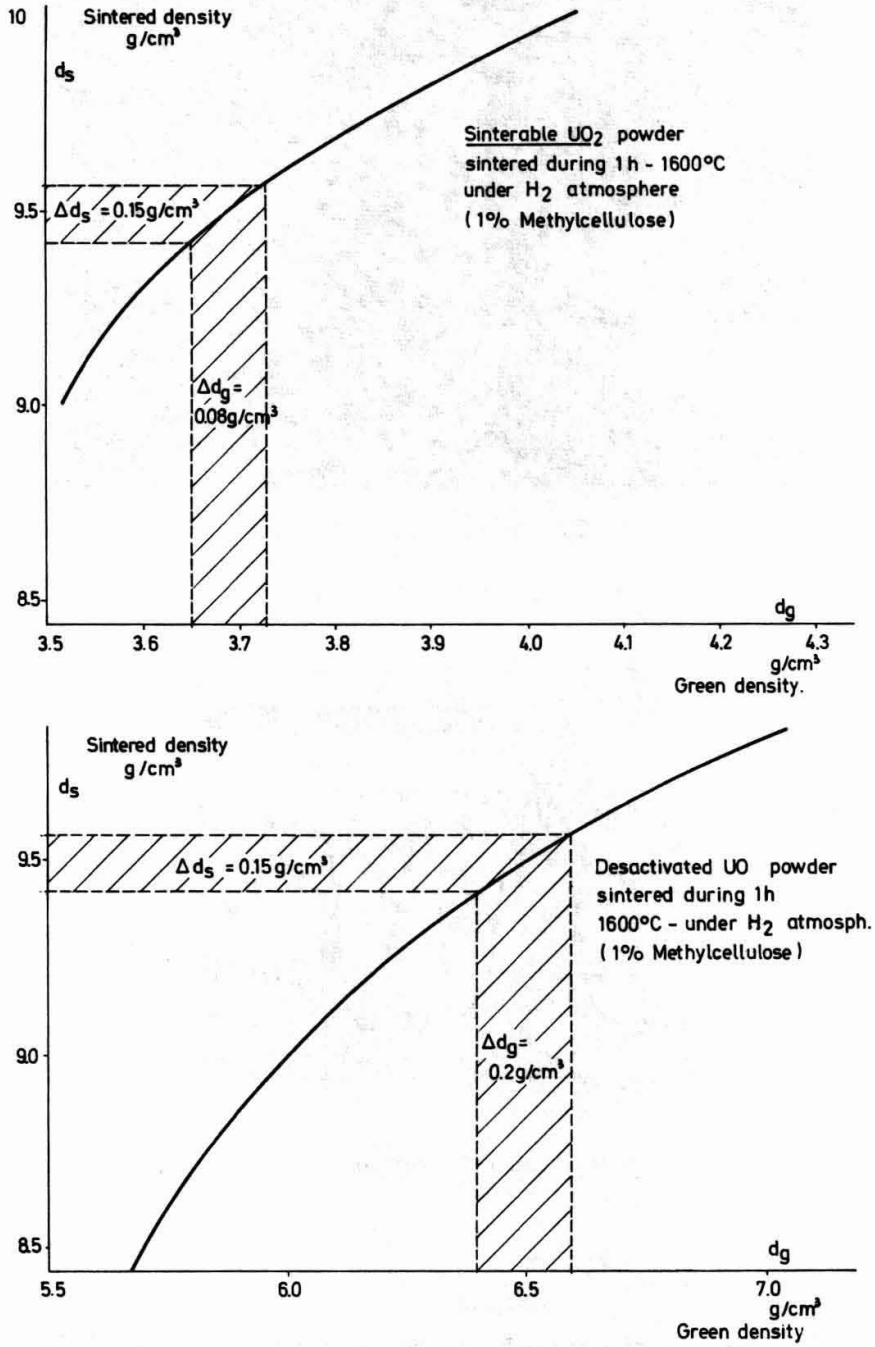

FIGURE 4: GREEN DENSITY VERSUS SINTERED DENSITY FOR SINTERABLE AND DESACTIVATED POWDERS

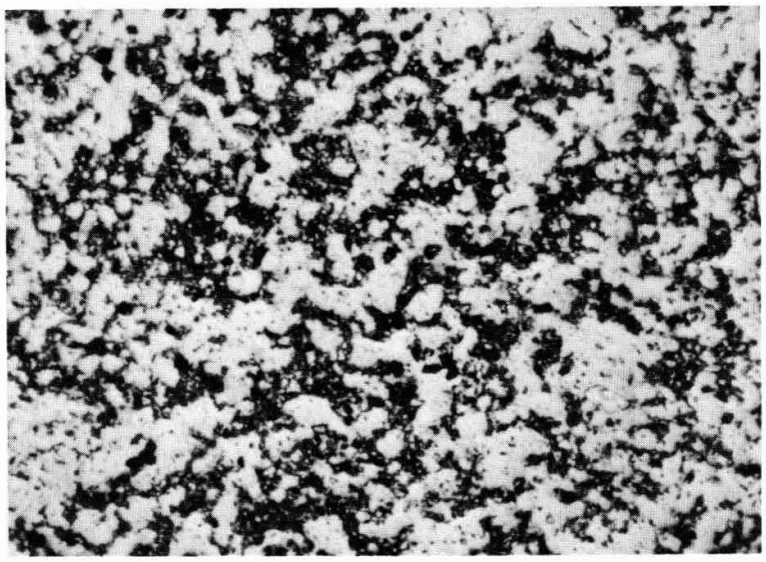

Ceramography : 200 x

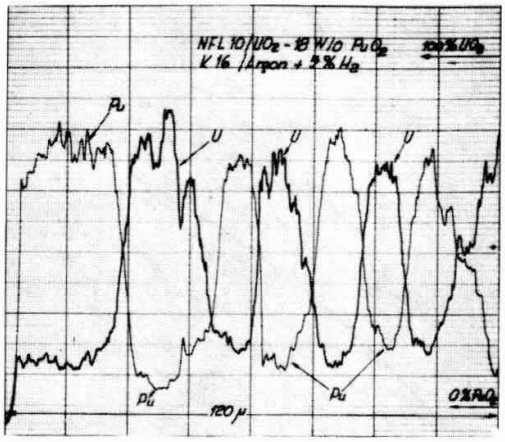

Electron microprobe scan

Figure 5

Electron microprobe scan and ceramography of UO_2 - 18 w/o PuO_2 pellets sintered under reducing atmosphere (Argon + 5 % H_2)

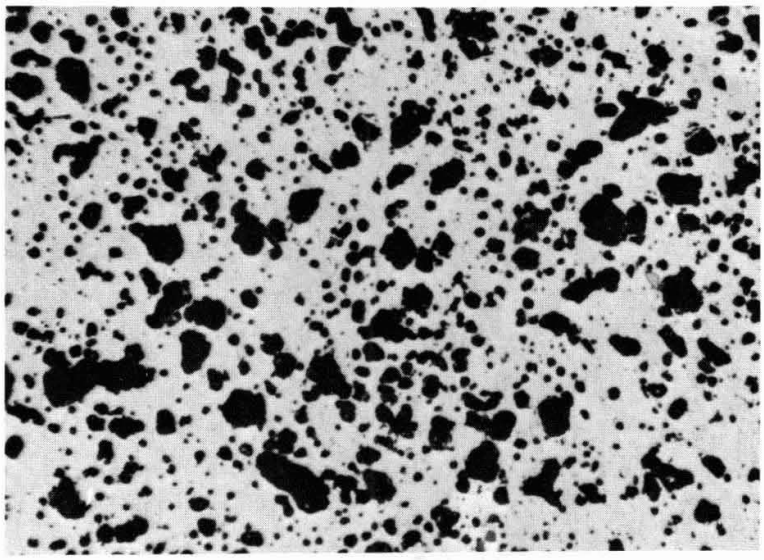

Ceramography : 200 x

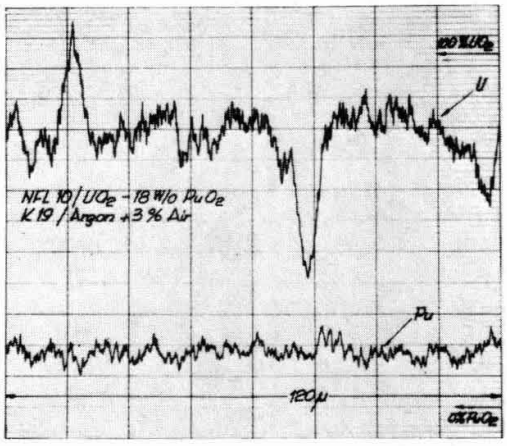

Electron microprobe scan

Figure 6

Electron microprobe scan and ceramography of UO_2 - 18 w/o PuO_2 pellets sintered under oxidizing atmosphere (Argon + 3 % Air)

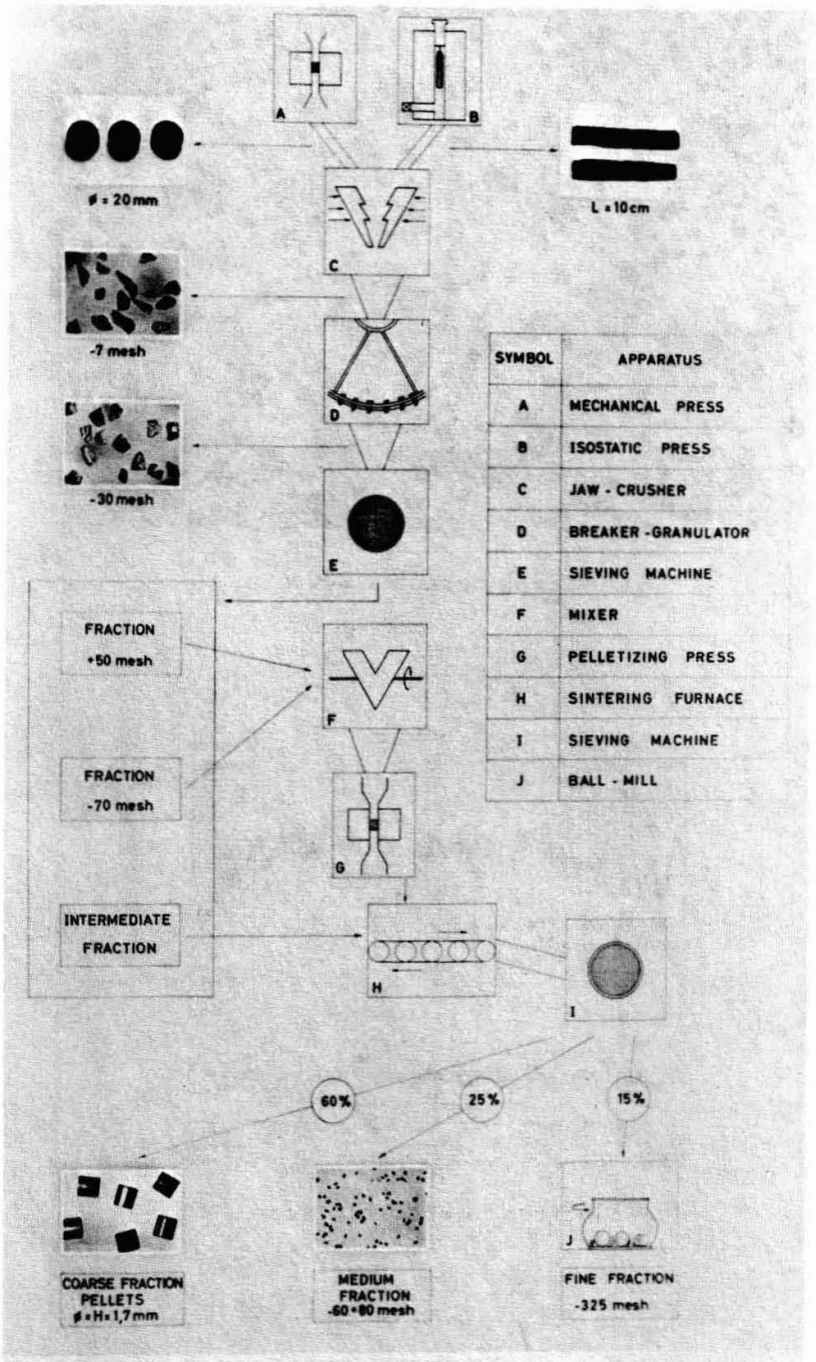

Figure 7

Flow sheet for dense powder preparation according to the sintering process

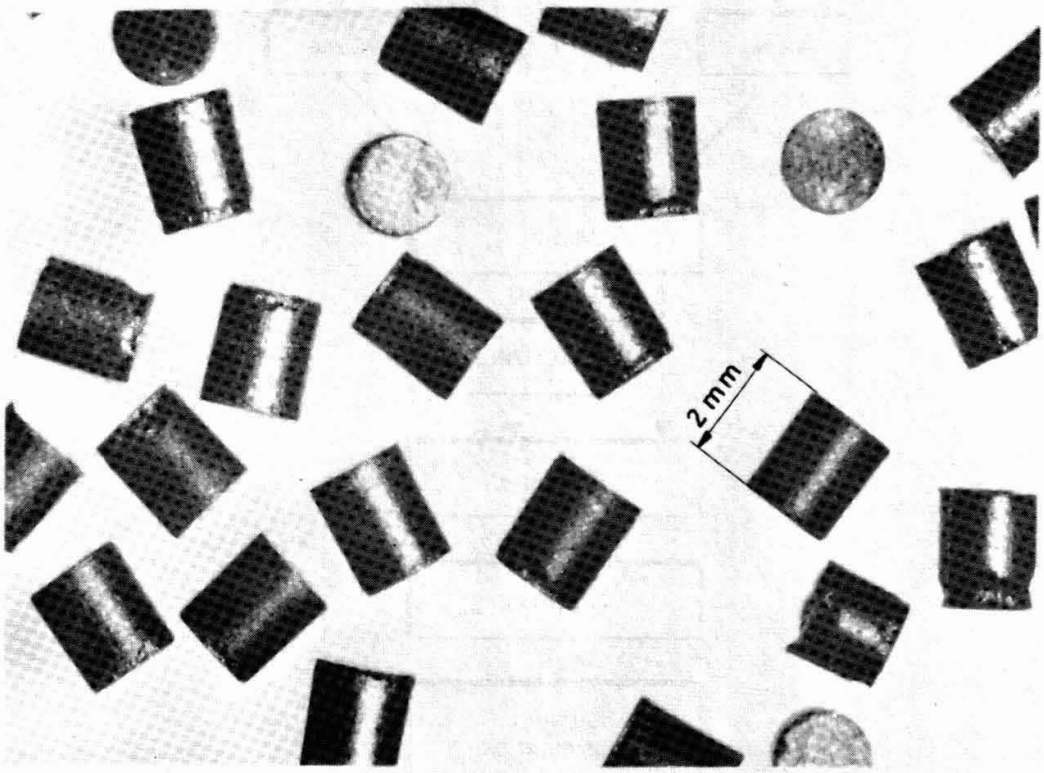

Figure 8
High density small pellets (nodules) coarse fraction
for Vipac fuels

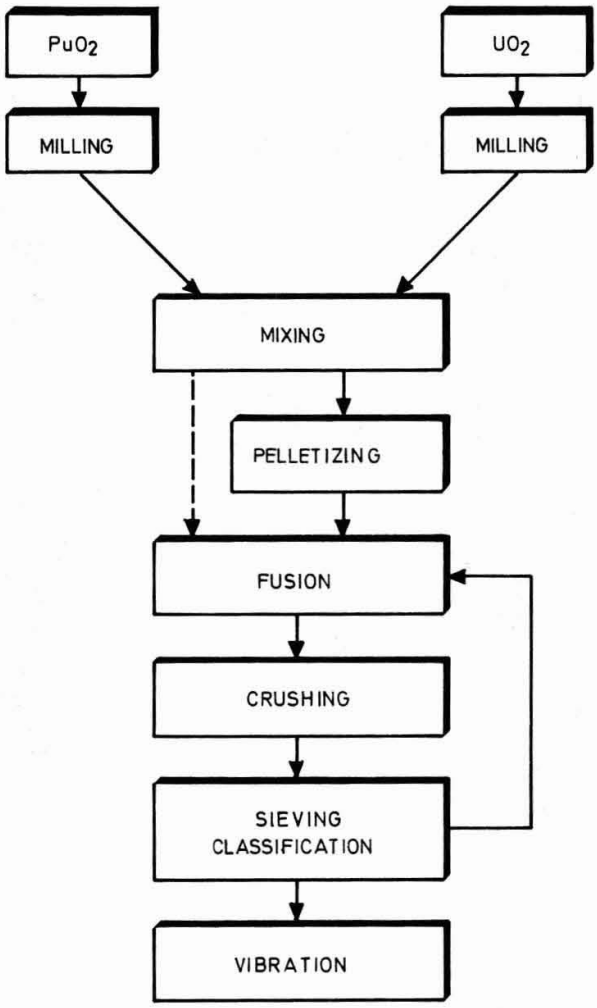

FIGURE. 9: FLOW SHEET FOR DENSE POWDER PREPARATION ACCORDING TO THE FUSION PROCESS

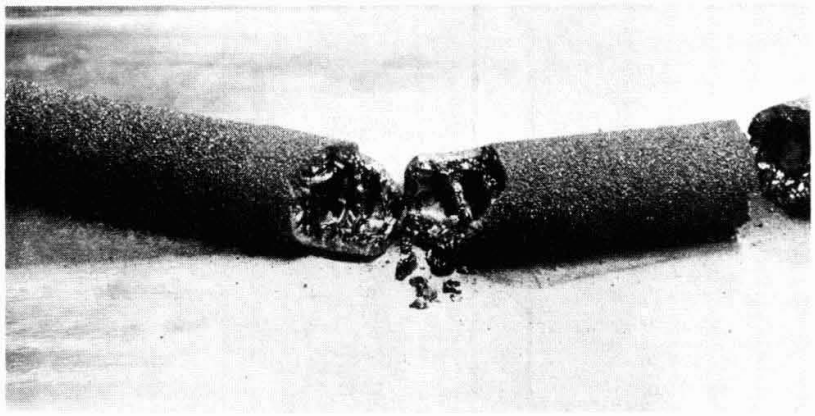

Figure 10
UO_2 - 18 w/o PuO_2 fused ingot

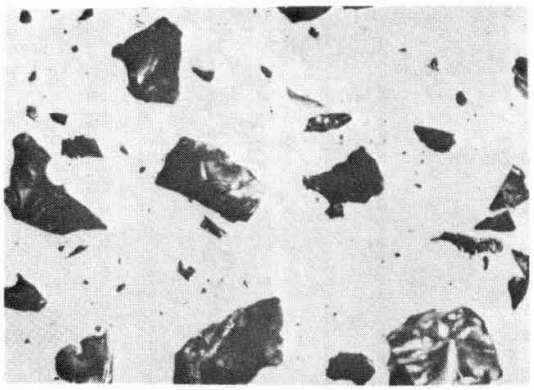

Figure 11
UO_2 - 18 w/o PuO_2 fused particles coming from crushed fused ingot

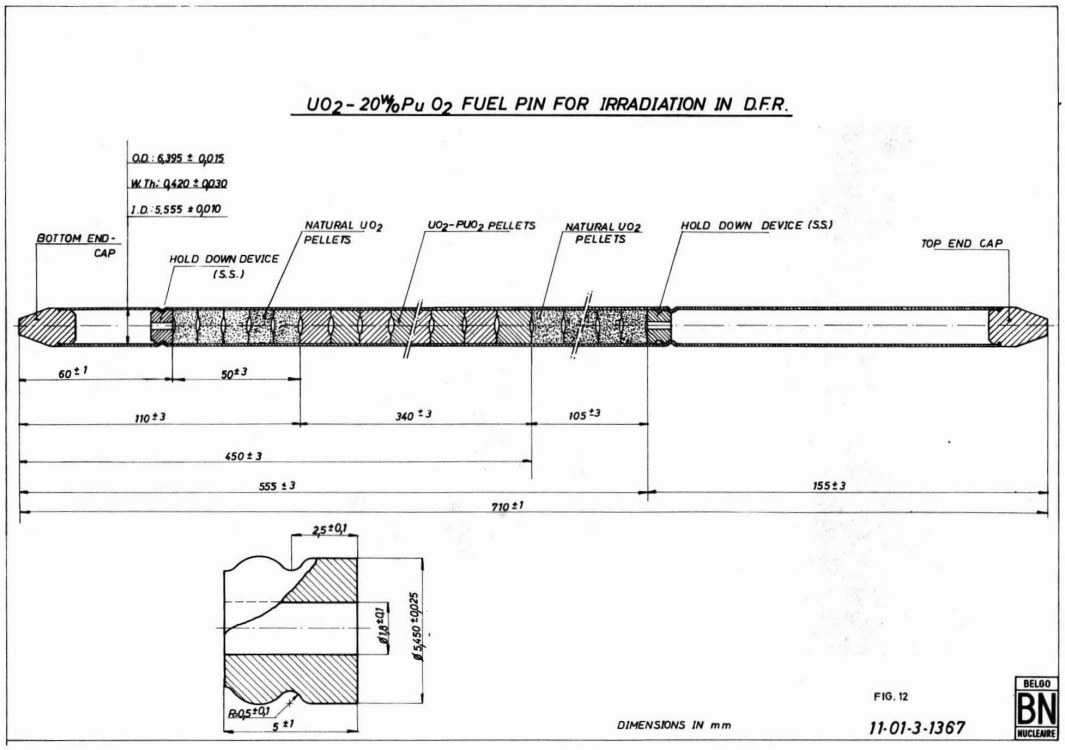
UO2 - 20 w% Pu O2 FUEL PIN FOR IRRADIATION IN D.F.R.
O.D : 6,395 ± 0,015
W.Th: 0,420 ± 0,030
I.D : 5,555 ± 0,010
BOTTOM END-CAP
HOLD DOWN DEVICE (S.S.)
NATURAL UO2 PELLETS
UO2-PUO2 PELLETS
NATURAL UO2 PELLETS
HOLD DOWN DEVICE (S.S.)
TOP END CAP
60 ± 1
50 ± 3
110 ± 3
340 ± 3
105 ± 3
450 ± 3
555 ± 3
155 ± 3
710 ± 1
2,5 ± 0,1
Ø 1,8 ± 0,1
Ø 5,450 ± 0,025
R 0,5 ± 0,1
5 ± 1
DIMENSIONS IN mm
FIG. 12
11-01-3-1367
BELGO BN NUCLEAIRE

U.S. EXPERIENCE ON IRRADIATION PERFORMANCE OF UO_2-PuO_2 FAST REACTOR FUEL

R. E. Skavdahl
C. N. Spalaris
E. L. Zebroski

Abstract

The data thus far add further confidence that UO_2-PuO_2 fuel elements can be designed to achieve high burnup at economical performance conditions in a safe, reliable manner. An increasing number of high-burnup specimens were examined during the past year, which included thermal flux samples at high burnup (>10 atom %) and fast flux specimens at medium burnup ($\sim$6 atom %). Detailed analysis of fuel pins irradiated to burnups up to 6.3 atom % in fast flux, generally confirm the low swelling rates observed in thermal flux. The largest diametral strain was associated with strong axial restraint. Thermal reactor irradiations of vented-to-coolant fuel pins demonstrated an effective holdup time of several days for fission gas release with a simple one-stage vent. Vented fuel is believed to have promise for significantly lengthening fuel lifetime. Transient irradiations show no fuel damage occurs with or without pre-irradiation until energy inputs sufficient to melt about half of the fuel are reached.

Worked Performed Under Contract AT(04-3)-189, Project Agreement 10, Between the U.S. Atomic Energy Commission and the General Electric Company, Advanced Products Operation, Sunnyvale, California.

R. E. Skavdahl is Project Engineer, Fast Ceramic Reactor Development Program; C. N. Spalaris is Manager, Fast Reactor Fuels & Materials Subsection; and E. L. Zebroski is Manager, Sodium Reactor Technology Section for the General Electric Company, Advanced Products Operation, 310 DeGuigne Drive, Sunnyvale, California.

SUMMARY

The data thus far add further confidence that UO_2-PuO_2 fuel elements can be designed to achieve high burnup at economical performance conditions in a safe, reliable manner.

An increasing number of high-burnup specimens were examined during the past year, which included thermal flux samples at high burnup (>10 atom %) and fast flux specimens at medium burnup (~6 atom %). These results are expected to provide the bases for development of more quantitative models for fuel rod design.

Capsules incorporating strongly radially restrained fuel pins yielded data on the effect of temperature and burnup on fuel swelling. The rate of swelling (~0.3% $\Delta V/V$ per 10^{20} fissions/cc) was found to be substantially lower than that found in prior measurements (~0.7% $\Delta V/V$ per 10^{20} fissions/cc) at lower temperatures with UO_2. The maximum swelling rate was exhibited by fuel in the intermediate temperature range (~1800°C).

Fuel pins with more prototypic fuel densities and degree of radial restraint (irradiated in thermal neutron fluxes) displayed similar swelling rates to burnups of 120,000 MWd/Te. The swelling was largely accommodated by the axial expansion of the short fuel columns, rather than being manifested in diametral cladding strain.

Detailed analysis of fuel pins irradiated to burnups up to 6.3 atom % in fast flux, generally confirm the low swelling rates observed in thermal flux. The swelling was manifested in part by larger diametral cladding strains, which is believed to be caused by the partial axial restraint afforded by longer fuel columns. For burnups of ~50,000 MWd/Te, diametral strain was seen to be a strong function of fuel pin smeared density for densities above ~93% T.D. A reduced dependence was observed for densities less than ~93% T.D. Apparently a large part of the initial swelling is accommodated by in-fuel voidage, but in the later stage the remaining voidage is not utilized. Reducing radial restraint (by reducing cladding thickness) results in only moderate increase in diametral strain. The largest diametral strain was associated with strong axial restraint. Few fuel-pin failures have been observed, and those observed thus far in EBR-II have been encapsulated specimens in which the encapsulation itself may have contributed to the failure mechanism.

Thermal reactor irradiations of vented-to-coolant fuel pins demonstrated an effective holdup time of several days for fission gas release with a simple one-stage vent. Vented fuel is believed to have promise for significantly lengthening fuel lifetime by reducing the fission gas pressure within the pin, resulting in less stress on the cladding. Initial failed-fuel behavior tests show differences in fuel distortion and loss from over-power and over-temperature operation.

Transient irradiations show no fuel damage occurs with or without pre-irradiation until energy inputs sufficient to melt about half of the fuel are reached. Axial restraint and increased fuel density lower the threshold energy level which results in fuel damage.

Burnups in the fast flux in EBR-II are expected to reach 75,000 MWd/Te by the end of 1967 and 100,000 MWd/Te by mid-1968. Fast flux irradiations to date have emphasized parametric testing of encapsulated fuel pins. Experiments now planned feature: (1) statistical testing of unencapsulated fuel pins, (2) high risk tests which include fuel pins with purposely defected cladding, and (3) tests designed to achieve higher cladding temperatures.

THERMAL FLUX IRRADIATIONS

Introduction

High burnup experiments in thermal neutron spectra have been underway for the last three years to permit parametric and scoping experiments on the behavior of mixed oxide fuels, which could not be accommodated in fast-flux tests. In addition to various structural and properties investigations, information being obtained includes data on the amount of fuel swelling and cladding strain that can occur at very high burnups. The thermal neutron irradiations are atypical only in that radiation damage to the cladding is too small relative to fast flux tests. However, fuel swelling data are believed to be valid, after making adjustments for self-shielding effects.

Fuel Swelling

Until recently, information on the swelling behavior of oxide fuels has been based on the early BAPD plate fuel and LSBR data which suggest bulk swelling rates in excess of 0.7% $\Delta V/V$ per 10^{20} fissions/cc; the available data has too large a range of scatter to permit correlations with temperature or configuration. The early favorable results from mixed oxide irradiations, however, suggested that in cylindrical geometries operating with fuel surface temperatures greater than 900°C, there may be lower net swelling rates because of better restraint conditions, higher average fuel temperature, greater plasticity of fuel, and more effective utilization of available void space (1).

Basic fuel swelling studies have been performed using strong radial restraint to force all swelling to occur in the axial direction. The experiments employed fuel pins with 0.100-inch fuel pellet diameter and 0.460-inch wall thickness, and provided information on the rate of "inexorable" swelling and the effect of peak fuel temperatures ranging from 1400°C to 2200°C. The data are shown plotted in Fig. 1. The swelling rates with strong radial restraint are seen to be substantially lower than prior data for UO_2, and sharply dependent upon temperature.

At burnups to 15 atom %, the swelling rate is found to be maximum at 1800°C central temperature and lower at lower temperatures. The hypothesis is that at lower temperatures (1400°C peak temperature), fission gases are largely retained; but the growth of fission gas bubbles is restricted by the strength of the mixed oxide lattice and the accommodation of fission gas atoms in interstitial lattice positions similar to those occupied by oxygen in slightly hyperstoichiometric oxide. As the temperature is increased, the interstitial atoms combine to form bubbles, and as the creep strength of the lattice becomes lower, the fission gas bubbles grow more rapidly, which leads to a threefold increase in swelling rate at 1800°C versus the 1400°C central temperature. At temperatures above 1800°C, fission gas is released by diffusion so only a small inventory of gas is retained at steady state. The major portion of further swelling arises from solid fission products.

Included in Fig. 1, and summarized in Table I, are swelling data from thermal flux irradiations of fuel pins with limited radial restraint typical of 0.015-inch-thick cladding. The swelling rates are in surprisingly close agreement with those from the basic swelling studies. The results indicate that (a) no diametral swelling (<0.0002 inch) has been

recorded to date in near-prototype fuels (between 84 and 92% of theoretical density) irradiated to burnups ranging from 80,000 to 120,000 MWd/Te, and (b) some axial expansion, caused by a combination of fuel swelling and axial flux peaking is observed. The volumetric swelling was determined from the change in length of the fuel and resulted in a high value, because axial flux peaking caused a conical central void near the end of the fuel, which was not subtracted from the final volume.

The swelling rate value of about 0.3% $\Delta V/V$ per 10^{20} fissions/cc displayed by these fuel pins implies that smeared fuel densities as high as 88 to 90% of theoretical might be utilized for LMFBR fuel designs for 100,000 MWd/Te burnup, provided that axial restraint is limited.

Fission Gas Release

Fission gas release measurements have indicated that gas release increases with burnup, and releases of 80 to 90% are typical beyond 4% burnup. The increased gas release is believed to work to advantage in minimizing fuel swelling.

Fuel Stoichiometry

Physical property measurements have shown that the melting point and thermal conductivity of mixed oxides are affected by stoichiometry (2). Fuel irradiations at low burnup indicated that hypostoichiometric fuel had a higher thermal conductivity than stoichiometric mixed oxide (3,4). It is recognized that stoichiometry may change within the fuel element during reactor exposure. Anselin and Baily (5) calculated that after high burnups, the stoichiometry is maintained at 2.00, primarily because of thermodynamic equilibria involving chemical reactions of the excess oxygen (from fissions) distributed among the fission products and inner surface of the cladding.

Experiment E2D (Table I) was designed to investigate the effect of stoichiometry upon fuel performance at high burnups. The two fuel specimens contained mixed oxide pellets with average stoichiometries of O/M = 1.96 (1.954, 1.959, 1.960) and 2.006 (2.003, 2.009). The fuel specimens were operated under identical conditions of time, heat flux, power cycling, and neutron flux spectra. They showed similar post-irradiation microstructural characteristics - identical center-hold diameter and location, and columnar grain growth. These results are consistent with the theoretical analysis mentioned above. It is concluded that the initial advantage of using hypostoichiometric fuel (for higher thermal conductivity and higher melting point) may diminish with increasing burnup.

Fuel Density

One of the experiments in Table I (E2C) had fuel density as a prominent variable, with all other parameters held nearly constant. Fig. 2 shows comparative sizes of central void formation observed after reactor exposure. Fuel pellets which were initially 94.3% of theoretical density displayed a central void volume of 3.8%. Pellets of initially 84.5% theoretical density displayed a central void which occupied 10.5% of the original fuel element volume. The absence of porosity in the columnar grain growth region of the low density fuel indicates that it had a higher central temperature, perhaps early in life because both specimens exhibited columnar grain growth to about 75% of the radius. The usual high porosity, believed to be produced by fission gas bubbles, was found

to be present in the structure immediately adjacent to the cladding where fuel burnup was the highest. It is concluded that the difference in the effective thermal conductivities of the two fuels is not significant at very high burnup. A significant difference between low and high density fuels has been demonstrated at low burnup (6).

Fuel-to-Cladding Gap

Fabrication of large quantities of fuel rods (approximately 38,000 rods or about 1×10^6 inches of fuel for a 300 MWe power reactor) under glove-box conditions required simple assembly techniques. Ease of assembly requires a diametral gap range of 3 to 7 mils. Numerous experiments were conducted to explore fuel performance behavior as a function of initial pellet-to-cladding gap. In one specific case, diametral gaps of 2, 4, and 10 mils were investigated at low burnups (45 hours). Thermocouple measurements yielded derived contact conductance values of 2000, 1100, and 600 Btu/h-ft^2-°F for the gaps mentioned; but the 4- and 10-mil gaps were reduced to one-half their initial value in 45 hours (7).

Recent results shown in Table I were obtained from fuel experiments carried out to high burnups. Post-irradiation metallography indicated small or no gaps remaining. These results confirmed those obtained earlier in experiments conducted at low burnups, and show that diametral gaps cannot be used to accommodate fuel swelling.

FAST FLUX IRRADIATIONS

Introduction

A total of 20 mixed oxide fuel pins have completed irradiation in EBR-II at burnups of 0.2 to 6.3%, and have been subjected to post-irradiation examination (Table II). An addition 93 specimens, ranging in burnup from 1.5 to 6.4 atom %, are currently being irradiated in EBR-II.

The first six pins listed in Table II were removed from EBR-II in May, 1965, following a short-term irradiation as a proof-of-principle test (8). In November, 1966, two fuel rods containing vibrationally compacted UO_2-20%PuO_2 were removed from EBR-II after a burnup of ∿2.7% (9). In February, 1967, a significant milestone was reached when the first pins to achieve greater than 5 atom % burnup were removed (10). This batch of 12 pins included 11 pins which had reached burnups of from 5.0 to 6.3 atom % and one pin at 3.6 atom %. It is expected that the first pins to reach 10 atom % burnup will be removed from EBR-II in mid-1968.

Fuel Swelling

The maximum diametral strain observed on 11 of the 12 F2 series of fuel pins ranged from 0.40% (0.0010 inch ΔD) to 1.72% (0.0043 inch ΔD); the latter for a fuel pin with an axially restrained fuel column. Excluding the axially-restrained specimen and the lower burnup (3.6%) specimen, the maximum diametral strains all fall in the range 0.40% to 0.92%. The corresponding fuel pin gross volumetric swelling rates ($\Delta V/10^{20}$ fissions/cc) are well below the minimum rate observed for the basic swelling capsules, and indicate that fuel swelling is being accommodated to a great extent in some manner other than diametral strain. The nearly-double strain exhibited by the axially-restrained specimen tends to confirm that axial expansion is a significant mechanism in accommodating fuel swelling.

Fig. 3 shows the maximum diametral strains plotted as a function of initial fuel pin average smear density, and indicates that the degree of fuel pin swelling is not a strong function of the degree of initial void volume in the fuel. A detailed pellet-by-pellet analysis of the data was performed. The ΔD at each pellet location in the fuel column was obtained by subtracting the local pre-irradiation diameter (determined by a micrometer) from the post-irradiation diameter (determined by detailed profilometry) at two rod orientations (0° and 90°). Each ΔD was actually a range of values, because the profilometer trace is continuous and rod diameter variation over even one pellet length was detected. Using as-fabricated values of pellet density and pellet-cladding gap, local smear densities were calculated for each pellet location. The data are plotted in Fig. 4, where the data points are vertical lines representing the range of the local ΔD at pellet locations of indicated smear density. The data in Fig. 4 represent all the pellets in fuel rods F2A, F2E, F2Q, and F2U. Two items are particularly apparent:

1. The scatter in the data is quite large, indicating the value of more closely controlling fabrication of parametric test pins (more closely match pellet densities and sizes, more closely control and select cladding dimensions) and of obtaining more detailed pre-irradiation dimensional measurements (profilometer rather than micrometer).

2. The gradual trend of increased diametral strain with increased density, exhibited by Fig. 3, appears in Fig. 4 to be replaced by a two-stage dependence (at ∿50,000 MWd/Te burnup). At the low densities (from ∿86% T.D. to 93% T.D.), reducing smear density does not result in greatly reduced diametral swelling, the dependence being only about $\frac{0.02\%\ \Delta D/D}{1\%\ \text{T.D.}}$. At higher densities, the relationship is about $\frac{0.20\%\ \Delta D/D}{1\%\ \text{T.D.}}$. The large difference is probably caused by the occurrence of an "induction" period of burnup, during which the larger amount of in-fuel voidage in the lower density pins partially accommodates the swelling and delays its manifestation as diametral cladding strain. Differential thermal expansion between the fuel pellets and cladding accounts for a portion of the strain at the high-smeared densities (>95% T.D.).

Similar plots were made of the pellets in the other fuel rods from the F2 series. Using the center-of-mass of the data from each pin as a data point, it appears that reducing cladding thickness from 0.015 inch to 0.010 inch increased diametral strain from ∿0.3% to ∿0.7% (at ∿92.6% T.D., average).

Fission Gas Release

Fig. 5 shows the fission gas release values plotted against fuel pin smear density. Two trends are apparent: (1) decreasing gas release with increasing smear density (decreasing fuel temperature), and (2) increasing gas release with increasing burnup. Comparison with British data (11) shows general agreement for vibrationally compacted fuel, but the F2 release values for solid pellet fuel are somewhat higher than the British values for annular pellet fuel, as might be expected. The fission gas release data for pins irradiated in EBR-II, although not so abundant as for pins irradiated in thermal flux, tend to confirm the saturation effect indicated by the latter data.

Fuel Pin Failures

On neutron radiographic examinations of the 12 encapsulated pins irradiated to >5% burnup, it was observed that one pin had failed. At least one additional encapsulated-pin failure has been detected in a subsequent group of pins, but examinations other than neutron radiography have not yet been done.

Structural Changes in Mixed Oxide

In all cases, structural changes (central void formation, columnar grain growth, etc.) occurred which were consistent with those observed in thermal flux irradiations having similar design and operating parameters.

Metallic inclusions were observed throughout a cross-section of pin SOV-6 (12) (vipac, 83.3% theoretical density, 18.4kW/ft, 2.9% peak burnup), as well as in the bottom of the central void. The latter corresponded to a peak in a gamma-scan for ruthenium-103 activity, while the former were identified (13) to consist mainly of ruthenium and molybdenum, with smaller amounts of technetium, rhodium, and palladium. Similar inclusions were observed in the cross-sections of the F2 group of pins, but not in the bottom of the central void. The concentration of inclusions found in the bottom of SOV-6 probably resulted from the fuel having been molten at some time during its irradiation, which was not the case for the F2 pins.

A gray phase located in the grain boundaries of the fuel in SOV-6 was identified (13) to contain significant amounts of barium, strontium, and cerium. A similar gray phase has been observed in the F2 pins, but not nearly so extensive.

Fig. 6 shows the transverse cross-sections of pelleted fuel pins F2Q and F2U. The pins had smeared densities of 96.7% and 87.0%, and operated at 16.7 kW/ft and 16.3 kW/ft, to peak burnups of 6.0% and 5.9%, respectively. The structures are consistent with expectation, the larger central void in F2U reflecting its higher fuel temperatures (lower smear density) and higher fission gas release (63% versus 47% for F2Q).

BEHAVIOR OF OXIDE FUELS DURING POWER TRANSIENTS

The availability of a large, prompt, negative Doppler coefficient in fast reactor cores fueled with mixed oxide, makes it important to establish the magnitude of the power pulse which oxide fuel can withstand without suffering gross mechanical distortion. This data is important in the hazards analysis of a reactor because it determines the amount of reactivity insertion which can be safely offset by the Doppler coefficient without having to take into account further reactivity effects caused by fuel motion. It is of further importance to determine the nature of the phenomena in the vicinity of the damage threshold of the fuel, and how the threshold of damage varies with the details of the fuel design and its prior exposure history. A program of such tests, primarily utilizing the TREAT facility to provide power transients, has been underway for six years in connection with the Fast Ceramic Reactor Development Program.*

The effort to date has reasonably well established the threshold damage limits for unirradiated fuel and preliminary data on fuel pre-

*Sponsored by the United States Atomic Energy Commission under Contract AT(04-3)-189, Project Agreement 10, with the Gen. Elect. Co., Sunnyvale, Calif.

irradiated to 60,000 MWd/Te in thermal fluxes. All of the energy inputs at failure thresholds observed so far are substantially higher than those calculated for credible excursions in current U.S. fast reactor designs. The mechanisms by which thresholds are exceeded have been determined. Further irradiations of typical fuel is underway in EBR-II to establish the influence on transient behavior of pre-irradiation in a fast flux. Effects of (1) the reduced ductility of the cladding caused by exposures of the order of 5 to 8 x 10^{22} nvt, and (2) the different inventory and radial distribution of fission gases, will be explored for the fast flux irradiations.

Three recent transient tests of mixed oxide pins in TREAT are tabulated in Table III. Examination of these experiments leads to the following conclusions (applicable to fuel which is not irradiated prior to the transient).

1. The transient failure mechanism for zero burnup fuel is cladding melting caused by contact with molten fuel. High internal pressure does not appear to contribute significantly to failure (no appreciable cladding deformation is found in areas adjacent to the failure zones).
2. Axial restraint of the fuel column significantly (10 to 15%) reduces the threshold energy level for cladding failure. Unavailability of axial expansion space results in earlier contact of molten fuel and cladding.
3. Decreased fuel density partially offsets the effect of axial restraint and allows accommodation of melting of most of the fuel (70 to 80%) without cladding failure.

For pre-irradiated fuels, the mechanism of failure in transients is considerably different. Table IV summarizes pre-irradiated test results (14).

1. The fission gases released from molten fuel contribute significantly to the stress of the cladding, even at low strain levels.
2. Pressure from suddenly released fission gas can cause redistribution of part of the molten fuel, but "foaming" of molten fuel does not occur appreciably.
3. Fuel pins survive transients producing extensive fuel melting, even after extensive pre-irradiation (in thermal flux). Fast flux pre-irradiation tests are in progress.

VENTED FUEL BEHAVIOR

Vented fuel is a strong candidate for current reference fuel designs for several 1000 MWe plant design studies sponsored by ANL, and is under active consideration for first generation demonstration plants of about 300 MWe. The potential benefits of venting are:

1. Lower stress level in the cladding at high burnups.
2. Elimination of the possibility of gas blanketing damage of nearby fuel from the release of high pressure fission gases at the inception of a fuel defect.
3. Lower failure rate of fuel at high burnups with consequent lower contamination of system by mixed fission products.

The intentional emission of fission gases from vented fuel need not be considered a disadvantage for plant operation or maintenance. In a practical system, the effect of fixed radioactivity on maintenance operations at high burnup may actually be less with properly designed vented fuel than with nonvented fuel, because of the reduced failure rate of the former.

Prior tests with short pins (5-inch fuel length) have been encouraging because the predominant activity appearing in the sodium was Cs-134 via the chain:

$$\text{Xe-133} \xrightarrow{\beta^-} \underset{5.7\text{d (stable)}}{\text{Cs-133}} \xrightarrow{n,\gamma} \text{Cs-134} \xrightarrow{\beta^-} \underset{2.3\text{y (stable)}}{\text{Ba-134}} .$$

The cesium-134 activity was of the same order as the limiting level of Na-22 activity expected in a large fast reactor. The distribution of the fission gases released suggested an average delay time of about 5 days for the particular geometry tested.

Fission product escape rates are being determined from more typical pins (20-inch and 23-inch fueled regions - 8 to 12-inch axial blanket) under conditions simulating central and core-edge positions. Results are available for one specimen (B3F in Table V).

With the longer pin, the release of short-lived fission gases is somewhat greater than in the short-pin test. (A simple one-stage vent was used for both cases). This effect is tentatively attributed to the different ratios of free volume in the pin to the volume of the vent and vent plenum. The breathing of gas with cycling of power and temperature, results in a smaller effective delay time during a power cycle.

Analysis of delay times attainable indicates that, with several vent chambers in series, effective holdup times of 10^2 to 10^3 hours are attainable. Additional holdup time of the vented gas is normally provided by the reactor cell atmospheres.

Venting to atmosphere is possible because the amount of activity released can be made very small, and essentially only Kr-85 would be emitted. Release rates well within typical 10CFR-20 limits appear feasible for a 3000 MWt reactor.

Failed Fuel Behavior

The mechanism of propagation of defects is of importance in both safety analysis and in the definition of effective fuel lifetime. The objective is to find operating conditions and fuel configurations such that continued reactor operation is practical until the next convenient refueling time. It is also essential, for safety analysis, to be able to describe the behavior of fuel under overpower and low-flow conditions.

Some fuel defects have occurred in the course of testing fuel in capsules, but these have been difficult to interpret because of the influence of the capsule itself on the nature of the failure. Transient defect testing with circulating sodium is planned for 1968. Two interesting examples of probable steady-state overpower or over-temperature failures are available which occurred in low velocity flowing coolant (natural convection NaK at $\sim$1 fps). The conditions of the tests are given in Table VII. For B3B, the initial failure occurred during a three-hour

period of over-power operation near 30 kW/ft. For B3C, failure was caused by over-temperature operation for a period of 11 days at 1300°F (at the outer surface of the cladding). The volume increase on melting in B3B was greater than could be accommodated by the design, resulting in local necking and rupture of the cladding. For the specimen which continued prolonged operation after failure (24 weeks) further increase in fuel diameter took place because of the penetration of sodium into the fuel. For stoichiometric fuel, density changes up to 12% have been observed in out-of-pile tests (21), depending on the initial density and O/M ratio.

While the conditions of these tests only roughly approximate actual power reactor operation, it is provisionally concluded that:

1. Limited operation after over-power failure may be feasible with respect to acceptable escape of fuel and fission products.
2. Over-temperature operation (1300 to 1350°F local cladding peak) is not acceptable because of gross emission of fuel after failure occurs. Tests of failure effects in various forced circulation loops are planned to determine behavior of defected fuel under the following conditions:
   a. steady-state over-power,
   b. steady-state over-temperature (low flow),
   c. loss of flow and meltdown, and
   d. transient over-power from full power.

REFERENCES

1. J. M. Gerhart, The Post-Irradiation Examination of a PuO_2-UO_2 Fast Reactor Fuel, GEAP-3824, November, 1961.
2. W. E. Baily, E. A. Aitken, R. R. Asamoto, and C. N. Craig, Thermal Conductivity of Uranium-Plutonium Dioxide Fuels, Proceedings of AIME Nuclear Metallurgy Symposium, October, 1967.
3. C. N. Craig, and W. E. Baily, In-Pile Comparison of the Effective Thermal Conductivity of PuO_2-UO_2 Mixed Oxide, forthcoming topical report.
4. S. A. Rabin, W. W. Kendall, and W. E. Baily, Short-Term Fast Flux (EBR-II Irradiation of PuO_2-UO_2 Fuel Pins, GEAP-4473 (In Publication).
5. F. Anselin and W. E. Baily, Trans. Am. Nuc. Soc., 1967, Vol. 10, No. 1, p. 103.
6. Fast Ceramic Reactor Development Program Quarterly Report, February-April, 1966, GEAP-5158, June, 1966.
7. W. E. Baily, C. N. Craig, and E. L. Zebroski, Trans. Am. Nuc. Soc., 1966, Vol. 9, No. 1, p. 40.
8. S. A. Rabin, R. W. Darmitzel, and W. W. Kendall, Trans. Am. Nuc. Soc., 1966, Vol. 9, No. 1, p. 41.
9. Argonne National Laboratory, Reactor Development Program Progress Report, November, 1966, ANL-7279, p. 26.
10. Fast Ceramic Reactor Development Program Quarterly Report, February-April, 1967, GEAP-5491, May, 1967.
11. H. Lawton, et al., The Irradiation Behavior in a Fast Flux of Plutonium Bearing Ceramic Fuels, BNES Conference, May, 1966, Paper No. 4B/4.
12. Argonne National Laboratory, Reactor Development Program Progress Report, February, 1967, ANL-7308, p. 29.
13. Argonne National Laboratory, Reactor Development Program Progress Report, May, 1967, ANL-7342, p. 71.
14. J. H. Field and J. E. Hanson, Experimental Studies of Transient Effects in Fast Reactor Fuels. Series III, Pre-Irradiated Mixed Oxide (PuO_2-UO_2) Irradiations. Final Report, Transient Irradiations, GEAP-4469, October, 1967.
15. Argonne National Laboratory, Reactor Development Program Progress Report, June, 1967, ANL-7349, p. 76-78.
16. Argonne National Laboratory, Reactor Development Program Progress Report, March, 1967, ANL-7317, p. 52-53.
17. E. L. Zebroski, H. Kittel, and D. Moss, Reviews of Status of Technology of Fast Reactor Fuels, Proceedings of Fast Reactor National Topical Meeting, April, 1967, ANS-101, p. 2-63.
18. Fast Ceramic Reactor Development Program Quarterly Report, May-July, 1967, GEAP-5522, September, 1967.

REFERENCES (Continued)

19. R. C. Nelson, B. F. Rubin, W. W. Kendall, and W. E. Baily, Performance of Mixed Oxide Fuel Pins Irradiated in a Fast Reactor to 50,000 MWD/Te, Trans. Am. Nuc. Soc., 1967, Vol. 10, No. 2.

20. M. L. Bleiberg, R. M. Berman, and B. Lustman, Effects of High Burnup on Oxide Ceramic Fuels, March, 1962, WAPD-T 1455.

21. Fast Ceramic Reactor Development Program Quarterly Report, November, 1965-January, 1966, GEAP-5098, April, 1966.

TABLE I

FUEL PINS IRRADIATED TO HIGH BURNUPS IN THERMAL FLUX

Pin No.	Cladding	O/M	Smear Density, % Theoretical	kW/ft	Cladding Temperature (°F)	Burnup (MWd/Te)	$\frac{\Delta L}{L}$* (%)	Inital Diametral Gap (mils)	Final Diametral Gap (mils)	Fission Gas Release (%)
E1E-1		2.00	94.7	∿20	∿650	∿87,000	4.4			
E1F-1		2.00	94.6	∿20	∿650	∿80,000	4.2			
E2C-1	347 SS	2.00	85	20	1060	120,000	6.1	3.2	0	83
E2C-2	347 SS	2.00	95	20	1060	120,000	8.0	3.7	0	83
E2D-1	316 SS	2.00	90	17	1050	117,000	8.3	2.0-2.9	0 - 1	86
E2D-2	316 SS	1.96	92	17	1050	117,000	4.5	2.2-3.5	0 - 1	91
E5B-1	347 SS	2.00	86	20	1100-1150	115,000	4.7	3.2-3.7		
E5B-2	347 SS	1.999	84	20	1100-1150	115,000	3.0			

*ΔD <0.0002 inch on all pins.

TABLE II

RESULTS OF POST-IRRADIATION EXAMINATION OF UO_2-20% PuO_2

FUEL PINS IRRADIATED IN EBR-II

			Design Parameters						Operating Parameters		
			Cladding			Gaps (in.)		Average Smear Density	Maximum Linear Power	Maximum Cladding Temp.	Peak Burnup
Pin No.	O/M	Fuel Form	Type	O.D. (in.)	Thick (in.)	Diameter	Axial	(%)	(kW/ft)	(°F)	(atom %) (5)
F1A	2.00	Pellet	347 SS	0.250	0.015	0.0039	0.49	93	16.1	1086	0.2
F1B	2.00	Pellet	347 SS	0.250	0.015	0.0025	0.48	95	16.4	1091	0.2
F1C	2.03	Pellet	Incoloy-800	0.250	0.015	0.0022	0.002	94	16.8	1097	0.2
F1D	1.98	Pellet	Incoloy-800	0.250	0.015	0.0030	0.48	93	16.2	1088	0.2
F1E	1.98	Pellet	316 SS	0.250	0.015	0.0030	0.50	87	14.8	1066	0.2
F1F	1.99	Vipac	Incoloy-800	0.250	0.015	N.A.	0.31	85	16.4	1091	0.2
SOV-5	>2.00	Vipac	304 SS	0.296	0.021	N.A.		83.4	17.2	1049	2.7
SOV-6	>2.00	Vipac	304 SS	0.296	0.021	N.A		83.3	18.4	1076	2.9
F2A	2.00	Pellet	347 SS	0.250	0.015	0.0025		94.0	16.1	1140	5.8
F2B	2.00	Pellet	316 SS	0.250	0.015	0.0026		94.6	16.4	1154	6.0
F2E	1.98	Pellet	316 SS	0.250	0.015	0.0032		94.4	16.7	1161	6.0
F2F	1.98	Pellet	Incoloy-800	0.250	0.015	0.0030		94.8	16.8	1165	6.1
F2N	2.00	Pellet	347 SS	0.250	0.010	0.0034		92.6	16.6	1160	6.0
F2P	2.00	Pellet	347 SS	0.250	0.015	0.0030		94.5	9.9	975	3.6
F2Q	2.00	Pellet	347 SS	0.250	0.015	0.0012		96.7	16.7	1161	6.0
F2S	2.00	Pellet	347 SS	0.250	0.030	0.0012		96.7	17.5	1184	6.3
F2U	1.98	Pellet	347 SS	0.250	0.015	0.0034		87.0	16.3	1150	5.9
F2W	1.99	Vipac	347 SS	0.250	0.015	N.A.		83.8	14.1	1092	5.1
F2Y	1.99	Vipac	316 SS	0.250	0.015	N.A.		83.9	13.8	1084	5.0
F2Z	1.99	Pellet	316 SS	0.250	0.015	0.0029		87.2	16.1	1140	5.8

TABLE II (Continued)

Pin No.	Post-Irradiation Results: Maximum Δ Diameter (inches)	Δ Density (%)	Δ Length (inches)	% Fission Gas Release	General Condition	References	Remarks
F1A	<0.001[1]		-0.013[2]	11	Good	4,8	
F1B	<0.001[1]		-0.008[2]	5	Good		
F1C	<0.001[1]		+0.002[2]	7	Good		
F1D	<0.001[1]		-0.007[2]	8	Good		
F1E	<0.001[1]		-0.017[2]	26	Good		
F1F	<0.001		-0.013[2]	28	Good		
SOV-5	not significant	<0.03%[3]	+0.54%[4]		Good	12,15,16	Not destructively examined; to be re-irrad. in TREAT.
SOV-6	not significant	<0.03%[3]	+0.54%[4]	65	Good		
F2A	0.0014		+0.033[2]	49	Good	10,17,18,19	
F2B	0.0017		+0.026[2]	48	Good		
F2E	0. 021		+0.022[2]	50	Good		
F2F					Failed		
F2N	0.0022		+0.028[2]	50	Good		
F2P	0.0013		+0.029[2]	32	Good		
F2Q	0.0023		+0.032[2]	47	Good		
F2S	0.0043		+0.014[2]	55	Good		Axially restrained fuel column.
F2U	0.001		+0.017[2]	63	Good		
F2W	0.0011		+0.013[2]	58	Good		
F2Y	0.0010		+0.006[2]	56	Good		
F2Z	0.0016		+0.011[2]	58	Good		

(1) Exhibited ridging (<0.0002 inch) at some pellet interfaces.
(2) Of ∿35.5 inches long fuel pin.
(3) Of jacketed fuel column.
(4) Of ∿11.5 in. long fuel column .
(5) Peak/Average = 1.14.

TABLE III

TRANSIENT OVER-POWER TESTS OF MIXED OXIDE FUELS PINS

Specimen	C2B	C4A	C4C
Design:			
Smeared density	90%	90%	80%
Length	6 inches	14 inches	14 inches
Axial Restraint	None	(space provided for expansion only up to melting)	
Operation:			
Pre-irradiation	None	None	None
Peak transient specimen power	200 kW/ft	160 kW/ft	150 kW/ft
Total specimen energy release	150 kW-sec/ ft	130 kW-sec/ft	120 kW-sec/ft
Maximum fuel temperature (calculated)	∿3000°C	3500°C	3500°C
Results:			
Fuel volume melted	∿75%	70-75%	75-80%
Cladding failure	No	Yes*	No
Cladding deformation	No	No**	No

*Approximately 10% of the fuel was expelled from the pin.
**Two additional pins failed at still higher energy inputs. Failure was also cladding melting, but no cladding deformation could be measured in unmelted regions.

TABLE IV

TRANSIENT TESTS OF PRE-IRRADIATED MIXED OXIDE FUEL PINS

Sample(1)	Pre-Irradiated (MWd/Te)	Transient Power Peak (kW/ft)	Transient Power Total (kW-sec/ft)	% Fuel Melted	Observations
C3B	8,100	112	143	30	(2)
C3C	64,000	166	147	67	(3)
C4E	63,000	76	97	22	(4)

(1) All samples fuel length 6 inches, 0.250 inch nominal O.D., 0.015 inch wall, thickness SS Type-347, 28% PuO_2 in UO_2.
(2) Prior calibration transient to 55 kW-sec/ft; final cladding diameter increase 2 to 3 mils.
(3) Fuel cladding intact after transient, average diameter increase 3 mils. (The failure of a pressure transducer diaphragm allowed molten fuel (11 gms) to flow via a 0.033-inch tube to a plenum below the pin.)
(4) Minor axial displacement of part of molten fuel, no diametral changes.

TABLE V

RADIOACTIVITY LEVELS IN VENTED FUEL TEST B3F
(Natural Convection NaK)

Species Observed	dps/gm NaK x 10^6	Rare Gas Parent Isotope	Rare Gas Parent Half-Life
Cs-134	1.6	Xe-133	5.3d
Cs-136	0.14	Xe-135	9m
Cs-137	0.6*	Xe-137	3.9m
I-131	$<40 \times 10^{-5}$	-	-
Na-22	0.016	-	-
Ba-140**	$<10^{-3}$	Xe-140	16s
Ce-144**	$<10^{-4}$	Xe-144	∿1s
Zr-95**	$<10^{-4}$	Kr-95	short

* This is ∿0.1% of total inventory formed.
**Most of these activities in the cold trap; release fractions about 10^{-9}.

TABLE VI

CURRENT VENTED FUEL TESTS

Sample (5)	Active Fuel Length (inches)	Density	kW/ft (peak)	Core Region Simulated	Peak Cladding Surf.Temp. (°F)	Status
B3D	20	85	18	center	1200	(1)
B3E	23	83	18	edge	1200	(2)
B3F	23	84	15	edge	1100	(3)
B4D	20	84	15	center	1100	(4)

(1) Present burnup ∿7,000 MWd/Te.
Target burnup ∿50,000 MWd/Te.
(2) Present burnup ∿7,000 MWd/Te.
Target burnup ∿50,000 MWd/Te.
(3) F.P. release data obtained at 23,500 MWd/Te.
(4) Neutron radiograph at 38,000 MWd/Te; F.P. release to be measured at ∿45,000 MWd/Te.
(5) All samples nominal 0.250-inch O.D. clad with 0.015-inch wall, Type-316 SS. Fuel is 25% PuO_2-75% UO_2, flowing NaK (natural convection) capsules. Inverted "U" tube or "diving bell" type single-stage vents.

TABLE VII

DEFECT TESTING - STEADY STATE OVER-TEMPERATURE OPERATION

Sample[1]	Burnup at Failure (MWd/Te)	Steady State (kW/ft)	Peak Power (kW/ft)	Peak Local Temperature (°F)	Final Burnup (MWd/Te)	Fuel in Cold Trap	Observations
B3B	15,000	21	>25[2]	1250	18,000	trace	Multiple fissures 1/4 in. to 1-1/2 inches. Diameter changes 1 to 2% next to fissures; 14% at fissure.
B3C	∿16,000	19	19	1350	47,000	∿ 15g (8%)	5-inch long fissure in cladding; 4 to 9% diameter changes adjacent to fissure; 38% at fissure.

(1) Both samples nominal 0.250-inch O.D., 0.015-inch cladding thickness, 20-inch active fuel length, 25% PuO_2-75% UO_2, 85% smeared density, O/M ratio 2.00.

(2) Location of molten zone indicates local peak power may have been ∿ 30 kW/ft. The over-power operation continued for 3 hours, followed by four weeks of operation at 5 kW/ft.

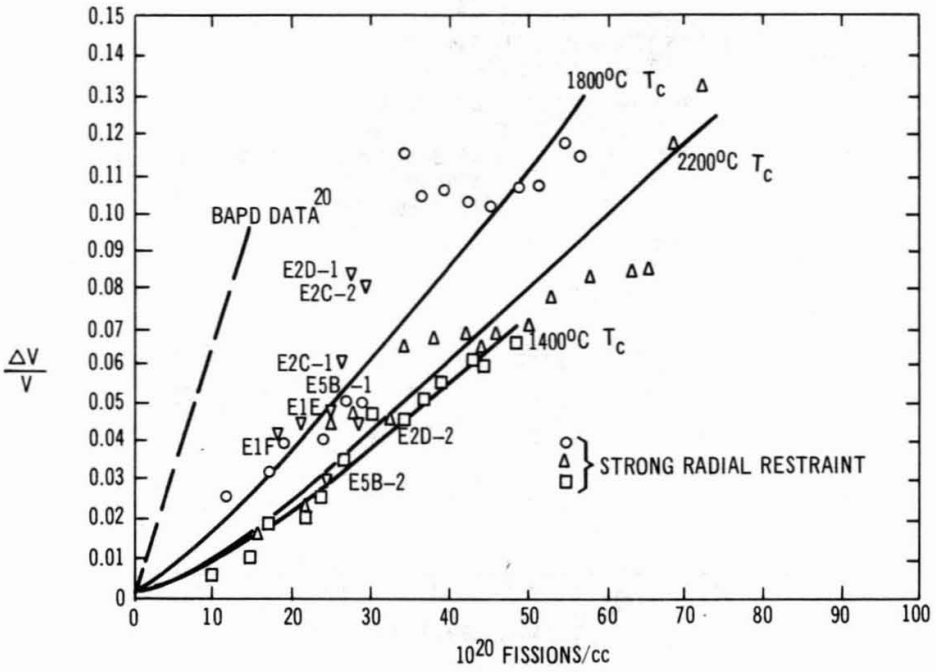

FIGURE 1. VOLUMETRIC SWELLING IN PuO_2–UO_2 FUEL IRRADIATED IN THERMAL FLUX

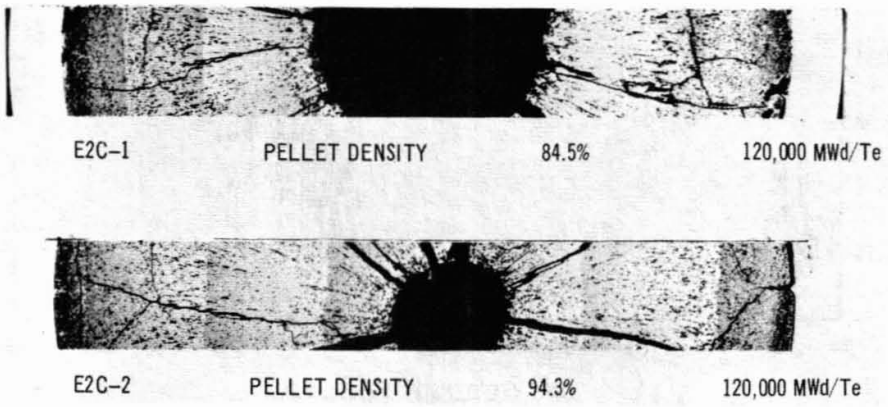

FIGURE 2. TRANSVERSE CROSS SECTIONS OF FUEL PINS FROM CAPSULE E2C IRRADIATED IN THERMAL FLUX

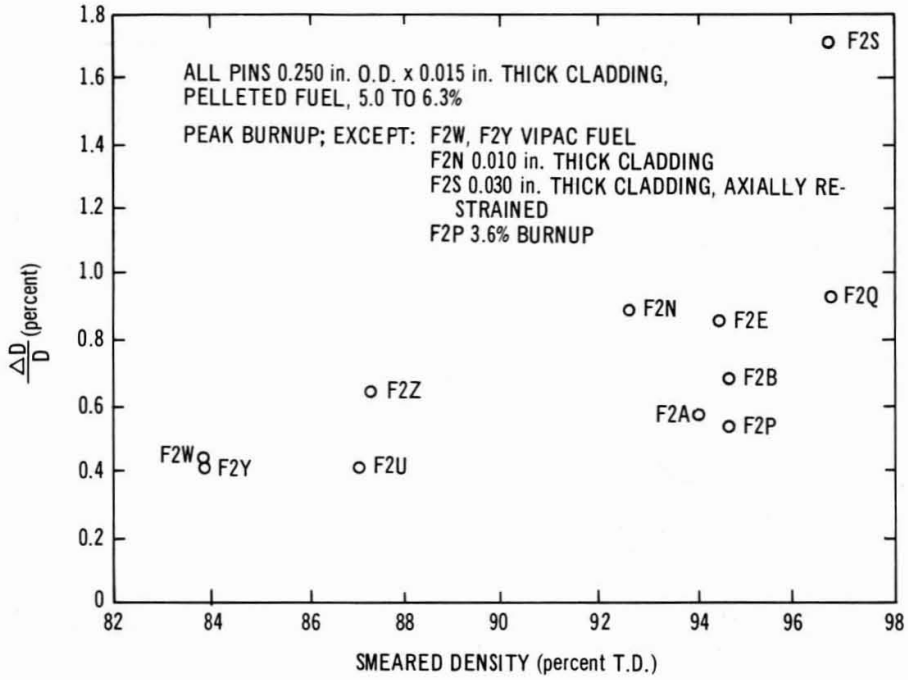

FIGURE 3. DIAMETRAL STRAIN IN FUEL PINS IRRADIATED IN EBR-II

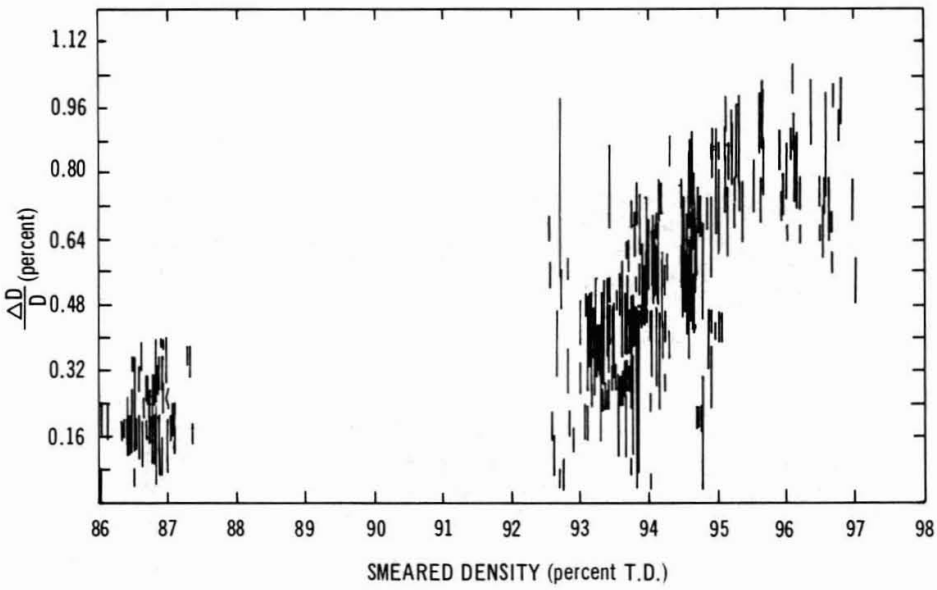

FIGURE 4. DETAILED DIAMETRAL STRAIN IN FUEL PINS IRRADIATED IN EBR-II

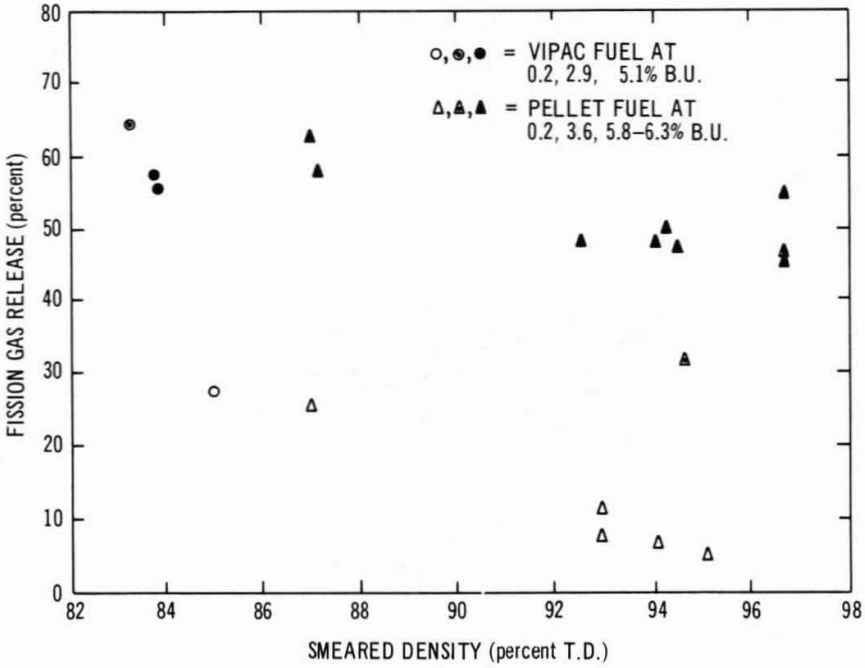

FIGURE 5. FISSION GAS RELEASE IN FUEL PINS IRRADIATED IN EBR–II

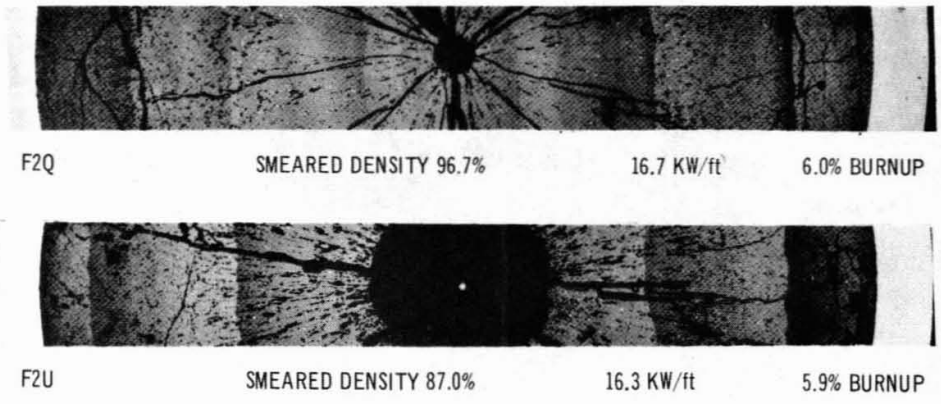

FIGURE 6. TRANSVERSE CROSS SECTIONS OF FUEL PINS F2Q AND F2U IRRADIATED IN EBR–II

IRRADIATION PERFORMANCE OF URANIUM-PLUTONIUM CARBIDE FUELS – THE USA EXPERIENCE

A. A. Strasser
J. H. Kittel

ABSTRACT

Uranium-plutonium carbides have been irradiated in thermal and fast reactors, in the form of high and low density pellets and vibratory compacted powders. Maximum performance levels achieved are 36×10^{20} fiss/cc (114,000 Mwd/T), and 470 w/g.

The fuel performed without significant microstructural changes, such as melting or grain growth. Plutonium redistribution or significant fission product segregation did not occur. Voids due to fission gas agglomeration formed at high temperatures and burnups. The maximum clad OD increase was 0.9% per 10,000 Mwd/T. One percent of the fission gases was released from high density pellets below 16×10^{20} fiss/cc, and 40% above 32×10^{20} fiss/cc.

The thermodynamic compatibility of the carbides with stainless steel, niobium, and vanadium clads was excellent up to 10,600 hours of operation.

A. A. Strasser is Manager, Plutonium Fuels Department at United Nuclear Corporation's Research and Engineering Center, Elmsford, N. Y.
J. H. Kittel is Head of the Fuels Development Section in the Metallurgy Division of Argonne National Laboratory, Argonne, Illinois.

INTRODUCTION

Carbide fuels have the potential to reduce fast breeder reactor fuel cycle costs by virtue of their high thermal conductivity and high fuel density. The high fuel density provides a high breeding ratio. The high thermal conductivity can be used to advantage for:

1. High specific power operation – to reduce inventory costs and decrease doubling time;
2. High linear power operation with larger diameter, fewer, mechanically more stable fuel rods – to reduce fabrication cost;
3. Lower fuel temperature which decreases fission gas release, swelling, and fuel redistribution – to increase burnup potential.

The near-term performance goals of carbide fuels are expected to produce fuel cycle costs of <1 mill/kwh. The extent to which the performance goals have been achieved in irradiation experiments is indicated below.

	Goal (Avg)	Achievement (Avg)
Specific Power, w/g	150-400	150-280
Linear Power, w/cm	500-1300	300-800
Burnup, fiss/cm^3	17-34 $\times 10^{20}$	3-38 $\times 10^{20}$

Many of the early tests were not with prototypical fuel elements in that short specimens, some refractory metal clads, and some very thick clads were used in a thermal flux. However, the recent irradiation of six prototypical fuel rods in a fast flux confirmed the basic data obtained by the nonprototypical specimens. This paper summarizes and evaluates the irradiation test results obtained in the past five years in the USA.

PRE-IRRADIATION CHARACTERIZATION OF FUELS

Structural characterization of carbides is complicated by the difficulty in making pure, stoichiometric (U,Pu)C. The range of carbon solubility in (U,Pu)C is small. Therefore, small changes in carbon content from stoichiometric monocarbide will generate additional phases. In addition, the generally present oxygen and nitrogen impurities can re-

place carbon in the lattice and the resulting equivalent carbon content* can affect the structural stoichiometry in the same manner as the carbon content itself. The constituents in the microstructure, produced in increasing order of either carbon or equivalent carbon content, are: M† + MC, MC, MC + M_2C_3, and MC + MC_2. Because the solubility of oxygen and nitrogen in the carbide is large, it is possible to have a hypostoichiometric carbon content in a hyperstoichiometric structure. Use of nickel sintering aid also makes this situation possible by promoting M_2C_3 formation. Therefore, it is important to differentiate between structural and carbon stoichiometry in the characterization of carbides.

The structural stoichiometry appears to have a significantly stronger effect on irradiation performance than the carbon stoichiometry. Uranium carbide irradiations[1] showed that hypostoichiometric structures of U + UC were prone to greater swelling and fission gas release rates than stoichiometric UC or hyperstoichiometric UC + UC_2 or UC + U_2C_3 structures. For this reason, the majority of the mixed carbide irradiation tests have been with stoichiometric or hyperstoichiometric structure fuel.

Containing fuel swelling without clad rupture for long periods of time is a requirement for economical, fast reactor fuels. A number of methods to minimize fuel swelling of carbides have been proposed:

1. Providing void space for fuel swelling;
2. Releasing and venting the fission gases that are a major cause of swelling;
3. Increasing the strength of the fuel (resistance to swelling) by additives.

Irradiation experience to date is limited to the first method only. The types of fuel rods tested and examined include: high- and low-density pellets with varying size helium annuli between fuel and clad, and vibratorily compacted particles in helium. Tests in process include in addition to the above: annular high-density pellets and sodium-bonded pellets.

*Equivalent carbon = C + (12/16 O) + (12/14 N).
†M = (U,Pu).

HIGH-DENSITY PELLETS

Early thermal flux irradiations[2,3] compared the performance of MC + 15 v/o M_2C_3 sintered at 96% of theoretical density with the aid of 0.1 w/o nickel and MC + <5 v/o MC_2 sintered to 91% of theoretical density without nickel sintering aid. The incentive to use nickel sintering aid is to provide a fabrication method that has a minimum sensitivity to processing variables, and therefore, is more economical than a process without sintering aid. Since the trace of MC_2 disappeared at burnups of less than 7×10^{20} fiss/cc and the M_2C_3 was stable up to 38×10^{20} fiss/cc, the irradiations also compared the behavior of the MC + M_2C_3 vs single-phase MC structure. Current fast reactor irradiations of high-density pellets are concentrating on the MC + M_2C_3 structure made with nickel sintering aid, since the thermal irradiations and out-of-pile property measurements[4,5] did not show any significant differences between the two-phase and single-phase structures.

The fuel characterization is summarized in Table I.

The fuel was fabricated by the carbothermic reduction of the mixed oxides followed by cold pressing, sintering, and centerless grinding.[5]

LOW-DENSITY PELLETS

Arc-melted buttons of $(U_{0.8}\text{-}Pu_{0.2})C$ were crushed to various particle sizes in glove boxes that contained a high-purity nitrogen atmosphere.[6] The powder was cold pressed into pellets. Pellets of the desired density (85%) were obtained by sintering at 1900°C for two hours. The shrinkage of the pellets was controlled so that they could be loaded into fuel cladding without grinding to size.

Chemical analyses of the pellets showed 4.64 to 4.72 w/o carbon, 1100 to 1200 ppm oxygen, and 140 to 200 ppm nitrogen. The microstructure of pellets was entirely single-phase monocarbide.

VIBRATORILY COMPACTED PARTICLES

The vibratory compaction process is of particular interest for the fabrication of fast reactor ceramic fuels because: (1) the process is amenable to remote operation, as would be required with fuels containing substantial quantities of the higher isotopes of plutonium, and (2) the process inherently provides the uniformly distributed void space required to accommodate fuel swelling for high burnups.

Two vibratorily compacted uranium-plutonium-carbide systems are

under study: (1) solid-solution (U,Pu)C particles, and (2) mixed particles of UC and PuC. The solid-solution particles are presently made in the same way as described above for feed for the low-density pellets. The use of solid-solution particles has the advantage of assuring maximum uniformity of plutonium distribution in the fuel matrix. On the other hand, the mixed particles are subject to plutonium segregation should particle segregation occur. Primarily for this reason, emphasis is being shifted to the use of solid-solution particles, although irradiations are also being made to a limited extent on mixed carbide particles.

Vibratory compaction presently is being done by an infiltration technique.[7] This technique enables reproducible packing densities to be achieved in minimum time. The fuel columns are characterized by uniform particle densities. Packing densities in the range of 80 to 85% are normally specified.

FUEL SPECIMEN PERFORMANCE

The irradiations to date have covered all but the highest ranges of desirable thermal performance. The most recent tests were with prototypical fuel rods in a fast reactor (EBR-II). They were preceded by the irradiation of smaller samples in thermal reactors that pointed out some of the problems to be encountered in high-power, long burnup fuels.

HIGH-DENSITY PELLETS

Initial thermal irradiations by the United Nuclear Corporation tested fuel configurations with a minimum fuel-to-clad helium gap to minimize fuel temperature and swelling, and thick clads to maximize the clad strength. The clad used was cold worked (half hard), thick type 316 stainless steel and niobium. At the time the specimens were designed (1960), high fission gas pressure was considered a very likely cause of failure.

The results of the irradiation experiments showed that fission gas release was low and would not be the primary cause of failure. All of the niobium clad specimens were intact to the maximum burnup of 30×10^{20} fiss/cc (113,000 Mwd/T) and the clad appearance was the same as prior to irradiation. The stainless steel clad specimens were intact to about 8×10^{20} fiss/cc (24,000 Mwd/T), and above that failed from a combination of fuel swelling and clad embrittlement. The niobium clad was

able to accommodate the relatively small amount of fuel swelling: 0.3% per 10,000 Mwd/T burnup. However, the ductility of the stainless steel was decreased so drastically by the test that it could not accommodate the strain due to fuel swelling. Results are summarized in Table II.

The results indicated that void to accommodate fuel swelling must be provided in the fuel rod, and for high-density pellets this meant a larger fuel-to-clad gap, at the cost of higher initial fuel temperatures. Also, the clad composition and structure must be designed for maximum ductility at some adequate strength. The stainless steel clad specimens allowed for essentially no expansion space and the cold-worked cladding was later found to be prone to the greatest ductility losses.[8]

Accordingly, the next set of experiments by the United Nuclear Corporation was designed with a larger fuel-to-clad gap and maximum ductility stainless steel. The specimens were full-length rods irradiated in EBR-II. The diametral fuel-to-clad gap was 5 to 6 mils, providing smear densities of ~93%. The gap size was a compromise between "acceptable" cladding strains, based on fuel swelling rates from the previous experiments, and "acceptable" fuel temperatures. "Acceptable" was based on best estimates of current knowledge.

The clads were all annealed, and the stainless steel had a minimum grain size number of ASTM-6. The finer grain size is reported to help retain ductility.[9]

The three rods were irradiated in EBR-II to peak burnups of 10.1×10^{20} fiss/cc (29,000 Mwd/T) at essentially the design powers, and performed as predicted. Preliminary results are summarized in Table II and below. The final data are published in Reference 10.

The clad strains were the magnitude predicted within the accuracy of measurement: 0.0 to 0.2% for the type 316 rod, 0.1 to 0.6% for the vanadium and vanadium-20% titanium rod.

During the initial irradiation period, the fuel swells into the fuel-clad gap and no clad strain occurs to 20,000 to 30,000 Mwd/T. Above this burnup, the fuel contacts the clad and the subsequent swelling is accommodated by clad strain. The current data are sufficient to give a fair degree of confidence in the swelling rate numbers for high-density pellets.

In low-density pellets, some of the swelling is accommodated in the internal fuel porosity; however, the efficiency of the swelling accomo-

dation by internal voids is as yet unknown.

The clad diameter changes were highest at the maximum power positions, as expected: 0.7 mils at 625 w/cm for the type 316 clad rod, and 2.3 mils at 920 w/cm for the vanadium clad rods. This is equivalent to an average clad OD increase of 0.07%/10,000 Mwd/T and 0.15%/10,000 Mwd/T, respectively.

Whole fuel pellets were recovered from the V-20 Ti clad rod and larger fuel chunks from the other rods. Fuel density decreases measured by immersion ranged from 2 to 3% at the lower power rod extremities to 5 to 6% at the higher power rod center. The average density decrease in the fast reactor irradiations is compared to thermal reactor irradiations (Fig. 1).

The density decrease and the swelling rates (Table II) compare favorably with the earlier thermal reactor irradiations. If, however, the swelling rates are plotted vs maximum calculated fuel temperature at startup, these rates are much lower than would be expected from UC data. The reason is that with large initial fuel-to-clad gaps, the calculated temperature is high but drops rapidly as the fuel swells and contact is made with the clad. A typical calculated temperature history of a pellet is given (Fig. 2). As the fuel temperature decreases, the swelling rate and temperature become difficult to define during the initial irradiation period. After fuel-to-clad contact is made, the lowered fuel temperatures probably will fit into the accepted carbide swelling-temperature relationship.

LOW-DENSITY PELLETS

Initial interest at Argonne National Laboratory in the use of low-density pellets developed during the design of a series of high-burnup ceramic fuel elements for fast breeder reactors. It was recognized that inexorable swelling would result from solid fission products with an additional increment of volume change resulting from nucleation of fission gas bubbles. The swelling due to fission gas effects was expected to be highly temperature-sensitive, as had been noted in metallic fuels. Internal void space in the fuel appeared to be a feasible solution to the problem of accommodating fuel swelling.

A group of experimental fuel elements of single-phase monocarbide is being irradiated in EBR-II. The first element has been removed with

a peak burnup of 16,000 Mwd/T and is undergoing post-irradiation examination. The element operated at a maximum cladding temperature of 575°C with a peak linear heat rating of 515 w/cm (16 kw/ft). The irradiation conditions are summarized in Table II.

No significant dimensional changes were noted in the fully annealed type 316 stainless steel cladding. Nondestructive examinations of the element by neutron radiography and by gamma scanning showed that pellets were loose within the cladding and could be axially shifted to some extent. The fuel element had originally been assembled with a diametral clearance of 0.004 in. between the fuel and cladding.

VIBRATORILY COMPACTED PARTICLES

Experimental specimens of the mixed carbide particles were investigated first because of the earlier availability of UC and PuC starting materials. Thermal reactor irradiations were made on mixed UC and PuC particles in the form of small prototype fuel elements.[11] Results from these experiments were highly encouraging in that they showed that fuel burnups up to at least 18×10^{20} fiss/cc (58,000 Mwd/T) could be achieved in thin (0.009-in.) cladding without excessive cladding strain. The results from these experiments also are summarized in Table II.

More recently, experimental elements fabricated by vibratory compaction have been placed under irradiation in EBR-II. Both mixed particles and solid-solution material are represented. One element of each type has been removed from the reactor and is being subjected to detailed post-irradiation inspection.

The element containing mixed particles of UC and PuC achieved a peak burnup of 22,000 Mwd/T with a maximum cladding temperature of 630°C at a peak linear heat rating of 690 w/cm (21 kw/ft). No diametral changes occurred in the type 316 stainless steel cladding. Neutron radiography and gamma scans showed no indication of fuel movement from the originally assembled configuration. The effective density of the fuel prior to irradiation was 80.0%.

The element containing solid-solution $(U,Pu)C_{1+x}$ particles reached a peak burnup of 26,000 Mwd/T at a maximum cladding temperature of 645°C with a peak linear heat rating of 850 w/cm (26 kw/ft). The vanadium jacket elongated 0.31% and increased in diameter a maximum of 0.83%. Neutron radiography disclosed that the fuel column had elongated

slightly more than the cladding. The as-fabricated effective density of the element was 85.9%.

FUEL STRUCTURE

HIGH-DENSITY PELLETS

With some minor exceptions, fuel microstructures are not changed by irradiation. At the power levels and burnups tested, there is no central core formation or increase in the fuel grain size at the pellet center. Macro examination of cross sections shows relatively little cracking (Fig. 3).

The (U,Pu)C without nickel sintering aid was single-phase monocarbide after the thermal reactor irradiation, having lost the trace of original dicarbide.

The (U,Pu)C with nickel sintering aid retained its original $MC + M_2C_3$ structure in thermal flux irradiations up to an average 38×10^{20} fiss/cc (113,000 Mwd/T) and 570 w/cm. The porosity in the fuel increased with increasing burnup. Through burnups of 13×10^{20} fiss/cc, the porosity was slight. After 38×10^{20} fiss/cc, there was a significant increase in the amount of intergranular porosity at the fuel center of the highest power specimens. The pores are caused by fission gas agglomeration.

The fast flux irradiations did not affect the structure to about 9×10^{20} fiss/cc and 670 w/cm. In the range of 700 to 850 w/cm, the M_2C_3 phase disappeared at the pellet center and porosity appeared both in the grains and at grain boundaries (Fig. 4). The amount or shape of the M_2C_3 in other parts of the pellet did not change.

LOW-DENSITY PELLETS

With the exception of cracks (noted in some of the high-density pellets also) there was no change in the appearance of the low density pellets irradiated in EBR-II (Fig. 5). These cracks are attributed to thermal stresses that developed on cooling from operating temperatures.

The pellets were single-phase $(U,Pu)C_{1.0}$ before irradiation. Preliminary optical metallography has disclosed no new phases that appeared as a result of irradiation. The shape, size, and distribution of the pores in the material were also unchanged by irradiation.

VIBRATORILY COMPACTED PARTICLES

As mentioned previously, most results presently available on the irradiation behavior of vibratorily compacted particles are on mixed particles of uranium carbide and plutonium carbide because of the earlier availability of this type of material. The preliminary thermal reactor irradiations showed that the PuC particles swelled, as expected, into adjacent void spaces between fuel particles.[11] In the higher burnup specimens the PuC phase formed almost a continuous network around the coarser unenriched UC particles.

Fast reactor irradiation of mixed carbide particles shows structural changes similar in most respects to those described above for thermal reactor irradiations. A transverse section of the fuel element irradiated in EBR-II to 22,000 Mwd/T is shown (Fig. 6). The PuC particles have swelled and formed a continuous network around the coarser UC particles.

In contrast to the thermal reactor study, the material irradiated in the fast reactor experiments contained fully-enriched UC, so that the fission density in the UC was comparable to that in the PuC. As a result, fission gas bubbles formed in the UC particles near the center of the rod, although not to the extent that porosity developed in the PuC phase.

The most rigorous fast reactor irradiation conditions to which vibratorily compacted particles have been subjected have been on solid-solution particles of $(U,Pu)C_{1+x}$. As a result, gross structural alterations were more extensive than those described above for the mixed particles. This is illustrated (Fig. 7). At the point of maximum burnup and temperature, 40% of the fuel volume was sintered into a porous structure similar in some respects to that of the low density pellets described previously. A few random cracks were noted in this structure, which contained no trace of the original particles from which it was formed. The M_2C_3 phase in the outer zone of the sintered area was evident without etching. Preliminary metallographic studies indicate that fission gas bubbles in the solid-solution particles are significantly smaller than those observed in the mixed particles.

FUEL AND FISSION PRODUCT DISTRIBUTION

Gamma scanning and neutron radiography did not show any significant axial fuel or fission product migration in any of the mixed carbide specimens irradiated to date.

Alpha autoradiography, used for studying radial fuel distribution, disclosed no plutonium migration in any of the specimens. Fuel irradiated in thermal reactors typically showed greater burnout of plutonium near the pellet OD (Fig. 8), as would be expected by the thermal flux depression. Fuel irradiated in a fast flux showed the even plutonium distribution to be expected from the uniform flux across the diameter of the pellet (Figs. 3, 5, 6, 7).

The beta-gamma autoradiographs of high-density pellets disclosed no fission product migration. Again, due to the flux depression, more fission products were seen at the OD of pellets irradiated in thermal flux (Fig. 8), whereas a uniform fission product distribution was seen in a fast flux (Fig. 3). Low-density pellets showed a slight radial migration of fission products from the center of the rod when irradiated in fast flux (Fig. 5). This was more evident in vibratory-compacted particles, especially mixed-carbide particles (Fig. 6). The element containing solid solution particles (Fig. 7) operated at a higher heat rating and temperature.

FISSION GAS RELEASE

HIGH-DENSITY PELLETS

The fission gas release from (U,Pu)C up through 13×10^{20} fiss/cc is very low even to powers as high as 500 w/cm. The limited data at 30 to 38×10^{20} fiss/cc indicate a sharp increase to about 30% of theoretical. The data are summarized (Fig. 9).

Fission gas release from the recent irradiations in EBR-II to 10.1×10^{20} fiss/cc and between 625 and 920 w/cm indicated good agreement with the low release obtained in earlier thermal reactor irradiations. The low gas release during the initial irradiation period helps to keep the fuel-clad gap conductivity high at a time when that gap is the largest. After $\sim 9 \times 10^{20}$ fiss/cc, the fuel and clad are in good contact and further gas release has little effect on gap conductivity.

LOW DENSITY PELLETS

Low density pellets, as anticipated, release fission gas more readily than high density pellets. Fig. 9 shows that the one element examined to date after irradiation in EBR-II had released 4.1% of its theoretical yield of fission gas at 5.1×10^{20} fiss/cc. The maximum linear heat rating of the element was 520 w/cm.

VIBRATORILY COMPACTED PARTICLES

Thermal reactor irradiations of mixed particles of UC and PuC, in which virtually all fissions occurred in the PuC fraction, showed that fission gas release was dependent on the carbon content of the PuC. Compacts containing PuC_{1-x} released more gas and had larger bubble sizes than compacts containing PuC_{1+x}.[11] The fission density in the PuC fraction was 110×10^{20} fiss/cc.

The recently completed EBR-II irradiation of an element of mixed UC and PuC particles showed that under fast reactor operating conditions, this type of fuel releases fission gas at a greater rate than either of the other two forms of low-density fuel evaluated (low-density pellets and vibratorily compacted solid-solution particles). As shown in Fig. 9, 13.4% of the fission gas had been released at 5.1×10^{20} fiss/cc, at a maximum linear heat rating of 690 w/cm. The relatively high fission gas release rate in this material is attributed to the extensive swelling of the PuC phase, and consequent interconnection of bubbles.

A lower gas release rate was shown by the element containing solid-solution particles of $(U,Pu)C_{1+x}$ that was irradiated in EBR-II. This element showed 8.6% gas release at 8.7×10^{20} fiss/cc with a maximum linear heat rating of 850 w/cm.

FUEL-CLAD COMPATIBILITY

The in-pile compatibility of MC and MC + M_2C_3 type structures, helium contact-bonded to stainless steel, niobium, and vanadium, is excellent. The maximum length tests in thermal and fast reactors are summarized in Table III. The in-pile results are similar to previously reported out-of-pile results.[4,12]

Some reaction products were found in the failed thermal reactor stainless steel specimens, but these are believed to be due to fuel-to-clad transfer of unknown elements by the sodium that entered through the

rupture.[2,3] The quantity of reaction products was too small to be identified by microprobe analysis.

A reaction zone was found on the ID of V-20 Ti fueled with high-density MC + M_2C_3 pellets. However, this was expected based on reactions found in out-of-pile compatibility tests.[13] The interactions indicate that V-20 Ti alloy is not a desirable clad for carbides.

No fuel-clad reactions have been observed to date in the low-density pellet or vibratory-compacted particle irradiations.

CLAD PERFORMANCE

Evaluation of the irradiated clad has been limited to visual and microscopic examination, chemical analysis, and cold bend tests.

Visual examination and cold bend tests indicated, that up to 5.4×10^{20} nvt thermal or 1.7×10^{22} nvt fast neutrons, type 316 retains its good ductility. At 2.0×10^{21} nvt thermal and above, type 316 suffers a drastic ductility decrease to less than 3%, as indicated by the brittle longitudinal ruptures. Analyses for the transmutation products of helium and hydrogen indicate that some helium is retained, but the hydrogen diffuses out of the steel.[3]

Microscopic examination of type 316 revealed the structures to be expected by the thermal treatment in the reactor. The initially all-austenitic structure transformed to austenite with sigma and carbides. A typical clad section from the recently examined EBR-II irradiation is shown (Fig. 10). The crack initiation and propagation in the failed thermal reactor specimens were typical of out-of-pile tests where a steel is strained very slowly at a high temperature.[3]

The niobium and vanadium clads both retained their ductility and their original single-phase structure. Niobium was irradiated to 3.3×10^{21} nvt thermal and vanadium to 1.7×10^{22} nvt fast.

The V-20 Ti alloy had a circumferential hairline crack in the weld zone of one end plug, but retained its cold bend ductility.

PERFORMANCE POTENTIAL OF CARBIDE FUELS

In order to achieve the performance goals, outlined at the beginning of this paper, with helium-bonded rods, the clad will have to restrain

fuel swelling and be able to take a strain in the range of 0.2 to 2.0%.

Swelling data on high-density pellets indicate that 33×10^{20} fiss/cc (2×10^{21} nvt) at 600 to 1000 w/cm can be achieved with maximum clad strains on the order of 2%. Clad irradiations in turn indicate that strains of 20% are feasible for 5×10^{22} nvt.[14]

A similar analysis of low density pellets shows[15] that the same performance goals can be achieved with maximum clad strains of 0.2%, assuming that 50% of the available void space will accommodate fuel swelling. Smear densities in the range of 70 to 93% are being studied to determine the optimum distribution of void.

Vibratorily compacted particles are analogous to low-density pellets with mostly interconnected, rather than closed, voids. Sufficient data have not been developed to determine differences in performance potential of the two different types of fuel structures. There is sufficient experience to date, however, to indicate that vibratorily compacted, solid-solution particles release less fission gas and show more uniform plutonium and fission product distribution than do physically mixed particles of UC and PuC.

Annular, high-density pellets also have a potential to achieve the carbide performance goals, but their behavior is unknown at this time.

The reasonable (U,Pu)C swelling rates, the excellent (U,Pu)C-stainless steel compatibility, and the reliability of the helium bond, all make the near-term achievement of the helium-bonded carbide fuel rod performance goals possible.

The sodium-bonded carbide fuel rod is an advanced concept which is estimated could reach even higher performance goals than those projected here. The major advantage is the considerable increase in burnup potential by providing very large space for expansion without significant increase in fuel temperatures or clad strains. In addition, an increase of power to 1500 w/cm, in the range of 200 to 300 w/g, is possible because the fuel temperatures are decreased. These powers represent limits set by the thermal stresses in the clad and the current state-of-the-art in transferring large quantities of heat to sodium. The major disadvantage of the sodium bond is the potential fuel rod failure caused by disruption of the bond by gas bubbles. The facility with which sodium transfers elements from fuel to clad is another disadvantage. The car-

bon transfer problem may soon be solved;[13,16] however, transfer of a multitude of fission products may pose additional problems.

Irradiation tests are continuing at an accelerated pace to determine the proper design of a carbide fuel rod that will meet the performance goals. Most of the approaches to solve the fuel-clad mechanical interaction problem are being investigated. Current irradiation tests, in pile or under construction, include:

High-density, solid helium-bonded pellets

High-density, helium-bonded annular pellets

Low-density, helium-bonded pellets

Sodium-bonded, high-density pellets

Vibratorily-compacted, helium-bonded particles

Vibratorily-compacted, sodium-bonded particles.

ACKNOWLEDGEMENT

The work summarized in this paper was sponsored by the U. S. Atomic Energy Commission. The contributions of the many staff members of Argonne National Laboratory, United Nuclear Corporation, Battelle Memorial Institute, and the General Electric Test Reactor, that made the results possible, are gratefully acknowledged.

REFERENCES

1. J. Crane, E. Gordon, J. Gates,: Effects of Fabrication and Composition on the Irradiation Stability of Uranium Carbide. Compounds of Interest in Nuclear Reactor Technology, Nuclear Metallurgy, Vol. X. AIME 1964 (Also UNC-5080, Feb. 1964.)

2. A. Strasser, J. Cihi, W. Sheridan, and V. Storhok: Irradiation Behavior of Solid Solution Uranium-Plutonium Monocarbides. Compounds of Interest in Nuclear Reactor Technology, Nuclear Metallurgy, Vol. X, AIME 1964. (Also UNC-5134, Vol. II, Oct. 1965.)

3. A. Strasser, J. Cihi, S. Hurwitz, and R. Martin: Irradiation Behavior of Solid Solution Uranium-Plutonium Monocarbides at High Burnups. Plutonium 1965. Chapman and Hall, London 1967. (Also UNC-5134, Vol. II, Oct. 1965.)

4. D. Stahl, A. Strasser: Properties of Solid Solution Uranium-Plutonium Carbides, "Carbides in Nuclear Energy," Vol. I, Macmillan &Co., London, 1964.

5. A. Strasser, D. Stahl: Carbide Fuel Development, UNC-5134, Vol. I (Oct. 1965).

6. L. A. Neimark, J. E. Ayer, O. L. Kruger, T. W. Latimer, and C. M. Walter: Mixed Carbide Fuels for Fast Reactors, Proceedings Conference on Safety, Fuels, and Core Design in Large Fast Power Reactors, Argonne National Laboratory, ANL-7120, 314-327 (1965).

7. J. E. Ayer, F. E. Soppet, G. J. Talaber, and B. N. Bieler: Nuclear Fuel Element Loading by Vibratory Compaction – Uranium-Carbide Specimens for EBR-II Irradiation, ANL-7075 (1966).

8. W. R. Martin, J. R. Weir: Influence of Pre-Irradiation Heat Treatment on the Post-Irradiation Ductility of Stainless Steel, Nuclear Applications, Vol. I (Oct. 1965).

9. W. R. Martin, J. R. Weir: Solutions to the Problems of High Temperature Irradiation Embrittlement, presented at the 69th Annual ASTM Meeting, Atlantic City, June 1966.

10. A. Strasser, D. Stahl, R. Martin: Fast Reactor Irradiation of (UPu)C Fuel Rods. ANS Transactions, Vol. 10, No. 2. Nov. 1967.

11. Y. K. Yoon, H. Watanabe, and J. H. Kittel: Electron Microscopic Studies of Structural Changes in High Burnup UC-PuC, Proceedings IAEA Symposium on Use of Plutonium as a Reactor Fuel, Brussels, Mar. 13-17, 1966 (to be published).

12. W. Batey, D. M. Donaldson, M. B. Finlayson: The Compatibility of Type 316L Stainless Steel with Mixed Uranium-Plutonium Carbides. Plutonium 1965. Chapman and Hall, London, 1967.

13. R. M. Powers, A. A. Strasser: Compatibility of Sodium and Helium Bonded Uranium-Plutonium Carbide Fuels with Several Cladding Materials. Presented at the ANS Meeting, Chicago, Ill., Nov. 1967.

14. I. P. Bell et al.: The Effects of Irradiation on the High Temperature Properties of Austenitic Steels and a Precipitation Hardened Alloy, presented at the 69th Annual ASTM Meeting, Atlantic City, June 1966.

15. B. H. Cherry, C. A. Beaulieu, and A. H. Kazi: Design for Helium-Bonded (UPu)C Fuel Pin Capsules for Fast Flux Irradiations, Transactions of the ANS, Vol. 9, No. 2 (Oct. 1966).

16. R. Pascard: Properties of Carbides and Carbonitrides. Presented at the AIME Nuclear Metallurgy Symposium on Plutonium Fuels Technology, Phoenix, Arizona, October 4-6, 1967.

TABLE I. CHARACTERIZATION OF MIXED CARBIDES USED IN IRRADIATION TESTS

Fuel Type	Structure*	Effective Fuel Density, %	C, w/o	Equivalent C, w/o†	Pu, w/o	O, w/o	N, w/o	Ni, w/o	Irradiations to Date
High-density pellets (>90% T.D.)	MC	91	4.5-4.6	4.8	19	0.2-0.3	0.02	—	Thermal
	MC + M_2C_3	96	4.6-4.8	4.9-5.1	19	0.3-0.5	0.01-0.1	0.1	Thermal and fas
Low-density pellets (<90% T.D.)	MC	81	4.7	4.8	19	0.1	0.01	—	Fast
Vibratorily compacted particles	UC_{1+X} + PuC + Pu	80	3.4-4.2‡	3.6-4.4§	19	—	—	—	Thermal
	UC + PuC	80	4.8	4.9	19	0.1	0.01	—	Fast
	UC_{1+X} + PuC + Pu_2C_3	80	6.2-6.4‡	6.4-6.6§	19	—	—	—	Thermal
	MC + M_2C_3	86	5.1	5.1	19	0.06	0.01	—	Fast

*M = (U,Pu).
†Equivalent C = C + (12/16 O) + (12/14 N).
‡PuC fraction only. The uranium carbide was UC_{1+X}.
§Estimated from microstructure.

TABLE II. SUMMARY OF MIXED CARBIDE IRRADIATION TESTS

Fuel Type	Structure	Average Burnup, Mwd/T	Average Clad Diameter Increase, %/10,000 Mwd/T	Clad Material and Thickness, in.		Average Power w/cm	Average Power w/g	Irradiation Type
High-density pellets	MC or MC + M_2C_3	23,000	0	0.036	Type 316	390	170	Thermal
		22,000-35,000	0	0.036	Nb	340	150	
		38,000-49,000	0.7-0.9	0.036	Type 316	470-540	210-250	
		100,000	0.6-0.5	0.036	Type 316	560	240	
		114,000	0.17-0.28	0.036	Nb	500	260	
	MC + M_2C_3	18,000	0.07	0.022	Type 316	540	135	Fast
		25,000	0.15	0.022	V and V-20 Ti	800	200	
Low-density pellets	MC	14,000	0	0.024	Type 316	460	140	Fast
Vibratorily compacted pellets	UC_{1+x} + PuC + Pu	12,000-58,000	0.4-0.8	0.009	Type 304	195	155	Thermal
		19,000-58,000	0.07-0.16	0.009	Nb-1 Zr	210	170	
	UC + PuC	19,000	0	0.024	Type 316	610	175	Fast
	UC_{1+x} + PuC + Pu_2C_3	11,000-49,000	0.3-0.6	0.009	Type 304	180	140	Thermal
		10,000-58,000	0.03-0.05	0.009	Nb-1 Zr	180	140	
	MC + M_2C_3	23,000	0.32	0.024	Vanadium	750	200	Fast

TABLE III. MIXED CARBIDE-CLAD COMPATIBILITY IN THE MAXIMUM LENGTH IN-PILE TESTS

Clad	Flux	Fuel Type	Length of Test, hr	Average Clad ID Temperature, °C	Results	Test Identification
Type 316	Thermal	MC + M_2C_3 pellet	8,730	715	No reaction	UNC 66T
		MC pellet	8,730	570	No reaction	UNC 66B
Type 316	Fast	MC + M_2C_3 pellet	2,850	650	No reaction	UNC 79
		MC pellet	2,850	575	No reaction	SMP-1
		UC + PuC Vipac	2,850	630	No reaction	SMV-1
Type 304	Thermal	UC_{1+x} + PuC_{1-x} Vipac	10,600	675	No reaction	F-20
		UC_{1+x} + PuC_{1+x} Vipac	10,600	600	No reaction	F-19
Vanadium	Fast	MC + M_2C_3 pellet	2,850	660	No reaction	UNC 80
		MC + M_2C_3 Vipac	2,850	645	No reaction	VMV-1
V-20 Ti	Fast	MC + M_2C_3 pellet	2,850	700	Reaction	UNC 78
Niobium	Thermal	MC + M_2C_3 pellet	9,200	605	No reaction	UNC 63T
		MC pellet	9,200	520	No reaction	UNC 63B
Nb-1 Zr	Thermal	UC_{1+x} + PuC_{1-x} Vipac	10,600	660	No reaction	C-72
		UC_{1+x} + PuC_{1+x} Vipac	10,600	680	No reaction	C-70

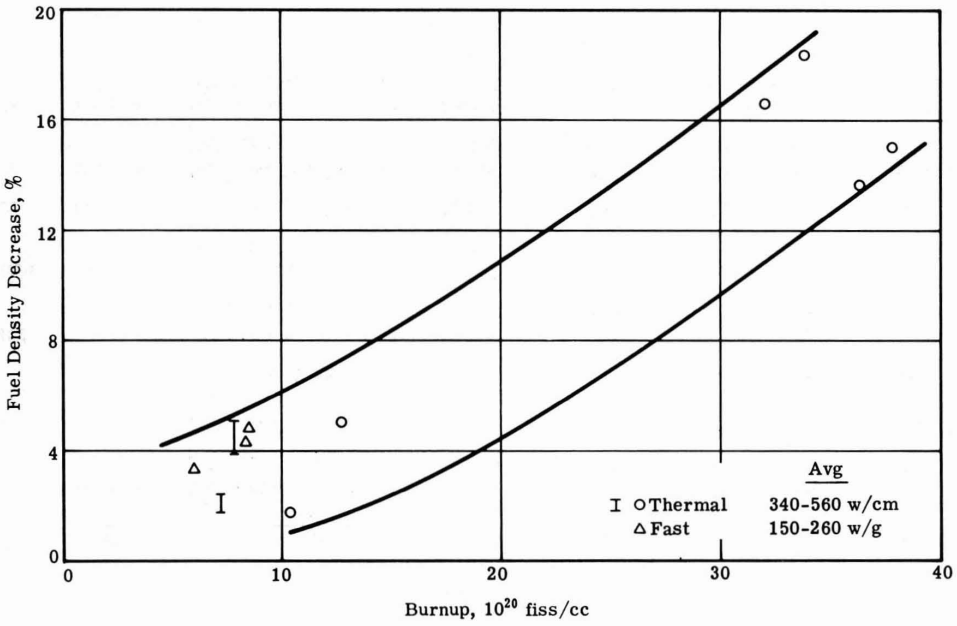

Fig. 1 — Effect of Burnup on Mixed Carbide Fuel Density
(High-Density Pellets)

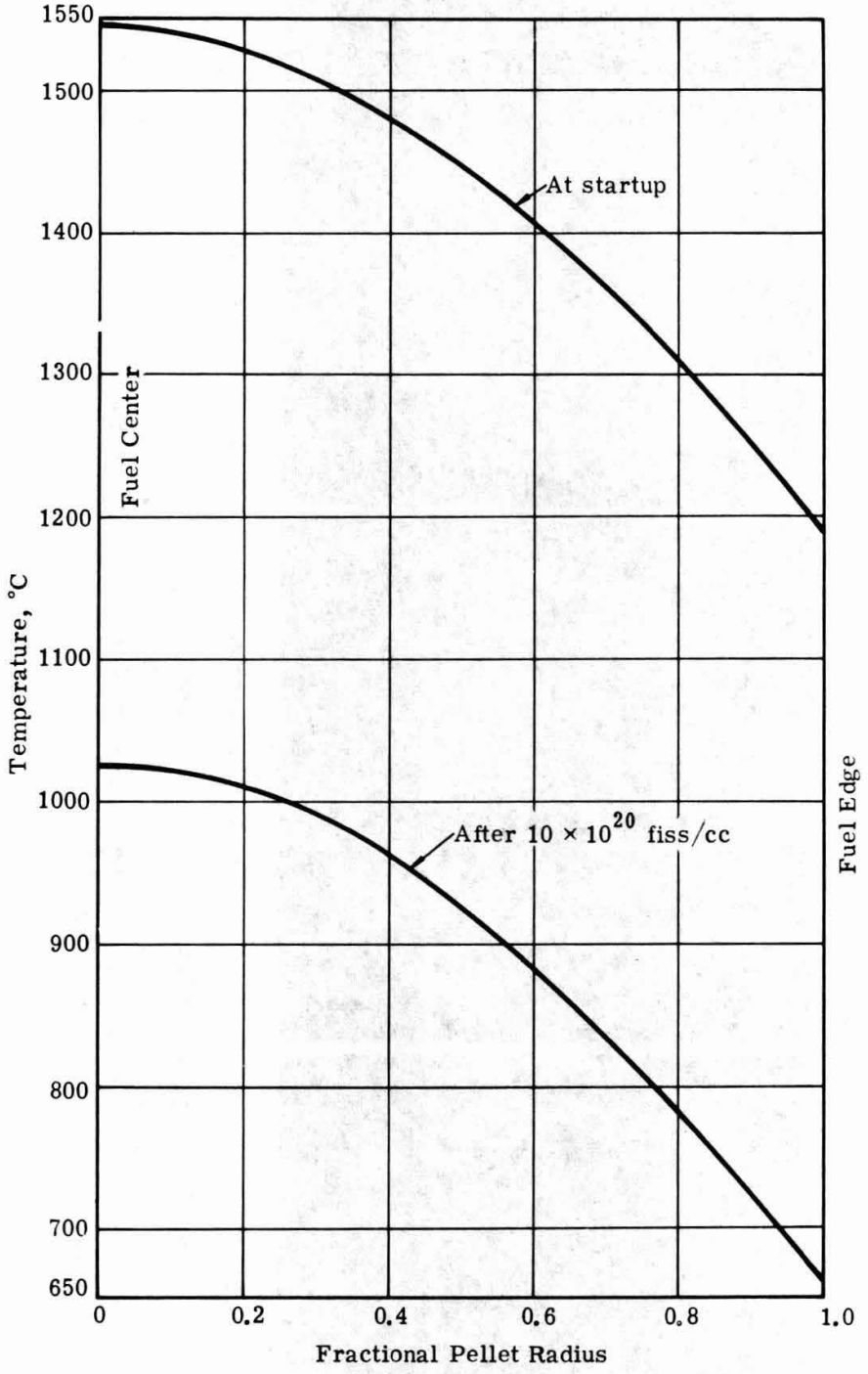

Fig. 2 — Change in Helium-Bonded Carbide, Radial Temperature Distribution with Time (UNC Rod 80, Pellet 27, 920 w/cm)

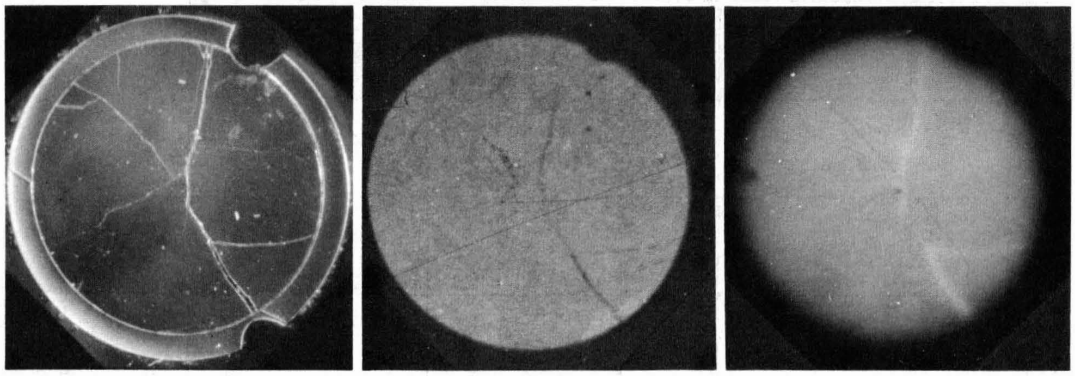

Metallographic Section | Alpha Autoradiograph | Beta-Gamma Autoradiograph

Fig. 3 — Typical Transverse Section of High Density Pellet Fuel Element $(U_{0.8}Pu_{0.2})C$ after Irradiation in EBR-II to a Burnup of 20,000 Mwd/T at 620 w/cm (19 kw/ft). The effective density of the fuel before irradiation was 96% of theoretical (UNC-78).

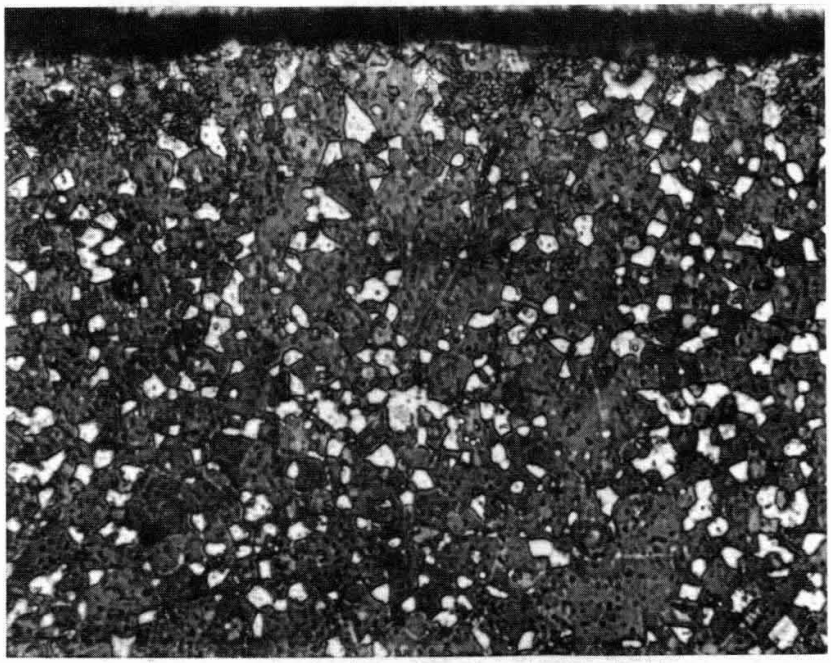

Pellet OD (structure is gray MC and white M_2C_3)

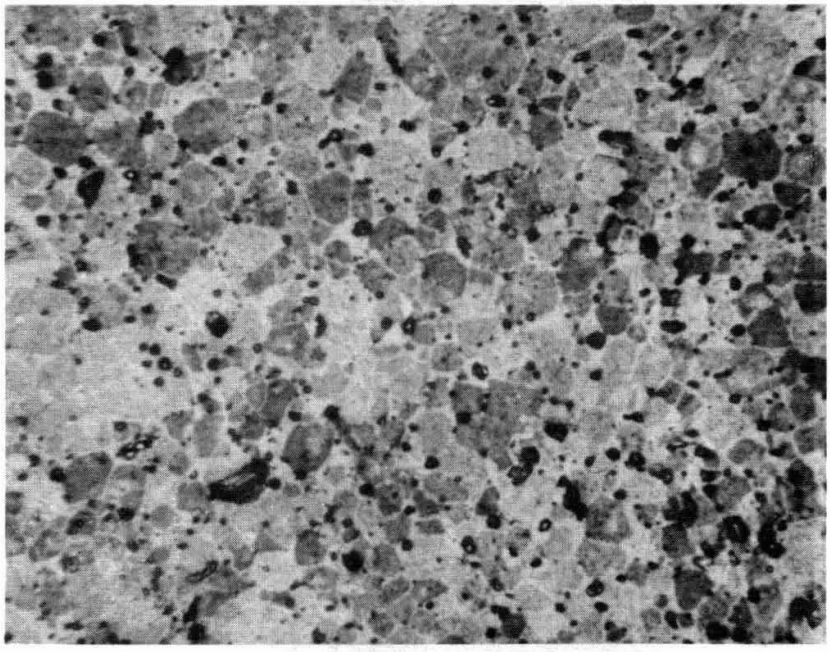

Pellet Center (structure is gray MC and dark voids)

Fig. 4 — Microstructure of a High Density Pellet $(U_{0.8}Pu_{0.2})C$ at 500× after Irradiation in EBR-II to 25,000 Mwd/T at 760 w/cm (23 kw/ft) and 220 w/g (UNC-80)

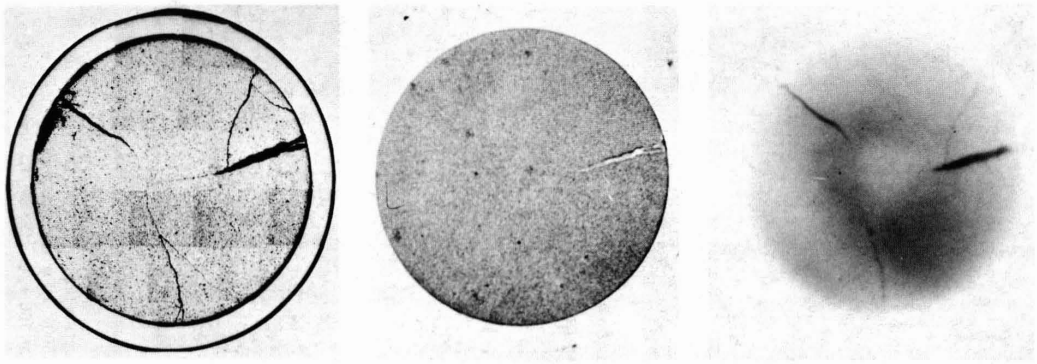

Metallographic Section | Alpha Autoradiograph | Beta-Gamma Autoradiograph

Fig. 5 — Transverse Section of Low Density Pellet Fuel Element $(U_{0.8}Pu_{0.2})C_{1.0}$ after Irradiation in EBR-II to a Burnup of 16,000 Mwd/T at 525 w/cm (16 kw/ft). The effective density of the fuel before irradiation was 81.4% of theoretical.

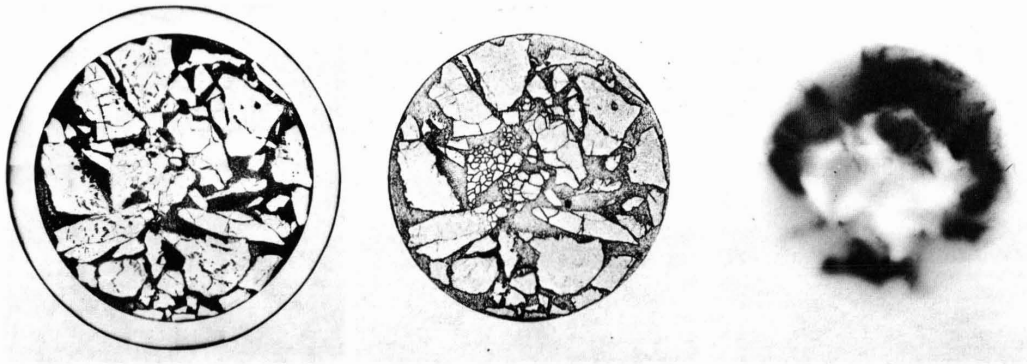

Metallographic Section | Alpha Autoradiography | Beta-Gamma Autoradiograph

Fig. 6 — Transverse Section of Vibratorily Compacted $UC_{1.0}$-20 w/o $PuC_{1.0}$ Fuel Element after Irradiation in EBR-II to a Burnup of 22,000 Mwd/T at 690 w/cm (21 kw/ft). The effective density of the mixed UC and PuC particles before irradiation was 80.0% of theoretical.

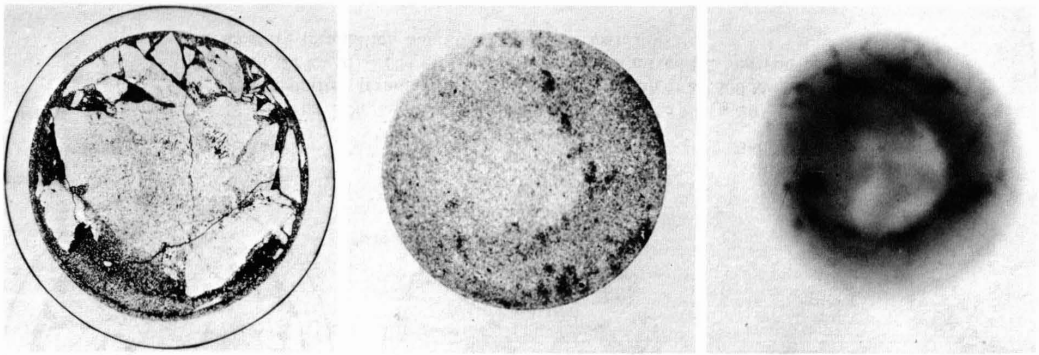

Metallographic Section | Alpha Autoradiography | Beta-Gamma Autoradiograph

Fig. 7 — Transverse Section of Vibratorily Compacted Fuel Element of $(U_{0.8}Pu_{0.2})C_{1.1}$ after Irradiation in EBR-II to a Peak Burnup of 26,000 Mwd/T at 850 w/cm (26 kw/ft). The effective density of the solid-solution particles before irradiation was 85.9% of theoretical.

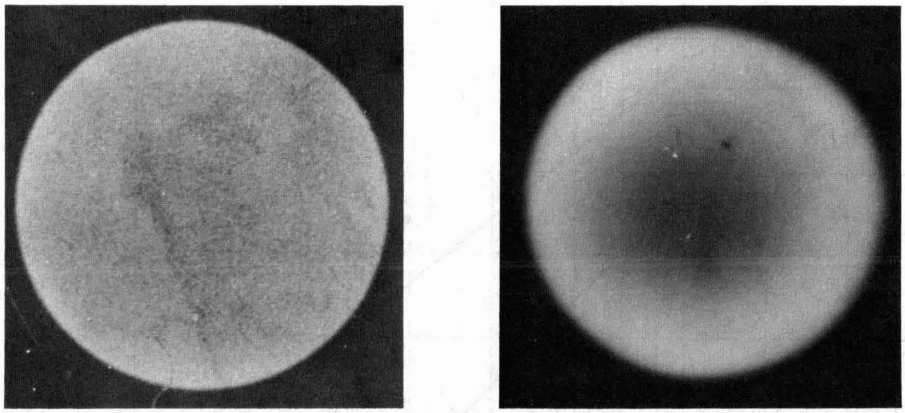

Alpha Autoradiograph

Beta-Gamma Autoradiograph

Fig. 8 — Typical Transverse Section of High Density Pellet Fuel $(U_{0.8}Pu_{0.2})C$ after Thermal Irradiation to 114,000 Mwd/T at 500 w/cm and 270 w/g (UNC-63B)

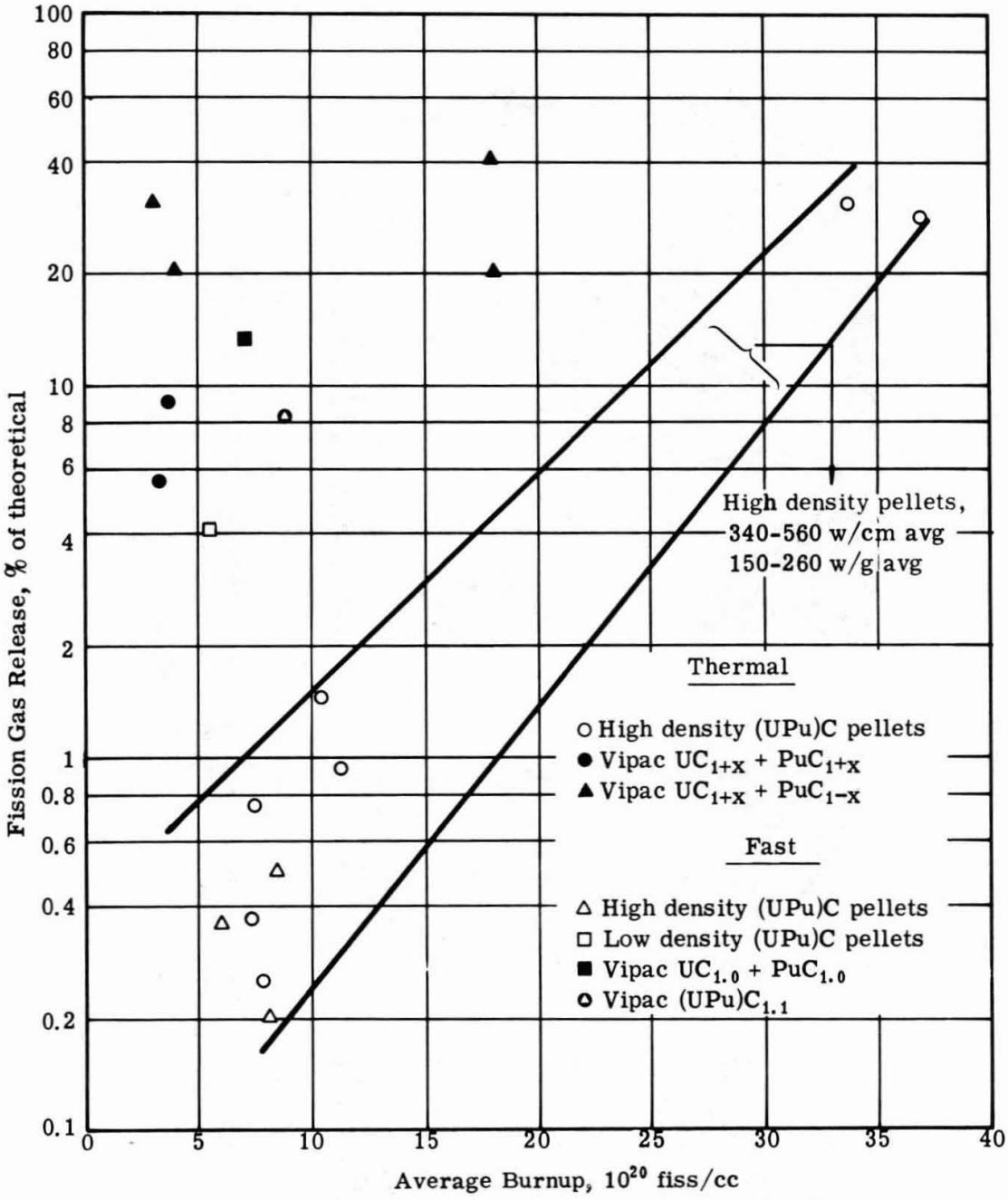

Fig. 9 — Effect of Burnup on Fission Gas Release from Mixed Carbide Fuels

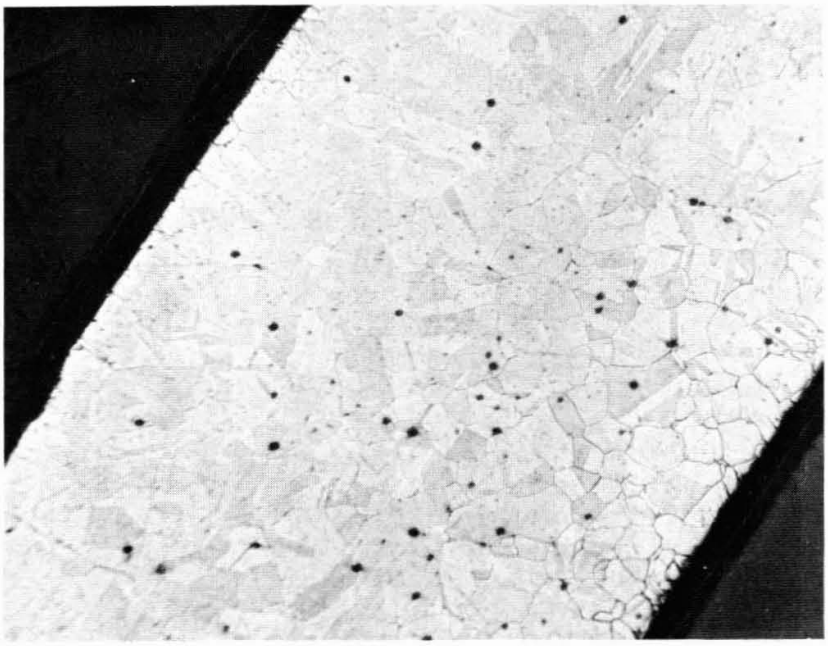

Clad OD 150× Clad ID

Fig. 10 — Microstructure of Type 316 Clad from High Density Pellet $(U_{0.8}Pu_{0.2})C$ Fuel Element Irradiated in EBR-II to 18,000 Mwd/T (UNC-79)

IRRADIATION BEHAVIOUR OF URANIUM-PLUTONIUM CARBIDE FUELS

B. R. T. Frost, J. M. Horspool and R. G. Bellamy

Abstract

Preliminary studies of the irradiation behaviour of (U,Pu)C under conditions typical of those in a sodium-cooled fast breeder reactor have been made at Harwell and Dounreay. With the fuel element geometry typical of oxide fuels carbide displays a high retention of fission gases and a high swelling rate, leading to early clad failure. The experiments suggest that operation below 1000°C, as in a sodium bonded design, operation at very high fuel temperatures, or the use of a single size fraction powder may lead to improved performance from carbide fuel in a sodium cooled fast reactor.

B. R. T. Frost and R. G. Bellamy are members of the Metallurgy Division, A.E.R.E., Harwell, and J. M. Horspool is a member of the Chemistry Division, D.E.R.E., Dounreay.

Introduction

The fuel chosen for the first charge of the U.K.A.E.A.'s prototype fast reactor (P.F.R.) is $(U,Pu)O_2$. It is also very probable that it will be used in the early charges of the first commercial fast reactors. The technology of this fuel has evolved naturally and rapidly from the large background of experience on UO_2 in thermal reactors and its performance has proved to be satisfactory in a fast reactor environment. However, mixed oxide has the disadvantages of a low fissile atom density and a low thermal conductivity which limits the maximum diameter of the fuel. (U,Pu)C has a high thermal conductivity, which can be used to advantage in appropriate pin designs, and a high fissile atom density. Accordingly, the U.K.A.E.A. laboratories at Dounreay and Harwell have been making a study of the fabrication technology, properties and irradiation behaviour of (U,Pu)C over the past few years. The fabrication technology is now well established and has been reported elsewhere (1). In this paper the results of the early studies of irradiation performance are reported.

The main problem in the development of carbide as a fast reactor fuel is one of design philosophy; must one adopt a different design from the oxide case to take advantage of its different properties? To help to answer this question three types of experiment have been performed:

1. Short pin irradiations in a thermal neutron flux (in a materials testing reactor).
2. Short pin experiments in the Dounreay Fast Reactor (D.F.R.) core.
3. Long pin (up to 28 in.) irradiations in the D.F.R. core.

The objectives of these experiments were, in the first two cases, to establish the optimum fuel form (composition, density and fabrication route) and in the third to establish performance limits, including an assessment of fission gas release and swelling behaviour.

Short Pin Irradiations

A total of 23 short pins were irradiated to study the effect of fuel form on its irradiation behaviour and to determine the form on which to concentrate future efforts. Eleven pins were irradiated in D.F.R. and twelve in DIDO at Harwell. Details of these experiments were given in an earlier paper (2) and only a brief outline will be given here, including some results which were obtained subsequent to that meeting.

The fuels irradiated were arc-cast and sintered, stoichiometric, carbon-rich and metal-rich. Each of the two series included two low density (60-65% T.D.) powders made from a single size range ($\sim$100μ) of crushed arc-cast material. The standard plutonium content was 15w/o.

In the D.F.R. experiment the pins were between 0.26 in. and 0.33 in. diameter to achieve a constant linear rating along the varying flux profile in the reactor core. The fuel was clad in a nickel base alloy (Nimonic 90) lined with 0.002 in. tantalum to prevent fuel-clad reactions. Mild steel cylinders acted as heat transfer media to the outer stainless steel cans and imposed heavy radial restraint on the fuel. The arrangement of the capsules is shown in Figure 1a and the irradiation data are listed in Table I. Nine of the eleven cans failed by longitudinal cracks - as shown in Figure 2 - the cause being high strain produced by thermal stresses combined with fuel swelling stresses induced in a cladding material which was considerably embrittled by neutron irradiation. It is significant that the two low density powder specimens did not fail.

The pins irradiated in DIDO were of small (0.1 in.) fuel diameter and were clad in 0.020 in. wall type 316 stainless steel. Four pins were housed in an aluminium block which contained an electric heater as shown in Figure 3. The small fuel diameter was chosen to minimize flux depression in the fuel. The irradiation data are given in Table II. In this case none of the pins failed and the measured gas releases were all low, except for the metal-rich powder specimen. Surprisingly good agreement was obtained between the measured gas release levels and the value predicted on the basis of a diffusion model, using D' values determined by the short irradiation and anneal technique (3). The predicted results are listed in the final column of Table II. The main conclusions drawn from these experiments were:

1. The use of low density fuel of a single size range appears to accommodate fuel swelling without excessive clad strain.
2. An irradiation temperature of less than 1000°C gives low swelling and gas release rates up to a radiochemical burn-up of 7.6% heavy atoms.
3. Sintered stoichiometric or slightly carbon-rich fuel gives the best performance in terms of swelling, gas release and compatibility.

A further comparison of arc-cast and sintered carbide is being made in an experiment in the D.F.R. core in which four 4 in. long pins are being irradiated. The rig design is shown in Figure 1b. 0.25 in. diameter carbide is clad in 0.015 in. wall niobium cladding which is contained in a sodium filled capsule. Two of the specimens are sintered ~95% T.D. $(U_{0.85}Pu_{0.15})C$ and two are arc-cast ~98% T.D., the compositions being slightly hyperstoichiometric. The rig was unloaded from the reactor for non-destructive examination at a peak burn-up of 6.2%. Radiographs, of which Figure 4 is a representative example, showed axial swelling of the fuel with little radial movement. The extent of axial swelling can, therefore, be used as a measure of the swelling rate; this is seen as the dimension ΔL in the figure. The results are plotted in Figure 5. It will be noted that the two capsules furthest from the core centre are in a lower flux and achieved only 4.2% burn-up. The results show very approximately that all four specimens have a similar swelling rate with

an incubation period up to 2% burn-up, but that the total change recorded in the arc-cast material is greater than in the sintered, implying some accommodation of swelling in pores or voids in the latter. This test will continue to higher burn-up levels.

An important parameter in these irradiation experiments is the fuel centre temperature since it determines the rate of thermally activated processes such as gas release, swelling and fission product movement. It is not possible, nor desirable, to attach centre thermocouples to many experiments in the D.F.R. and in general centre temperatures are calculated from a knowledge of the fuel thermal conductivity and the fuel-clad gap conductance. To check such calculations two experiments in which fuel centre line temperatures have been measured have been performed in the D.F.R. core. In each case four capsules of the type shown in Figure 1c were mounted in a stainless steel element identical in shape and size to a driver element. A tungsten-tungsten 26% rhenium thermocouple was inserted in the central molybdenum pocket and chromel-alumel thermocouples were attached to the can wall. In the first experiment two mixed carbide and two mixed oxide pins were irradiated for one reactor cycle (40 days). The central thermocouples were insulated with MgO which contained impurities. Consequently the readings showed a steady downward drift for about 28 days after which open circuit conditions were obtained. In the second test pure Al_2O_3 insulator was used on four carbide specimens. The thermocouples showed a gradual rise in temperature for about 14 days followed by a downward drift for the remainder of the 40 day cycle. A tentative explanation is that the helium filling gas is initially diluted with fission gases, lowering its conductivity, while subsequently fuel swells or moves outwards to decrease the fuel-can gap width. In this experiment the calculated fuel temperatures agrees well with the measured values if a fuel-clad gap conductance of $2 w/cm^2/^oC$ is used.

Long Pin Irradiations

The first long pin irradiations were designed to test the behaviour of carbide as a direct substitute for oxide in the same 'reference' fuel pin design. Five pins were irradiated in the D.F.R. core. All were 28 in. long and were clad in 20% cold worked type M316L steel. Approximately 20 in. of the pin contained fuel, the rest being a plenum. Two of the pins were loaded with vibrocompacted fuel and three with hollow (annular) pellets, designed in both cases to give a fuel stack density of ~80% theoretical.

The vibrocompacted fuel contained 15% plutonium and was made by crushing and sieving arc melted buttons to give three size ranges of particle which were added simultaneously during the filling operation. The composition range was 4.8% to 5.3% carbon, although the analysis of one 'rogue' button ran as high as 5.8%C.

The pellet pins contained near-stoichiometric material of 94-95% theoretical density prepared by sintering in hydrogen using a nickel sintering aid. In one pin the pellets were 0.1985 in. O.D. and 0.067 in. I.D., the initial cold fuel-clad gap being 0.0008 in. radially. In the two others the pellet dimensions were 0.270 in. O.D. and ~0.080 in. I.D; the initial cold fuel-clad radial gaps were 0.0015 in.

The pins were irradiated in direct contact with the reactor NaK coolant which entered at 230°C and, due to flow restrictors, attained an outlet temperature of ~600°C. Details of the irradiation conditions are given in Table III. The ratings of ~200 w/gm were attained by using fully enriched uranium in the fuel. The temperatures listed were calculated on the same basis as discussed above. It will be seen that three of the five specimens failed by longitudinal splits in the cladding due to excessive strain induced by fuel swelling. The typical appearance of the failures is shown in Figure 6. In Figure 7 the cross section of a vibrocompacted pin is shown at the point of failure. The absence of any change in wall thickness at the point of fracture indicates low non-uniform elongation at failure.

Gamma scans of all the pins showed few abnormal features. No evidence suggesting gross fuel movement or fission product migration was discerned. Diameter changes were measured on all pins. These are summarized in Figure 8 and in Table IV together with other data. A characteristic value of cladding strain for the 0.2 in. and 0.27 in. pins was estimated to be 0.3% to 0.4% per 1% burn-up, with an induction period of about 1% burn-up. However, the absolute values of the strain rates are still open to question and a longer induction period and a higher strain rate than 0.4% is indicated by some of the data (Figure 9).

Metallographic examination of the fuel in CV002 and CV003 showed no signs of sintering and, apart from a few fragments in CV003, no apparent increase in porosity. The great variety of fuel structures revealed on etching all matched the pre-irradiation structures, most of the fuel showed the dedritic structure of arc cast carbide as seen in Figure 10. There was no correlation between structure and position of a fragment radially within the fuel section. The conclusion is drawn that the fuel temperature in these pins was certainly below 1600°C and probably below 1400°C. No conclusions could be drawn on changes in fuel stoichiometry during irradiation.

In the annular pelleted fuel CA002 little change in the fuel-can clearance from the pre-irradiation value could be detected at the ends of the fuel column, despite perceptible clad diameter increases at these positions. In CA003 and the fractured regions of CA002, the gap width had been reduced to less than half its original value. There was essentially no change in the central hole diameter at the bottom end of either pin but at the top ends, small decreases were detected. The smallest central holes in both pins were found in the fractured regions. All sections of both pins showed fine porosity near the surface and larger, more abundant porosity near the centre, where both intergranular and intragrannular pores were found. The fuel structures were generally very similar to those of unirradiated samples as shown in Figure 11.

All the pins examined were reputedly clad in 20% cold-worked M316L steel. Metallographic data, however, suggest that the cladding in CV002 had a much lower cold-worked fraction than 20%. The grain size was about 30 microns in CA003 and about 15-20 microns in CV002 and CV003. Several very fine cracks were detected in the clad from CA003 and CV002; though traversing the clad wall, they were too small to be detected other than by metallographic polishing. All cracks were clearly intergranular. Associated with a transverse crack in CV002 was a gross increase in grain size, severe pitting at the inner surface and a curious etching effect at the outer surface. These effects are attributed to a 'hot spot' produced by the anchoring of a bubble of gas ascending from an earlier failure lower down the pin.

Summary and Conclusions

From the series of experiments described above it has been possible to draw a number of conclusions which form the basis of a further series of experiments on more specific design concepts:

1. The primary cause of failure in small diameter, sealed carbide-stainless steel fuel pins is fuel swelling. The swelling rate appears to be somewhat higher than in oxide fuel, due to the greater retention of gaseous fission products and to the higher fissile atom density.
2. The swelling and gas release is markedly temperature and burn-up dependent; below 1000°C the rates are low, suggesting that sodium bonding may be an attractive design concept. Increasing the fuel diameter from 0.2 in. to 0.27 in. in pelletted carbide to give centre temperatures around 1600° gives no apparent reduction in swelling rate. It is probable that the fuel surface temperature must be raised to at least 1200°C to show an appreciable effect.
3. A stoichiometric, or slightly hyperstoichiometric, composition gives the minimum structural change on irradiation and negligible fuel-clad interaction below 700°C. With strong cladding fuel containing sinter pores absorbs some of the swelling, in contrast to denser arc cast material. A low density powder (60-65% T.D.) of a single particle size accommodates swelling much better than a vibro-compacted powder (80-85% T.D.) made up from two particle sizes.
4. In summary, a design of fuel pin for carbide must be sought in which the effects or extent of the temperature region 1000-1600°C are minimized or eliminated.

Acknowledgements: The authors wish to stress that the work described in this paper was the result of the efforts of their colleagues in the U.K.A.E.A. who are too numerous to name.

REFERENCES

1. 'Carbides in Nuclear Energy' ed. L. E. Russell, McMillan, London 1964, pages 540 to 647.

2. B. T. Bradbury and B. R. T. Frost, Radiation Performance of Plutonium-Uranium Monocarbide Fast Reactor Fuels, A.I.M.E. Nuclear Metallurgy Symposium, Delavan, Wis., 1966.

3. B. T. Bradbury, B. R. T. Frost and J. R. Findlay, Plutonium 1965, The Institute of Metals, London.

TABLE I. FAST REACTOR EXPERIMENT - SPECIMEN IRRADIATION DETAILS

Can No. and Fuel type	Spec No.	Spec. Length Diam (in.)	Specimen Composition (wt %)					Equivalent Carbon Content	Microstructure	Density (gm/cm^3)		Spec. Rating (W/gm)	Est. Surface Temp. (°C)	Est. Centre Temp. (°C)	Est. Burnup (% heavy atoms)	Fission Gas Release (%)
			C	O	N	Pu	U			Sintered Bulk	Theoretical					
1 Sintered	8139	1.024 0.32	4.76	0.24	0.04	13.0	82.0	4.97	MC + M_2C_3	12.9	13.4	144	1040	1610	3.95	-
2 Sintered	8140	1.018 0.29	5.32	0.07	0.02	12.6	81.99	5.38	MC + M_2C_3	12.8	13.3	162	940	1440	4.45	-
3 Sintered	8141	1.015 0.27	4.73	0.09	0.07	13.2	81.90	4.86	MC + M_2C_3	13.0	13.4	180	950	1460	4.95	-
4 Sintered	8142	1.013 0.26	5.32	0.07	0.02	12.6	81.99	5.38	MC + M_2C_3	12.8	13.3	190	930	1430	5.20	-
5 Arc-cast	8143	1.068 0.25	4.76	-	-	-	-	-	MC + trace of free metal	-	-	199	940	1420	5.40	-
6 Sintered	8144	1.024 0.25	4.76	0.24	0.04	13.0	82.0	4.97	MC + M_2C_3	12.9	13.4	201	950	1430	5.50	-
7 Powder	8145	1.023 0.25	5.32	0.07	0.02	12.6	82.0	5.39	-	60% T.D.	13.3	199	800	1270	5.40	0.2-0.5
8 Powder	8146	1.016 0.26	5.32	0.07	0.02	12.6	82.0	5.39	-	60% T.D.	13.3	190	800	1250	5.20	1.25-2.5
9 Arc-cast	8147	1.017 0.27	4.75	-	-	14.2	-	-	MC + trace of free metal	13.36	13.6	180	930	1410	4.95	-
10 Sintered	8148	1.022 0.29	4.00	0.07	0.10	14.3	81.53	4.14	MC in metal matrix	13.5	14.2	162	990	1530	4.45	-
11 Arc-cast	8149	1.016 0.32	4.80	-	-	-	-	-	MC + trace of free metal	13.54	13.6	144	1020	1610	3.95	-

TABLE II. BURN-UP AND GAS RELEASE VALUES

Sheath Number	Specimen Number	Material	Rating			Estimated Temperatures °C		Burn-up (% H.A.) MWd/teV		Gas Release Based on		Xe/Kr	Predicted Release Findlay (4) %
			W/gm.	W/cm.	∫kdθ W/cm.	Can Surface	Fuel Centre	Monitors and Reactor Opn.	Radiochem.	Monitors %	Radiochem. %		
4A	8090	Sintered 'Stoich'	283	187	15	630	820	5.4% 46700 MWd/teV	-	0.96	-	18.0	1.1
3C	8084	Powder 'Stoich'	400	164	13	630	1100	7.4% 64000 MWd/teV	6.01 52,000	6.2	7.6	17.6	-
3B	8083	Powder C	430	176	14	630	1170	8.1% 70000 MWd/teV	5.75 49,700	18.8	26.4	17.8	-
3A	8082	Sintered 'Stoich'	358	234	19	630	840	6.7% 58000 MWd/teV	5.75 49,700	2.12	2.48	17.6	1.1
2D	8081	Arc-cast C⁻	435	297	24	650	940	8.8% 76000 MWd/teV	6.08 52,500	2.02	2.88	17.2	1.6
2C	8080	Arc-cast 'Stoich'	435	297	24	650	940	8.8% 76000 MWd/teV	6.16 53,200	0.64	0.92	16.5	1.8
2B	8079	Arc-cast C⁺	435	297	24	650	940	8.8% 76000 MWd/teV	6.19 53,500	0.70	1.00	17.1	1.2
2A	8078	Sintered 'Stoich'	435	282	23	650	940	8.8% 76000 MWd/teV	6.31 54,500	0.56	0.78	16.7	1.1
1D	8089	Sintered C⁻	538	348	28	675	980	10.6% 90000 MWd/teV	7.57 65,500	2.5	3.5	16.4	2.5
1C	8088	Sintered C⁺	538	348	28	675	980	10.6% 90000 MWd/teV	7.16 62,000	0.23	0.34	17.3	1.7
1B	8087	Sintered 'Stoich'	538	348	28	675	980	10.6% 90000 MWd/teV	7.16 62,000	0.32	0.475	17.8	1.1
1A	8086	Sintered 'Stoich'	538	348	28	675	980	10.6% 90000 MWd/teV	6.96 60,000	0.19	0.29	17.1	1.1

TABLE III. IRRADIATION CONDITIONS - 28 IN. CARBIDE PINS IN D.F.R.

Pin Designation	Fuel Diameter (in.)	Density of Fuel Stack (% of theory)	Initial Fuel Rating		Max. Can Mid-wall temp. °C	Estimated Irradiation Conditions at point of Maximum Flux			Burn-up at End of Irradiation (% h.a.)		Condition on Discharge
			W/gm	W/cm		Can Mid-wall Temp °C	Fuel Surface Temp °C	Fuel Centre Temp °C	Mean	Max.	
CV002	0.200	83.1	165	376	580	480	615	1300	7.1	8.0	FAILED
CV003	0.200	81.1	182	404	560	470	615	1390	4.6	5.2	INTACT
CA001	0.1985 0.067	83.6	226	517	630	500	720	890	5.4	6.1	INTACT
CA002	0.270	83.4	226	970	655	540	1290	1635	3.6	4.0	FAILED
CA003	0.082	83.5	222	955	650	540	1275	1625	5.3	5.8	FAILED

TABLE IV. POST-IRRADIATION DATA - 28 IN. CARBIDE PINS IN D.F.R.

Pin Designation	Max. B.U. %	Characteristic Diameter Increase, (%) over Length				Max. Diam. Change (%)	Estimated Max. Clad Strain (%)	Diam. Change at Plenum (%)	Pin Extention (%)	Fission Gas Release
		0-5 in.	5-10 in.	10-15 in.	15-20 in.					
CA002	4.0	0.64	0.67	0.58	0.32	1.05(at crack)	1.0	0.09	0.24	-
CA003	5.8	1.1	Split	1.3	0.45	8.0 (at crack)	1.4	Nil	-	-
CA001	6.1	0.73	1.30	1.11	0.67	1.40	1.4	0.26	0.8	0.11
CV002	8.0	1.9	Split	Split	1.5	8.0 (at crack)	1.4-1.9	0.2	-	-

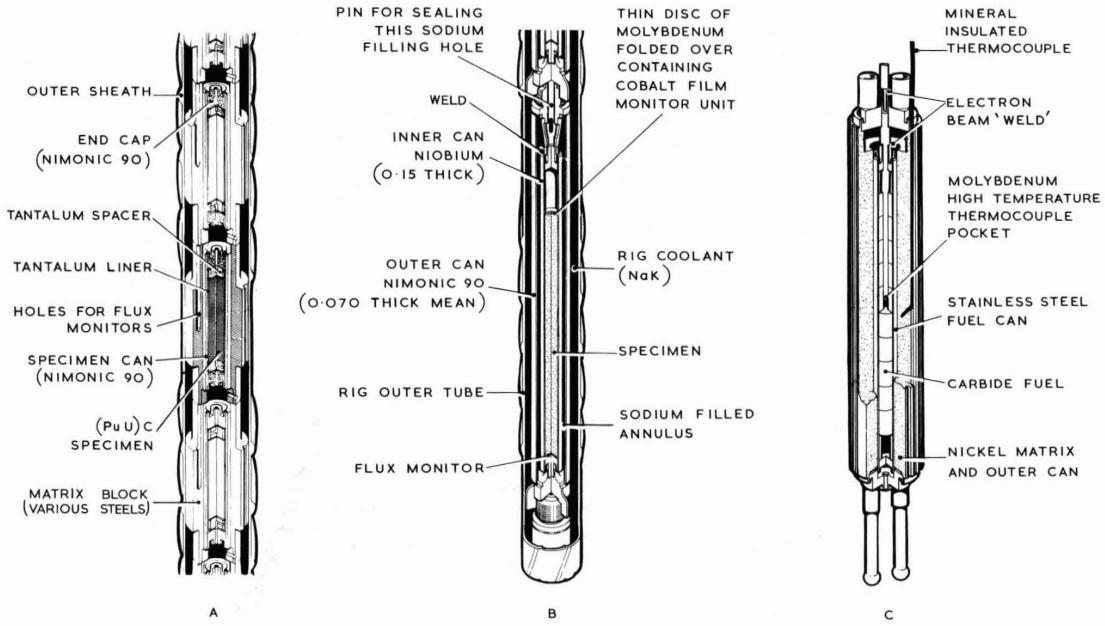

FIG. 1 SECTIONAL VIEWS OF FAST REACTOR CAPSULES

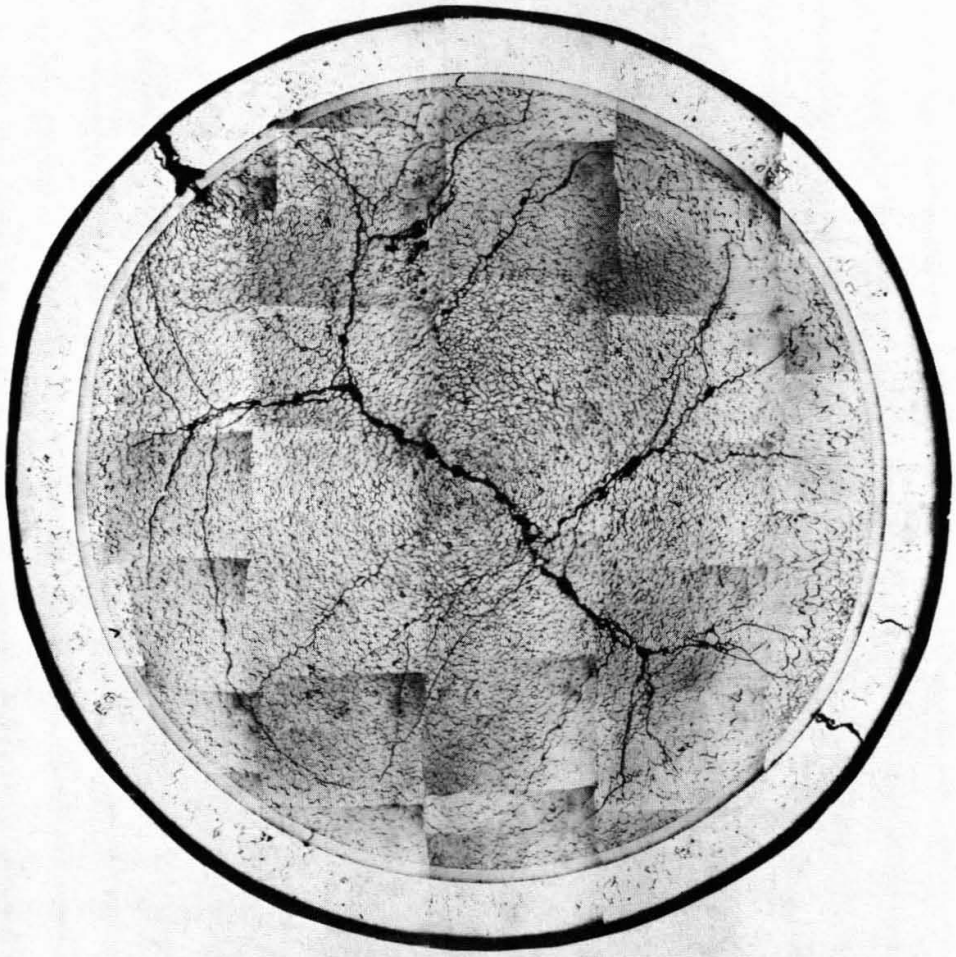

Mag ×60

D.F.R. 26/1 EXPERIMENT CAN Nº11.

CROSS SECTION OF ARC CAST STOICHIOMETRIC (PuU)C MATERIAL.

FIG. 2

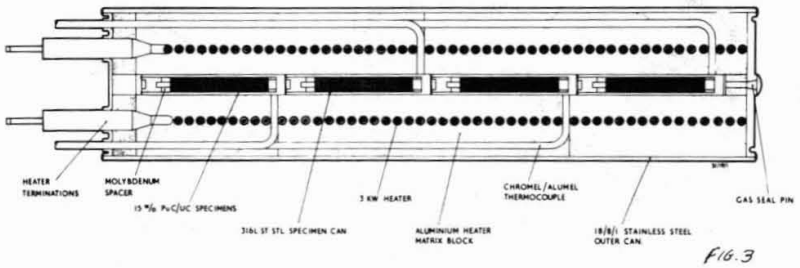
HEATER TERMINATIONS
MOLYBDENUM SPACER
15 % PuC/UC SPECIMENS
316L ST STL SPECIMEN CAN
3 KW HEATER
ALUMINIUM HEATER MATRIX BLOCK
CHROMEL/ALUMEL THERMOCOUPLE
18/8/1 STAINLESS STEEL OUTER CAN
GAS SEAL PIN

FIG.3

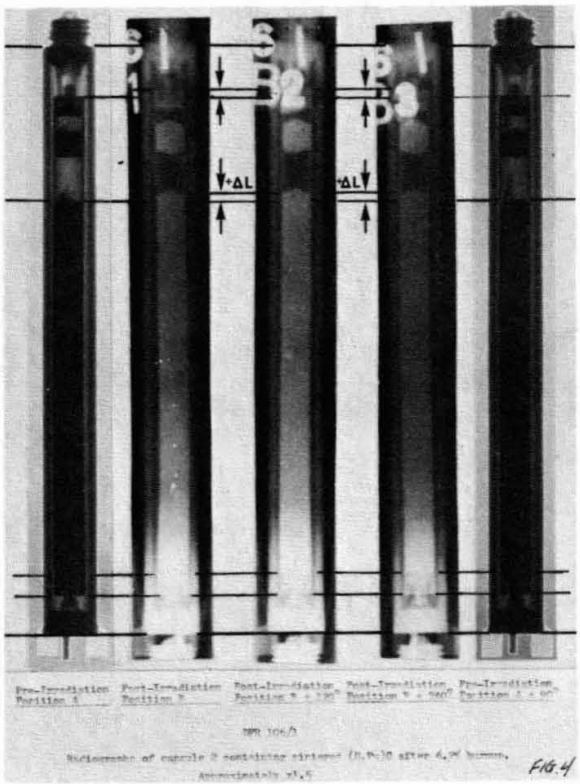
B1
B2
B3
+ΔL
+ΔL
Pre-Irradiation Position 1
Post-Irradiation Position 2
Post-Irradiation Position 3 + 120°
Post-Irradiation Position 3 + 240°
Pre-Irradiation Position 3 + 0°

FIG.4

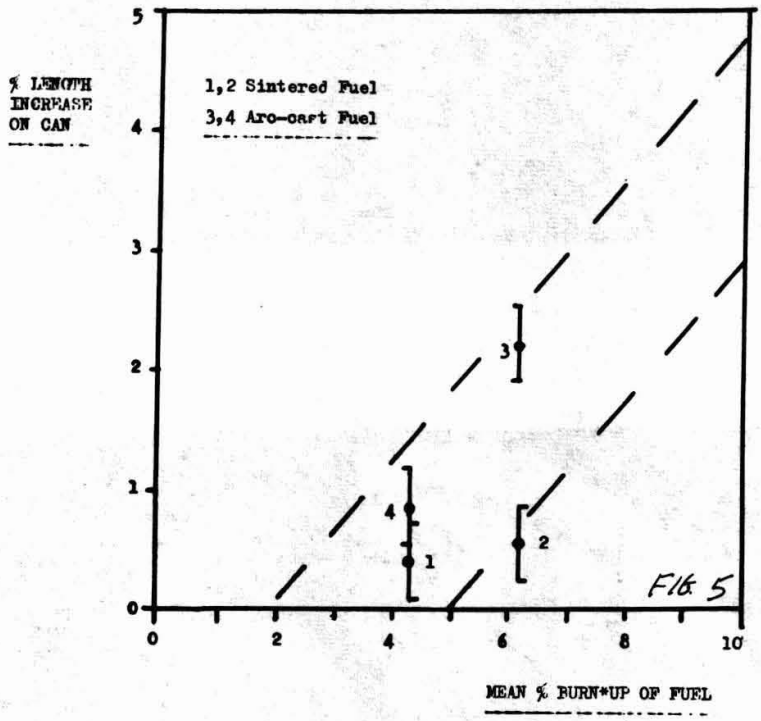

Length increase against burn-up for niobium-clad (U,Pu)C from DFR 106/1

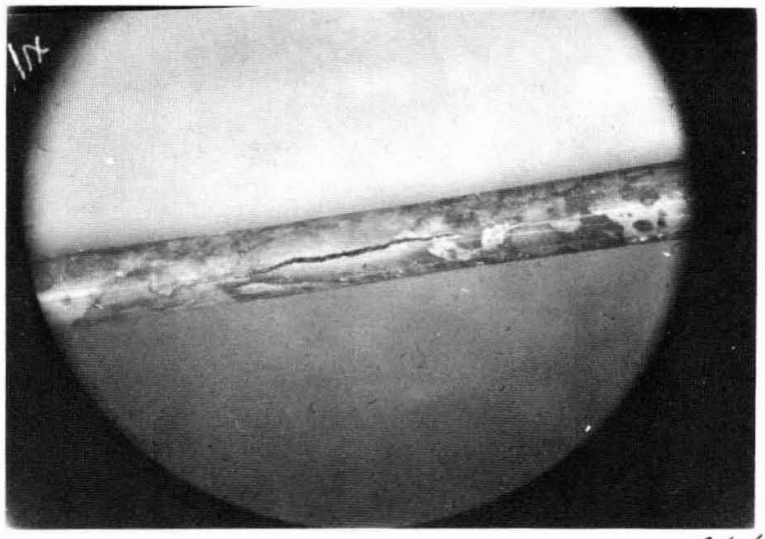

FIG. 6

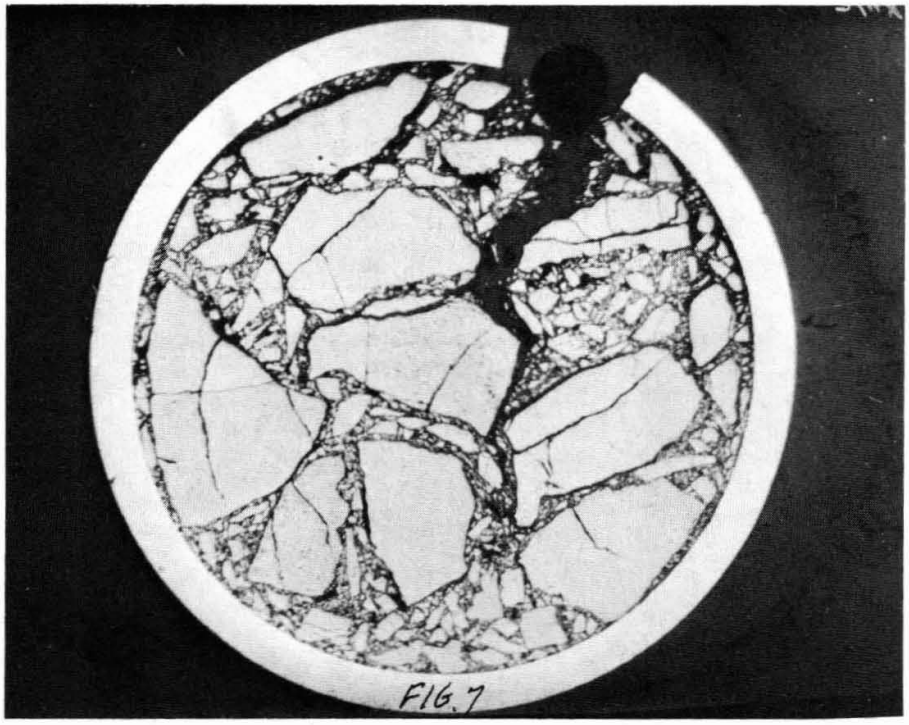

FIG. 7

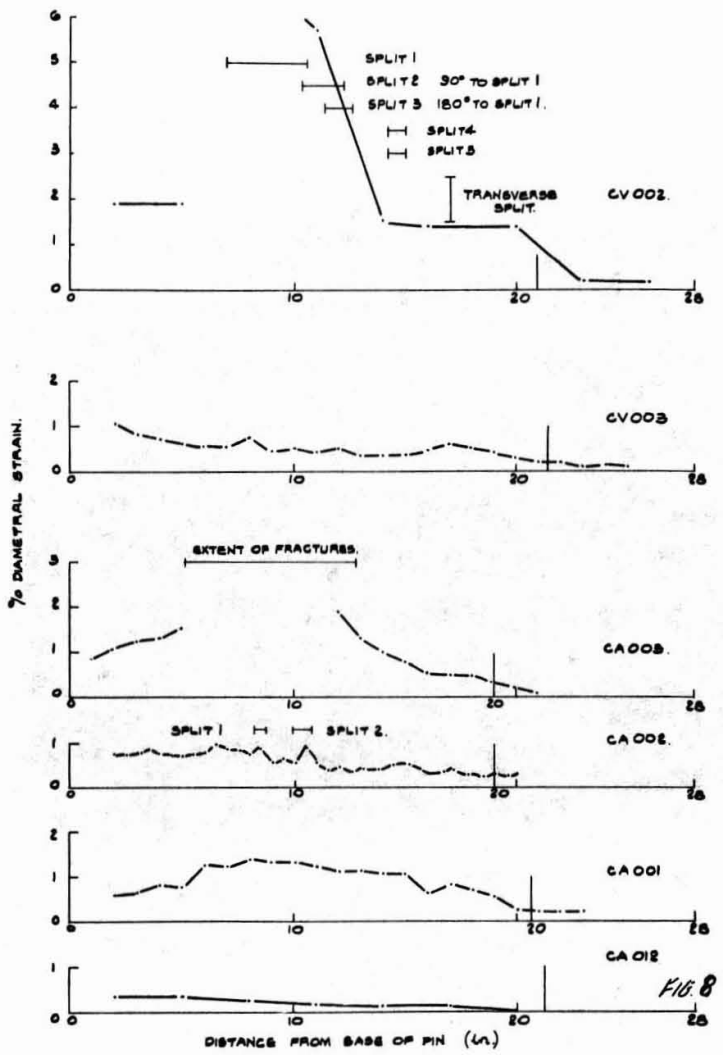
SPLIT 1
SPLIT 2 90° TO SPLIT 1
SPLIT 3 180° TO SPLIT 1.
SPLIT 4
SPLIT 5
TRANSVERSE SPLIT.
CV002.
CV003
EXTENT OF FRACTURES.
CA005.
SPLIT 1
SPLIT 2.
CA006.
CA001
CA012
% DIAMETRAL STRAIN.
DISTANCE FROM BASE OF PIN (in.)

FIG. 8

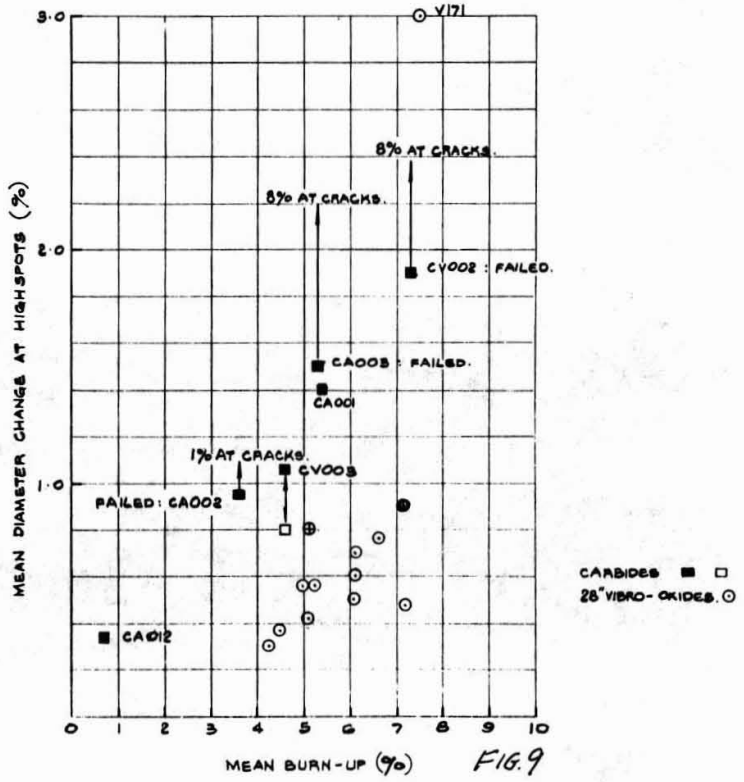
V171
8% AT CRACKS.
8% AT CRACKS.
CV002 : FAILED.
CA005 : FAILED.
CA001
1% AT CRACKS.
CV003
FAILED: CA002
CA012
MEAN DIAMETER CHANGE AT HIGH SPOTS (%)
MEAN BURN-UP (%)
CARBIDES
28" VIBRO-OXIDES.

FIG. 9

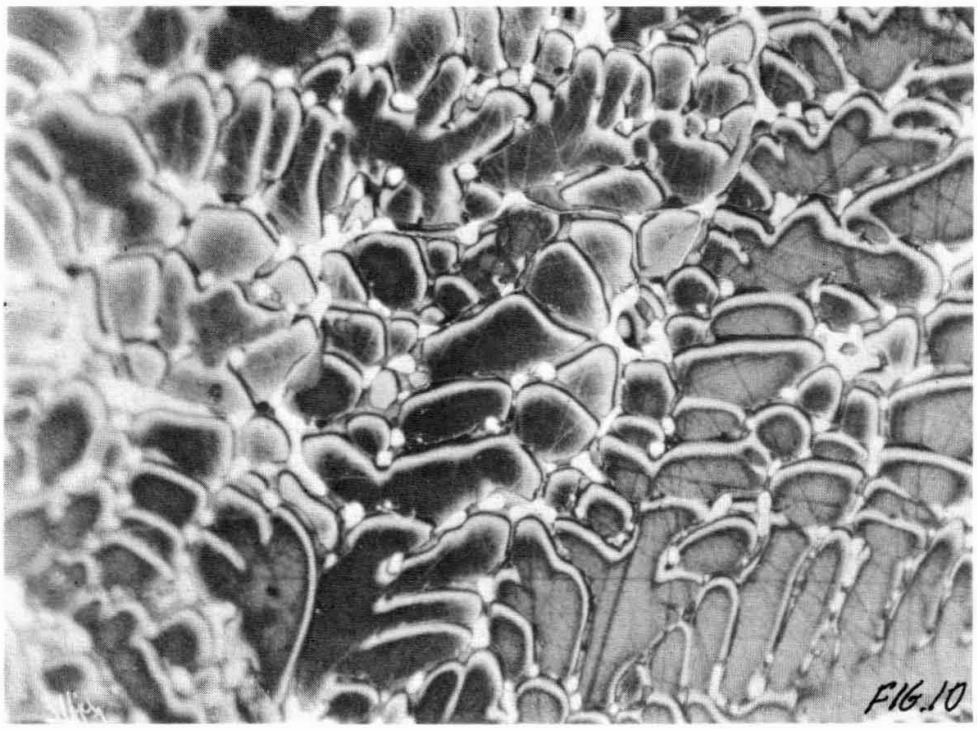

FIG. 10

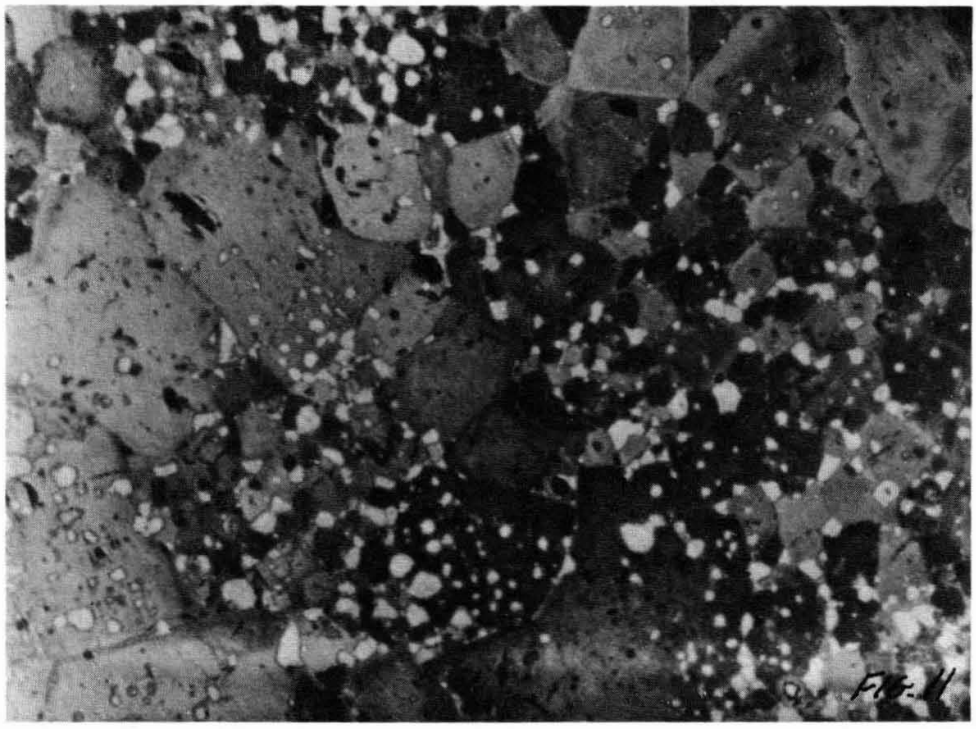

FIG. 11

IRRADIATION PERFORMANCE OF FAST REACTOR URANIUM-PLUTONIUM METAL FUELS

W. N. Beck, F. L. Brown, B. J. Koprowski, and J. H. Kittel

Irradiation studies are being performed on uranium-plutonium alloys as fuels for fast breeder reactors. The irradiation performance of the alloys is being evaluated as prototype elements in thermal reactors, and as full-size elements, in the fast reactor EBR-II. of the alloys tested, the U-Pu-Zr system is the most attractive because of its good compatibility with stainless steel cladding and its greater resistance to fuel swelling. The alloy has been successfully irradiated to 12.5 a/o burnup at maximum clad temperatures of 655°C and at linear heat ratings of 11 kw/ft. Experiments are in the planning stage that will evaluate the performance of this alloy at linear heat ratings of 15 to 20 kw/ft.

The authors are members of the Metallurgy Division, Argonne National Laboratory, Argonne, Illinois.

Introduction

Uranium-plutonium metal fuels are attractive for large fast reactors because of their high fertile-fissile atom densities, high breeding ratio, good thermal conductivity, and large thermal expansion coefficients. In addition, the alloys are easily fabricated to close tolerances and are amenable to pyrorefining.

Previous irradiation studies that were reported on the uranium-plutonium systems were principally on unclad fuel and not at the temperatures and burnup values that are of interest for future fast breeder reactors. The principal alloys that were evaluated in the previous studies may be summarized as follows:

1. Uranium-plutonium, with plutonium concentrations as high as 20 wt.%, were tested to 1.9 at.% burnup (1). A comparison of cast with extruded alloys showed that the extruded 20 wt.% plutonium alloy yielded the best results.

2. Zirconium-plutonium with plutonium concentrations of 5 wt.% to 7 wt.% were irradiated at maximum temperatures of 500°C to burnups of 1.8 at.% (2). The pins were fabricated by forging and rolling arc-melted buttons. These pins showed preferred axial elongation with length changes as high as 400%.

3. Aluminum-plutonium and aluminum-plutonium-nickel alloys have been irradiated in Zircaloy tubing (3-6). The alloys were found to be stable under conditions appropriate for water-cooled reactors.

4. Uranium-plutonium-molybdenum with plutonium concentrations up to 18% and molybdenum additions to 13% were found to have a high swelling rate at low temperatures (7,8). The alloy was successfully contained in 0.016 in. thick jacket material to burnups up to 1 at.% (9,10).

5. Uranium-plutonium-fissium alloys have been investigated by ANL for use in the EBR-II reactor. Irradiation experiments on unclad pins with plutonium concentrations of 20 wt.% and fissium contents near 10 wt.% showed that the alloy swelled rapidly at a temperature of about 370°C (11).

In addition, a compatibility problem exists between U-Pu-Fs fuel alloy and nickel-base or iron-base cladding materials at the desired operating temperatures. It was apparent that considerable reliance would have to be placed on the jacket and that the jackets would have to be made of refractory alloys which do not form low melting eutectic alloys with the fuel (12).

Irradiations performed on prototype elements of U-Pu-Fs alloy jacketed in various refractory alloy tubing having a wall thickness of

0.009 in. and an effective fuel density ~81% indicated that burnups on the order of 4 at.% could be achieved (13).

The most significant results, with regard to improving the performance of metallic fuel elements, were obtained from irradiation studies in which the fuel was permitted various degrees of unrestrained swelling (14). The results supported the theoretical prediction (15) that metal fuels would release substantial amounts of fission gas after their volume has increased approximately 30%. Metallographic examination of irradiated fuel having this volume increase indicated that fission gas bubbles became interconnected so that the fission gas could escape to the surface of the fuel.

A fuel volume increase of 33% can be obtained by using an element design having an effective fuel density of 75%. The necessary voidage is provided by the sodium-filled annulus between the fuel pin and the jacket. Sufficient plenum volume is provided into which the fission gas can be released and into which the bond sodium can be displaced.

Utilizing this design criterion, successful irradiations were performed on prototype elements to burnups up to 12.5 at.%.

Figure 1 is a graph showing fission gas release vs. fuel volume expansion for U-Fs, U-Pu-Fs, and U-Pu-Zr. Analyses of the results indicate that the fission gas release is largely independent of burnup and temperature and depends principally on the amount of fuel swelling. The points which are plotted in Fig. 1 represent burnups between 2.7 and 12.5 at.% and maximum fuel temperatures between 450°C and 840°C.

With the development of fuel reprocessing schemes where all the fission products could be remotely removed from uranium and plutonium, other uranium-plutonium alloys were considered for use in fast breeder reactors. The emphasis was on compositions with relatively high melting points. Alloying elements that were investigated included Se, Ti, Y, Zn, Nb, Mo, Pd, and Th. Of these, the ones which were most effective in raising the solidus temperature of the U+Pu system were zirconium and titanium. These two alloy additions were most desirable from physics considerations.

The last two mentioned alloys, i.e., U-Pu-Zr and U-Pu-Ti, will be discussed in greater detail.

Irradiations of U-Pu-Zr and U-Pu-Ti Alloys

Alloy Properties

Studies of the properties of these alloys disclosed that the U-Pu-Zr system was compatible with Type 304 stainless steel up to 800°C (16). The use of Type 304 stainless steel as jacket material is attractive in sodium cooled fast reactors for its nuclear properties, compatibility with flowing sodium, and commercial availability as small-size tubing. A comparison of the melting temperatures of reaction products between

Type 304 stainless steel and U-Pu-Zr alloys with data on other alloys is shown in Fig. 2 (17).

Repeated thermal cycling of U-Pu-Zr and U-Pu-Ti alloys through their phase changes showed no significant effect. Length change increases varied from 0 to 5% but the errors in measuring slightly distorted rods were believed to be the cause of the length increase. Density changes varied from -0.6 to +0.8% but probably were due to homogenization of the cast structure rather than thermal cycling damage (18).

The U-Pu-Zr and U-Pu-Ti systems are similar in that both contain appreciable amounts of alpha-uranium and zeta U-Pu phases at room temperature, show extensive solubility for the alloy addition, and both will first form a body-centered-cubic gamma solid-solution on solidification (19). Table I lists the important physical properties of the U-Pu-Zr and U-Pu-Ti alloys investigated. Although these two alloy systems were studied extensively, emphasis was placed on the U-Pu-Zr alloy because of its excellent compatibility with stainless steel.

The phase transformation studies on the U-Pu-Zr system having nominal concentrations of 15 wt.% Pu and 10 to 14 wt.% Zr showed that the alloy contains alpha-uranium and zeta-uranium-plutonium + delta-UZr_2 up to a temperature of about 595°C, which is the first significant transformation (20). At this temperature the principal reaction is alpha + gamma → delta + zeta. Between 595°C and 655°C, the fuel contains three phases, alpha-uranium + zeta-uranium-plutonium + gamma. The reaction at this temperature is gamma + beta → alpha + zeta. Above the temperature of 655°C, the fuel is in a gamma phase. Dilatometry tests on the alloy showed these transformations to be pronounced and well-defined. As will be shown later, the phase transformation characteristics of the alloy are important in interpreting the structural changes that develop under irradiation.

Capsule Irradiations

Preliminary irradiations were performed on six U-15 wt.% Pu-12 wt.% Zr fuel alloy specimens jacketed in either Type 304 stainless steel, Type 316 stainless steel, or Hastelloy-X tubing. The effective density of the fuel was 75%. These specimens were irradiated to 2.4 at.% burnup in an instrumented, temperature-controlled capsule that was inserted in a vertical thimble of the CP-5 reactor. The maximum jacket temperature was 610°C.

The postirradiation metallographic examination of the specimens showed excellent compatibility between the fuel and the cladding. Photomicrographs of interfaces are shown in Fig. 3. The transverse macrosections of the fuel revealed three distinct bands that can be correlated with phase transformation temperatures. A typical transverse section is shown in Fig. 4. The outer zone is believed to correspond to the (alpha-uranium + delta + zeta) phase, the second band (alpha-uranium + zeta + gamma) phase and the central area principally

the gamma phase. As anticipated, the fuel had swelled to the internal diameter of the cladding and the bond sodium was entirely displaced into the gas plenum. Figure 4 also shows that the volume of the sodium-filled annulus around the solid metal fuel pin at the start of irradiation became redistributed throughout the fuel volume in the form of finely-divided porosity.

Before the excellent compatibility between U-Pu-Zr alloy and austenitic stainless steels had been established, an irradiation was performed on a U-18.5 wt.% Pu-14.1 wt.% Zr alloy pin jacketed in V-20 wt.% Ti tubing. The effective density of fuel was 63% and the plenum was 73% of the fuel volume.

The specimen achieved 12.5 at.% burnup (28×10^{20} fiss/cm^3) without jacket failure at a maximum clad temperature of 655°C. During the irradiation, periodic interim nondestructive examinations of the specimen were made by neutron radiography. These examinations showed that the fuel pin attained a maximum elongation of 3% within the jacket at 4.2 at.% burnup. This dimension did not change throughout the remainder of the irradiation.

Diameter changes of the jacketed specimen were calculated from volume changes measured by immersion. An average 0.0002 in. diameter increase was observed. No measurable length increase of the jacketed specimen was noted. The jacket was punctured and the recovered fission gas was analyzed for fission product isotopes. It was determined that 74% of the fission gas had been released to the plenum.

Metallographic examination showed that there was no significant penetration of the fuel into the jacket.

The condition of the fuel as well as the calculated final operating gas plenum pressures (~2200 psi) indicates that the specimen could have attained still higher burnups without jacket failure. Table II lists the design parameters and operating conditions for the U-Pu-Zr prototype elements irradiated in capsules in the CP-5 reactor.

U-Pu-Ti was regarded as secondary in importance and as such only one irradiation was performed on a U-15 wt.% Pu-10 wt.% Ti pin jacketed in V-20 wt.% Ti tubing.

The specimen reached 10.7 at.% burnup (25×10^{20} fiss/cm^3) without jacket failure at a maximum clad temperature of 630°C. Periodic nondestructive examination of the capsule by neutron radiography showed a maximum fuel pin elongation within the cladding of 14% which occurred at 4.6 at.% burnup. This dimension remained the same throughout the remainder of the irradiation.

The cessation of lengthwise growth in the U-Pu-Zr and U-Pu-Ti specimens is not unusual, as similar behavior has been observed in other metal irradiation specimens where release of the fission gases in the fuel had occurred (21).

An average clad diameter increase of 0.0016 in. was calculated from volume changes by immersion. No measurable length change was noted. The jacket was punctured for fission gas recovery but the gas sample was lost in the hot cell because of equipment failure.

The metallographic examination of the specimen shows that there was no significant penetration of the fuel into the jacket. In isolated areas there was occasional evidence of surface reaction in the fuel occurring to a depth of ~0.005 in. A transverse section of the specimen can be seen in Fig. 5. The central area which is characteristically different from the rest of the fuel is believed to be indicative of a $(U,Pu)_2Ti + \gamma$ phase which is stable above the temperature of 710°C.

Completed Fast Reactor Irradiations

Successful irradiations have been completed on 16 full-length elements of U-Pu-Zr alloy in the EBR-II reactor (Group XA07) (22). These elements measured 33 in. in length and 0.196 in. OD. The fuel alloys were U-15 wt.% Pu-9 wt.% Zr or U-15 wt.% Pu-12 wt.% Zr pins sodium-bonded in either Type 304 stainless steel, Type 316 stainless steel, Hastelloy-X, or Hastelloy-X-280 tubing. The effective fuel densities in most of the elements were from 73 to 75%. They were operated at a maximum clad temperature of 630°C and a maximum heat rating of 10.9 kw/ft. The elements attained burnups of up to 4.6 at.%.

External dimensional measurements of the elements showed no significant changes as a result of irradiation. No jacket failures occurred. Fuel pin length dimensions within the cladding were determined by neutron radiography and disclosed an average fuel length increase of 1.9%. The fuel pins were not seated on the bottom closures of the jackets, but were elevated an average of 0.20 in. These elements had been intentionally assembled without fuel restrainers to observe possible axial fuel movement. The neutron radiographs of the elements also revealed one or two partial separations in most of the fuel pins within the cladding that varied from ~0.020 in. to 0.050 in. in width.

Fission gas recovery data established that ~57% of the fission gas had been released from the fuel pins to the plenum above the bond sodium. These results are in agreement with the previously reported data on fission gas release rates on small prototype elements (Fig. 1). A calculation of the plenum pressures in the specimens revealed that, at reactor operating temperatures, the average gas pressure was 485 psi.

Transverse as well as longitudinal metallographic sections of the fuel elements showed no penetration of the fuel into the cladding materials. A detailed metallographic and microprobe examination of the fuel/clad interfaces did show what appeared to be a carbide precipitation zone that had a depth of 140μ in the Type 304 stainless steel, and a diffusion zone of 20μ in the Type 316 stainless steel. The fuel adjacent to the Type 304 stainless steel was U-15 wt.% Pu-9 wt.% Zr while the fuel adjacent to the Type 316 stainless steel was

U-15 wt.% Pu-12 wt.% Zr. Alpha autoradiographs as well as microprobe analyses showed no plutonium in the jacket materials. Detailed information on the design of these elements is listed in Table III, along with a summary of irradiation conditions.

Fast Reactor Irradiations in Progress

Two full-length U-Pu alloy fuel elements are presently being irradiated in the EBR-II reactor. One element is fueled with U-15 wt.% Pu-10 wt.% Zr and the other with U-15 wt.% Pu-10 wt.% Ti. Both pins are jacketed in V-20 wt.% Ti, 0.206 in. OD and having a wall thickness of 0.016 in. The average effective fuel density is 65%. The elements have been irradiated at a maximum clad temperature of 540°C and to a calculated 5.5 at.% burnup. The target burnup for the fuel is 10 at.%.

Two additional elements, which are duplicates of those described above, have been irradiated at jacket temperatures near 540°C and to 5 at.% burnup. An interim examination of the two encapsulated elements by neutron radiography showed the elements to be in excellent condition. Irradiation will be continued to the target 10 at.% burnup.

A group of fifteen U-15 wt.% Pu-10 wt.% Zr elements (Group M-3) has been prepared for insertion in EBR-II. These elements are similar in design to the XA07 group irradiated to 4.6 at.% burnup. Group M-3 will be irradiated with higher initial plenum pressures and to 10 at.% burnup.

A group of forty U-15 wt.% Pu-12 wt.% Zr elements (Group M-4) is in preparation. These elements will have larger diameters than used heretofore so that the performance of U-Pu alloy fuels can be evaluated at linear heat ratings up to approximately 15 kw/ft.

Other experiments are in the planning stage that will evaluate the performance of U-Pu-Zr alloy elements at linear heat ratings in the range of 15 to 20 kw/ft.

Acknowledgement

This work was performed under the auspices of the United States Atomic Energy Commission.

REFERENCES

1. Reactor Handbook, Volume I (Materials) 1960, p. 282.

2. J. A. Horak and H. V. Rhude, Irradiation Growth of Zirconium-Plutonium Alloys, 1961, J. Nucl. Mat'ls 3, (1) pp. 111-112.

3. T. I. Jones, The Irradiation of Aluminum-Plutonium Alloys in Zircaloy-2 Sheathing, 1962, AECL-1589.

4. R. Carlander, J. H. Kittel, and R. J. Dunworth, Postirradiation Examination of EBR-I Core IV Prototype Fuel Rods, 1963, ANL-6770.

5. M. D. Freshley and Staff, PRTR Fuel Element Experience, 1964, ANS Trans. 7, (2).

6. R. K. Koler, M. D. Freshley, W. J. Bailey, Irradiation Testing of Injection-Cast Al/Pu/Ni Alloy Fuel Rods, 1963, ANS Trans. 6, (1) p. 159.

7. M. B. Waldron, et al., Plutonium Technology for Reactors, 1958, Proceedings Second International Conference on the Peaceful Uses of Atomic Energy, 6, 690-696.

8. B.R.T. Frost, P. G. Margon, and L. E. Russell, Research on the Fabrication, Properties, and Irradiation Behavior of Plutonium Fuels for the U.K. Reactor Programme, 1962, HW-75007, 4.1-4.38.

9. F. Sebilleau and C. P. Zaleski, Plutonium as a Fuel for the Fast Reactor Rapsodie, 1962, HW-75007, 15.1-15.17.

10. J. P. Mustelier, Quelques Resultats d'Irradiation sur les Combustibles Envisages Pour Rapsodie, 1963, New Nuclear Mat'ls Including Non-Metallic Fuels, II, 163-183, IAEA, Vienna.

11. J. A. Horak, J. H. Kittel, and R. J. Dunworth, The Effects of Irradiation on Uranium-Plutonium-Fissium Fuels Alloys, 1962, ANL-6429.

12. J. H. Kittel and W. N. Beck, Behavior of Refractory Metal-Clad Plutonium Alloy Fuel Under Irradiation, 1963, Proceedings AIME Conference on Applied Aspects of Refractory Metals, 597-607.

13. W. N. Beck, J. H. Kittel, and R. J. Fousek, Irradiations of U-20Pu-10Fs Alloy Fuel Rods, 1965, ANL-6750.

14. W. N. Beck and R. J. Fousek, Fission Gas Release and Microstructural Changes in High Burnup U-Pu Fast Breeder Alloys, 1966, Trans. ANS 9, (2) 415.

15. R. S. Barnes, A Theory of Swelling and Gas Release for Reactor Materials, 1964, J. Nucl. Mat'ls, 11, (2) 135-148.

16. L. R. Kelman, et al., Status of Metallic Plutonium Fast Power Breeder Fuels, Third International Conference on Plutonium, London, November 22-26, 1965.

17. C. M. Walter, et al., Compatibility of U-Pu-Zr and U-Pu-Ti Alloys with Potential Cladding Materials, Annual Progress Report for 1965, Metallurgy Division, ANL-7155, p. 22.

18. R. J. Dunworth, Thermal Cycling of U-Pu-Zr and U-Pu-Ti Alloys, Annual Progress Report for 1965, Metallurgy Division, ANL-7155, p. 19.

19. S. T. Zegler, Structure and Transformations in U-Pu-Zr and U-Pu-Ti Alloys, Annual Progress Report for 1965, Metallurgy Division, ANL-7155, p. 14.

20. D. R. O'Boyle, private communication.

21. W. N. Beck, Irradiations of Uranium-Plutonium Alloys, Annual Progress Report for 1965, Metallurgy Division, ANL-7155, p. 80.

22. W. N. Beck, F. L. Brown, B. J. Koprowski, and J. H. Kittel, Performance of Advanced U-Pu-Zr Alloy Fuel Elements Under Fast Reactor Conditions, 1967, Trans. Am. Nucl. Soc. 10, (1) 106.

Table 1. Properties of U-Pu-Zr and U-Pu-Ti Alloys

	U Pu Zr	U Pu Zr	U Pu Zr	U Pu Zr	U Pu Ti	U Pu Ti
Nominal Composition:						
wt.%	11.1 6.3	15 10	18.4 14.1	17.1 3.4	15 6.5	15 10
at.%	10 15	12.9 22.5	15 30	15 15	11.9 25.7	10.7 35.6
Approx. Liquidus Temp. (°C)	1200	1250	1290	1200	1300	1340
Approx. Solidus Temp. (°C)	1120	1155	1170	1075	1160	1200
Solid Transformation						
Temp. Range (°C)	595-680	595-665	595-660	570-780	570-850	680-850
Density at 25°C As-Cast (g/cm^3)	17.0	16.0	15.1	17.0	15.6	14.4
Thermal Expansion						
Avg. Coef. x 10^6 ($°C^{-1}$)						
25°C to 1st trans.	18.3	17.6	17.5	21.2	18.9	19.2
End of trans. to 950°C	18.1	20.1	20.0	16.4*	20.0	19.2
In Trans. Range $\Delta\ell/\ell \times 10^3$ ($°C^{-1}$)	5.1	5.2	5.0	9.3	17	13.7
Thermal Cycling						
Density Change (%)	0	-0.1	0	+0.1	-	-
Hardness at 25°C As-Cast (DPH)	470	540	410	430	-	400
Thermal Conductifity (w/cm-°C)						
200°C	-	0.12	0.11	0.13	0.13	0.13
400°C	-	0.18	0.17	0.20	0.17	0.16
600°C	-	0.22	0.21	0.25	0.21	0.20
800°C	-	0.25	0.24	0.30	0.24	0.23
Tensile Strength (kg/mm^2)						
25°C	18.1	6.7	7.7	-	4.5	6.5
675°C	1.2	2.1	2.9	3.6	2.6	7
Compressive Strength (kg/mm^2)						
25°C	164	129	116	96	130	90
675°C	4	5.6	5.6	3.8	6.3	10

*To 860°C.

Table 2. Design Parameters and Operating Conditions for U-Pu-Zr Prototype Elements Irradiated in Capsules in the CP-5 Reactor

	Design Parameters						Operating Conditions			
									Burnup	
Spec. No.	Fuel Composition, w/o	Eff. Density, %	Clad. Comp., w/o	Clad. OD, in.	Clad. Thick., in.	Plenum Vol. %	Max. Clad. Temp., °C	Max. Fuel Temp., °C	a/o,U+Pu	fiss/cc x 10^{-20} (a)
48-2	U-15Pu-12Zr	75	304 SS	0.196	0.015	96	610	700	2.4	6.2
48-5	U-15Pu-12Zr	75	304 SS	0.196	0.015	92	660	810	2.4	6.2
48-3	U-15Pu-12Zr	75	316 SS	0.196	0.015	97	610	700	2.4	6.2
48-6	U-15Pu-12Zr	75	316 SS	0.196	0.015	97	660	810	2.4	6.2
48-1	U-15Pu-12Zr	75	Hast.-X	0.196	0.015	95	610	700	2.4	6.2
48-4	U-15Pu-12Zr	75	Hast.-X	0.196	0.015	98	660	810	2.4	6.2
45-1	U-18.5Pu-14.1Zr	63	V-20Ti	0.208	0.016	73	655	840	12.5	28.0

(a) Based on effective density.

Table 3. Irradiation Conditions for U-Pu-Zr Alloy Fuel Elements Irradiated in EBR-II in Subassembly XA07

Spec. No.	Fuel Composition, w/o	Cladding Alloy	Effective Density %	Clad. OD, in.	Clad. Thick., in.	Max. kw/ft	Max. Fuel Temp.,°C	Max. Clad. Temp.,°C	Estimated Burnup, at.%
ND-28	U-15Pu-9Zr	304 SS	73.1	0.205	0.019	10.9	745	630	4.6
ND-41	U-15Pu-9Zr	304 SS	73.8	0.205	0.019	10.4	735	625	4.4
ND-32	U-15Pu-9Zr	316 SS	73.8	0.196	0.015	9.9	715	605	4.2
ND-43	U-15Pu-9Zr	Hast.-X	74.5	0.196	0.015	10.4	725	615	4.4
ND-25	U-15Pu-12Zr	304 SS	73.5	0.205	0.019	9.5	710	600	4.0
ND-27	U-15Pu-12Zr	304 SS	73.1	0.205	0.019	9.7	715	605	4.1
ND-26	U-15Pu-12Zr	316 SS	73.9	0.196	0.015	9.5	695	590	4.0
ND-29	U-15Pu-12Zr	316 SS	72.2	0.196	0.015	9.5	700	595	4.0
ND-30	U-15Pu-12Zr	316 SS	72.3	0.196	0.015	10.4	700	615	4.4
ND-31	U-15Pu-12Zr	316 SS	74.1	0.196	0.015	9.9	720	610	4.2
ND-33	U-15Pu-12Zr	Hast.-X	72.8	0.196	0.015	9.9	715	605	4.2
ND-34	U-15Pu-12Zr	Hast.-X	72.6	0.196	0.015	9.9	720	610	4.2
ND-35	U-15Pu-12Zr	Hast.-X	74.9	0.197	0.015	10.4	725	615	4.4
ND-37	U-15Pu-12Zr	Hast.-X-280	63.8	0.207	0.015	10.4	720	610	4.4
ND-39	U-15Pu-12Zr	Hast.-X-280	65.4	0.207	0.015	10.2	720	610	4.3
ND-44	U-15Pu-12Zr	Hast.-X-280	66.4	0.208	0.015	9.9	710	600	4.2

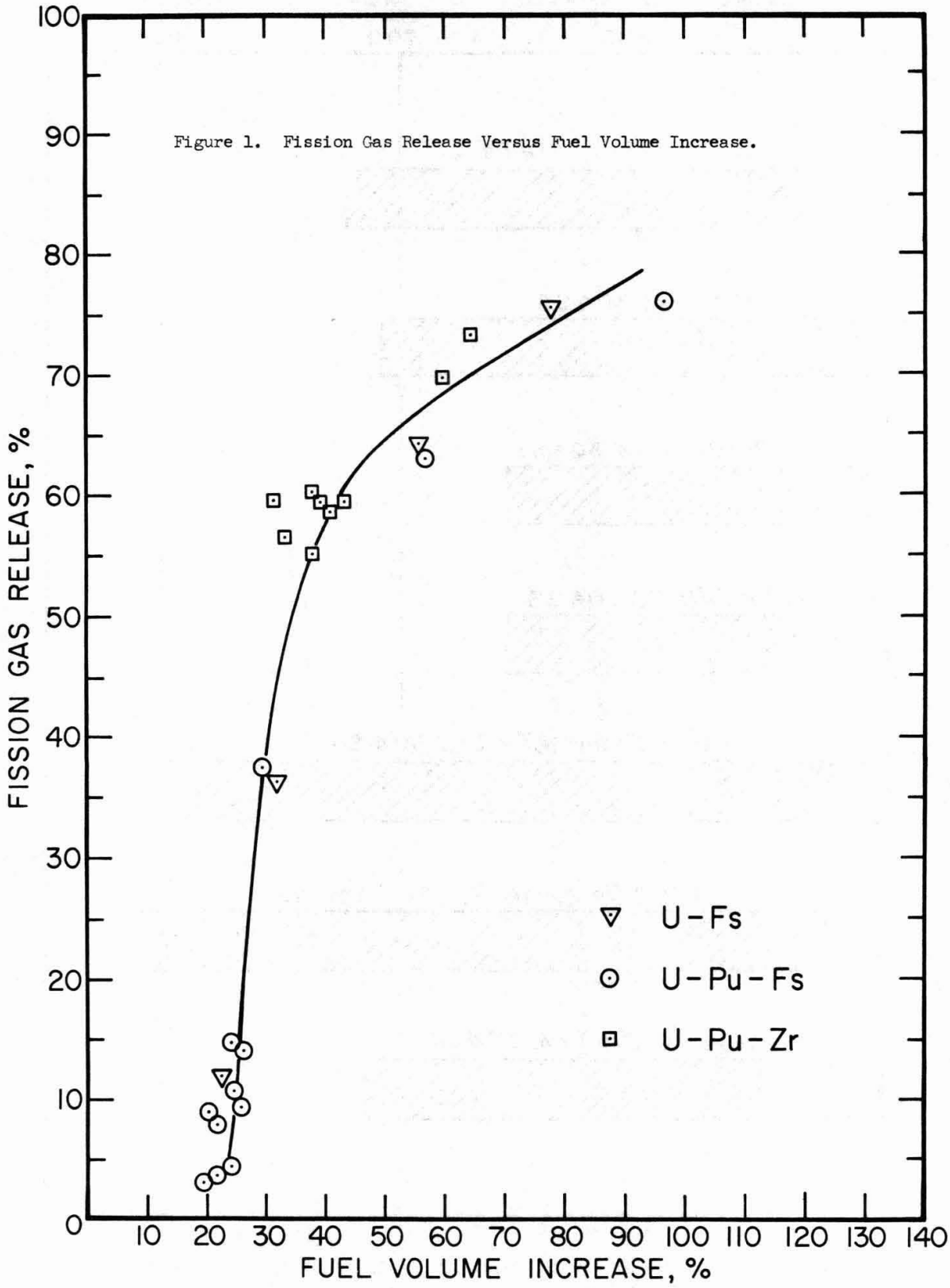

Figure 1. Fission Gas Release Versus Fuel Volume Increase.

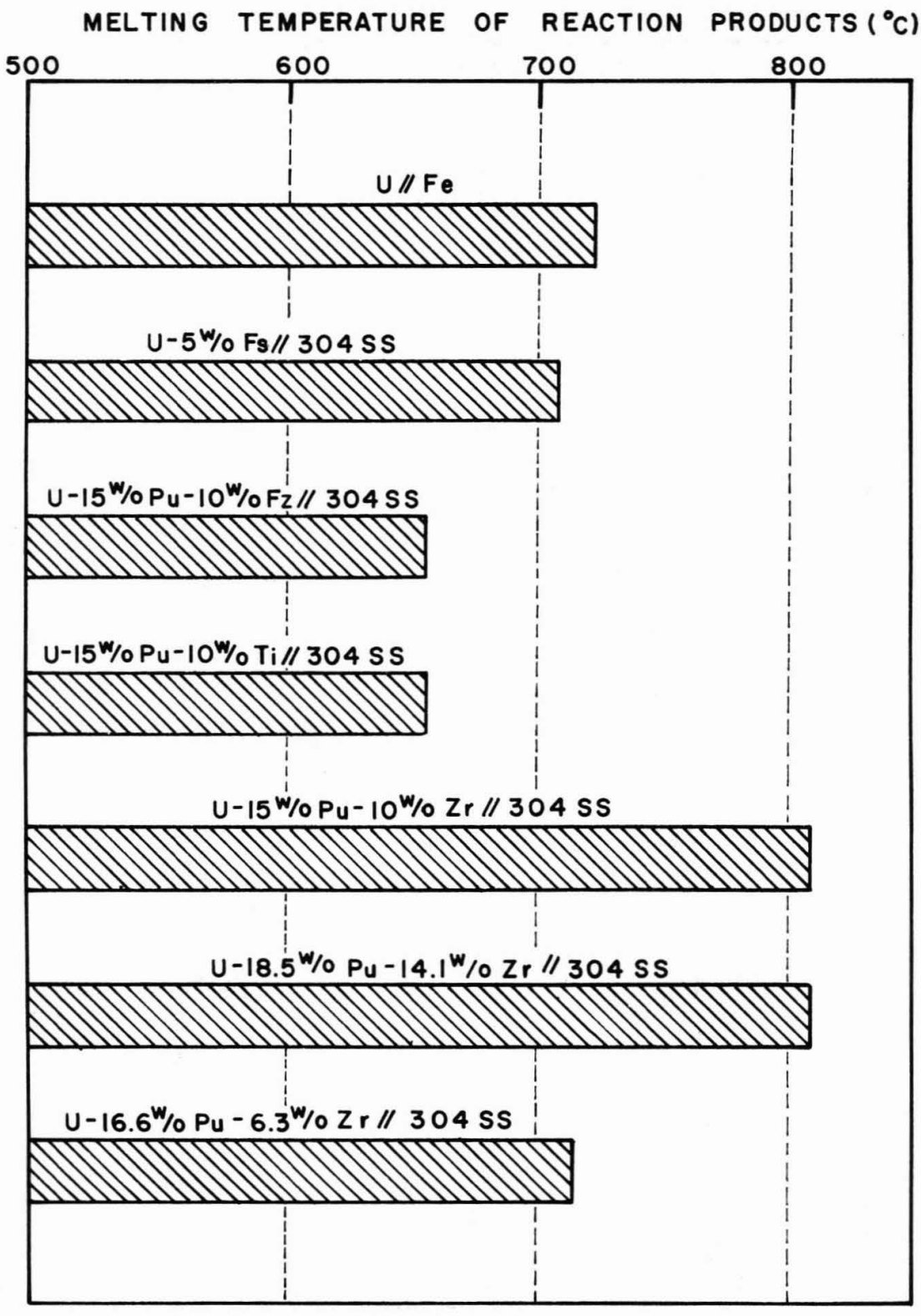

Figure 2. Melting Temperature of Reaction Products of Type 304 Stainless Steel with Several Fuels.

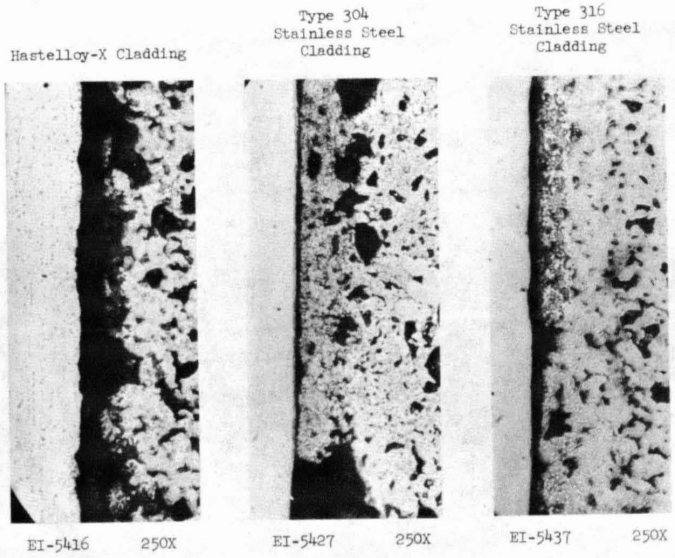

Figure 3. Clad-Fuel Interface of U-15 wt.% Pu-12 wt.% Zr and Hastelloy-X, Type 304 Stainless Steel, and Type 316 Stainless Steel Irradiated at Maximum Jacket Temperatures of 610°C for 2.4 at.% Burnup.

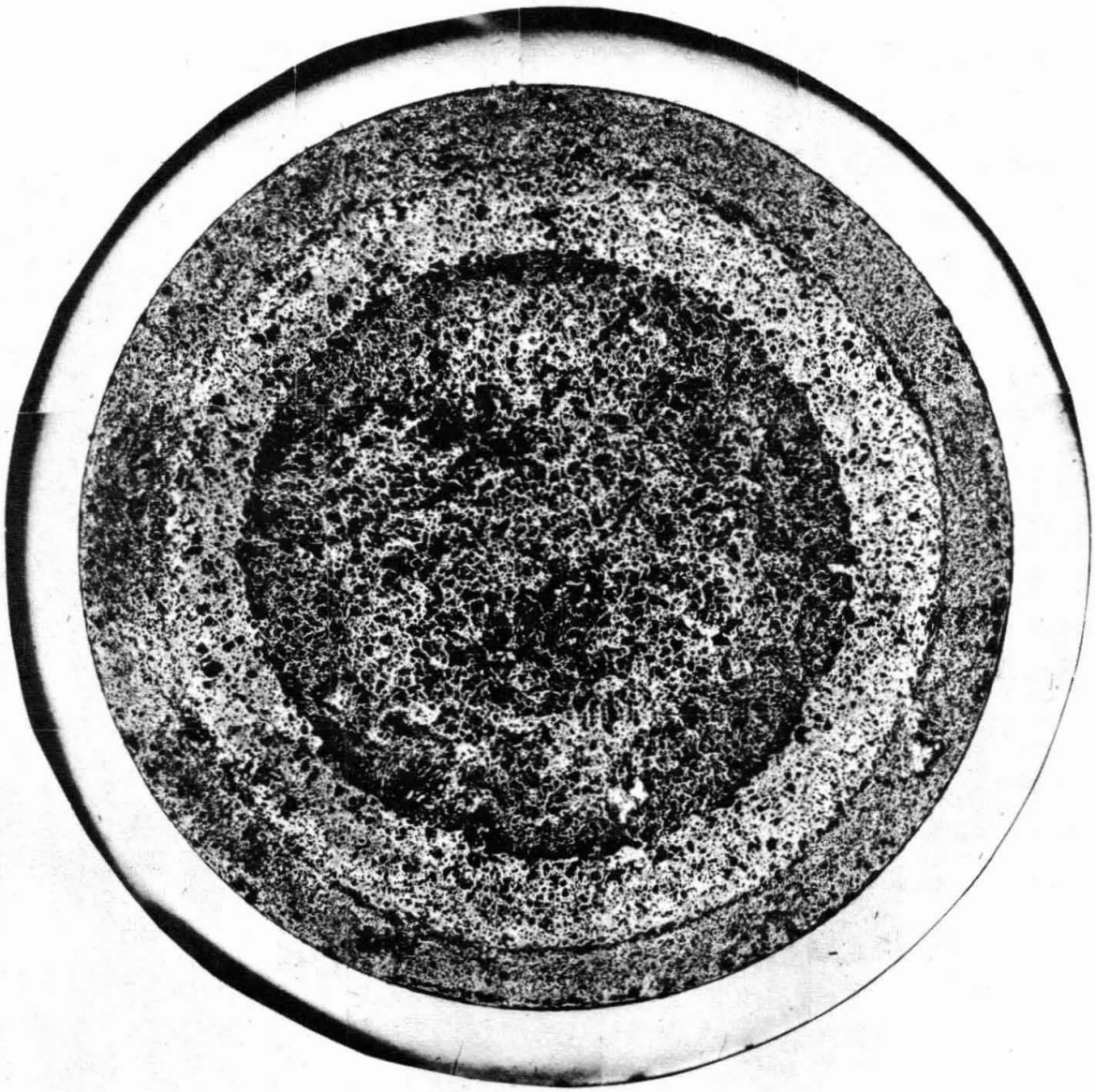

106-8919 32X

Figure 4. Transverse Section of U-15 wt.% Pu-12 wt.% Zr Alloy Jacketed in Hastelloy-X. The concentric bands in the fuel were correlated to phase transformation temperatures.

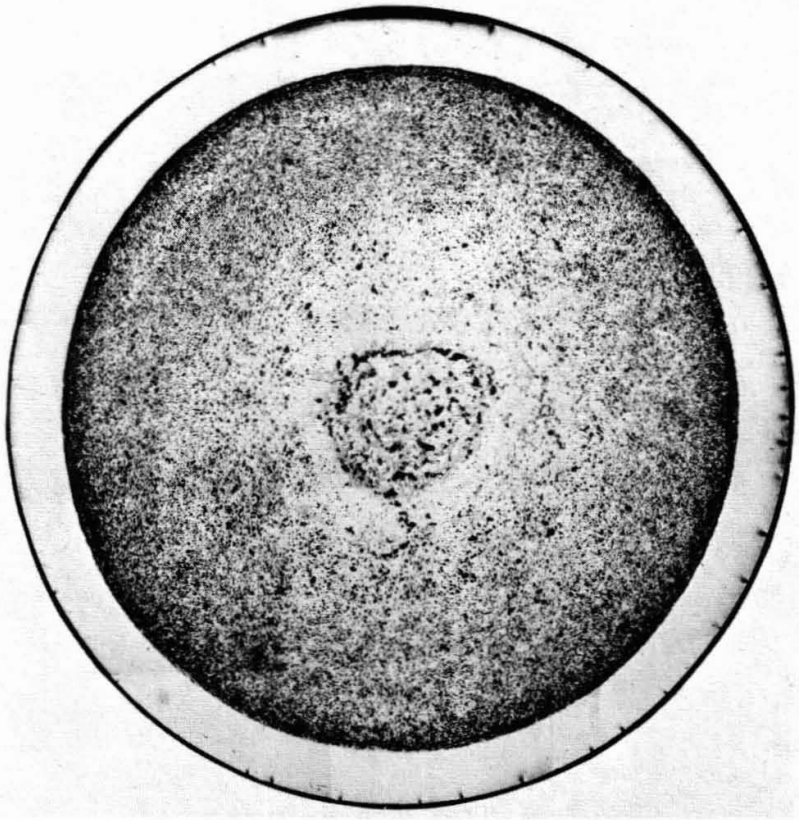

EI-5887 20X

Figure 5. Transverse Section of U-15 wt.% Pu-10 wt.% Ti Clad in V-20 wt.% Ti Tubing and Irradiated to 10.7 at.% Burnup at Maximum Clad Temperatures of 630°C.